INTERNATIONAL ATOMIC ENERGY AGENCY

INDC(CCP)-434
Distr.: IE/EL

I N D C **INTERNATIONAL NUCLEAR DATA COMMITTEE**

Experimental and Theoretical Study of the Yields of Residual Product Nuclei Produced in Thin Targets Irradiated by 100-2600 MeV Protons

Yu.E. Titarenko
(Project manager)
Institute for Theoretical and Experimental Physics (ITEP)

Co-authors: V.F. Batyaev, E.I. Karpikhin, R.D. Mulambetov, A.B. Koldobsky, V.M. Zhivun, S.V. Mulambetova, K.A. Lipatov, Yu.A. Nekrasov, A.V. Belkin, N.N. Alexeev, V.A. Schegolev, Yu.M. Goryachev, V.E. Luk'yashin, E.N. Firsov

September 2002

IAEA NUCLEAR DATA SECTION, WAGRAMER STRASSE 5, A-1400 VIENNA

Documents in the EL series are available in only limited quantities in hardcopy form. They may be downloaded in electronic form from http://www-nds.iaea.org/indc_sel.html or sent as an e-mail attachment. Requests for hardcopy or e-mail transmittal should be directed to services@iaeand.iaea.org or to:

Nuclear Data Section
International Atomic Energy Agency
PO Box 100
Wagramer Strasse 5
A-1400 Vienna
Austria

September 2002

Final
Project Technical Report
of ISTC 839B-99

Experimental and Theoretical Study of the Yields of Residual Product Nuclei Produced in Thin Targets Irradiated by 100-2600 MeV Protons

(From 1 January 1999 to 31 December 2000 for 24 months)

Yury Efimovich Titarenko
(Project manager)
Institute for Theoretical and Experimental Physics (ITEP)

Co-authors: V.F. Batyaev, E.I. Karpikhin, R.D. Mulambetov, A.B. Koldobsky, V.M. Zhivun, S.V. Mulambetova, K.A. Lipatov, Yu.A. Nekrasov, A.V. Belkin, N.N. Alexeev, V.A. Schegolev, Yu.M. Goryachev, V.E. Luk'yashin, E.N. Firsov.

February 2001

The work was supported financially by EU, Norway, and Japan and performed under the contract to the International Science and Technology Center (ISTC), Moscow.

Experimental and theoretical study of the yields of residual product nuclei produced in thin targets irradiated by 100-2600 MeV protons
(From 1 January 1999 to 31 December 2000 for 24 months)

Yury Efimovich Titarenko
(Project manager)
Institute for Theoretical and Experimental Physics (ITEP)[1]

The objective of the project is measurements and computer simulations of independent and cumulative yields of residual product nuclei in thin targets relevant as target materials and structure materials for hybrid accelerator-driven systems coupled to high-energy proton accelerators. The yields of residual product nuclei are of great importance when estimating such basic radiation-technology characteristics of hybrid facility targets as the total target activity, target “poisoning", buildup of long-lived nuclides that, in turn, are to be transmuted, product nuclide (Po) α-activity, content of low-pressure evaporated nuclides (Hg), content of chemically-active nuclides that spoil drastically the corrosion resistance of the facility structure materials, etc.

In view of the above, radioactive product nuclide yields from targets and structure materials were determined by an experiment using the ITEP U-10 proton accelerator in 47 irradiation runs for different thin targets: ^{182,183,184,186}W at proton energies 0.2, 0.8, and 1.6 GeV; ^{nat}W, ^{56}Fe, ^{58}Ni, and ^{93}Nb at 2,6 GeV; ^{232}Th, ^{nat}U, ^{99}Tc, at 0.1, 0.2, 0.8, and 1.6 GeV; ^{59}Co and ^{63,65}Cu at 0.2, 1.2, 1.6, and 2.6 GeV; ^{nat}Hg at 0.1, 0.2, 0.8, and 2.6 GeV and, additionally, ^{208}Pb at 1.0 GeV. As a result, 4050 cumulative and independent yields of residual radioactive product nuclei, whose lifetimes range from 8 minutes to 32 years, have been measured. Besides, the monitor ^{27}Al(p,x)^{24}Na and ^{27}Al(p,x)^{7}Be reaction cross sections have been measured at proton energies from 0.07 GeV to 2.6 GeV. The experimental nuclide yields were determined by the direct γ-spectrometry method. The γ-spectrometer resolution is of 1.8 keV at the 1332 keV γ-line. The experimental γ-spectra were processed by the GENIE2000 code. The γ-lines were identified, and the cross sections calculated, by the ITEP-developed SIGMA code using the PCNUDAT database. The proton fluence was monitored by the ^{27}Al(p,x)^{22}Na reaction.

Some of the results have been compared with the data obtained elsewhere, in particular with the recent GSI inverse kinematics experiments.

The measured data are compared with the simulations by the LAHET, CEM95, CEM2k, CASCADE, CASCADE/INPE, YIELDX, HETC, and INUCL codes. The predictive power of the tested codes is different but was found to be satisfactory for most of the nuclides in the spallation region, though none of the benchmarked codes agree well with the data in the whole mass region of product nuclides and all should be improved further. On the whole, the predictive power of all codes for the data in the fission product region is worse than in the spallation region; therefore, development of better models for fission-fragment formation is of first priority.

Keywords: nuclear reaction, spallation, fission, fragmention, yields, residual nuclides, cross sections, simulation, Monte-Carlo codes, comparison

[1]B. Cheremushkinskaya 25, 117259 Moscow, Russia, Phone +7-095-123-6383, Fax +7-095-127-0543, E-mail: Yury.Titarenko@itep.ru

The work has been performed by the following institutes and collaborators:

1. Participating institutes:

   1. Leading Institute: Institute for Theoretical and Experimental Physics (ITEP), B. Cheremushkinskaya 25, 117259, Moscow, Russia, Phone +7-095-123-6383, Fax +7-095-127-0543, E-mail Yury.Titarenko@itep.ru

2. Foreign Collaborators:

   1. Dr. W. Gudowski, The Royal Institute of Technology, Dep. of Neutron & Reactor Physics, Lindstedtvgen 30, S-10044 Stockholm, Fax 46 8 105 519, 46 8 106 948.

   2. Prof. M. Salvatores, Commissariat a l'Energy Atomique, Direction des Reacteurs Nucleaires, CEN - Cadarache, F - 13108 Saint Paul Lez Durance Cedex, France, Fax 33 4 42 25 33 65.

   3. Prof. R. Michel, Zentrum fuer Strahlenschutz und Radiooekologie, University of Hannover, Am Kleinen Felde 30, D - 30167 Hannover, Germany, Fax 49 511 762 3319.

   4. Dr. G. Benamati, ENEA (Ente Nazionale per le Nuove Tecnologie L'Energia e l'Ambiente) Fusion Division, C.R. Brasimone, I-40032 Camugnano (BO) Italy, Fax 39 534 80 12 25.

   5. Dr. H. Yasuda, Accelerator Radiation Laboratory, Japan Atomic Energy Research Institute, Shirakata-shirane 2-4, Tokai-mura, Ibaraki-ken 319-11, Japan, Fax 81 29 282 64 96.

   6. Dr. H. Takada, Center for Neutron Science, Japan Atomic Energy Research Institute, Tokai-mura, Naka-gun, Ibaraki-ken, 319-1195, Japan, E-mail : takada@omega.tokai.jaeri.go.jp

Contents

1 INTRODUCTION

This work is the final report on the ISTC Project#839B "Experimental and theoretical study of the yields of residual product nuclei produced in thin targets irradiated by 100-2600 MeV protons"[1].

The values of the yields of residual product nuclei in the medium- and high-energy proton-irradiated thin targets are extensively used in various fundamental and applied researches. The yield values are used to optimize the isotope production in accelerators, to design, develop, and operate high-current accelerators, and to interpret residual product nuclide yields formed in meteorites by cosmic ray-induced nuclear reactions. The yields of residual product nuclei are used also in astrophysics and medicine.

In recent years, the residual product yield data have been widely adopted in the feasibility analyses of accelerator-driven systems (ADS) applicable, for instance, to nuclear waste transmutation [2, 3, 4]. This is related primarily to the information on the applicability scope of the various simulation codes used to calculate high-energy interactions in the ADS structure elements with a view to more reliable calculations of the ADS nuclear physical parameters and performances.

The reported Project is aimed at experimental determination and computer-aided simulation of independent and cumulative yields of residual product nuclei in the ADS target and structure materials. Table 1 lists the proton energies and the target materials studied under the Project.

Table 1: Target materials and proton energies.

Target	Proton energy (GeV)						
	0.1	0.2	0.8	1.0	1.2	1.6	2.6
^{182}W		+	+			+	
^{183}W		+	+			+	
^{184}W		+	+			+	
^{186}W		+	+			+	
^{232}Th	+	+	+		+	+	
^{nat}U	+	+	+		+	+	
^{99}Tc	+	+	+		+	+	
^{59}Co		+			+	+	+
^{63}Cu		+			*	+	+
^{65}Cu		+			*	+	+
^{nat}Hg	+	+	+				+
^{56}Fe							+
^{58}Ni							+
^{93}Nb							+
^{nat}W							+
^{208}Pb				**			

* irradiated during the Feasibility Study stage of the Project (ISTC Project 839-0).
** additional 1.0 GeV proton irradiation of ^{208}Pb for comparing between the results of the direct (p $\rightarrow$ $^{208}_{82}$Pb; ITEP, Moscow), and inverse ($^{208}_{82}$Pb $\rightarrow$ $^{1}_{1}$H; GSI, Darmstadt) kinematics.

2 EXPERIMENTAL DETERMINATION TECHNIQUES

The techniques for experimental determining the reaction product yields are described in detail in [5, 6]. As the techniques have been persistently in progress since the publication [5] of 1998, this report is the first to present their most updated version the latest version of the techniques.

Any of the measured reaction products generated in different-energy proton interactions with matter can originate both in the reaction proper and in the decays of its chain precursors. Thus, the set of terms used in studying the mass and charge distributions of fission products can conveniently be used to process and interpret experimental results In terms of the set, the independent and cumulative yields of reaction products underlie the formalism. Conforming to the adopted terminology, the independent yield $\sigma_{ind}(A, Z)$ of a reaction product with mass number A and charge Z is meant to be a probability for the nuclide to be produced directly as a reaction proceeds. The cumulative yield $\sigma_{cum}(A, Z)$ is meant to be a probability for the nuclide (A,Z) to be produced in all the appropriate processes that can lead to its production.

Some applications make use also of the concept of mass yield $\sigma_{mass}(A)$, which is the sum of all independent yields of the elements of a given mass, $\sigma_{mass}(A) = \sum_z \sigma_{ind}(A, Z)$, or, equivalently, is the sum of cumulative yields of the stable nuclides of a given mass.

2.1 Mathematical representation of the reaction product yield values

Generation of residual product nuclei in proton interactions with a target nucleus is governed by intranuclear processes, namely, spallation, fission, fragmentation, emission of light nuclei and nucleons, decays of the residual product chain precursors.

The general form of proton interactions with a target nucleus is

$$ {}^{A_T}_{Z_T}T(p, x){}^{A}_{Z}N \ , $$

where T and N are the chemical symbols of the target and product nuclei; A_T and Z_T are, respectively, the mass number and charge of the target nuclide; A and Z are mass number and charge of a nuclide produced in the respective nuclear reaction. During the irradiation, the variations in the concentrations of two chain nuclides produced in an irradiated thin target may be presented as

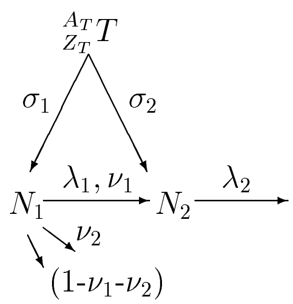

$$ \begin{cases} \dfrac{dN_1(t)}{dt} = \sigma_1 N_T \Phi - \lambda_1 N_1(t) \ , \\[2ex] \dfrac{dN_2(t)}{dt} = \sigma_2 N_T \Phi + \nu_1 \lambda_1 N_1(t) - \lambda_2 N_2(t) \ , \end{cases} \qquad (1) $$

with the initial conditions $N_1(0) = 0$ and $N_2(0) = 0$.

In (1), N_1 and N_2 are the numbers of nuclei produced; σ_1 and σ_2 are their independent yields; λ_1 and λ_2 are the decay constants; ν_1 is the probability for nuclide 1 to decay into nuclide 2, i.e., the branching ratio; N_T is the number of nuclei ${}^{A_M}_{Z_M}T$ in an experimental sample; Φ is the mean proton flux density; t is the actual time elapsed from the irradiation start to a current moment within the irradiation.

Given a pulsed irradiation mode, the solution for the set of differential equations (1) at the irradiation stop moment $t_{irr} = (K-1)T + \tau$ is described as

$$N_1\left((K-1)T+\tau\right) = \frac{N_T \Phi \sigma_1 F_1}{\lambda_1} , \tag{2}$$

$$N_2\left((K-1)T+\tau\right) = N_T \Phi \nu_1 \frac{1}{\lambda_2-\lambda_1}\sigma_1 F_1 + \frac{N_T\Phi}{\lambda_2}\left[\sigma_2 - \frac{\lambda_1}{\lambda_2-\lambda_1}\nu_1\sigma_1\right] F_2 , \tag{3}$$

where τ is the duration of a single proton pulse; T is the pulse repetition period; K is the number of irradiation pulses; F_j is the function

$$F_j = \left(1 - e^{-\lambda_j \tau}\right) \frac{1 - e^{-\lambda_j K T}}{1 - e^{-\lambda_j T}} , \qquad j = 1, 2 . \tag{4}$$

The after-irradiation decay of the product nuclides is described by the set

$$\begin{cases} \dfrac{dN_1(t)}{dt} &= -\lambda_1 N_1(t) , \\ \\ \dfrac{dN_2(t)}{dt} &= \nu_1\lambda_1 N_1(t) - \lambda_2 N_2(t) . \end{cases} \tag{5}$$

with initial conditions $N_1(0)=N_{1_0}$ and $N_2(0)=N_{2_0}$.

Here, N_{1_0} and N_{2_0} are numbers of product nuclei as radioactive cooling starts (irradiation stops); t is the current time elapsed from the irradiation stop moment.

The solution for (5) at any moment within the decay time t is

$$N_1(t) = N_{1_0} e^{-\lambda_1 t} , \tag{6}$$

$$N_2(t) = \left[N_{2_0} + \frac{\lambda_1}{\lambda_1-\lambda_2}\nu_1 N_{1_0}\right] e^{-\lambda_2 t} - \frac{\lambda_1}{\lambda_1-\lambda_2} N_{1_0}\nu_1 e^{-\lambda_1 t} , \tag{7}$$

The number of product nuclei at the irradiation stop moment is the same as their number at the decay start moment. In this case, the following condition is satisfied:

$$N_{1_0} = N_1\left((K-1)T+\tau\right) \ , \ N_{2_0} = N_2\left((K-1)T+\tau\right) \ . \tag{8}$$

The actual experiment measures the count rates $\tilde{S}_{1_i}$ and $\tilde{S}_{2_i}$ in the total absorption peaks at γ-line energies E_1 and E_2 making allowance for dead time. These same count rate can be expressed via the values of $N_1(t)$ and $N_2(t)$, which solve the set (5):

$$S_{1_i} = \frac{1}{t_{true_i}} \int_{t_{b_i}}^{t_{e_i}} N_1(t)\lambda_1\eta_1\varepsilon_1 dt , \quad S_{2_i} = \frac{1}{t_{true_i}} \int_{t_{b_i}}^{t_{e_i}} N_2(t)\lambda_2\eta_2\varepsilon_2 dt, \tag{9}$$

where η_1 and η_2 are the γ-abundances per decay (number of emitted photons per decay). ε_1 and ε_2 are the spectrometric efficiencies at γ energies E_1 and E_2; t_{b_i}, t_{e_i} are the start and stop moments of the i-th measurement run; t_{true_i} is the duration of the i-th measurement run (which is identical for $\tilde{S}_{1_i}$ and $\tilde{S}_{2_i}$ because they both are measured in one and the same spectrum).

Applying, then, equation (8) to the cooling start moment $t = t_{decay_i}$ of the i-th measurement run for S_{1_i} and S_{2_i}, we get

$$S_{1_i} = A_0 \frac{1 - e^{-\lambda_1 t_{true_i}}}{\lambda_1 t_{true_i}} e^{-\lambda_1 t_{decay_i}} \tag{10}$$

$$S_{2_i} = A_1 \frac{1 - e^{-\lambda_1 t_{true_i}}}{\lambda_1 t_{true_i}} e^{-\lambda_1 t_{decay_i}} + A_2 \frac{1 - e^{-\lambda_2 t_{true_i}}}{\lambda_2 t_{true_i}} e^{-\lambda_2 t_{decay_i}} \tag{11}$$

where

$$A_0 = N_T \Phi \sigma_1 \eta_1 \varepsilon_1 F_1 \ , \tag{12}$$

$$A_1 = N_T \Phi \sigma_1 \eta_2 \varepsilon_2 \frac{\lambda_2}{\lambda_2 - \lambda_1} \nu_1 F_1 \ , \tag{13}$$

$$A_2 = N_T \Phi \eta_2 \varepsilon_2 \left(\sigma_2 - \sigma_1 \nu_1 \frac{\lambda_1}{\lambda_2 - \lambda_1} \right) F_2 \ . \tag{14}$$

The coefficients A_0, A_1, and A_2, which carry information on the cross sections σ_1 and σ_2, are determined by least-squares fit of the measured S_{1i} and S_{2i} via the functions

$$g(t) = A_0 \frac{1 - e^{-\lambda_1 t_{true}}}{\lambda_1 t_{true}} e^{-\lambda_1 t} \ , \tag{15}$$

$$f(t) = A_1 \frac{1 - e^{-\lambda_1 t_{true}}}{\lambda_1 t_{true}} e^{-\lambda_1 t} + A_2 \frac{1 - e^{-\lambda_2 t_{true}}}{\lambda_2 t_{true}} e^{-\lambda_2 t} \ . \tag{16}$$

On introducing the quadratic functionals R_1 and R_2

$$R_1 = \sum_{i=1}^{L_1} (\tilde{S}_{1_i} - S_{1_i})^2 / \Delta \tilde{S}_{1_i}^2 = \sum_{i=1}^{L_1} \left(\tilde{S}_{1_i} - A_0 h_{1i} e^{-\lambda_1 t_{decay_i}} \right)^2 / \Delta \tilde{S}_{1_i}^2 \ , \tag{17}$$

$$R_2 = \sum_{i=1}^{L_2} (\tilde{S}_{2_i} - S_{2_i})^2 / \Delta \tilde{S}_{2_i}^2 = \sum_{i=1}^{L_2} \left(\tilde{S}_{2_i} - A_1 h_{1i} e^{-\lambda_1 t_{decay_i}} - A_2 h_{2i} e^{-\lambda_2 t_{decay_i}} \right)^2 / \Delta \tilde{S}_{2_i}^2 \ , \tag{18}$$

$$h_{ji} = \frac{1 - e^{-\lambda_j t_{true_i}}}{\lambda_j t_{true_i}} . \tag{19}$$

where $\Delta\tilde{S}_{1i}$ and $\Delta\tilde{S}_{2i}$ are the absolute errors in $\tilde{S}_{1i}$ and $\tilde{S}_{2i}$; L_1 and L_2 are numbers of experimental points for the first and second nuclide, respectively; h_{ji} is the set of the coefficients that allow for the decay of the j-th nuclide (j=1,2) in the i-th measurement run (i=1,..,L_1 for the first nuclide and i=1,..,L_2 for the second nuclide). Using, then, the condition of minimizing the functionals R_1 and R_2, we get the following expressions to find the parameters A_0, A_1, and A_2 together wth their errors:

$$A_0 = \frac{\sum_{i=1}^{L_1} \left(\tilde{S}_{1_i} e^{-\lambda_1 t_{decay_i}} h_{1i} / \Delta \tilde{S}_{1_i}^2 \right)}{\sum_{i=1}^{L_1} \left(e^{-2\lambda_1 t_{decay_i}} h_{1i}^2 / \Delta \tilde{S}_{1_i}^2 \right)} \ , \qquad \Delta A_0 = \left(\sum_{i=1}^{L_1} \frac{e^{-2\lambda_1 t_{decay_i}} h_{1i}^2}{\Delta \tilde{S}_{1_i}^2} \right)^{-1/2} \ , \tag{20}$$

$$\vec{A} = M^{-1} \vec{Z} \ , \qquad \Delta A_i = \sqrt{M_{ii}^{-1}} \ , \qquad (i = 1, 2) \ , \tag{21}$$

where

$$\vec{A} = \begin{Bmatrix} A_1 \\ A_2 \end{Bmatrix}, \qquad \vec{Z} = \begin{Bmatrix} Z_1 \\ Z_2 \end{Bmatrix} .$$

The matrix M and the vector $\overrightarrow{Z}$ in the right-hand side of the initial set of linear equations are

$$M_{ij} = \sum_{k=1}^{L_2} \left(e^{-(\lambda_i+\lambda_j)t_{decay_k}} h_{ik} h_{jk} / \Delta S_{2k}^2 \right) , \tag{22}$$

$$Z_i = \sum_{k=1}^{L_2} \left(S_{2k} e^{-\lambda_i t_{decay_k}} h_{ik} / \Delta S_{2k}^2 \right) , \qquad i,j = 1,2 . \tag{23}$$

Calculating the cross sections necessitates determination of the proton flux density Φ. With that purpose, an experimental sample was irradiated together with the Al monitor, for which we have, by analogy with expressions (2), (10) and (12):

$$S_{Na_i} = \frac{1}{t_{true_i}} \int_{t_{b_i}}^{t_{e_i}} N_{Al} \Phi \sigma_{st} F_{Na} \eta_{Na} \varepsilon_{Na} e^{-\lambda_{Na} t} dt = B e^{-\lambda_{Na} t_{b_i}} \frac{1 - e^{-\lambda_{Na} t_{true_i}}}{\lambda_{Na} t_{true_i}} , \tag{24}$$

where σ_{st} is either $^{27}Al(p,x)^{24}Na$ or $^{27}Al(p,x)^{22}Na$ monitor reaction cross section. The parameter B is also determined by least-squares fit of the experimental points through a dependence of the form (15) using formulas (20). The number of Na nuclei produced in the monitor will, then, be

$$N_{Na} = \frac{B}{\eta_{Na} \varepsilon_{Na} \lambda_{Na}} = N_{Al} \Phi \sigma_{st} \frac{F_{Na}}{\lambda_{Na}} ,$$

This permits the mean proton flux density Φ to be calculated as

$$\Phi = \frac{N_{Na} \lambda_{Na}}{N_{Al} \sigma_{st} F_{Na}} . \tag{25}$$

Formulas (12), (20), and (25) can be used to obtain an expression for calculating the cumulative (or independent) yield of the first nuclide. The yield of the first nuclide will be regarded as cumulative if that nuclide has its short-lived precursors producible in a given nuclear reaction:

$$\sigma_1^{cum} = \frac{A_0}{\eta_1 \varepsilon_1 F_1 N_{Na}} \frac{N_{Al}}{N_T} \frac{F_{Na}}{\lambda_{Na}} \sigma_{st} . \tag{26}$$

At the same time, formulas (13), (14), (21), and (25) can be used to obtain expressions for calculating the cumulative yield of the first nuclide, as well as the independent and cumulative yields of the second nuclide:

$$\sigma_1^{cum} = \frac{A_1}{\nu_1 \eta_2 \varepsilon_2 F_1 N_{Na}} \frac{N_{Al}}{N_T} \frac{\lambda_2 - \lambda_1}{\lambda_2} \frac{F_{Na}}{\lambda_{Na}} \sigma_{st} , \tag{27}$$

$$\sigma_2^{ind} = \left(\frac{A_2}{F_2} + \frac{A_1}{F_1} \frac{\lambda_1}{\lambda_2} \right) \frac{1}{\eta_2 \varepsilon_2 N_{Na}} \frac{N_{Al}}{N_T} \frac{F_{Na}}{\lambda_{Na}} \sigma_{st} , \tag{28}$$

$$\sigma_2^{cum} = \sigma_2^{ind} + \nu_1 \sigma_1^{cum} = \left(\frac{A_1}{F_1} + \frac{A_2}{F_2} \right) \frac{1}{\eta_2 \varepsilon_2 N_{Na}} \frac{N_{Al}}{N_T} \frac{F_{Na}}{\lambda_{Na}} \sigma_{st} . \tag{29}$$

Obviously, the yields calculated by formulas (26) and (27) must be the same. However, the yield obtained by formula (26) is usually included in the final results because the calculation reliability of (26) is higher.

The errors in the cross sections $\Delta\sigma_1^{cum}$, $\Delta\sigma_2^{ind}$, and $\Delta\sigma_2^{cum}$ may be calculated by the error transfer formula making allowance for all the errors in the terms of expressions (27), (28), (29). Considering that $\Delta A_i^2 = M_{i,i}^{-1}$, the errors in the functions $G_1(\overrightarrow{A})$ and $G_2(\overrightarrow{A})$,

$$G_1(\overrightarrow{A}) = \frac{A_2}{F_2} + \frac{A_1}{F_1}\frac{\lambda_1}{\lambda_2} \tag{30}$$

$$G_2(\overrightarrow{A}) = \frac{A_1}{F_1} + \frac{A_2}{F_2}, \tag{31}$$

of the parameters A_1 and A_2, which are obtained by the least-squares fit and enter expressions (28) and (29), were calculated as

$$\Delta G_i^2 = grad\ G_i \cdot M^{-1} \cdot (grad\ G_i)^T, \qquad i = 1, 2,$$

where

$$gradG_i = \left(\frac{\partial G_i}{\partial A_1}, \frac{\partial G_i}{\partial A_2}\right)$$

The calculations having been made, the errors may be presented as

$$\Delta G_1^2 = \sum_{i,j=1}^{2} M_{i,j}^{-1}\left(\frac{\lambda_1}{\lambda_2}\right)^{4-i-j}\frac{1}{F_i}\frac{1}{F_j} \tag{32}$$

$$\Delta G_2^2 = \sum_{i,j=1}^{2} M_{i,j}^{-1}\frac{1}{F_i}\frac{1}{F_j} \tag{33}$$

If a few nuclides of different half-lives are of the same γ-line energy (within the spectrometric resolution) and, besides, the precursors of the nuclides either are absent or have half-lives much smaller (or, in the "shielding"case, much longer) compared with any of the said nuclides, then the total count rate in the total absorption peak at moment t_{decay_i} equals the sum of the γ-line count rates for each of the nuclides:

$$S_{1sum_i} = \sum_{k=1}^{n}\frac{A_k}{t_{true\ i}}\int_{t_{b_i}}^{t_{e_i}} e^{-\lambda_k t}dt = \sum_{k=1}^{n} A_k\frac{1-e^{-\lambda_k t_{true\ i}}}{\lambda_k t_{true\ i}}e^{-\lambda_k t_{decay_i}}$$

$$A_k = N_T\Phi\sigma_k\eta_k\varepsilon F_k$$

where n is the number of the nuclides, ε is the detection efficiency that corresponds to their common γ-energy.

The coefficients A_i may be found from the approximation curve through the least-squares method by minimizing the functional

$$R = \sum_{i=1}^{L}\left(\tilde{S}_{1sum_i} - S_{1sum_i}\right)^2/\Delta\tilde{S}_{1sum_i}^2 = \sum_{i=1}^{L}\left(\tilde{S}_{1sum_i} - \sum_{k=1}^{n} A_k h_{ki} e^{-\lambda_k t_{decay_i}}\right)^2/\Delta\tilde{S}_{1sum_i}^2 \tag{34}$$

$$h_{ki} = \frac{1-e^{-\lambda_k t_{true\ i}}}{\lambda_k t_{true\ i}} \tag{35}$$

in the parameters A_i. Here, $\tilde{S}_{1sum_i}$ and $\Delta\tilde{S}_{1sum_i}$ are, respectively, the measured total count rate in the total absorption peak at the moment t_k and the error in the measured total counting rate; L is the number of experimental points In such a manner, we get the set of linear equations

$$\vec{Z} = M \times \vec{A}$$

where

$$\vec{A} = \begin{Bmatrix} A_1 \\ A_2 \\ \vdots \\ A_n \end{Bmatrix} , \qquad \vec{Z} = \begin{Bmatrix} Z_1 \\ Z_2 \\ \vdots \\ Z_n \end{Bmatrix}$$

$$Z_i = \sum_{k=1}^{L} \tilde{S}_{1sum_k} h_{ik} e^{-\lambda_i t_{decay_k}} / \Delta\tilde{S}^2_{1sum_k}$$

$$M_{ij} = \sum_{k=1}^{L} e^{-(\lambda_i+\lambda_j)t_{decay_k}} h_{ik} h_{jk} / \Delta\tilde{S}^2_{1sum_k}$$

The solution for the set is

$$\vec{A} = M^{-1} \times \vec{Z}$$

So, the production cross section of each of the nuclides may be presented as

$$\sigma_k^{cum} = \frac{A_k}{\eta_k \varepsilon F_k N_{Na}} \times \frac{N_{Al}}{N_T} \frac{F_{Na}}{\lambda_{Na}} \sigma_{st}. \qquad (36)$$

It should be noted that formulas (27) – (29) are deduced on assumption that the γ-count rates of each nuclide produced under irradiation are determined to within a desired accuracy throughout the time interval from the irradiation stop moment to the actual intensity detection threshold. In practice, however, the above requirement may (or may not) be met, thus resulting in the situation that can be either favourable or unfavourable for measurements and data analysis. Since any such situation is determined fully by the numerical values of nuclear constants of the given nuclides, the situations are expedient to analyze in terms of definite examples.

Curve 1 in Fig. 1 illustrates the most favourable situation, as regards the discussed analysis. The situation corresponds to the ^{192}Hg ($T_{1/2}$ = 4.85 h) $\rightarrow$ ^{192}Au ($T_{1/2}$=4.94 h) decay chain, with measuring the ^{192}Au γ-line at E_γ = 316.5 keV (η_γ=58%). Despite the similar half-lives, the absence of any addends to the measured γ-line (i.e., null contribution from γ-lines of any other nuclide whose energy is the same as the measured γ-line energy within the spectrometer resolution) provides for sufficiently accurate determination of the cumulative ^{192}Hg yield, as well as the independent and cumulative ^{192}Au yields.

The real situation often gets complicated, however, because the decay curve of the second nuclide cannot be measured correctly in every case within the desired (in the same sense as mentioned above) time interval. Its γ-line intensity is often difficult to measure in the beginning of a measurement run, right after the irradiation stops. In the case of short-lived nuclides, this is due to the fact that, within the period from the end of irradiation to the beginning of a measurement run (the cooling time), the nuclide N_1 (precursor) can partly or fully decay (if $\lambda_1 > \lambda_2$), or else a full or partial equilibrium occurs (if $\lambda_1 < \lambda_2$) between nuclides N_1 and N_2.

The contribution from nuclide N_1 will, then, never be reflected in the experimental decay curve of nuclide N_2. The situation gets even more complicated because a great number of the reaction products may include the nuclides whose half-lives are close to the half-life of a shorter-lived nuclide, either N_1 or N_2. In that case, as noted above, if the γ-line energy of such nuclides is the same (within the spectrometer resolution) as the measured γ-line energy of nuclide N_2, then one of the factors A_1 and A_2 cannot be determined at all, or can be determined with a great uncertainty and, thus, becomes useless when calculating the yields.

Fig. 1 is also a good illustration of a possible unfavourable situation for analyzing the nuclides of similar half-lives (Curve 1). If the ^{192}Au decay curve begins being measured in more than two days after the irradiation, the ^{192}Hg contribution becomes uncertain, resulting in erroneous calculations of the ^{192}Au yield. Such a situation is most probably responsible for the fact that the ^{192}Au yields measured in the reported work (see Table 46 below) and in work [8] differ by more than a factor 3 (46.9±6.6 mb and 160±50 mb, respectively).

Analyzing the possible structures of radioactive chains permits the following two very common situations to be singled out.

First, assume that $\lambda_1 < \lambda_2$. This situation is exemplified in by Curve 2 Fig. 1, which shows the decay of chain nuclides ^{188}Pt($T_{1/2}$=10.2 days)→^{188}Ir($T_{1/2}$=41.5 hours) detected by measuring the 2214.6 keV γ-line of the ^{188}Ir daughter nuclide. In this case, the decay curve of nuclide ^{188}Ir can be used to obtain fairly accurate values of the factors A_1 and A_2 and, hence, of σ_1^{cum}, σ_2^{ind}, and σ_2^{cum} ($\sigma_{^{188}Pt}^{cum}$, $\sigma_{^{188}Ir}^{ind}$, and $\sigma_{^{188}Ir}^{cum}$). Should this favourable situation get complicated (for example, the measurements began in 2 days after irradiation), then, even without observing the knee, the conclusion concerning the ^{188}Pt production is quite obvious because the 2214.6 keV γ-line of ^{188}Ir is measured with the ^{188}Pt halflife period. In this case, formula (27) may be used to calculate the

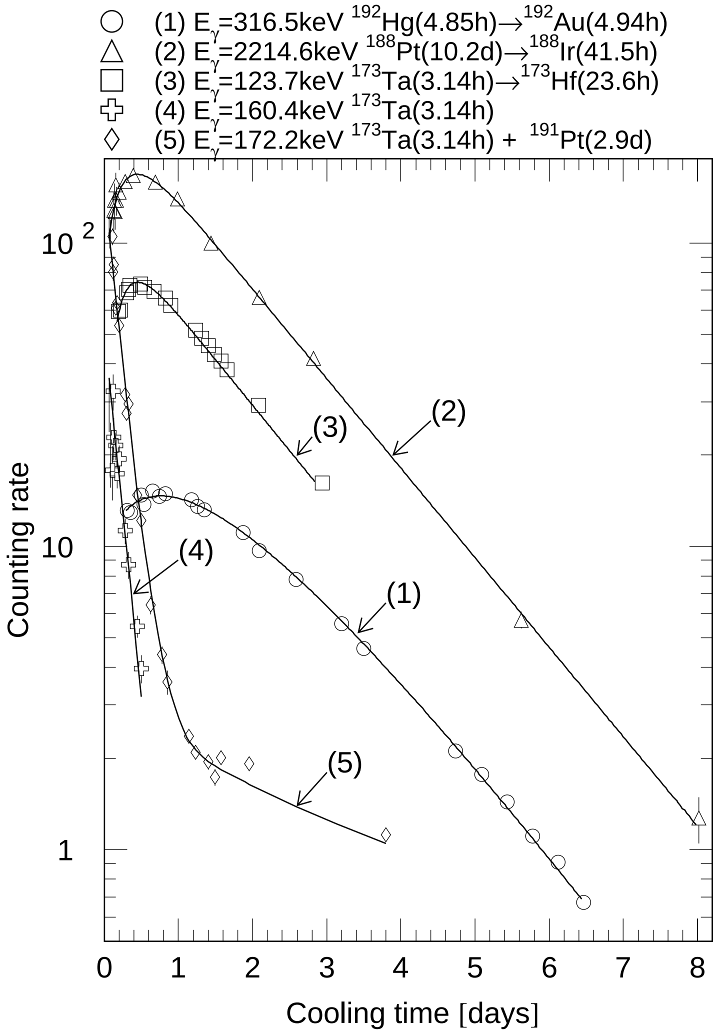

Fig. 1: The typical examples of the decay curves. Curve (1) is for the chain ^{192}Hg→ ^{192}Au. Curve (2) is for ^{188}Pt → ^{188}Ir. Curve (3) is for ^{173}Ta → ^{173}Hf. Curve (4) is for the independent ^{173}Ta decay. Curve (5) is for the independent ^{173}Ta + ^{191}Pt decay. (Scale factors x and X have been introduced, respectively, along the Y and X axes).

$\sigma^{cum}_{^{188}Pt}$ value, whereas the ^{188}Ir data are lost.

It should be noted that there even exists a nuclear decay data library that presents the ^{188}Pt γ-abundances corrected for the $(\lambda_2 - \lambda_1)/\lambda_2$ value [26]. The corrected yields are marked with an index (D) to notify the validity of using the daughter nuclide γ-lines when calculating the number of mother nuclei.

The inverse situation ($\lambda_1 > \lambda_2$) permits the factor A_2 alone to be determined reliably. This is exemplified by Curve 3 in Fig. 1, which is the decay curve of the chain nuclides ^{173}Ta ($T_{1/2}$=3.14 hours)→^{173}Hf ($T_{1/2}$=23.6 hours) recorded by measuring the 123.7 keV γ-line of ^{173}Hf. In this case, the factor A_2 alone can be determined to within the desired accuracy.

If, however, the eigen γ-line is used (this is shown in Fig. 1 by Curve 4, which is the ^{173}Ta decay curve measured via the 160.4 keV ^{173}Ta γ-line, or by Curve 5, which is the same, but inferred from the 172.3 keV ^{173}Ta γ-line with an addend contributed by the ^{191}Pt decay), then the factor A_0 can well be calculated, and the missing factor A_1 proves to be

$$A_1 = A_0 \frac{\eta_2 \varepsilon_2}{\eta_1 \varepsilon_1} \nu_1 \frac{\lambda_2}{\lambda_2 - \lambda_1} \; , \tag{37}$$

whereupon formulas (27)–(29) can be used to find σ^{cum}_1, σ^{ind}_2, and σ^{cum}_2 ($\sigma^{cum}_{^{173}Ta}$, $\sigma^{ind}_{^{173}Hf}$, and $\sigma^{cum}_{^{173}Hf}$).

If, however, the factor A_1 cannot be found, we may use the factor A_2 together with expression (14) to determine the constant ($\sigma^{cum^*}_2$), which we call the supra-cumulative yield. The latter can be presented as

$$\sigma^{cum^*}_2 = \sigma_2 + \frac{\lambda_1}{\lambda_1 - \lambda_2} \nu_1 \sigma^{cum}_1 = \frac{A_2}{\eta_2 \varepsilon_2 F_2 N_{Na}} \frac{N_{Al}}{N_T} \frac{F_{Na}}{\lambda_{Na}} \sigma_{st} \tag{38}$$

It should be noted that the difference between σ^{cum}_2 and $\sigma^{cum^*}_2$ is not specified in many of the relevant publications, despite the fact that $\sigma^{cum^*}_2$ is always greater than σ^{cum}_2. The explanation is that, the irradiation having ended, the nuclei of the second nuclide still keep being produced due to the decay of the first nuclide. This is formally equivalent to a shift Δt of the decay start moment:

$$\Delta t = \frac{1}{\lambda_2} \left[1 + \frac{\nu_1 \sigma^{cum}_1}{\sigma^{ind}_2 + \nu_1 \sigma^{cum}_1} \left(\frac{\lambda_2}{\lambda_1 - \lambda_2} \right) \right] \tag{39}$$

From formula (39), it is seen that Δt depends on the yields σ^{cum}_1 and σ^{ind}_2, thereby preventing the time correction Δt from being allowed for in the general case when determining σ^{cum}_2. At the same time, in the prevailing cases of $\sigma^{ind}_2 \ll \nu_1 \sigma^{cum}_1$, the time shift Δt can be presented to depend on the decay constants only:

$$\Delta t \cong \Delta t' = \frac{1}{\lambda_2} \left[1 + \left(\frac{\lambda_2}{\lambda_1 - \lambda_2} \right) \right] \tag{40}$$

Therefore, the cumulative yield of the second nuclide can be determined after a post-irradiation period sufficient for N_1 to decay into N_2 (normally, this equals from 6 to 10 half-lives of the first nuclide) by measuring the decay curve of the second nuclide with due allowance for the time shift Δt:

$$\sigma^{cum}_2 = \frac{A_2}{\eta_2 \varepsilon_2 F_2 N_{Na}} \frac{N_{Al}}{N_T} \frac{F_{Na}}{\lambda_{Na}} \sigma_{st} e^{-\lambda_2 \Delta t} \cong \frac{A_2}{\eta_2 \varepsilon_2 F_2 N_{Na}} \frac{N_{Al}}{N_T} \frac{F_{Na}}{\lambda_{Na}} \sigma_{st} \left(1 - \frac{\lambda_2}{\lambda_1} \right) \tag{41}$$

In case the condition $\sigma^{ind}_2 \ll \sigma^{cum}_1 \nu_1$ is not satisfied and the σ^{cum}_2 value cannot be calculated in any way accurately, we may estimate the difference

$$\Delta \sigma^{cum^*}_2 = \sigma^{cum^*}_2 - \sigma^{cum}_2 = \frac{\lambda_2}{\lambda_1 - \lambda_2} \nu_1 \sigma^{cum}_1 \tag{42}$$

Basing on the condition $\sigma_2^{cum^*} \geq \sigma_2^{cum} \geq \sigma_1^{cum}\nu_1$, we may estimate the upper limit for $\Delta\sigma_2^{cum^*}$:

$$\Delta\sigma_2^{cum^*} \leq \frac{\lambda_2}{\lambda_1 - \lambda_2}\sigma_2^{cum^*} \tag{43}$$

or, in the relative form,

$$\delta\sigma_2^{cum} = \frac{\Delta\sigma_2^{cum^*}}{\sigma_2^{cum^*}} \cdot 100\% \leq \frac{\lambda_2}{\lambda_1 - \lambda_2} \cdot 100\% \tag{44}$$

From formula (43) it is seen that the measured value of the supra-cumulative yield $\sigma_2^{cum^*}$ may sometimes be very different from its true value σ_2^{cum}. In the case of ^{179}Re, for example, formula (44) (see the data for ^{208}Pb in Table (46))indicates that $\delta\sigma_2^{cum}$ may reach $\sim$ 50%.

The $\delta\sigma_2^{cum}$ value was always estimated in case any unfavourable situation occurs. If the estimate exceeded the relative experimental error for a given nuclide, the type of the presented experimental yield value was designated cum^*. This fact was always borne in mind when comparing between experimental and simulated data (see formulas (90) and (91) in section 4.1).

2.2 Manufacture, certification, and irradiation of experimental samples

The eperimental samples and monitors were manufactured by cutting them from ^{nat}W, ^{232}Th, ^{nat}U, ^{99}Tc, ^{63}Cu, ^{65}Cu, ^{93}Nb, ^{208}Pb, and ^{27}Al metal foils, by pressing fine-dispersed (^{182}W, ^{183}W, ^{184}W, ^{186}W, ^{59}Co, ^{56}Fe, and ^{58}Ni) metal powders, or by pressing ^{nat}HgO oxide. Tc was chemically extracted from the irradiated reactor fuel elements.

All the samples and monitors were manufactured to be of the same 10.5-mm diameter. Table 2 presents the isotopic composition of all the experimental samples used in irradiations.

From Table 2 it is seen that the reported researches are characterised by predominant usage of high-enriched isotopic samples. Surely, the reported results can have been much affected by any chemical impurities in the experimental samples. Therefore, all the experimental materials were strictly tested and certified accordingly. Tables 3 – 6 present the full chemical composition of all experimental samples.

The total impurity content percentages of the high-enriched (^{56}Fe, ^{58}Ni, ^{63}Cu, ^{65}Cu, ^{182}W, ^{183}W, ^{184}W, and ^{186}W, ^{208}Pb) samples are presented in Tables 3 and 4 to conform to the quality certificate issued by the Stable Isotopes Scientific-Research Center, wherefrom the experimental sample materials were received. The bottom rows of Tables 3 and 4 show the identification numbers of the certificates.

Table 5 presents the results of analyzing the total impurity content in the experimental samples of natural stable isotopes. The analysis was made at the Laboratory of Mass-Spectrometry and Chromatography (MS&GS Lab) of the State Rare Earth Institute by spark mass-spectrometry method using a Japanese (JEOL Co)-made JMS-01-BM2 double-focus spark mass spectrometer. The mass-spectra were recorded on Ilford-Q high mass-spectrum resolution photo plates. The mass-spectra were quantitatively interpreted using a British (Joyce Loebl Co)-made MDM6 micro-densitometer coupled to an American-made NOVA-4 minicomputer. The impurity content was calculated using the MS&GC Lab-developed mathematical software. The random error in the analysis results is characterized by a relative standard deviation 0.15-0.30. The content of noble gases and transuranics in each given sample is below their detection threshold (0.001 ppm). The analysis results are reported in units of mass part per million relative to metal base (1 ppm = 0.0001%).

The isotopic and elemental compositions of radioactive experimental samples were analyzed at VNIINM. The chemical impurity content of all samples, the ^{230}Th content of natural thorium,

Table 2: Isotopic composition of targets

Isotope	State	Certificate identification number	Isotopic composition, %				
			^{180}W	^{182}W	^{183}W	^{184}W	^{186}W
^{182}W	metal	70-5	< 0.03	90.7	5.71	2.62	0.97
^{183}W	metal	78-8	0.07	4.62	73.3	20.08	1.93
^{184}W	metal	31-3.a	0.3	1.9	3.9	90.3	3.6
^{186}W	metal	85-2.a	<0.02	0.66	0.49	2.45	96.4
^{nat}W	metal	[9]*	0.13	26.3	14.3	30.67	28.6
^{232}Th	metal	VNIINM certificate	^{232}Th-99.9995 %; ^{232}Th-$5{\cdot}10^{-4}$ %.				
^{nat}U	metal	VNIINM certificate	^{234}U – 0.006 %; ^{235}U – 0.721±0.004 %; ^{236}U – <0.005 %; ^{238}U – 99.27±0.01 %.				
^{99}Tc	metal	VNIINM certificate	^{97}Tc - $<10^{-4}$; ^{98}Tc - $<10^{-4}$; ^{99}Tc - >99.9999 %.				
^{59}Co	metal	[9]*	100 %				
^{63}Cu**	metal	90	^{63}Cu – 99.6±0.1 %; ^{65}Cu – 0.4 %.				
^{65}Cu**	metal	135	^{63}Cu – 1.3 %; ^{65}Cu – 98.7±0.1 %.				
^{63}Cu	metal	93-5	^{63}Cu – 99.5 %; ^{65}Cu – 0.5 %.				
^{65}Cu	metal	52-5	^{63}Cu – 0.3 %; ^{65}Cu – 99.7 %.				
^{nat}Hg	oxide	[9]*	^{196}Hg – 0.14 %; ^{198}Hg – 10.02 %; ^{199}Hg – 16.84 %; ^{200}Hg – 23.13 %; ^{201}Hg – 13.22%; ^{202}Hg – 29.80%; ^{204}Hg – 6.85%.				
^{56}Fe	metal	284	^{54}Fe–0.3%; ^{56}Fe–99.5±0.1%; ^{57}Fe–0.2%; ^{58}Fe–< 0.05%.				
^{58}Ni	metal	165	^{58}Ni – 99.8±0.1 %; ^{60}Ni – 0.19 %; ^{61}Ni - < 0.01 %; ^{62}Ni – 0.01 %; ^{64}Ni – < 0.01 %.				
^{93}Nb	metal	[9]*	100 %				
^{208}Pb	metal	334-12	^{204}Pb - <0.01 %; ^{206}Pb - 0.87 %; ^{207}Pb - 1.93 %; ^{208}Pb - 97.2 %.				

* Isotopic composition is taken from [9].
**Irradiated at 1.2 GeV.

and the ^{97}Tc and ^{98}Tc content of technetium were determined by spark mass-spectrometry technique using a JEOL JMS-01-BM spark mass-spectrograph. The error of the results is 30%. The uranium isotopic composition was determined using a British (Micromac Co)-made Sector-54 thermal-ionizing mass spectrometer. Table 2 presents the isotopic composition analysis results. The chemical impurity content results of Table 6 are expressed in units of mass part per million (1ppm=0.0001%) relative to metallic base.

The occurrences of the long lived ^{98}Tc isotope ($T_{1/2} \sim 4.2 \times 10^6$ years) in the experimental samples were also monitored by the γ-spectrometry method. Fig. 2 shows the non-irradiated Tc–spectrum with two γ-lines of ^{98}Tc: 652.41 keV (η_γ=100%) and 745.35 keV (η_γ=102%). These lines were used to determine the ^{98}Tc content of the technetium samples ($< 10^{-4}$ at. %). The results of the two methods have proved to be the same within the experimental errors

Table 3: Chemical impurity content of high-enriched experimental samples

Chemical impurity, %	Target					
	^{56}Fe	^{58}Ni	^{63}Cu	^{63}Cu*	^{65}Cu	^{65}Cu*
Na	<0.001	0.005				
Mg	0.007	0.005				
Al	0.009	0.001				
Si	0.020	0.003				
S			<0.005	0.005		0.005
Cl	0.005					
K		0.001				
Ca	0.005	0.004				
Cr	0.013					
Fe		0.005	0.009	0.005	0.006	0.012
Co	<0.01					
Ni	0.001		0.005	0.01	<0.003	0.027
Cu	0.018	0.006				
Zn			0.032	<0.004	<0.004	<0.004
As			<0.004	<0.0005		<0.0005
Cd		<0.001				
Sn			0.001	0.006	<0.001	<0.003
Sb	0.002		<0.006	<0.006	0.023	<0.006
Pb		0.001	0.003	<0.001	0.002	0.003
Bi			<0.001	<0.001	<0.001	<0.001
Certificate Identification Number	284	165	93-5	90	52-5	135

*1.2 GeV proton-irradiated.

Table 4: Chemical impurity content of high-enriched experimental samples

Chemical impurity, %	Target				
	^{182}W	^{183}W	^{184}W	^{186}W	^{208}Pb
Na	<0.003	<0.003	<0.01	<0.003	0.0005
Mg	<0.003	<0.003	<0.01	<0.003	0.0004
Al	<0.003	<0.003	0.013	0.003	<0.001
Si	0.008	0.017	0.02	0.01	0.002
K	<0.01	<0.01	–	<0.01	
Ca	<0.003	<0.003	<0.01	0.003	0.0009
Cr	<0.005	<0.005	<0.01	<0.005	<0.003
Mn	<0.002	<0.002	–	<0.002	
Fe	0.013	0.02	0.01	0.01	0.002
Ni	<0.003	<0.003	0.01	<0.003	0.0003
Cu	<0.002	0.004	<0.01	0.003	0.0003
Zn					<0.001
Mo	0.007	0.06	<0.03	0.017	
Ag					<0.0002
Sn					<0.0003
Sb					<0.001
Bi					<0.0003
Certificate Identification Number	70-5	78-8	31-3.a	85-2.a	334-12

Table 5: Chemical impurity content of cobalt, niobium, mercury oxide, and natural tungsten

Chemical imourity, ppm	Target			
	Co	Nb	^{nat}HgO	^{nat}W
H	ND	ND	ND	ND
Li	<0.1	<0.07	0.08	40
Be	<0.05	<0.05	<0.07	<0.01
B	1	0.1	0.6	0.4
C	ND	ND	ND	ND
N	ND	ND	ND	ND
O	ND	ND	Base	ND
F	3	1	10	0.1
Na	10	<1	2	60
Mg	80	3	80	9
Al	200	10	60	20
Si	200	20	100	20
P	4	ND	0.6	2
S	50	8	10	40
Cl	3	4	300	50
K	20	<1	1	100
Ca	4	2	200	30
Sc	0.1	<0.6	<0.5	<0.3
Ti	200	6	400	2
V	2	<0.3	<0.3	5
Cr	50	3	20	30
Mn	900	0.9	7	2
Fe	300	200	300	2000
Co	Base	0.2	10	9
Ni	3000	0.4	40	900
Cu	2000	4	50	10
Zn	4000	2	60	<1
Ga	<0.3	20	<1	<0.6
Ge	<0.4	<0.5	<1	<0.7
As	<0.9	<0.2	<0.3	2
Se	<0.4	<0.4	<1	<0.5
Br	<0.2	<0.4	2	<0.8
Rb	<0.4	<0.5	<0.5	<0.6
Sr	6	<0.2	5	<0.3
Y	<0.3	<0.6	<0.7	<0.4
Zr	<0.4	7	20	<1
Nb	1	Base	<2	<3
Mo	7	30	<3	100
Ru	<2	<0.4	<1	<1
Rh	<0.5	<0.6	<0.5	<0.5
Pd	<2	<7	<1	<2
Ag	<0.9	<4	<2	<0.9
Cd	<3	<2	20	9

Table 5, cont'd

Chemical impurity, ppm	Target			
	Co	Nb	^{nat}HgO	^{nat}W
In	<0.8	<0.4	<0.5	<0.7
Sn	<2	<2	60	<2
Sb	<1	<2	<2	1
Te	<2	<3	<2	<2
I	<0.06	<0.5	3	<0.5
Cs	<0.4	<0.5	<0.5	<0.4
Ba	7	<1	100	<1
La	3	<0.4	<0.4	<0.4
Ce	9	<0.5	<0.4	<0.5
Pr	1	<0.4	<0.3	<0.4
Nd	20	<0.8	<0.7	<0.8
Sm	10	<0.9	<0.8	<0.9
Eu	<2	<0.5	<0.3	<0.5
Gd	<4	<0.8	<0.8	<0.8
Tb	<1	<0.4	<0.4	<0.4
Dy	<3	<0.8	<0.9	<0.8
Ho	<0.7	<0.5	<0.4	<0.5
Er	<3	<0.9	<0.9	<0.9
Tm	<0.8	<0.5	<0.5	<0.5
Yb	<2	<0.9	<1	<0.9
Lu	<1	<0.5	<0.5	<0.5
Hf	<3	<1	<1	<1
Ta	<1	300	ND	<0.8
W	1000	20	<2	Base
Re	<1	<0.9	<1	<0.9
Os	<3	<0.8	<2	<0.8
Ir	<2	<0.6	<1	<0.6
Pt	<2	<0.8	<3	<0.8
Au	<1	<0.6	<2	<0.6
Hg	<3	<1	Base	<1
Tl	<0.8	<0.7	<0.8	<0.7
Pb	800	<2	20	<2
Bi	<2	<0.7	<1	<0.7
Th	<2	<0.9	<1	<0.9
U	<1	<0.9	<1	<0.9

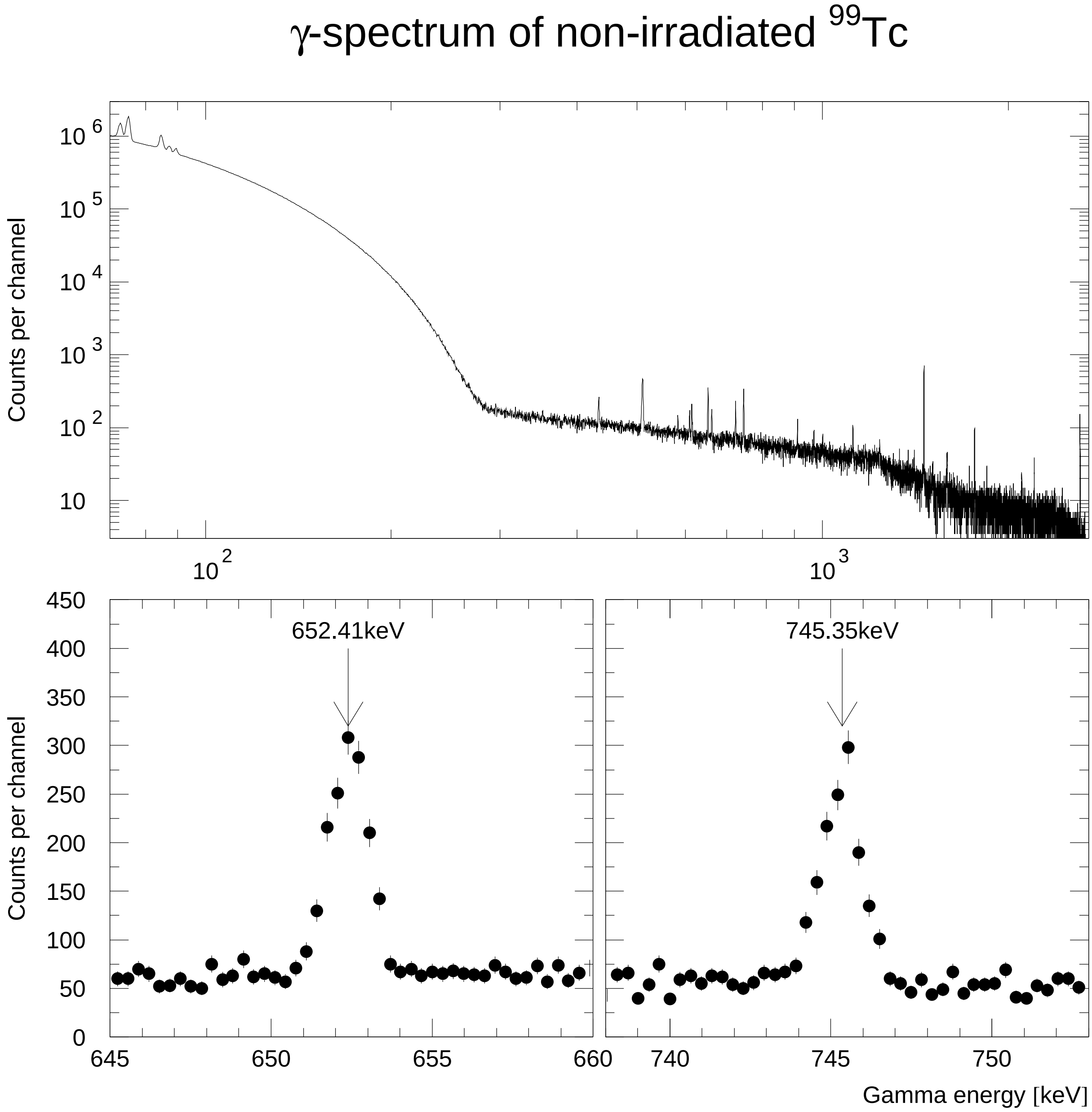

Fig. 2: γ-spectra of non-irradiated ^{99}Tc.

Having been manufactured, the experimental samples and monitors were weighed with a SARTORIUS Co-made BP-61 analytical balance (a $1 \cdot 10^{-4} g$ weighing accuracy) and, then, were "soldered"tight into polyethylene envelopes to form the Al monitor-Al interlayer-experimental sample sandwiches to be irradiated.

In each irradiation run, a sandwich was placed normally to proton beam. The sample and monitor manufacture precision has provided for identical geometrical dimensions of both.

In the latest experiments, the sandwich assembly and irradiation pattern was opposite to the above, namely, the experimental sample-Al interlayer-Al monitor arrangement was used.

Table 6: Chemical impurity content of natural Uranium, Thorium, and Technetium.

Chemical impurities	Target		
	U	Th	Tc
B	0.2	0.2	0.08
Mg	0.6	2	20
Al	30	30	50
Si	30	30	80
P	<1	<1	<1
Ca	16	16	40
Sc	<1	<1	<1
Ti	<1	<1	<1
V	<0.5	<0.5	<0.5
Cr	6.0	0.9	3.0
Mn	5.0	3.0	
Fe	200	70	100
Co	<1	<1	
Ni	9	1	20
Cu	10	4	50
Zn	2	2	2
Ga	<0.5	<0.5	<0.5
Ge	<0.5	<0.5	<0.5
As	<0.5	<0.5	<0.5
Se	<0.5	<0.5	<0.5
Br	<0.5	<0.5	<0.5
Sr	<0.5	<0.5	<0.5
Zr	3	3	6.0
Mo	<0.5	<0.5	<0.5
Rh	<0.5	<0.5	<0.5
Pd	<0.5	<0.5	<0.5
Ag	<0.5	<0.5	<0.5
Sb	<0.5	<0.5	<0.5
Te	<0.5	<0.5	<0.5
Hf	1	1	2.0
W	<1	<1	1.0
Th	<1	Base	<50
U	Base	<50	<50
REE *	<1	<1	<1

* Rare earth elements.

The arrangement was chosen to preclude any additional contribution from ^{22}Na and ^{24}Na to the experimental samples due to emission of the two nuclides from Al monitor.

The experimental samples were irradiated by two independent proton beams from the ITEP U-10 synchrotron, namely, the high-energy (800-2600 MeV) and low-energy (80-200 MeV) beams. Figs. 3 and 4 are the beam extraction system flowcharts

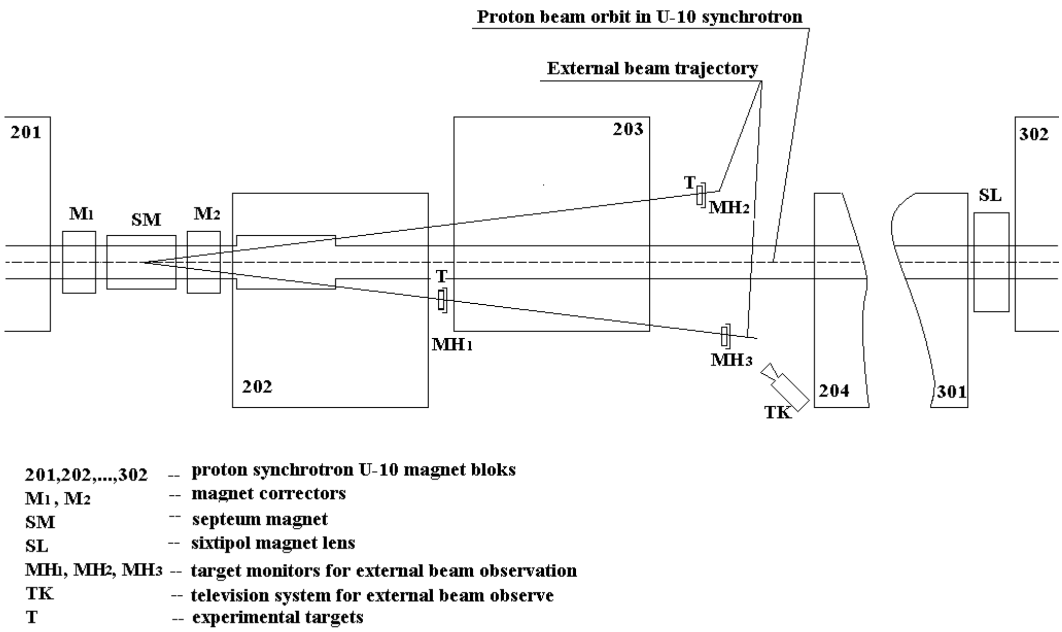

Fig. 3: The 800-2600 MeV proton beam extraction system flowchart

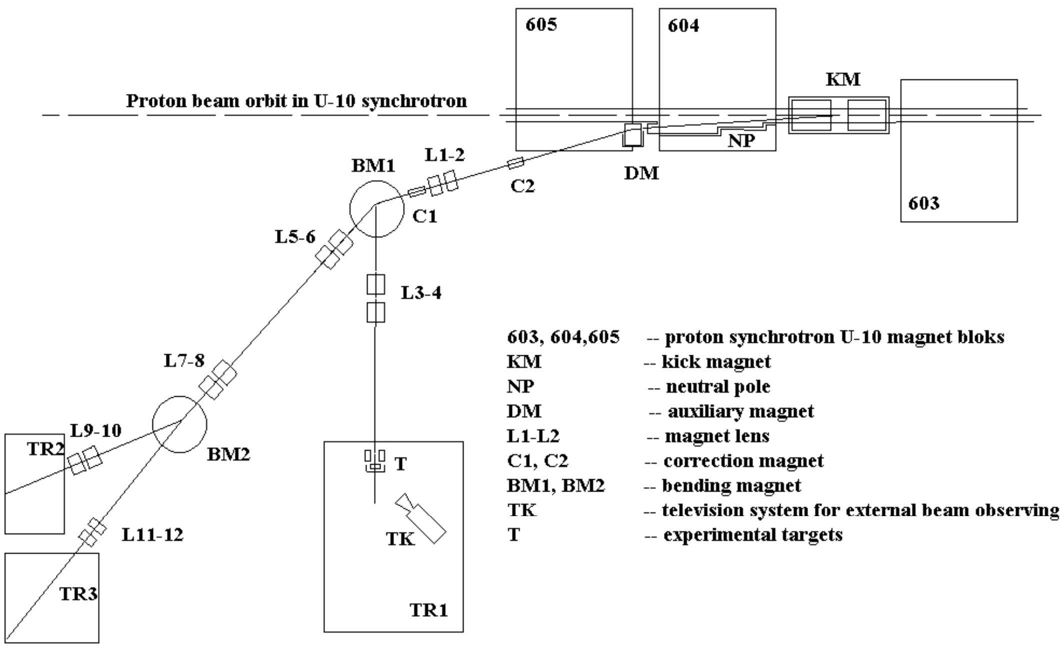

Fig. 4: The 70-200 MeV proton beam extraction system flowchart.

The high-energy beam section is ellipsis-shaped with $\sim 20{\times}12$ mm axes, $\sim 2{\cdot}10^{11}$ proton/pulse intensity, $\sim$ 16 min^{-1} pulse repetition rate, and $\sim$0.5 s pulse duration

The low-energy beam section is $\sim$ 30 mm diameter circle-shaped with $\sim 5\cdot10^{9}$ proton/pulse intensity, $\sim$ 16 min^{-1} pulse repetition rate, and 100 ns pulse duration

The geometric parameters of the beams were measured by the techniques describes in subsection 2.6.

Quite a different experimental design was used in 1200 MeV proton irradiations of high-enriched ^{63}Cu and ^{65}Cu samples. The irradiated sandwiches were stacked up, so as to order the Al monitor #1 - sample #1 - Al interlayer - Al monitor #2 - sample #2 arrangement. Two successive and independent irradiation runs were carried out. The sandwiches with ^{63}Cu samples were irradiated in the first run, and the sandwiches with ^{65}Cu samples in the second. After the irradiations, the experimental samples and the monitors were repacked into the hermetically sealed polyethylene envelopes. The samples and monitors labelled #1 were gamma-specrometered at ITEP. The samples and monitors labelled #2 were sent to JAERI, (Japan) to be processed there.

The time interval between irratiations of the ^{63}Cu and ^{65}Cu sandwiches was sufficient for the ITEP team to measure short-lived nuclides in ^{63}Cu sample #1.

2.3 γ-spectra: measurements and processing

After the irradiation runs, the experimental samples and monitors were measured using the CANBERRA PACKARD Trading Corp.-made gamma-spectrometering facility (a 1.8 keV energy resolution in the 1332 keV ^{60}Co) γ-line) based on a coaxial GC-2518 Ge detector, a 1510 integrated signal processor (a 6000 V power supply, a spectrometric amplifier, and a 100-MHz 8192-channel ADC), and a SYSTEM-100 master board that emulates the multichannel analyzer performance in IBM PC (full size PC compatible board that plugs into 8- or 16-bit slot).

FIg. 5 presents the measured γ-spectra of the ^{63}Cu(p,x) and ^{65}Cu(p,x) reaction products together with the background γ-spectrum measured inside the lead shield measured without any sample. Not a single unidentifiable γ-line was observed in the measured spectra

The background spectrum shows the presence of natural radionuclides alone, which are members of the ^{238}U, ^{235}U, ^{232}Th series, except for γ-line energy of 661keV (^{137}Cs) and 344.9, 722.9keV (^{108}Ag). Occurrences of ^{137}Cs and ^{108}Ag is due probably to the many-year operations of the heavy-water reactor in the laboratory house, where the measurements were taken.

During the initial stage of the researches, the γ-spectra were processed by the ASPRO code, which sought for the peaks, separated the multiplets in automatic mode, and Gaussian-approximated the photopeaks [20].

However, the actual experiments have shown that the potentialities of the automatic-mode processing codes get restricted when applied to the experimental γ-spectra of, particularly, heavy nuclides, which are very complicated because of a great number of γ-lines and, besides, are very unstable. Despite the fact that the Ge detector was used actually at its ultimate resolution level, the spectra still contained numerous unstable multiplets.

In view of the above, the ASPRO code was replaced with the GENIE2000 γ-spectrum processing code [21]. The latter is advantageous in that, after a set of experimental γ-spectra have been automatically processed by interactive fitting the peaks in each spectrum, the results of the tentative processing beyond the set can well be examined. Namely, we can find out whether the peak regions are the multiplets or the true peaks that do not meet the search requirements, or the spurious peaks, etc. The fitting quality is displayed as dots representing the normalized differences between data and fitting. This particular processing mode has much improved the quality of analyzing the measured γ-spectra.

Figs. 6 and 7, together with table 7 exemplify the GENIE2000 operation beyond the set by presenting the working window of the code with a fraction of the analyzed spectrum of the 800 MeV proton–irradiated ^{nat}U in 15 hours after the irradiation and by displaying the processing

Fig. 5: The measured γ-spectra of the ^{63,65}Cu(p,x) reaction products and the background γ-spectrum inside the lead shield.

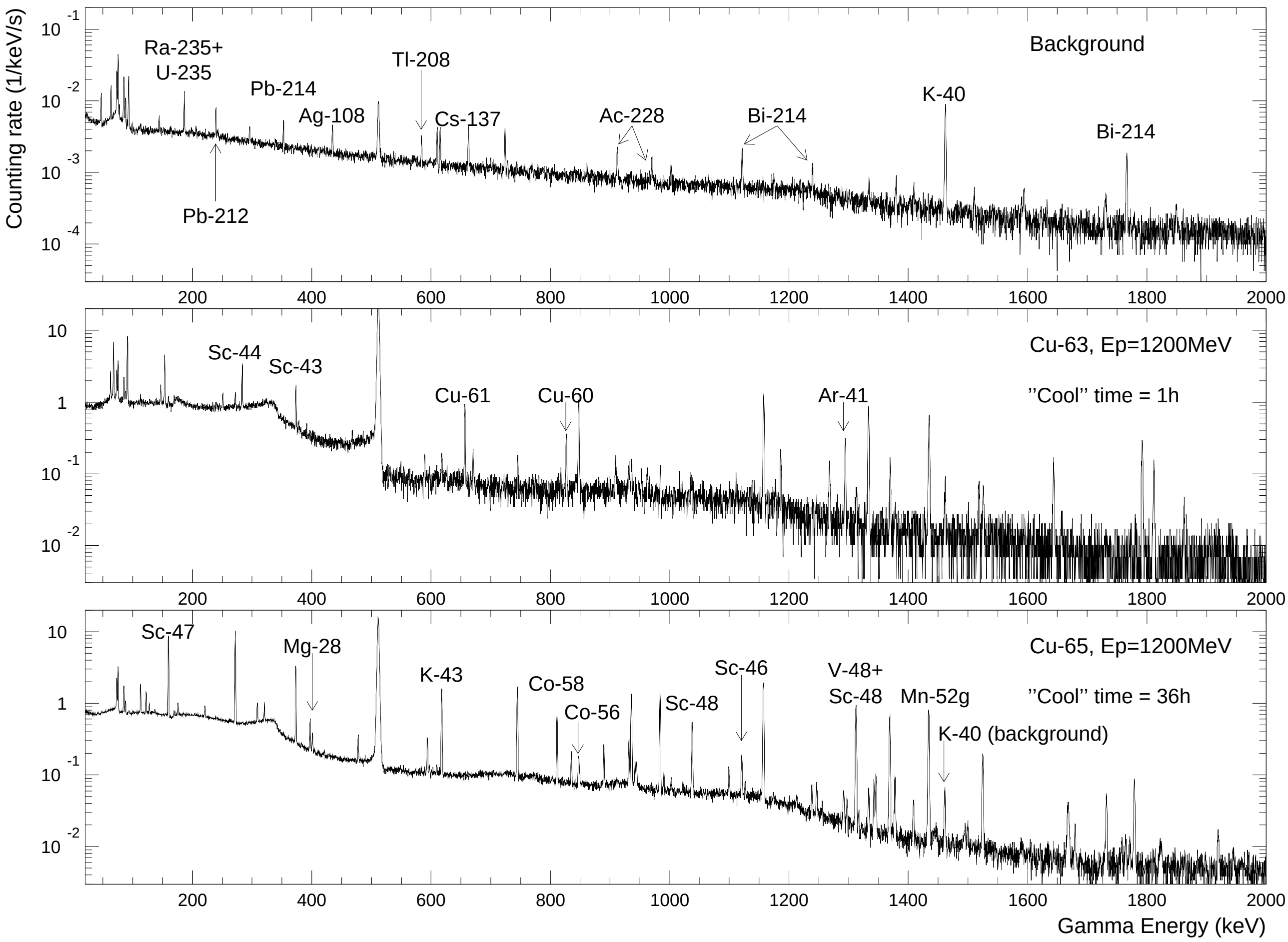

reports. The energies of the displayed γ-spectrum fragment are ranging from 770.6 kV to 796.1 kV.

The upper parts of the figures show the primary GENIE2000 processing in the automatic mode. It is seen that the multiplets are poorly separated, the fact confirmed by the code report (see Fig. 7). The bottom parts of the figures show the results of the additional manual fitting in the interactive fit mode. Table 7 presents the nuclear physics characteristics of the identified nuclides from [17] and the positions of the peaks calculated in terms of the energy calibration of the spectrometer for all ten peaks determined by GENIE2000.

Obviously the multiplet resolution quality has got improved, permitting the codes to separate the peaks differing by ~ 1 keV. This, in turn, permits five additional extra nuclides to be identified, thus providing for a substantial improvement of the determination quality of the reaction product yields.

The above processing conditions have made it possible to raise the accuracy and reliability when analyzing the measured γ-spectra, in particular the poorly resolved γ-spectra supported by scanty statistics.

The processed γ–spectra are united to form a single file that becomes the input file for the ITEP-developed SIGMA code. The SIGMA code plots the intensity variations of a selected γ-line versus time. After that, the γ–line energy and the calculated half-life are used to identify the produced nuclides and to calculate their cross sections by formulas (26-29),(36) using nuclear a

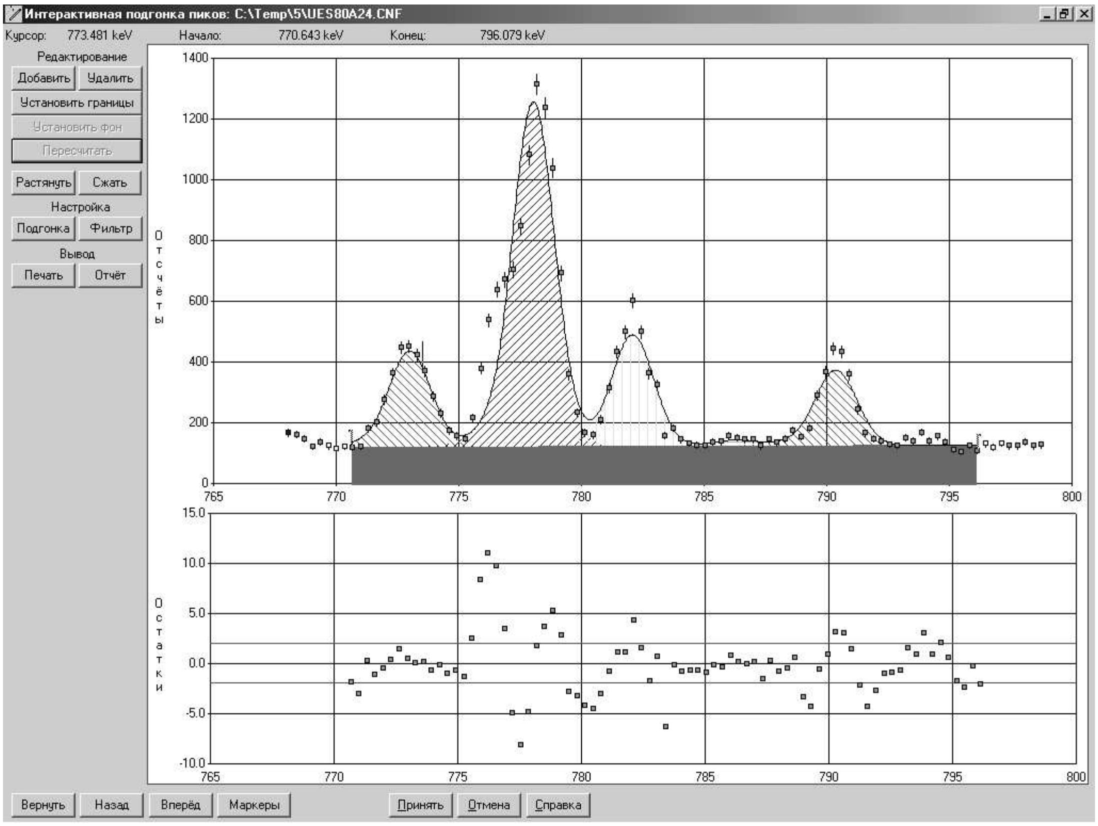

b

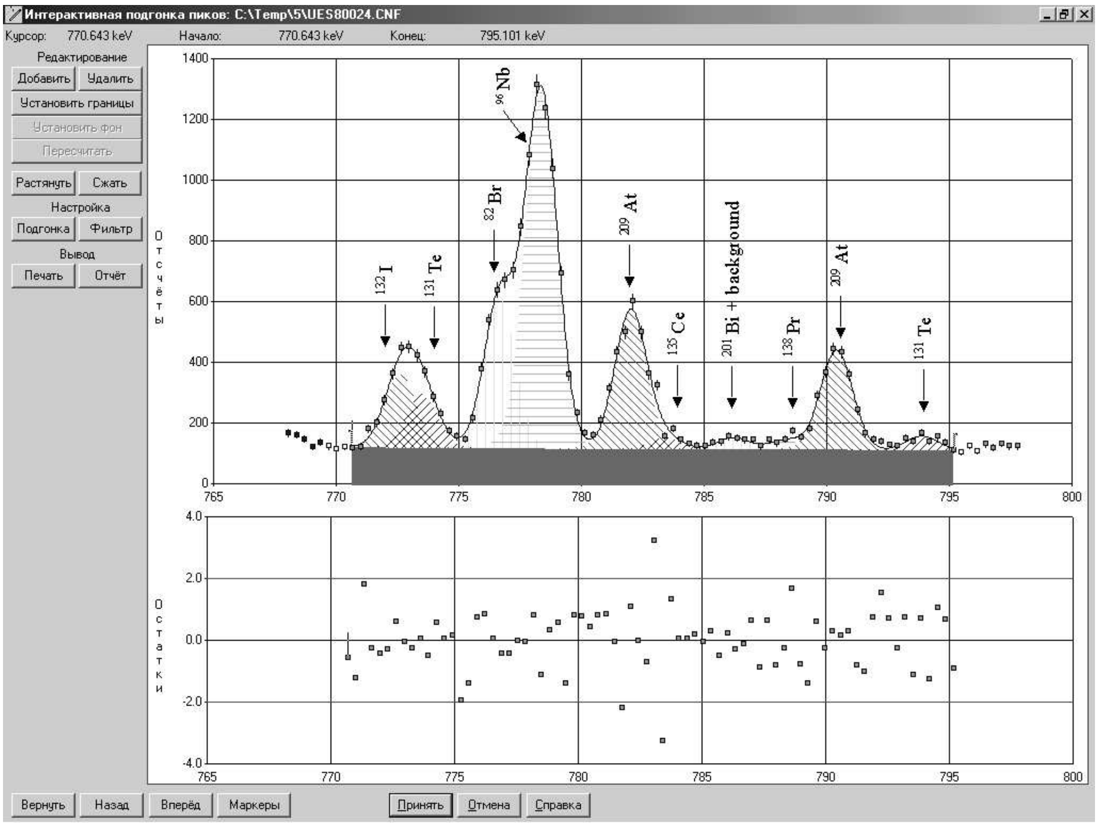

Fig. 6: Results of primary processing the of γ-spectrun by GENIE2000 in automatic mode (a) and of additional manual processing in interactive fit mode (b).

decay data from the PCNUDAT database [17], [18]. It should be noted that the information a

b

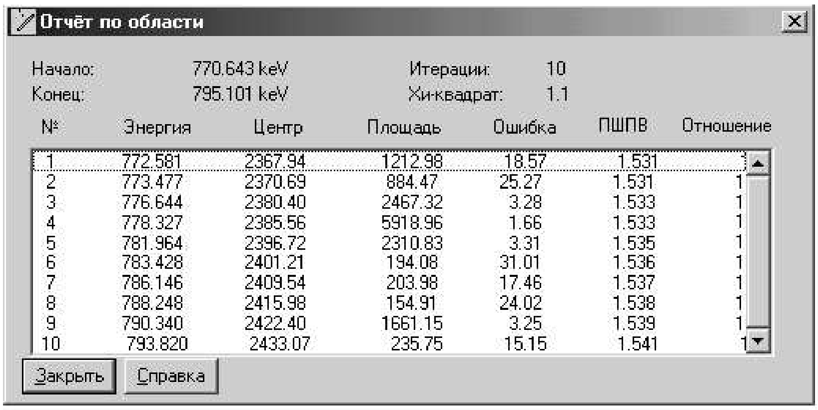

Fig. 7: The GENIE2000 report on the parameters of processing the found peaks. The legend in (a) (b) is the same as in Fig. 6.

Table 7: Nuclear physics characteristics of identified nuclides

	Nuclide	$T_{1/2}$	Energy, keV (PCNUDAT)	Energy, keV (GENIE)	γ-abundance, %
1	^{132}I	2.295 h	772.60	772.58	75.6
2	^{131}Te	30 h	773.67	773.48	38.9
3	^{82}Br	35.30 h	776.517	776.64	83.5
4	^{96}Nb	23.35 h	778.224	778.33	96.45
5	^{209}At	5.41 h	781.90	781.96	83.5
6	^{135}Ce	17.7 h	783.590	783.43	10.6
7	^{201}Bi	108 m	786.4	786.15	9.5
8	^{138}Pr	2.12 h	788.70	788.25	100.
9	^{209}At	5.41 h	790.20	790.34	63.5
10	^{131}Te	30 h	793.75	793.82	14.1

(experimental design, experimental sample parameters, spectrometer calibration data, measured γ-spectra, γ-spectrum processing results, calculation results, etc.) to be used in the measurements can be retrieved from the ExpData laboratory database. The format of the stored and continuously refreshed data is selected in such a way that the easiest access is reached with minimum storage space.

2.4 Determination of the spectrometer characteristics

The very great number of radioactive reaction products from proton irradiation of experimental samples generate a high-intensity γ-radiation, particularly in the very beginning of the post-irradiation period. Therefore, the measured γ-spectra are explicitly of extremely complicated form.

Any possible instability of the spectrometer performances is able not only to hamper the data acquisition and processing, but also to distort the eventual results. That is why the stability of the spectrometer performances was very carefully analyzed throughout the reported researches.

2.4.1 Determination of admissible measurement conditions

The parameters that define the admissible measurement conditions include

- The time-temperature stability,
- cascade effect summation,
- ultimate spectrometer load,
- height and energy dependences of the absolute spectrometer detection efficiency.

The temperature stability was maintained by producing stable microclimatic environment in the measurement room of the laboratory.

Spectrometer stability is assessed by regular measurements of ^{152}Eu γ-spectrum. The many-year observations (see Fig. 8) indicate that the position fluctuations of the photo peak detection maximum of the 121.78 keV, 778.90 keV, and 1408.01 keV γ-lines in the channels around their means are mostly within 0.10 %.

The observed temperature drift of the instrumental line in the measured γ-spectra is allowed for by continuous calibration of the spectrometer, thereby making it possible to keep the errors at a 0.1-0.3 keV level when measuring the γ-line energy of irradiated samples. This permits a significant reduction of the number of the nuclide γ-lines, which must be included as contributing additionally to the cross section of a respective reaction yield.

Fig. 9 presents the overall statistics for the spectrometer stability.

Quantitative estimates of detection loss due to high loads of the spectrometer were obtained by the two-source method. One of the sources (^{137}Cs) was placed at a fixed height H that determines the γ-source - Ge detector distance, while another source (^{152}Eu) was at a height that decreased during measurements. The position of the first source provided for a moderate load of the spectrometer, and the position of the second source imitated an increasing load inherent to the measurements.

Fig. 10 shows the variations of the peak area and energy resolution of the ^{137}Cs γ-line versus spectrometer load.

Conforming to these results, the ultimate load of the spectrometer did not exceed 5% in all of the measurements.

To remain within that limitation, we started monitoring the experimental samples at a ~500 mm height and, as the load decreased, the monitoring descended down to the ultimate height of 40 mm. In such a way, the cascade summation effects were reduced.

Experimental estimates of the cascade summation effects obtained using ^{24}Na and ^{60}Co at a 40 mm height have shown that the effects are within statistical errors. The independent and cumulative yields of the reaction products in formulas (26)-(29), (36) were calculated using the

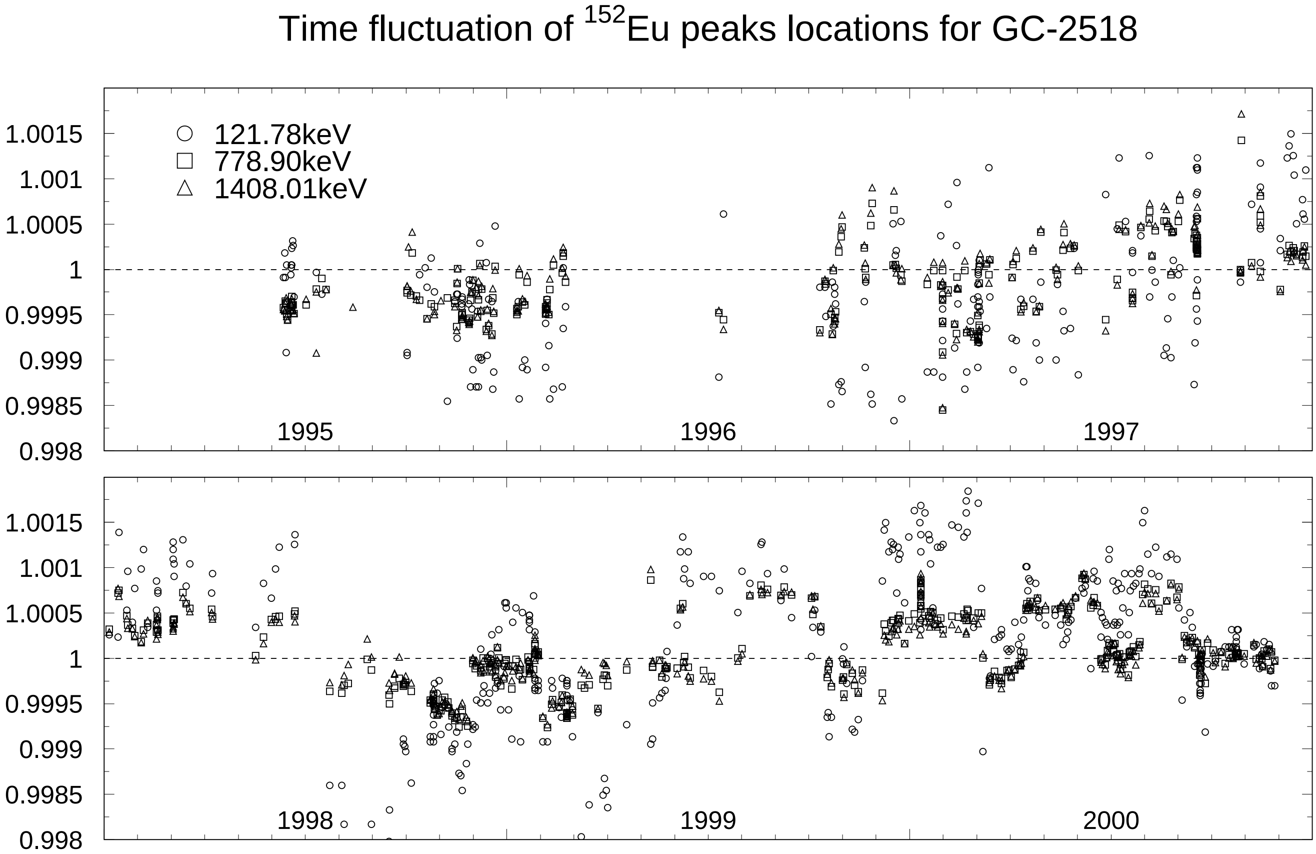

Fig. 8: Positions of the photo peak detection maxima of the 121.78 keV, 778.90 keV, and 1408.01 kev γ-lines

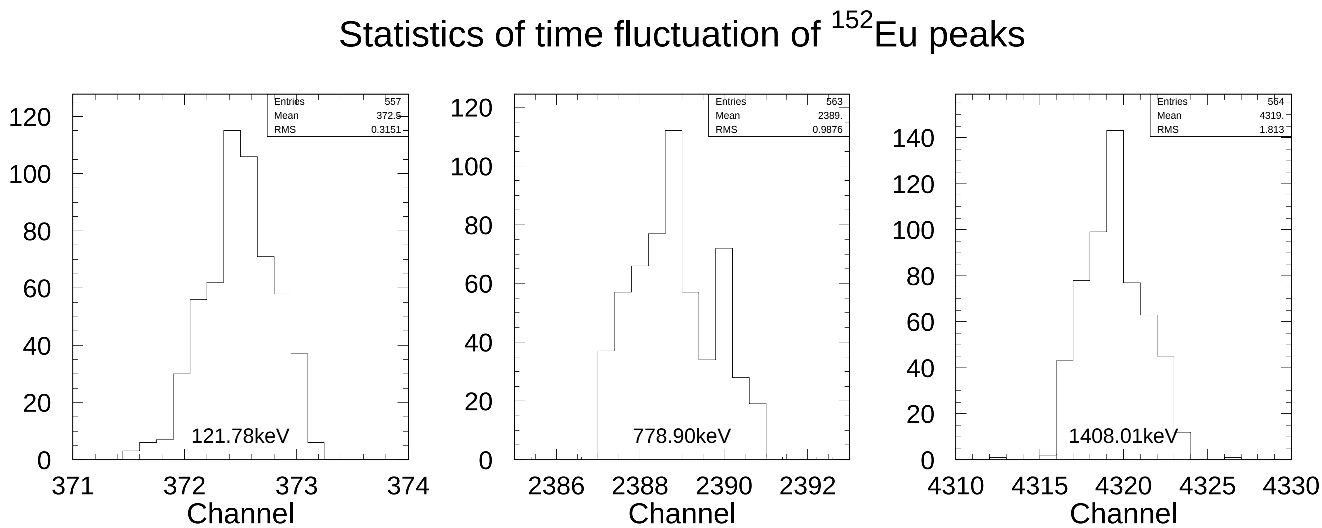

Fig. 9: The overall statistics of the spectrometer time stability.

height-energy dependence of the absolute spectrometer efficiency. Therefore, this characteristic was very carefully tested and traced.

2.4.2 Determination of the absolute height-energy detection efficiency of spectrometer.

The absolute spectrometer detection efficiency for the energy, which corresponds to the γ-

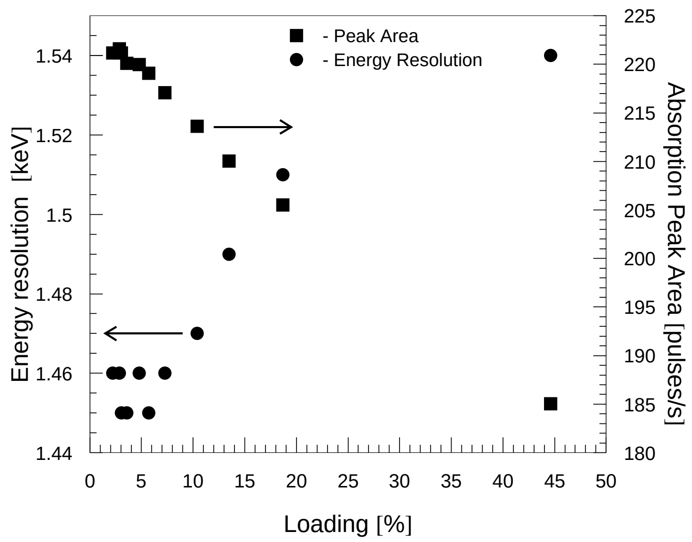

Fig. 10: Load characteristics of spectrometer.

energy of the measured source, can be presented as

$$\varepsilon_{abs}^{E} = \frac{S_0}{A \cdot \eta} \tag{45}$$

where S_0 is the count rate in the total absorption peak (count/s); η is the absolute γ-abundance A is the rated γ-source activity reduced to the measurement moment The rated γ-source is taken to be the OSGI-3 #9402 set of samples certified by the D.I.Mendeleev VNIIM institute. The set comprises ^{54}Mn, ^{57}Co, ^{60}Co, ^{88}Y, ^{109}Cd, ^{113}Sn, ^{133}Ba, ^{137}Cs, ^{139}Ce, ^{152}Eu, ^{228}Th, and^{241}Am. Besides, ^{22}Na was used from the OSGI #237 set certified by VNIIFTRI.

The source activity and the nuclear data used to calculate the absolute efficiency were taken to conform to the their technical certificate [22].

Fig.11 shows the results of experimental determining the absolute detection efficiency of the spectrometer at different heights.

In practice, a high accuracy has to be attained in the analytical energy dependences of the detection efficiency. The dependences were calculated as follows.

When taken at each fixed height H on double logarithmic scale, the energy dependence of the absolute spectrometer detection efficiency is well-known to be a smooth curve that approach a straight line and turns into a linear dependence above 100 keV. The dependence can conveniently be simulated using the spline-least squares technique, i.e., fitting the experimental dots by polynomials within some energy ranges and by joining the polynomials over their eigenvalues and first derivative. The polynomial coefficients are determined by the least squares method and are used then to find the absolute spectrometer efficiency for the desired energy and height.

If the entire measured energy range is broken into two intervals, the polynomial coefficients

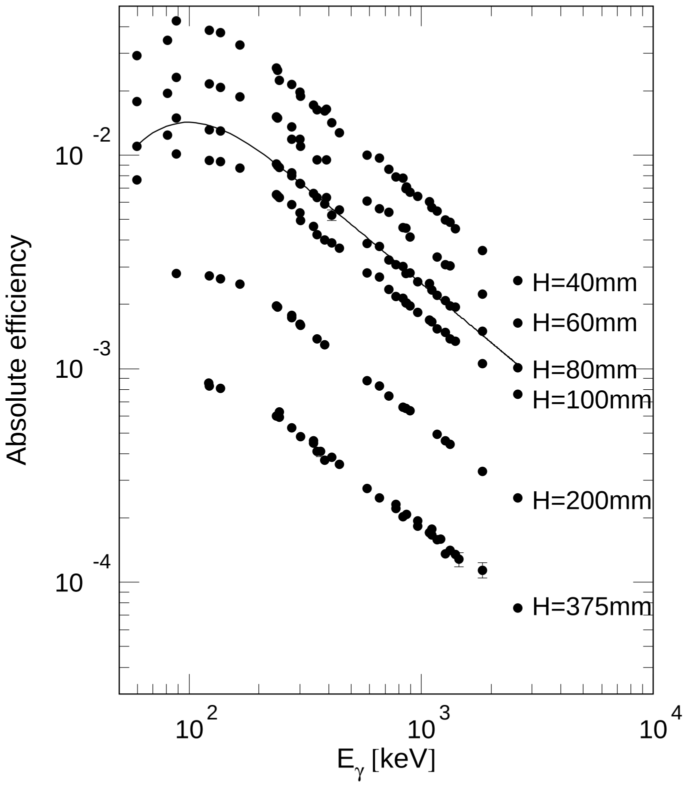

Fig. 11: Experimental absolute detection efficiency of the spectrometer versusγ-source position height above the detector. The spline-least squares simulated absolute efficiency at H = 80 mm at is also shown.

will be found by minimizing the quadratic functional:

$$R=\sum_{i=1}^{N_1}\left(\ln(\varepsilon_i)-\sum_{j=1}^{m_1+1}P_j\cdot(\ln E)^{j-1}\right)^2\cdot W_i+\sum_{i=1}^{N_2}\left(\ln(\varepsilon_i)-\sum_{j=1}^{m_2+1}P_{m_1+j+1}\cdot(\ln E)^{j-1}\right)^2\cdot W_i+$$
$$+P_{m_1+m_2+3}\cdot\left(\sum_{j=1}^{m_1+1}P_j\cdot(\ln E_0)^{j-1}-\sum_{j=1}^{m_2+1}P_{m_1+j+1}\cdot(\ln E_0)^{j-1}\right)+$$
$$+P_{m_1+m_2+4}\cdot\left(\sum_{j=2}^{m_1+1}(j-1)\cdot P_j\cdot(\ln E_0)^{j-2}-\sum_{j=2}^{m_2+1}(j-1)\cdot P_{m_1+j+1}\cdot(\ln E_0)^{j-2}\right),\quad(46)$$

where N_1 and N_2 - are the numbers of experimental dots in the first and second intervals, respectively; m_1 and m_2 are the degrees of polynomials in the two intervals; ε_i are the experimental values of the absolute detection efficiency at energy E_i; W_i is inverse to the squared relative error ε_i; E_0 is the energy range boundary point; $P_1,...,P_{m_1+m_2+2}$ are the polynomial coefficients; $P_{m_1+m_2+3},...,P_{m_1+m_2+k+2}$ are the indefinite Lagrangian coefficients for the jointing up to the (k-1)-th derivative, inclusive.

Minimizing the functional R as

$$\frac{\partial R}{\partial P_i}=0,\qquad i=1,2,\cdots,m_1+m_2+k+2\qquad(47)$$

leads to the set of linear equations

$$M\cdot\vec{P}=\vec{B},\qquad(48)$$

with the matrix M for third-degree polynomial and jointing at the boundary point over the values of the functions and their first derivatives

$$\begin{pmatrix} M_{11} & M_{12} & M_{13} & M_{14} & 0 & 0 & 0 & 0 & \frac{1}{2} & 0 \\ M_{21} & M_{22} & M_{23} & M_{24} & 0 & 0 & 0 & 0 & \frac{\ln E_0}{2} & \frac{1}{2} \\ M_{31} & M_{32} & M_{33} & M_{34} & 0 & 0 & 0 & 0 & \frac{(\ln E_0)^2}{2} & \ln E_0 \\ M_{41} & M_{42} & M_{43} & M_{44} & 0 & 0 & 0 & 0 & \frac{(\ln E_0)^3}{2} & \frac{3}{2}(\ln E_0)^2 \\ 0 & 0 & 0 & 0 & M_{55} & M_{56} & M_{57} & M_{58} & -\frac{1}{2} & 0 \\ 0 & 0 & 0 & 0 & M_{65} & M_{66} & M_{67} & M_{68} & -\frac{\ln E_0}{2} & -\frac{1}{2} \\ 0 & 0 & 0 & 0 & M_{75} & M_{76} & M_{77} & M_{78} & -\frac{(\ln E_0)^2}{2} & -\ln E_0 \\ 0 & 0 & 0 & 0 & M_{85} & M_{86} & M_{87} & M_{88} & -\frac{(\ln E_0)^3}{2} & -\frac{3}{2}(\ln E_0)^2 \\ \frac{1}{2} & \frac{\ln E_0}{2} & \frac{(\ln E_0)^2}{2} & \frac{(\ln E_0)^3}{2} & -\frac{1}{2} & -\frac{\ln E_0}{2} & -\frac{(\ln E_0)^2}{2} & -\frac{(\ln E_0)^3}{2} & 0 & 0 \\ 0 & \frac{1}{2} & \ln E_0 & \frac{3}{2}(\ln E_0) & 0 & -\frac{1}{2} & -LnE_0 & -\frac{3}{2}(\ln E_0)^2 & 0 & 0 \end{pmatrix} \quad (49)$$

where

$$\begin{cases} M_{ij} = \sum\limits_{k=1}^{N_1} W_k \cdot (\ln E)_k^{i+j-2} & i,j = 1, \cdots, 4; \\ M_{ij} = \sum\limits_{k=1}^{N_2} W_k \cdot (\ln E)_k^{i+j-10} & i,j = 5, \cdots, 8; \end{cases}$$

Vector $\vec{B}$ in the right-hand part of (48) may be presented as

$$\begin{cases} B_{ij} = \sum\limits_{k=1}^{N_1} W_k \cdot \ln(\varepsilon_k) \cdot (\ln E)_k^{i-1} & i,j = 1, \cdots, 4; \\ B_{ij} = \sum\limits_{k=1}^{N_2} W_k \cdot \ln(\varepsilon_k) \cdot (\ln E)_k^{i-5} & i,j = 5, \cdots, 8; \end{cases}$$

Solving (48), we get the sought parameters $\vec{P}$ of spline function:

$$\vec{P} = M^{-1} \cdot \vec{B}, \quad (50)$$

The calculated absolute detection efficiency at energy E is

$$\varepsilon(E) = exp\left[\sum_{i=k}^{k+3} P_i \cdot (\ln E)^{i-k}\right] \quad (51)$$

where

$$k = \begin{cases} 1, \text{ for } \ln E < \ln E_0 \\ 5, \text{ for } \ln E \geqslant \ln E_0 \end{cases}$$

The error of the calculated spectrometer detection efficiency is calculated as

$$\Delta_\varepsilon = \varepsilon \cdot \sqrt{\frac{\chi^2}{F}} \cdot \sqrt{\sum_{i=k}^{k+3} \sum_{j=k}^{k+3} M_{ij}^{-1} \cdot (\ln E)^{i-k} \cdot (\ln E)^{j-k}} \quad (52)$$

$$\chi^2 = \sum_{i=1}^{N_1+N_2} \left[\varepsilon^{exp}(E_i) - \varepsilon^{calc}(E_i)\right]^2 \cdot \frac{1}{\Delta_i^2}, \quad (53)$$

where $\varepsilon^{calc}(E_i)$ is calculated by formula (51); Δ_i is the absolute error in the experimental value of detection efficiency at energy E_i. $F = N_1 + N_2 - m_1 - m_2 + k - 3$,

Here, k-1 is the highest order of the derivative for jointing at point $\ln E_0$ (E_0=300 keV). Table 8 presents the results of experimental determining the parameters of the analytical dependence of detection efficiency. The errors in the results are presented in Table 9.

Table 8: The values of the analytical dependence parameters of the detection efficiency curve for H = 80 mm.

	P_1	P_2	P_3	P_4
E≤300keV	-46.631378174	23.883819580	-4.3730840683	0.25755405426
	P_5	P_6	P_7	P_8
E>300keV	-3.5564117432	0.77763748169	-0.24309635162	0.011581897736

Table 9: The error matrix of the analytical dependence parameters of the detection efficiency curve for H = 80 mm.

Matrix elements for E≤300 keV			
M_{11}=17.465349666	M_{12}=-10.492000118	M_{13}= 2.0872481010	M_{14}=-0.13747284173
M_{21}=-10.492000118	M_{22}=6.3094165872	M_{23}=-1.2563955076	M_{24}= 0.082824350573
M_{31}= 2.0872481010	M_{32}=-1.2563955076	M_{33}= 0. 2.5041482285	M_{34}=-0.016521865357
M_{41}=-0.13747284173	M_{42}= 0.082824350573	M_{43}=-0.016521865357	M_{44}= 0.0010909378058
Matrix elements for E>300 keV			
M_{55}=12.828705422	M_{56}=-5.8112015601	M_{57}=0.87201911548	M_{58}=-0.043361273067
M_{65}=-5.8112015601	M_{66}= 2.6347925077	M_{67}=-0.39573831006	M_{68}=0.019696373292
M_{75}=0.87201911548	M_{76}=-0.39573831006	M_{77}=0.059494783759	M_{78}=-0.0029639407716
M_{85}=-0.043361273067	M_{86}=0.019696373292	M_{87}=-0.0029639407716	M_{88}=0.00014780140661

Fig.11 presents also the shape of the analytical dependence of the absolute spectrometer detection efficiency at H =80 mm, as calculated using the above coefficients.

As seen from Fig. 11, the above techniques can be used to calculate the analytical dependence parameters of the detection efficiency at other heights (H = 40, 60, 100, 200, and 375 mm).

This approach was not realized in terms of the given techniques because the actual conservation requirements of the peak spectrometer load have forced measurements at different heights, so the situation got much deteriorated also because the measurements had to be made often at intermediate heights.

Since the coefficients A_0, A_1, A_2 in formulas (17) and (18), or A_k in formula (34), are determined by fitting the γ-ray intensities $\tilde{S}_{1_i}$ и $\tilde{S}_{2_i}$ or $\tilde{S}_{1sum_i}$, the γ-spectrum processing must be followed by renormalization of all the coefficients to a single height (say, 80 mm), whose analytical dependence of absolute detection efficiency is known. This procedure is realized using the relative coefficients, which can be calculated by different techniques. The simplest technique is to calculate the desired "height"coefficients for each of the energies via the respective curves of the analytical dependences of the absolute detection efficiency.

As mentioned above, however, the measurement procedure is difficult to unify because the experimental sample compositions and the irradiation conditions vary significantly, so the intermediate heights of measurements occur actually in all cases. Therefore, the approach has been developed, which avoids any extra measurements in determining the analytical dependences of the analytical dependences of absolute detection efficiency at intermediate heights.

The dependence of the absolute spectrometer detection efficiency on height H was simulated further by analyzing the detection efficiency ratios $\varepsilon_{60}^{E_i}/\varepsilon_{40}^{E_i}$, $\varepsilon_{80}^{E_i}/\varepsilon_{40}^{E_i}$, $\varepsilon_{100}^{E_i}/\varepsilon_{40}^{E_i}$, $\varepsilon_{200}^{E_i}/\varepsilon_{40}^{E_i}$, $\varepsilon_{375}^{E_i}/\varepsilon_{40}^{E_i}$ as functions of energy logarithm.

The analysis results displayed in Fig.12, demonstrate that the slope of the detection efficiency curve varies (increases) with height H.

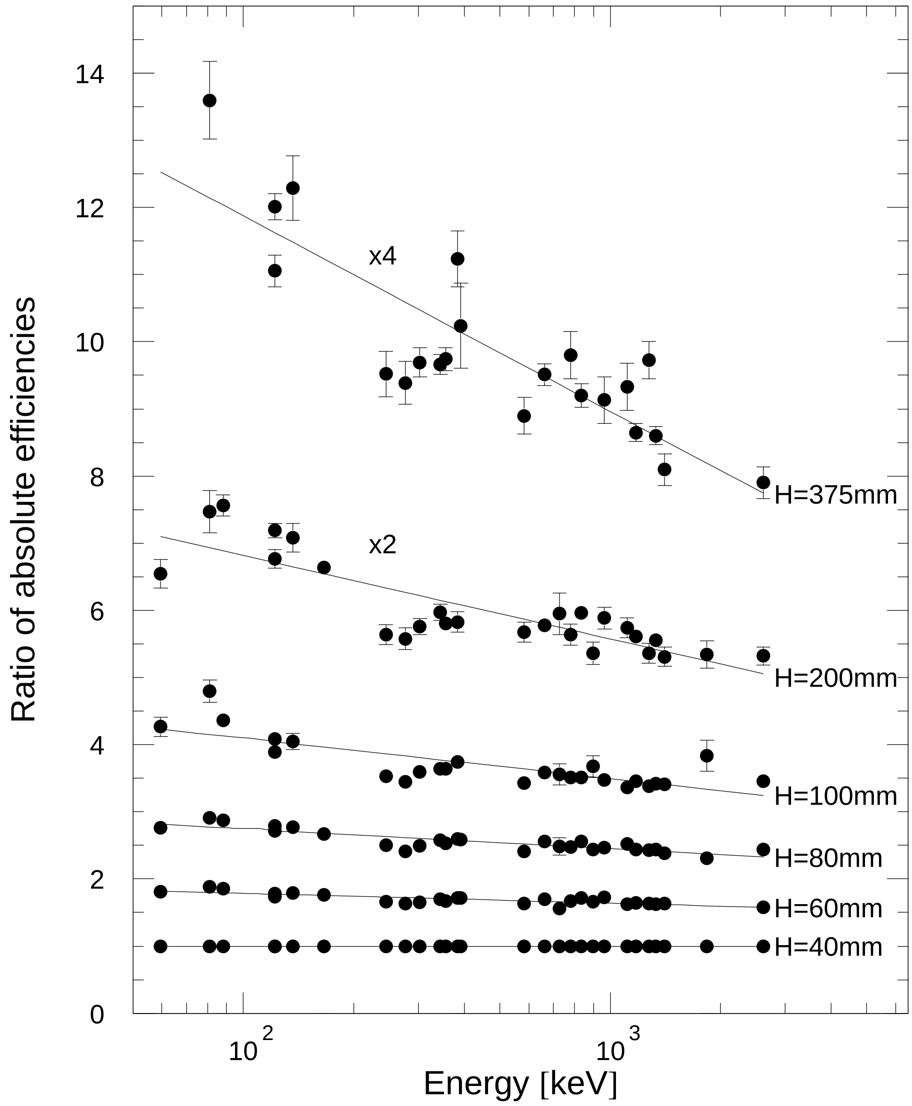

Fig. 12: The detection efficiency ratios at heights H = 60, 80, 100, 200, and 375 mm, as reduced to H=40 mm.

The dependence of the efficiency curve slope on height H was determined by treating the variations in the detection efficiency as a function of H at fixed values of γ–energy. Fig.13 shows the typical plots of the dependence at 121.78 keV, 778.90 keV, and 1408.01 keV, which can properly be described by the function

$$G^*(H) = A \cdot (B + H)^2 \tag{54}$$

where $G^*(H)$ is inverse to the spectrometer detection efficiency at distance H; A and B are parameters.

At each γ–energy, the parameters A and B were determined by minimizing the quadratic functional

$$R_1 = \sum_{i=1}^{N} \left[G_i^* - A \cdot (B + H_i)^2\right]^2 \cdot \frac{1}{\Delta_i^2} \tag{55}$$

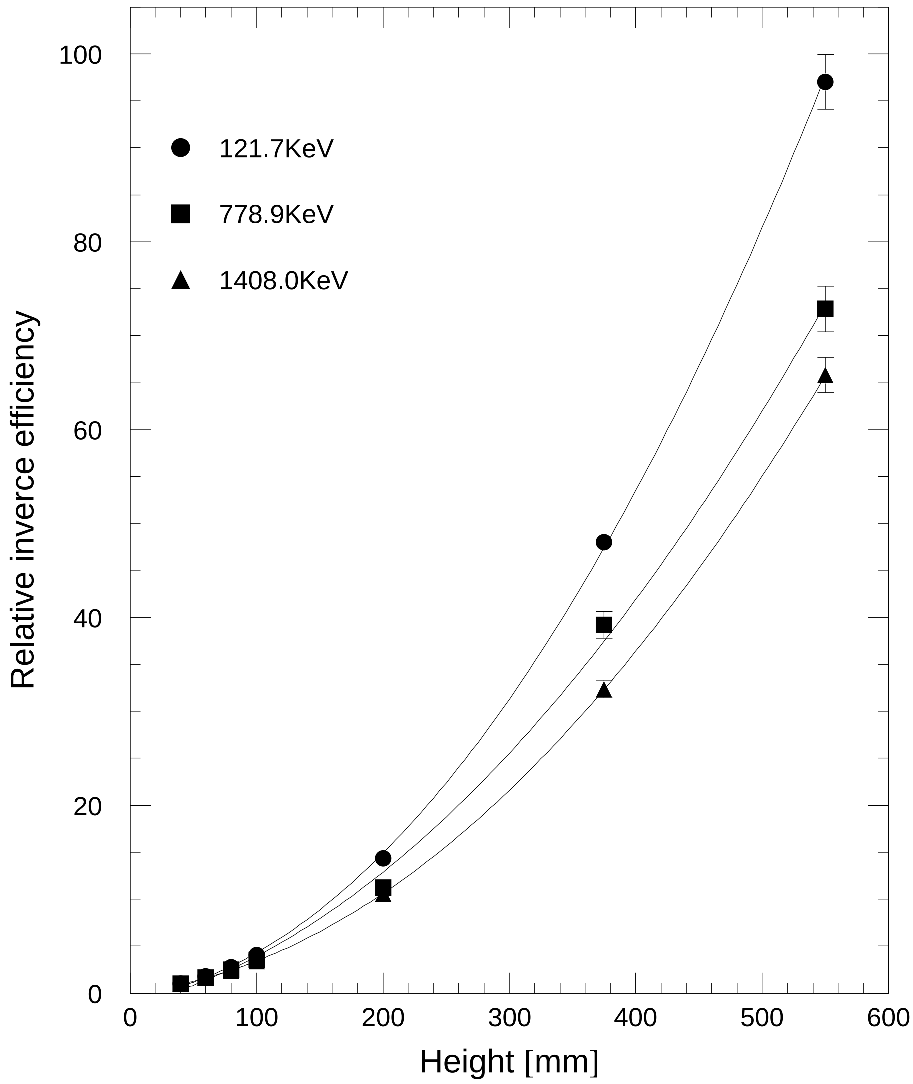

Fig. 13: Relative value of inverse detection efficiency versus distance at different γ-quantum energies.

where N is the number of experimental height points at each of the energies; Δ_i is the absolute error in G_i.

The functional R_1 was minimized by nonlinear least squares method, so the function presented by formula (54) was Taylor series-expanded in the parameters A and B up to linear terms in the vicinity of point (A_0, B_0), which is the initial approximation for the iteration process. In this case, the functional R_1 takes the form

$$R_1 = \sum_{i=1}^{N} \left[G_i^* - A_0 \cdot (B_0 + H_i)^2 - (B_0 + H_i)^2 \cdot \xi_A - 2A_0 \cdot (B_0 + H_i) \cdot \xi_B\right]^2 \cdot \frac{1}{\Delta^2_{G_i}} \qquad (56)$$

where ξ_A, ξ_B are some addends to the initial values of the parameters A_0 and B_0, which linearly enter the approximating function and, hence, can be found from the set of linear equations resultant from the condition of R_1 minimum in ξ_A, ξ_B:

$$\frac{\partial R_1}{\partial \xi_A} = 0\,; \frac{\partial R_1}{\partial \xi_B} = 0\,. \qquad (57)$$

On substituting (56), the set (57) takes the form

$$M1\begin{pmatrix}\xi_A\\ \xi_B\end{pmatrix} = \vec{Z} \tag{58}$$

where

$$M1_{11} = \sum_{i=1}^{N} \frac{(B_0 + H_i)^4}{\Delta_i^2}$$

$$M1_{12} = M1_{21} = \sum_{i=1}^{N} \frac{2(B_0 + H_i)^3}{\Delta_i^2} \cdot A_0$$

$$M1_{22} = \sum_{i=1}^{N} \frac{4(B_0 + H_i)^2}{\Delta_i^2} \cdot A_0^2$$

$$Z_1 = \sum_{i=1}^{N} \left[G_i^* - A_0 \cdot (B_0 + H_i)^2\right] \cdot (B_0 + H_i)^2 \cdot \frac{1}{\Delta_i^2}$$

$$Z_2 = \sum_{i=1}^{N} \left[G_i^* - A_0 \cdot (B_0 + H_i)^2\right] \cdot 2A_0 \cdot (B_0 + H_i) \cdot \frac{1}{\Delta_i^2}$$

The augmentations ξ_A, ξ_B are determined from the set of linear equations (58)

$$\begin{pmatrix}\xi_A\\ \xi_B\end{pmatrix} = M1^{-1} \cdot \vec{Z} \tag{59}$$

After that, we obtain the following approximation of the parameters A and B

$$\begin{cases} A_1 = A_0 + \xi_A \\ B_1 = B_0 + \xi_B \end{cases}$$

and the process is repeated ab initio, with A_1 and B_1 being substituted for A_0 and B_0 in formulas (56) – (59), untill the conditions

$$\frac{\xi_A}{A} < eps, \qquad \frac{\xi_B}{B} < eps, \tag{60}$$

are satisfied. Here, *eps* is small, for instance, 10^{-6}.

After that, the parameters A and B are taken to be their values from the last approximation, while the errors are calculated as

$$\Delta_A^2 = M1_{11}^{-1} \cdot \frac{\chi^2}{F} \qquad \Delta_B^2 = M1_{22}^{-1} \cdot \frac{\chi^2}{F} \tag{61}$$

where

$$\chi^2 = \sum_{i=1}^{N} \left[G_i^* - A \cdot (B + H_i)^2\right]^2 \cdot \frac{1}{\Delta_i^2}\ ; \tag{62}$$

$M1_{11}^{-1}, M1_{22}^{-1}$ are the diagonal elements of the inverse matrix of the set of linear equations (58) for the last iteration step; $F = N - 3$.

This procedure of determining the parameters A and B was realized for the γ–energies supported by experimental data (see Fig. 11). Fig. 14 shows the resultant dependences of the parameters $A(E_i)$ and $B(E_i)$.

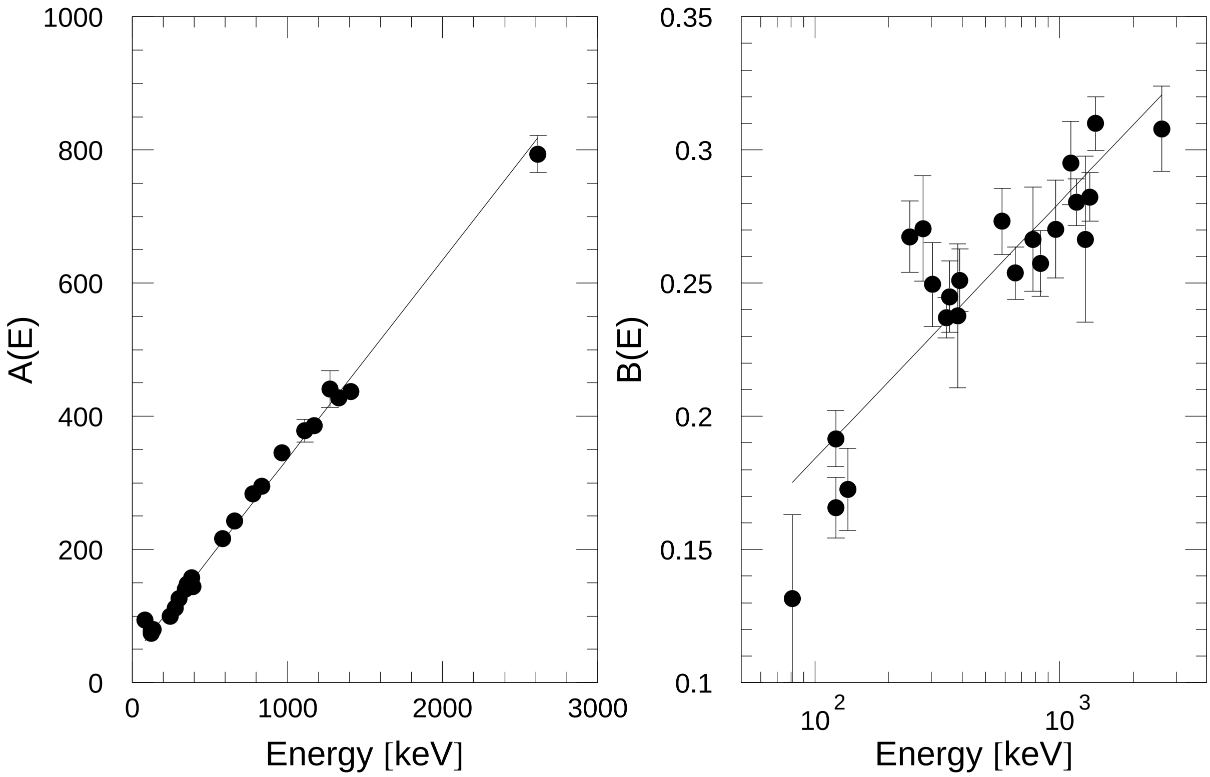

Fig. 14: The approximation coefficients A and B versus energy

From Fig. 14 it is follows that the parameter A is quite properly described by linear function within a broad energy range, while the parameter B can be represented by the linear function of energy logarithm:

$$\begin{cases} A(E) = q_1 + q_2 \cdot E \\ B(E) = q_3 + q_4 \cdot \ln(E) \end{cases} \tag{63}$$

The parameters q_1 and q_2, q_3, and q_4 were determined by least squares method using the above-obtained values of A_i and Δ_{A_i}, as well as B_i и Δ_{B_i}, via minimization of R_2 and R_3, respectively:

$$R_2 = \sum_{i=1}^{N} (A_i - q_1 - q_2 \cdot E_i)^2 \cdot \frac{1}{\Delta^2_{A_i}} \tag{64}$$

$$R_3 = \sum_{i=1}^{N} (B_i - q_3 - q_4 \cdot \ln E_i)^2 \cdot \frac{1}{\Delta^2_{B_i}} \tag{65}$$

where N is the number of experimental points.

Minimizing the functionals R_2 and R_3 leads to two sets of linear equations:

$$\begin{cases} \dfrac{\partial R_2}{\partial q_1} = 0 \\ \dfrac{\partial R_2}{\partial q_2} = 0 \end{cases} \qquad \begin{cases} \dfrac{\partial R_3}{\partial q_1} = 0 \\ \dfrac{\partial R_3}{\partial q_2} = 0 \end{cases} \tag{66}$$

or

$$M2_{ij} \cdot \begin{pmatrix} q_1 \\ q_2 \end{pmatrix} = \vec{Z}_2 \ ; \qquad M3_{ij} \cdot \begin{pmatrix} q_3 \\ q_4 \end{pmatrix} = \vec{Z}_3 \ , \tag{67}$$

where

$$\begin{cases} M2_{ij} = \sum_{i=1}^{N} \frac{1}{\Delta^2_{A_k}} \cdot E_i^{\;i+j-2} & Z2_i = \sum_{i=1}^{N} \frac{1}{\Delta^2_{A_k}} \cdot A_k \cdot E_k^{\;i-1} \\ M3_{ij} = \sum_{i=1}^{N} \frac{1}{\Delta^2_{B_k}} \cdot (\ln(E_k))^{i+j-2} & Z3_i = \sum_{i=1}^{N} \frac{1}{\Delta^2_{B_k}} \cdot (\ln E_k)^{i-1} \end{cases} \quad (68)$$

On solving the set (68), we get the sought parameters q_1, q_2, q_3, q_4 and their errors:

$$\begin{pmatrix} q_1 \\ q_2 \end{pmatrix} = M2^{-1} \cdot \vec{Z}_2 \; ; \qquad \begin{pmatrix} q_3 \\ q_4 \end{pmatrix} = M3^{-1} \cdot \vec{Z}_3 \; ; \quad (69)$$

$$\Delta^2_{q_i} = M2^{-1}_{ii} \cdot \frac{\chi^2_A}{F} \quad (i = 1\,, 2)\;; \qquad \Delta^2_{q_i} = M3^{-1}_{ii} \cdot \frac{\chi^2_B}{F} \quad (i = 3\,, 4)\;, \quad (70)$$

where

$$\chi^2_A = \sum_{i=1}^{N} (A_i - q_1 - q_2 \cdot E_i)^2 \cdot \frac{1}{\Delta^2_{A_i}}\;; \qquad \chi^2_B = \sum_{i=1}^{N} (B_i - q_3 - q_4 \cdot \ln E_i)^2 \cdot \frac{1}{\Delta^2_{B_i}} \qquad F = N-3\,. \quad (71)$$

The resultant values of the parameters are summarized in Table 10.

Table 10: Values of parameters

Parameter	Value	Parameter	Value	Parameter	Value
q_1	38.16	$M2_{11}$	2.8638	$M3_{11}$	3.881×10^{-4}
q_2	0.2982	$M2_{12} = M2_{21}$	- 1.108×10^{-2}	$M3_{12} = M3_{21}$	- 6.094×10^{-5}
q_3	-8.663×10^{-3}	$M2_{22}$	5.610×10^{-5}	$M3_{22}$	9.751×10^{-6}
q_4	4.184×10^{-2}	χ^2_A	1.989	χ^2_B	1.436

It should be noted that the expression (54) can be used to calculate the absolute spectrometer detection efficiency ε and the error σ_ε basing on the above-tabulated parameters and using the formula

$$\varepsilon(E, H) = \frac{1}{(q_1 + q_2 \cdot E) \cdot [q_3 + q_4 \cdot \ln E + H]^2} \quad (72)$$

$$\Delta^2_\varepsilon = \sum_{i=1}^{2}\sum_{j=1}^{2} \frac{\partial\varepsilon}{\partial q_i}\frac{\partial\varepsilon}{\partial q_j} M2^{-1}_{ij} \cdot \frac{\chi^2_A}{F} + \sum_{i=1}^{2}\sum_{j=1}^{2} \frac{\partial\varepsilon}{\partial q_{i+2}}\frac{\partial\varepsilon}{\partial q_{j+2}} M3^{-1}_{ij} \cdot \frac{\chi^2_B}{F} \quad (73)$$

The folowing techniques are proposed to use in practice when determining the absolute spectrometer efficiency. At height H = 80 mm, which has been supported by sufficient experimental data and affected but little by the cascading effects, the spline – function coefficients have been obtained, and the values of the absolute spectrometer efficiency and its errors are calculated by formulas (51) and (52).

At the remaining heights, the absolute spectrometer efficiency can be calculated in terms of (72) using the expression

$$\varepsilon_H = \varepsilon_{80} \cdot \left[\frac{(q_3 + q_4 \cdot \ln E + 80/100)}{(q_3 + q_4 \cdot \ln E + H/100)}\right]^2 \quad (74)$$

where ε_{80} is the detection efficiency at H= 80 mm.

The error ε_H can be calculated by the error transfer formula:

$$\Delta^2_{\varepsilon_H} = \left[\frac{\Delta\varepsilon_{80}}{\varepsilon_{80}}\right]^2 + 4\cdot\frac{(H/100-80/100)^2\cdot(M3^{-1}_{11}+2M3^{-1}_{12}\cdot\ln E+M3^{-1}_{22}\cdot(\ln E)^2)\cdot\chi^2_B}{[q_3+q_4\cdot\ln E+80/100]^2\cdot[q_3+q_4\cdot\ln E+H/100]^2} \quad (75)$$

where q_3 and q_4 are the parameters determined by formula (69); $M3^{-1}_{ij}$ is the inverse matrix $M3_{ij}$ determined by formula (67).

Fig. 15 shows the simulated curves of absolute spectrometer efficiency calculated by formula (74) at the reference 80-mm height. Additional measuring the absolute detection efficiency at some intermediate heights (H = 150, 250, and 550 mm) has testified a high reliability of the above techniques

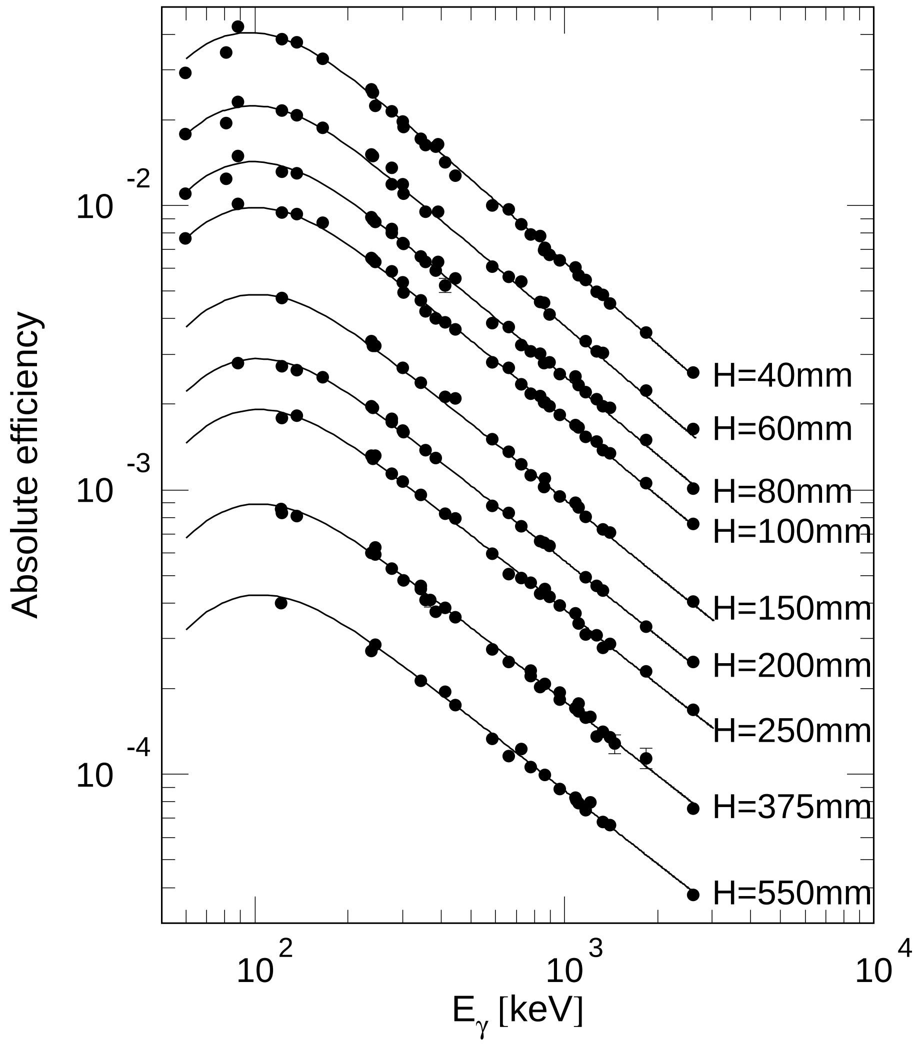

Fig. 15: The simulated absolute spectrometer detection efficiency calculated by the spline-least squares method.

From Figs. 11 and 15 it follows that the above techniques permit quite an adequate description of the experimental values of the absolute spectrometer efficiency at any height and can correctly reproduce the variations induced by height H in the slope of the energy dependence curve of the spectrometer efficiency on double logarithmic scale.

The proposed techniques permits calculations of the absolute spectrometer efficiency in the 100 keV ÷ 2600 keV range at heights 40 mm ÷ 550 mm within a relative error of 3-10%. At relatively low energies (<120 keV) and in the energy ranges supported by scanty experimental points, the error approaches 10%. This is quite sufficient in practical usage because the reaction product γ-lines analyzed here belong to the range above 100 keV.

2.5 Extracted proton beam energies

Knowledge of the extracted proton beam energy is very urgent because our experiments are eventually aimed at obtaining the energy dependence, i.e. the excitation functions of the proton-induced reactions.

As mentioned above, our experiments are made using the ITEP proton synchrotron, wherefrom monoenergetic proton beams are extracted. The ITEP proton synchrotron is a cycling ring machine that accelerates protons to a maximum energy of up to 9.3 GeV. The injection energy of the synchrotron is 25 MeV, so the 70-200 MeV and 800-2600 MeV protons are quite acceptable for experiments and applications. During acceleration, the proton energy is measured allowing for one of the basic synchrotron characteristics, namely, the unchangeable closed orbit length for the circling protons. So, the proton energy can readily be estimated by measuring the proton rotation frequency f_r:

$$E_k = \frac{E_0 c}{\sqrt{c^2 - L^2 f_r^2}} - E_0, \tag{76}$$

where E_k is kinetic energy of the circling proton; E_0=938.26 MeV is proton mass; L=251.21 m is the closed orbit length, $c = 2.99776 \times 10^8$ m/s is speed of light. The f_r value is multiple to the accelerating radio frequency:

$$f_a = h f_r \tag{77}$$

where h=4 is a harmonic number: f_a is the accelerating radio frequency that varies within a 1.07 MHz - 4.85 MHz range. The f_a signal is formed properly, so there is no problem in measuring the f_a values accurated within 10^{-4} and even better. The error of energy measurements is energy-dependent and can be calculated as

$$\frac{\Delta E_k}{E_k} = \beta^2 \frac{\gamma^3}{\gamma - 1} \sqrt{\left(\frac{\Delta f_a}{f_a}\right)^2 + \left(\frac{\Delta L}{L}\right)^2}, \tag{78}$$

where β is the proton velocity equal to Lf_a/hc; γ is the relativistic factor equal to $1/\sqrt{1-\beta^2}$. The value of L is known up to a relative error of 10^{-4}.

The proton beam is transferred to the low-energy transport channel using a fast extraction system with a kicker magnet, and to the high-energy transport channel using a slow extraction system with a septum magnet placed behind the vacuum chamber aperture. The bending angles of the above magnets are 20 mrad and 17 mrad, respectively.

Since, in transporting the beam to the experimental sample irradiation site, a small fraction of the beam energy gets lost in proton interactions with the transport channel structure materials, the loss is allowed for as

$$E_k^{'} = E_k - \delta E_k \tag{79}$$

where $E_k^{'}$ is the proton beam kinetic energy at the experimental sample location; δE_k is the energy loss in the channel between the extraction and the target calculated by formula $\delta E_k = (dE/dx)X$, which is valid because the total thickness (X) of the structure materials along the beam path is insignificant and, hence, the specific loss for ionization dE/dx may well be assumed to be constant.

The geometry and composition of the transport channel structure elements are known to within a very high accuracy, so the expression for calculating the error in the incident proton energy is

$$dE_k' = \sqrt{(dE_k)^2 + [d(dE/dx)X]^2} \tag{80}$$

Table 11 presents the experimental proton beam energies and their errors as calculated by formulas (76-80).

The energy of the extracted low-energy beam can readily be checked experimentally by measuring the longitudinal dose distribution (the Bragg curve) in a water-filled phantom.

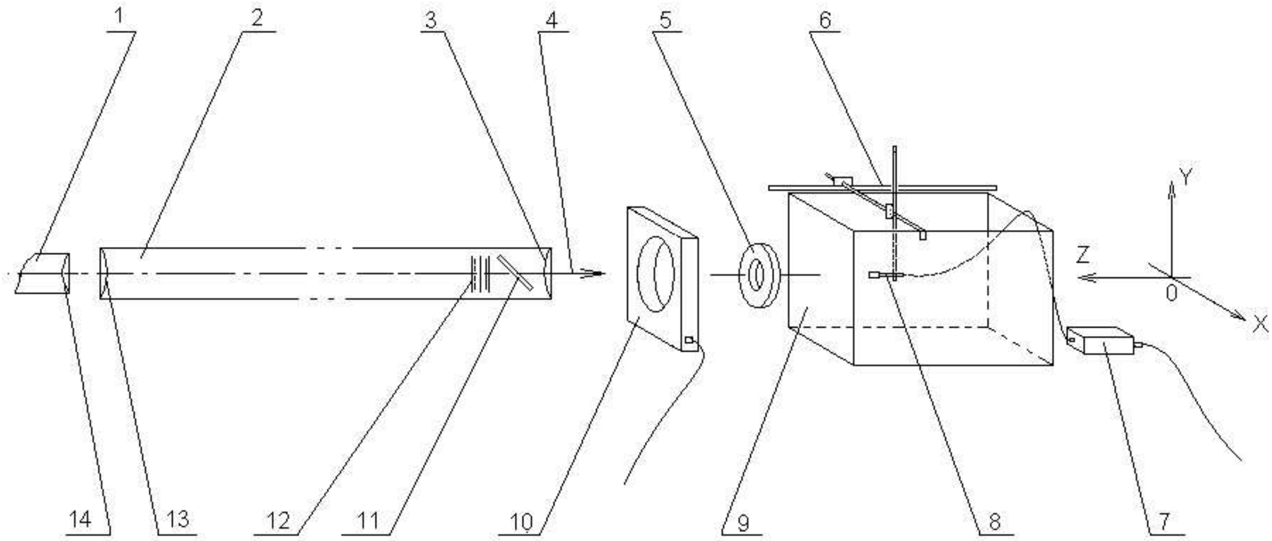

Fig. 16: A schematic of proton beam transport and experimental equipment for determining the longitudinal dose distribution. 1, 2, 3, 4, 5, 6, 7, 8, 9, 10, 11, 12, 13, 14.

Fig. 16 is a schematic of the experimental facility used in the measurements. The facility is a three-coordinate displacement system of a quasi-point semiconductor (SC) dosimeter, which is a purpose-designed 1.25×1.25×1.25 mm^3 silicon-based SC detector of a 0.25 micron sensitive volume depth placed inside a homogenous medium called the water-filled phantom. The sensitive volume is located on the silicon crystal surface and is separated from water by a 12-micron thick opaque polymer foil. The phantom front wall is 3-mm thick lucid plate. The accuracy of the SC dosimeter displacement along a given coordinate is 0.25 mm. The SCD was oriented normally to the proton beam. The SCD signal was normalized to the signal from the induction sensor of proton flux.

Four curves presented in Fig. 17 have been plotted from the runs of measuring the longitudinal dose distribution (the Bragg curve) of the 0.07, 0.10, 0.13,and 0.2 GeV proton beams. The proton range length is defined by the abscisa that corresponds to 83% of the highest dose at some point of the Bragg curve descending segment. The proton beam energy at the phantom inlet point was found by comparing the resultant proton range length in water with the tabulated data of [32].

Within the experimental errors, the coincidence between the energies measured by two independent methods indicates that the value of energy is true and that the measured excitation function represents that value quite correctly.

Another parameter affecting the character of the presented values is the incident proton

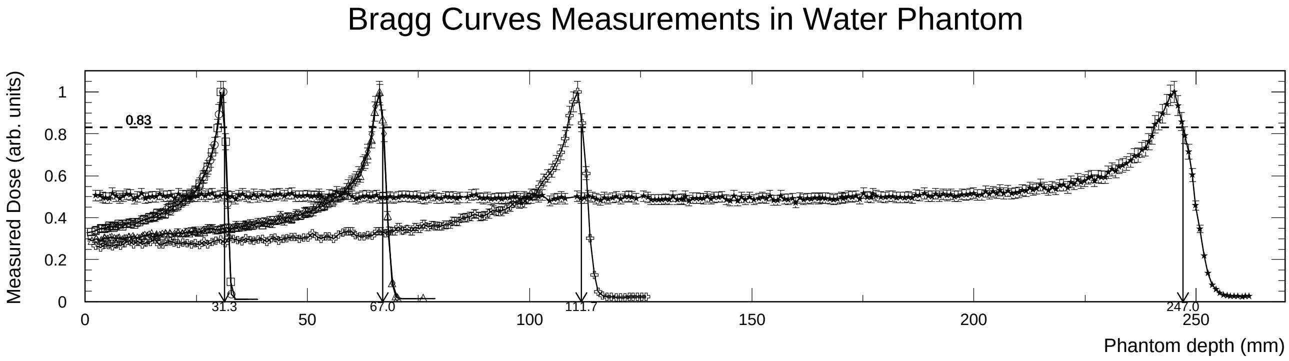

Fig. 17: Longitude dose distributions in a water-filled phantom.

beam energy spread ΔE_k found usually through the momentum spread dp/p.

The dp/p value for the ITEP synchrotron beam is close to $\pm 0.5\%$ during injection (E_k=25 MeV, p_0=220 MeV/c) and decreases as a function of $k = \sqrt{p_0/p}$ during acceleration in the relevant energy range.

The proton beam energy spread $\Delta E_k/E_k$ is an additional parameter of the beam, which has to be taken into account when analyzing the experimental results. The ΔE_k values are presented in Table 11.

Table 11: Energy and spread of energies in the experimental proton beam.

Proton beam energy in ring, (GeV)	Proton energy at sample irradiation point points, (GeV)	Energy spread ΔE, (GeV)
0.070	0.0672	0.0006
0.100	0.0970	0.0006
0.130	0.1267	0.0007
0.150	0.1468	0.0008
0.200	0.1966	0.0011
0.8	0.802	0.002
1.0	0.995	0.003
1.2	1.119	0.003
1.4	1.393	0.003
1.5	1.500	0.003
1.6	1.600	0.003
2.6	2.602	0.004

2.6 Neutron background

The proton beams extracted from accelerators include not only primary protons, but also secondary particles (neutrons, protons, π mesons, and gammas) produced in the primary proton interactions with the structure materials of the transport channels and shielding. Identical reaction products can be produced in interactions of various secondaries with an experimental sample. Since any particular nuclear reaction, which generates a given nuclide, cannot be identified in the measurements, the extracted proton beams have to be tested and specified thoroughly.

Solid state nuclear track detectors (SSNTD) were used earlier in the experiments to discriminate the neutron component in the proton beams [6]. Later, direct γ spectrometry was used for the purpose. The SSNTDs of an improved geometry with a collimating grid were used to record the fission fragments from a fissile layer, thereby improving the absolute detector efficiency.

An SSNTD with a 61.5 μg/cm^2 ^{209}Bi layer was used to measure the proton flux density. The ^{209}Bi was selected because the cross section for its fission induced by secondary neutrons is small compared with that induced by primary protons ($\overline{\sigma_{^{209}Bi(n,f)}} << \sigma_{^{209}Bi(p,f)}$). The neutron flux density was measured using an SSNTD with a 880 μg/cm^2 ^{237}Np layer. Glass was used to record the fission fragments.

The following experimental design was adopted. An extracted proton beam irradiates a ^{209}Bi-containing a sandwich (Bi layer + collimator + glass), while similar sandwiches with ^{237}Np layers are placed along a line normal to, and at distances of 20–435 mm from, the beam axis. In the experiments, the neutron-to-proton flux density ratio, Φ_n/Φ_p, was determined as

$$\overline{\Phi}_n/\overline{\Phi}_p = \frac{T_1}{T_2} \cdot \frac{\sigma_{p,f}^{^{209}Bi}}{\overline{\sigma}_{n,f}^{^{237}Np}} \cdot \frac{N^{^{209}Bi}}{N^{^{237}Np}} \cdot \frac{\xi_2}{\xi_1} \tag{81}$$

where T_1 and T_2 are numbers of measured tracks of ^{237}Np and ^{209}Bi fission products, respectively; $N^{^{237}Np}$ and $N^{^{209}Bi}$ are numbers of the ^{237}Np and ^{209}Bi nuclei; ξ_1 and ξ_2 are, respectively, corrections to the ^{237}Np and ^{209}Bi layers, which allow for the anisotropy of fission-fragment ejection and for the variations of the solid angle of fission-fragment ejection through the collimator grid; $\sigma_{p,f}^{^{209}Bi}$ is the cross section for proton-induced ^{209}Bi fission; $\overline{\sigma}_{n,f}^{^{237}Np}$ is the weighted mean ^{237}Np neutron-induced fission cross section calculated as

$$\overline{\sigma}_x = \frac{\int \sigma_x(E)\Phi(E)dE}{\int \Phi(E)dE} \tag{82}$$

where x - ^{209}Bi(n,f), ^{237}Np(n,f), ^{27}Al(n,p)^{27}Mg, ^{27}Al(n,α)^{24}Na, and ^{27}Al(n,x)^{22}Na.

The calculated mean-weighted cross section $\overline{\sigma}_{n,f}^{^{237}Np}$ was taken to be 550 mbarn. The cross section for the proton-induced ^{209}Bi fission, $\sigma_{p,f}^{^{209}Bi}$, was taken from [23].

The experiments were made with 200, 800, and 2600 MeV proton beams. Fig. 18 shows the resultant Φ_n/Φ_p ratios as functions of the the distance perpendicular to the proton beam. The Φ_n/Φ_p ratio right in the proton beam was estimated by extrapolating the peripheral results to the center and proved to be about (0.3-2)%.

The feasibility of distinguishing the (n,p) reactions from (p,x) reactions has permitted an alternative pattern of direct γ–spectrometry. Namely, Al samples were irradiated, and ^{27}Al(n,p)^{27}Mg (a $\sim$ 2.5MeV threshold), [^{27}Al(n,α)^{24}Na (a $\sim$5.5 MeV threshold) + ^{27}Al(p,x)^{24}Na (a $\sim$25 MeV threshold)], ^{27}Al(^n_p,x)^{22}Na (a $\sim$25 MeV threshold), and ^{27}Al(^n_p,x)^{7}Be (a $\sim$25 MeV threshold) reaction rates were measured, in the beam center and periphery. The ^{27}Al(n,p)^{27}Mg reaction characteristics have made it possible to detect ^{27}Mg in the experimental ^{27}Al samples positioned normally to the proton beam axis in the beam center and at distances of 40–430 mm from the beam axis.

The experimental design was as follows. Three rectangular 35×40 мм^2 Al plates were irradiated. The proton beam was focuses on a a 10.5-cm diameter Al sample fastened at the plate centre. The plates and the experimental sample were all of the same 100-mm thickness. Five peripheral 10.5-m diameter, 1.6-mm thick Al samples, together with five SSNTDs (a sandwich of a glass plate, a collimating grid, and a thin ^{237}Np fissile target) were placed normally to the proton beam at distances of 20-460 mm from the central sample. After irradiation, two rectangular plates were cut to form the vertical and horizontal 2-mm thick strips. Measurements of their γ-spectra made it possible to determine the ^{24}Na yields in the vertical and horizontal projections. Since

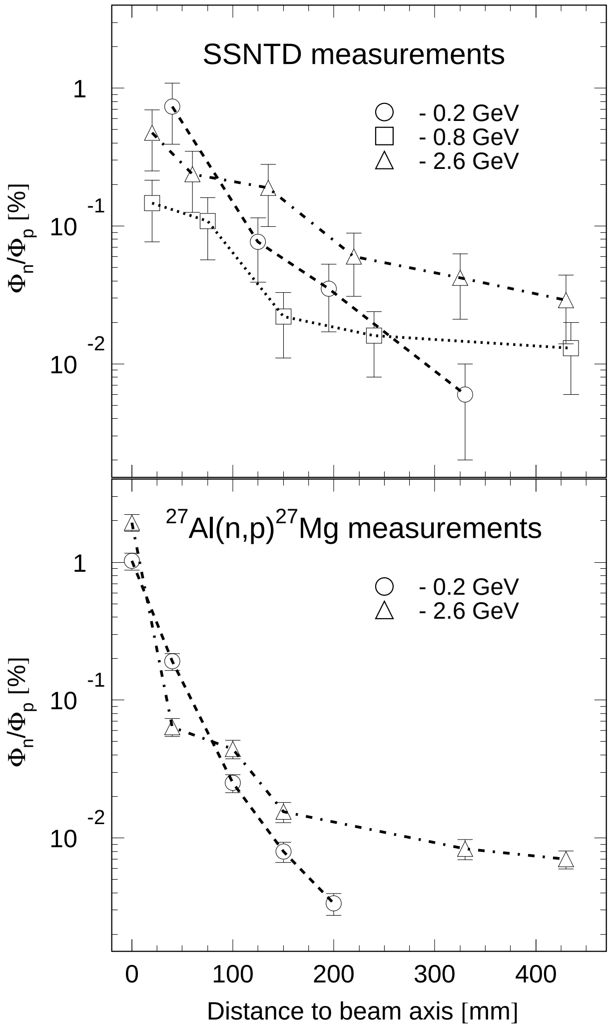

Fig. 18: The neutron-to-proton mean flux density ratios versus distance from the proton beam axis calculated using: (1) the SSNTD measurements (upper plot); (2) ^{27}Al(n,p)^{27}Mg measurements (bottom plot).

the concentration of ^{24}Na in Al plates is proportional to proton beam intensity, the geometric dimensions of the beam can be determined accordingly

The third plate and the central sample were used to determine the proton fluence incident onto the central sample and the total fluence of the beam particles. In this case, the mean neutron-to-proton flux density ratio in the beam is estimated as

$$\frac{\overline{\Phi}_n}{\overline{\Phi}_p} = \frac{\sigma_{p,x}^{^7Be,^{22}Na,^{24}Na} / \overline{\sigma}_{n,p}^{\;^{27}Mg}}{N^{^7Be,^{22}Na,^{24}Na} / N^{^{27}Mg} - \overline{\sigma}_{n,x}^{\;^7Be,^{22}Na,^{24}Na} / \overline{\sigma}_{n,p}^{\;^{27}Mg}} \tag{83}$$

where $\overline{\sigma}_{n,p}^{\;^{27}Mg}, \overline{\sigma}_{n,x}^{\;^{22}Na}, \overline{\sigma}_{n,\alpha}^{\;^{24}Na}$, $\overline{\sigma}_{n,x}^{\;^7Be}$ are the above reaction cross sections mean weighted with respect to the neutron spectrum, as calculated by formula (82): $\sigma_{p,x}^{^{22}Na}, \sigma_{p,x}^{^{24}Na}$ and $\sigma_{p,x}^{^7Be}$ are the ^{27}Al(p,x)^{24}Na, ^{27}Al(p,x)^{22}Na, ^{27}Al(p,x)^{7}Be; reaction cross sections N$^{^{24}Na}$, N$^{^{22}Na}$, N$^{^{27}Mg}$ и N$^{^7Be}$ are numbers of ^{24}Na, ^{22}Na, ^{27}Mg, and ^{7}Be nuclei produced in Al samples, with due allowance for their decay under irradiation.

The techniques described above were used in the experiments with the 70, 100, 130, 200, 800, 1000, and 2600 MeV proton beams The neutron spectrum $\Phi(E)$) used to calculate the mean-weighted ^{209}Bi(n,f), ^{237}Np(n,f), ^{27}Al(n,p)^{27}Mg, ^{27}Al(n,α)^{24}Na, and ^{27}Al(n,x)^{22}Na reaction cross

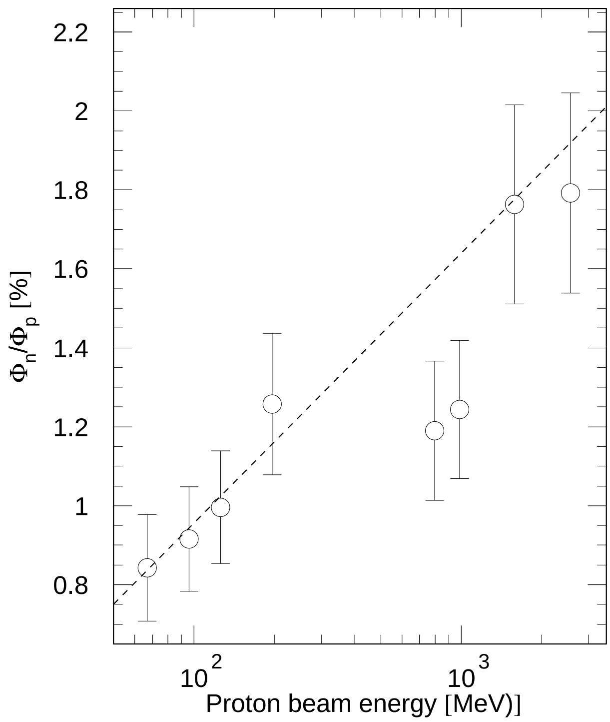

Fig. 19: The mean neutron-to-proton flux density ratio in the proton flux versus proton beam energy. The calculations were made using the experimental γ-spectrometry data.

sections was estimated by the LAHET code. The excitation function of theses reaction were retrieved from the MENDL2 database [29]. The ^{27}Al(p,x)^{24}Na reaction cross section used in the reported researches has been obtained under the reported Project (see below, Table 12). The results are presented in Fig. 19, which demonstrates that the neutron-to-proton flux ratio is 0.8-2%.

As seen from Fig. 18, the neutron component estimates obtained by the both techniques (SSNTD and γ–spectrometry) are alike.

It should be noted that the neutron background effect must be allowed for (via the (n, x) reactions) in some of the targets. The allowance can essentially be made using, for example, the background neutron spectra simulated by the LAHET Code System for appropriate proton energies and the excitation functions from the MENDL2 database. However, this particular type of researches falls outside the scope of the agreed workplan and technological assignment under the given Project. On the other hand, the accuracy of the like predictions is now dubious in virtue of the below-discussed imperfection of the simulation codes and their associate databases as applied to the studied class of nuclear reactions. This is why the said allowance is subject to separate researches, which may be realized later (using, in particular the Uppsala neutron beams)

Beside the neutron background estimation, the above descibed method allows the shape and cross section of proton beams to be determined. The shapes of the 0.2, 0.8, and 2.6 GeV beams are presented in Fig. 20. It should be noted that the 0.8 GeV beam was defocused deliberately to confirm the validity of the method.

2.7 Monitor reactions

The ^{27}Al(p,x)^{22}Na monitor reaction was used in most cases, and the ^{27}Al(p,x)^{24}Na reaction in but a few cases of short-term irradiations. At present, the use of the latter reaction is not regarded as quite correct when monitoring proton flux because the (n,α) reaction can contribute

Table 12: The monitor reaction cross sections averaged over irradiation runs

Proton energy, GeV	The ^{27}Al(p,x)^{22}Na monitor cross sections [10]	The measured reaction cross sections. Shown in brackets are the errors disregarding/allowing for the ^{27}Al(p,x)^{22}Na reaction cross section error	
		^{27}Al(p,x)^{24}Na	^{27}Al(p,x)^{7}Be
0.067	24.4 ± 1.4	11.3 ± (0.5 / 0.8)	0.76 ± (0.20 / 0.21)
0.097	19.1 ± 1.3	11.0 ± (0.3 / 0.8)	0.97 ± (0.07 / 0.10)
0.127	17.0 ± 1.3	10.1 ± (0.3 / 0.8)	1.14 ± (0.06 / 0.11)
0.147	16.1 ± 1.2	9.8 ± (0.4 / 0.8)	1.44 ± (0.11 / 0.16)
0.197	15.1 ± 0.9	9.8 ± (0.4 / 0.7)	1.48 ± (0.04 / 0.10)
0.8	15.5 ± 0.9	12.7 ± (0.3 / 0.8)	6.4 ± (0.3 / 0.4)
1.0	15.0 ± 0.9	13.0 ± (0.8 / 1.1)	7.5 ± (0.3 / 0.5)
1.2	14.6 ± 1.0	12.9 ± (0.3 / 0.9)	8.3 ± (0.2 / 0.6)
1.4	13.9 ± 1.0	12.8 ± (0.4 / 1.0)	9.0 ± (0.3 / 0.7)
1.5	13.5 ± 1.0	12.4 ± (0.3 / 1.0)	8.8 ± (0.3 / 0.7)
1.6	13.2 ± 1.0	11.6 ± (0.3 / 0.9)	8.9 ± (0.2 / 0.7)
2.6	11.7 ± 0.9	10.6 ± (0.3 / 0.9)	9.2 ± (0.2 / 0.7)

to the ^{24}Na production, resulting in an overestimation of the mean proton flux density. That is why the neuton background generated during proton irradiation of experimental samples was measured to a high accuracy, as described in Subsection 2.6.

As noted above, an extremely low neutron background was recorded, thus refuting the claim that the ^{27}Al(p,x)^{24}Na monitor reaction cannot be used. In turn, this has led to the idea that the $^{24\mathrm{Na}}\sigma/^{22\mathrm{Na}}\sigma$ and $^{7\mathrm{Be}}\sigma/^{22\mathrm{Na}}\sigma$ ratios should be measured additionally and, respectivelly, $^{24\mathrm{Na}}\sigma$ and $^{7\mathrm{Be}}\sigma$ should be calculated, because the recommended ^{27}Al(p,x)^{24}Na, ^{27}Al(p,x)^{7}Be, and ^{27}Al(p,x)^{22}Na monitor reaction data, which were obtained and used elsewhere to joint the short- and long-term irradiation data, can lead to significant systematic errors.

Since ^{24}Na, ^{7}Be, and ^{22}Na are produced when irradiating one and the same experimental sample, the ratio of their cross sections can be presented as

$$\frac{\sigma^{^{24}\mathrm{Na},^{7}\mathrm{Be}}}{\sigma^{^{22}\mathrm{Na}}} = \frac{A_0^{^{24}Na,^{7}\mathrm{Be}}}{A_0^{^{22}Na}} \frac{(\lambda\eta\varepsilon)^{^{22}Na}}{(\lambda\eta\varepsilon)^{^{24}Na,^{7}\mathrm{Be}}} \frac{F^{^{22}Na}}{F^{^{24}Na,^{7}\mathrm{Be}}} \times \frac{1+\left(\overline{\sigma}_{n,x}^{^{22}Na}\Phi_n/\sigma_{p,x}^{^{22}Na}\Phi_p\right)}{1+\left(\overline{\sigma}_{n,x}^{^{24}Na,^{7}\mathrm{Be}}\Phi_n/\sigma_{p,x}^{^{24}Na,^{7}\mathrm{Be}}\Phi_p\right)} \quad . \tag{84}$$

where t_{irr} is irradiation time of a single sample; $t_{irr} = [(K-1)T + \tau]$.

Since the Φ_n/Φ_p ratio is $\sim 0.8 - 2\%$ at proton beam energies 0.07-3.0 GeV, the calculations of the cross section ratio get simplified:

$$\frac{\sigma^{^{24}\mathrm{Na},^{7}\mathrm{Be}}}{\sigma^{^{22}\mathrm{Na}}} = \frac{A_0^{^{24}Na,^{7}\mathrm{Be}}}{A_0^{^{22}Na}} \frac{(\lambda\eta\varepsilon)^{^{22}Na}}{(\lambda\eta\varepsilon)^{^{24}Na,^{7}\mathrm{Be}}} \frac{F^{^{22}Na}}{F^{^{24}Na,^{7}\mathrm{Be}}} \tag{85}$$

The measurement results are presented in Table 12 and displayed in Fig. 21.

Table 13 presents the nuclear-physics characteristics of the given nuclides used in the calculations by formula (85).

Table 13: Nuclear-physics characteristics of the nuclides produced in the ^{27}Al(p,x) monitor reactions.

Product	γ– energy (keV)	γ–abundance (%)	$T_{1/2}$
^{24}Na	1369.0	100	(14.9590±0.0012) h
^{22}Na	1274.5	99.944±0.014	(2.6088±0.0014) y
^{7}Be	477.6	10.5±0.6	(53.29±0.07) d

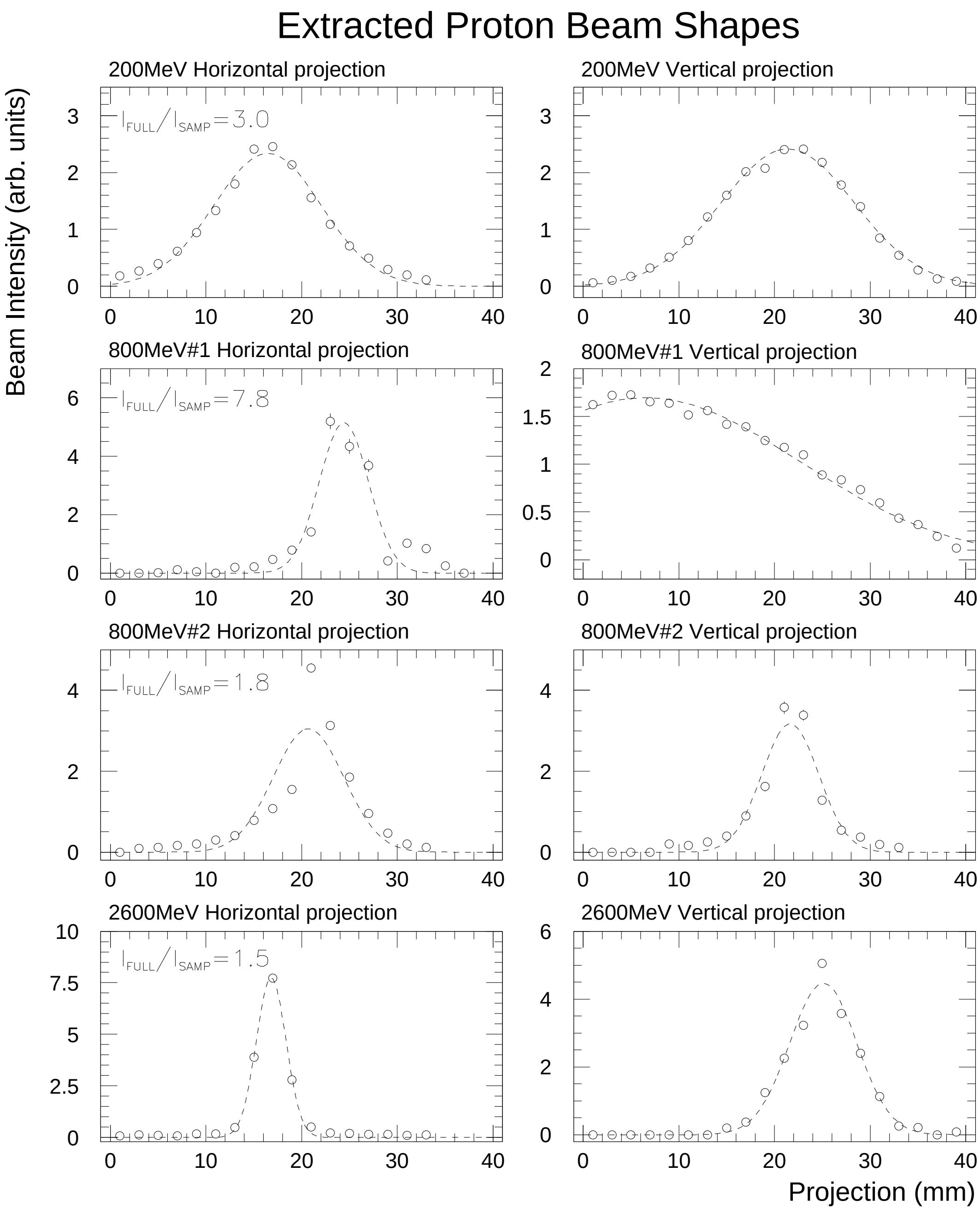

Fig. 20: Vertical and Horizontal projections of extracted proton beams.

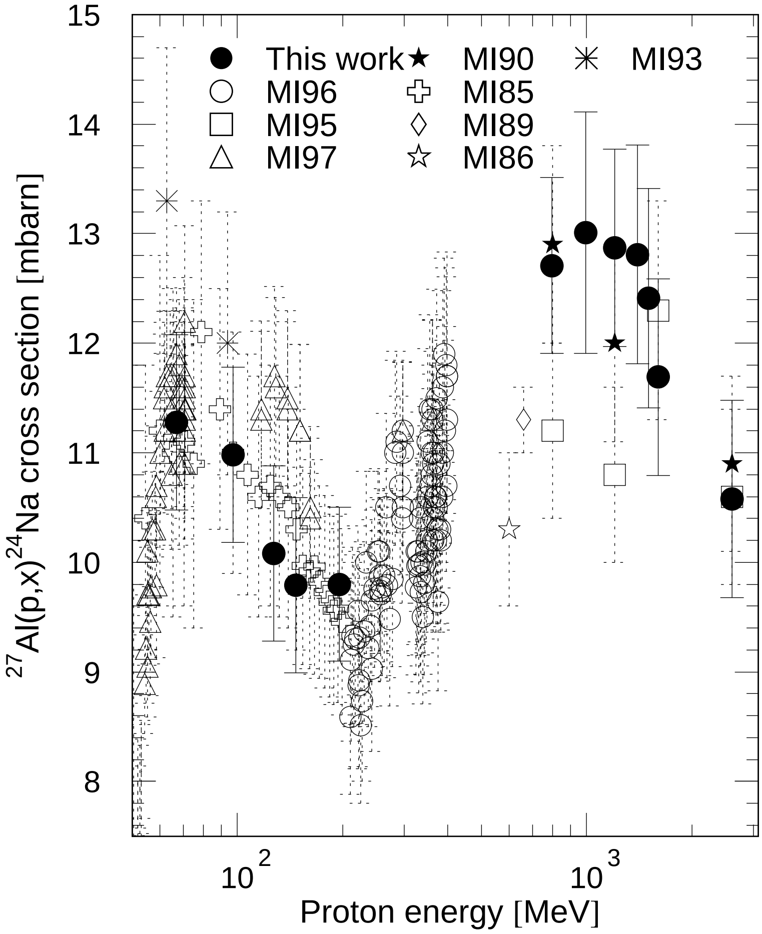

Fig. 21: ^{27}Al(p,x)^{24}Na reaction cross sections measured at ITEP and elsewhere.

3 EXPERIMENTAL RESULTS.

The results of determining the yields of reaction products in the targets listed in Table 1 are presented in Tables 16, 18, 20, 22, 24, 26, 28, 30, 32, 34, 36, 38, 40, 42, 44, 46. Table 14 shows total amount of measured reaction product yields different types in each experiment.

It should be emphasized that in some of the isobaric chains (about 1% of the data), the cumulative yield of parent nuclide exceeds the cumulative yield of its daughter (^{188}Pt and ^{188}Ir, for example). Surely, this fact cannot be explained essentially in terms of the physics of the studied processes. Nevertheless, in case the excess is within the experimental errors, the appropriate data are presented in the tables of yields. The common case is a sufficient smallness of the independent yield of daughter nuclide compared with the cumulative yield of its precursor. The cases of the excess beyond the experimental errors are excluded from the tabulated results. The discrepancies are most probably due to, for instance, inadequate values of the absolute γ-abundances of the analyzed nuclides and/or the fact that the daughter nuclide has a still unidentified short-lived isomeric state with a high branching ratio of the mother nuclide decay into an isomeric state and a low branching ratio for isomeric transition. These cases are to be analyzed in the pending researches.

The ^{27}Al(p,x)^{22}Na reaction was used in all the experiments to monitor the proton flux, except for some cases (^{nat}Pb 1.5 GeV) where the ^{27}Al(p,x)^{24}Na reaction was used. Table 12 presents the cross sections of the two monitor reactions.

3.1 Experimental errors

As seen from Tables 16 – 46, the experimental errors are within $\sim (6 \div 35)\%$. The experimental errors were calculated as follows. Since the reported results were mostly obtained by averaging a few $(\sigma_i \pm \Delta\sigma_i)$ values, which were calculated on the basis of their γ-lines, their mean and the experimental errors were calculated as

$$\overline{\sigma} = \frac{\sum_i \sigma_i W_i}{\sum_i W_i}, \qquad \text{where} \qquad W_i = 1/\Delta\sigma_i^2 \ . \tag{86}$$

The $\Delta\overline{\sigma}$ value was calculated by the techniques [19]. The $\Delta\overline{\sigma}$ was taken to be the highest of the $\Delta\overline{\sigma}'$ and $\Delta\overline{\sigma}''$ values calculated as:

$$\Delta\overline{\sigma}\ ' = \sqrt{\frac{\sum_i W_i \left(\overline{\sigma} - \sigma_i\right)^2}{(n-1)\sum_i W_i}}\ , \tag{87}$$

$$\Delta\overline{\sigma}\ '' = \sqrt{\frac{1}{\sum_i W_i}}\ . \tag{88}$$

The total error in the measured yields was calculated making allowance for the monitor error:

$$\frac{\Delta\overline{\sigma}}{\overline{\sigma}} = \sqrt{\left(\frac{\Delta\overline{\sigma}}{\overline{\sigma}}\right)^2 + \left(\frac{\Delta\sigma_{st}}{\sigma_{st}}\right)^2}\ . \tag{89}$$

The errors in the independent and cumulative yields of the reaction products for separate γ-lines, which vere obtained via formulas (32) and (33), were determined using the error transfer formulas [19].

Table 14: Number of measured reaction product yields of different types in each experiment.

Experiment	Yield type					Total
	i	c	c*	i(Σm_j)	i(Σm_j+g)	
^{182}W, E$_p$=0.2 GeV	3	22	3	1	3	32
^{182}W, E$_p$=0.8 GeV	5	52	6	1	6	70
^{182}W, E$_p$=1.6 GeV	10	84	3	6	6	109
^{183}W, E$_p$=0.2 GeV	4	23	3	1	4	35
^{183}W, E$_p$=0.8 GeV	6	55	6	2	7	76
^{183}W, E$_p$=1.6 GeV	12	84	3	6	6	111
^{184}W, E$_p$=0.2 GeV	4	23	3	1	5	36
^{184}W, E$_p$=0.8 GeV	7	55	6	2	7	77
^{184}W, E$_p$=1.6 GeV	12	85	3	7	7	114
^{186}W, E$_p$=0.2 GeV	4	23	3	1	5	36
^{186}W, E$_p$=0.8 GeV	4	48	5	1	4	62
^{186}W, E$_p$=1.6 GeV	13	87	3	8	8	119
^{nat}W, E$_p$=2.6 GeV	10	100	4	9	6	129
^{232}Th, E$_p$=0.1 GeV	10	58	2	9	8	87
^{232}Th, E$_p$=0.2 GeV	16	80	4	18	10	128
^{232}Th, E$_p$=0.8 GeV	15	78	11	15	11	130
^{232}Th, E$_p$=1.2 GeV	22	140	13	19	20	214
^{232}Th, E$_p$=1.6 GeV	22	143	13	18	16	212
^{nat}U, E$_p$=0.1 GeV	12	74	3	9	10	108
^{nat}U, E$_p$=0.2 GeV	15	77	3	15	13	123
^{nat}U, E$_p$=0.8 GeV	21	122	15	17	20	195
^{nat}U, E$_p$=1.2 GeV	22	146	15	22	21	226
^{nat}U, E$_p$=1.6 GeV	23	151	15	22	20	231
^{99}Tc, E$_p$=0.1 GeV	4	9	0	3	2	18
^{99}Tc, E$_p$=0.2 GeV	4	21	0	9	5	39
^{99}Tc, E$_p$=0.8 GeV	10	40	3	11	8	72
^{99}Tc, E$_p$=1.2 GeV	8	39	2	12	6	67
^{99}Tc, E$_p$=1.6 GeV	10	44	3	11	10	78
^{59}Co, E$_p$=0.2 GeV	6	17	0	3	3	29
^{59}Co, E$_p$=1.2 GeV	7	26	0	4	4	41
^{59}Co, E$_p$=1.6 GeV	7	26	0	4	4	41
^{59}Co, E$_p$=2.6 GeV	7	26	0	4	4	41
^{63}Cu, E$_p$=0.2 GeV	9	12	1	3	4	29
^{63}Cu, E$_p$=1.2 GeV	10	27	2	4	4	47
^{63}Cu, E$_p$=1.6 GeV	11	22	1	4	4	42
^{63}Cu, E$_p$=2.6 GeV	11	22	1	4	4	42
^{65}Cu, E$_p$=0.2 GeV	8	13	1	4	3	29
^{65}Cu, E$_p$=1.2 GeV	13	29	2	5	5	54
^{65}Cu, E$_p$=1.6 GeV	10	26	1	5	5	47
^{65}Cu, E$_p$=2.6 GeV	10	27	1	5	5	48
^{nat}Hg, E$_p$=0.1 GeV	4	17	1	10	12	44
^{nat}Hg, E$_p$=0.2 GeV	6	27	6	12	14	65
^{nat}Hg, E$_p$=0.8 GeV	9	57	11	12	14	103
^{nat}Hg, E$_p$=1.6 GeV	8	90	13	16	14	141
^{56}Fe, E$_p$=2.6 GeV	5	24	1	3	3	36
^{58}Ni, E$_p$=2.6 GeV	9	21	1	3	4	38
^{93}Nb, E$_p$=2.6 GeV	6	56	2	12	8	85
^{208}Pb, E$_p$=1.0 GeV	8	65	11	15	15	114
Total	**472**	**2593**	**209**	**388**	**387**	**4050**

i – independent yields of ground states, **c** – cumulative yields, **c*** - supra-cumulative yields,
i(Σm_j) – independent yields of metastable states,
i(Σm_j+**g**) – summed independent yields of metastable and ground states.

The uncertainties in the nuclear data (absolute values of γ–abundances and monitor reaction cross sections) were found in the relevant analysis to make the major contribution to the total error.

It should be noted that all the experimental reaction product yields have been obtained using the nuclear decay data from the PCNUDAT database, or if not found there, from the Tables of Isotopes Handbook (8th Ed.) [17, 18].

3.2 Experimental yields for ^{182}W irradiated with 0.2, 0.8, 1.6 GeV protons.

Table 15 presents the parameters of ^{182}W irradiations. Table 16 presents the yields of residual nuclide products measured.

Table 15: Parameters of ^{182}W irradiation.

E_p (GeV)	Sample weight (mg)	Monitor weight (mg)	Irradiation duration (min)	Proton Flux p/cm^2	Number of measured γ -spectra of sample/monitor	EXPDATA index
0.2	143.1	109.2	60	2.1×10^{13}	48 / 8	w182200
0.8	178.6	109.9	60	4.1×10^{13}	47 / 8	w182800
1.6	170.4	109.8	60	3.1×10^{13}	49 / 11	w18216g

Table 16: Experimental yields from ^{182}W irradiated with 0.2, 0.8, 1.6 GeV protons.

Product	$T_{1/2}$	Type	Yields [mbarn] at		
			0.2 GeV	0.8 GeV	1.6 GeV
^{181}Re	19,9h	i	13.2 ± 1.8	4.58 ± 0.72	3.71 ± 0.61
^{179}Re	19,5m	i	21.7 ± 2.5	–	–
^{178}W	21,6d	c	70.6 ± 8.2	–	–
^{177}W	135m	c	70.4 ± 8.0	25.4 ± 2.9	19.4 ± 2.4
^{176}W	2,5h	c	84.1 ± 7.1	–	–
^{174}W	31m	c	80.6 ± 9.0	–	–
^{183}Ta	5,1d	c	0.548 ± 0.117	1.14 ± 0.22	–
^{182}Ta	114,43d	c	–	2.04 ± 0.24	2.24 ± 0.34
^{178m}Ta	2,36h	i(m1+m2)	9.02 ± 0.61	9.39 ± 0.98	7.98 ± 0.71
^{176}Ta	8,09h	i(m+g)	25.3 ± 3.1	–	–
^{176}Ta	8,09h	c	112. ± 8.	50.9 ± 4.3	38.9 ± 3.9
^{175}Ta	10,5h	c	109. ± 8.	49.3 ± 4.8	29.4 ± 4.2
^{174}Ta	1,14h	c	105. ± 11.	51.5 ± 5.5	43.9 ± 5.9
^{174}Ta	1,14h	i	24.2 ± 4.3	38.1 ± 4.8	–
^{173}Ta	3,14h	c*	113. ± 8.	–	–
^{173}Ta	3,14h	c	–	–	31.5 ± 3.4
^{172}Ta	36,8m	c*	51.2 ± 4.3	–	–
^{171}Ta	23,3m	c*	10.0 ± 1.4	–	–
^{181}Hf	42,39d	c	–	–	0.187 ± 0.025
^{175}Hf	70d	c	120. ± 9.	56.3 ± 4.1	39.0 ± 3.4
^{173}Hf	23,6h	c	115. ± 8.	60.2 ± 4.4	38.6 ± 3.2
^{173}Hf	23,6h	i	–	–	6.20 ± 2.75
^{172}Hf	1,87y	c	86.8 ± 5.8	47.9 ± 3.3	30.5 ± 2.9
^{171}Hf	12,1h	c	72.3 ± 5.7	48.1 ± 4.8	30.5 ± 3.3

Table 16, continued.

Product	$T_{1/2}$	Type	Yields [mbarn] at		
			0.2 GeV	0.8 GeV	1.6 GeV
^{170}Hf	16,01h	c	58.4 ± 4.3	49.0 ± 4.3	27.6 ± 2.9
^{173}Lu	1,37y	c	106. ± 8.	56.7 ± 4.0	38.5 ± 3.5
^{172}Lu	6,70d	i(m1+m2+g)	1.17 ± 0.09	3.68 ± 0.40	2.95 ± 0.26
^{172}Lu	6,70d	c	87.9 ± 6.0	51.7 ± 3.6	33.9 ± 3.5
^{171}Lu	8,24d	i(m+g)	12.6 ± 3.1	9.61 ± 3.79	4.72 ± 2.23
^{171}Lu	8,24d	c	84.9 ± 5.8	57.8 ± 3.9	35.2 ± 2.9
^{170}Lu	2,012d	i(m+g)	–	4.04 ± 2.25	7.25 ± 1.97
^{170}Lu	2,012d	c	60.8 ± 3.9	51.1 ± 4.1	32.2 ± 2.7
^{169}Lu	34,06h	c	41.5 ± 3.3	50.3 ± 3.8	26.9 ± 2.2
^{167}Lu	51,5m	c	–	53.5 ± 4.8	27.4 ± 4.4
^{169}Yb	32,026d	c	48.6 ± 3.1	58.0 ± 4.4	32.1 ± 2.6
^{167}Yb	17,5m	c	–	54.9 ± 5.3	–
^{166}Yb	56,7h	c	16.3 ± 1.1	52.3 ± 3.6	31.5 ± 3.1
^{162}Yb	18,87m	c	–	44.9 ± 6.2	39.5 ± 5.7
^{167}Tm	9,25d	c	–	60.6 ± 12.2	36.3 ± 5.2
^{166}Tm	7,70h	c	15.9 ± 1.1	56.2 ± 4.0	31.8 ± 3.2
^{166}Tm	7,70h	i	–	3.71 ± 0.76	0.264 ± 0.357
^{165}Tm	30,06h	c	10.7 ± 0.8	57.3 ± 4.2	32.1 ± 2.8
^{163}Tm	1,810h	c*	–	57.5 ± 3.8	37.4 ± 3.7
^{161}Tm	33m	c*	–	41.2 ± 7.1	–
^{161}Tm	33m	c	–	–	33.5 ± 6.8
^{161}Er	3,21h	c	–	47.3 ± 4.2	28.2 ± 3.8
^{160}Er	28,58h	c	–	54.4 ± 4.3	32.7 ± 3.2
^{159}Er	36m	c*	–	59.4 ± 4.2	40.3 ± 6.0
^{156}Er	19,5m	c	–	30.2 ± 3.1	–
^{160m}Ho	5,02h	c	–	56.5 ± 4.7	32.6 ± 3.2
^{159}Ho	33,05m	c	–	54.4 ± 4.2	–
^{156}Ho	56m	c	–	38.1 ± 3.0	24.6 ± 4.9
^{157}Dy	8,14h	c	–	44.6 ± 3.4	31.5 ± 2.9
^{155}Dy	9,9h	c*	–	36.2 ± 3.9	–
^{155}Dy	9,9h	c	–	–	29.2 ± 2.6
^{153}Dy	6,4h	c	–	21.3 ± 1.8	22.3 ± 2.5
^{152}Dy	2,38h	c	–	20.1 ± 1.3	20.3 ± 1.7
^{155}Tb	5,32d	c	–	36.7 ± 3.3	30.0 ± 2.5
^{153}Tb	2,34d	c*	–	29.0 ± 2.6	–
^{153}Tb	2,34d	c	–	–	25.5 ± 2.7
^{152}Tb	17,5h	c	–	22.9 ± 2.0	20.6 ± 2.1
^{151}Tb	17,609h	c	–	23.5 ± 3.1	20.7 ± 1.8
^{150}Tb	3,48h	c	–	12.4 ± 1.9	13.2 ± 2.1
^{149}Tb	4,118h	c	–	10.3 ± 0.8	10.1 ± 0.8

Table 16, continued.

Product	$T_{1/2}$	Type	Yields [mbarn] at		
			0.2 GeV	0.8 GeV	1.6 GeV
^{148}Tb	60m	c	–	13.4 ± 1.0	14.9 ± 1.3
^{147}Tb	1,7h	c	–	–	3.43 ± 0.41
^{153}Gd	240,4d	c	–	28.0 ± 2.4	24.1 ± 2.4
^{151}Gd	124d	c	–	–	20.6 ± 2.0
^{149}Gd	9,28d	c	–	26.0 ± 2.3	27.6 ± 2.3
^{147}Gd	38,06h	c	–	19.4 ± 1.3	25.6 ± 2.2
^{146}Gd	48,27d	c	–	19.1 ± 1.2	26.3 ± 2.1
^{145}Gd	23,0m	c	–	–	21.0 ± 2.2
^{149}Eu	93,1d	c	–	–	30.6 ± 2.5
^{148}Eu	54,5d	i	–	1.14 ± 0.23	–
^{147}Eu	24,1d	c	–	22.5 ± 1.9	28.8 ± 2.4
^{146}Eu	4,61d	c	–	–	33.6 ± 3.0
^{146}Eu	4,61d	i	–	–	7.22 ± 1.00
^{145}Eu	5,93d	c	–	13.9 ± 1.0	22.8 ± 1.9
^{144}Pm	363d	i	–	–	0.569 ± 0.074
^{143}Pm	265d	c	–	–	22.8 ± 2.3
^{139m}Nd	5,5h	i(m)	–	–	2.51 ± 0.34
^{137}Nd	38,5m	c	–	–	37.3 ± 5.1
^{136}Nd	50,65m	c	–	–	17.6 ± 1.8
^{139}Ce	137,640d	c	–	6.02 ± 0.39	21.8 ± 1.8
^{135}Ce	17,7h	c	–	–	18.2 ± 1.4
^{134}Ce	3,16d	c	–	–	17.0 ± 1.6
^{133}Ce	4,9h	i	–	–	3.02 ± 0.34
^{132}Ce	3,51h	c	–	–	13.8 ± 1.6
^{132}La	4,8h	c	–	–	13.6 ± 1.5
^{133}Ba	3848,9d	c	–	–	17.2 ± 2.5
^{131}Ba	11,50d	c	–	–	14.8 ± 1.1
^{128}Ba	2,43d	c	–	–	11.6 ± 1.1
^{129}Cs	32,06h	c	–	–	14.7 ± 1.4
^{127}Xe	36,4d	c	–	0.936 ± 0.086	11.1 ± 0.9
^{125}Xe	16,9h	c	–	–	9.84 ± 0.80
^{123}Xe	2,08h	c	–	–	10.9 ± 1.0
^{121m}Te	154d	i(m)	–	–	0.314 ± 0.041
^{121}Te	19,16d	c	–	–	6.88 ± 0.58
^{119m}Te	4,70d	c	–	–	1.11 ± 0.10
^{119}Te	16,05h	c	–	–	4.82 ± 0.40
^{113}Sn	115,09d	c	–	–	3.05 ± 0.27
^{106m}Ag	8,28d	i(m)	–	–	0.872 ± 0.093
^{105}Ag	41,29d	c	–	–	1.69 ± 0.18
^{96}Tc	4,28d	i(m+g)	–	0.330 ± 0.030	0.745 ± 0.066

Table 16, continued.

Product	$T_{1/2}$	Type	Yields [mbarn] at		
			0.2 GeV	0.8 GeV	1.6 GeV
^{93m}Mo	6,85h	i(m)	–	–	0.662 ± 0.066
^{90}Nb	14,60h	c	–	–	1.12 ± 0.11
^{89}Zr	78,41h	c	–	–	1.61 ± 0.13
^{88}Zr	83,4d	c	–	0.346 ± 0.074	1.19 ± 0.13
^{88}Y	106,65d	i(m+g)	–	0.486 ± 0.054	0.550 ± 0.143
^{88}Y	106,65d	c	–	0.836 ± 0.066	2.24 ± 0.25
^{87}Y	79,8h	c*	–	0.978 ± 0.096	–
^{85}Sr	64,84d	c	–	0.912 ± 0.082	1.93 ± 0.18
^{87}Rb	79,8h	c*	–	–	2.01 ± 0.17
^{84}Rb	32,77d	i(m+g)	–	0.552 ± 0.045	0.735 ± 0.084
^{83}Rb	86,2d	c	–	0.890 ± 0.122	2.12 ± 0.28
^{75}Se	119,779d	c	–	–	1.57 ± 0.23
^{74}As	17,77d	i	–	0.563 ± 0.066	0.921 ± 0.108
^{69m}Zn	13,76h	i(m)	–	–	0.319 ± 0.033
^{59}Fe	44,472d	c	–	0.281 ± 0.030	0.503 ± 0.051
^{52}Fe	8,275h	c	–	–	0.265 ± 0.109
^{54}Mn	312,11d	i	–	–	1.08 ± 0.21
^{52}Mn	5,591d	c	–	–	0.220 ± 0.049
^{48}V	15,9735d	c	–	–	0.252 ± 0.038
^{48}Sc	43,67h	i	–	–	0.429 ± 0.045
^{28}Mg	20,915h	c	–	–	0.388 ± 0.042
^{24}Na	14,9590h	c	–	–	1.84 ± 0.15
^{7}Be	53,29d	i	–	–	5.12 ± 0.58

3.3 Experimental yields for ^{183}W irradiated with 0.2, 0.8, 1.6 GeV protons.

Table 17 presents the parameters of ^{183}W irradiations. Table 18 presents the yields of residual nuclide products measured.

Table 17: Parameters of ^{183}W irradiation.

E_p (GeV)	Sample weight (mg)	Monitor weight (mg)	Irradiation duration (min)	Proton Flux p/cm^2	Number of measured γ -spectra of sample/monitor	EXPDATA index
0.2	141.0	120.6	60	9.5×10^{12}	40 / 7	w183200
0.8	137.8	107.9	52	4.0×10^{13}	52 / 10	w183800
1.6	140.8	108.2	45	4.2×10^{13}	33 / 8	w18316g

Table 18: Experimental yields from ^{183}W irradiated with 0.2, 0.8, 1.6 GeV protons.

Product	$T_{1/2}$	Type	Yields [mbarn] at		
			0.2 GeV	0.8 GeV	1.6 GeV
^{183}Re	70,0d	i(m+g)	5.20 ± 0.46	1.69 ± 0.33	–
^{182}Re	64,0h	i	3.91 ± 0.41	–	–
^{181}Re	19,9h	i	22.4 ± 2.9	6.29 ± 0.99	4.60 ± 0.76
^{179}Re	19,5m	i	19.8 ± 3.7	–	–
^{178}W	21,6d	c	65.5 ± 10.5	–	–
^{177}W	135m	c	64.9 ± 7.8	24.6 ± 2.8	17.7 ± 2.2
^{176}W	2,5h	c	74.9 ± 10.1	–	–
^{174}W	31m	c	71.8 ± 8.4	–	–
^{184}Ta	8,7h	c	–	0.564 ± 0.123	–
^{183}Ta	5,1d	c	2.71 ± 0.29	5.53 ± 0.39	4.69 ± 0.45
^{182}Ta	114,43d	c	12.3 ± 1.0	20.9 ± 1.3	19.0 ± 1.5
^{178m}Ta	2,36h	i(m1+m2)	11.5 ± 0.8	10.9 ± 1.5	8.79 ± 0.77
^{176}Ta	8,09h	i(m+g)	39.2 ± 8.1	–	–
^{176}Ta	8,09h	c	118. ± 9.	54.1 ± 4.7	43.1 ± 4.3
^{175}Ta	10,5h	c	108. ± 8.	52.2 ± 5.1	30.2 ± 4.4
^{174}Ta	1,14h	c	104. ± 11.	53.8 ± 5.8	30.1 ± 3.9
^{174}Ta	1,14h	i	32.0 ± 5.5	45.4 ± 5.8	16.1 ± 5.4
^{173}Ta	3,14h	c*	94.8 ± 8.2	–	–
^{173}Ta	3,14h	c	–	51.2 ± 8.0	30.0 ± 3.2
^{172}Ta	36,8m	c*	48.0 ± 5.2	–	–
^{171}Ta	23,3m	c*	8.16 ± 1.22	–	–
^{181}Hf	42,39d	c	–	0.653 ± 0.074	0.581 ± 0.064
^{179m}Hf	25,05d	i(m2)	–	0.305 ± 0.063	–
^{175}Hf	70d	c	121. ± 9.	60.2 ± 4.3	42.1 ± 3.7

Table 18, continued.

Product	$T_{1/2}$	Type	Yields [mbarn] at		
			0.2 GeV	0.8 GeV	1.6 GeV
^{173}Hf	23,6h	c	107. ± 7.	62.8 ± 4.6	41.3 ± 3.5
^{173}Hf	23,6h	i	–	–	8.77 ± 2.73
^{172}Hf	1,87y	c	76.2 ± 5.4	51.8 ± 3.6	33.7 ± 2.9
^{171}Hf	12,1h	c	69.9 ± 5.2	48.4 ± 4.2	31.0 ± 3.8
^{170}Hf	16,01h	c	50.1 ± 4.1	46.7 ± 4.1	25.4 ± 2.8
^{173}Lu	1,37y	c	101. ± 8.	59.6 ± 5.7	42.1 ± 3.8
^{172}Lu	6,70d	i(m1+m2+g)	1.68 ± 0.18	5.56 ± 0.45	4.01 ± 0.35
^{172}Lu	6,70d	c	79.0 ± 5.6	57.0 ± 4.0	38.2 ± 3.3
^{171}Lu	8,24d	i(m+g)	5.12 ± 1.25	15.6 ± 3.0	8.40 ± 3.05
^{171}Lu	8,24d	c	75.0 ± 5.4	64.0 ± 4.3	39.4 ± 3.3
^{170}Lu	2,012d	i(m+g)	–	13.6 ± 2.4	13.0 ± 2.8
^{170}Lu	2,012d	c	51.5 ± 3.6	58.4 ± 4.7	34.9 ± 3.0
^{169}Lu	34,06h	c	35.4 ± 4.2	53.2 ± 4.0	29.7 ± 2.4
^{167}Lu	51,5m	c	–	53.1 ± 4.7	28.4 ± 3.5
^{169}Yb	32,026d	c	38.0 ± 2.6	62.9 ± 5.0	36.2 ± 3.0
^{167}Yb	17,5m	c	–	60.8 ± 5.9	–
^{166}Yb	56,7h	c	11.0 ± 0.8	56.9 ± 4.0	35.0 ± 3.5
^{162}Yb	18,87m	c	–	40.9 ± 5.3	21.7 ± 4.0
^{168}Tm	93,1d	i	–	–	0.676 ± 0.101
^{167}Tm	9,25d	c	–	64.4 ± 13.0	40.4 ± 5.6
^{166}Tm	7,70h	c	11.6 ± 0.8	61.2 ± 4.3	36.0 ± 3.6
^{166}Tm	7,70h	i	–	6.78 ± 1.39	1.08 ± 0.50
^{165}Tm	30,06h	c	6.75 ± 0.69	63.6 ± 4.6	36.4 ± 3.2
^{163}Tm	1,810h	c*	–	60.9 ± 5.1	36.7 ± 4.1
^{161}Tm	33m	c*	–	42.2 ± 7.4	–
^{161}Tm	33m	c	–	–	26.6 ± 4.9
^{161}Er	3,21h	c	–	51.8 ± 4.6	33.4 ± 3.5
^{160}Er	28,58h	c	–	59.6 ± 5.3	36.6 ± 3.6
^{159}Er	36m	c*	–	60.6 ± 4.2	36.0 ± 5.5
^{156}Er	19,5m	c	–	25.3 ± 2.8	–
^{160m}Ho	5,02h	c	–	58.9 ± 5.2	39.1 ± 3.9
^{159}Ho	33,05m	c	–	54.1 ± 5.6	–
^{156}Ho	56m	c	–	38.4 ± 3.2	22.5 ± 2.6
^{156}Ho	56m	i	–	12.8 ± 3.5	–
^{157}Dy	8,14h	c	–	47.3 ± 3.6	35.5 ± 3.3
^{155}Dy	9,9h	c*	–	38.1 ± 2.8	–
^{155}Dy	9,9h	c	–	–	32.5 ± 2.8
^{153}Dy	6,4h	c	–	22.9 ± 2.0	26.2 ± 3.0
^{152}Dy	2,38h	c	–	20.2 ± 1.3	22.5 ± 1.9
^{155}Tb	5,32d	c	–	37.6 ± 3.3	32.7 ± 2.8

Table 18, continued.

Product	$T_{1/2}$	Type	Yields [mbarn] at		
			0.2 GeV	0.8 GeV	1.6 GeV
^{153}Tb	2,34d	c*	–	30.6 ± 2.7	–
^{153}Tb	2,34d	c	–	–	29.3 ± 3.3
^{152}Tb	17,5h	c	–	22.7 ± 2.0	24.1 ± 2.5
^{151}Tb	17,609h	c	–	23.7 ± 2.5	23.9 ± 2.1
^{150}Tb	3,48h	c	–	12.0 ± 1.8	13.7 ± 2.2
^{149}Tb	4,118h	c	–	9.67 ± 0.66	10.7 ± 0.9
^{148}Tb	60m	c	–	11.0 ± 0.9	14.2 ± 1.3
^{147}Tb	1,7h	c	–	–	3.10 ± 0.51
^{153}Gd	240,4d	c	–	27.2 ± 2.1	28.8 ± 2.7
^{151}Gd	124d	c	–	–	23.4 ± 2.2
^{149}Gd	9,28d	c	–	25.3 ± 2.3	30.8 ± 2.5
^{147}Gd	38,06h	c	–	19.4 ± 1.3	27.7 ± 2.3
^{146}Gd	48,27d	c	–	17.6 ± 1.1	28.3 ± 2.3
^{145}Gd	23,0m	c	–	–	13.1 ± 2.3
^{149}Eu	93,1d	c	–	–	35.1 ± 2.9
^{148}Eu	54,5d	i	–	1.48 ± 0.34	–
^{147}Eu	24,1d	c	–	21.5 ± 1.8	30.9 ± 2.7
^{146}Eu	4,61d	c	–	–	36.5 ± 3.2
^{146}Eu	4,61d	i	–	–	6.93 ± 1.02
^{145}Eu	5,93d	c	–	13.3 ± 1.0	25.0 ± 2.1
^{144}Pm	363d	i	–	–	0.521 ± 0.138
^{143}Pm	265d	c	–	–	26.1 ± 2.7
^{139m}Nd	5,5h	i(m)	–	–	3.16 ± 0.46
^{137}Nd	38,5m	c	–	–	29.5 ± 3.4
^{136}Nd	50,65m	c	–	–	15.9 ± 1.7
^{139}Ce	137,640d	c	–	5.65 ± 0.36	24.0 ± 2.0
^{135}Ce	17,7h	c	–	–	19.4 ± 1.5
^{134}Ce	3,16d	c	–	–	17.1 ± 1.7
^{133}Ce	4,9h	i	–	–	3.99 ± 0.47
^{132}Ce	3,51h	c	–	–	15.9 ± 1.3
^{132}La	4,8h	c	–	–	14.6 ± 1.6
^{133}Ba	3848,9d	c	–	–	17.1 ± 1.8
^{131}Ba	11,50d	c	–	–	15.8 ± 1.2
^{128}Ba	2,43d	c	–	–	12.4 ± 1.2
^{129}Cs	32,06h	c	–	–	15.9 ± 1.6
^{127}Xe	36,4d	c	–	0.907 ± 0.091	12.0 ± 1.0
^{125}Xe	16,9h	c	–	–	10.3 ± 0.8
^{123}Xe	2,08h	c	–	–	11.2 ± 1.0
^{121m}Te	154d	i(m)	–	–	0.404 ± 0.075
^{121}Te	19,16d	c	–	–	7.50 ± 0.65

Table 18, continued.

Product	$T_{1/2}$	Type	Yields [mbarn] at		
			0.2 GeV	0.8 GeV	1.6 GeV
^{119m}Te	4,70d	c	–	–	1.19 ± 0.13
^{119}Te	16,05h	c	–	–	5.22 ± 0.45
^{113}Sn	115,09d	c	–	–	3.18 ± 0.27
^{106m}Ag	8,28d	i(m)	–	–	0.794 ± 0.072
^{105}Ag	41,29d	c	–	–	1.54 ± 0.15
^{96}Tc	4,28d	i(m+g)	–	0.323 ± 0.026	0.827 ± 0.075
^{93m}Mo	6,85h	i(m)	–	–	0.624 ± 0.071
^{90}Nb	14,60h	c	–	–	1.68 ± 0.23
^{89}Zr	78,41h	c	–	–	1.72 ± 0.14
^{88}Zr	83,4d	c	–	0.308 ± 0.116	1.17 ± 0.10
^{88}Y	106,65d	i(m+g)	–	0.649 ± 0.115	1.04 ± 0.10
^{88}Y	106,65d	c	–	0.970 ± 0.074	2.20 ± 0.18
^{87}Y	79,8h	c*	–	1.04 ± 0.07	–
^{85}Sr	64,84d	c	–	1.06 ± 0.16	1.92 ± 0.18
^{87}Rb	79,8h	c*	–	–	2.00 ± 0.25
^{84}Rb	32,77d	i(m+g)	–	0.641 ± 0.055	0.750 ± 0.074
^{83}Rb	86,2d	c	–	0.968 ± 0.113	1.84 ± 0.21
^{75}Se	119,779d	c	–	–	1.90 ± 0.22
^{74}As	17,77d	i	–	0.582 ± 0.058	0.917 ± 0.120
^{69m}Zn	13,76h	i(m)	–	–	0.367 ± 0.044
^{59}Fe	44,472d	c	–	0.405 ± 0.050	0.659 ± 0.063
^{54}Mn	312,11d	i	–	–	1.21 ± 0.13
^{52}Mn	5,591d	c	–	–	0.190 ± 0.038
^{48}V	15,9735d	c	–	–	0.276 ± 0.032
^{48}Sc	43,67h	i	–	–	0.410 ± 0.059
^{28}Mg	20,915h	c	–	–	0.362 ± 0.070
^{24}Na	14,9590h	c	–	–	2.04 ± 0.18
^{7}Be	53,29d	i	–	–	4.52 ± 0.51

3.4 Experimental yields for ^{184}W irradiated with 0.2, 0.8, 1.6 GeV protons.

Table 19 presents the parameters of ^{184}W irradiations. Table 20 presents the yields of residual nuclide products measured.

Table 19: Parameters of ^{184}W irradiation.

E_p (GeV)	Sample weight (mg)	Monitor weight (mg)	Irradiation duration (min)	Proton Flux p/cm^2	Number of measured γ -spectra of sample/monitor	EXPDATA index
0.2	182.6	20.6	60	1.0×10^{13}	44 / 8	w184200
0.8	181.5	108.7	40	2.5×10^{14}	43 / 12	w184800
1.6	181.2	109.2	60	3.1×10^{13}	46 / 10	w18416g

Table 20: Experimental yields from ^{184}W irradiated with 0.2, 0.8, 1.6 GeV protons.

Product	$T_{1/2}$	Type	Yields [mbarn] at		
			0.2 GeV	0.8 GeV	1.6 GeV
^{184}Re	38,0d	i(m+g)	3.03 ± 0.43	–	–
^{183}Re	70,0d	i(m+g)	11.5 ± 1.1	3.61 ± 0.33	3.14 ± 0.71
^{182}Re	64,0h	i	6.22 ± 0.64	–	–
^{181}Re	19,9h	i	23.9 ± 3.1	7.42 ± 1.16	4.84 ± 0.79
^{179}Re	19,5m	i	18.2 ± 2.0	–	–
^{178}W	21,6d	c	76.0 ± 9.3	–	–
^{177}W	135m	c	58.3 ± 6.9	23.4 ± 2.7	15.0 ± 1.9
^{176}W	2,5h	c	73.1 ± 6.4	–	–
^{174}W	31m	c	60.0 ± 6.9	–	–
^{184}Ta	8,7h	c	–	0.950 ± 0.085	0.763 ± 0.097
^{183}Ta	5,1d	c	9.71 ± 0.73	21.2 ± 1.5	19.4 ± 1.6
^{182}Ta	114,43d	c	12.1 ± 1.1	18.6 ± 1.2	16.7 ± 1.4
^{178m}Ta	2,36h	i(m1+m2)	12.2 ± 0.9	12.1 ± 1.8	9.84 ± 0.83
^{176}Ta	8,09h	i(m+g)	34.1 ± 4.0	–	–
^{176}Ta	8,09h	c	$109. \pm 8.$	45.6 ± 4.2	33.9 ± 3.7
^{175}Ta	10,5h	c	$100. \pm 8.$	45.7 ± 5.3	27.4 ± 3.9
^{174}Ta	1,14h	c	88.0 ± 9.6	50.0 ± 5.5	29.3 ± 3.6
^{174}Ta	1,14h	i	27.9 ± 4.4	40.2 ± 5.6	22.0 ± 4.1
^{173}Ta	3,14h	c*	85.9 ± 6.5	–	–
^{173}Ta	3,14h	c	–	46.8 ± 4.4	28.2 ± 3.0
^{172}Ta	36,8m	c*	40.5 ± 4.4	–	–
^{171}Ta	23,3m	c*	5.59 ± 0.80	–	–
^{181}Hf	42,39d	c	–	1.24 ± 0.11	1.18 ± 0.10
^{179m}Hf	25,05d	i(m2)	–	0.294 ± 0.036	0.372 ± 0.051

Table 20, continued.

Product	$T_{1/2}$	Type	Yields [mbarn] at		
			0.2 GeV	0.8 GeV	1.6 GeV
^{175}Hf	70d	c	111. ± 9.	56.7 ± 4.2	38.0 ± 3.3
^{173}Hf	23,6h	c	93.3 ± 6.5	58.6 ± 4.4	36.6 ± 3.2
^{173}Hf	23,6h	i	–	11.5 ± 2.7	8.68 ± 2.34
^{172}Hf	1,87y	c	65.9 ± 4.8	47.5 ± 3.3	28.4 ± 2.8
^{171}Hf	12,1h	c	44.1 ± 3.6	44.4 ± 5.0	27.5 ± 2.8
^{170}Hf	16,01h	c	32.8 ± 2.8	51.3 ± 4.9	24.4 ± 2.2
^{173}Lu	1,37y	c	85.0 ± 6.8	58.9 ± 4.4	39.3 ± 3.6
^{172}Lu	6,70d	i(m1+m2+g)	1.77 ± 0.14	5.89 ± 0.60	4.46 ± 0.38
^{172}Lu	6,70d	c	67.8 ± 5.0	55.8 ± 3.7	33.1 ± 3.4
^{171}Lu	8,24d	i(m+g)	14.5 ± 2.1	16.7 ± 4.2	8.69 ± 1.75
^{171}Lu	8,24d	c	58.6 ± 4.2	61.1 ± 4.2	36.2 ± 3.0
^{170}Lu	2,012d	i(m+g)	–	5.77 ± 3.70	9.60 ± 2.06
^{170}Lu	2,012d	c	38.9 ± 2.7	54.0 ± 4.4	32.9 ± 2.8
^{169}Lu	34,06h	c	25.0 ± 2.4	50.7 ± 3.5	27.5 ± 2.2
^{167}Lu	51,5m	c	–	53.9 ± 5.0	25.9 ± 3.7
^{169}Yb	32,026d	c	28.0 ± 1.9	61.4 ± 4.5	34.0 ± 2.7
^{167}Yb	17,5m	c	–	61.2 ± 5.8	–
^{166}Yb	56,7h	c	6.51 ± 0.49	53.9 ± 3.8	32.7 ± 3.3
^{162}Yb	18,87m	c	–	42.7 ± 4.6	25.1 ± 6.0
^{168}Tm	93,1d	i	–	–	0.900 ± 0.112
^{167}Tm	9,25d	c	–	61.4 ± 12.4	37.1 ± 5.1
^{166}Tm	7,70h	c	6.98 ± 0.59	59.0 ± 4.2	34.2 ± 3.4
^{166}Tm	7,70h	i	–	5.18 ± 0.76	1.53 ± 0.38
^{165}Tm	30,06h	c	3.89 ± 0.31	59.3 ± 4.4	33.9 ± 3.0
^{163}Tm	1,810h	c*	–	59.9 ± 4.5	36.8 ± 3.7
^{161}Tm	33m	c*	–	42.7 ± 7.4	–
^{161}Tm	33m	c	–	–	29.4 ± 5.7
^{161}Er	3,21h	c	–	48.0 ± 4.3	28.2 ± 3.0
^{160}Er	28,58h	c	–	54.6 ± 4.6	34.4 ± 3.4
^{159}Er	36m	c*	–	56.0 ± 3.9	35.7 ± 5.4
^{156}Er	19,5m	c	–	20.0 ± 2.9	–
^{160m}Ho	5,02h	c	–	56.2 ± 4.7	36.7 ± 3.6
^{159}Ho	33,05m	c	–	54.1 ± 3.9	–
^{156}Ho	56m	c	–	37.9 ± 2.9	23.2 ± 2.8
^{156}Ho	56m	i	–	17.5 ± 4.6	–
^{157}Dy	8,14h	c	–	43.6 ± 3.4	33.0 ± 3.0
^{155}Dy	9,9h	c*	–	35.1 ± 2.6	–
^{155}Dy	9,9h	c	–	–	29.4 ± 2.5
^{153}Dy	6,4h	c	–	21.6 ± 1.8	25.0 ± 2.3
^{152}Dy	2,38h	c	–	18.5 ± 1.2	20.8 ± 1.7

Table 20, continued.

Product	$T_{1/2}$	Type	Yields [mbarn] at		
			0.2 GeV	0.8 GeV	1.6 GeV
^{155}Tb	5,32d	c	–	35.3 ± 3.2	31.8 ± 2.7
^{153}Tb	2,34d	c*	–	27.1 ± 2.5	–
^{153}Tb	2,34d	c	–	–	26.2 ± 2.9
^{152}Tb	17,5h	c	–	20.1 ± 1.9	22.5 ± 2.3
^{151}Tb	17,609h	c	–	20.0 ± 1.5	22.5 ± 1.9
^{150}Tb	3,48h	c	–	10.2 ± 1.6	12.6 ± 2.0
^{149}Tb	4,118h	c	–	7.79 ± 0.55	9.12 ± 0.77
^{148}Tb	60m	c	–	8.61 ± 0.72	13.2 ± 1.1
^{147}Tb	1,7h	c	–	–	2.77 ± 0.28
^{153}Gd	240,4d	c	–	25.5 ± 2.2	27.6 ± 2.7
^{151}Gd	124d	c	–	–	21.6 ± 2.4
^{149}Gd	9,28d	c	–	22.1 ± 2.0	27.8 ± 2.3
^{147}Gd	38,06h	c	–	17.2 ± 1.1	25.7 ± 2.2
^{146}Gd	48,27d	c	–	15.0 ± 1.0	25.1 ± 2.0
^{145}Gd	23,0m	c	–	–	19.7 ± 2.3
^{149}Eu	93,1d	c	–	–	31.5 ± 2.6
^{148}Eu	54,5d	i	–	1.39 ± 0.29	–
^{147}Eu	24,1d	c	–	18.5 ± 1.5	28.6 ± 2.5
^{146}Eu	4,61d	c	–	–	35.7 ± 3.5
^{146}Eu	4,61d	i	–	–	10.1 ± 1.8
^{145}Eu	5,93d	c	–	10.9 ± 0.8	22.7 ± 1.9
^{144}Pm	363d	i	–	–	0.612 ± 0.177
^{143}Pm	265d	c	–	–	23.5 ± 2.4
^{139m}Nd	5,5h	i(m)	–	–	3.46 ± 0.49
^{137}Nd	38,5m	c	–	–	28.4 ± 3.4
^{136}Nd	50,65m	c	–	–	15.2 ± 1.5
^{139}Ce	137,640d	c	–	4.69 ± 0.31	22.1 ± 1.8
^{135}Ce	17,7h	c	–	–	18.1 ± 1.4
^{134}Ce	3,16d	c	–	–	15.0 ± 1.4
^{133}Ce	4,9h	i	–	–	3.27 ± 0.36
^{132}Ce	3,51h	c	–	–	14.5 ± 1.2
^{132}La	4,8h	c	–	–	14.2 ± 1.4
^{133}Ba	3848,9d	c	–	–	16.6 ± 1.8
^{131}Ba	11,50d	c	–	–	14.3 ± 1.1
^{128}Ba	2,43d	c	–	–	11.6 ± 1.1
^{129}Cs	32,06h	c	–	–	14.4 ± 1.4
^{127}Xe	36,4d	c	–	0.710 ± 0.117	10.8 ± 0.9
^{125}Xe	16,9h	c	–	–	9.15 ± 0.76
^{123}Xe	2,08h	c	–	–	9.73 ± 0.84
^{121m}Te	154d	i(m)	–	–	0.475 ± 0.052

Table 20, continued.

Product	$T_{1/2}$	Type	Yields [mbarn] at		
			0.2 GeV	0.8 GeV	1.6 GeV
^{121}Te	19,16d	c	–	–	6.65 ± 0.56
^{119m}Te	4,70d	c	–	–	1.03 ± 0.11
^{119}Te	16,05h	c	–	–	4.48 ± 0.52
^{113}Sn	115,09d	c	–	–	2.71 ± 0.25
^{106m}Ag	8,28d	i(m)	–	–	0.849 ± 0.104
^{105}Ag	41,29d	c	–	–	1.46 ± 0.15
^{96}Tc	4,28d	i(m+g)	–	0.261 ± 0.024	0.706 ± 0.066
^{93m}Mo	6,85h	i(m)	–	–	0.728 ± 0.067
^{90}Nb	14,60h	c	–	–	0.841 ± 0.146
^{89}Zr	78,41h	c	–	–	1.42 ± 0.12
^{88}Zr	83,4d	c	–	0.341 ± 0.133	1.03 ± 0.10
^{88}Y	106,65d	i(m+g)	–	0.441 ± 0.095	0.804 ± 0.286
^{88}Y	106,65d	c	–	0.782 ± 0.079	1.74 ± 0.38
^{87}Y	79,8h	c*	–	0.664 ± 0.063	–
^{85}Sr	64,84d	c	–	0.866 ± 0.128	1.63 ± 0.16
^{87}Rb	79,8h	c*	–	–	1.59 ± 0.14
^{84}Rb	32,77d	i(m+g)	–	0.496 ± 0.050	0.758 ± 0.087
^{83}Rb	86,2d	c	–	0.756 ± 0.078	1.51 ± 0.18
^{74}As	17,77d	i	–	0.453 ± 0.054	0.796 ± 0.090
^{69m}Zn	13,76h	i(m)	–	–	0.280 ± 0.034
^{59}Fe	44,472d	c	–	0.287 ± 0.034	0.502 ± 0.062
^{52}Fe	8,275h	c	–	–	0.278 ± 0.057
^{54}Mn	312,11d	i	–	–	0.859 ± 0.100
^{52}Mn	5,591d	c	–	–	0.184 ± 0.023
^{48}V	15,9735d	c	–	–	0.209 ± 0.042
^{48}Sc	43,67h	i	–	–	0.511 ± 0.048
^{28}Mg	20,915h	c	–	–	0.444 ± 0.042
^{24}Na	14,9590h	c	–	–	1.90 ± 0.16
^{7}Be	53,29d	i	–	–	4.27 ± 0.46

3.5 Experimental yields for ^{186}W irradiated with 0.2, 0.8, 1.6 GeV protons.

Table 21 presents the parameters of ^{186}W irradiations. Table 22 presents the yields of residual nuclide products measured.

Table 21: Parameters of ^{186}W irradiation.

E_p (GeV)	Sample weight (mg)	Monitor weight (mg)	Irradiation duration (min)	Proton Flux p/cm^2	Number of measured γ -spectra of sample/monitor	EXPDATA index
0.2	135.0	120.6	60	2.2×10^{13}	44 / 7	w186200
0.8	135.6	110.2	30	1.4×10^{13}	37 / 9	w186800
1.6	138.0	108.6	40	5.4×10^{13}	35 / 9	w18616g

Table 22: Experimental yields from ^{186}W irradiated with 0.2, 0.8, 1.6 GeV protons.

Product	$T_{1/2}$	Type	Yields [mbarn]		
			0.2 GeV	0.8 GeV	1.6 GeV
^{184}Re	38,0d	i(m+g)	14.4 ± 1.0	–	3.29 ± 0.30
^{184}Re	38,0d	i	–	–	2.93 ± 0.26
^{183}Re	70,0d	i(m+g)	26.5 ± 2.1	10.5 ± 1.7	3.70 ± 0.64
^{182}Re	64,0h	i	12.0 ± 1.0	–	–
^{181}Re	19,9h	i	28.8 ± 3.8	7.48 ± 1.18	4.40 ± 0.72
^{179}Re	19,5m	i	20.5 ± 4.0	–	–
^{178}W	21,6d	c	76.4 ± 9.2	–	–
^{177}W	135m	c	66.8 ± 7.8	15.9 ± 1.8	11.8 ± 1.4
^{176}W	2,5h	c	62.8 ± 9.7	–	–
^{174}W	31m	c	50.2 ± 6.0	–	–
^{184}Ta	8,7h	c	–	15.1 ± 1.0	15.5 ± 1.3
^{183}Ta	5,1d	c	16.1 ± 1.3	20.5 ± 1.6	20.2 ± 1.7
^{182}Ta	114,43d	c	17.5 ± 1.2	26.9 ± 2.6	17.1 ± 1.4
^{178m}Ta	2,36h	i(m1+m2)	16.5 ± 1.2	13.1 ± 2.9	10.5 ± 1.3
^{176}Ta	8,09h	i(m+g)	39.0 ± 6.4	–	–
^{176}Ta	8,09h	c	106. ± 9.	40.0 ± 4.3	31.2 ± 2.9
^{175}Ta	10,5h	c	91.4 ± 7.4	38.9 ± 3.8	23.6 ± 3.4
^{174}Ta	1,14h	c	74.4 ± 8.3	43.1 ± 4.8	28.6 ± 3.6
^{174}Ta	1,14h	i	24.2 ± 4.1	41.2 ± 5.1	28.0 ± 4.8
^{173}Ta	3,14h	c*	60.2 ± 6.5	–	–
^{173}Ta	3,14h	c	–	40.2 ± 3.8	21.4 ± 2.2
^{172}Ta	36,8m	c*	28.4 ± 3.4	–	–
^{171}Ta	23,3m	c*	3.63 ± 0.61	–	–
^{181}Hf	42,39d	c	–	3.17 ± 0.41	3.01 ± 0.24

Table 22, continued.

Product	$T_{1/2}$	Type	Yields [mbarn]		
			0.2 GeV	0.8 GeV	1.6 GeV
^{180m}Hf	5,5h	i(m)	–	–	1.51 ± 0.14
^{179m}Hf	25,05d	i(m2)	–	–	0.709 ± 0.069
^{175}Hf	70d	c	103. ± 8.	53.0 ± 4.0	36.0 ± 3.1
^{173}Hf	23,6h	c	71.9 ± 5.3	51.5 ± 3.8	34.3 ± 2.9
^{173}Hf	23,6h	i	–	11.7 ± 2.4	14.6 ± 2.7
^{172}Hf	1,87y	c	44.3 ± 3.3	49.9 ± 8.4	28.1 ± 2.4
^{171}Hf	12,1h	c	26.3 ± 2.9	28.6 ± 3.2	25.3 ± 2.6
^{170}Hf	16,01h	c	14.8 ± 2.0	40.7 ± 5.5	18.7 ± 2.4
^{173}Lu	1,37y	c	66.9 ± 5.5	70.2 ± 8.5	38.1 ± 3.5
^{172}Lu	6,70d	i(m1+m2+g)	2.13 ± 0.16	7.80 ± 0.60	5.97 ± 0.49
^{172}Lu	6,70d	c	46.2 ± 3.4	53.6 ± 8.0	34.5 ± 2.9
^{171}Lu	8,24d	i(m+g)	9.73 ± 2.23	29.2 ± 3.1	10.5 ± 1.9
^{171}Lu	8,24d	c	36.0 ± 2.7	57.8 ± 4.1	35.8 ± 3.0
^{170}Lu	2,012d	i(m+g)	–	17.0 ± 5.0	14.1 ± 1.9
^{170}Lu	2,012d	c	22.5 ± 1.8	50.9 ± 4.4	32.2 ± 2.7
^{169}Lu	34,06h	c	13.5 ± 1.4	44.2 ± 3.6	26.9 ± 2.2
^{167}Lu	51,5m	c	–	42.2 ± 3.8	21.0 ± 3.2
^{169}Yb	32,026d	c	15.3 ± 1.1	58.5 ± 4.0	34.0 ± 2.7
^{167}Yb	17,5m	c	–	50.8 ± 4.7	–
^{166}Yb	56,7h	c	2.10 ± 0.17	49.0 ± 3.4	31.9 ± 3.2
^{162}Yb	18,87m	c	–	31.7 ± 4.8	22.3 ± 2.8
^{168}Tm	93,1d	i	–	–	1.42 ± 0.18
^{167}Tm	9,25d	c	–	58.2 ± 11.8	37.1 ± 5.1
^{166}Tm	7,70h	c	2.19 ± 0.37	55.6 ± 3.8	34.8 ± 3.5
^{166}Tm	7,70h	i	–	6.67 ± 0.60	2.94 ± 0.46
^{165}Tm	30,06h	c	1.58 ± 0.16	53.5 ± 4.0	34.6 ± 3.0
^{163}Tm	1,810h	c*	–	49.9 ± 4.2	31.6 ± 3.0
^{161}Tm	33m	c*	–	38.7 ± 6.8	–
^{161}Tm	33m	c	–	–	24.4 ± 4.6
^{161}Er	3,21h	c	–	44.8 ± 4.1	31.1 ± 3.2
^{160}Er	28,58h	c	–	44.3 ± 3.7	34.7 ± 3.4
^{159}Er	36m	c*	–	45.8 ± 3.2	34.4 ± 5.1
^{160m}Ho	5,02h	c	–	47.1 ± 4.3	35.2 ± 3.5
^{159}Ho	33,05m	c	–	45.9 ± 3.5	–
^{156}Ho	56m	c	–	29.2 ± 2.5	35.0 ± 3.4
^{157}Dy	8,14h	c	–	36.3 ± 2.9	34.5 ± 3.1
^{155}Dy	9,9h	c*	–	29.4 ± 2.5	–
^{155}Dy	9,9h	c	–	–	32.1 ± 2.8
^{153}Dy	6,4h	c	–	14.9 ± 1.4	24.8 ± 2.6
^{152}Dy	2,38h	c	–	13.6 ± 0.9	20.0 ± 1.6

Table 22, continued.

Product	$T_{1/2}$	Type	Yields [mbarn]		
			0.2 GeV	0.8 GeV	1.6 GeV
^{155}Tb	5,32d	c	–	29.8 ± 2.7	31.7 ± 2.6
^{153}Tb	2,34d	c*	–	23.2 ± 2.2	–
^{153}Tb	2,34d	c	–	–	28.5 ± 3.4
^{152}Tb	17,5h	c	–	14.8 ± 1.3	23.9 ± 2.4
^{151}Tb	17,609h	c	–	13.9 ± 1.1	21.0 ± 1.9
^{150}Tb	3,48h	c	–	6.19 ± 0.96	11.3 ± 1.8
^{149}Tb	4,118h	c	–	4.69 ± 0.38	7.77 ± 0.65
^{148}Tb	60m	c	–	5.88 ± 0.49	10.9 ± 1.2
^{147}Tb	1,7h	c	–	–	2.18 ± 0.29
^{153}Gd	240,4d	c	–	21.8 ± 2.6	28.1 ± 2.6
^{151}Gd	124d	c	–	–	24.5 ± 2.3
^{149}Gd	9,28d	c	–	15.6 ± 1.1	27.1 ± 2.2
^{147}Gd	38,06h	c	–	12.2 ± 0.9	24.0 ± 2.2
^{146}Gd	48,27d	c	–	10.7 ± 0.8	23.3 ± 1.9
^{145}Gd	23,0m	c	–	–	13.1 ± 1.9
^{149}Eu	93,1d	c	–	–	32.9 ± 2.7
^{147}Eu	24,1d	c	–	13.1 ± 1.3	29.0 ± 2.6
^{146}Eu	4,61d	c	–	–	34.9 ± 3.0
^{146}Eu	4,61d	i	–	–	10.7 ± 1.1
^{145}Eu	5,93d	c	–	8.64 ± 0.83	21.5 ± 1.8
^{144}Pm	363d	i	–	–	0.899 ± 0.090
^{143}Pm	265d	c	–	–	23.0 ± 2.3
^{139m}Nd	5,5h	i(m)	–	–	3.66 ± 0.49
^{137}Nd	38,5m	c	–	–	25.8 ± 2.6
^{136}Nd	50,65m	c	–	–	12.7 ± 1.3
^{139}Ce	137,640d	c	–	3.55 ± 0.49	21.4 ± 1.7
^{135}Ce	17,7h	c	–	–	16.8 ± 1.4
^{134}Ce	3,16d	c	–	–	14.3 ± 1.4
^{133}Ce	4,9h	i	–	–	3.59 ± 0.33
^{132}Ce	3,51h	c	–	–	12.5 ± 1.0
^{132}La	4,8h	c	–	–	12.3 ± 1.2
^{133}Ba	3848,9d	c	–	–	13.5 ± 1.5
^{131}Ba	11,50d	c	–	–	13.4 ± 1.1
^{128}Ba	2,43d	c	–	–	9.99 ± 0.95
^{129}Cs	32,06h	c	–	–	12.9 ± 1.3
^{127}Xe	36,4d	c	–	–	9.83 ± 0.81
^{125}Xe	16,9h	c	–	–	8.25 ± 0.67
^{123}Xe	2,08h	c	–	–	8.47 ± 0.71
^{121m}Te	154d	i(m)	–	–	0.486 ± 0.066
^{121}Te	19,16d	c	–	–	5.93 ± 0.49

Table 22, continued.

Product	$T_{1/2}$	Type	Yields [mbarn]		
			0.2 GeV	0.8 GeV	1.6 GeV
^{119m}Te	4,70d	c	–	–	1.05 ± 0.14
^{119}Te	16,05h	c	–	–	3.84 ± 0.35
^{113}Sn	115,09d	c	–	–	2.38 ± 0.21
^{106m}Ag	8,28d	i(m)	–	–	0.693 ± 0.070
^{105}Ag	41,29d	c	–	–	1.12 ± 0.11
^{96}Tc	4,28d	i(m+g)	–	–	0.677 ± 0.060
^{93m}Mo	6,85h	i(m)	–	–	0.577 ± 0.087
^{90}Nb	14,60h	c	–	–	0.689 ± 0.124
^{89}Zr	78,41h	c	–	–	1.22 ± 0.10
^{88}Zr	83,4d	c	–	–	0.887 ± 0.079
^{88}Y	106,65d	i(m+g)	–	–	0.651 ± 0.075
^{88}Y	106,65d	c	–	–	1.53 ± 0.15
^{85}Sr	64,84d	c	–	–	1.50 ± 0.14
^{87}Rb	79,8h	c*	–	–	1.53 ± 0.13
^{84}Rb	32,77d	i(m+g)	–	–	0.679 ± 0.068
^{83}Rb	86,2d	c	–	–	1.60 ± 0.28
^{75}Se	119,779d	c	–	–	1.38 ± 0.25
^{74}As	17,77d	i	–	–	0.732 ± 0.080
^{69m}Zn	13,76h	i(m)	–	–	0.299 ± 0.041
^{59}Fe	44,472d	c	–	–	0.657 ± 0.064
^{52}Fe	8,275h	c	–	–	0.316 ± 0.060
^{54}Mn	312,11d	i	–	–	0.792 ± 0.110
^{52}Mn	5,591d	c	–	–	0.172 ± 0.035
^{48}V	15,9735d	c	–	–	0.183 ± 0.023
^{48}Sc	43,67h	i	–	–	0.469 ± 0.061
^{28}Mg	20,915h	c	–	–	0.406 ± 0.059
^{24}Na	14,9590h	c	–	–	1.79 ± 0.15
^{22}Na	2,6019y	c	–	–	1.36 ± 0.18
^{7}Be	53,29d	i	–	–	4.16 ± 0.59

3.6 Experimental yields for ^{nat}W irradiated with 2.6 GeV protons.

Table 23 presents the parameters of ^{nat}W irradiation. Table 24 presents the yields of residual nuclide products measured.

Table 23: Parameters of ^{nat}W irradiation.

E_p (GeV)	Sample weight (mg)	Monitor weight (mg)	Irradiation duration (min)	Proton Flux p/cm^2	Number of measured γ -spectra of sample/monitor	EXPDATA index
2.6	33.0	120.4	30	5.4×10^{13}	48 / 8	wnat26g

Table 24: Experimental yields from ^{nat}W irradiated with 2.6 GeV protons.

Product	$T_{1/2}$	Type	Yields [mbarn]
^{181}Re	19,9h	i	3.51 ± 0.58
^{177}W	135m	c	13.0 ± 1.6
^{176}W	2,5h	c	7.86 ± 2.51
^{184}Ta	8,7h	c	4.39 ± 0.44
^{183}Ta	5,1d	c	10.4 ± 1.0
^{182}Ta	114,43d	c	12.8 ± 1.3
^{178m}Ta	2,36h	i(m1+m2)	7.98 ± 1.34
^{176}Ta	8,09h	c	29.3 ± 3.4
^{175}Ta	10,5h	c	25.7 ± 2.8
^{174}Ta	1,14h	c	25.5 ± 2.8
^{173}Ta	3,14h	c	23.9 ± 3.2
^{181}Hf	42,39d	c	1.24 ± 0.12
^{180m}Hf	5,5h	i(m)	0.688 ± 0.085
^{175}Hf	70d	c	33.0 ± 3.0
^{173}Hf	23,6h	c	29.5 ± 2.5
^{173}Hf	23,6h	i	5.52 ± 2.43
^{172}Hf	1,87y	c	21.7 ± 2.1
^{171}Hf	12,1h	c	19.4 ± 2.4
^{170}Hf	16,01h	c	19.4 ± 4.0
^{173}Lu	1,37y	c	33.4 ± 3.3
^{172}Lu	6,70d	i(m1+m2+g)	3.68 ± 0.50
^{172}Lu	6,70d	c	25.5 ± 2.4
^{171}Lu	8,24d	i(m+g)	10.7 ± 2.0
^{171}Lu	8,24d	c	29.7 ± 2.5

Table 24, continued.

Product	$T_{1/2}$	Type	Yields [mbarn]
^{170}Lu	2,012d	c	24.5 ± 2.2
^{169}Lu	34,06h	c	21.9 ± 1.8
^{167}Lu	51,5m	c	23.1 ± 2.5
^{169}Yb	32,026d	c	27.4 ± 2.5
^{167}Yb	17,5m	c	24.6 ± 2.9
^{166}Yb	56,7h	c	24.3 ± 2.1
^{162}Yb	18,87m	c	18.6 ± 3.3
^{167}Tm	9,25d	c	28.9 ± 6.0
^{166}Tm	7,70h	c	26.9 ± 2.4
^{166}Tm	7,70h	i	2.34 ± 0.45
^{165}Tm	30,06h	c	26.8 ± 2.5
^{163}Tm	1,810h	c*	26.0 ± 3.3
^{161}Tm	33m	c	20.8 ± 2.5
^{161}Er	3,21h	c	24.0 ± 2.5
^{160}Er	28,58h	c	23.6 ± 2.2
^{159}Er	36m	c*	25.0 ± 3.8
^{157}Er	18,65m	c	20.2 ± 3.5
^{156}Er	19,5m	c	15.7 ± 2.4
^{160m}Ho	5,02h	c	24.6 ± 2.3
^{157}Ho	12,6m	c	21.8 ± 4.0
^{156}Ho	56m	c	19.4 ± 1.8
^{157}Dy	8,14h	c	23.9 ± 2.3
^{155}Dy	9,9h	c	21.9 ± 1.9
^{153}Dy	6,4h	c	13.9 ± 1.9
^{152}Dy	2,38h	c	15.4 ± 1.3
^{155}Tb	5,32d	c	22.4 ± 1.9
^{153}Tb	2,34d	c	18.7 ± 1.8
^{152}Tb	17,5h	c	16.1 ± 1.4
^{151}Tb	17,609h	c	16.5 ± 1.4
^{150}Tb	3,48h	c	9.23 ± 1.23
^{149}Tb	4,118h	c	6.77 ± 0.63
^{147}Tb	1,7h	c	2.13 ± 0.33
^{153}Gd	240,4d	c	26.7 ± 2.6
^{151}Gd	124d	c	18.8 ± 2.2
^{149}Gd	9,28d	c	20.2 ± 1.7
^{147}Gd	38,06h	c	18.4 ± 1.6
^{146}Gd	48,27d	c	18.6 ± 1.6
^{145}Gd	23,0m	c	12.7 ± 1.5
^{149}Eu	93,1d	c	26.4 ± 3.4
^{147}Eu	24,1d	c	22.2 ± 2.0

Table 24, continued.

Product	$T_{1/2}$	Type	Yields [mbarn]
^{146}Eu	4,61d	c	22.2 ± 1.9
^{146}Eu	4,61d	i	3.60 ± 0.32
^{145}Eu	5,93d	c	17.6 ± 1.6
^{143}Pm	265d	c	20.1 ± 2.2
^{139m}Nd	5,5h	i(m)	2.84 ± 0.49
^{139}Ce	137,640d	c	19.6 ± 1.7
^{135}Ce	17,7h	c	17.6 ± 1.5
^{134}Ce	3,16d	c	17.7 ± 1.8
^{133}Ce	4,9h	i	3.77 ± 0.39
^{132}Ce	3,51h	c	16.1 ± 2.7
^{132}La	4,8h	c	14.3 ± 1.7
^{133}Ba	3848,9d	c	18.2 ± 4.1
^{131}Ba	11,50d	c	16.0 ± 1.3
^{128}Ba	2,43d	c	15.4 ± 1.5
^{126}Ba	100m	c	7.86 ± 1.12
^{129}Cs	32,06h	c	18.6 ± 1.7
^{127}Xe	36,4d	c	15.2 ± 1.3
^{125}Xe	16,9h	c	14.1 ± 1.2
^{123}Xe	2,08h	c	15.5 ± 1.3
^{122}Xe	20,1h	c	11.6 ± 1.0
^{121m}Te	154d	i(m)	0.449 ± 0.072
^{121}Te	19,16d	c	10.8 ± 1.0
^{119m}Te	4,70d	c	1.94 ± 0.17
^{119}Te	16,05h	c	9.06 ± 0.76
^{117}Te	62m	c	8.71 ± 0.79
^{118m}Sb	5,00h	i(m)	1.07 ± 0.22
^{115}Sb	32,1m	c*	9.74 ± 0.89
^{113}Sn	115,09d	c	7.35 ± 0.64
^{111}In	2,8047d	c	7.33 ± 0.63
^{110}In	4,9h	i	3.25 ± 0.30
^{109}In	4,2h	c	5.06 ± 0.44
^{106m}Ag	8,28d	i(m)	1.68 ± 0.16
^{105}Ag	41,29d	c	5.27 ± 0.69
^{100}Pd	3,63d	c	1.18 ± 0.26
^{100}Rh	20,8h	i(m+g)	2.53 ± 0.30
^{100}Rh	20,8h	c	3.74 ± 0.48
^{99m}Rh	4,7h	c	2.38 ± 0.29
^{97}Ru	2,791d	c	3.08 ± 0.30
^{96}Tc	4,28d	i(m+g)	1.71 ± 0.20
^{93m}Mo	6,85h	i(m)	1.59 ± 0.14

Table 24, continued.

Product	$T_{1/2}$	Type	Yields [mbarn]
^{90}Nb	14,60h	c	2.55 ± 0.23
^{89}Zr	78,41h	c	3.42 ± 0.29
^{88}Zr	83,4d	c	2.53 ± 0.27
^{88}Y	106,65d	i(m+g)	1.54 ± 0.22
^{88}Y	106,65d	c	3.45 ± 0.34
^{87}Y	79,8h	c*	4.08 ± 0.35
^{85}Sr	64,84d	c	3.76 ± 0.39
^{83}Sr	32,41h	c	1.94 ± 0.92
^{84}Rb	32,77d	i(m+g)	1.29 ± 0.14
^{83}Rb	86,2d	c	3.30 ± 0.58
^{82m}Rb	6,472h	i(m)	1.87 ± 0.17
^{77}Kr	74,4m	c	1.69 ± 0.18
^{75}Se	119,779d	c	2.35 ± 0.22
^{73}Se	7,15h	c	1.06 ± 0.12
^{74}As	17,77d	i	1.37 ± 0.16
^{69m}Zn	13,76h	i(m)	0.416 ± 0.039
^{59}Fe	44,472d	c	0.845 ± 0.103
^{54}Mn	312,11d	i	2.48 ± 0.41
^{51}Cr	27,7025d	c	4.48 ± 1.34
^{48}V	15,9735d	c	0.551 ± 0.060
^{48}Sc	43,67h	i	0.660 ± 0.088
^{43}K	22,3h	c	0.673 ± 0.081
^{28}Mg	20,915h	c	0.899 ± 0.087
^{24}Na	14,9590h	c	4.04 ± 0.34
^{7}Be	53,29d	i	8.61 ± 1.01

3.7 Experimental yields for ^{232}Th irradiated with 0.1, 0.2, 0.8, 1.2, 1.6 GeV protons.

Table 25 presents the parameters of ^{232}Th irradiations. Table 26 presents the yields of residual nuclide products measured.

Table 25: Parameters of ^{232}Th irradiation.

E_p (GeV)	Sample weight (mg)	Monitor weight (mg)	Irradiation duration (min)	Proton Flux p/cm^2	Number of measured γ -spectra of sample/monitor	EXPDATA index
0.1	87.5	169.4	40	5.4×10^{12}	34 / 10	th100
0.2	115.9	48.4	45	2.1×10^{13}	36 / 11	th200
0.8	89.6	160.3	30	3.7×10^{13}	44 / 17	th800
1.2	114.1	119.0	30	5.7×10^{13}	48 / 10	th12g
1.6	111.6	119.0	20	3.6×10^{13}	42 / 11	th16g

Table 26: Experimental yields from ^{232}Th irradiated with 0.1, 0.2, 0.8, 1.2, 1.6 GeV protons.

Product	$T_{1/2}$	Type	Yields [mbarn] at				
			0.1 GeV	0.2 GeV	0.8 GeV	1.2 GeV	1.6 GeV
^{233}Pa	26,967d	i	–	1.67 ± 0.22	–	2.81 ± 0.33	3.12 ± 0.30
^{227}Th	18,72d	c	51.0 ± 6.4	28.1 ± 3.5	–	13.5 ± 1.6	12.3 ± 1.6
^{229}Ac	62,7m	c	–	0.828 ± 0.126	1.30 ± 0.21	1.23 ± 0.18	1.09 ± 0.17
^{228}Ac	6,15h	i	19.8 ± 1.7	21.2 ± 2.1	20.1 ± 2.1	19.3 ± 1.5	17.8 ± 1.6
^{226}Ac	29,37h	i	8.29 ± 0.87	17.0 ± 1.8	16.6 ± 1.6	17.1 ± 1.7	15.1 ± 1.6
^{225}Ac	10,0d	c	–	19.4 ± 1.6	20.3 ± 5.1	19.5 ± 1.5	18.5 ± 1.5
^{224}Ac	2,78h	i	5.72 ± 0.72	17.0 ± 1.4	12.0 ± 0.9	12.5 ± 1.0	11.8 ± 1.1
^{225}Ra	14,9d	c	–	–	–	4.18 ± 0.37	3.87 ± 0.41
^{223}Ra	11,435d	c	–	36.0 ± 3.2	–	21.8 ± 1.7	20.6 ± 2.0
^{211}Rn	14,6h	c	–	3.21 ± 0.26	9.89 ± 0.75	9.76 ± 0.76	7.57 ± 0.63
^{210}At	8,1h	c	–	4.82 ± 0.39	11.0 ± 0.8	10.6 ± 0.8	8.92 ± 0.74
^{209}At	5,41h	c*	–	4.35 ± 0.37	17.8 ± 1.2	19.3 ± 1.4	16.5 ± 1.3
^{208}At	1,63h	c*	–	1.40 ± 0.16	10.5 ± 0.9	9.95 ± 0.88	7.94 ± 0.66
^{207}At	1,80h	c	–	–	16.5 ± 1.4	14.2 ± 1.4	11.6 ± 1.2
^{206}At	30,6m	c*	–	–	10.3 ± 0.8	9.08 ± 0.83	8.31 ± 0.82
^{206}Po	8,8d	c	–	2.81 ± 0.27	20.0 ± 1.5	18.6 ± 1.4	15.5 ± 1.2
^{205}Po	1,66h	c*	–	–	15.5 ± 1.7	9.22 ± 1.38	8.74 ± 2.15
^{204}Po	3,53h	c	–	–	13.5 ± 1.1	14.6 ± 1.2	11.9 ± 1.3
^{203}Po	36,7m	c*	–	–	10.7 ± 1.2	9.60 ± 0.96	8.48 ± 0.94
^{202}Po	44,7m	c	–	–	8.81 ± 0.87	9.94 ± 1.63	8.28 ± 1.22
^{206}Bi	6,243d	c	–	2.78 ± 0.23	20.1 ± 1.5	18.9 ± 1.4	15.7 ± 1.3
^{205}Bi	15,31d	c	–	–	18.2 ± 1.7	14.2 ± 1.1	11.8 ± 1.0
^{204}Bi	11,22h	c	–	0.498 ± 0.063	13.2 ± 1.0	15.2 ± 1.2	12.2 ± 1.1
^{203}Bi	11,76h	c	–	–	10.3 ± 0.8	11.1 ± 0.8	8.64 ± 0.72

Table 26, continued.

Product	$T_{1/2}$	Type	Yields [mbarn] at				
			0.1 GeV	0.2 GeV	0.8 GeV	1.2 GeV	1.6 GeV
^{202}Bi	1,72h	c	–	–	11.2 ± 0.8	12.2 ± 0.9	10.5 ± 0.9
^{200}Bi	36,4m	c	–	–	6.29 ± 2.50	8.87 ± 2.41	4.87 ± 1.01
^{198}Bi	11,6m	c*	–	–	–	8.66 ± 1.49	5.61 ± 1.05
^{203}Pb	51,873h	i(m1+m2+g)	–	–	–	1.14 ± 0.46	–
^{203}Pb	51,873h	c	–	–	10.3 ± 0.7	11.7 ± 0.9	9.88 ± 0.81
^{201}Pb	9,33h	i(m+g)	–	–	7.22 ± 2.56	3.45 ± 1.05	5.79 ± 1.07
^{201}Pb	9,33h	c	–	–	9.62 ± 0.99	11.2 ± 1.1	10.0 ± 1.0
^{200}Pb	21,5h	c	–	–	7.70 ± 0.56	9.35 ± 0.72	7.97 ± 0.69
^{199}Pb	90m	c*	–	–	15.7 ± 2.8	22.7 ± 4.0	19.1 ± 3.5
^{200}Tl	26,1h	i(m+g)	–	–	0.980 ± 0.204	1.36 ± 0.16	1.08 ± 0.16
^{200}Tl	26,1h	c	–	–	8.44 ± 0.60	10.6 ± 0.8	8.89 ± 0.71
^{192}Hg	4,85h	c	–	–	6.11 ± 0.55	11.6 ± 1.0	11.0 ± 1.4
^{190}Hg	20,0m	c*	–	–	–	9.61 ± 1.26	9.62 ± 1.20
^{190}Hg	20,0m	c	–	–	3.64 ± 1.27	–	–
^{190}Au	42,8m	c*	–	–	5.48 ± 0.79	–	–
^{190}Au	42,8m	c	–	–	–	11.1 ± 1.3	11.3 ± 1.3
^{191}Pt	2,802d	c	–	–	–	9.98 ± 1.13	10.1 ± 1.5
^{188}Pt	10,2d	c	–	–	–	11.0 ± 1.0	11.9 ± 1.1
^{186}Pt	2,08h	c	–	–	2.88 ± 0.83	10.8 ± 2.5	12.2 ± 2.8
^{188}Ir	41,5h	c	–	–	–	8.65 ± 1.25	9.14 ± 1.31
^{186}Ir	16,64h	i	–	–	1.80 ± 0.21	4.84 ± 0.40	5.09 ± 0.46
^{185}Ir	14,4h	c	–	–	–	8.14 ± 1.36	9.33 ± 1.59
^{184}Ir	3,09h	c*	–	–	2.65 ± 0.33	9.71 ± 0.95	12.9 ± 1.3
^{185}Os	93,6d	c	–	–	–	11.2 ± 0.9	13.1 ± 1.2
^{183m}Os	9,9h	c	–	–	–	5.89 ± 0.47	7.17 ± 0.62
^{183}Os	13,0h	c	–	–	1.39 ± 0.18	–	–
^{182}Os	22,10h	c	–	–	2.76 ± 0.29	11.1 ± 1.0	14.3 ± 1.2
^{183}Re	70,0d	c	–	–	–	9.69 ± 0.82	12.7 ± 1.1
^{182m}Re	12,7h	c	–	–	–	10.7 ± 0.9	14.0 ± 1.2
^{181}Re	19,9h	c	–	–	2.13 ± 0.35	9.96 ± 1.40	13.1 ± 1.9
^{180}Re	21,5m	c	–	–	–	10.8 ± 1.0	12.8 ± 1.3
^{177}W	135m	c	–	–	–	5.85 ± 0.72	9.66 ± 1.20
^{176}W	2,5h	c	–	–	–	7.66 ± 1.52	8.56 ± 1.72
^{182}Ta	114,43d	c	–	–	–	–	16.7 ± 3.7
^{176}Ta	8,09h	c	–	–	–	6.31 ± 0.83	12.0 ± 1.4
^{175}Ta	10,5h	c	–	–	–	5.86 ± 0.77	12.4 ± 1.6
^{174}Ta	1,14h	c	–	–	–	6.36 ± 0.76	10.4 ± 1.3
^{175}Hf	70d	c	–	–	–	6.43 ± 0.54	11.2 ± 1.0
^{173}Hf	23,6h	c	–	–	–	5.55 ± 0.57	10.8 ± 1.1
^{170}Hf	16,01h	c	–	–	–	–	8.02 ± 1.30

Table 26, continued.

Product	$T_{1/2}$	Type	Yields [mbarn] at				
			0.1 GeV	0.2 GeV	0.8 GeV	1.2 GeV	1.6 GeV
^{171}Lu	8,24d	c	–	–	–	4.76 ± 0.38	10.7 ± 0.9
^{170}Lu	2,012d	c	–	–	–	4.58 ± 0.50	7.89 ± 0.79
^{169}Lu	34,06h	c	–	–	–	3.49 ± 0.30	7.43 ± 0.64
^{169}Yb	32,026d	c	–	–	–	5.75 ± 0.47	9.66 ± 0.90
^{166}Yb	56,7h	c	–	–	–	3.03 ± 0.30	7.98 ± 0.82
^{167}Tm	9,25d	c	–	–	–	3.43 ± 0.71	8.40 ± 1.75
^{166}Tm	7,70h	c	–	–	–	3.12 ± 0.36	–
^{160}Er	28,58h	c	–	–	–	2.20 ± 0.24	6.11 ± 0.66
^{160m}Ho	5,02h	i(m)	–	–	–	2.59 ± 0.49	–
^{160m}Ho	5,02h	c	–	–	–	4.80 ± 0.76	6.50 ± 0.96
^{157}Dy	8,14h	c	–	–	–	1.63 ± 0.17	4.27 ± 0.41
^{155}Dy	9,9h	c*	–	–	–	1.49 ± 0.13	3.70 ± 0.35
^{152}Dy	2,38h	c	–	–	–	0.702 ± 0.156	2.24 ± 0.21
^{152}Tb	17,5h	c*	–	–	0.864 ± 0.115	1.34 ± 0.14	2.81 ± 0.29
^{151}Tb	17,609h	c	–	–	–	1.12 ± 0.13	1.95 ± 0.21
^{150}Tb	3,48h	c	–	–	–	–	1.00 ± 0.20
^{149}Gd	9,28d	c	–	–	–	1.26 ± 0.13	2.94 ± 0.46
^{147}Gd	38,06h	c	–	–	–	1.10 ± 0.16	2.47 ± 0.23
^{146}Gd	48,27d	c	–	–	–	0.677 ± 0.068	1.98 ± 0.18
^{147}Eu	24,1d	c	–	–	–	1.11 ± 0.17	2.84 ± 0.41
^{146}Eu	4,61d	c	–	–	–	1.27 ± 0.11	2.86 ± 0.25
^{146}Eu	4,61d	i	–	–	–	0.589 ± 0.054	0.879 ± 0.092
^{145}Eu	5,93d	c	–	–	–	–	3.87 ± 0.89
^{147}Nd	10,98d	c	–	2.99 ± 0.61	–	–	–
^{146}Pr	24,15m	c	–	2.59 ± 0.57	–	–	–
^{138m}Pr	2,12h	i(m)	–	–	1.33 ± 0.31	2.13 ± 0.20	2.65 ± 0.28
^{143}Ce	33,039h	c	14.8 ± 1.1	7.78 ± 0.63	4.15 ± 0.30	4.05 ± 0.31	3.75 ± 0.31
^{141}Ce	32,501d	c	24.2 ± 2.6	12.3 ± 1.0	–	6.41 ± 0.49	5.66 ± 0.53
^{139}Ce	137,640d	c	–	–	–	4.54 ± 0.55	6.40 ± 0.53
^{135}Ce	17,7h	c	–	–	1.94 ± 0.20	3.11 ± 0.27	3.52 ± 0.32
^{132}Ce	3,51h	c	–	–	0.563 ± 0.215	1.28 ± 0.20	1.89 ± 0.26
^{142}La	91,1m	c	16.5 ± 1.3	8.15 ± 0.69	–	–	–
^{140}La	1,6781d	c	20.4 ± 1.6	11.2 ± 0.9	6.69 ± 0.85	6.82 ± 0.52	5.98 ± 0.52
^{140}La	1,6781d	i	4.93 ± 0.38	2.64 ± 0.27	1.47 ± 0.15	1.24 ± 0.10	0.986 ± 0.092
^{132}La	4,8h	i(m+g)	–	–	1.27 ± 0.37	1.21 ± 0.28	0.770 ± 0.251
^{132}La	4,8h	c	–	–	1.84 ± 0.25	2.49 ± 0.30	2.66 ± 0.32
^{141}Ba	18,27m	c	15.6 ± 2.0	7.65 ± 1.03	–	–	–
^{140}Ba	12,752d	c	15.5 ± 1.3	8.91 ± 0.85	5.24 ± 0.91	5.57 ± 0.42	5.00 ± 0.43
^{139}Ba	83,06m	c	20.2 ± 3.8	11.6 ± 2.2	–	–	–
^{135m}Ba	28,7h	i(m)	2.72 ± 0.32	3.20 ± 0.30	–	–	–

Table 26, continued.

Product	$T_{1/2}$	Type	Yields [mbarn] at				
			0.1 GeV	0.2 GeV	0.8 GeV	1.2 GeV	1.6 GeV
^{133m}Ba	38,9h	i(m)	–	1.69 ± 0.17	–	–	–
^{131}Ba	11,50d	c	–	–	–	4.97 ± 0.42	5.15 ± 0.49
^{128}Ba	2,43d	c	–	–	–	2.40 ± 0.22	3.15 ± 0.30
^{138}Cs	33,41m	c	12.8 ± 1.8	6.61 ± 1.14	–	–	–
^{136}Cs	13,16d	i(m+g)	9.97 ± 0.81	5.08 ± 0.40	–	2.18 ± 0.16	1.87 ± 0.17
^{134m}Cs	2,903h	i(m)	6.79 ± 0.73	4.85 ± 0.53	–	–	–
^{132}Cs	6,479d	i	–	2.85 ± 0.69	–	3.50 ± 0.29	4.14 ± 0.45
^{138}Xe	14,08m	c	–	4.54 ± 0.76	–	–	–
^{135m}Xe	15,29m	i(m)	11.6 ± 1.2	5.38 ± 0.53	–	–	–
^{135}Xe	9,14h	i(m+g)	13.4 ± 1.1	7.17 ± 0.69	3.93 ± 0.40	3.00 ± 0.35	2.25 ± 0.46
^{135}Xe	9,14h	c	23.1 ± 1.9	12.3 ± 1.1	6.86 ± 0.54	6.91 ± 0.59	6.11 ± 0.60
^{133m}Xe	2,19d	c	11.0 ± 1.1	6.83 ± 0.60	–	–	–
^{127}Xe	36,4d	c	–	1.76 ± 0.18	8.38 ± 0.98	8.91 ± 0.71	8.42 ± 0.69
^{125}Xe	16,9h	c	–	0.317 ± 0.039	4.26 ± 0.32	6.04 ± 0.47	6.51 ± 0.55
^{135}I	6,57h	c	10.1 ± 0.8	5.42 ± 0.47	2.93 ± 0.28	3.65 ± 0.45	3.65 ± 0.46
^{134}I	52,5m	i(m+g)	7.95 ± 1.20	3.63 ± 0.68	–	–	–
^{134}I	52,5m	c	13.4 ± 1.2	6.78 ± 0.64	–	–	–
^{133}I	20,8h	c	17.9 ± 1.5	9.28 ± 0.80	4.59 ± 0.35	4.52 ± 0.37	4.29 ± 0.38
^{131}I	8,02070d	c	25.4 ± 1.9	13.9 ± 1.1	6.82 ± 0.52	6.31 ± 0.47	5.60 ± 0.45
^{130}I	12,36h	i(m+g)	12.4 ± 1.0	7.45 ± 0.58	4.13 ± 0.34	3.53 ± 0.26	2.79 ± 0.24
^{126}I	13,11d	i	–	4.28 ± 0.60	–	5.80 ± 0.67	4.07 ± 0.54
^{124}I	4,1760d	i	–	2.07 ± 0.42	4.67 ± 0.69	5.37 ± 0.50	4.61 ± 0.45
^{121}I	2,12h	c	–	–	3.07 ± 0.27	4.61 ± 0.36	5.48 ± 0.47
^{134}Te	41,8m	c	5.41 ± 0.68	3.16 ± 0.42	–	–	–
^{133m}Te	55,4m	c	5.51 ± 0.69	3.17 ± 0.39	–	–	–
^{132}Te	3,204d	c	9.60 ± 0.85	5.07 ± 0.43	2.55 ± 0.22	2.76 ± 0.21	2.57 ± 0.23
^{131m}Te	30h	c	5.55 ± 0.93	4.03 ± 0.39	–	1.28 ± 0.28	1.20 ± 0.27
^{131}Te	25,0m	c	5.68 ± 0.74	3.22 ± 0.33	–	–	–
^{131}Te	25,0m	i	4.49 ± 1.11	2.65 ± 0.43	–	–	–
^{129m}Te	33,6d	c	–	–	–	1.50 ± 0.62	5.23 ± 1.92
^{123m}Te	119,7d	i(m)	–	3.93 ± 0.37	–	6.60 ± 0.55	6.68 ± 0.57
^{121m}Te	154d	c	–	–	–	5.30 ± 0.46	4.41 ± 0.38
^{121}Te	19,16d	c	–	–	–	9.90 ± 0.82	10.1 ± 0.9
^{119m}Te	4,70d	c	–	–	–	3.14 ± 0.23	2.95 ± 0.24
^{119}Te	16,05h	c	–	–	–	1.92 ± 0.15	2.29 ± 0.19
^{130m}Sb	39,5m	c	–	1.32 ± 0.16	–	–	–
^{129}Sb	4,40h	c	5.66 ± 0.60	3.11 ± 0.39	–	–	–
^{128}Sb	9,01h	c	6.27 ± 0.68	3.26 ± 0.29	–	–	–
^{127}Sb	3,85d	c	16.4 ± 1.5	8.75 ± 0.77	5.11 ± 0.51	3.82 ± 0.32	3.35 ± 0.31
^{126m}Sb	19,15m	i(m1+m2)	–	2.04 ± 0.29	–	–	–

Table 26, continued.

Product	$T_{1/2}$	Type	Yields [mbarn] at				
			0.1 GeV	0.2 GeV	0.8 GeV	1.2 GeV	1.6 GeV
^{126}Sb	12,46d	i(m1+m2+g)	12.5 ± 0.9	7.11 ± 0.56	3.22 ± 0.33	3.20 ± 0.24	–
^{124}Sb	60,20d	i(m1+m2+g)	18.1 ± 1.7	11.7 ± 0.9	8.50 ± 2.42	6.39 ± 0.47	–
^{122}Sb	2,7238d	i(m+g)	6.20 ± 0.48	8.25 ± 0.65	8.72 ± 0.61	8.03 ± 0.60	6.89 ± 0.57
^{120m}Sb	5,76d	i(m)	–	2.56 ± 0.22	7.04 ± 0.48	6.33 ± 0.48	5.22 ± 0.42
^{118m}Sb	5,00h	i(m)	–	0.571 ± 0.065	4.62 ± 0.34	5.64 ± 0.46	4.93 ± 0.45
^{116m}Sb	60,3m	i(m)	–	–	2.86 ± 0.38	2.69 ± 0.37	2.96 ± 0.32
^{128}Sn	59,07m	c	2.43 ± 0.35	1.24 ± 0.12	–	–	–
^{127}Sn	2,10h	c	3.83 ± 0.85	2.10 ± 0.43	–	–	–
^{125}Sn	9,64d	c	–	5.13 ± 1.65	–	–	–
^{123m}Sn	40,06m	c	11.7 ± 0.9	6.90 ± 0.56	3.85 ± 0.31	3.56 ± 0.30	3.29 ± 0.34
^{117m}Sn	13,60d	c	–	3.00 ± 0.26	7.00 ± 1.12	9.42 ± 0.77	9.56 ± 0.80
^{113}Sn	115,09d	c	–	–	–	3.17 ± 0.29	3.65 ± 0.35
^{116m}In	54,29m	i(m1+m2)	–	6.82 ± 0.58	13.9 ± 1.0	11.3 ± 0.9	8.83 ± 0.80
^{114m}In	49,51d	i(m1+m2)	24.8 ± 4.6	6.32 ± 1.10	–	9.96 ± 0.80	9.03 ± 0.85
^{111}In	2,8047d	c	–	–	3.02 ± 0.33	4.87 ± 0.38	5.70 ± 0.47
^{110}In	4,9h	i	–	–	1.41 ± 0.42	2.50 ± 0.21	2.64 ± 0.25
^{117m}Cd	3,36h	c	25.4 ± 1.9	18.8 ± 1.5	10.9 ± 1.1	9.95 ± 0.94	9.04 ± 1.17
^{117}Cd	2,49h	c	16.8 ± 1.3	11.3 ± 0.9	–	6.26 ± 0.66	5.39 ± 0.74
^{115}Cd	53,46h	c	49.4 ± 3.7	35.0 ± 2.8	21.1 ± 1.6	19.1 ± 1.4	16.5 ± 1.3
^{111m}Cd	48,30m	i(m)	–	1.39 ± 0.20	–	–	–
^{113}Ag	5,37h	c	71.0 ± 5.3	55.9 ± 4.5	37.6 ± 2.7	36.3 ± 2.8	30.4 ± 2.6
^{112}Ag	3,130h	c	69.5 ± 8.5	57.0 ± 6.5	49.4 ± 5.9	42.1 ± 7.8	35.0 ± 7.0
^{112}Ag	3,130h	i	11.0 ± 1.6	14.3 ± 1.7	22.8 ± 3.0	19.1 ± 3.8	15.2 ± 3.9
^{111}Ag	7,45d	c	72.4 ± 8.0	54.6 ± 5.5	–	45.0 ± 4.3	36.7 ± 3.7
^{110m}Ag	249,76d	i(m)	–	3.31 ± 0.68	–	–	–
^{110m}Ag	249,76d	i	–	–	–	11.1 ± 0.9	9.56 ± 0.82
^{106m}Ag	8,28d	i(m)	–	–	–	3.40 ± 0.27	3.57 ± 0.31
^{105}Ag	41,29d	c	–	3.50 ± 0.43	–	2.66 ± 0.26	3.35 ± 0.32
^{94}Ag	293m	i	–	–	–	1.40 ± 0.18	1.48 ± 0.21
^{112}Pd	21,03h	c	57.5 ± 7.0	42.5 ± 4.9	27.0 ± 3.1	23.0 ± 4.2	19.7 ± 3.7
^{111m}Pd	5,5h	i(m)	12.6 ± 1.8	12.0 ± 1.7	–	–	–
^{107}Rh	21,7m	c*	66.2 ± 7.9	55.9 ± 6.8	–	–	–
^{106m}Rh	131m	i(m)	4.33 ± 0.64	6.08 ± 0.53	14.9 ± 1.2	15.6 ± 1.4	12.4 ± 1.1
^{105}Rh	35,36h	i(m+g)	–	–	–	24.8 ± 4.2	14.4 ± 4.6
^{105}Rh	35,36h	c	54.9 ± 4.3	49.8 ± 4.3	52.1 ± 3.9	54.3 ± 4.4	44.4 ± 3.9
^{101m}Rh	4,34d	c	–	–	3.08 ± 0.50	4.99 ± 0.49	6.07 ± 0.66
^{100}Rh	20,8h	i(m+g)	–	–	–	2.41 ± 0.20	2.77 ± 0.26
^{106}Ru	373,59d	c	–	43.1 ± 5.1	–	38.4 ± 3.1	26.6 ± 6.6
^{105}Ru	4,44h	c	58.6 ± 4.3	50.0 ± 3.9	43.0 ± 2.9	38.2 ± 3.0	31.6 ± 2.6
^{103}Ru	39,26d	c	53.4 ± 4.1	48.0 ± 3.9	61.0 ± 4.4	52.4 ± 4.0	44.0 ± 3.7

Table 26, continued.

Product	$T_{1/2}$	Type	Yields [mbarn] at				
			0.1 GeV	0.2 GeV	0.8 GeV	1.2 GeV	1.6 GeV
^{104}Tc	18,3m	c	49.9 ± 4.2	37.2 ± 3.2	30.5 ± 2.8	26.1 ± 2.3	19.7 ± 2.1
^{101}Tc	14,22m	c	50.1 ± 9.8	45.4 ± 5.1	61.3 ± 7.0	54.2 ± 5.9	33.2 ± 4.0
^{101}Tc	14,22m	i	–	7.49 ± 3.97	32.1 ± 7.0	26.5 ± 4.9	8.76 ± 3.39
^{99m}Tc	6,01h	i(m)	0.010 ± 0.087	0.707 ± 0.119	2.49 ± 0.21	3.70 ± 0.34	3.60 ± 0.34
^{99m}Tc	6,01h	c	40.8 ± 3.1	35.9 ± 2.9	41.8 ± 2.8	41.4 ± 3.2	35.5 ± 2.9
^{96}Tc	4,28d	i(m+g)	–	–	2.95 ± 0.90	3.92 ± 0.31	4.20 ± 0.36
^{95}Tc	20,0h	c*	–	–	1.04 ± 0.12	2.34 ± 0.18	3.00 ± 0.25
^{101}Mo	14,61m	c	51.7 ± 5.0	38.4 ± 3.4	32.8 ± 5.7	28.2 ± 3.0	25.1 ± 2.6
^{99}Mo	65,94h	c	46.7 ± 3.5	40.3 ± 3.3	45.0 ± 3.1	43.0 ± 3.3	36.4 ± 3.0
^{93m}Mo	6,85h	i(m)	–	–	0.774 ± 0.213	1.82 ± 0.14	2.12 ± 0.19
^{98m}Nb	51,3m	i(m)	9.78 ± 0.93	11.1 ± 0.9	16.8 ± 1.5	16.0 ± 1.5	11.8 ± 1.1
^{96}Nb	23,35h	i	2.08 ± 0.23	5.37 ± 0.42	14.8 ± 1.0	17.6 ± 1.4	14.3 ± 1.4
^{95}Nb	34,975d	i(m+g)	–	3.13 ± 0.30	12.7 ± 1.3	17.0 ± 1.2	16.1 ± 1.3
^{95}Nb	34,975d	c	43.7 ± 3.6	35.3 ± 2.8	42.0 ± 4.5	47.9 ± 3.5	39.7 ± 3.2
^{92m}Nb	10,15d	i(m)	–	–	4.08 ± 0.69	0.706 ± 0.058	0.869 ± 0.086
^{90}Nb	14,60h	c	–	–	0.820 ± 0.097	1.83 ± 0.14	2.29 ± 0.20
^{97}Zr	16,744h	c	36.1 ± 2.6	26.4 ± 2.1	19.1 ± 1.3	18.2 ± 1.3	15.3 ± 1.2
^{95}Zr	64,02d	c	41.6 ± 3.4	32.4 ± 2.5	31.5 ± 2.9	30.8 ± 2.2	25.2 ± 2.1
^{89}Zr	78,41h	c	–	–	–	5.61 ± 0.41	6.59 ± 0.53
^{88}Zr	83,4d	c	–	–	–	2.29 ± 0.18	2.96 ± 0.28
^{94}Y	18,7m	i	37.8 ± 3.8	23.7 ± 2.4	20.0 ± 2.3	15.8 ± 1.6	14.6 ± 1.6
^{93}Y	10,18h	c	38.9 ± 5.1	28.1 ± 3.6	23.5 ± 3.9	–	–
^{92}Y	3,54h	c	48.2 ± 6.7	32.3 ± 4.6	30.5 ± 4.6	34.2 ± 4.8	29.8 ± 4.4
^{92}Y	3,54h	i	19.0 ± 3.8	7.10 ± 2.08	13.0 ± 5.0	11.5 ± 2.8	12.6 ± 3.3
^{91m}Y	49,71m	i(m)	–	–	14.3 ± 1.1	16.2 ± 1.2	14.1 ± 1.2
^{91m}Y	49,71m	c	–	–	26.0 ± 1.8	27.6 ± 2.1	23.9 ± 1.9
^{90m}Y	3,19h	i(m)	0.793 ± 0.109	2.25 ± 0.18	11.9 ± 0.9	14.6 ± 1.4	13.3 ± 1.4
^{88}Y	106,65d	i(m+g)	–	–	–	10.4 ± 0.8	–
^{88}Y	106,65d	c	–	–	–	12.6 ± 0.9	13.2 ± 1.2
^{87m}Y	13,37h	c	–	–	2.83 ± 0.52	5.39 ± 0.50	6.38 ± 0.67
^{87}Y	79,8h	c	–	0.248 ± 0.073	3.54 ± 0.25	6.56 ± 0.49	7.66 ± 0.62
^{86}Y	14,74h	c	–	–	1.28 ± 0.12	2.54 ± 0.19	3.24 ± 0.26
^{92}Sr	2,71h	c	32.7 ± 3.3	22.8 ± 2.2	15.9 ± 1.5	14.9 ± 1.5	12.9 ± 1.4
^{91}Sr	9,63h	c	40.5 ± 3.2	27.9 ± 2.6	22.8 ± 2.1	20.7 ± 1.6	17.1 ± 1.7
^{85}Sr	64,84d	c	–	–	–	6.01 ± 0.78	7.08 ± 0.77
^{89}Rb	15,15m	c*	35.8 ± 3.6	24.0 ± 2.2	23.6 ± 3.3	20.2 ± 2.2	17.4 ± 1.9
^{88}Rb	17,78m	c	–	27.0 ± 3.1	–	–	–
^{88}Rb	17,78m	i	–	8.74 ± 1.95	–	–	–
^{86}Rb	18,631d	i(m+g)	–	–	–	16.6 ± 1.3	16.5 ± 1.4
^{84m}Rb	20,26m	i(m)	–	–	5.43 ± 0.69	8.05 ± 0.71	7.95 ± 0.82

Table 26, continued.

Product	$T_{1/2}$	Type	Yields [mbarn] at				
			0.1 GeV	0.2 GeV	0.8 GeV	1.2 GeV	1.6 GeV
^{83}Rb	86,2d	c	–	–	–	8.74 ± 0.75	10.1 ± 0.9
^{82m}Rb	6,472h	i(m)	–	–	1.49 ± 0.20	3.37 ± 0.32	4.02 ± 0.37
^{88}Kr	2,84h	c	26.9 ± 2.1	16.0 ± 1.3	10.6 ± 0.9	9.65 ± 0.76	8.48 ± 0.81
^{87}Kr	76,3m	c	29.7 ± 3.3	20.2 ± 1.9	13.4 ± 1.5	12.6 ± 1.4	11.1 ± 1.3
^{85m}Kr	4,480h	c	24.8 ± 2.0	15.9 ± 1.3	11.2 ± 1.1	10.1 ± 1.0	8.97 ± 0.96
^{84}Br	31,80m	c	21.9 ± 2.8	12.2 ± 1.6	–	–	–
^{82}Br	35,30h	i(m+g)	1.97 ± 0.16	3.25 ± 0.26	8.59 ± 0.66	10.7 ± 0.8	9.21 ± 0.75
^{77}Br	57,036h	c	–	–	–	2.47 ± 0.21	2.70 ± 0.24
^{83}Se	22,3m	c	12.8 ± 1.2	8.10 ± 0.70	–	–	–
^{75}Se	119,779d	c	–	–	–	2.98 ± 0.28	3.47 ± 0.29
^{78}As	90,7m	c	7.17 ± 1.04	6.19 ± 0.76	10.0 ± 1.5	11.2 ± 1.6	9.38 ± 1.32
^{78}As	90,7m	i	2.63 ± 0.78	2.95 ± 0.64	7.09 ± 1.61	8.43 ± 1.42	7.12 ± 1.09
^{76}As	1,0778d	i	–	–	5.03 ± 0.43	7.54 ± 0.65	7.88 ± 0.73
^{74}As	17,77d	i	–	–	–	4.90 ± 0.49	5.50 ± 0.59
^{78}Ge	88m	c	4.23 ± 0.37	3.30 ± 0.29	2.94 ± 0.87	2.74 ± 0.60	2.26 ± 0.41
^{77}Ge	11,30h	c	2.71 ± 0.21	2.60 ± 0.21	3.15 ± 0.27	3.31 ± 0.32	2.16 ± 0.23
^{73}Ga	4,86h	c	1.87 ± 0.16	2.38 ± 0.21	4.55 ± 0.36	5.50 ± 0.49	4.20 ± 0.55
^{72}Ga	14,10h	i(m+g)	–	0.871 ± 0.120	–	5.31 ± 0.47	5.22 ± 0.53
^{72}Ga	14,10h	c	–	2.59 ± 0.23	–	7.95 ± 0.65	7.41 ± 0.66
^{72}Zn	46,5h	c	–	1.72 ± 0.18	2.00 ± 0.20	2.48 ± 0.20	2.22 ± 0.19
^{71m}Zn	3,96h	c	0.547 ± 0.087	1.09 ± 0.10	2.41 ± 0.34	2.99 ± 0.28	2.57 ± 0.26
^{69m}Zn	13,76h	i(m)	–	0.398 ± 0.036	3.01 ± 0.20	4.42 ± 0.33	4.47 ± 0.36
^{58}Co	70,86d	i(m+g)	–	–	–	0.851 ± 0.081	1.26 ± 0.12
^{59}Fe	44,472d	c	–	–	–	3.42 ± 0.29	3.97 ± 0.35
^{56}Mn	2,5789h	c	–	–	–	3.99 ± 0.55	3.50 ± 0.59
^{48}V	15,9735d	c	–	–	–	0.232 ± 0.025	0.283 ± 0.084
^{48}Sc	43,67h	i	–	–	0.940 ± 0.180	0.923 ± 0.071	1.21 ± 0.10
^{46}Sc	83,79d	i(m+g)	–	–	–	0.980 ± 0.094	1.42 ± 0.16
^{43}K	22,3h	c	–	–	–	1.19 ± 0.10	1.66 ± 0.15
^{28}Mg	20,915h	c	–	–	–	0.562 ± 0.048	0.894 ± 0.075
^{24}Na	14,9590h	c	–	–	0.806 ± 0.131	1.51 ± 0.12	2.62 ± 0.22

3.8 Experimental yields for ^{nat}U irradiated with 0.1, 0.2, 0.8, 1.2, 1.6 GeV protons.

Table 27 presents the parameters of ^{nat}U irradiations. Table 28 presents the yields of residual nuclide products measured.

Table 27: Parameters of ^{nat}U irradiation.

E_p (GeV)	Sample weight (mg)	Monitor weight (mg)	Irradiation duration (min)	Proton Flux p/cm^2	Number of measured γ -spectra of sample/monitor	EXPDATA index
0.1	159.2	47.9	60	8.5×10^{12}	48 / 15	ues100
0.2	160.0	47.8	28.5	1.3×10^{13}	41 / 12	ues200
0.8	160.9	48.0	60	5.7×10^{13}	51 / 13	ues800
1.2	160.6	47.8	40	6.1×10^{13}	42 / 9	ues12g
1.6	160.4	48.2	30	4.5×10^{13}	44 / 11	ues16g

Table 28: Experimental yields from ^{nat}U irradiated with 0.1, 0.2, 0.8, 1.2, 1.6 GeV protons.

Product	$T_{1/2}$	Type	Yields [mbarn] at				
			0.1 GeV	0.2 GeV	0.8 GeV	1.2 GeV	1.6 GeV
^{239}Np	2,3565d	i	–	–	3.46 ± 0.28	3.69 ± 0.32	3.51 ± 0.47
^{238}Np	2,117d	i	2.93 ± 0.28	1.09 ± 0.12	–	–	–
^{237}U	6,75d	c	95.3 ± 8.0	76.9 ± 6.0	107. ± 9.	115. ± 9.	108. ± 10.
^{234}Pa	6,70h	i	3.26 ± 0.66	6.39 ± 0.63	7.88 ± 1.05	10.7 ± 1.8	9.39 ± 1.48
^{233}Pa	26,967d	c	5.09 ± 0.41	9.87 ± 0.68	14.2 ± 0.9	14.0 ± 1.1	12.7 ± 1.1
^{232}Pa	1,31d	i	3.75 ± 0.33	8.52 ± 0.64	8.88 ± 0.63	7.95 ± 0.70	7.18 ± 0.70
^{230}Pa	17,4d	i	–	3.88 ± 0.48	3.60 ± 0.34	2.99 ± 0.37	2.73 ± 0.34
^{228}Pa	22h	c	2.45 ± 0.37	1.55 ± 0.21	1.98 ± 0.64	–	1.25 ± 0.32
^{227}Th	18,72d	c	3.66 ± 0.81	2.63 ± 0.49	3.87 ± 0.60	4.28 ± 0.63	2.95 ± 0.44
^{226}Ac	29,37h	i	–	–	2.18 ± 0.22	2.34 ± 0.29	1.80 ± 0.21
^{225}Ac	10,0d	c	–	–	3.31 ± 0.23	2.99 ± 0.23	–
^{223}Ra	11,435d	c	–	–	4.45 ± 0.40	3.66 ± 0.33	2.65 ± 0.50
^{211}Rn	14,6h	c	–	–	4.03 ± 0.28	3.88 ± 0.31	3.17 ± 0.30
^{210}At	8,1h	c	–	–	4.67 ± 0.32	4.49 ± 0.34	3.54 ± 0.32
^{209}At	5,41h	c	–	–	9.02 ± 0.58	8.93 ± 0.66	7.03 ± 0.62
^{208}At	1,63h	c*	–	–	4.73 ± 0.51	4.84 ± 0.56	4.20 ± 0.47
^{207}At	1,80h	c	–	–	8.43 ± 0.84	8.12 ± 0.87	6.07 ± 0.85
^{206}At	30,6m	c*	–	–	4.82 ± 0.38	5.17 ± 0.50	4.65 ± 0.54
^{206}Po	8,8d	c	–	–	8.85 ± 0.55	9.29 ± 0.66	7.66 ± 0.65
^{205}Po	1,66h	c*	–	–	7.10 ± 0.79	8.19 ± 0.90	7.27 ± 0.98
^{204}Po	3,53h	c*	–	–	8.11 ± 0.57	8.72 ± 0.82	7.53 ± 0.69
^{203}Po	36,7m	c*	–	–	5.17 ± 0.58	6.35 ± 0.73	7.42 ± 0.89
^{202}Po	44,7m	c	–	–	3.68 ± 0.42	6.69 ± 0.65	5.24 ± 0.72
^{206}Bi	6,243d	c	–	–	8.63 ± 0.53	9.02 ± 0.64	7.55 ± 0.63

Table 28, continued.

Product	$T_{1/2}$	Type	Yields [mbarn] at				
			0.1 GeV	0.2 GeV	0.8 GeV	1.2 GeV	1.6 GeV
^{205}Bi	15,31d	c	–	–	6.68 ± 0.41	7.79 ± 0.56	6.53 ± 0.56
^{204}Bi	11,22h	c	–	–	7.21 ± 0.57	8.22 ± 0.84	6.90 ± 0.80
^{203}Bi	11,76h	c	–	–	4.52 ± 0.59	6.15 ± 0.68	5.27 ± 0.52
^{202}Bi	1,72h	c	–	–	5.24 ± 0.37	7.26 ± 0.56	6.69 ± 0.61
^{203}Pb	51,873h	i(m1+m2+g)	–	–	1.24 ± 0.24	1.34 ± 0.40	–
^{203}Pb	51,873h	c	–	–	5.25 ± 0.35	6.69 ± 0.50	5.66 ± 0.48
^{201}Pb	9,33h	i(m+g)	–	–	3.86 ± 0.92	5.64 ± 0.99	4.07 ± 0.93
^{201}Pb	9,33h	c	–	–	4.94 ± 0.47	7.12 ± 0.70	6.21 ± 0.67
^{200}Pb	21,5h	c	–	–	3.21 ± 0.28	5.36 ± 0.53	4.88 ± 0.42
^{199}Pb	90m	c*	–	–	8.40 ± 1.67	12.5 ± 2.2	14.5 ± 2.1
^{200}Tl	26,1h	i(m+g)	–	–	1.29 ± 0.13	1.58 ± 0.22	0.923 ± 0.362
^{200}Tl	26,1h	c	–	–	4.39 ± 0.42	6.75 ± 0.58	5.63 ± 0.58
^{193m}Hg	11,8h	i(m)	–	–	–	1.12 ± 0.47	1.29 ± 0.37
^{192}Hg	4,85h	c	–	–	2.37 ± 0.24	6.68 ± 0.66	8.00 ± 0.80
^{192}Au	4,94h	c	–	–	–	8.91 ± 1.20	10.8 ± 1.6
^{191}Pt	2,802d	c	–	–	1.48 ± 0.52	5.82 ± 0.60	6.27 ± 0.87
^{188}Pt	10,2d	c	–	–	1.29 ± 0.13	5.72 ± 0.61	6.94 ± 0.85
^{186}Pt	2,08h	c	–	–	–	5.30 ± 1.23	7.82 ± 1.82
^{190}Ir	11,78d	i(m1+g)	–	–	1.01 ± 0.12	–	–
^{188}Ir	41,5h	c	–	–	–	4.88 ± 0.57	6.58 ± 0.78
^{186}Ir	16,64h	i	–	–	–	3.10 ± 0.26	3.89 ± 0.36
^{185}Ir	14,4h	c	–	–	–	4.80 ± 0.84	7.19 ± 1.27
^{184}Ir	3,09h	c	–	–	–	5.44 ± 0.55	8.24 ± 0.87
^{185}Os	93,6d	c	–	–	2.59 ± 0.31	5.32 ± 1.44	7.54 ± 1.52
^{183m}Os	9,9h	c	–	–	–	4.10 ± 0.35	5.79 ± 0.53
^{182}Os	22,10h	c	–	–	1.20 ± 0.13	6.27 ± 0.49	10.0 ± 0.9
^{183}Re	70,0d	c	–	–	–	5.84 ± 0.51	8.81 ± 0.85
^{182m}Re	12,7h	c	–	–	–	6.31 ± 0.53	10.2 ± 0.9
^{181}Re	19,9h	c	–	–	–	5.99 ± 0.84	9.61 ± 1.41
^{177}W	135m	c	–	–	2.13 ± 0.30	4.85 ± 0.58	7.20 ± 0.90
^{176}W	2,5h	c	–	–	–	3.20 ± 1.06	6.35 ± 1.46
^{174}W	31m	c	–	–	–	3.01 ± 0.64	7.04 ± 1.05
^{176}Ta	8,09h	c	–	–	–	3.79 ± 0.54	7.93 ± 1.02
^{175}Ta	10,5h	c	–	–	–	3.45 ± 0.52	6.81 ± 0.94
^{174}Ta	1,14h	c	–	–	–	3.59 ± 0.49	8.15 ± 1.03
^{172}Ta	36,8m	c*	–	–	1.86 ± 0.26	4.04 ± 0.58	6.54 ± 0.98
^{175}Hf	70d	c	–	–	0.578 ± 0.071	3.67 ± 0.32	7.73 ± 0.72
^{172}Hf	1,87y	c	–	–	–	2.77 ± 0.66	6.80 ± 0.70
^{173}Lu	1,37y	c	–	–	–	4.42 ± 0.61	5.99 ± 0.88
^{172}Lu	6,70d	c	–	–	–	2.82 ± 0.65	6.96 ± 0.71

Table 28, continued.

Product	$T_{1/2}$	Type	Yields [mbarn] at				
			0.1 GeV	0.2 GeV	0.8 GeV	1.2 GeV	1.6 GeV
^{171}Lu	8,24d	c	–	–	0.938 ± 0.103	3.08 ± 0.26	7.22 ± 0.64
^{170}Lu	2,012d	c	–	–	–	–	5.94 ± 1.01
^{169}Lu	34,06h	c	–	–	–	2.27 ± 0.20	4.91 ± 0.45
^{169}Yb	32,026d	c	–	–	–	–	6.44 ± 0.62
^{166}Yb	56,7h	c	–	–	–	1.70 ± 0.21	5.43 ± 0.53
^{160}Er	28,58h	c	–	–	–	1.91 ± 0.23	4.22 ± 0.48
^{160m}Ho	5,02h	i(m)	–	–	–	–	2.18 ± 0.52
^{160m}Ho	5,02h	c	–	–	–	–	6.22 ± 1.03
^{157}Dy	8,14h	c	–	–	0.752 ± 0.107	1.29 ± 0.15	3.38 ± 0.33
^{155}Dy	9,9h	c*	–	–	0.722 ± 0.137	1.32 ± 0.17	2.66 ± 0.28
^{152}Dy	2,38h	c	–	–	–	–	1.52 ± 0.15
^{156}Tb	5,35d	i(m1+m2+g)	–	–	0.472 ± 0.051	–	–
^{155}Tb	5,32d	c	–	–	1.48 ± 0.23	2.98 ± 0.40	4.38 ± 0.48
^{153}Tb	2,34d	c*	–	–	1.05 ± 0.13	1.90 ± 0.21	2.81 ± 0.32
^{152}Tb	17,5h	c*	–	–	0.907 ± 0.093	1.48 ± 0.15	2.65 ± 0.29
^{150}Tb	3,48h	c	–	–	–	0.401 ± 0.111	0.675 ± 0.158
^{149}Gd	9,28d	c	–	–	0.840 ± 0.082	1.50 ± 0.13	2.88 ± 0.27
^{146}Gd	48,27d	c	–	–	0.309 ± 0.050	0.804 ± 0.081	1.71 ± 0.16
^{147}Eu	24,1d	c	–	–	–	0.772 ± 0.226	2.65 ± 0.31
^{146}Eu	4,61d	c	–	–	0.876 ± 0.078	1.66 ± 0.15	2.75 ± 0.25
^{146}Eu	4,61d	i	–	–	0.567 ± 0.053	0.858 ± 0.088	1.05 ± 0.10
^{145}Eu	5,93d	c	–	–	–	–	2.19 ± 0.31
^{144}Pm	363d	i	–	–	1.32 ± 0.23	1.50 ± 0.14	1.28 ± 0.16
^{147}Nd	10,98d	c	–	9.16 ± 0.98	6.56 ± 0.64	6.16 ± 0.78	6.28 ± 0.74
^{139m}Nd	5,5h	i(m)	–	–	–	–	1.86 ± 0.34
^{146}Pr	24,15m	c	15.3 ± 2.3	12.4 ± 1.4	–	–	–
^{146}Pr	24,15m	i	–	7.60 ± 2.06	–	–	–
^{138m}Pr	2,12h	i(m)	–	–	2.22 ± 0.34	2.34 ± 0.22	–
^{144}Ce	284,893d	c	–	–	11.6 ± 1.0	12.1 ± 1.1	11.6 ± 1.3
^{143}Ce	33,039h	c	24.9 ± 1.9	17.3 ± 1.2	12.4 ± 0.8	11.7 ± 0.9	10.4 ± 0.9
^{141}Ce	32,501d	c	34.1 ± 2.7	25.0 ± 1.8	19.0 ± 1.3	17.5 ± 1.4	15.4 ± 1.3
^{139}Ce	137,640d	c	1.46 ± 0.22	3.58 ± 0.32	8.20 ± 0.54	8.33 ± 0.62	7.82 ± 0.68
^{135}Ce	17,7h	c	–	–	3.08 ± 0.25	4.28 ± 0.36	4.64 ± 0.43
^{132}Ce	3,51h	c	–	–	0.701 ± 0.186	1.45 ± 0.20	2.01 ± 0.21
^{142}La	91,1m	c	25.1 ± 2.4	17.1 ± 1.6	13.3 ± 1.0	11.5 ± 1.0	10.4 ± 1.1
^{140}La	1,6781d	c	31.9 ± 2.4	22.6 ± 1.5	16.6 ± 1.0	15.4 ± 1.1	14.2 ± 1.2
^{140}La	1,6781d	i	7.23 ± 0.62	5.13 ± 0.42	3.22 ± 0.23	2.60 ± 0.24	2.18 ± 0.30
^{132}La	4,8h	i(m+g)	–	–	–	2.02 ± 0.31	1.73 ± 0.27
^{132}La	4,8h	c	–	–	2.02 ± 0.33	3.50 ± 0.39	3.71 ± 0.44
^{141}Ba	18,27m	c	23.6 ± 2.8	16.0 ± 1.8	–	–	–

Table 28, continued.

Product	$T_{1/2}$	Type	Yields [mbarn] at				
			0.1 GeV	0.2 GeV	0.8 GeV	1.2 GeV	1.6 GeV
^{140}Ba	12,752d	c	24.9 ± 1.9	17.6 ± 1.1	13.5 ± 0.8	12.7 ± 0.9	11.7 ± 1.0
^{139}Ba	83,06m	c	32.1 ± 5.9	21.2 ± 3.8	–	–	–
^{135m}Ba	28,7h	i(m)	2.56 ± 0.30	3.98 ± 0.33	–	–	–
^{133m}Ba	38,9h	i(m)	2.78 ± 0.25	2.77 ± 0.26	5.11 ± 0.40	4.55 ± 0.41	2.88 ± 0.39
^{131}Ba	11,50d	c	–	–	6.51 ± 0.45	7.28 ± 0.58	6.67 ± 0.64
^{128}Ba	2,43d	c	–	–	2.16 ± 0.28	3.05 ± 0.45	3.54 ± 0.46
^{138}Cs	33,41m	i(m+g)	–	15.4 ± 2.6	–	–	–
^{138}Cs	33,41m	c	24.9 ± 2.4	18.6 ± 1.7	14.2 ± 1.6	–	–
^{136}Cs	13,16d	i(m+g)	13.9 ± 1.1	9.79 ± 0.66	5.96 ± 0.36	4.83 ± 0.34	3.87 ± 0.33
^{134m}Cs	2,903h	i(m)	9.58 ± 0.99	7.44 ± 0.65	–	–	–
^{134}Cs	2,0648y	i(m+g)	9.31 ± 1.20	10.1 ± 2.1	6.43 ± 0.52	4.78 ± 0.43	3.97 ± 0.38
^{132}Cs	6,479d	i	3.48 ± 0.40	5.30 ± 0.43	6.95 ± 0.48	5.72 ± 0.56	4.94 ± 0.48
^{135m}Xe	15,29m	i(m)	16.2 ± 1.6	11.0 ± 0.9	–	–	–
^{135}Xe	9,14h	i(m+g)	17.8 ± 1.6	13.0 ± 1.0	8.19 ± 0.66	6.94 ± 0.60	5.88 ± 0.58
^{135}Xe	9,14h	c	37.2 ± 3.1	26.2 ± 2.0	20.0 ± 1.5	18.7 ± 1.5	16.8 ± 1.5
^{133m}Xe	2,19d	c	16.6 ± 1.3	11.5 ± 0.8	7.34 ± 0.52	6.03 ± 0.50	4.69 ± 0.46
^{127}Xe	36,4d	c	–	2.08 ± 0.22	11.6 ± 0.8	13.0 ± 0.9	11.8 ± 1.0
^{125}Xe	16,9h	c	–	–	6.09 ± 0.39	7.57 ± 0.58	7.83 ± 0.67
^{135}I	6,57h	c	19.0 ± 1.5	13.3 ± 0.9	12.0 ± 0.8	11.9 ± 1.0	11.0 ± 0.9
^{134}I	52,5m	i(m+g)	14.5 ± 1.7	10.8 ± 1.1	–	–	–
^{134}I	52,5m	c	25.7 ± 2.1	18.4 ± 1.3	–	–	–
^{133}I	20,8h	c	32.4 ± 2.7	22.3 ± 1.7	16.7 ± 1.2	15.8 ± 1.3	14.5 ± 1.3
^{131}I	8,02070d	c	43.1 ± 3.3	30.2 ± 2.0	20.4 ± 1.3	18.2 ± 1.3	15.6 ± 1.3
^{130}I	12,36h	i(m+g)	15.0 ± 1.1	11.4 ± 0.7	8.85 ± 0.56	6.84 ± 0.50	5.54 ± 0.47
^{126}I	13,11d	i	2.38 ± 0.39	5.45 ± 0.63	9.74 ± 0.89	8.62 ± 1.02	6.40 ± 0.73
^{124}I	4,1760d	i	–	–	7.83 ± 0.52	7.90 ± 0.61	6.29 ± 0.67
^{121}I	2,12h	c	–	–	3.16 ± 0.23	5.01 ± 0.40	6.14 ± 0.54
^{134}Te	41,8m	c	11.4 ± 1.0	7.93 ± 0.67	–	–	–
^{133m}Te	55,4m	c	11.4 ± 1.3	7.55 ± 0.75	–	–	–
^{132}Te	3,204d	c	18.1 ± 1.4	12.5 ± 0.8	10.3 ± 0.7	10.0 ± 0.8	8.93 ± 0.78
^{131m}Te	30h	c	13.6 ± 1.1	9.50 ± 0.74	5.29 ± 0.40	4.73 ± 0.39	4.19 ± 0.61
^{131}Te	25,0m	c	10.9 ± 1.2	8.29 ± 0.70	–	–	–
^{131}Te	25,0m	i	2.02 ± 1.54	2.98 ± 0.77	–	–	–
^{129m}Te	33,6d	c	17.1 ± 2.8	12.4 ± 1.5	7.74 ± 0.85	6.66 ± 0.91	6.11 ± 0.88
^{123m}Te	119,7d	i(m)	1.13 ± 0.21	3.96 ± 0.35	–	9.05 ± 0.68	7.12 ± 0.63
^{121m}Te	154d	c	–	–	6.28 ± 0.44	6.87 ± 0.52	5.90 ± 0.53
^{121}Te	19,16d	c	–	–	9.79 ± 0.74	12.0 ± 0.9	10.9 ± 1.0
^{119m}Te	4,70d	c	–	–	2.90 ± 0.19	4.39 ± 0.36	3.91 ± 0.34
^{119}Te	16,05h	c	–	–	1.21 ± 0.09	2.23 ± 0.17	2.66 ± 0.23
^{131}Sb	23,03m	c	8.91 ± 1.04	5.32 ± 0.57	–	–	–

Table 28, continued.

Product	$T_{1/2}$	Type	Yields [mbarn] at				
			0.1 GeV	0.2 GeV	0.8 GeV	1.2 GeV	1.6 GeV
^{130m}Sb	39,5m	c*	7.45 ± 0.62	4.91 ± 0.36	3.05 ± 0.36	2.42 ± 0.32	2.58 ± 0.40
^{129}Sb	4,40h	c	11.8 ± 1.2	8.17 ± 0.80	–	–	–
^{128}Sb	9,01h	c	10.7 ± 0.9	7.15 ± 0.55	5.21 ± 0.43	4.32 ± 0.44	3.71 ± 0.40
^{127}Sb	3,85d	c	27.0 ± 2.3	19.2 ± 1.5	12.0 ± 0.8	10.5 ± 0.9	9.13 ± 0.85
^{126}Sb	12,46d	i(m1+m2+g)	15.9 ± 1.2	11.8 ± 0.8	7.80 ± 0.47	6.32 ± 0.45	5.18 ± 0.43
^{125}Sb	2,75856y	c	46.4 ± 5.4	34.7 ± 4.2	24.3 ± 2.1	19.7 ± 1.6	14.9 ± 1.8
^{124}Sb	60,20d	i(m1+m2+g)	16.1 ± 1.2	15.4 ± 1.0	13.1 ± 0.9	10.4 ± 0.8	8.22 ± 0.73
^{122}Sb	2,7238d	i(m+g)	5.78 ± 0.44	9.45 ± 0.63	14.0 ± 0.9	11.6 ± 0.9	9.26 ± 0.79
^{120m}Sb	5,76d	i(m)	0.604 ± 0.050	2.55 ± 0.18	9.10 ± 0.55	8.65 ± 0.61	6.94 ± 0.57
^{118m}Sb	5,00h	i(m)	–	0.584 ± 0.064	6.14 ± 0.44	7.05 ± 0.56	6.34 ± 0.57
^{116m}Sb	60,3m	i(m)	–	–	–	3.07 ± 0.26	3.82 ± 0.36
^{128}Sn	59,07m	c	6.48 ± 0.59	4.03 ± 0.40	–	–	–
^{127}Sn	2,10h	c	9.44 ± 1.61	5.97 ± 0.96	4.80 ± 1.36	3.82 ± 1.11	4.49 ± 1.28
^{125}Sn	9,64d	c	15.7 ± 3.5	10.5 ± 2.4	7.80 ± 1.41	7.34 ± 1.65	5.46 ± 1.25
^{123m}Sn	40,06m	c	18.3 ± 1.4	13.0 ± 0.9	8.57 ± 0.58	7.72 ± 0.62	7.70 ± 0.69
^{117m}Sn	13,60d	c	0.476 ± 0.068	2.45 ± 0.19	12.5 ± 1.4	11.6 ± 0.9	10.1 ± 0.9
^{113}Sn	115,09d	c	–	–	2.02 ± 0.18	3.45 ± 0.32	3.84 ± 0.37
^{116m}In	54,29m	i(m1+m2)	–	7.23 ± 0.57	15.6 ± 1.1	15.7 ± 1.2	13.1 ± 1.2
^{114m}In	49,51d	i(m1+m2)	–	3.53 ± 0.66	10.6 ± 0.7	12.4 ± 1.0	10.1 ± 0.9
^{111}In	2,8047d	c	–	–	3.47 ± 0.27	5.45 ± 0.43	6.47 ± 0.56
^{110}In	4,9h	i	–	–	1.35 ± 0.10	2.55 ± 0.21	2.98 ± 0.27
^{117m}Cd	3,36h	c	23.9 ± 1.8	21.0 ± 1.4	18.2 ± 1.1	14.6 ± 1.2	12.6 ± 1.1
^{117}Cd	2,49h	c	18.6 ± 1.6	13.8 ± 1.1	10.9 ± 0.9	8.72 ± 0.81	6.91 ± 0.86
^{115}Cd	53,46h	c	48.5 ± 3.7	40.6 ± 2.7	33.4 ± 2.1	27.8 ± 2.0	22.0 ± 1.9
^{111m}Cd	48,30m	i(m)	–	1.36 ± 0.16	–	–	–
^{115}Ag	20,0m	c	33.9 ± 15.6	27.0 ± 12.2	–	–	–
^{113}Ag	5,37h	c	62.9 ± 4.8	57.8 ± 3.9	58.2 ± 3.8	52.5 ± 4.1	40.2 ± 3.4
^{112}Ag	3,130h	c	65.8 ± 8.1	60.8 ± 7.2	67.3 ± 7.7	58.2 ± 6.4	48.7 ± 6.2
^{112}Ag	3,130h	i	9.10 ± 1.60	14.2 ± 1.8	26.5 ± 3.2	23.2 ± 2.6	18.8 ± 2.4
^{111}Ag	7,45d	c	57.5 ± 5.6	56.5 ± 5.1	66.7 ± 5.8	57.7 ± 5.4	46.6 ± 4.8
^{110m}Ag	249,76d	i(m)	–	3.16 ± 0.29	13.3 ± 0.8	13.6 ± 1.0	11.3 ± 0.9
^{106m}Ag	8,28d	i(m)	–	–	2.47 ± 0.16	3.94 ± 0.28	4.15 ± 0.36
^{105}Ag	41,29d	c	–	–	1.53 ± 0.18	2.82 ± 0.28	3.56 ± 0.32
^{112}Pd	21,03h	c	55.5 ± 6.8	46.7 ± 5.5	40.6 ± 4.6	34.9 ± 3.8	29.9 ± 3.8
^{111m}Pd	5,5h	i(m)	10.2 ± 1.4	11.3 ± 1.5	14.7 ± 2.0	14.1 ± 2.0	9.58 ± 1.51
^{107}Rh	21,7m	c*	63.7 ± 7.6	57.1 ± 6.5	63.4 ± 7.1	58.2 ± 6.9	52.3 ± 6.6
^{106m}Rh	131m	i(m)	–	5.70 ± 0.43	18.6 ± 1.3	18.0 ± 1.5	14.8 ± 1.3
^{105}Rh	35,36h	i(m+g)	–	–	–	10.4 ± 3.6	18.0 ± 3.7
^{105}Rh	35,36h	c	57.5 ± 4.6	53.9 ± 4.0	73.9 ± 5.3	67.9 ± 5.4	56.7 ± 5.1
^{101m}Rh	4,34d	c	–	–	2.38 ± 0.22	3.95 ± 0.54	5.32 ± 0.57

Table 28, continued.

Product	$T_{1/2}$	Type	Yields [mbarn] at				
			0.1 GeV	0.2 GeV	0.8 GeV	1.2 GeV	1.6 GeV
^{100}Rh	20,8h	i(m+g)	–	–	1.34 ± 0.11	2.38 ± 0.19	3.08 ± 0.27
^{106}Ru	373,59d	c	59.8 ± 5.7	39.8 ± 4.1	44.0 ± 6.1	38.8 ± 3.1	31.3 ± 2.9
^{105}Ru	4,44h	c	60.8 ± 4.9	56.1 ± 3.8	60.0 ± 3.7	52.4 ± 3.8	42.3 ± 3.5
^{103}Ru	39,26d	c	61.1 ± 4.7	57.0 ± 3.8	75.9 ± 4.7	70.1 ± 5.4	57.0 ± 4.8
^{104}Tc	18,3m	c	55.1 ± 4.8	45.4 ± 3.4	41.4 ± 3.3	34.2 ± 2.9	35.8 ± 3.6
^{101}Tc	14,22m	c	64.2 ± 7.5	55.3 ± 5.2	63.5 ± 7.3	52.7 ± 8.9	50.8 ± 9.0
^{101}Tc	14,22m	i	–	7.19 ± 2.89	–	–	–
^{99m}Tc	6,01h	i(m)	–	–	3.95 ± 0.35	3.95 ± 0.38	3.30 ± 0.34
^{99m}Tc	6,01h	c	54.5 ± 4.4	47.6 ± 3.4	60.1 ± 4.2	57.3 ± 4.5	48.3 ± 4.2
^{96}Tc	4,28d	i(m+g)	–	–	2.16 ± 0.18	3.84 ± 0.36	4.34 ± 0.41
^{95}Tc	20,0h	c*	–	–	0.964 ± 0.077	2.23 ± 0.17	3.15 ± 0.27
^{101}Mo	14,61m	c	62.6 ± 5.5	49.8 ± 3.7	50.2 ± 4.0	48.2 ± 5.0	45.5 ± 5.6
^{99}Mo	65,94h	c	62.9 ± 5.0	54.7 ± 3.9	65.7 ± 4.6	61.0 ± 4.4	51.5 ± 4.5
^{93m}Mo	6,85h	i(m)	–	–	0.951 ± 0.074	1.88 ± 0.15	2.45 ± 0.22
^{98m}Nb	51,3m	i(m)	8.96 ± 0.80	11.4 ± 0.8	18.5 ± 1.2	16.7 ± 1.3	14.0 ± 1.2
^{96}Nb	23,35h	i	1.86 ± 0.16	4.45 ± 0.32	17.6 ± 1.1	19.3 ± 1.4	16.5 ± 1.5
^{95}Nb	34,975d	i(m+g)	–	1.88 ± 0.58	16.7 ± 1.1	19.5 ± 1.4	17.7 ± 1.5
^{95}Nb	34,975d	c	54.6 ± 4.6	48.6 ± 4.3	70.1 ± 4.4	67.9 ± 4.9	60.3 ± 5.0
^{92m}Nb	10,15d	i(m)	–	–	0.496 ± 0.044	0.609 ± 0.090	0.869 ± 0.082
^{90}Nb	14,60h	c*	–	–	0.807 ± 0.064	1.89 ± 0.14	2.51 ± 0.21
^{97}Zr	16,744h	c	50.1 ± 3.8	39.5 ± 2.6	35.3 ± 2.3	31.9 ± 2.3	27.1 ± 2.3
^{95}Zr	64,02d	c	52.8 ± 3.9	46.2 ± 3.0	50.9 ± 3.2	46.3 ± 3.3	39.4 ± 3.5
^{89}Zr	78,41h	c	–	–	3.05 ± 0.20	5.83 ± 0.43	6.98 ± 0.58
^{88}Zr	83,4d	c	–	–	1.04 ± 0.08	2.27 ± 0.18	2.96 ± 0.25
^{94}Y	18,7m	i	46.3 ± 4.4	34.6 ± 3.1	34.0 ± 2.9	34.2 ± 3.2	31.7 ± 3.5
^{93}Y	10,18h	c	44.8 ± 5.8	38.6 ± 4.7	38.7 ± 6.4	37.3 ± 4.7	33.4 ± 5.7
^{92}Y	3,54h	c	50.4 ± 7.0	44.6 ± 6.0	50.5 ± 6.7	45.9 ± 6.4	40.8 ± 5.9
^{92}Y	3,54h	i	15.0 ± 2.7	15.7 ± 2.8	20.8 ± 3.7	15.4 ± 3.5	17.4 ± 3.5
^{91m}Y	49,71m	i(m)	–	–	16.5 ± 1.1	17.9 ± 1.3	–
^{91m}Y	49,71m	c	–	–	36.2 ± 2.3	35.1 ± 2.6	13.8 ± 23.7
^{90m}Y	3,19h	i(m)	0.765 ± 0.077	2.12 ± 0.14	12.3 ± 0.8	14.8 ± 1.1	14.5 ± 1.5
^{88}Y	106,65d	i(m+g)	–	1.14 ± 0.34	6.74 ± 0.52	10.9 ± 0.8	11.2 ± 0.9
^{88}Y	106,65d	c	–	2.44 ± 0.45	7.62 ± 0.50	12.9 ± 0.9	14.2 ± 1.2
^{87}Y	79,8h	c	–	–	3.28 ± 0.22	6.54 ± 0.48	7.75 ± 0.65
^{86}Y	14,74h	c	–	–	1.10 ± 0.08	2.56 ± 0.19	3.21 ± 0.27
^{92}Sr	2,71h	c	37.4 ± 3.6	30.7 ± 2.7	28.3 ± 2.4	25.9 ± 2.7	21.6 ± 2.2
^{91}Sr	9,63h	c	40.3 ± 3.3	34.5 ± 2.5	34.4 ± 2.1	30.6 ± 2.3	25.5 ± 2.2
^{85}Sr	64,84d	c	–	–	3.96 ± 0.32	7.16 ± 0.62	8.69 ± 0.82
^{83}Sr	32,41h	c	–	–	–	1.33 ± 0.63	1.69 ± 0.80
^{89}Rb	15,15m	c*	35.7 ± 3.3	28.9 ± 2.3	29.6 ± 2.4	28.1 ± 3.2	31.1 ± 4.4

Table 28, continued.

Product	$T_{1/2}$	Type	Yields [mbarn] at				
			0.1 GeV	0.2 GeV	0.8 GeV	1.2 GeV	1.6 GeV
^{88}Rb	17,78m	c	36.5 ± 3.6	31.7 ± 2.6	–	–	–
^{88}Rb	17,78m	i	10.3 ± 2.1	9.79 ± 1.41	–	–	–
^{86}Rb	18,631d	i(m+g)	–	–	15.8 ± 1.0	18.6 ± 1.4	17.5 ± 1.5
^{84m}Rb	20,26m	i(m)	–	–	–	7.85 ± 0.71	10.6 ± 1.0
^{83}Rb	86,2d	c	–	–	4.75 ± 0.40	8.99 ± 0.76	10.2 ± 1.0
^{82m}Rb	6,472h	i(m)	–	–	–	3.61 ± 0.35	4.17 ± 0.43
^{88}Kr	2,84h	c	24.2 ± 1.9	20.1 ± 1.4	16.4 ± 1.1	14.4 ± 1.3	13.0 ± 1.1
^{87}Kr	76,3m	c	26.0 ± 2.9	22.4 ± 2.3	20.6 ± 1.8	18.4 ± 1.7	15.8 ± 1.9
^{85m}Kr	4,480h	c	18.0 ± 1.5	15.5 ± 1.2	15.3 ± 1.4	13.9 ± 1.4	11.4 ± 1.2
^{84}Br	31,80m	c	14.4 ± 1.8	12.3 ± 1.5	–	–	–
^{82}Br	35,30h	i(m+g)	1.34 ± 0.13	2.88 ± 0.19	10.9 ± 0.7	12.1 ± 0.9	10.4 ± 0.9
^{77}Br	57,036h	c	–	–	1.13 ± 0.10	1.57 ± 0.15	2.42 ± 0.25
^{83}Se	22,3m	c	7.78 ± 1.00	6.81 ± 0.62	–	–	–
^{75}Se	119,779d	c	–	–	1.38 ± 0.17	2.99 ± 0.26	3.75 ± 0.34
^{78}As	90,7m	c	5.86 ± 1.00	6.04 ± 0.95	10.8 ± 1.2	11.0 ± 1.8	11.1 ± 1.5
^{78}As	90,7m	i	–	–	7.10 ± 0.94	8.23 ± 1.53	9.02 ± 1.36
^{76}As	1,0778d	i	–	–	5.68 ± 0.45	8.12 ± 0.70	8.36 ± 0.79
^{74}As	17,77d	i	–	–	2.85 ± 0.27	4.99 ± 0.50	5.96 ± 0.64
^{78}Ge	88m	c	3.61 ± 0.35	3.42 ± 0.26	3.70 ± 0.38	3.18 ± 0.38	2.78 ± 0.50
^{77}Ge	11,30h	c	2.38 ± 0.19	2.74 ± 0.19	4.21 ± 0.33	3.91 ± 0.34	2.85 ± 0.28
^{73}Ga	4,86h	c	1.68 ± 0.15	2.46 ± 0.18	6.32 ± 0.47	6.61 ± 0.54	6.74 ± 0.68
^{72}Ga	14,10h	i(m+g)	0.434 ± 0.174	0.747 ± 0.096	4.83 ± 0.39	5.84 ± 0.47	5.69 ± 0.55
^{72}Ga	14,10h	c	1.70 ± 0.17	2.51 ± 0.19	7.88 ± 0.57	8.97 ± 0.68	8.27 ± 0.82
^{72}Zn	46,5h	c	1.27 ± 0.18	1.77 ± 0.16	2.89 ± 0.21	2.88 ± 0.24	2.34 ± 0.23
^{71m}Zn	3,96h	c	0.600 ± 0.087	0.941 ± 0.075	3.07 ± 0.23	3.55 ± 0.30	3.05 ± 0.28
^{69m}Zn	13,76h	i(m)	–	–	3.33 ± 0.22	4.68 ± 0.34	4.70 ± 0.40
^{65}Zn	244,26d	c	–	–	–	1.41 ± 0.16	1.74 ± 0.26
^{66}Ni	54,6h	c	–	–	2.62 ± 0.24	3.23 ± 0.43	2.81 ± 0.44
^{58}Co	70,86d	i(m+g)	–	–	0.334 ± 0.043	0.831 ± 0.068	1.30 ± 0.16
^{59}Fe	44,472d	c	–	–	2.96 ± 0.28	4.34 ± 0.35	4.50 ± 0.39
^{56}Mn	2,5789h	c	–	–	–	3.72 ± 0.40	4.00 ± 0.45
^{54}Mn	312,11d	i	–	–	–	–	1.56 ± 0.22
^{48}V	15,9735d	c	–	–	0.203 ± 0.030	0.141 ± 0.038	0.252 ± 0.040
^{48}Sc	43,67h	i	–	–	0.573 ± 0.065	1.17 ± 0.11	1.40 ± 0.12
^{46}Sc	83,79d	i(m+g)	–	–	–	1.00 ± 0.10	1.77 ± 0.15
^{43}K	22,3h	c	–	–	0.503 ± 0.057	1.42 ± 0.11	1.91 ± 0.17
^{28}Mg	20,915h	c	–	–	0.295 ± 0.027	0.608 ± 0.052	1.02 ± 0.09
^{24}Na	14,9590h	c	0.386 ± 0.046	0.196 ± 0.023	–	1.27 ± 0.11	2.42 ± 0.22
^{7}Be	53,29d	i	–	–	3.91 ± 0.47	5.78 ± 1.23	5.82 ± 0.61

3.9 Experimental yields for ^{99}Tc irradiated with 0.1, 0.2, 0.8, 1.2, 1.6 GeV protons.

Table 29 presents the parameters of ^{99}Tc irradiations. Table 30 presents the yields of residual nuclide products measured.

Table 29: Parameters of ^{99}Tc irradiation.

E_p (GeV)	Sample weight (mg)	Monitor weight (mg)	Irradiation duration (min)	Proton Flux p/cm^2	Number of measured γ -spectra of sample/monitor	EXPDATA index
0.1	56.6	163.1	50	7.0×10^{12}	37 / 11	tc99100
0.2	48.4	169.5	40	1.8×10^{13}	31 / 10	tc99200
0.8	57.7	122.9	60	4.0×10^{13}	41 / 20	tc99800
1.2	47.6	186.0	16	1.1×10^{13}	44 / 9	tc9912g
1.6	52.5	49.9	45	2.3×10^{13}	32 / 10	tc9916g

Table 30: Experimental yields from ^{99}Tc irradiated with 0.1, 0.2, 0.8, 1.2, 1.6 GeV protons.

Product	$T_{1/2}$	Type	Yields [mbarn] at				
			0.1 GeV	0.2 GeV	0.8 GeV	1.2 GeV	1.6 GeV
^{97}Ru	2,791d	i	32.4 ± 2.5	14.0 ± 1.0	3.58 ± 0.23	4.02 ± 0.33	2.28 ± 0.23
^{95}Ru	1,643h	i	18.1 ± 1.6	6.30 ± 0.60	1.66 ± 0.17	1.40 ± 0.11	1.05 ± 0.21
^{94}Ru	51,8m	i	7.28 ± 0.80	2.31 ± 0.30	0.692 ± 0.176	–	–
^{99m}Tc	6,01h	i(m)	–	7.42 ± 0.60	7.22 ± 0.48	8.78 ± 0.78	7.20 ± 0.63
^{96}Tc	4,28d	i(m+g)	98.0 ± 7.4	50.0 ± 3.4	26.7 ± 1.6	27.2 ± 2.1	21.0 ± 1.8
^{95m}Tc	61d	i(m)	–	–	4.10 ± 0.33	–	–
^{95}Tc	20,0h	c	107. ± 8.	49.0 ± 3.4	21.2 ± 1.3	20.1 ± 1.5	15.2 ± 1.3
^{94m}Tc	52,0m	i(m)	16.3 ± 1.6	8.68 ± 0.78	–	–	–
^{94m}Tc	52,0m	c	23.3 ± 1.8	10.8 ± 0.8	3.92 ± 0.29	3.35 ± 0.29	2.40 ± 0.25
^{94}Tc	293m	i	62.4 ± 4.7	27.4 ± 1.8	10.7 ± 0.6	9.58 ± 0.71	7.73 ± 0.65
^{93m}Tc	43,5m	c	2.76 ± 0.25	1.58 ± 0.16	–	–	–
^{93}Tc	2,75h	c	50.9 ± 4.0	21.7 ± 1.5	8.03 ± 0.51	6.85 ± 0.62	5.21 ± 0.47
^{93m}Mo	6,85h	i(m)	16.0 ± 1.2	10.9 ± 0.8	6.51 ± 0.41	6.06 ± 0.47	4.65 ± 0.40
^{90}Mo	5,56h	c	4.50 ± 0.39	7.06 ± 0.59	4.56 ± 0.35	3.96 ± 0.36	2.78 ± 0.36
^{97}Nb	72,1m	i(m+g)	–	0.447 ± 0.054	–	–	–
^{96}Nb	23,35h	i	–	–	3.21 ± 0.21	3.30 ± 0.38	2.97 ± 0.28
^{95m}Nb	86,6h	i(m)	–	–	4.30 ± 0.77	–	–
^{95}Nb	34,975d	i(m+g)	–	–	5.85 ± 0.36	6.27 ± 0.85	5.09 ± 0.46
^{95}Nb	34,975d	i	–	–	1.55 ± 0.73	–	–
^{92m}Nb	10,15d	i(m)	6.96 ± 0.66	5.47 ± 0.42	4.38 ± 0.27	5.18 ± 0.60	3.55 ± 0.38
^{90}Nb	14,60h	i(m1+m2+g)	27.0 ± 2.2	35.0 ± 2.4	27.9 ± 1.7	25.1 ± 2.0	19.1 ± 1.6
^{90}Nb	14,60h	c	31.6 ± 2.4	41.9 ± 2.8	32.6 ± 2.0	28.4 ± 2.2	21.5 ± 1.9
^{89m}Nb	66m	i(m)	–	1.97 ± 0.36	–	1.98 ± 0.21	1.34 ± 0.18
^{89}Nb	2,03h	c	–	26.5 ± 3.8	25.0 ± 4.0	26.5 ± 6.5	15.6 ± 2.9

Table 30, continued.

Product	$T_{1/2}$	Type	Yields [mbarn] at				
			0.1 GeV	0.2 GeV	0.8 GeV	1.2 GeV	1.6 GeV
^{88m}Nb	7,8m	i(m)	–	–	–	3.23 ± 0.56	–
^{89}Zr	78,41h	c	8.80 ± 0.75	43.2 ± 2.9	44.8 ± 2.7	39.1 ± 2.9	29.6 ± 2.5
^{88}Zr	83,4d	c	–	28.3 ± 2.2	35.4 ± 2.2	31.4 ± 2.5	24.3 ± 2.1
^{87}Zr	1,68h	c	–	15.6 ± 1.2	23.5 ± 1.7	20.5 ± 1.9	12.8 ± 1.6
^{86}Zr	16,5h	c	–	5.09 ± 0.36	11.0 ± 0.7	9.44 ± 0.78	6.66 ± 0.59
^{90m}Y	3,19h	i(m)	–	–	1.28 ± 0.09	1.54 ± 0.13	1.30 ± 0.12
^{88}Y	106,65d	i(m+g)	–	8.43 ± 1.12	11.8 ± 0.8	13.2 ± 3.7	8.00 ± 0.75
^{88}Y	106,65d	c	–	34.6 ± 4.1	46.6 ± 3.1	36.9 ± 6.7	32.7 ± 3.4
^{87m}Y	13,37h	i(m)	–	8.83 ± 0.85	17.8 ± 1.5	16.2 ± 1.6	14.7 ± 1.6
^{87m}Y	13,37h	c	3.98 ± 0.34	24.5 ± 1.6	41.3 ± 2.5	36.7 ± 2.8	28.0 ± 2.4
^{87}Y	79,8h	c	4.05 ± 0.32	25.9 ± 1.8	44.2 ± 2.6	39.7 ± 2.9	30.2 ± 2.5
^{86m}Y	48m	i(m)	–	7.56 ± 0.54	16.7 ± 1.1	15.7 ± 1.2	11.2 ± 1.0
^{86}Y	14,74h	i(m+g)	–	11.1 ± 0.8	25.0 ± 1.5	22.8 ± 1.7	17.2 ± 1.5
^{86}Y	14,74h	c	–	15.8 ± 1.1	35.8 ± 2.1	31.6 ± 2.4	23.6 ± 2.0
^{85m}Y	4,86h	c	–	5.16 ± 0.97	14.1 ± 1.3	15.4 ± 2.0	11.2 ± 1.9
^{85}Y	2,68h	c	–	2.06 ± 0.21	5.66 ± 0.99	5.98 ± 0.63	4.51 ± 0.50
^{84}Y	39,5m	c	–	2.64 ± 0.19	11.3 ± 0.7	10.5 ± 0.8	7.47 ± 0.65
^{85}Sr	64,84d	c	–	14.1 ± 1.5	41.0 ± 3.1	35.7 ± 4.9	32.8 ± 3.1
^{83}Sr	32,41h	c	–	4.06 ± 1.96	28.1 ± 7.6	27.9 ± 7.8	20.5 ± 5.7
^{82}Sr	25,55d	c	–	–	17.4 ± 1.4	–	13.5 ± 1.4
^{81}Sr	22,3m	c	–	–	3.83 ± 0.70	4.69 ± 0.76	4.22 ± 0.73
^{80}Sr	106,3m	c	–	–	1.70 ± 0.27	1.53 ± 0.29	1.49 ± 0.31
^{84m}Rb	20,26m	i(m)	–	0.626 ± 0.109	3.52 ± 0.31	3.78 ± 0.37	2.73 ± 0.31
^{84}Rb	32,77d	i(m+g)	–	–	4.99 ± 0.34	–	4.20 ± 0.39
^{83}Rb	86,2d	c	–	–	39.8 ± 2.9	39.6 ± 4.2	28.4 ± 2.8
^{82m}Rb	6,472h	i(m)	–	2.08 ± 0.17	14.9 ± 0.9	15.1 ± 1.1	11.1 ± 1.0
^{81}Rb	4,576h	c	–	2.12 ± 0.18	28.0 ± 2.0	28.7 ± 2.5	21.1 ± 2.0
^{79}Rb	22,9m	c*	–	–	6.63 ± 0.88	7.62 ± 0.71	5.12 ± 0.55
^{79}Kr	35,04h	c	–	–	22.6 ± 1.5	24.2 ± 1.9	20.0 ± 1.8
^{77}Kr	74,4m	c	–	–	8.22 ± 0.65	10.0 ± 0.9	7.72 ± 0.77
^{76}Kr	14,8h	c	–	–	2.48 ± 0.38	3.76 ± 0.89	2.94 ± 0.96
^{82}Br	35,30h	i(m+g)	–	–	–	–	0.370 ± 0.099
^{77}Br	57,036h	c	–	–	18.9 ± 1.3	23.6 ± 1.9	17.8 ± 1.6
^{76}Br	16,2h	i(m+g)	–	–	11.4 ± 0.8	13.7 ± 1.7	13.1 ± 1.6
^{76}Br	16,2h	c	–	–	13.4 ± 1.0	15.4 ± 2.5	17.3 ± 2.5
^{74m}Br	46m	i(m)	–	–	2.45 ± 0.28	3.18 ± 0.36	2.80 ± 0.34
^{75}Se	119,779d	c	–	–	18.1 ± 1.3	26.7 ± 3.3	21.4 ± 1.8
^{73m}Se	39,8m	c	–	–	–	5.80 ± 1.66	4.47 ± 1.44
^{73}Se	7,15h	c	–	–	7.35 ± 0.46	10.6 ± 0.8	9.27 ± 0.80
^{73}Se	7,15h	i	–	–	6.33 ± 0.87	6.36 ± 1.34	6.00 ± 1.17

Table 30, continued.

Product	$T_{1/2}$	Type	Yields [mbarn] at				
			0.1 GeV	0.2 GeV	0.8 GeV	1.2 GeV	1.6 GeV
^{72}Se	8,40d	c	–	–	2.93 ± 0.21	2.49 ± 1.10	–
^{74}As	17,77d	i	–	–	3.53 ± 0.33	6.27 ± 0.82	4.66 ± 0.51
^{72}As	26,0h	c	–	–	10.9 ± 0.7	16.0 ± 1.5	12.8 ± 1.8
^{72}As	26,0h	i	–	–	7.97 ± 0.55	11.5 ± 1.1	11.3 ± 1.3
^{71}As	65,28h	c	–	–	7.77 ± 0.52	13.1 ± 1.1	11.6 ± 1.0
^{70}As	52,6m	c	–	–	–	5.35 ± 0.56	3.82 ± 0.44
^{70}As	52,6m	i	–	–	–	4.70 ± 0.66	2.78 ± 0.57
^{69}Ge	39,05h	c	–	–	4.66 ± 0.50	–	8.92 ± 1.82
^{67}Ge	18,9m	c	–	–	0.840 ± 0.138	1.53 ± 0.17	1.43 ± 0.24
^{67}Ga	3,2612d	c	–	–	5.28 ± 0.52	14.8 ± 2.4	13.0 ± 1.2
^{66}Ga	9,49h	c*	–	–	2.80 ± 0.22	6.79 ± 0.63	6.77 ± 0.78
^{69m}Zn	13,76h	i(m)	–	–	–	1.11 ± 0.17	1.21 ± 0.22
^{65}Zn	244,26d	c	–	–	4.35 ± 0.53	–	12.8 ± 1.4
^{58}Co	70,86d	i(m+g)	–	–	1.33 ± 0.14	–	6.31 ± 0.56
^{56}Co	77,233d	c	–	–	–	–	1.56 ± 0.30
^{56}Mn	2,5789h	c	–	–	–	0.811 ± 0.098	1.12 ± 0.11
^{54}Mn	312,11d	i	–	–	–	–	7.24 ± 0.81
^{52}Mn	5,591d	c	–	–	0.273 ± 0.029	–	1.33 ± 0.12
^{48}V	15,9735d	c*	–	–	0.333 ± 0.029	–	1.71 ± 0.16
^{46}Sc	83,79d	i(m+g)	–	–	–	–	1.91 ± 0.27
^{41}Ar	109,34m	c	–	–	–	–	0.443 ± 0.073
^{24}Na	14,9590h	c	–	–	0.341 ± 0.038	0.911 ± 0.100	1.06 ± 0.12
^{7}Be	53,29d	i	–	–	4.16 ± 0.91	–	9.89 ± 1.77

3.10 Experimental yields for ^{59}Co irradiated with 0.2, 1.2, 1.6, 2.6 GeV protons.

Table 31 presents the parameters of ^{59}Co irradiations. Table 32 presents the yields of residual nuclide products measured.

Table 31: Parameters of ^{59}Co irradiation.

E_p (GeV)	Sample weight (mg)	Monitor weight (mg)	Irradiation duration (min)	Proton Flux p/cm^2	Number of measured γ -spectra of sample/monitor	EXPDATA index
0.2	199.4	108.7	60	2.3×10^{13}	41 / 8	co59200
1.2	202.7	95.9	45	5.1×10^{13}	45 / 10	co5912g
1.6	197.0	140.2	60	8.5×10^{13}	40 / 10	co5916g
2.6	200.5	118.2	30	6.4×10^{13}	44 / 10	co5926g

Table 32: Experimental yields from ^{59}Co irradiated with 0.2, 1.2, 1.6, 2.6 GeV protons.

Product	$T_{1/2}$	Type	Yields [mbarn] at			
			0.2 GeV	1.2 GeV	1.6 GeV	2.6 GeV
^{57}Ni	35,60h	c	0.781 ± 0.074	0.274 ± 0.021	0.246 ± 0.020	0.223 ± 0.020
^{58m}Co	9,15h	i(m)	40.7 ± 3.7	32.9 ± 2.6	32.9 ± 3.0	29.5 ± 2.7
^{58}Co	70,86d	i(m+g)	63.5 ± 5.7	51.3 ± 3.7	50.1 ± 4.1	47.8 ± 3.9
^{58}Co	70,86d	i	22.8 ± 2.2	18.5 ± 1.7	17.3 ± 2.0	18.2 ± 1.8
^{57}Co	271,79d	c	49.2 ± 4.4	27.2 ± 1.9	26.0 ± 2.1	24.2 ± 2.0
^{56}Co	77,233d	c	15.8 ± 1.4	6.91 ± 0.48	6.31 ± 0.50	5.63 ± 0.45
^{55}Co	17,53h	c	2.53 ± 0.23	1.00 ± 0.08	0.905 ± 0.076	0.762 ± 0.065
^{59}Fe	44,472d	c	–	0.555 ± 0.043	0.583 ± 0.049	0.537 ± 0.048
^{52}Fe	8,275h	c	0.255 ± 0.024	0.165 ± 0.013	0.138 ± 0.012	0.120 ± 0.011
^{56}Mn	2,5789h	c	4.54 ± 0.41	5.94 ± 0.42	5.61 ± 0.45	4.99 ± 0.41
^{54}Mn	312,11d	i	35.8 ± 3.2	26.8 ± 1.9	24.5 ± 2.0	21.3 ± 1.8
^{52m}Mn	21,1m	i(m)	4.57 ± 0.43	3.17 ± 0.25	2.99 ± 0.26	2.45 ± 0.22
^{52m}Mn	21,1m	c	4.82 ± 0.45	3.37 ± 0.26	3.19 ± 0.28	2.61 ± 0.23
^{52}Mn	5,591d	c	12.0 ± 1.1	8.39 ± 0.59	7.29 ± 0.58	6.14 ± 0.50
^{51}Cr	27,7025d	c	31.4 ± 2.9	29.0 ± 2.2	25.3 ± 2.1	21.4 ± 1.8
^{49}Cr	42,3m	c	2.82 ± 0.28	3.64 ± 0.30	3.25 ± 0.29	2.61 ± 0.24
^{48}Cr	21,56h	c	0.252 ± 0.023	0.456 ± 0.034	0.390 ± 0.033	0.317 ± 0.027
^{48}V	15,9735d	c	8.43 ± 0.75	14.9 ± 1.0	13.0 ± 1.0	10.6 ± 0.9
^{48}Sc	43,67h	i	0.186 ± 0.017	0.785 ± 0.055	0.693 ± 0.058	0.625 ± 0.051
^{47}Sc	3,3492d	c	1.14 ± 0.10	4.11 ± 0.30	3.71 ± 0.30	3.20 ± 0.27
^{47}Sc	3,3492d	i	1.09 ± 0.10	4.03 ± 0.30	3.60 ± 0.30	3.12 ± 0.26
^{46}Sc	83,79d	i(m+g)	2.52 ± 0.26	9.91 ± 0.70	8.84 ± 0.71	7.42 ± 0.60
^{44m}Sc	58,6h	i(m)	1.28 ± 0.11	7.91 ± 0.58	7.01 ± 0.58	5.85 ± 0.48
^{44}Sc	3,927h	i(m+g)	2.41 ± 0.22	14.7 ± 1.1	13.2 ± 1.1	10.9 ± 0.9

Table 32, continued.

Product	$T_{1/2}$	Type	Yields [mbarn] at			
			0.2 GeV	1.2 GeV	1.6 GeV	2.6 GeV
^{44}Sc	3,927h	i	1.17 ± 0.11	7.10 ± 0.52	6.47 ± 0.53	5.30 ± 0.44
^{43}Sc	3,891h	c	0.491 ± 0.048	4.64 ± 0.37	4.22 ± 0.37	3.46 ± 0.31
^{47}Ca	4,536d	c	0.051 ± 0.009	0.087 ± 0.010	0.099 ± 0.010	0.082 ± 0.010
^{43}K	22,3h	c	0.107 ± 0.010	1.70 ± 0.12	1.64 ± 0.13	1.42 ± 0.11
^{42}K	12,360h	i	0.357 ± 0.033	5.15 ± 0.38	4.81 ± 0.39	4.17 ± 0.35
^{41}Ar	109,34m	c	0.036 ± 0.004	0.929 ± 0.068	0.918 ± 0.075	0.836 ± 0.070
^{39}Cl	55,6m	c	–	0.608 ± 0.045	0.630 ± 0.053	0.566 ± 0.049
^{38}Cl	37,24m	i(m+g)	–	2.01 ± 0.15	2.14 ± 0.18	1.93 ± 0.17
^{38}Cl	37,24m	c	–	2.07 ± 0.16	2.20 ± 0.19	2.00 ± 0.17
^{34m}Cl	32,00m	i(m)	–	0.670 ± 0.051	0.745 ± 0.064	0.704 ± 0.061
^{38}S	170,3m	c	–	0.064 ± 0.006	0.064 ± 0.006	0.066 ± 0.007
^{29}Al	6,56m	c	–	1.48 ± 0.20	2.36 ± 0.23	2.56 ± 0.24
^{28}Mg	20,915h	c	–	0.264 ± 0.019	0.353 ± 0.028	0.432 ± 0.035
^{27}Mg	9,462m	c	–	0.819 ± 0.089	1.43 ± 0.18	1.53 ± 0.14
^{24}Na	14,9590h	c	–	2.13 ± 0.16	2.88 ± 0.23	3.77 ± 0.31
^{22}Na	2,6019y	c	–	1.35 ± 0.16	1.74 ± 0.15	2.46 ± 0.22
^{7}Be	53,29d	i	–	5.52 ± 0.52	6.58 ± 0.66	8.78 ± 0.89

3.11 Experimental yields for ^{63}Cu irradiated with 0.2, 1.2, 1.6, 2.6 GeV protons.

Table 33 presents the parameters of ^{63}Cu irradiations. Table 34 presents the yields of residual nuclide products measured.

Table 33: Parameters of ^{63}Cu irradiation.

E_p (GeV)	Sample weight (mg)	Monitor weight (mg)	Irradiation duration (min)	Proton Flux p/cm^2	Number of measured γ -spectra of sample/monitor	EXPDATA index
0.2	85.3	118.6	54	1.5×10^{13}	38 / 7	cu63200
1.2	80.2	49.4	70	8.5×10^{13}	44 / 23	cu6312g
1.6	87.6	120.4	60	8.5×10^{13}	48 / 10	cu6316g
2.6	87.3	118.5	60	2.2×10^{13}	44 / 7	cu6326g

Table 34: Experimental yields from ^{63}Cu irradiated with 0.2, 1.2, 1.6, 2.6 GeV protons.

Product	$T_{1/2}$	Type	Yields [mbarn] at			
			0.2 GeV	1.2 GeV	1.6 GeV	2.6 GeV
^{63}Zn	38,47m	i	2.17 ± 0.33	1.33 ± 0.20	–	–
^{62}Zn	9,26h	i	2.06 ± 0.17	0.481 ± 0.053	0.328 ± 0.036	0.336 ± 0.035
^{61}Cu	3,333h	c	29.5 ± 3.0	14.9 ± 1.7	12.2 ± 1.5	12.6 ± 1.5
^{60}Cu	23,7m	c*	8.44 ± 0.57	3.46 ± 0.25	2.76 ± 0.23	2.62 ± 0.22
^{57}Ni	35,60h	c	2.16 ± 0.19	1.18 ± 0.10	0.824 ± 0.069	0.777 ± 0.074
^{56}Ni	5,9d	i	0.147 ± 0.011	0.086 ± 0.012	–	–
^{61}Co	1,650h	c	–	5.29 ± 1.92	–	–
^{60}Co	5,2714y	i(m+g)	9.43 ± 1.30	9.27 ± 0.68	6.74 ± 0.55	8.39 ± 0.88
^{58m}Co	9,15h	i(m)	26.8 ± 2.0	20.0 ± 2.9	12.1 ± 2.3	15.2 ± 1.6
^{58}Co	70,86d	i(m+g)	42.2 ± 2.8	31.0 ± 2.2	23.7 ± 1.9	23.1 ± 1.9
^{58}Co	70,86d	i	15.5 ± 1.4	11.0 ± 2.6	11.6 ± 2.2	7.97 ± 1.12
^{57}Co	271,79d	c	44.0 ± 2.9	29.5 ± 2.1	22.1 ± 1.8	21.5 ± 1.8
^{57}Co	271,79d	i	–	27.1 ± 2.0	–	–
^{56}Co	77,233d	c	14.1 ± 0.9	9.68 ± 0.67	7.10 ± 0.57	6.94 ± 0.57
^{55}Co	17,53h	c	2.28 ± 0.16	1.73 ± 0.13	1.28 ± 0.11	1.17 ± 0.10
^{59}Fe	44,472d	c	0.468 ± 0.065	0.931 ± 0.070	0.757 ± 0.065	0.757 ± 0.078
^{53}Fe	8,51m	c*	–	2.19 ± 0.37	–	–
^{52}Fe	8,275h	c	–	0.264 ± 0.021	–	–
^{52}Fe	8,275h	i	0.158 ± 0.012	–	0.194 ± 0.017	0.174 ± 0.016
^{56}Mn	2,5789h	c	1.73 ± 0.11	2.56 ± 0.18	2.03 ± 0.16	1.91 ± 0.16
^{54}Mn	312,11d	i	17.4 ± 1.2	21.7 ± 1.5	16.4 ± 1.3	15.4 ± 1.3
^{52m}Mn	21,1m	i(m)	2.25 ± 0.17	3.26 ± 0.26	2.53 ± 0.22	2.11 ± 0.19
^{52m}Mn	21,1m	c	2.39 ± 0.18	3.54 ± 0.28	2.75 ± 0.24	2.26 ± 0.20
^{52}Mn	5,591d	c	–	9.91 ± 0.70	–	–

Table 34, continued.

Product	$T_{1/2}$	Type	Yields [mbarn] at			
			0.2 GeV	1.2 GeV	1.6 GeV	2.6 GeV
^{52}Mn	5,591d	i	5.99 ± 0.39	–	7.35 ± 0.59	6.54 ± 0.54
^{51}Cr	27,7025d	c	12.8 ± 0.9	28.8 ± 2.2	21.7 ± 1.8	19.8 ± 1.7
^{49}Cr	42,3m	c	1.04 ± 0.09	4.08 ± 0.34	3.20 ± 0.29	2.78 ± 0.26
^{48}Cr	21,56h	c	–	0.558 ± 0.041	–	–
^{48}Cr	21,56h	i	0.084 ± 0.006	–	0.427 ± 0.035	0.383 ± 0.033
^{48}V	15,9735d	c	2.67 ± 0.17	15.2 ± 1.1	11.6 ± 0.9	10.6 ± 0.9
^{48}Sc	43,67h	i	–	0.581 ± 0.041	0.483 ± 0.039	0.451 ± 0.040
^{47}Sc	3,3492d	c	0.241 ± 0.017	3.31 ± 0.24	2.64 ± 0.22	2.50 ± 0.21
^{47}Sc	3,3492d	i	–	–	2.56 ± 0.21	2.43 ± 0.21
^{46}Sc	83,79d	i(m+g)	0.605 ± 0.062	8.29 ± 0.58	6.68 ± 0.55	6.37 ± 0.56
^{44m}Sc	58,6h	i(m)	0.308 ± 0.022	7.49 ± 0.58	6.44 ± 0.53	5.93 ± 0.51
^{44}Sc	3,927h	i(m+g)	0.548 ± 0.038	13.5 ± 1.0	11.0 ± 0.9	10.0 ± 0.8
^{44}Sc	3,927h	i	0.266 ± 0.019	6.34 ± 0.46	5.18 ± 0.42	4.57 ± 0.38
^{43}Sc	3,891h	c	–	4.72 ± 0.87	–	–
^{47}Ca	4,536d	c	–	0.071 ± 0.009	0.064 ± 0.009	0.065 ± 0.014
^{43}K	22,3h	c	–	1.28 ± 0.09	1.13 ± 0.09	1.10 ± 0.09
^{42}K	12,360h	i	–	4.09 ± 0.30	3.57 ± 0.30	3.51 ± 0.30
^{41}Ar	109,34m	c	–	0.708 ± 0.053	0.645 ± 0.053	0.683 ± 0.058
^{39}Cl	55,6m	c	–	0.442 ± 0.034	0.436 ± 0.037	0.479 ± 0.050
^{38}Cl	37,24m	c	–	1.50 ± 0.12	1.55 ± 0.13	1.64 ± 0.15
^{34m}Cl	32,00m	i(m)	–	0.585 ± 0.050	0.591 ± 0.053	0.676 ± 0.066
^{29}Al	6,56m	c	–	1.13 ± 0.14	1.56 ± 0.17	1.83 ± 0.49
^{28}Mg	20,915h	c	–	0.195 ± 0.014	0.245 ± 0.020	0.357 ± 0.030
^{27}Mg	9,462m	c	–	0.503 ± 0.074	0.713 ± 0.079	1.15 ± 0.15
^{24}Na	14,9590h	c	–	1.73 ± 0.12	2.16 ± 0.18	3.31 ± 0.28
^{22}Na	2,6019y	c	–	1.39 ± 0.20	1.45 ± 0.13	2.72 ± 0.90
^{7}Be	53,29d	i	–	5.47 ± 0.51	5.85 ± 0.59	8.71 ± 0.92

3.12 Experimental yields for ^{65}Cu irradiated with 0.2, 1.2, 1.6, 2.6 GeV protons.

Table 35 presents the parameters of ^{65}Cu irradiations. Table 36 presents the yields of residual nuclide products measured.

Table 35: Parameters of ^{65}Cu irradiation.

E_p (GeV)	Sample weight (mg)	Monitor weight (mg)	Irradiation duration (min)	Proton Flux p/cm^2	Number of measured γ -spectra of sample/monitor	EXPDATA index
0.2	80.0	120.3	60	1.7×10^{13}	40 / 8	cu65200
1.2	92.6	49.8	70	1.1×10^{14}	45 / 20	cu6512g
1.6	80.1	120.1	60	4.0×10^{13}	43 / 9	cu6516g
2.6	80.0	119.5	60	2.5×10^{13}	41 / 7	cu6526g

Table 36: Experimental yields from ^{65}Cu irradiated with 0.2, 1.2, 1.6, 2.6 GeV protons.

Product	$T_{1/2}$	Type	Yields [mbarn] at			
			0.2 GeV	1.2 GeV	1.6 GeV	2.6 GeV
^{65}Zn	244,26d	i	2.88 ± 0.22	1.73 ± 0.13	1.54 ± 0.15	2.19 ± 0.25
^{63}Zn	38,47m	i	4.34 ± 0.33	1.32 ± 0.26	–	–
^{62}Zn	9,26h	i	0.970 ± 0.087	0.219 ± 0.027	0.159 ± 0.023	0.147 ± 0.022
^{64}Cu	12,700h	i	68.1 ± 4.8	61.4 ± 4.7	62.5 ± 5.4	60.2 ± 5.4
^{61}Cu	3,333h	c	14.0 ± 1.5	5.42 ± 0.62	4.98 ± 0.60	4.06 ± 0.51
^{60}Cu	23,7m	c*	3.10 ± 0.21	1.08 ± 0.08	0.893 ± 0.076	0.770 ± 0.070
^{65}Ni	2,51719h	c	–	0.390 ± 0.043	–	0.348 ± 0.036
^{57}Ni	35,60h	c	0.572 ± 0.040	0.392 ± 0.035	0.311 ± 0.026	0.251 ± 0.023
^{56}Ni	5,9d	i	–	0.356 ± 0.084	–	–
^{62m}Co	13,91m	i(m)	1.17 ± 0.10	1.63 ± 0.11	1.63 ± 0.15	1.38 ± 0.13
^{61}Co	1,650h	c	5.11 ± 0.68	6.52 ± 0.87	7.40 ± 0.89	6.25 ± 1.11
^{60}Co	5,2714y	i(m+g)	19.9 ± 1.5	16.8 ± 1.2	15.7 ± 1.3	14.4 ± 1.3
^{58m}Co	9,15h	i(m)	23.9 ± 1.7	19.9 ± 2.2	16.0 ± 2.3	12.9 ± 1.5
^{58}Co	70,86d	i(m+g)	34.3 ± 2.3	25.4 ± 1.8	22.0 ± 1.8	19.4 ± 1.6
^{58}Co	70,86d	i	10.4 ± 1.0	5.47 ± 1.68	6.04 ± 1.96	6.44 ± 1.14
^{57}Co	271,79d	c	24.6 ± 1.6	18.6 ± 1.3	15.9 ± 1.3	13.7 ± 1.2
^{57}Co	271,79d	i	–	18.5 ± 1.3	–	–
^{56}Co	77,233d	c	5.95 ± 0.40	5.08 ± 0.36	4.35 ± 0.35	3.70 ± 0.32
^{55}Co	17,53h	c	0.681 ± 0.049	0.739 ± 0.056	0.600 ± 0.062	0.498 ± 0.046
^{59}Fe	44,472d	c	2.65 ± 0.19	4.19 ± 0.33	4.01 ± 0.33	3.75 ± 0.33
^{53}Fe	8,51m	c*	–	1.30 ± 0.43	–	–
^{52}Fe	8,275h	c	–	0.098 ± 0.016	0.074 ± 0.008	0.069 ± 0.006
^{56}Mn	2,5789h	c	3.49 ± 0.23	6.04 ± 0.43	5.53 ± 0.45	4.92 ± 0.41
^{54}Mn	312,11d	i	13.1 ± 0.9	22.5 ± 1.6	19.4 ± 1.6	16.4 ± 1.4

Table 36, continued.

Product	$T_{1/2}$	Type	Yields [mbarn] at			
			0.2 GeV	1.2 GeV	1.6 GeV	2.6 GeV
^{52m}Mn	21,1m	i(m)	0.802 ± 0.062	2.06 ± 0.16	1.77 ± 0.15	1.38 ± 0.13
^{52m}Mn	21,1m	c	0.839 ± 0.064	2.20 ± 0.17	1.87 ± 0.16	1.46 ± 0.14
^{52}Mn	5,591d	c	2.42 ± 0.16	6.69 ± 0.47	5.82 ± 0.47	4.70 ± 0.39
^{51}Cr	27,7025d	c	6.06 ± 0.46	23.5 ± 1.8	20.5 ± 1.7	17.1 ± 1.5
^{49}Cr	42,3m	c	–	2.40 ± 0.20	2.13 ± 0.20	1.75 ± 0.17
^{48}Cr	21,56h	c	–	0.260 ± 0.019	0.233 ± 0.019	0.192 ± 0.017
^{48}V	15,9735d	c	0.906 ± 0.061	11.0 ± 0.8	9.79 ± 0.78	8.21 ± 0.69
^{48}Sc	43,67h	i	0.055 ± 0.006	1.21 ± 0.09	1.16 ± 0.09	1.03 ± 0.09
^{47}Sc	3,3492d	c	0.248 ± 0.018	4.99 ± 0.36	4.77 ± 0.39	4.15 ± 0.36
^{47}Sc	3,3492d	i	–	4.81 ± 0.35	4.60 ± 0.38	4.00 ± 0.34
^{46}Sc	83,79d	i(m+g)	–	9.77 ± 0.68	9.34 ± 0.75	7.82 ± 0.66
^{44m}Sc	58,6h	i(m)	0.102 ± 0.009	5.91 ± 0.43	6.00 ± 0.50	5.17 ± 0.45
^{44}Sc	3,927h	i(m+g)	0.187 ± 0.015	10.4 ± 0.7	10.1 ± 0.8	8.75 ± 0.74
^{44}Sc	3,927h	i	0.084 ± 0.007	4.80 ± 0.35	4.66 ± 0.38	3.93 ± 0.33
^{43}Sc	3,891h	c	–	3.10 ± 0.76	–	–
^{47}Ca	4,536d	c	–	0.182 ± 0.014	0.174 ± 0.017	0.168 ± 0.020
^{43}K	22,3h	c	–	1.98 ± 0.14	2.07 ± 0.16	1.91 ± 0.16
^{42}K	12,360h	i	–	4.82 ± 0.35	5.25 ± 0.43	4.77 ± 0.41
^{41}Ar	109,34m	c	–	1.08 ± 0.08	1.22 ± 0.10	1.20 ± 0.10
^{39}Cl	55,6m	c	–	0.679 ± 0.051	0.788 ± 0.066	0.812 ± 0.071
^{38}Cl	37,24m	i(m+g)	–	1.90 ± 0.14	2.23 ± 0.19	2.10 ± 0.19
^{38}Cl	37,24m	c	–	1.99 ± 0.15	2.30 ± 0.19	2.21 ± 0.20
^{34m}Cl	32,00m	i(m)	–	0.329 ± 0.032	0.425 ± 0.042	0.483 ± 0.048
^{38}S	170,3m	c	–	0.073 ± 0.008	0.136 ± 0.025	0.111 ± 0.011
^{29}Al	6,56m	c	–	1.32 ± 0.14	1.71 ± 0.21	2.08 ± 0.22
^{28}Mg	20,915h	c	–	0.251 ± 0.018	0.385 ± 0.031	0.531 ± 0.045
^{27}Mg	9,462m	c	–	0.452 ± 0.068	1.08 ± 0.12	1.30 ± 0.19
^{24}Na	14,9590h	c	–	1.61 ± 0.13	2.54 ± 0.21	3.76 ± 0.32
^{22}Na	2,6019y	c	–	1.12 ± 0.11	–	–
^{7}Be	53,29d	i	–	4.50 ± 0.42	5.68 ± 0.58	7.40 ± 0.80

3.13 Experimental yields for ^{nat}Hg irradiated with 0.1, 0.2, 0.8, 2.6 GeV protons.

Table 37 presents the parameters of ^{nat}Hg irradiations. Table 38 presents the yields of residual nuclide products measured.

Table 37: Parameters of ^{nat}Hg irradiation.

E_p (GeV)	Sample weight (mg)	Monitor weight (mg)	Irradiation duration (min)	Proton Flux p/cm^2	Number of measured γ -spectra of sample/monitor	EXPDATA index
0.1	501.0	119.6	60	9.9×10^{12}	37 / 9	hgo100
0.2	502.3	118.8	45	2.0×10^{13}	48 / 8	hgo200
0.8	494.7	120.4	15	1.3×10^{13}	44 / 8	hgo800
1.6	501.2	118.6	30	8.4×10^{13}	45 / 8	hgo26g

Table 38: Experimental yields from ^{nat}Hg irradiated with 0.1, 0.2, 0.8, 2.6 GeV protons.

Product	$T_{1/2}$	Type	Yields [mbarn] at			
			0.1 GeV	0.2 GeV	0.8 GeV	2.6 GeV
^{202}Tl	12,23d	i	4.73 ± 0.37	2.00 ± 0.14	0.811 ± 0.070	–
^{201}Tl	72,912h	i(m+g)	13.7 ± 1.1	5.93 ± 0.47	–	–
^{200}Tl	26,1h	i(m+g)	23.7 ± 2.3	9.53 ± 0.87	5.00 ± 0.48	2.79 ± 1.43
^{199}Tl	7,42h	i(m+g)	38.8 ± 5.4	14.9 ± 2.0	4.70 ± 0.97	–
^{198m}Tl	1,87h	i(m1+m2)	39.6 ± 5.5	17.2 ± 2.3	–	–
^{197}Tl	2,84h	i(m+g)	112. ± 37.	35.9 ± 11.7	–	–
^{196m}Tl	1,41h	i(m)	158. ± 27.	39.2 ± 6.5	11.5 ± 2.0	8.29 ± 1.45
^{195}Tl	1,16h	i(m+g)	100. ± 10.	22.9 ± 2.6	–	–
^{194m}Tl	32,8m	i(m)	98.9 ± 9.2	18.2 ± 1.7	–	–
^{194}Tl	32,8m	i(m+g)	125. ± 16.	22.9 ± 2.3	6.30 ± 0.74	–
^{203}Hg	46,612d	c	9.63 ± 0.75	6.80 ± 0.48	8.99 ± 0.62	9.22 ± 0.78
^{199m}Hg	42,6m	i(m)	53.0 ± 6.1	26.9 ± 3.0	25.3 ± 2.1	23.2 ± 2.1
^{197m}Hg	23,8h	i(m)	88.5 ± 8.7	48.4 ± 4.5	29.8 ± 2.7	26.2 ± 2.7
^{197}Hg	64,14h	c	194. ± 18.	96.8 ± 9.4	–	–
^{195m}Hg	41,6h	i(m)	75.9 ± 7.2	47.7 ± 4.2	24.2 ± 2.4	17.8 ± 2.8
^{195}Hg	9,9h	c	194. ± 25.	69.2 ± 8.6	–	–
^{193m}Hg	11,8h	i(m)	56.3 ± 5.0	59.4 ± 4.9	20.8 ± 1.4	12.3 ± 1.0
^{192}Hg	4,85h	c	107. ± 9.	83.4 ± 6.8	26.8 ± 2.2	14.8 ± 1.5
^{190}Hg	20,0m	c*	8.48 ± 1.96	61.9 ± 10.8	15.8 ± 2.0	–
^{200m}Au	18,7h	i(m)	0.215 ± 0.036	0.343 ± 0.037	0.707 ± 0.114	0.664 ± 0.096
^{199}Au	3,139d	c	6.83 ± 0.56	11.8 ± 0.9	19.4 ± 1.4	–
^{198m}Au	2,27d	i(m)	1.01 ± 0.09	1.64 ± 0.12	1.91 ± 0.19	1.41 ± 0.31
^{198}Au	2,69517d	i(m+g)	7.80 ± 0.61	13.2 ± 0.9	18.8 ± 1.3	16.2 ± 1.4
^{198}Au	2,69517d	i	7.01 ± 0.59	11.7 ± 0.8	17.1 ± 1.2	14.8 ± 1.4

Table 38, continued.

Product	$T_{1/2}$	Type	Yields [mbarn] at			
			0.1 GeV	0.2 GeV	0.8 GeV	2.6 GeV
^{196m}Au	9,7h	i(m2)	2.71 ± 0.42	5.65 ± 0.82	–	–
^{196}Au	6,183d	i(m1+m2+g)	9.58 ± 0.75	18.7 ± 1.4	20.5 ± 1.4	17.1 ± 1.4
^{195}Au	186,098d	c	284. ± 33.	141. ± 15.	–	–
^{194}Au	38,02h	i(m1+m2+g)	10.6 ± 0.9	26.9 ± 2.0	24.9 ± 2.0	20.8 ± 2.1
^{192}Au	4,94h	i(m1+m2+g)	13.3 ± 5.2	27.8 ± 6.5	24.6 ± 4.3	17.6 ± 2.7
^{192}Au	4,94h	c	132. ± 13.	118. ± 14.	50.6 ± 8.1	34.8 ± 5.1
^{191}Au	3,18h	i(m+g)	–	68.6 ± 8.6	–	–
^{191}Au	3,18h	c	58.3 ± 9.6	100. ± 8.	44.7 ± 3.5	–
^{190}Au	42,8m	c	–	85.7 ± 9.1	42.7 ± 4.2	–
^{190}Au	42,8m	i	–	–	27.2 ± 3.7	–
^{189}Au	28,7m	c*	–	3.32 ± 0.69	–	–
^{191}Pt	2,802d	c	48.7 ± 4.4	94.2 ± 7.9	47.1 ± 4.9	26.0 ± 3.0
^{189}Pt	10,87h	c	9.22 ± 0.96	85.9 ± 7.6	53.8 ± 4.3	29.0 ± 3.5
^{188}Pt	10,2d	c	3.14 ± 0.27	60.1 ± 4.4	54.1 ± 4.1	25.2 ± 2.3
^{187}Pt	2,35h	c	–	37.2 ± 4.3	35.8 ± 6.6	–
^{186}Pt	2,08h	c	–	28.9 ± 2.2	42.9 ± 3.2	17.6 ± 1.6
^{194}Ir	171d	i(m2)	–	–	–	0.201 ± 0.020
^{192}Ir	73,831d	i(m1+g)	–	–	0.927 ± 0.071	0.749 ± 0.061
^{190}Ir	11,78d	i(m1+g)	–	0.506 ± 0.041	1.85 ± 0.14	1.27 ± 0.11
^{189}Ir	13,2d	c	–	–	58.3 ± 7.7	27.6 ± 3.6
^{188}Ir	41,5h	c	3.55 ± 0.37	64.3 ± 6.0	62.5 ± 6.8	28.1 ± 3.7
^{188}Ir	41,5h	i	0.217 ± 0.090	1.90 ± 0.43	6.92 ± 0.99	3.02 ± 0.88
^{187}Ir	10,5h	c	–	57.8 ± 5.9	–	–
^{186}Ir	16,64h	i	–	13.8 ± 1.1	27.8 ± 2.1	13.6 ± 1.2
^{185}Ir	14,4h	c*	–	17.8 ± 1.3	44.4 ± 3.1	20.0 ± 1.7
^{184}Ir	3,09h	c*	–	–	49.2 ± 4.5	20.8 ± 1.8
^{185}Os	93,6d	c	–	21.6 ± 1.5	55.8 ± 4.0	25.8 ± 2.1
^{183m}Os	9,9h	c*	–	5.75 ± 0.72	31.1 ± 2.1	13.5 ± 1.3
^{182}Os	22,10h	c	–	6.34 ± 0.60	58.6 ± 4.2	28.3 ± 2.3
^{181m}Os	105m	c	–	–	14.5 ± 3.4	–
^{183}Re	70,0d	c	–	9.72 ± 0.73	59.1 ± 4.1	25.9 ± 2.3
^{182}Re	12,7h	c	–	6.76 ± 0.70	60.0 ± 4.5	28.6 ± 2.8
^{181}Re	19,9h	c*	–	3.76 ± 0.51	57.9 ± 7.7	19.8 ± 3.4
^{179}Re	19,5m	c*	–	–	59.2 ± 5.9	24.5 ± 6.2
^{178}W	21,6d	c	–	–	–	17.7 ± 2.5
^{177}W	135m	c	–	–	46.9 ± 6.4	19.0 ± 2.7
^{176}Ta	8,09h	c	–	–	43.5 ± 4.0	19.9 ± 2.4
^{175}Ta	10,5h	c	–	–	44.5 ± 4.6	20.9 ± 2.6
^{174}Ta	1,14h	c	–	–	41.9 ± 4.4	22.1 ± 2.5
^{175}Hf	70d	c	–	–	44.3 ± 3.3	21.3 ± 1.9

Table 38, continued.

Product	$T_{1/2}$	Type	Yields [mbarn] at			
			0.1 GeV	0.2 GeV	0.8 GeV	2.6 GeV
^{173}Hf	23,6h	c*	–	–	46.9 ± 5.4	25.5 ± 2.3
^{172}Hf	1,87y	c	–	–	34.3 ± 2.4	19.1 ± 1.6
^{170}Hf	16,01h	c	–	–	29.7 ± 3.9	18.5 ± 2.0
^{173}Lu	1,37y	c	–	–	39.2 ± 3.1	22.2 ± 2.2
^{172}Lu	6,70d	i(m1+m2+g)	–	–	0.178 ± 0.050	–
^{172}Lu	6,70d	c	–	–	34.6 ± 2.4	19.2 ± 1.7
^{171}Lu	8,24d	c*	–	–	35.7 ± 2.5	22.3 ± 1.9
^{170}Lu	2,012d	c	–	–	32.6 ± 2.3	20.5 ± 1.8
^{169}Lu	34,06h	c	–	–	27.5 ± 1.9	17.6 ± 1.6
^{169}Yb	32,026d	c	–	–	32.4 ± 2.2	21.9 ± 1.9
^{166}Yb	56,7h	c	–	–	21.3 ± 1.5	20.0 ± 1.8
^{167}Tm	9,25d	c	–	–	27.3 ± 5.7	21.5 ± 3.0
^{165}Tm	30,06h	c	–	–	20.4 ± 1.6	21.7 ± 2.2
^{163}Tm	1,810h	c	–	–	16.6 ± 2.3	24.1 ± 2.5
^{161}Tm	33m	c*	–	–	–	17.0 ± 3.1
^{160}Er	28,58h	c	–	–	11.8 ± 1.4	21.1 ± 2.6
^{160m}Ho	5,02h	c	–	–	11.2 ± 1.7	21.6 ± 2.7
^{157}Dy	8,14h	c	–	–	6.91 ± 0.55	19.6 ± 1.8
^{155}Dy	9,9h	c*	–	–	5.34 ± 0.40	18.1 ± 1.6
^{152}Dy	2,38h	c	–	–	–	11.9 ± 1.0
^{155}Tb	5,32d	c	–	–	5.87 ± 0.58	18.4 ± 1.9
^{153}Tb	2,34d	c*	–	–	2.60 ± 0.25	14.5 ± 1.4
^{152}Tb	17,5h	c*	–	–	–	12.1 ± 1.1
^{151}Tb	17,609h	c	–	–	–	13.0 ± 1.2
^{150}Tb	3,48h	c	–	–	–	7.89 ± 1.30
^{149}Tb	4,118h	c	–	–	–	5.13 ± 0.45
^{148}Tb	60m	c	–	–	–	9.31 ± 0.74
^{153}Gd	240,4d	c	–	–	2.85 ± 0.55	15.5 ± 1.9
^{151}Gd	124d	c	–	–	–	13.6 ± 1.5
^{149}Gd	9,28d	c	–	–	2.09 ± 0.23	17.6 ± 1.5
^{147}Gd	38,06h	c	–	–	–	17.2 ± 1.7
^{146}Gd	48,27d	c	–	–	1.29 ± 0.12	16.0 ± 1.4
^{145}Gd	23,0m	c	–	–	–	10.5 ± 1.4
^{149}Eu	93,1d	c	–	–	–	17.0 ± 1.6
^{148}Eu	54,5d	i	–	–	–	0.725 ± 0.062
^{147}Eu	24,1d	c	–	–	1.83 ± 0.23	18.8 ± 1.6
^{146}Eu	4,61d	c	–	–	1.68 ± 0.23	18.4 ± 1.5
^{146}Eu	4,61d	i	–	–	0.430 ± 0.219	2.59 ± 0.23
^{145}Eu	5,93d	c	–	–	–	13.2 ± 1.2
^{139m}Nd	5,5h	i(m)	–	–	–	1.65 ± 0.26

Table 38, continued.

Product	$T_{1/2}$	Type	Yields [mbarn] at			
			0.1 GeV	0.2 GeV	0.8 GeV	2.6 GeV
^{136}Nd	50,65m	c	–	–	–	9.34 ± 1.09
^{139}Ce	137,640d	c	–	–	0.557 ± 0.058	14.7 ± 1.3
^{135}Ce	17,7h	c	–	–	–	12.9 ± 1.3
^{130}Ce	25m	c	–	–	–	6.53 ± 0.65
^{132}La	4,8h	c	–	–	–	8.73 ± 0.85
^{131}Ba	11,50d	c	–	–	–	10.9 ± 0.9
^{129}Cs	32,06h	c	–	–	–	12.1 ± 1.2
^{127}Xe	36,4d	c	–	–	–	9.61 ± 0.79
^{123}Xe	2,08h	c	–	–	–	10.4 ± 1.2
^{121m}Te	154d	i(m)	–	–	0.287 ± 0.050	0.523 ± 0.052
^{121}Te	19,16d	c	–	–	–	8.01 ± 0.80
^{119m}Te	4,70d	i(m)	–	–	0.321 ± 0.044	1.38 ± 0.12
^{119}Te	16,05h	c	–	–	–	5.23 ± 0.69
^{117}Te	62m	c	–	–	–	5.09 ± 0.51
^{120m}Sb	5,76d	i(m)	–	0.191 ± 0.018	–	–
^{118m}Sb	5,00h	i(m)	–	–	–	1.07 ± 0.11
^{115}Sb	32,1m	c*	–	–	–	5.53 ± 0.49
^{113}Sn	115,09d	c	–	–	–	4.33 ± 0.38
^{111}In	2,8047d	c	–	–	0.802 ± 0.081	4.66 ± 0.47
^{109}In	4,2h	c	–	–	–	3.43 ± 0.31
^{110m}Ag	249,76d	i(m)	–	0.429 ± 0.042	0.587 ± 0.060	0.347 ± 0.033
^{106m}Ag	8,28d	i(m)	–	–	0.876 ± 0.149	1.43 ± 0.14
^{105}Ag	41,29d	c	–	–	–	3.29 ± 0.27
^{100}Pd	3,63d	c	–	–	–	0.818 ± 0.082
^{101m}Rh	4,34d	c	0.093 ± 0.028	0.149 ± 0.017	–	2.92 ± 0.35
^{100}Rh	20,8h	i(m+g)	–	–	–	2.25 ± 0.39
^{100}Rh	20,8h	c	–	–	–	3.10 ± 0.47
^{99m}Rh	4,7h	c	–	–	–	1.80 ± 0.22
^{103}Ru	39,26d	c	1.05 ± 0.09	1.55 ± 0.11	1.78 ± 0.13	0.967 ± 0.111
^{97}Ru	2,791d	c	–	–	–	2.01 ± 0.25
^{96}Tc	4,28d	i(m+g)	–	–	0.947 ± 0.074	1.59 ± 0.16
^{96}Nb	23,35h	i	0.378 ± 0.064	0.954 ± 0.069	1.39 ± 0.12	–
^{95}Nb	34,975d	i(m+g)	0.205 ± 0.067	0.978 ± 0.070	1.84 ± 0.13	1.02 ± 0.10
^{95}Nb	34,975d	c	1.35 ± 0.20	1.93 ± 0.13	2.89 ± 0.19	1.53 ± 0.13
^{97}Zr	16,744h	c	0.411 ± 0.035	0.284 ± 0.020	–	–
^{95}Zr	64,02d	c	1.15 ± 0.23	0.956 ± 0.075	1.03 ± 0.08	0.512 ± 0.046
^{89}Zr	78,41h	c	–	0.173 ± 0.020	1.75 ± 0.12	3.27 ± 0.27
^{88}Zr	83,4d	c	–	–	0.843 ± 0.062	2.31 ± 0.21
^{88}Y	106,65d	i(m+g)	–	–	2.46 ± 0.23	2.21 ± 0.19
^{88}Y	106,65d	c	–	0.461 ± 0.037	3.06 ± 0.24	4.48 ± 0.37

Table 38, continued.

Product	$T_{1/2}$	Type	Yields [mbarn] at			
			0.1 GeV	0.2 GeV	0.8 GeV	2.6 GeV
^{87}Y	79,8h	c*	–	0.154 ± 0.013	2.57 ± 0.23	4.33 ± 0.35
^{85}Sr	64,84d	c	–	–	2.41 ± 0.20	3.94 ± 0.38
^{83}Sr	32,41h	c	–	–	–	1.66 ± 0.79
^{82}Sr	25,55d	c	–	–	–	0.945 ± 0.101
^{84}Rb	32,77d	i(m+g)	–	–	–	2.08 ± 0.18
^{83}Rb	86,2d	c	–	–	2.73 ± 0.28	4.19 ± 0.42
^{82m}Rb	6,472h	i(m)	–	–	1.51 ± 0.16	1.82 ± 0.17
^{82}Br	35,30h	i(m+g)	0.329 ± 0.034	0.664 ± 0.067	1.27 ± 0.10	0.720 ± 0.073
^{77}Br	57,036h	c	–	–	0.983 ± 0.176	2.50 ± 0.25
^{75}Se	119,779d	c	–	–	1.31 ± 0.11	2.69 ± 0.23
^{74}As	17,77d	i	–	0.195 ± 0.029	1.51 ± 0.16	1.97 ± 0.21
^{65}Zn	244,26d	c	–	–	–	1.88 ± 0.17
^{59}Fe	44,472d	c	–	–	0.717 ± 0.063	1.23 ± 0.11
^{54}Mn	312,11d	i	–	–	–	1.74 ± 0.14
^{52}Mn	5,591d	c	–	–	–	0.276 ± 0.028
^{51}Cr	27,7025d	c	–	–	–	1.26 ± 0.14
^{48}V	15,9735d	c	–	–	–	0.419 ± 0.034
^{48}Sc	43,67h	i	–	–	0.380 ± 0.042	0.843 ± 0.092
^{46}Sc	83,79d	i(m+g)	–	–	–	1.82 ± 0.16
^{44m}Sc	58,6h	i(m)	–	–	–	0.620 ± 0.068
^{28}Mg	20,915h	c	–	–	–	1.18 ± 0.11
^{24}Na	14,9590h	c	–	–	0.303 ± 0.042	4.46 ± 0.37
^{22}Na	2,6019y	c	–	–	–	0.677 ± 0.071

3.14 Experimental yields for ^{56}Fe irradiated with 2.6 GeV protons.

Table 39 presents the parameters of ^{56}Fe irradiation. Table 40 presents the yields of residual nuclide products measured.

Table 39: Parameters of ^{56}Fe irradiation.

E_p (GeV)	Sample weight (mg)	Monitor weight (mg)	Irradiation duration (min)	Proton Flux p/cm^2	Number of measured γ -spectra of sample/monitor	EXPDATA index
2.6	200.0	120.2	30	3.0×10^{13}	44 / 10	fe26g

Table 40: Experimental yields from ^{56}Fe irradiated with 2.6 GeV protons.

Product	$T_{1/2}$	Type	Yields [mbarn]
^{57}Co	271,79d	c	0.365 ± 0.033
^{56}Co	77,233d	c	1.02 ± 0.09
^{55}Co	17,53h	c	0.274 ± 0.025
^{53}Fe	8,51m	c*	2.44 ± 0.32
^{52}Fe	8,275h	c	0.232 ± 0.020
^{56}Mn	2,5789h	c	0.861 ± 0.072
^{54}Mn	312,11d	i	32.8 ± 2.7
^{52m}Mn	21,1m	i(m)	5.50 ± 0.49
^{52m}Mn	21,1m	c	5.73 ± 0.51
^{52}Mn	5,591d	c	7.02 ± 0.59
^{51}Cr	27,7025d	c	27.9 ± 2.4
^{49}Cr	42,3m	c	4.00 ± 0.35
^{48}Cr	21,56h	c	0.506 ± 0.043
^{48}V	15,9735d	c	13.4 ± 1.1
^{48}Sc	43,67h	i	0.428 ± 0.039
^{47}Sc	3,3492d	c	2.69 ± 0.23
^{46}Sc	83,79d	i(m+g)	7.18 ± 0.61
^{44m}Sc	58,6h	i(m)	6.40 ± 0.54
^{44}Sc	3,927h	i(m+g)	12.6 ± 1.1
^{44}Sc	3,927h	i	6.67 ± 0.56
^{43}Sc	3,891h	c	4.11 ± 0.37
^{47}Ca	4,536d	c	0.067 ± 0.017
^{43}K	22,3h	c	1.17 ± 0.10
^{42}K	12,360h	i	3.91 ± 0.33
^{41}Ar	109,34m	c	0.703 ± 0.060
^{39}Cl	55,6m	c	0.521 ± 0.045
^{38}Cl	37,24m	i(m+g)	1.72 ± 0.16
^{38}Cl	37,24m	c	1.77 ± 0.16
^{34m}Cl	32,00m	i(m)	0.870 ± 0.078
^{38}S	170,3m	c	0.055 ± 0.008
^{29}Al	6,56m	c	1.63 ± 0.30
^{28}Mg	20,915h	c	0.387 ± 0.033
^{27}Mg	9,462m	c	1.56 ± 0.15
^{24}Na	14,9590h	c	3.70 ± 0.32
^{22}Na	2,6019y	c	3.10 ± 0.29
^{7}Be	53,29d	i	8.95 ± 0.91

3.15 Experimental yields for ^{58}Ni irradiated with 2.6 GeV protons.

Table 41 presents the parameters of ^{58}Ni irradiation. Table 42 presents the yields of residual nuclide products measured.

Table 41: Parameters of ^{58}Ni irradiation.

E_p (GeV)	Sample weight (mg)	Monitor weight (mg)	Irradiation duration (min)	Proton Flux p/cm^2	Number of measured γ-spectra of sample/monitor	EXPDATA index
2.6	339.8	120.8	30	6.8×10^{13}	40 / 10	ni58-26g

Table 42: Experimental yields from ^{58}Ni irradiated with 2.6 GeV protons.

Product	$T_{1/2}$	Type	Yields [mbarn]
^{57}Ni	35,60h	c	30.7 ± 2.6
^{56}Ni	5,9d	i	2.56 ± 0.21
^{58}Co	70,86d	i(m+g)	6.21 ± 0.52
^{57}Co	271,79d	c	82.1 ± 6.7
^{57}Co	271,79d	i	50.8 ± 4.4
^{56}Co	77,233d	c	36.5 ± 3.0
^{56}Co	77,233d	i	33.5 ± 2.8
^{55}Co	17,53h	c	11.1 ± 0.9
^{53}Fe	8,51m	c*	4.12 ± 0.78
^{52}Fe	8,275h	c	1.55 ± 0.13
^{54}Mn	312,11d	i	9.90 ± 0.82
^{52m}Mn	21,1m	i(m)	7.09 ± 0.62
^{52m}Mn	21,1m	c	8.68 ± 0.75
^{52}Mn	5,591d	c	11.8 ± 1.0
^{51}Cr	27,7025d	c	28.4 ± 2.5
^{49}Cr	42,3m	c	8.08 ± 0.74
^{48}Cr	21,56h	c	1.65 ± 0.14
^{48}V	15,9735d	c	17.4 ± 1.4
^{48}Sc	43,67h	i	0.076 ± 0.017
^{47}Sc	3,3492d	c	0.794 ± 0.067
^{46}Sc	83,79d	i(m+g)	3.63 ± 0.30
^{44m}Sc	58,6h	i(m)	6.96 ± 0.59
^{44}Sc	3,927h	i(m+g)	13.9 ± 1.1
^{44}Sc	3,927h	i	7.11 ± 0.59
^{43}Sc	3,891h	c	6.21 ± 0.55
^{43}K	22,3h	c	0.411 ± 0.034
^{42}K	12,360h	i	1.94 ± 0.16
^{38}K	7,636m	i	0.957 ± 0.125
^{41}Ar	109,34m	c	0.240 ± 0.021
^{39}Cl	55,6m	c	0.183 ± 0.019
^{38}Cl	37,24m	i(m+g)	0.886 ± 0.078
^{34m}Cl	32,00m	i(m)	1.47 ± 0.12
^{29}Al	6,56m	c	1.28 ± 0.15
^{28}Mg	20,915h	c	0.206 ± 0.018
^{27}Mg	9,462m	c	0.710 ± 0.087
^{24}Na	14,9590h	c	2.92 ± 0.28
^{22}Na	2,6019y	c	3.64 ± 0.32
^{7}Be	53,29d	i	12.4 ± 1.3

3.16 Experimental yields for ^{93}Nb irradiated with 2.6 GeV protons.

Table 43 presents the parameters of ^{93}Nb irradiation. Table 44 presents the yields of residual nuclide products measured.

Table 43: Parameters of ^{93}Nb irradiation.

E_p (GeV)	Sample weight (mg)	Monitor weight (mg)	Irradiation duration (min)	Proton Flux p/cm^2	Number of measured γ -spectra of sample/monitor	EXPDATA index
2.6	9.0	119.5	40	1.1×10^{14}	39 / 10	nb93-26g

Table 44: Experimental yields from ^{93}Nb irradiated with 2.6 GeV protons.

Product	$T_{1/2}$	Type	Yields [mbarn]
^{93m}Mo	6,85h	i(m)	0.298 ± 0.044
^{90}Mo	5,56h	c	0.584 ± 0.069
^{92m}Nb	10,15d	i(m)	19.1 ± 1.6
^{90}Nb	14,60h	c	21.1 ± 1.7
^{89m}Nb	66m	i(m)	1.43 ± 0.15
^{88}Nb	14,5m	c*	2.36 ± 0.35
^{89}Zr	78,41h	c	39.4 ± 3.3
^{88}Zr	83,4d	c	27.8 ± 2.2
^{87}Zr	1,68h	c	13.8 ± 1.6
^{86}Zr	16,5h	c	5.92 ± 0.48
^{90m}Y	3,19h	i(m)	1.60 ± 0.14
^{88}Y	106,65d	i(m+g)	12.8 ± 1.1
^{88}Y	106,65d	c	40.9 ± 3.3
^{87m}Y	13,37h	i(m)	16.5 ± 1.8
^{87m}Y	13,37h	c	31.9 ± 3.1
^{87}Y	79,8h	c	34.9 ± 3.0
^{86m}Y	48m	i(m)	10.9 ± 1.0
^{86}Y	14,74h	i(m+g)	17.6 ± 1.4
^{86}Y	14,74h	c	23.3 ± 1.9
^{85m}Y	4,86h	c	9.91 ± 1.02
^{85}Y	2,68h	c	4.11 ± 0.42
^{84}Y	39,5m	c	7.04 ± 0.59
^{85}Sr	64,84d	c	30.8 ± 2.9
^{83}Sr	32,41h	c	18.8 ± 3.9

Table 44, continued.

Product	$T_{1/2}$	Type	Yields [mbarn]
^{82}Sr	25,55d	c	12.3 ± 1.2
^{81}Sr	22,3m	c	4.37 ± 0.80
^{84m}Rb	20,26m	i(m)	2.61 ± 0.24
^{84}Rb	32,77d	i(m+g)	3.86 ± 0.34
^{83}Rb	86,2d	c	28.5 ± 2.6
^{82m}Rb	6,472h	i(m)	10.3 ± 0.8
^{81}Rb	4,576h	c*	20.2 ± 1.8
^{79}Rb	22,9m	c	6.67 ± 0.73
^{85m}Kr	4,480h	c	0.166 ± 0.047
^{79}Kr	35,04h	c	18.9 ± 1.7
^{77}Kr	74,4m	c	7.60 ± 0.65
^{76}Kr	14,8h	c	2.27 ± 0.20
^{77}Br	57,036h	c	17.0 ± 1.4
^{76}Br	16,2h	i(m+g)	10.6 ± 0.9
^{76}Br	16,2h	c	12.9 ± 1.1
^{74m}Br	46m	i(m)	2.89 ± 0.37
^{75}Se	119,779d	c	19.6 ± 1.6
^{73}Se	7,15h	c	7.99 ± 0.68
^{72}Se	8,40d	c	3.62 ± 0.44
^{74}As	17,77d	i	3.83 ± 0.37
^{72}As	26,0h	c	14.9 ± 1.4
^{72}As	26,0h	i	11.3 ± 1.0
^{71}As	65,28h	c	11.8 ± 1.0
^{70}As	52,6m	c	4.75 ± 0.49
^{69}Ge	39,05h	c	9.65 ± 1.22
^{67}Ge	18,9m	c	1.91 ± 0.22
^{67}Ga	3,2612d	c	14.5 ± 1.2
^{65}Ga	15,2m	c	2.32 ± 0.60
^{69m}Zn	13,76h	i(m)	0.205 ± 0.031
^{65}Zn	244,26d	c	14.4 ± 1.3
^{62}Zn	9,26h	c	1.44 ± 0.23
^{61}Cu	3,333h	c	5.19 ± 0.99
^{60}Cu	23,7m	c	0.832 ± 0.138
^{57}Ni	35,60h	c	0.207 ± 0.026
^{60}Co	5,2714y	i(m+g)	9.24 ± 0.99
^{58}Co	70,86d	i(m+g)	8.97 ± 0.77
^{57}Co	271,79d	c	7.68 ± 0.66
^{56}Co	77,233d	c	2.46 ± 0.26
^{55}Co	17,53h	c	0.318 ± 0.044
^{59}Fe	44,472d	c	0.779 ± 0.088

Table 44, continued.

Product	$T_{1/2}$	Type	Yields [mbarn]
^{56}Mn	2,5789h	c	1.54 ± 0.14
^{52m}Mn	21,1m	c	0.547 ± 0.090
^{52}Mn	5,591d	c	2.62 ± 0.23
^{51}Cr	27,7025d	c	7.86 ± 0.77
^{48}Cr	21,56h	c	0.084 ± 0.010
^{48}V	15,9735d	c	3.44 ± 0.28
^{48}Sc	43,67h	i	0.388 ± 0.033
^{47}Sc	3,3492d	c	1.62 ± 0.14
^{46}Sc	83,79d	i(m+g)	2.91 ± 0.26
^{44m}Sc	58,6h	i(m)	2.40 ± 0.21
^{44}Sc	3,927h	i(m+g)	3.18 ± 0.27
^{44}Sc	3,927h	i	0.787 ± 0.130
^{43}K	22,3h	c	0.760 ± 0.080
^{42}K	12,360h	i	1.79 ± 0.17
^{41}Ar	109,34m	c	0.505 ± 0.058
^{39}Cl	55,6m	c	0.464 ± 0.086
^{34m}Cl	32,00m	i(m)	1.93 ± 0.30
^{28}Mg	20,915h	c	0.326 ± 0.037
^{27}Mg	9,462m	c	0.634 ± 0.140
^{24}Na	14,9590h	c	2.50 ± 0.21
^{7}Be	53,29d	i	10.0 ± 1.1

3.17 Experimental yields for ^{208}Pb irradiated with 1.0 GeV protons.

Table 45 presents the parameters of ^{208}Pb irradiation. Table 46 presents the yields of residual nuclide products measured.

Table 45: Parameters of ^{208}Pb irradiation.

E_p (GeV)	Sample weight (mg)	Monitor weight (mg)	Irradiation duration (min)	Proton Flux p/cm^2	Number of measured γ -spectra of sample/monitor	EXPDATA index
1.0	120.7	120.9	60	5.2×10^{13}	47 / 10	pb081g

Table 46: Measured residual nuclide yields [mbarn] in в ^{208}Pb irradiated with 1.0 GeV protons together with results obtained at GSI [36] in inverce kimematics experiments and at ZSR on ^{nat}Pb [7].

Product	$T_{1/2}$[17], [18]	Type	Yield (this work)	Work [36]	Work [7]
^{206}Bi	6.243d	i	4.60 ± 0.29	–	5.36 ± 0.67
^{205}Bi	15.31d	i	6.20 ± 0.40	–	7.09 ± 0.90
^{204}Bi	11.22h	i(m1+m2+g)	5.29 ± 0.80	–	6.03 ± 0.95
^{203}Bi	11.76h	i(m+g)	4.84 ± 0.59	–	–
^{204m}Pb	67.2m	i(m)	11.0 ± 1.0	–	–
^{203}Pb	51.873h	c	31.5 ± 2.1	28.7 ± 3.1	–
^{201}Pb	9.33h	c*	26.9 ± 2.4	20.4 ± 1.9	–
^{200}Pb	21.5h	c	18.2 ± 1.2	18.2 ± 2.0	27.8 ± 3.5
^{198}Pb	2.4h	c	8.9 ± 2.1	14.0 ± 1.3	–
^{197m}Pb	43m	c*	17.9 ± 4.0	–	–
^{202}Tl	12.23d	c	18.8 ± 1.2	40.0 ± 4.0	22.0 ± 2.7
^{201}Tl	72.912h	c	43.7 ± 2.9	37.3 ± 3.7	53.5 ± 6.6
^{200}Tl	26.1h	c	40.6 ± 2.6	35.2 ± 3.7	–
^{200}Tl	26.1h	i(m+g)	22.7 ± 1.5	17.0 ± 1.7	22.3 ± 6.1
^{199}Tl	7.42h	c	38.5 ± 5.2	34.3 ± 3.4	–
^{198m1}Tl	1.87h	i(m1+m2)	17.6 ± 3.6	–	–
^{198}Tl	5.3h	c	35.9 ± 5.0	–	–
^{196m}Tl	1.41h	i(m)	34.8 ± 4.4	–	–
^{203}Hg	46.612d	c	4.03 ± 0.27	–	3.66 ± 0.45
^{197m}Hg	23.8h	i(m)	10.7 ± 0.7	–	–
^{195m}Hg	41.6h	i(m)	13.6 ± 2.0	–	13.3 ± 1.8
^{193m}Hg	11.8h	i(m)	18.9 ± 2.5	–	10.8 ± 2.3
^{192}Hg	4.85h	c	35.2 ± 2.8	31.3 ± 3.4	–
^{198m}Au	2.27d	i(m)	1.01 ± 0.14	–	1.25 ± 1.11
^{198}Au	2.69517d	i(m+g)	2.11 ± 0.22	1.96 ± 0.23	–
^{198}Au	2.69517d	i	1.09 ± 0.30	–	–
^{196}Au	6.183d	i(m1+m2+g)	4.13 ± 0.35	4.02 ± 0.47	3.88 ± 0.47
^{195}Au	186.09d	c	48.7 ± 5.5	28.4 ± 3.3	51.1 ± 6.6

Table 46 cont'd.

Product	$T_{1/2}$	Type	Yield (this work)	Work [36]	Work [7]
^{194}Au	38.02h	i(m1+m2+g)	7.06 ± 0.75	6.33 ± 0.75	6.85 ± 0.92
^{192}Au	4.94h	c	46.9 ± 6.6	39.9 ± 4.6	–
^{192}Au	4.94h	i(m1+m2+g)	11.6 ± 1.7	9.2 ± 1.1	–
^{191}Pt	2.9d	c	40.1 ± 4.4	44.4 ± 5.5	37.9 ± 4.8
^{189}Pt	10.87h	c	46.8 ± 4.8	40.4 ± 5.0	–
^{188}Pt	10.2d	c	40.5 ± 2.9	38.4 ± 4.7	42.8 ± 5.4
^{186}Pt	2.0h	c*	34.5 ± 2.4	32.9 ± 4.1	–
^{190}Ir	11.78d	i(m1+g)	0.69 ± 0.06	–	–
^{188}Ir	41.5h	c	43.2 ± 3.2	40.9 ± 5.4	–
^{188}Ir	41.5h	i	2.93 ± 0.69	2.48 ± 0.33	–
^{186}Ir	16.64h	i	20.8 ± 1.9	–	22.5 ± 3.1
^{185}Ir	14.4h	c*	34.8 ± 2.3	39.4 ± 5.2	39.4 ± 7.9
^{184}Ir	3.09h	c*	39.5 ± 3.0	36.9 ± 4.8	–
^{185}Os	93.6d	c	41.8 ± 2.8	38.1 ± 5.3	43.0 ± 5.3
^{183m}Os	9.9h	c	23.2 ± 1.5	–	–
^{182}Os	22.10h	c	42.0 ± 2.8	34.2 ± 4.8	–
^{183}Re	70.0d	c	41.7 ± 2.9	36.3 ± 5.3	38.2 ± 4.8
^{182m}Re	12.7h	c	45.2 ± 3.7	–	–
^{181}Re	19.9h	c	43.1 ± 5.9	37.0 ± 5.4	45.9 ± 5.9
^{179}Re	19.5m	c*	48.2 ± 4.2	44.7 ± 6.6	–
^{177}W	2.25h	c	30.1 ± 3.5	23.4 ± 3.6	–
^{176}W	2.5h	c	28.0 ± 3.9	29.0 ± 4.5	–
^{176}Ta	8.09h	c	35.0 ± 3.6	28.8 ± 4.7	–
^{173}Ta	3.14h	c	31.0 ± 3.9	26.3 ± 4.3	–
^{172}Ta	36.8m	c*	17.3 ± 2.3	27.4 ± 4.5	–
^{175}Hf	70d	c	31.3 ± 2.3	28.3 ± 4.8	34.1 ± 4.1
^{173}Hf	23.6h	c	28.4 ± 2.6	25.2 ± 4.3	39.0 ± 4.9
^{172}Hf	1.87y	c	24.1 ± 1.6	24.6 ± 4.2	24.4 ± 3.1
^{171}Hf	12.1h	c	18.2 ± 2.8	22.9 ± 3.9	–
^{170}Hf	16.01h	c	22.1 ± 6.8	20.3 ± 3.5	21.2 ± 3.0
^{172}Lu	6.70d	c	23.9 ± 1.7	24.7 ± 4.4	–
^{172}Lu	6.70d	i(m1+m2+g)	0.19 ± 0.05	0.183 ± 0.037	–
^{171}Lu	8.24d	c	26.1 ± 1.8	16.6 ± 3.0	31.3 ± 3.9
^{170}Lu	2.012d	c	21.7 ± 2.9	20.9 ± 3.7	–
^{169}Lu	34.06h	c	18.6 ± 1.2	12.1 ± 2.2	26.4 ± 3.7
^{169}Yb	32.026d	c	20.9 ± 1.5	18.1 ± 3.4	24.3 ± 3.0
^{166}Yb	56.7h	c	16.1 ± 1.1	13.7 ± 2.6	16.4 ± 2.3
^{167}Tm	9.25d	c	19.4 ± 4.0	14.0 ± 2.7	21.2 ± 2.6
^{165}Tm	30.06h	c	14.4 ± 1.4	13.3 ± 2.6	–
^{160}Er	28.58h	c	8.8 ± 0.6	7.2 ± 1.5	–
^{157}Dy	8.14h	c	5.73 ± 0.45	5.0 ± 1.1	–
^{155}Dy	9.9h	c*	3.66 ± 0.27	2.86 ± 0.63	–

Table 46 cont'd.

Product	$T_{1/2}$	Type	Yield (this work)	Work [36]	Work [7]
^{155}Tb	5.32d	c	4.16 ± 0.39	2.72 ± 0.62	5.52 ± 0.70
^{153}Tb	2.34d	c*	2.52 ± 0.25	2.40 ± 0.54	2.51 ± 0.40
^{152}Tb	17.5h	c*	2.10 ± 0.17	–	–
^{153}Gd	241.6d	c	2.60 ± 0.23	2.18 ± 0.51	3.10 ± 0.38
^{149}Gd	9.28d	c	2.24 ± 0.18	–	3.06 ± 0.38
^{146}Gd	48.27d	c	1.26 ± 0.09	1.23 ± 0.29	1.68 ± 0.21
^{147}Eu	24d	c	0.98 ± 0.31	1.18 ± 0.29	1.97 ± 0.29
^{146}Eu	4.59d	c	1.63 ± 0.11	1.17 ± 0.28	–
^{146}Eu	4.59d	i	0.37 ± 0.05	0.181 ± 0.047	–
^{143}Pm	265d	c	1.02 ± 0.13	0.85 ± 0.22	1.00 ± 0.13
^{139}Ce	137.640d	c	0.83 ± 0.06	0.45 ± 0.13	0.82 ± 0.10
^{121m}Te	154d	i(m)	0.44 ± 0.04	–	0.53 ± 0.07
^{121}Te	16.78d	c	1.11 ± 0.11	–	0.79 ± 0.10
^{119m}Te	4.70d	i(m)	0.40 ± 0.04	–	–
^{120m}Sb	5.76d	i(m)	0.54 ± 0.05	–	0.53 ± 0.07
^{114m}In	49.51d	i(m1+m2)	0.95 ± 0.19	–	1.07 ± 0.16
^{110m}Ag	249.79d	i(m)	1.12 ± 0.09	–	1.32 ± 0.17
^{106m}Ag	8.28d	i(m)	0.89 ± 0.08	–	0.92 ± 0.14
^{105}Ag	41.29d	c	0.65 ± 0.12	0.74 ± 0.17	1.04 ± 0.14
^{105}Rh	35.36h	c	4.63 ± 0.54	3.13 ± 0.51	–
^{101m}Rh	4.34d	c	1.29 ± 0.16	–	–
^{103}Ru	39.26d	c	3.84 ± 0.26	3.03 ± 0.50	4.11 ± 0.53
^{96}Tc	4.28d	i(m+g)	1.20 ± 0.09	–	1.49 ± 0.19
^{95}Tc	20.0h	c	1.38 ± 0.13	–	–
^{96}Nb	23.35h	i	2.31 ± 0.19	2.13 ± 0.34	–
^{95}Nb	34.975d	c	5.41 ± 0.34	–	–
^{95}Nb	34.975d	i(m+g)	3.03 ± 0.20	–	3.58 ± 0.56
^{95}Zr	64.02d	c	2.34 ± 0.15	1.58 ± 0.28	2.32 ± 0.29
^{89}Zr	78.41h	c	2.30 ± 0.16	–	2.82 ± 0.35
^{88}Zr	83.4d	c	0.76 ± 0.08	0.97 ± 0.15	1.19 ± 0.15
^{90m}Y	3.19h	i(m)	4.82 ± 0.39	–	–
^{88}Y	106.65d	c	4.03 ± 0.27	3.72 ± 0.58	–
^{88}Y	106.65d	i(m+g)	3.41 ± 0.25	2.76 ± 0.44	3.74 ± 0.46
^{87}Y	79.8h	c*	2.94 ± 0.23	–	3.36 ± 0.42
^{85}Sr	64.84d	c	2.76 ± 0.22	–	3.42 ± 0.41
^{86}Rb	18.631d	i(m+g)	5.48 ± 0.66	2.43 ± 0.38	4.39 ± 0.61
^{83}Rb	86.2d	c	3.46 ± 0.28	2.82 ± 0.45	3.96 ± 0.49
^{82m}Rb	6.472h	i(m)	2.73 ± 0.30	–	–
^{82}Br	35.30h	i(m+g)	2.17 ± 0.14	1.55 ± 0.24	2.62 ± 0.50
^{75}Se	119.770d	c	1.34 ± 0.09	1.18 ± 0.19	1.61 ± 0.20
^{74}As	17.77d	i	1.86 ± 0.18	1.66 ± 0.27	2.24 ± 0.28
^{59}Fe	44.503d	c	0.91 ± 0.08	0.69 ± 0.11	1.05 ± 0.14
^{65}Zn	244.26d	c	0.79 ± 0.19	0.42 ± 0.07	0.66 ± 0.17
^{46}Sc	83.810d	i(m+g)	0.35 ± 0.06	–	0.37 ± 0.05

3.18 Comparison of the reported results with the results obtained elesewhere

As shown by analyzing the EXFOR database, the data obtained elsewhere, which could have been compared with the reported results, are actually absent because the isotopic compositions of the irradiated samples are discordant and the interaction energies are not identical. Nevertheless, Tables 47, 46, and 49 present the comparison results for three experiments, which are alike as regards the above parameters (see Table 50), for this seems to be essential for confirming the reliability of the results obtained,

The criteria for comparison between the experimental data sets obtained at ITEP and elsewhere were chosen to be the "coincidence criteria" described in detail in Subsections 4.1: (1) Statistics of the respective ratios and (2) their mean squared deviation factor <F> (considering that $\sigma_{cal,i}$ was replaced by $\sigma_{exp,i}$ elsewhere). In this case, therefore, criterion (2) is interpreted to be the mean deviation of a dataset obtained at a laboratory from an identical dataset obtained at another laboratory.

It should be noted that the extent, to which the compared results prove to coincide when analyzing their statistical distributions (see Figs. 22 and 23), is determined by the deviation of the center of mass of the respective histogram from unity (in case the values obtained at diffrent laboratories are the same).

It should be borne in mind, however, that the physical and methodological features of the intercompared experiments preclude their treatment as equivalued parts in the comparison. In this sense, the analysis of the comparison results is expedient to begin with Table 47, which presents the results of the inter-laboratory comparison between the results obtained at ITEP (102 yields) and JAERI (45 yields measured with a VHTRC detector and 25 yields measured with a FNS detector; the two detectors have measured 50 nuclides) for the reaction product yields in the ITEP 1.2 GeV proton-irradiated ^{63}Cu and ^{65}Cu samples. Fig. 22 shows the comparison histogram. The disagreement in results is readily seen to be due only to the methodological features of the respective γ-spectrometric measurements, so the relevant histograms must be expected to approach a symmetry with respect to unity.

The validity of this conclusion is supported by the nuclear data of Table 48, which are used to calculate the ^{65,63}Cu(p,x) reaction product yields. The respective monitor reaction cross sections are presented in Table 12. The comparison results displayed in Fig. 22 are quite accordant with the expectation (the mean <F> value is 1.08).

A somewhat larger deviation of the comparison histogram centers from unity should be expected when comparing between the results obtained at ITEP and ZSR (Zentrum fuer Strahlenschuts und Radiooekologie der Universitaet Hannover); see Tables 46 and 49. Despite the fact that the results of the two groups have been obtained by the same experimental technique (direct gamma-spectrometry), the disagreement in the data may have arisen from the differences in the isotopic composition (the upper left-hand panel in Fig. 23), in the projectile proton energies (the upper right-hand panel in Fig. 23), in the selected monitor reactions, in the nuclear data used, etc. As should be expected, the mean squared deviation factor <F> = 1.23 in the case of ITEP-ZSR comparison is markedly higher than in the case of ITEP-JAERI comparison.

Unlike this report and ZSR, the GSR group (see Table 46) make use of quite a different methodological approach to determining the reaction product yields, namely, they use the inverse kinematics and physical detection of outgoing products. At the same time, the fact is worth emphasizing that the composition and energy (scaled per a nucleon in the case of a heavy-ion beam) were actually identical in the ITEP and GSI experiments.

So, any possible difference in the compared results can well be claimed to result solely from

Table 47: The experimental yields of metastable and ground states of ^{63,65}Cu(p,x) reaction products at E_p = 1.2 GeV measured at ITEP and JAERI.

Prod	$T_{1/2}$	Type	^{65}Cu			^{63}Cu		
			ITEP	JAERI		ITEP	JAERI	
			GC-2518	VHTRC	FNS	GC-2518	VHTRC	FNS
^{65}Zn	244.26d	i	1.73 ± 0.13	–	–	–	–	–
^{63}Zn	38.47m	i	1.32 ± 0.25	–	–	1.33 ± 0.21	–	–
^{62}Zn	9.26h	i	0.219 ± 0.020	0.33 ±0.08	–	0.481 ± 0.053	0.45 ± 0.14	–
^{64}Cu	12.700h	i	61.4 ± 4.7	–	–	–	–	–
^{61}Cu	3.333h	c	5.42 ± 0.62	–	–	14.9 ± 1.7	–	–
^{60}Cu	23.7m	c*	1.08 ± 0.08	–	–	3.46 ± 0.25	–	–
^{65}Ni	2.51719h	c	0.390 ± 0.040	–	–	–	–	–
^{57}Ni	35.60h	c	0.392 ± 0.035	0.38 ±0.05	–	1.18 ± 0.10	1.20 ± 0.13	–
^{56}Ni	5.9d	i	0.356 ± 0.080	–	–	0.086 ± 0.012	–	–
^{62m}Co	13.91m	i(m)	1.63 ± 0.11	–	–	–	–	–
^{61}Co	1.650h	c	6.52 ± 0.86	–	–	5.29 ± 1.92	–	–
^{60}Co	5.2714y	i(m+g)	16.8 ± 1.2	–	17.0 ± 1.9	9.27 ± 0.68	–	9.5 ± 1.1
^{58m}Co	9.15h	i(m)	19.9 ± 2.2	–	–	20.0 ± 2.9	–	–
^{58}Co	70.916d	i(m+g)	25.4 ± 1.8	25.8 ±2.8	25.4 ± 2.8	31.0 ± 2.2	31.1 ± 2.7	30.3 ± 3.4
^{58}Co	70.916d	i	5.47 ± 1.70	–	–	11.0 ± 2.6	–	–
^{57}Co	271.79d	c	18.6 ± 1.3	18.1 ± 2.0	18.7 ± 2.1	29.5 ± 2.1	28.3 ± 3.2	29.3 ± 3.3
^{57}Co	271.79d	i	18.5 ± 1.3	–	–	27.1 ± 2.0	–	–
^{56}Co	77.27d	c	5.08 ± 0.35	5.2 ± 0.6	5.2 ± 0.6	9.68 ± 0.67	10.0 ± 1.2	10.0 ± 1.1
^{55}Co	17.53h	c	0.739 ± 0.050	0.87 ± 0.11	–	1.73 ± 0.13	1.83 ± 0.23	–
^{59}Fe	44.503d	c	4.19 ± 0.33	4.5 ± 0.5	4.3 ± 0.5	0.931 ± 0.070	0.87 ± 0.13	1.0 ± 0.1
^{53}Fe	8.51m	c*	1.30 ± 0.42	–	–	2.19 ± 0.37	–	–
^{52}Fe	8.275h	c	0.098 ± 0.016	0.12 ± 0.02	–	0.264 ± 0.021	0.23 ± 0.05	–
^{56}Mn	2.5785h	c	6.04 ± 0.43	–	–	2.56 ± 0.18	–	–
^{54}Mn	312.12d	i	22.5 ± 1.6	22.6 ± 2.5	22.4 ± 2.5	21.7 ± 1.5	21.7 ± 2.5	20.9 ± 2.4
^{52}Mn	5.591d	c	6.69 ± 0.47	7.2 ± 0.8	6.6 ± 0.8	9.91 ± 0.70	10.3 ± 1.2	9.8 ± 1.2
^{52m}Mn	21.1m	c	2.20 ± 0.17	–	–	3.54 ± 0.28	–	–
^{52m}Mn	21.1m	i(m)	2.06 ± 0.16	–	–	3.26 ± 0.26	–	–
^{51}Cr	27.704d	c	23.5 ± 1.8	25.5 ± 2.8	24.1 ± 2.7	28.8 ± 2.2	31.3 ± 3.6	28.9 ± 3.2
^{49}Cr	42.3m	c	2.40 ± 0.20	–	–	4.08 ± 0.34	–	–
^{48}Cr	21.56h	c	0.260 ± 0.019	0.30 ± 0.04	–	0.558 ± 0.041	0.62 ± 0.07	–
^{48}V	15.9735d	c	11.0 ± 0.8	11.3 ± 1.3	10.8 ± 1.2	15.2 ± 1.1	15.4 ± 1.8	14.7 ± 1.7
^{48}Sc	43.67h	i	1.21 ± 0.09	1.32 ± 0.19	–	0.581 ± 0.041	0.60 ± 0.18	–
^{47}Sc	80.381h	c	4.99 ± 0.36	5.7 ± 0.6	–	3.31 ± 0.24	3.70 ± 0.15	–
^{47}Sc	80.381h	i	4.81 ± 0.35	–	–	3.18 ±0.23	–	–
^{46}Sc	83.810d	i(m+g)	9.77 ± 0.68	10.0 ± 1.1	9.8 ± 1.1	8.29 ± 0.58	8.4 ± 1.0	8.1 ± 0.9
^{44m}Sc	58.6h	i(m)	5.91 ± 0.43	6.5 ± 0.7	–	7.49 ± 0.58	8.1 ± 1.0	–
^{44}Sc	3.927h	i(m+g)	10.4 ± 0.7	–	–	13.5 ± 1.0	–	–
^{44}Sc	3.927h	i	4.80 ± 0.35	–	–	6.34 ± 0.46	–	–
^{43}Sc	3.891h	c	3.10 ± 0.76	–	–	4.72 ± 0.87	–	–
^{47}Ca	4.536d	c	0.182 ± 0.014	0.15 ± 0.02	–	0.071 ± 0.009	0.11 ± 0.04	–
^{43}K	22.3h	c	1.98 ± 0.14	2.16 ± 0.25	–	1.28 ± 0.09	1.39 ± 0.15	–
^{42}K	12.360h	i	4.82 ± 0.35	4.6 ± 0.5	–	4.09 ± 0.30	4.0 ± 0.5	–
^{41}Ar	109.34m	c	1.08 ± 0.07	–	–	0.708 ± 0.053	–	–
^{39}Cl	55.6m	c	0.679 ± 0.050	–	–	0.442 ± 0.034	–	–
^{38}Cl	37.24m	c	1.99 ± 0.15	–	–	1.50 ± 0.12	–	–
^{38}Cl	37.24m	i(m+g)	1.90 ± 0.14	–	–	–	–	–
^{34m}Cl	32.00m	i(m)	0.329 ± 0.030	–	–	0.585 ± 0.050	–	–
^{38}S	170.3m	c	0.073 ± 0.008	–	–	–	–	–
^{29}Al	6.56m	c	1.32 ± 0.14	–	–	1.13 ± 0.14	–	–
^{28}Mg	20.91h	c	0.251 ± 0.018	0.26 ± 0.05	–	0.195 ± 0.014	0.18 ± 0.05	–
^{27}Mg	9.462m	c	0.452 ± 0.068	–	–	0.503 ± 0.074	–	–
^{24}Na	14.9590h	c	1.61 ± 0.13	1.98 ± 0.23	–	1.73 ± 0.12	1.68 ± 0.19	–
^{22}Na	2.6019y	c	1.12 ± 0.11	–	0.98 ± 0.14	1.39 ± 0.20	–	1.34 ± 0.24
^{7}Be	53.29d	i	4.50 ± 0.42	5.0 ± 0.6	4.5 ± 0.6	5.47 ± 0.51	5.3 ± 0.7	5.7 ± 0.7

Table 48: Nuclear data used to calculate the ^{63,65}Cu(p,x) reaction products at E_p=1.2 GeV.

Nucleus	Half-life.	E_γ (кэВ)	η_γ^{ITEP} (%)	$\Delta\eta_\gamma^{ITEP}$ (%)	η_γ^{JAERI} (%)	$\Delta\eta_\gamma^{JAERI}$ (%)
^{65}Zn	243.9d	1115.5	50.6	2.4	50.6	0.24
^{62}Zn	9.26h	548.35	15.3	1.5		
		596.56	26.0	2.0	26.0	2.0
^{64}Cu	12.700h	1345.77	0.473	0.010		
^{61}Cu	3.408h	282.96	12.2	2.3		
		656.01	10.8	2.0		
		1185.23	3.7	0.7		
^{60}Cu	24.39m	826.4	21.7	1.1		
		1332.5	88.0	1.0		
		1791.6	45.4	2.4		
^{57}Ni	35.65h	127.1	16.7	0.5		
		1377.6	81.7	2.4	81.7	2.36
		1919.43	12.3	0.4		
^{62m}Co	13.91m	1163.5	69.6	0.8		
		1172.9	100.0	0.0		
^{60}Co	5.270y	1173.23	99.9736	0.0007	99.90	0.02
		1332.5	99.9956	0.0004		
^{58}Co	70.916d	810.77	99.448	0.008	99.45	0.01
^{58m}Co	9.11h	–	–	–		
^{57}Co	271.80d	122.06	85.60	1.70	85.6	0.17
		136.47	10.68	0.08		
^{56}Co	77.12d	846.76	100.00	0.03	99.94	0.03
		1037.84	14.13	0.05		
		1238.29	66.07	0.19		
		1771.35	15.48	0.05		
		2598.46	16.96	0.06		
^{55}Co	17.53h	477.20	20.20	1.70	20.18	1.79
		931.10	75.00	4.00	75.00	4.0
		1408.5	16.90	0.80		
^{59}Fe	44.496d	192.36	3.08	0.12		
		1099.25	56.50	1.90	56.5	1.84
		1291.6	43.2	1.4		
^{53}Fe	8.51 m	377.9	42	3		
^{52}Fe	8.275h	168.68	99.00	3.00	99.20	0.03
^{56}Mn	2.5785h	846.75	98.9	0.3		
		1810.7	27.2	0.8		
		2113.0	14.3	0.4		

Table 48 cont'd.

Nucleus	Half-life.	E_γ (кэВ)	η_γ^{ITEP} (%)	$\Delta\eta_\gamma^{ITEP}$ (%)	η_γ^{JAERI} (%)	$\Delta\eta_\gamma^{JAERI}$ (%)
^{54}Mn	312.12d	834.8	99.976	0.010	99.98	0.03
^{52}Mn	5.591d	744.2	90.0	0.9	89.05	0.39
		935.5	94.5	1.0		
		1333.61	5.07	0.06		
		1434.1	100.0	0.6		
^{52m}Mn	21.12m	1434.1	98.3	2		
^{51}Cr	27.704d	320.08	10.08	0.23	9.86	0.05
^{49}Cr	42.3m	90.63	53.2	1.9		
		152.93	30.3	1.1		
^{48}Cr	21.56h	112.31	96.0	2.1		
		308.24	100.0	2.0	100.0	2.0
^{48}V	15.974d	944.13	7.76	0.1		
		983.52	100.0	0.3	99.98	0.28
		1312.1	97.5	0.9		
		2240.4	2.41	0.04		
^{48}Sc	43.7h	175.36	7.48	0.1	7.48	0.10
		983.52	100.1	0.6	100.10	0.58
		1037.5	97.6	0.7		
		1312.1	100.1	0.7		
^{47}Sc	3.345d	159.38	68.3	0.4	67.9	1.5
^{46}Sc	83.810d	889.28	99.984	0.010	99.98	0.00
		1120.5	99.987	0.010		
^{44m}Sc	2.442d	271.24	86.7	0.3	86.75	0.30
		1157.0	1.20	0.07		
^{44}Sc	3.927h	1157.0	99.9	0.0		
^{43}Sc	3.891h	372.81	22.5	0.7		
^{47}Ca	4.537d	1297.09	71.0	7.0	74.1	9.0

Table 49: Experimental yields (in mbarn) of the metastable and ground states of ^{nat}Pb(p,x) reaction products obtained at ITEP at E_p = 1.5 GeV and at ZSR (Hannover) at E_p = 1.6 GeV.

		ITEP		ZSR (Hannover)	
Product	$T_{1/2}$	Type	Yield (mbarn)	Type	Yield (mbarn)
^{207} Bi	31.55y			i	4.09 ± 0.58
^{206} Bi	6.243d	i	3.54 ± 0.30	i	5.16 ± 0.61
^{205} Bi	15.31d	i	6.07 ± 0.59	i	7.18 ± 0.84
^{204} Bi	11.22h	i	5.00 ± 0.55		
^{204m} Pb	67.2m	c	13.2 ± 1.1		
^{204m} Pb	67.2m	i(m)	12.4 ± 1.1		
^{203} Pb	51.873h	c	36.5 ± 3.1	c	39.0 ± 4.3
^{203} Pb	51.873h	i	35.5 ± 3.4		
^{202m} Pb	3.53h	c	12.4 ± 1.4		
^{201} Pb	9.33h	c	27.0 ± 2.9		
^{200} Pb	21.5h	c	20.1 ± 1.9	c	19.2 ± 2.1
^{199} Pb	90m	c*	32.8 ± 6.1		
^{197m} Pb	43m	c*	14.8 ± 3.3		
^{202} Tl	12.23d	c	18.5 ± 1.6	c	19.7 ± 2.0
^{201} Tl	72.912h	c*	47.3 ± 4.1	c	46.2 ± 5.9
^{200} Tl	26.1h	c	40.7 ± 4.3		
^{200} Tl	26.1h	i	21.2 ± 2.5		
^{199} Tl	7.42h	c*	40.4 ± 4.9		
^{198} Tl	5.3h	c	29.8 ± 6.5		
^{194m} Tl	33.0m	i(m)	10.1 ± 1.2		
^{203} Hg	46.612d	c	3.72 ± 0.36		
^{197m} Hg	23.8h	i(m)	9.39 ± 0.91	c	8.32 ± 0.91
^{195m} Hg	41.6h	i(m)	14.4 ± 2.3	c	16.6 ± 1.8
^{193m} Hg	11.8h	i(m)	19.8 ± 3.4		
^{192} Hg	4.85h	c	30.4 ± 2.9		
^{199} Au	3.139d			c	6.02 ± 0.82
^{198} Au	2.69517d	i(m+g)	1.65 ± 0.76		
^{196} Au	6.183d	i(m1+m2+g)	3.47 ± 0.30	i	3.20 ± 0.35
^{195} Au	186.098d	c	58.2 ± 9.8	c	42.8 ± 4.8
^{194} Au	38.02h	i(m1+m2+g)	6.09 ± 0.73		
^{192} Au	4.94h	c	43.2 ± 6.4		
^{192} Au	4.94h	i(m1+m2+g)	9.63 ± 1.56		
^{191} Pt	2.802d	c	33.9 ± 3.7		
^{188} Pt	10.2d	c	32.2 ± 2.9	c	18.5 ± 2.1
^{192} Ir	73.827d			i	0.142 ± 0.032
^{186} Ir	16.64h	i	16.9 ± 1.5		
^{185} Ir	14.4h	c	25.0 ± 4.5		
^{184} Ir	3.09h	c*	33.6 ± 3.3		
^{185} Os	93.6d	c	33.6 ± 3.2	c	29.0 ± 3.3
^{183m} Os	9.9h	c*	18.7 ± 1.7		
^{182} Os	22.10h	c	37.6 ± 3.7		

Table 49, cont'd.

		ITEP		ZSR (Hannover)	
Product	$T_{1/2}$	Type	Yield (mbarn)	Type	Yield (mbarn)
^{183} Re	70.0d	c	34.5 ± 3.1		
^{182} Re	12.7h	c	41.0 ± 4.1		
^{181} Re	19.9h	c	32.9 ± 4.9		
^{179} Re	19.5m	c*	41.3 ± 4.2		
^{176} Ta	8.09h	c	34.1 ± 4.1		
^{175} Ta	10.5h	c	35.8 ± 4.2		
^{174} Ta	1.14h	c	24.5 ± 3.2		
^{173} Ta	3.14h	c	33.6 ± 4.7		
^{172} Ta	36.8m	c*	15.3 ± 2.1		
^{181} Hf	42.39d			i	0.192 ± 0.058
^{175} Hf	70d	c	31.9 ± 2.9	c	28.5 ± 3.0
^{173} Hf	23.6h	c	39.4 ± 3.6		
^{172} Hf	1.87y	c	27.9 ± 2.8	c	23.5 ± 2.5
^{170} Hf	16.01h	c	40.0 ± 9.0		
^{173} Lu	1.37y	c	34.3 ± 3.8	c	43.5 ± 4.7
^{171} Lu	8.24d	c	33.8 ± 3.0	c	30.7 ± 3.2
^{170} Lu	2.012d	c*	38.8 ± 4.3	c	39.8 ± 4.4
^{169} Lu	34.06h	c	26.0 ± 2.8		
^{169} Yb	32.026d	c	29.0 ± 2.9	c	28.0 ± 3.9
^{166} Yb	56.7h	c	27.3 ± 2.4	c	22.3 ± 3.4
^{168} Tm	93.1d			i	0.304 ± 0.077
^{167} Tm	9.25d	c	30.2 ± 6.3	c	28.2 ± 3.1
^{160} Er	28.58h	c	26.0 ± 4.3	c	23.3 ± 2.5
^{157} Dy	8.14h	c	21.1 ± 2.0		
^{155} Dy	9.9h	c	16.9 ± 1.6		
^{155} Tb	5.32d	c	16.4 ± 2.0	c	17.4 ± 2.1
^{153} Tb	2.34d	c*	13.7 ± 1.5	c	11.8 ± 1.3
^{151} Tb	17.609h	c	10.6 ± 1.4		
^{150} Tb	3.48h	c	4.89 ± 0.85		
^{153} Gd	241.4d	c	11.8 ± 1.2	c	11.8 ± 1.3
^{149} Gd	9.28d	c	11.7 ± 1.1		
^{147} Gd	38.06h	c	9.13 ± 1.02		
^{146} Gd	48.27d	c	9.07 ± 0.89	c	10.1 ± 1.0
^{152} Eu	13.537y			i	17.3 ± 3.2
^{147} Eu	24.1d	c	12.7 ± 2.5	c	10.8 ± 1.4
^{146} Eu	4.61d	c	10.5 ± 1.0		
^{146} Eu	4.61d	i	1.47 ± 0.19		
^{145} Eu	5.93d	c	7.31 ± 0.76	c	6.50 ± 0.90
^{144} Pm	363d			i	1.01 ± 0.16
^{143} Pm	265d	c	8.26 ± 0.97	c	6.77 ± 0.76
^{139} Ce	137.640d	c	5.20 ± 0.48	c	5.28 ± 0.55
^{133} Ba	3848.9d			c	3.49 ± 0.44

Table 49, cont'd.

		ITEP		ZSR (Hannover)	
Product	$T_{1/2}$	Type	Yield (mbarn)	Type	Yield (mbarn)
^{127} Xe	36.4d	c	2.37 ± 0.23		
^{123m} Te	119.7d			c	0.233 ± 0.035
^{121m} Te	154d			c	0.489 ± 0.071
^{121} Te	19.16d	c	1.82 ± 0.22	c	1.86 ± 0.21
^{119m} Te	4.70d	i(m)	0.616 ± 0.094	c	0.544 ± 0.094
^{124} Sb	60.20d			i	0.331 ± 0.057
^{120m} Sb	5.76d			i	0.430 ± 0.075
^{113} Sn	115.09d	c	1.18 ± 0.15		
^{114m} In	49.51d			i	1.01 ± 0.24
^{111} In	2.8047d	c	1.69 ± 0.16		
^{110m} Ag	249.79d			i	0.899 ± 0.119
^{106m} Ag	8.28d			i	1.02 ± 0.16
^{102} Rh	207d			i	1.49 ± 0.21
^{102m} Rh	2.9y			i	1.03 ± 0.16
^{101} Rh	3.3y			c	0.534 ± 0.085
^{101m} Rh	4.34d	c	2.14 ± 0.24	c	3.28 ± 0.40
^{103} Ru	39.26d	c	3.67 ± 0.34	c	2.92 ± 0.32
^{96} Tc	4.28d	i(m+g)	1.54 ± 0.16	i	1.61 ± 0.22
^{95m} Tc	61d			c	2.74 ± 0.43
^{99} Mo	65.94h	c	2.77 ± 0.36		
^{96} Nb	23.35h			i	7.34 ± 1.13
^{95} Nb	34.975d	c	4.98 ± 0.48		
^{95} Nb	34.975d	i	2.72 ± 0.30		
^{95} Zr	64.02d	c	2.26 ± 0.43	c	1.58 ± 0.18
^{89} Zr	78.41h	c	3.08 ± 0.27	c	2.64 ± 0.29
^{88} Zr	83.4d	c	1.44 ± 0.17		
^{90m} Y	3.19h	i(m)	3.24 ± 0.35		
^{88} Y	106.65d	c	2.99 ± 0.95		
^{87} Y	79.8h	c	4.27 ± 0.36		
^{85} Sr	64.84d	c	4.41 ± 0.50	c	3.77 ± 0.40
^{84} Rb	32.77d			i	5.71 ± 0.71
^{83} Rb	86.2d	c	5.21 ± 0.95	c	5.12 ± 0.69
^{82m} Rb	6.472h	i(m)	2.00 ± 0.27		
^{82} Br	35.30h	i(m+g)	1.89 ± 0.23	i	1.99 ± 0.31
^{75} Se	119.779d	c	1.67 ± 0.20	c	2.14 ± 0.26
^{74} As	17.77d	i	2.58 ± 0.30	i	2.29 ± 0.25
^{65} Zn	244.26d			c	1.14 ± 0.13
^{60} Co	5.2714y			c	1.18 ± 0.23
^{58} Co	70.86d			i	2.84 ± 0.31
^{59} Fe	44.503d			c	1.19 ± 0.15
^{54} Mn	312.11d	i	1.29 ± 0.21	i	0.860 ± 0.116
^{46} Sc	83.810d			i	0.834 ± 0.103

Table 50: Results of comparing among the experimental data obtained at ITEP, ZSR, and GSI.

Comparison set	Composition of irradiated samples, %	Energy (GeV)	<F>
ITEP JAERI	^{65}Cu (98.7)	1.2	1.14 (VHTRC) 1.04 (FNS)
	^{63}Cu (99.6)	1.2	1.12 (VHTRC) 1.03 (FNS)
Averaged <F> (ITEP-JAERI)			1.08
ITEP	^{nat}Pb	1.5	1.22
ZSR	^{nat}Pb	1.6	
ITEP	^{208}Pb (97.2)	1.0	1.24
ZSR	^{nat}Pb	1.0	
ITEP	^{208}Pb (97.2)	1.0	1.32
GSI	^{208}Pb (100)	1.0 A	
GSI	^{208}Pb (100)	1.0 A	1.46
ZSR	^{nat}Pb	1.0	

the methodological features of experimental design and from the selected nuclear data. The <F> value proved to be 1.32 (the bottom left-hand panel in Fig. 23). It may be tentatively concluded, therefore, that the methodological side of the measurements affects the consistency of the results to a greater extent in the given case, compared with the physical differences in the experimental designs (composition of samples, interaction energy).

At the same time, a possible effect of the above mentioned physical differences on the comparison results cannot be disregarded. This is corroborated, in particular, by a high <F> value (1.46) in the case of the ZSR-GSI comparison (the bottom right-hand panel in Fig. 23).

We are of the opinion that all the above is a ponderous argument for usage of isotopically pure samples to be irradiated in the reported type experiments, for they permit a correct comparison among the results obtained by different experimental techniques. At the same time, the accord of all the data analyzed here is, generally, quite satisfactory, the fact that may indicate a sufficiently high degree of reliability of the reported experimental data.

Table 46 compares between the results of ITEP (direct kinematics, p $\rightarrow$ $^{208}_{82}$Pb) and GSI (Inverse kinematics, $^{208}_{82}$Pb $\rightarrow$ $^{1}_{1}$H). In the given experiments, the energy of the extracted protons that irradiated the ^{208}Pb target, as well as the energy of each of the ^{208}Pb ion beam nucleons that irradiated the liquid hydrogen target, corresponded to 1 GeV.

Besides, Table 46 presents the reaction product yields obtained at ZSR in ^{nat}Pb interactions with 1 GeV protons. Since the ZSR data are the independent yields only, they were summarized with respect to the respective isobaric chains.

Fig. 23 shows the comparison histograms.

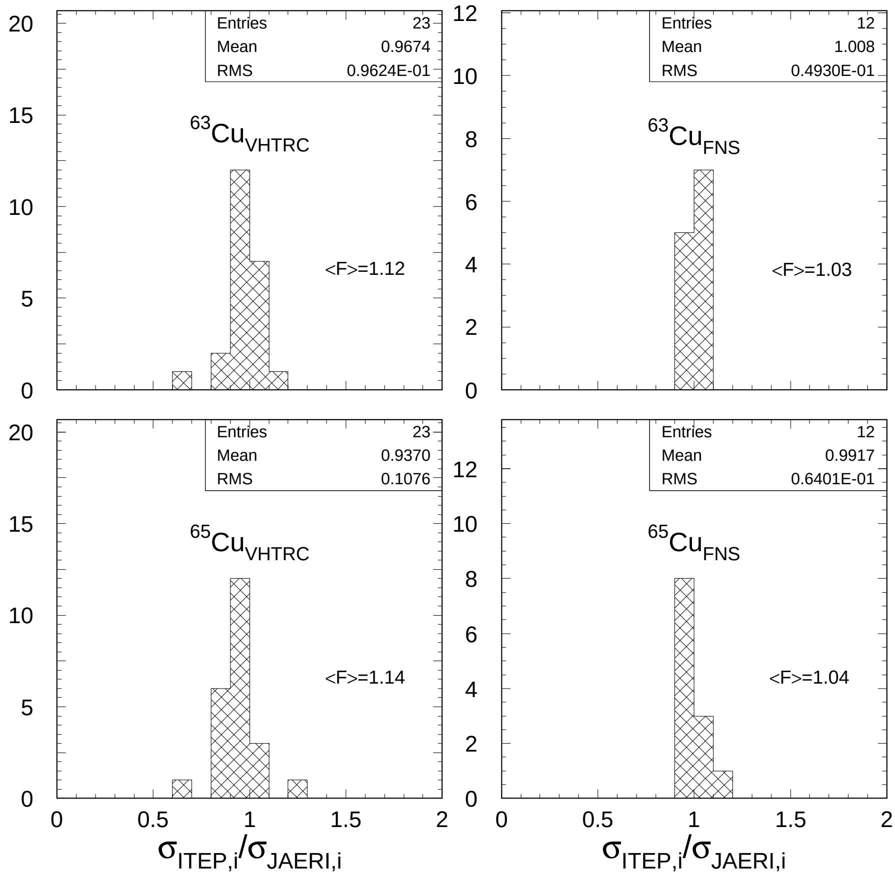

Fig. 22: Statistics of the ratios of the ITEP ^{63}Cu and ^{65}Cu results to the JAERI results.

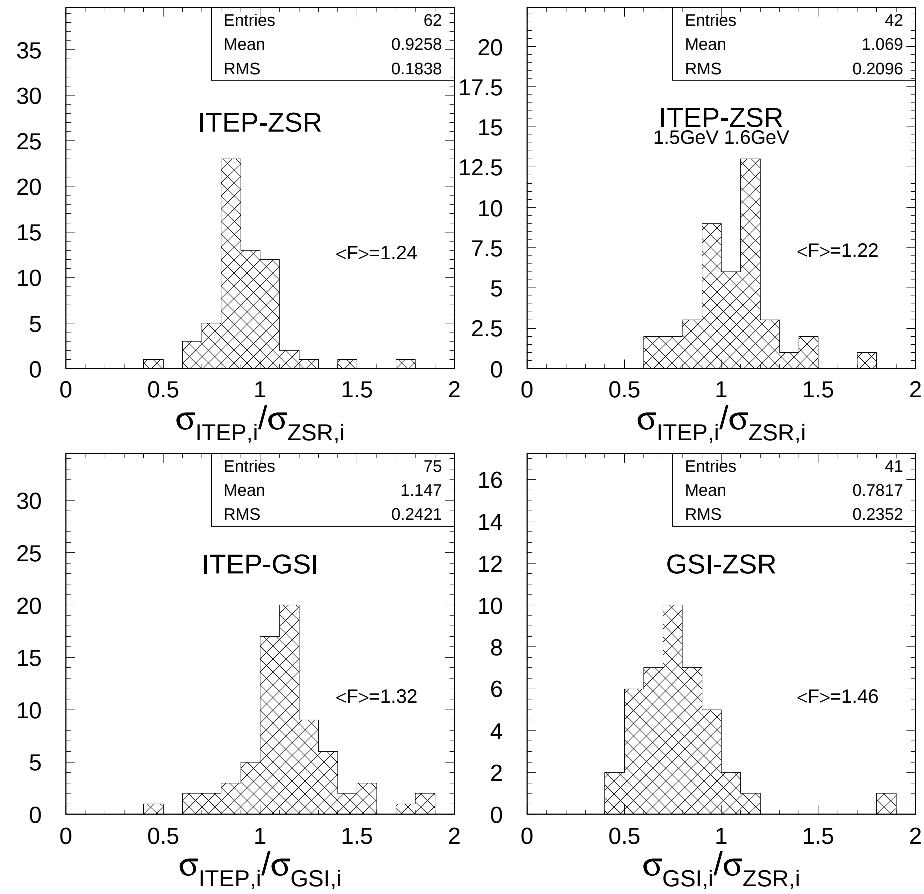

Fig. 23: Statistics of the ratios of : the ITEP ^{208}Pb results at E_p = 1.0 GeV to the ZSR ^{nat}Pb results at E_p = 1.0 GeV; the ITEP ^{nat}Pb results at E_p = 1.5 GeV to the ZSR ^{nat}Pb results at E_p = 1.6 GeV; the ITEP ^{208}Pb results at E_p = 1.0 GeV to the GSI ^{208}Pb results at E_p = 1.0 GeV; the GSI ^{208}Pb results at E_p = 1.0 GeV to the ZSR ^{208}Pb results at E_p = 1.0 GeV.

4 SIMULATION OF EXPERIMENTAL RESULTS BY THE CODES

4.1 The methods for comparing between experimental and simulated data

Contrary to the simulated data, the experimental results include not only independent, but also (and mainly) cumulative and supra cumulative, residual product nuclei yields. To get a correct comparison between the experimental and simulation data, the cumulative yields must be calculated on the basis of the simulated independent yields. If the production chain of n radioactive nuclei is presented as

$$\begin{array}{ccccccc} \sigma_1 & & \sigma_2 & & \dots & & \sigma_n \\ \downarrow & & \downarrow & & & & \downarrow \\ 1 & \xrightarrow{\nu_1} & 2 & \xrightarrow{\nu_2} & \dots & \xrightarrow{\nu_{n-1}} & n \end{array}$$

(where $\nu_1, ..., \nu_{n-1}$ are the branching ratios of the respective nuclides), the simulated cumulative and supra-cumulative yields of the n-th nuclide can be calculated as

$$\sigma_n^{cum} = \sigma_n^{ind} + \sum_{i=1}^{n-1} \left(\sigma_i^{ind} \prod_{j=i}^{n-1} \nu_j \right), \tag{90}$$

$$\sigma_n^{cum*} = \sigma_n^{ind} + \frac{\lambda_{n-1}}{\lambda_{n-1} - \lambda_n} \nu_{n-1} \times \left[\sigma_{n-1}^{ind} + \sum_{i=1}^{n-2} \left(\sigma_i^{ind} \prod_{j=i}^{n-2} \nu_j \right) \right] \quad . \tag{91}$$

The branching ratios of the decay chains were taken from [18], considering that the branched (due to isomeric transitions and α-decay) isobaric chains can always be presented to be a superposition of linear chains.

To get a correct comparison for the results obtained by different codes, the calculated yields values were renormalized to the same cross sections for inelastic proton-nucleus interactions. We calculated the cross sections via the semi-empirical formula [37] :

$$\begin{aligned} \sigma_{inel} &= 45A^{0.7} f(A) g(E), (\text{ in mb}) \\ f(A) &= 1 + 0.016 \sin(5.3 - 2.63 \log A), \\ g(E) &= 1 - 0.62 \exp(-E/200) \sin(10.9E^{-0.28}), \end{aligned} \tag{92}$$

where A is the mass number of the target, E is the energy (in MeV) of the projectile proton.

The calculated proton-nucleus inelastic cross sections of the targets are presented in Table 51.

The quantitative comparison between experimental and simulated yields is made by assessing the following two parameters (coincidence criteria):

- the number of "coincidences"taken to be the simulation-experiment difference not exceeding 30% ($N_{1.3}$: 0.77< $\sigma_{calc,i}/\sigma_{exp,i}$ <1.3) or factor 2 ($N_{2.0}$: 0.5< $\sigma_{calc}/\sigma_{exp}$ <2.0). The 30% level meets the accuracy requirements [38] of the cross sections for nuclide production to be used in designing the ADS plants. The simulation accuracy can be presented to be the ratio of the number of a such "coincidences"to the number of the comparison events.

- the mean-squared deviation factor between the simulated and experimental yields [6], [33]:

$$< F > = 10^{\sqrt{< \log{(\sigma_{cal,i}/\sigma_{exp,i})}^2 >}}, \tag{93}$$

with its standard deviation

$$S(< F >) = < (\log{(\sigma_{cal,i}/\sigma_{exp,i})} - \log(< F >))^2 >, \tag{94}$$

where <> designates averaging over all the experimental and simulated results used in the comparisons ($i = 1, ..., N_S$).

The mean-squared ratio $< F >$, together with its standard deviation $S(< F >)$, defines the interval $[< F > /S(< F >)\,, < F > \times S(< F >)]$ that covers about 2/3 of the simulation-to-experiment ratios. A logarithmic, rather than a linear, scale is preferable when determining the factor $< F >$, because the simulation-experiment differences may be as high as a few orders of magnitude.

Table 51: Inelastic proton-nucleus interaction cross sections [mbarn] calculated by formulae [37].

Target	Proton Energy (GeV)						
	0.1	0.2	0.8	1.0	1.2	1.6	2.6
^{182}W		1462	1683			1702	
^{183}W		1467	1690			1709	
^{184}W		1473	1696			1715	
^{186}W		1484	1709			1728	
^{232}Th	1924	1726	1989		2008	2011	
^{nat}U	1958	1757	2024		2044	2047	
^{99}Tc	1075	964	1110		1122	1123	
^{59}Co		677			789	789	789
^{63}Cu		708			824	825	825
^{65}Cu		724			842	843	843
^{nat}Hg	1741	1562	1799				1820
^{56}Fe							761
^{58}Ni							780
^{93}Nb							1076
^{nat}W							1714
^{208}Pb				1858			

4.2 The codes used to simulate the experimental results

The following 14 codes were used for simulation:

- the CEM95 cascade-exciton model code [39],
- the latest version of the improved cascade-exciton model [52] code, CEM2k, [53],
- the CASCADE cascade-evaporation-fission transport code [40],
- the INUCL cascade-preequilibrium-evaporation-fission code [41],
- the LAHET (both ISABEL and Bertini options) cascade-preequilibrium-evaporation-fission transport code [43],

– HETC cascade-evaporation transport code [42],

– the YIELDX semi-phenomenological code [44],

– the CASCADE/INPE cascade-evaporation-preequilibrium-fission-transport code [45].

– the CASCADO-IPPE cascade-evaporation-preequilibrium-fission-transport code.

– the GNASH code based on the Hauser-Feshbach and preequilibrium approach [46],

– the ALICE code with HMS precompound approach [47],

– the Quantum Molecular Dynamics (QMD) code [48],

– the NUCLEUS cascade – evaporation – fission code [49],

– the ALICE-IPPE code [55],

The detailed description of the codes may be found in [39]–[49], and a brief description in our earlier works [5], [6].

The default options were used in all the simulation codes without modifying the latter to get the optimal agreement with experimental data. All the calculations were made prio to obtaining any experimental results, except the results from CEM2k. With such an approach, our comparisons demonstrate the real predictive, rather than the descriptive power of the codes.

Since most of the simulation codes (except for GNASH) cannot simulate the metastable states of product nuclei, the respective nuclide chains used to calculate the cumulative yields of the product nuclei were simplified. It should be emphasized also, that the HETC and CEM95 codes were not used in comparisons with the experimental data for ^{nat}U and ^{232}Th as fission is the dominant mode of their reactions (CEM95 does not include description of fission reactions, it calculates only fission cross section but does not privide fission fragment yields).

4.3 Comparison of experiment with simulations

All the product nuclide yields simulated by the above codes are presented in Tables 65 – 113, together with the experimental values of the respective yields.

The results of quantitative comparison in two parameters described in section 4.1 are presented in Tables 52 – 61 which give quantitative information concerning the agreement of the simulated yields with experimental data for each of the simulation codes, namely:

– the total number of measured yields, N_E;

– of them, the number of the measured yields selected to be compared with calculations, N_G. For instance, in the case of 1 GeV proton-irradiated ^{208}Pb, some nuclides were discarded from the comparison in the following caSES:

1. The measured products are in metastable or just ground state, namely, ^{204m}Pb, ^{197m}Pb, ^{198m1}Tl, ^{196m}Tl, ^{197m}Hg, ^{195m}Hg, ^{193m}Hg, ^{198m}Au, ^{198g}Au, ^{186g}Ir, ^{183m}Os, ^{182m}Re, ^{121m}Te, ^{119m}Te, ^{120m}Sb, ^{114m}In, ^{110m}Ag, ^{106m}Ag, ^{101m}Rh, ^{90m}Y, and ^{82m}Rb;
2. Transfer of a metastable state to a product occurs outside the given decay chain, namely, ^{198}Tl, ^{190}Ir, ^{152}Tb, ^{149}Gd, ^{121}Te, ^{96}Tc, ^{95}Tc, ^{95}Nb, ^{95}Nb, ^{89}Zr, ^{82}Br, ^{87}Y, and ^{85}Sr;

3. A strong correlation occurs between a yield and the cumulative yield into which the former decays, namely, ^{188}Pt $\longrightarrow$ ^{188}Ir, ^{185}Ir $\longrightarrow$ ^{185}Os, ^{173}Ta $\longrightarrow$ ^{173}Hg, ^{172}Hf $\longrightarrow$ ^{172}Lu, ^{170}Hf $\longrightarrow$ ^{170}Lu, ^{169}Lu $\longrightarrow$ ^{169}Yb, ^{155}Dy $\longrightarrow$ ^{155}Tb, ^{153}Tb $\longrightarrow$ ^{153}Gd, and ^{146}Gd $\longrightarrow$ ^{146}Eu. The cumulative yields of the precursors in all the above chains are almost equal to the cumulative yields of the daughters. This is why the daughter yields alone were used in our comparisons, to prevent double counting. Also, in the case of a strong correlation between the cumulative and independent yields of a product (^{88}Y), only the independent yield was used in the comparison.

– of them, the number of the product nuclei whose yields were simulated by a particular code, N_S;

– the number of comparison events when the simulated results differ from the experimental data by not more than 30%, $N_{1.3}$, and the number of comparison events when the calculations differ from data by not more than factor 2.0, $N_{2.0}$;

– the mean squared deviation of the simulated results from experimental data, $< F >$, and its standard deviation, $S(< F >)$.

Moreover, the product yields simulated by the codes are displayed in three types of figures that visualize the simulation-to-experiment comparison:

– Figures 25, 34, 42, 50, 28, 36, 44, 52, 31, 39, 47, 55, 58, 91, 94, 96, 99, 102, 105, 108, 111, 114, 117, 120, 123, 126, 129, 132, 135, 138, 141, 144, 147, 150, 153, 156, 159, and 162, which show the results of a detailed comparison between the simulated and experimental independent and cumulative products;

– Figures 26, 28, 36, 44, 52, 32, 40, 48, 56, 59, 92, 97, 100, 103, 106, 109, 112, 115, 118, 121, 124, 127, 130, 133, 136, 139, 142, 145, 148, 151, 154, 157, 160, and 163, which show the statistics of the simulated-to-experimental data ratios;

– Figures 27, 35, 43, 51, 30, 38, 46, 54, 33, 41, 49, 57, 60, 93, 95, 98, 101, 104, 107, 110, 113, 116, 119, 122, 125, 128, 131, 134, 137, 140, 143, 146, 149, 152, 155, 158, 161, and 164, which show the simulated mass distributions of the products together with the measured cumulative and supra cumulative yields of the nuclides that are in immediate proximity to the stable isotope of a given mass (the sum of such yields from either side in the cases where both left- and right-hand branches of the chain are present). Obviously, the simulation results do not contradict the experimental data if the calculated values run above the experimental data and follow the general trend of the latter. This is because the direct γ-spectrometry identifies only the radioactive products, which generally form a significant fraction of the total mass yield, but are never equal to the total mass yield when a stable isobar is produced.

Table 52: Quantitative parameters of the simulation-experiment comparison for W.

Code	$N_{1.3}$/ $N_{2.0}$/N_S	$<F>$	S($<F>$)
^{182}W, E_p=200MeV, N_E=32, N_G=22			
CEM95	11 / 16 / 21	2.13	1.86
LAHET	15 / 17 / 21	1.88	1.80
CASCADE	9 / 16 / 21	2.60	2.34
HETC	7 / 12 / 19	2.18	1.82
INUCL	6 / 15 / 21	2.78	2.42
YIELDX	8 / 15 / 21	2.04	1.68
^{182}W, E_p=800MeV, N_E=70, N_G=50			
CEM95	24 / 31 / 35	1.55	1.50
LAHET	23 / 35 / 42	1.81	1.64
CASCADE	20 / 31 / 41	2.03	1.81
HETC	15 / 25 / 33	2.69	2.42
INUCL	12 / 22 / 39	2.15	1.65
YIELDX	15 / 29 / 42	1.79	1.42
^{182}W, E_p=1600MeV, N_E=109, N_G=65			
CEM95	28 / 44 / 49	1.91	1.83
LAHET	17 / 51 / 63	2.20	1.82
CASCADE	33 / 48 / 59	1.91	1.72
HETC	20 / 38 / 49	2.76	2.50
INUCL	16 / 35 / 55	2.89	2.28
YIELDX	17 / 33 / 62	2.66	1.89
^{183}W, E_p=200MeV, N_E=35, N_G=24			
CEM95	12 / 18 / 23	2.27	2.00
LAHET	14 / 20 / 23	1.81	1.71
CASCADE	10 / 17 / 23	2.49	2.09
HETC	7 / 13 / 21	3.12	2.56
INUCL	7 / 14 / 23	2.74	2.15
YIELDX	11 / 16 / 23	1.84	1.48
^{183}W, E_p=800MeV, N_E=76, N_G=47			
CEM95	23 / 32 / 38	1.65	1.51
LAHET	17 / 36 / 45	2.52	2.25
CASCADE	18 / 30 / 43	2.32	1.95
HETC	12 / 26 / 34	2.42	2.03
INUCL	11 / 20 / 42	2.61	1.86
YIELDX	12 / 29 / 45	2.03	1.51
^{183}W, E_p=1600MeV, N_E=111, N_G=68			
CEM95	28 / 46 / 52	1.58	1.39
LAHET	11 / 49 / 65	2.25	1.76
CASCADE	24 / 49 / 63	2.09	1.79
HETC	19 / 38 / 52	3.20	2.79
INUCL	18 / 35 / 59	2.90	2.26
YIELDX	21 / 33 / 67	2.62	1.88

Table 52, cont'd.

Code	$N_{1.3}$/ $N_{2.0}$/N_S	$< F >$	$S(< F >)$
^{184}W, E_p=200MeV, N_E=36, N_G=24			
CEM95	12 / 16 / 24	2.65	2.25
LAHET	15 / 19 / 24	1.95	1.80
CASCADE	6 / 17 / 24	2.82	2.26
HETC	7 / 11 / 21	3.14	2.39
INUCL	8 / 16 / 24	3.16	2.58
YIELDX	11 / 18 / 24	1.97	1.68
^{184}W, E_p=800MeV, N_E=77, N_G=49			
CEM95	24 / 32 / 40	1.76	1.61
LAHET	21 / 37 / 48	1.71	1.42
CASCADE	22 / 35 / 46	2.05	1.76
HETC	15 / 26 / 37	2.81	2.48
INUCL	12 / 23 / 44	2.53	1.81
YIELDX	14 / 35 / 48	1.83	1.40
^{184}W, E_p=1600MeV, N_E=114, N_G=69			
CEM95	30 / 47 / 55	1.81	1.65
LAHET	16 / 52 / 67	2.08	1.67
CASCADE	28 / 50 / 64	1.93	1.65
HETC	22 / 40 / 54	3.01	2.69
INUCL	18 / 36 / 58	2.50	2.01
YIELDX	14 / 37 / 68	2.61	1.82
^{186}W, E_p=200MeV, N_E=36, N_G=24			
CEM95	11 / 15 / 23	2.75	2.44
LAHET	19 / 22 / 24	1.60	1.56
CASCADE	7 / 17 / 24	2.54	2.13
HETC	7 / 12 / 20	3.08	2.47
INUCL	7 / 14 / 24	2.85	2.33
YIELDX	8 / 13 / 24	2.69	1.93
^{186}W, E_p=800MeV, N_E=62, N_G=41			
CEM95	24 / 32 / 39	2.00	1.88
LAHET	21 / 36 / 39	1.38	1.23
CASCADE	25 / 34 / 39	1.74	1.60
HETC	17 / 30 / 38	2.91	2.62
INUCL	10 / 20 / 39	2.10	1.48
YIELDX	7 / 25 / 39	1.98	1.43
^{186}W, E_p=1600MeV, N_E=119, N_G=71			
CEM95	25 / 49 / 55	1.61	1.39
LAHET	15 / 52 / 68	2.17	1.69
CASCADE	34 / 53 / 66	1.93	1.67
HETC	19 / 42 / 54	2.96	2.60
INUCL	19 / 37 / 60	2.52	1.93
YIELDX	13 / 33 / 71	2.86	1.93
^{nat}W, E_p=2600MeV, N_E=129, N_G=75			
LAHET	10 / 50 / 71	2.53	1.92
CEM95	28 / 53 / 63	2.40	2.23
CEM2k	18 / 51 / 65	2.13	1.68
CASCADE	38 / 56 / 73	2.29	2.12
INUCL	27 / 46 / 64	3.05	2.63
YIELDX	24 / 46 / 75	2.04	1.56
HETC	28 / 43 / 60	2.84	2.50

Table 53: Quantitative parameters of the simulation-experiment comparison for Th.

Code	$N_{1.3}$/ $N_{2.0}$/N_S	$< F >$	S($< F >$)
E_p=100MeV, N_E=87, N_G=44			
LAHET	15 / 34 / 44	1.81	1.46
INUCL	8 / 16 / 43	4.91	2.71
CASCADO-IPPE	14 / 28 / 44	2.98	2.35
ALICE-IPPE	1 / 2 / 4	2.40	1.70
CASCADE	3 / 10 / 44	8.11	3.43
E_p=200MeV, N_E=128, N_G=68			
LAHET	22 / 47 / 67	2.16	1.75
INUCL	5 / 22 / 63	5.55	2.88
ALICE-IPPE	0 / 6 / 12	3.57	2.17
CASCADE	5 / 15 / 66	8.25	3.48
E_p=800MeV, N_E=130, N_G=70			
LAHET	18 / 49 / 69	2.00	1.59
INUCL	12 / 23 / 61	4.40	2.66
CASCADO-IPPE	14 / 45 / 68	2.73	2.13
CASCADE	5 / 30 / 67	4.98	3.13
E_p=1200MeV, N_E=214, N_G=124			
LAHET	33 / 71 / 122	2.18	1.61
INUCL	12 / 34 / 96	6.74	4.11
CASCADE	22 / 54 / 112	4.87	3.30
E_p=1600MeV, N_E=212, N_G=124			
LAHET	35 / 80 / 122	2.08	1.60
INUCL	17 / 47 / 108	7.60	4.41
CASCADE	26 / 58 / 114	3.17	2.22

Table 54: Quantitative parameters of the simulation-experiment comparison for U.

Code	$N_{1.3}$/ $N_{2.0}$/N_S	$< F >$	S($< F >$)
E_p=100MeV, N_E=108, N_G=58			
LAHET	20 / 46 / 57	2.23	1.95
INUCL	5 / 15 / 53	5.67	2.86
CASCADO-IPPE	20 / 35 / 53	2.79	2.31
ALICE-IPPE	0 / 3 / 6	2.01	1.25
CASCADE	5 / 14 / 51	10.26	5.10
E_p=200MeV, N_E=123, N_G=65			
LAHET	21 / 55 / 64	1.70	1.40
INUCL	8 / 22 / 61	5.09	2.77
CASCADE	9 / 25 / 63	5.81	3.36
E_p=800MeV, N_E=195, N_G=116			
LAHET	29 / 84 / 113	1.87	1.44
INUCL	10 / 31 / 91	5.60	3.16
CASCADE	17 / 39 / 96	4.26	2.63
CASCADO-IPPE	21 / 64 / 112	2.72	1.94
E_p=1200MeV, N_E=226, N_G=131			
LAHET	28 / 71 / 128	2.09	1.49
INUCL	14 / 39 / 94	5.10	3.06
CASCADE	19 / 43 / 113	4.19	2.58
E_p=1600MeV, N_E=231, N_G=134			
LAHET	29 / 80 / 131	2.07	1.51
INUCL	13 / 44 / 100	5.74	3.47
CASCADE	22 / 53 / 121	4.18	2.61

Table 55: Quantitative parameters of the simulation-experiment comparison for Tc.

Code	$N_{1.3}$/ $N_{2.0}$/N_S	$< F >$	$S(< F >)$
E_p=100MeV, N_E=18, N_G=5			
CEM95	2 / 2 / 5	9.23	5.52
LAHET	2 / 3 / 5	2.14	1.56
INUCL	2 / 3 / 5	4.32	3.02
YIELDX	1 / 4 / 5	1.95	1.62
CASCADE	1 / 2 / 5	4.59	2.79
HETC	1 / 1 / 3	4.08	2.46
E_p=200MeV, N_E=39, N_G=12			
CEM95	3 / 5 / 12	4.20	2.72
LAHET	3 / 12 / 12	1.59	1.24
INUCL	1 / 4 / 12	4.29	2.22
YIELDX	3 / 7 / 12	2.15	1.60
CASCADE	2 / 4 / 12	3.29	2.01
ALICE(Fermi)	2 / 6 / 12	2.31	1.60
ALICE(Kataria)	2 / 3 / 12	2.77	1.66
HETC	0 / 4 / 9	3.21	1.86
GNASH	3/3/7	2.74	1.89
E_p=800MeV, N_E=72, N_G=37			
CEM95	17 / 25 / 34	2.23	1.89
LAHET	10 / 24 / 34	2.62	2.16
INUCL	3 / 12 / 34	3.64	2.09
YIELDX	15 / 30 / 36	1.95	1.70
CASCADE	8 / 20 / 34	2.87	2.15
HETC	7 / 18 / 30	4.57	3.56
E_p=1200MeV, N_E=67, N_G=31			
CEM95	12 / 20 / 30	2.68	2.20
LAHET	11 / 22 / 30	2.35	2.02
INUCL	2 / 11 / 29	3.54	2.13
YIELDX	2 / 14 / 31	2.45	1.55
CASCADE	6 / 14 / 30	3.35	2.30
HETC	9 / 16 / 26	3.53	2.83
E_p=1600MeV, N_E=78, N_G=41			
CEM95	16 / 27 / 38	2.20	1.88
LAHET	17 / 30 / 38	1.80	1.54
INUCL	6 / 14 / 35	4.12	2.78
YIELDX	9 / 24 / 40	2.34	1.71
CASCADE	11 / 22 / 38	3.15	2.35
HETC	11 / 19 / 31	4.30	3.40

Table 56: Quantitative parameters of the simulation-experiment comparison for ^{59}Co.

Code	$N_{1.3}$/ $N_{2.0}$/N_S	$< F >$	S($< F >$)
E_p=200MeV, N_E=29, N_G=19			
CEM95	6 / 10 / 15	2.22	1.75
LAHET	4 / 11 / 15	2.02	1.59
CASCADE	2 / 8 / 19	2.94	1.81
HETC	2 / 5 / 10	3.00	2.14
INUCL	6 / 14 / 19	2.28	1.82
YIELDX	7 / 13 / 19	1.81	1.44
E_p=1200MeV, N_E=41, N_G=29			
CEM95	9 / 16 / 26	2.30	1.79
LAHET	11 / 21 / 26	1.85	1.51
CASCADE	5 / 11 / 27	3.09	2.02
HETC	6 / 8 / 14	4.62	3.70
INUCL	5 / 22 / 27	1.93	1.46
YIELDX	18 / 27 / 28	1.56	1.44
NUCLEUS	6 / 15 / 28	2.21	1.52
QMD	1 / 13 / 17	2.41	1.70
E_p=1600MeV, N_E=41, N_G=29			
CEM95	6 / 14 / 26	2.54	1.84
LAHET	9 / 19 / 26	1.95	1.51
CASCADE	7 / 16 / 27	2.20	1.57
HETC	5 / 8 / 15	5.14	3.90
INUCL	6 / 20 / 27	1.95	1.50
YIELDX	17 / 27 / 28	1.55	1.47
E_p=2600MeV, N_E=41, N_G=29			
CEM95	5 / 14 / 26	2.73	1.91
LAHET	8 / 20 / 27	2.11	1.61
CASCADE	7 / 14 / 27	2.04	1.52
HETC	3 / 7 / 15	5.33	3.82
INUCL	7 / 18 / 27	2.03	1.51
YIELDX	19 / 26 / 28	1.53	1.45

Table 57: Quantitative parameters of the simulation-experiment comparison for ^{63}Cu and ^{65}Cu.

Code	$N_{1.3}$/ $N_{2.0}$/N_S	$< F >$	S($< F >$)
^{63}Cu E_p=200MeV, N_E=29, N_G=20			
CEM95	5 / 12 / 19	2.61	1.98
LAHET(Isabel)	8 / 12 / 20	2.25	1.73
LAHET(Bertini)	8 / 13 / 20	1.89	1.58
CASCADE	3 / 8 / 20	3.75	2.30
HETC	3 / 5 / 13	5.47	3.14
INUCL	6 / 11 / 20	2.22	1.65
YIELDX	3 / 14 / 20	2.27	1.65
^{65}Cu E_p=200MeV, N_E=29, N_G=20			
CEM95	7 / 13 / 18	2.04	1.63
LAHET	8 / 14 / 20	2.04	1.66
CASCADE	3 / 10 / 19	3.28	2.19
HETC	1 / 4 / 15	5.22	2.30
INUCL	3 / 12 / 20	2.34	1.72
YIELDX	7 / 14 / 20	1.89	1.47
^{63}Cu E_p=1200MeV, N_E=47, N_G=36			
CEM95	8 / 21 / 34	2.47	1.88
LAHET	10 / 27 / 34	1.79	1.41
CASCADE	4 / 13 / 35	3.98	2.46
HETC	5 / 12 / 20	4.23	3.00
INUCL	10 / 22 / 34	2.11	1.62
YIELDX	14 / 28 / 36	1.69	1.39
QMD	7 / 17 / 32	3.11	2.16
^{65}Cu E_p=1200MeV, N_E=54, N_G=40			
CEM95	10 / 18 / 35	2.83	1.97
LAHET	10 / 25 / 36	2.02	1.52
CASCADE	5 / 11 / 36	3.44	2.06
HETC	3 / 7 / 21	3.15	2.05
INUCL	13 / 22 / 37	2.03	1.57
YIELDX	13 / 30 / 38	1.71	1.37
QMD	7 / 16 / 32	3.18	2.13
^{63}Cu E_p=1600MeV, N_E=42, N_G=31			
CEM95	10 / 20 / 29	2.26	1.71
LAHET	12 / 22 / 29	1.70	1.39
CASCADE	6 / 17 / 30	2.40	1.75
HETC	3 / 7 / 16	3.13	2.18
INUCL	5 / 19 / 30	2.17	1.57
YIELDX	14 / 30 / 31	1.44	1.21
^{65}Cu E_p=1600MeV, N_E=47, N_G=34			
CEM95	9 / 16 / 31	2.62	1.82
LAHET	8 / 22 / 31	2.03	1.55
CASCADE	6 / 16 / 32	2.31	1.62
HETC	3 / 7 / 18	3.16	2.10
INUCL	10 / 22 / 32	1.97	1.55
YIELDX	10 / 30 / 34	1.58	1.27

Table 57, cont'd.

Code	$N_{1.3}$/ $N_{2.0}$/N_S	$< F >$	S($< F >$)
^{63}Cu E_p=2600MeV, N_E=42, N_G=31			
CEM95	8 / 16 / 28	2.36	1.79
LAHET	7 / 21 / 29	1.97	1.52
CASCADE	8 / 20 / 30	2.16	1.63
HETC	4 / 7 / 16	3.20	2.20
INUCL	7 / 17 / 30	2.13	1.55
YIELDX	16 / 31 / 31	1.31	1.17
^{65}Cu E_p=2600MeV, N_E=48, N_G=35			
CEM95	9 / 15 / 31	2.92	2.02
LAHET	7 / 18 / 33	2.21	1.61
CASCADE	10 / 18 / 32	2.07	1.59
HETC	3 / 7 / 19	3.34	2.07
INUCL	7 / 20 / 32	2.00	1.51
YIELDX	19 / 33 / 34	1.45	1.29

Table 58: Quantitative parameters of the simulation-experiment comparison for ^{nat}Hg

Code	$N_{1.3}$/ $N_{2.0}$/N_S	$<F>$	$S(<F>)$
E_p=2600MeV, N_E=141, N_G=82			
LAHET	7 / 15 / 24	2.35	1.88
CEM95	8 / 14 / 23	2.14	1.67
CEM2k	6 / 18 / 22	1.69	1.35
INUCL	8 / 15 / 25	2.74	2.07
CASCADE	11 / 16 / 25	2.47	2.03
HETC	4 / 7 / 18	3.75	2.58
E_p=800MeV, N_E=103, N_G=64			
LAHET	16 / 29 / 38	1.80	1.54
CEM95	11 / 26 / 33	2.16	1.86
CEM2k	18 / 27 / 33	1.61	1.43
INUCL	12 / 22 / 38	2.29	1.74
CASCADE	11 / 28 / 38	2.34	1.91
YIELDX	15 / 32 / 39	1.75	1.43
HETC	6 / 19 / 29	3.74	2.98
E_p=200MeV, N_E=65, N_G=39			
LAHET	34 / 49 / 63	1.98	1.73
CEM95	30 / 41 / 47	2.19	2.17
CEM2k	22 / 44 / 49	1.66	1.45
INUCL	23 / 35 / 59	2.56	1.97
CASCADE	29 / 47 / 60	2.11	1.86
YIELDX	23 / 47 / 64	2.10	1.73
HETC	14 / 34 / 42	2.33	2.06
E_p=100MeV, N_E=44, N_G=27			
LAHET	16 / 58 / 79	1.98	1.47
CEM95	31 / 52 / 61	1.93	1.77
CEM2k	21 / 52 / 66	2.48	2.10
INUCL	25 / 55 / 77	2.46	2.00
CASCADE	39 / 65 / 78	1.68	1.45
YIELDX	18 / 50 / 81	2.44	1.76
HETC	23 / 44 / 57	2.53	2.29

Table 59: Quantitative parameters of the simulation-experiment comparison for ^{56}Fe: N_E=36, N_G=27

Code	$N_{1.3}$/ $N_{2.0}$/N_S	$<F>$	$S(<F>)$
CEM95	2 / 10 / 22	2.65	1.70
LAHET	8 / 16 / 24	2.12	1.64
CASCADE	6 / 14 / 23	2.13	1.56
HETC	2 / 6 / 13	5.12	3.32
INUCL	9 / 15 / 23	1.96	1.62
YIELDX	9 / 20 / 25	1.62	1.31

Table 60: Quantitative parameters of the simulation-experiment comparison for ^{58}Ni: N_E=38, N_G=28

Code	$N_{1.3}$/ $N_{2.0}$/N_S	$< F >$	S($< F >$)
CEM95	7 / 13 / 26	3.46	2.73
LAHET	9 / 18 / 26	1.89	1.53
CASCADE	4 / 19 / 26	2.02	1.47
HETC	4 / 8 / 15	3.41	2.51
INUCL	9 / 18 / 26	2.34	1.84
YIELDX	22 / 25 / 27	1.40	1.32

Table 61: Quantitative parameters of the simulation-experiment comparison for ^{93}Nb: N_E=85, N_G=57

Code	$N_{1.3}$/ $N_{2.0}$/N_S	$< F >$	S($< F >$)
CEM95	8 / 28 / 52	2.56	1.82
LAHET	17 / 41 / 55	1.95	1.56
CASCADE	14 / 35 / 56	2.69	1.97
HETC	12 / 25 / 39	2.73	2.24
INUCL	12 / 31 / 56	2.59	1.77
YIELDX	22 / 42 / 57	1.91	1.56

Table 62: Statistics of comparison between experimental and simulated yields in 1.0 GeV proton-irradiated ^{208}Pb

Code	N_E = 114, N_G = 70		
	$N_{1.3}$/ $N_{2.0}$/N_S	$< F >$	$S(< F >)$
LAHET(Bertini)	30 / 51 / 70	2.03	1.69
LAHET(Isabel)	36 / 55 / 70	1.90	1.70
CEM95	27 / 43 / 51	2.06	1.91
CEM2k	30 / 51 / 55	1.61	1.43
CASCADE	26 / 51 / 66	2.09	1.79
CASCADE-INPE	27 / 51 / 64	1.84	1.56
INUCL	21 / 35 / 67	2.85	2.10
YIELDX	23 / 44 / 70	2.78	2.22
HETC	17 / 35 / 50	3.76	3.30

Table 63: Statistics of the simulation-to-experiment comparisons of the yields of the all presented reaction products.

Code	^{59}Co,^{63,65}Cu, E$_p$=0.2GeV ^{99}Tc, E$_p$ ≤0.2GeV N_E=144 N_G=76			^{59}Co,^{63,65}Cu, ^{59}Fe, ^{58}Ni, ^{93}Nb, E$_p$ ≥1.2GeV ^{99}Tc, E$_p$ ≥0.8GeV N_E=779 N_G=515		
	$N_{1.3}/N_{2.0}/N_S$	$\langle F\rangle$	$S(\langle F\rangle)$	$N_{1.3}/N_{2.0}/N_S$	$\langle F\rangle$	$S(\langle F\rangle)$
CEM95	23/42/69	3.04	2.39	136/273/468	2.57	1.94
LAHET	26/52/72	2.03	1.60	154/346/478	2.03	1.62
INUCL	18/45/76	2.72	2.00	112/283/479	2.47	1.84
HETC	7/19/50	4.37	2.51	81/162/308	3.81	2.85
CASCADE	11/32/75	3.40	2.15	107/260/483	2.71	1.96
YIELDX	21/52/76	2.02	1.55	219/417/504	1.75	1.50
NUCLEUS	–	–	–	6/15/28[1]	2.21	1.52
QMD	–	–	–	15/46/81[2]	2.99	2.06
GNASH	3/ 3/ 7[3]	2.74	1.89	–	–	–
ALICE(Kat)	2/3/12[3]	2.77	1.66	–	–	–
ALICE(Fer)	2/6/12[3]	2.31	1.60	–	–	–
Code	^{182,3,4,6}W,^{nat}Hg, E$_p$ ≤0.2GeV ^{232}Th,^{nat}U, E$_p$ ≤0.2GeV N_E=694 N_G=395			^{182,3,4,6,nat}W,^{nat}Hg, ^{208}Pb, E$_p$ ≥0.8GeV ^{232}Th,^{nat}U, E$_p$ ≥0.8GeV N_E=2433 N_G=1441		
	$N_{1.3}/N_{2.0}/N_S$	$\langle F\rangle$	$S(\langle F\rangle)$	$N_{1.3}/N_{2.0}/N_S$	$\langle F\rangle$	$S(\langle F\rangle)$
CEM95	65/105/147[4]	2.34	2.01	321/503/585[5]	1.90	1.77
LAHET	164/305/386	1.95	1.69	399/945/1334	2.04	1.62
INUCL	75/171/375	4.19	2.73	293/619/1213	4.05	2.92
HETC	39/74/128[4]	3.20	2.52	221/422/560[5]	2.88	2.55
CASCADE	78/176/379	5.46	3.53	451/828/1322	3.05	2.42
YIELDX	54/94/131[6]	2.03	1.65	201/443/732[5]	2.37	1.78
CASCADO^{IPPE}	34/63/97[7]	2.88	2.33	35/109/180[8]	2.73	2.01
ALICE-IPPE	1/8/16[9]	3.27	2.10	–	–	–
CEM2k	24/45/55[10]	1.64	1.40	91/198/235[11]	2.02	1.74
CASCADE^{INPE}	–	–	–	27/51/64[12]	1.84	1.56

[1] Here N_E=41 and N_G=29.
[2] Here N_E=152 and N_G=105.
[3] Here N_E=39 and N_G=12,
[4] Here N_E=248 and N_G=160.
[5] Here N_E=1225 and N_G=742.
[6] Here N_E=204 and N_G=133.
[7] Here N_E=195 and N_G=102.
[8] Here N_E=325 and N_G=186.
[9] Here N_E=195 and N_G=112.
[10] Here N_E=111 and N_G=66.
[11] Here N_E=552 and N_G=291.
[12] Here N_E=114 and N_G=70.

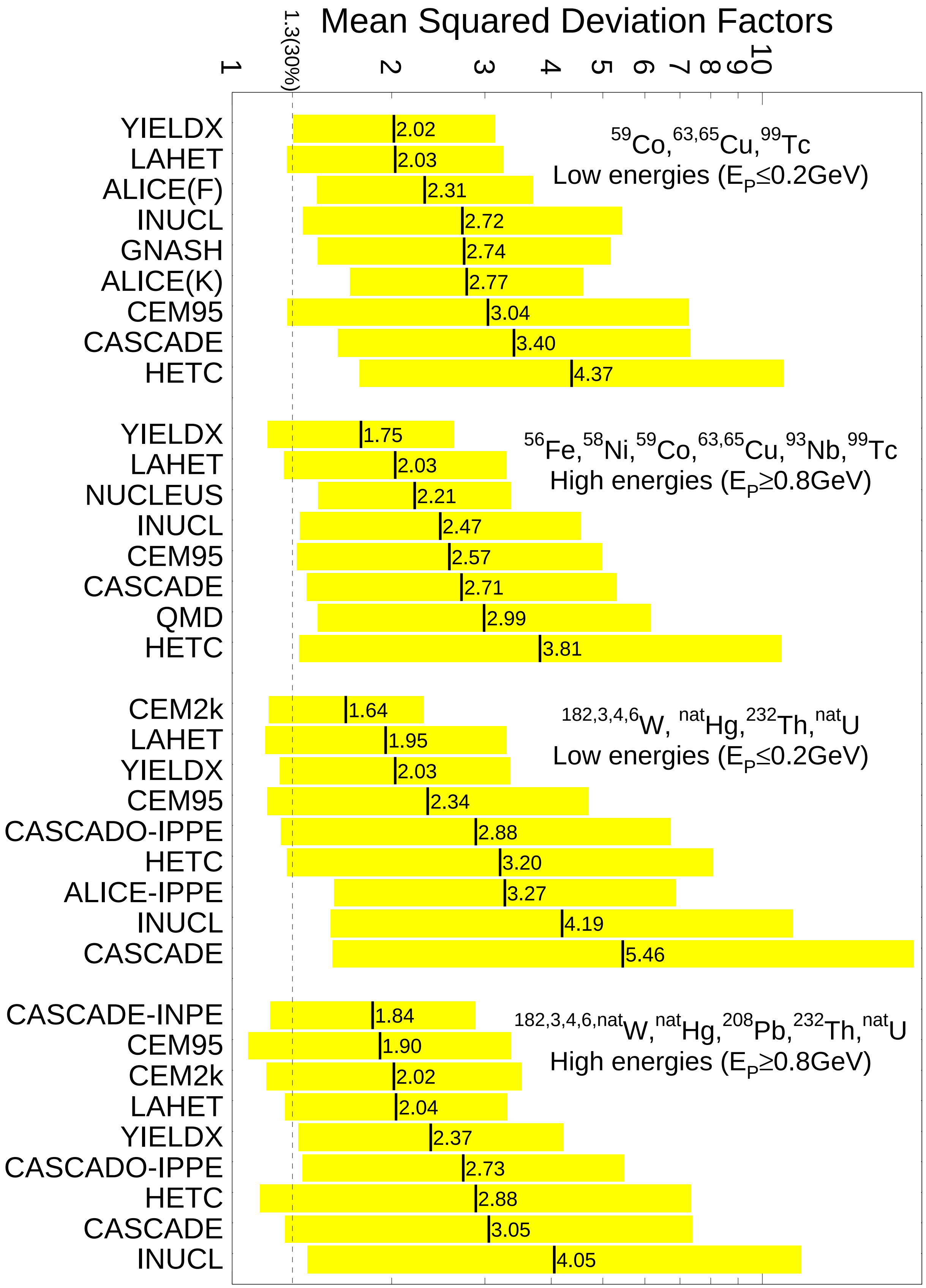

Fig. 24: The mean squared deviation factor for the unified comparison.

Table 64: Statistics of the experimental-to-simulated spallation and fission yield comparisons

Code	Spallation			Fission			All products (spallation+fission+frag-) mentation)		
^{208}Pb	N_T = 72, N_G = 50			N_T = 31, N_G= 14			N_T = 114, N_G = 70		
E_p=1.0GeV	$N_{1.3}/N_{2.0}/N_S$	$\langle F \rangle$	$S(\langle F \rangle)$	$N_{1.3}/N_{2.0}/N_S$	$\langle F \rangle$	$S(\langle F \rangle)$	$N_{1.3}/N_{2.0}/N_S$	$\langle F \rangle$	$S(\langle F \rangle)$
LAHET	32/46/50	1.41	1.32	1/3/14	3.50	1.68	36/55/70	1.90	1.70
CEM2k	29/48/50	1.42	1.25	–	–	–	30/51/55	1.61	1.43
CASCADE/INPE	23/42/46	1.54	1.35	4/8/14	2.29	1.73	27/51/64	1.84	1.56
CASCADE	22/43/49	1.55	1.32	4/8/14	2.67	1.94	26/51/66	2.09	1.79
YIELDX	21/37/50	1.85	1.55	1/3/14	6.87	2.63	23/44/70	2.78	2.22
CEM95	27/43/50	1.95	1.82	–	–	–	27/43/51	2.06	1.91
INUCL	14/25/50	2.63	1.91	7/10/13	1.99	1.75	21/35/67	2.85	2.10
HETC	17/35/47	3.48	3.22	–	–	–	17/35/50	3.76	3.30
^{nat}W	N_T = 100, N_G = 56			N_T = 18, N_G = 15			N_T = 129, N_G = 75		
E_p=2.6GeV	$N_{1.3}/N_{2.0}/N_S$	$\langle F \rangle$	$S(\langle F \rangle)$	$N_{1.3}/N_{2.0}/N_S$	$\langle F \rangle$	$S(\langle F \rangle)$	$N_{1.3}/N_{2.0}/N_S$	$\langle F \rangle$	$S(\langle F \rangle)$
CEM95	28/52/56	1.52	1.35	–	–	–	28/53/63	2.40	2.23
CASCADE	36/50/56	1.50	1.39	2/4/13	5.43	3.12	38/56/73	2.29	2.12
CEM2k	17/47/56	1.79	1.41	–	–	–	18/51/65	2.13	1.68
LAHET	10/46/56	1.80	1.35	0/3/11	6.36	2.97	10/50/71	2.53	1.92
YIELDX	21/35/56	1.92	1.49	3/8/15	2.32	1.68	24/46/75	2.04	1.56
INUCL	27/46/56	1.76	1.53	0/0/5	14.16	1.86	27/46/64	3.05	2.63
HETC	27/41/54	2.75	2.51	–	–	–	28/43/60	2.84	2.50
^{nat}Hg	N_T = 36, N_G = 23			N_T = 8, N_G = 4			N_T = 44, N_G = 27		
E_p=0.1GeV	$N_{1.3}/N_{2.0}/N_S$	$\langle F \rangle$	$S(\langle F \rangle)$	$N_{1.3}/N_{2.0}/N_S$	$\langle F \rangle$	$S(\langle F \rangle)$	$N_{1.3}/N_{2.0}/N_S$	$\langle F \rangle$	$S(\langle F \rangle)$
CEM2k	6/18/22	1.69	1.35	–	–	–	6/18/22	1.69	1.35
LAHET	7/15/22	1.79	1.43	0/0/2	9.36	1.38	7/15/24	2.35	1.88
INUCL	8/15/22	2.06	1.63	0/0/3	8.52	1.56	8/15/25	2.74	2.07
CASCADE	11/15/22	2.19	1.89	0/1/3	4.56	1.93	11/16/25	2.47	2.03
CEM95	8/14/23	2.14	1.67	–	–	–	8/14/23	2.14	1.67
HETC	4/7/18	3.75	2.58	–	–	–	4/7/18	3.75	2.58
^{nat}Hg	N_T = 52, N_G = 33			N_T = 13, N_G = 6			N_T = 65, N_G = 39		
E_p=0.2GeV	$N_{1.3}/N_{2.0}/N_S$	$\langle F \rangle$	$S(\langle F \rangle)$	$N_{1.3}/N_{2.0}/N_S$	$\langle F \rangle$	$S(\langle F \rangle)$	$N_{1.3}/N_{2.0}/N_S$	$\langle F \rangle$	$S(\langle F \rangle)$
LAHET	16/28/33	1.50	1.30	0/1/5	3.43	1.77	16/29/38	1.80	1.54
CEM2k	18/27/33	1.61	1.43	–	–	–	18/27/33	1.61	1.43
YIELDX	15/29/33	1.58	1.32	0/3/6	2.53	1.51	15/32/39	1.75	1.43
CASCADE	9/26/33	2.13	1.77	2/2/5	3.71	2.36	11/28/38	2.34	1.91
CEM95	11/26/33	2.16	1.86	–	–	–	11/26/33	2.16	1.86
INUCL	10/20/33	2.23	1.71	2/2/5	2.69	1.88	12/22/38	2.29	1.74
HETC	6/19/29	3.74	2.98	–	–	–	6/19/29	3.74	2.98
^{nat}Hg	N_T = 66, N_G = 44			N_T = 21, N_G = 13			N_T = 103, N_G = 64		
E_p=0.8GeV	$N_{1.3}/N_{2.0}/N_S$	$\langle F \rangle$	$S(\langle F \rangle)$	$N_{1.3}/N_{2.0}/N_S$	$\langle F \rangle$	$S(\langle F \rangle)$	$N_{1.3}/N_{2.0}/N_S$	$\langle F \rangle$	$S(\langle F \rangle)$
CASCADE	25/40/43	1.43	1.27	3/6/11	2.59	1.81	29/47/60	2.11	1.86
LAHET	29/41/44	1.46	1.33	1/1/11	4.03	1.61	34/49/63	1.98	1.73
CEM2k	21/42/44	1.46	1.27	–	–	–	22/44/49	1.66	1.45
CEM95	30/41/44	1.56	1.51	–	–	–	30/41/47	2.19	2.17
YIELDX	16/35/44	1.68	1.36	4/5/12	3.25	2.13	23/47/64	2.10	1.73
INUCL	21/32/43	1.89	1.59	2/3/10	4.17	2.32	23/35/59	2.56	1.97
HETC	14/33/40	2.21	1.98	–	–	–	14/34/42	2.33	2.06
^{nat}Hg	N_T = 92, N_G = 64			N_T = 30, N_G = 20			N_T = 141, N_G = 82		
E_p=2.6GeV	$N_{1.3}/N_{2.0}/N_S$	$\langle F \rangle$	$S(\langle F \rangle)$	$N_{1.3}/N_{2.0}/N_S$	$\langle F \rangle$	$S(\langle F \rangle)$	$N_{1.3}/N_{2.0}/N_S$	$\langle F \rangle$	$S(\langle F \rangle)$
CASCADE	34/49/54	1.52	1.40	4/10/16	2.08	1.46	39/65/78	1.68	1.45
CEM95	30/49/54	1.54	1.39	–	–	–	31/52/61	1.93	1.77
LAHET	11/44/53	1.70	1.25	5/10/18	2.52	1.85	16/58/79	1.98	1.47
CEM2k	16/45/54	1.75	1.37	–	–	–	21/52/66	2.48	2.10
INUCL	20/44/54	1.90	1.62	4/9/15	2.68	2.00	25/55/77	2.46	2.00
YIELDX	14/40/54	2.02	1.56	3/7/19	3.49	1.95	18/50/81	2.44	1.76
HETC	23/40/49	2.35	2.17	–	–	–	23/44/57	2.53	2.29

4.4 General conclusions on the agreement between the experimental and simulated product nuclide yields.

The comparison is expedient to make for two groups of nuclei: with a significant fission mode (the conditionally "heavy"nuclei ^{182,183,184,186}W, ^{nat}W, ^{nat}Hg, ^{208}Pb, ^{232}Th, ^{nat}U) and without any fission mode (the conditionally "light"nuclei ^{56}Fe, ^{58}Ni, ^{59}Co, ^{63,65}Cu, ^{93}Nb, ^{99}Tc). It should be noted that, beside the methodological convenience, this classification reflects (somewhat conditionally) the distinquishing design features of the materials as applied to the ADS (the target and structure materials). A total of 4050 experimental yields of proton reaction products have been obtained at ITEP under the ISTC Project 839B-99. Of them, 2427 yields were used to verify the simulation codes. Table 63 and Figure 24 summarize the information on the predictive power of the codes.

In the case of light nuclei, where nearly all product nuclides are formed by spallation, the predictive power of most of the Monte-Carlo codes is characterized by the mean squared deviation factor of at least 2, with the agreement being somewhat worse at low energies. The semi-phenomenological YIELDX code gives the best result when predicting the reaction product yields in light nuclei, and sometimes approaches the required 30% accuracy. It should be noted, however, that YIELDX does not generally use any physical model, but is based on the approximations for a large set of experimental data.

In the case of heavy nuclei, the physics of proton-nucleus interactions gets complicated because the fission process becomes significant. Production of high-energy fission product nuclides cannot be described by some of the tested codes (CEM95, HETC), or else the applied models are imperfect. Therefore, the mean squared deviation factor (see Table 64) is very high (commonly, at least 3.0 and sometimes about an order) for the fission products. From this it follows that, although the spallation products are described by the present-day codes somewhat better for heavy nuclei that for light nuclei (the mean squared deviation factor of about 1.5), the general agreement is about the same as in the case of light nuclei (the mean squared deviation factor about 2.0 and higher). From this it follows that the further development of fission models is a priority task in updating the simulation codes.

It should also be noted that, in the case of high-energy (E_p >1 GeV) projectile protons, most of the tested codes fail to satisfactorily describe the production of the nuclides whose nucleon compositions are close to the primary nuclei. This is also indicative of but imperfect physical models that are used to describe the $(p, xpyn)$–type processes, where $x+y \leq 3$ (the pre-equilibrium nucleon emission).

As a whole, it can be concluded that almost all the above-verified codes are applicable, during the stage of feasibility study and development work, but cannot be yet used to solve the applied problems that arise when designing and operating the ADS facilities. At the same time, the yields of numerous secondary products have to be known to within a very high accuracy for many reasons (large cross sections for neutron capture, a high radiotoxicity, chemical poisoning of structure elements, gas evolution, etc.). So, the codes have to be seriously improved to become a reliable tool for calculating the ADS parameters.

4.5 Methods for improving the simulation codes.

Most of the simulation codes, which describe the intermediate-energy nuclear reactions, make use of the Monte-Carlo method, are based on Intranuclear Cascade (INC) models , and treat a reaction to be a multistage procvess (INC, pre-equilibrium, equilibrium evaporation, and fission)

Since the intermediate energy range is very broad, different models are applied to different stages. The models describe the stages with different degree of rigor and are of different predictive powers. As a result, the simulation data of the codes, which are seemingly alike in their physical nature, differ much from each other.

The accuracy of describing the experimental yields of nuclear reaction products, as well as the predictive power of the simulation codes, can well be improved by updating the models realized in the codes when solving a set of the fundamental problems, of which the following is most important:

- Construction of a consistent nuclear fission model that would allow for the shell-to-liquid drop fission barrier transition and for the nuclear viscosity effects;
- Updating of the INC model aimed at effective allowance for the cluster emission during the pre-equilibrium stage of nuclear reactions;
- Development of consistent methods for calculating the spallation reaction cross sections and comparing the INC model with the optical-statistical calculation data in order to correctly include the nuclear structure effects in the energy range of 20–200 MeV.

It should be noted that the parametric fitting in terms of the present-day models, most of which do not reach any sufficient accuracy in representing the basic physical effects, can but partly solve the problem of constructing reliable models and codes. In some cases, such a fitting can distort the parameters and their physical sense, thereby considerably restricting the potentialities and predictive power of the codes.

5 Conclusion

The interest shown in the ADS facilities encourages us to anticipate that the accumulation and analysis of nuclear data for different ADS applications will have the same growth in academic interest and practical commitments as was the case for nuclear reactor data during the last five decades.

The experience gained in the reported researches indicates that the updating of the codes and the optimal selection of the parameters should better be applied to the promising materials and to the nuclei supported by as copious data as possible.

With the above purposes, we have proposed a new project (ISTC-#2002) aimed at studying in detail the yields of proton-induced reaction products from Pb and Bi isotopes in a broad energy range (0.04–2.6 GeV). Successful realization of the new project is expected to be an important step towards the goal of the reported researches, i.e., the desired accuracy of the models and codes used to calculate the nuclear-physics characteristics of ADS facilities and the reliable nuclear database compilation that can be used in other promising nuclear technologies

6 Acknowlegements

The authors are indebted to Drs. T. Enqvist and B. Mustapha for providing us with the cross sections measured at GSI, to Prof. R. Michel for sending us the nuclide production data obtained at ZSR, to Prof. V. Artisyuk for useful discussions and assistance, and to Prof. M. Blann, Drs. R.E. Prael, M.B. Chadwick, S.G. Mashnik, S. Chiba, H. Takada, T.A. Gabriel, and A.J. Sierk for their participating in the work with their code simulations.

References

[1] ISTC Project 839B-99 (http//www.istc.ru/website.nsf/fm/Project+by+number).

[2] Gregory J. Van Tuyle, ATW Technology Development & Demonstration Plan, LANL Report LA-UR-99-1061; Gregory J. Van Tuyle, ATW Technology & Scenarios, LANL Report LA-UR 99-771.

[3] T. Mukayama, OMEGA Program in Japan and ADS Development at JAERI, Proceedings of the Third International Conference on Accelerator-Driven Transmutation Technologies and Applications ADTT'99, Praha, June 1999. Mo-I-5.

[4] M. Salvatores, Strategies for the back-and of the fuel cycle: A scientific point of view, Proceedings of the Third International Conference on Accelerator-Driven Transmutation Technologies and Applications ADTT'99, Praha, June 1999, Mo-I-4.

[5] Yu. E. Titarenko, O. V. Shvedov, M. M. Igumnov, S. G. Mashnik, E. I. Karpikhin, V.D. Kazaritsky, V. F. Batyaev, A. B. Koldobsky, V. M. Zhivun, A.N. Sosnin, R. E. Prael, M. B. Chadwick, T. A. Gabriel, M. Blann, "Exerimental and theoretical Study of the Yields of Radionuclides Produced in ^{209}Bi thin target Irradiated by 1500 MeV and 130 MeV Protons", Los Alammos PrePrint LA-UR-97-3787; *nucl-th/9709056*, Nucl. Instr. and Meth. A414 (1998) 73-99.

[6] Yu. E.Titarenko, O. V. Shvedov, V. F. Batyaev, E. I. Karpikhin, V. M. Zhivun, A. B. Koldobsky, R. D. Mulambetov, D. V. Fischenko, S. V. Kvasova, A. N. Sosnin, S. G. Mashnik, R. E. Prael, A. J. Sierk T.A.Gabriel, M.Saito, H. Yasuda, "Cross sections for nuclide production in 1 GeV proton-irradiated ^{208}Pb", Los Alammos PrePrint LA-UR-00-4779; *nucl-th/0010083*; submitted to Phys.Rev.C.

[7] M. Gloris, R. Michel, F. Sudbrok, U. Herpers, P. Malmborg, B. Holmqvist, "Proton-Induced Production of Residual Radionuclides in Lead at Intermediate Energies". Submitted to Nucl. Instrum. Methods A (2000); EXFOR file O0500.

[8] Yu.V.Alexandrov, V.P.Eismont, R.V.Ivanov et. al. "Cross Section for the Production of Radionuclides in Lead Target Irradiated with 660 MeV Protons", Proceedings of the Second International Conference on Accelerator-Driven Transmutation Technologies and Applications. June 3-7, 1996, Kalmar, Sweeden, p.p. 576-578.

[9] N.E. Holden, R.L. Martin and I.L.Barnes, "Isotopic compositions of the elemnts 1983", Pure & Appl. Chem., Vol. 56, No. 6, pp. 675-694, 1984.

[10] J. Tobailem, "Sections Efficaces des Reactions Nucleaires Indutes par Protons, Deutrons, Particles Alphas. V. Silicium,"Note CEA-N-1466(5), Sacley, 1981.

[11] R. Michel, F. Peiffer, and R. Stück, Nucl. Phys. **A441**, 617 (1985).

[12] R. Michel, P. Dragovitsch, P. Englert, F. Peiffer, R. Stück, S. Theis, F. Begemann, H. Weber, P. Signer, R. Wieler, D. Filges, and P. Cloth, Nucl. Instrum. Methods B **16**, 61 (1986).

[13] R. Michel, B. Dittrich, U. Herpers, F. Peiffer, T. Schiffmann, P. Cloth, P. Dragovitsch, and D. Filges, Anayst **114**, 287 (1989).

[14] B. Dittrich, U. Herpers, M. Lüpke, R. Michel, P. Signer, R. Wieler, H. J. Hofmann, and W. Wölfli, in: Progress Report on Nuclear Data Research in the Federal Republic of Germany for the Period April 1, 1989 to March 31, 1990, NEANDC(E)-312-U Vol. V INDC(Ger)-35/LN+Special (1990), p. 45.

[15] R. Bodemann, H.-J. Lange, I. Leya, R. Michel, T. Schiekel, R. Rösel, U. Herpers, H. J. Hofmann, B. Dittrich, M. Suter, W. Wölfli, B. Holmqvist, H. Condé, and P. Malmborg, in: Progress Report on Nuclear Data Research in the Federal Republic of Germany for the Period April 1, 1992 to March 31, 1993, NEA/NDC/DOC(93) 17, INDC(Ger)-037/LN. Jul-2803 (1993), p. 49.

[16] Th. Sciekel, F. Sudbrock, U. Herpers, M. Gloris, H.-J. Lange, I. Leya, R. Michel, B. Dittrich-Hannen, H.-A. Synai, M. Suter, P. W. Kubik, M. Blann, and D. Filges, Nucl. Instrum. Methods B **114**, 91 (1996).

[17] R. R. Kinsey, et. al., Proc. 9th Int. Symp. of Capture-Gamma-Ray Spectroscopy and Related Topics, 8-12 October 1996, Budapest, Hungary.

[18] R. B. Firestone, in: *Tables of Isotopes, 8th ed.: 1998 Update (with CD ROM)* edited by S. Y. Frank Chu (CD-ROM Ed.), C. M. Baglin (Ed.), (Wiley Interscince, New York, 1996).

[19] D. J. Hudson, *Statistics Lectures on Elementary Statistics and Probability* (Geneva, 1964).

[20] V.V. Atrashkevich, Ya.K. Vaivade, V.P. Kolotov and V.V. Filippov, Analiticheskaya Khimiya 45 (1990) 5 (in Russian).

[21] Model S502 Genie-2000 Basic Spectroscopy Software. V1.X Russian; Model S561 Genie-2000 Batch Programming Support. V1.1.

[22] Certificate of complience #31/96/19826, D.I.Mendeleyev Institute for Metrology, State Center for Measuring Instrument Testing and Certification, Nov. 1995.

[23] H. Condé, V.P.Eismont, K.Elngren, A.I.Obukhov, A.N.Smirnov, "A Comparison of Proton- and Neutron-Induced Fission Cross Section of Heavy Nuclei of Intermediate Energies", in: Proc. Second Int. Conf. on Accelerator-Driven Transmutation Technologies and Applications, Kalmar, Sweden, June 3-7, 1996, ed. H. Condé (Uppsala University Press, 1997), Vol. 2, p. 599.

[24] M. Gloris, R. Michel, U. Herpers, F. Sudbrok, D. Filges, ”Production of residual nuclei from irradiation of thin Pb-targets with protons up to 1.6 GeV”, NIM B 113 (1996) 429-433

[25] R.Michel, M.Gloris, H.-J.Lange, I.Leya, M.Luepke, U.Herpers, B.Dittrich-Hannen, R.Roesel, Th.Schiekel, D.Filges, P.Dragovitsch, M.Suter, H.-J.Hofmann,W.Woelfli, P.W.Kubik, H.Baur, R.Wieler, ”Nuclide production by proton-induced reactions on elements (6<Z<29) in the energy range from 800 to 2600 MeV”, Nucl. Instr. Meth. B 103 (1995), 183-222.

[26] U. Reus and W.Westmeier, Catalog of gamma rays from radioactive decay, Atomic data and nuclear data tables, v. 29, part 1-2 (1983)

[27] A.Yu. Korovin et al., Report IAEA INDC(CCP)-384, 1995.

[28] V.P. Eismont et al., An experimental Database on proton-Induced Fission Cross Sections of Tantalum, Tungsten, Lead, Bismuth, Thorium and Uranium, Proceedings of the Second International Conference on Accelerator-Driven Transmutation Technologies and Applications. June 3-7, 1996, Kalmar, Sweeden, p.p. 592-598.

[29] Yu.N.Shubin, V.P.Lunev, A.Yu.Korovin, A.I.Dityuk, ”Cross Section Data Library MENDL-2 to Study Activation and Transmutation of Materials Irradiated by Neutrons of Intermediate Energies", Report IAEA, IC(CCP)-385, Vienna, 1995.

[30] J.B. Cumming, Monitor Reactions for High Energy Proton Beams, Annu. Rev. Nucl. Sci. No. 13, (1963) pp. 261-286.

[31] G.F. Steyn et al., Appl. Radiat. Isot. 41 (1990) 315.

[32] J.F.Janni, Proton Range-Energy Tables, Part 2, Nuclear Data and Nuclear Data Tables, 27, No.4/5 (1982) 339.

[33] R. Michel, R. Bodermann, H. Busemann, R. Daunke, M. Gloris, H.-J. Lange, B. Klug, A. Krins, I. Leya, M. Lüpke, S. Neumann, H. Reinhardt, M. Schnatz-Büttgen, U. Herpers, Th. Sciekel, F. Sudbrock, B. Holmqvist, H. Condé, P. Malmborg, M. Suter, B. Dittrich-Hannen, P.W. Kubik, H.-A. Synal and D. Filges, "Cross Sections for the Production of Residual Nuclides by Low- and Medium-Energy Protons from the Target Elements C, N, O, Mg, Al, Si, Ca, Ti, V, Mn, Fe, Co, Ni, Cu, Sr, Y, Zr, Nb, Ba and Au,"Nucl. Instr. and Meth. B. 129 (1997) 153 and references theirein. No. 2, pp. 153-193; see also the Web page at: http://sun1.rrzn-user.uni-hannover.de/zsr/survey.htm.

[34] Yu.E.Titarenko , V.F.Batyaev, N.V.Stepanov, V.D.Kazaritsky, S.G. Mashink, A.N.Sosnin, M.B.Chadwick, T.A.Gabriel, R.Michel, M.Gloris, R.E.Prael, M.Blann, "Experimental Study and Theoretical Simulation of Radionuclide Production in ^{99}Tc irradiated by protons of intermediate energies"Int. Conf. on Nuclear Data for Science and Technology, May 19-24, 1997, Trieste, Italy, p.1300

[35] R. Michel and P. Nagel, International Codes and Model Intercomparison for Intermediate Energy Activation Yields, NEA/OECD, Paris, 1997, NSC/DOC(97)-1; see also the Web page at: http://www.nea.fr/html/science/pt/ieay.

[36] W. Wlazlo, T. Enqvist, P. Armbruster et. al. "Isotope production in 1 A GeV ^{208}Pb on proton reactions", Proceedings of the Third International Conference on Accelerator-Driven Transmutation Technologies and Applications ADTT'99, Praha, June 1999; W. Wlazlo, T. Enqvist, P. Armbruster et. al. "Cross-sections of spallation residues produced in 1 A GeV ^{208}Pb on proton reactions"DAPNIA/SPHN-00-10 02/2000,p.1-4; W. Wlazlo, T. Enqvist, P. Armbruster, J. Benlliure, M. Bernas, A. Boudard, S. Czájkowski, R. Legrain, S. Leray, B. Mustapha, M. Pravikoff, F. Rejmund, K.-H. Schmidt, C. Stéphan, J. Taieb, L. Tassan-Got, and C. Volant, Phys. Rev. Lett. **84**, 5736 (2000); T. Enqvist, W. Wlazlo, P. Armbruster, J. Benlliure, M. Bernas, A. Boudard, S. Czájkowski, R. Legrain, S. Leray, B. Mustapha, M. Pravikoff, F. Rejmund, K.-H. Schmidt, C. Stéphan, J. Taieb, L. Tassan-Got, and C. Volant, "Isotopic Yields and Kinematic Energies of Primary Residues in 1A GeV ^{208}Pb + p Reactions,"GSI Preprint 2000-28, submitted to Nucl. Phys. A.

[37] J.R. Letaw et al. Ap. J. Suppl., 51 (1983) 271.

[38] A. Koning, Nuclear Data Evaluation for Accelerator-Driven Systems, Second International Conference on Accelerator-Driven Transmutation Technologies and Applications. June 3-7, 1996, Kalmar, Sweeden, p.p. 438-447.

[39] K.K. Gudima, S.G. Mashnik, V.D. Toneev, Nucl. Phys. A 401 (1983) 329–361; S.G. Mashnik, "User Manual for the Code CEM95", JINR, Dubna, 1995; OECD Nuclear Energy Agency Data Bank, Paris, France, 1995; http://www.nea.fr/abs/html/iaea1247.html; RSIC-PSR-357, Oak Ridge, 1995.

[40] V.S. Barashenkov, Le Van Ngok, L.G. Levchuk, Zh.Zh. Musul'manbekov, A.N. Sosnin, V.D. Toneev, S.Yu. Shmakov, JINR Report R2-85-173, Dubna, 1985; V.S. Barashenkov, F.G. Zheregi, Zh.Zh. Musul'manbekov, Yad. Fiz. 39 (1984) 1133 [Sov. J. Nucl. Phys. 39 (1984) 715]; V.S. Barashenkov, B.F. Kostenko, A.M. Zadorogny, Nucl. Phys. A 338 (1980) 413.

[41] G.A. Lobov, N.V. Stepanov, A.A. Sibirtsev, Yu.V. Trebukhovskii, ITEP Preprint ITEP- 91, Moscow, 1983; A.A. Sibirtsev, N.V. Stepanov, Yu.V. Trebukhovskii, ITEP Preprint ITEP-129, Moscow, 1985; N.V. Stepanov, ITEP Preprint ITEP-81, Moscow, 1987; N.V. Stepanov, ITEP Preprint ITEP-55-88, Moscow, 1988 (in Russian).

[42] T.W. Armstrong, K.C. Chandler, Nucl. Sci. Eng. 49 (1972) 110 and references therein.

[43] R.E. Prael, H. Lichtenstein, Los Alamos National Laboratory Report LA-UR-89-3014 (1989); see also the Web page at: http://www-xdiv.lanl.gov/XTM/lcs/lahet-doc.html.

[44] C.H. Tsao, Private communication, R. Silberberg, C.H. Tsao, Astrophys. J. 220 (1973) 315; ibid 335.

[45] Yu. A. Korovin, et al.: "Study of Accelerator-Driven Reactor systems", Kerntechnik, v.64 p.284 (1999); V. S. Barashenkov, A. Yu. Konobeev, Yu. A. Korovin, and V. N. Sosnin, Atomnaya Energiya **87**, 283 (1999) [Atomic Energy **87**, 742 (1999)].

[46] P.G. Young, E.D. Arthur and M.B.Chadwick, Los Alamos National Laboratory Report LA-12343-MS (1992); M.B. Chadwick and P.G. Young, Phys. Rev. C 47 (1993) 2255.

[47] M. Blann, Phys. Rev. C 54 (1996) 1341.

[48] Phys. Rev. C52 (1995) 2620; K. Niita, S. Chiba, H. Takada, and T. Maruyama, Proc. of the Third Workshop on Simulating Accelerator Radiation Environments, KEK Proceedings 97-5 (1997) edited by H. Hirayama, p.1.

[49] T. Nishida, Y. Nakahara, T. Tsutsui: "Development of a Nuclear Spallation Simulation Code and Calculations of Primary Spallation Products", JAERI-M 86-116, (1986), [in Japanese].

[50] V.S.Barashenkov, V.D.Toneev Interactions of High-Energy Particles and Atomic Nuclei with Nuclei, Moscow, 1972

[51] Wapstra A.H., Audi G. The 1995 Update to the Atomic Masses Evaluation // Nuclear Physics, 1995, v.A595, p.409

[52] S. G. Mashnik and A. J. Sierk, in *Proceedings of the Fourth International Workshop on Simulating Accelerator Radiation Environments (SARE4), Knoxville, TN, 1998*, edited by T. A. Gabriel, (ORNL, 1999), p. 29.

[53] The code CEM2k is briefly surveyed in S. G. Mashnik, L. S. Waters, and T. A. Gabriel, “Models and Codes for Intermediate Energy Nuclear Reactions,"in *Proceedings of the Fifth International Workshop on Simulating Accelerator Radiation Environments (SARE5), July 17-18, 2000, OECD Headquarters, Paris, France*, and will be described by S. G. Mashnik and A. J. Sierk in a future paper.

[54] V. S. Barashenkov, A. Yu. Konobeev, Yu. A. Korovin, and V. N. Sosnin, Atomnaya Energiya **87**, 283 (1999) [Atomic Energy **87**, 742 (1999)].

[55] A.I. Dityuk, A.Yu. Konobeyev, V.P. Lunev, and Yu.N. Shubin, New Version of the Advanced Computer Code ALICE-IPPE, Report INDC (CCP)-410, IAEA, Vienna, 1998.

7 Annex 1. Comparison between experimental and simulated data.

Table 65: Experimental and calculated yields from ^{182}W irradiated with 0.2 GeV protons.

Product	$T_{1/2}$	Type	Exp yield [mbarn]	Calculated Yields [mbarn] via CEM95	LAHET	CASCADE	HETC	INUCL	YIELDX
^{181}Re	19,9h	i	13.2 ± 1.8	23.5	30.7	40.3	22.3	25.1	11.2
^{179}Re	19,5m	i	21.7 ± 2.5	21.5	31.8	33.7	28.0	28.6	23.0
^{178}W	21,6d	c	70.6 ± 8.2	76.4	91.1	81.6	73.2	108.	80.9
^{177}W	135m	c	70.4 ± 8.0	79.4	84.3	79.2	73.8	93.6	68.9
^{176}W	2,5h	c	84.1 ± 7.1	80.3	91.1	91.3	75.8	96.1	57.5
^{174}W	31m	c	80.6 ± 9.0	72.2	85.5	92.6	77.8	71.7	35.9
^{183}Ta	5,1d	c	0.548 ± 0.117	–	–	–	–	–	0.753
^{176}Ta	8,09h	c	112. ± 8.	115.	114.	107.	84.7	130.	93.1
^{176}Ta	8,09h	i(m+g)	25.3 ± 3.1	35.8	24.2	16.4	10.0	34.2	36.2
^{174}Ta	1,14h	i	24.2 ± 4.3	46.0	28.9	20.6	10.4	27.5	29.9
^{172}Ta	36,8m	c*	51.2 ± 4.3	91.6	104.	121.	110.	72.7	62.1
^{171}Ta	23,3m	c*	10.0 ± 1.4	56.3	77.8	90.2	103.	45.9	47.5
^{175}Hf	70d	c	120. ± 9.	134.	116.	108.	89.1	118.	86.6
^{173}Hf	23,6h	c	115. ± 8.	132.	110.	109.	90.6	84.5	75.1
^{172}Hf	1,87y	c	86.8 ± 5.8	115.	102.	113.	93.6	69.4	74.4
^{171}Hf	12,1h	c	72.3 ± 5.7	87.1	86.0	96.1	97.5	49.8	65.0
^{172}Lu	6,70d	i(m1+m2+g)	1.17 ± 0.09	4.82	1.38	0.219	0.018	0.208	2.14
^{171}Lu	8,24d	i(m+g)	12.6 ± 3.1	6.11	2.63	0.668	0.035	0.327	2.10
^{170}Lu	2,012d	c	60.8 ± 3.9	57.6	65.6	85.5	90.7	34.8	31.8
^{169}Yb	32,026d	c	48.6 ± 3.1	38.8	53.2	64.8	106.	24.2	19.6
^{166}Tm	7,70h	c	15.9 ± 1.1	4.38	21.3	14.8	38.7	7.79	6.25
^{165}Tm	30,06h	c	10.7 ± 0.8	1.73	11.6	7.53	2.93	4.78	3.66

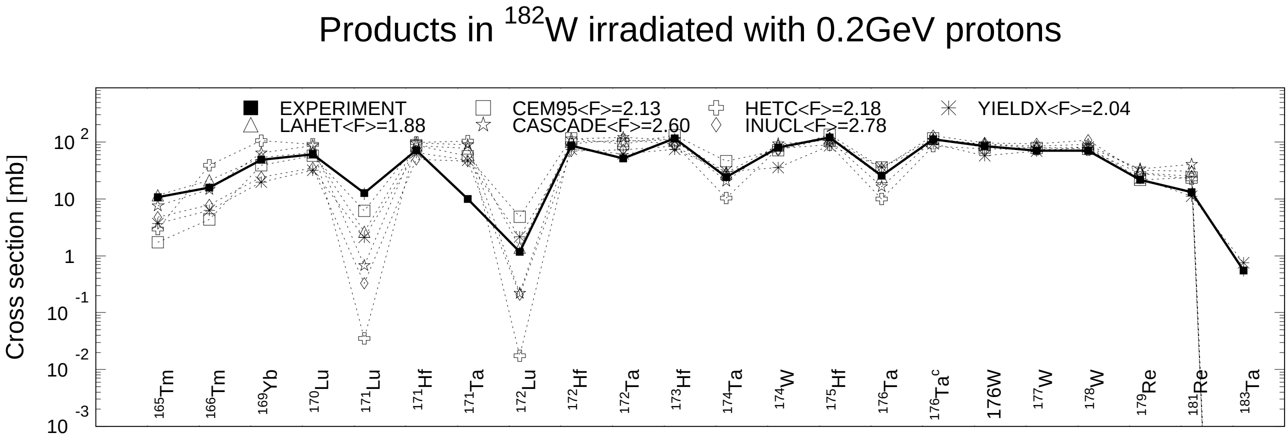

Fig. 25: Detailed comparison between experimental and simulated yields of radioactive reaction products in ^{182}W irradiated with 0.2 GeV protons. The cumulative yields are labeled -c when the respective independent yields are also shown.

Mass yields in ^{182}W,^{183}W, ^{184}W, and ^{186}W irradiated with 0.2GeV protons

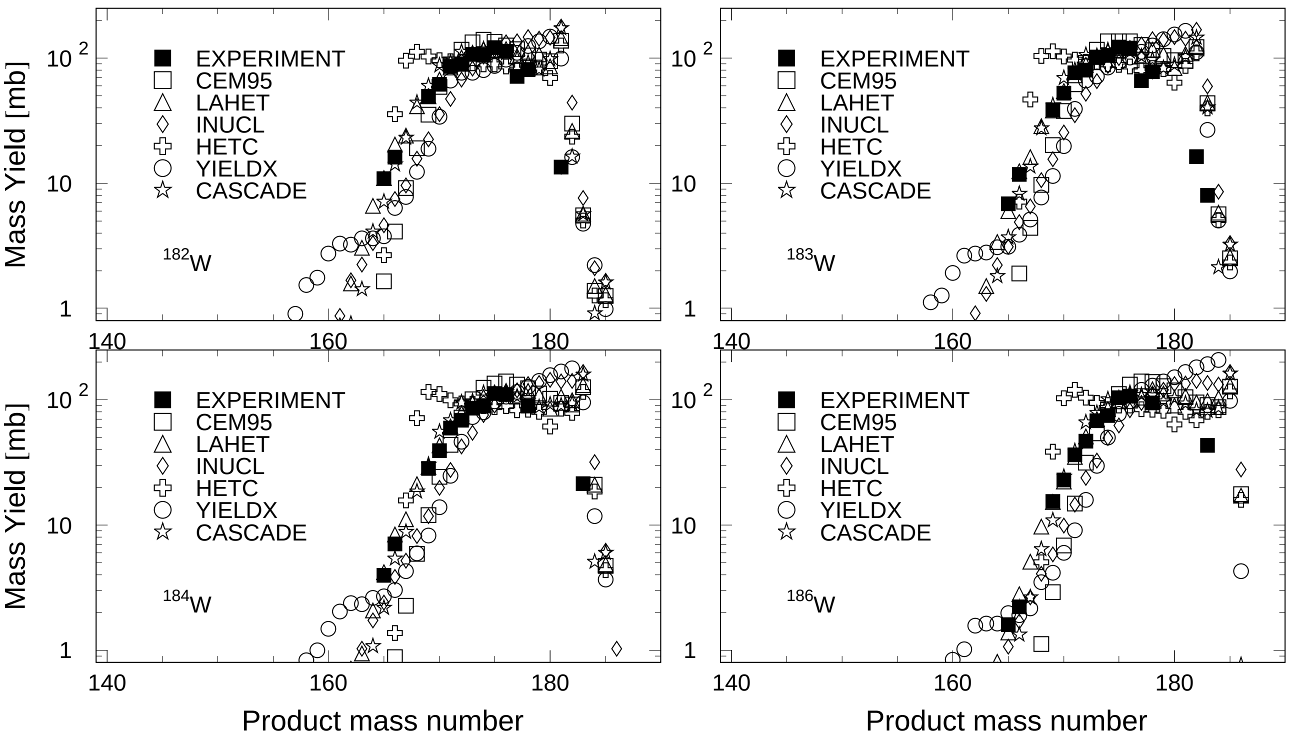

Fig. 26: The simulated mass distributions of reaction products together with the measured cumulative and supra-cumulative yields in ^{182,183,184,186}W irradiated with 0.2 GeV protons.

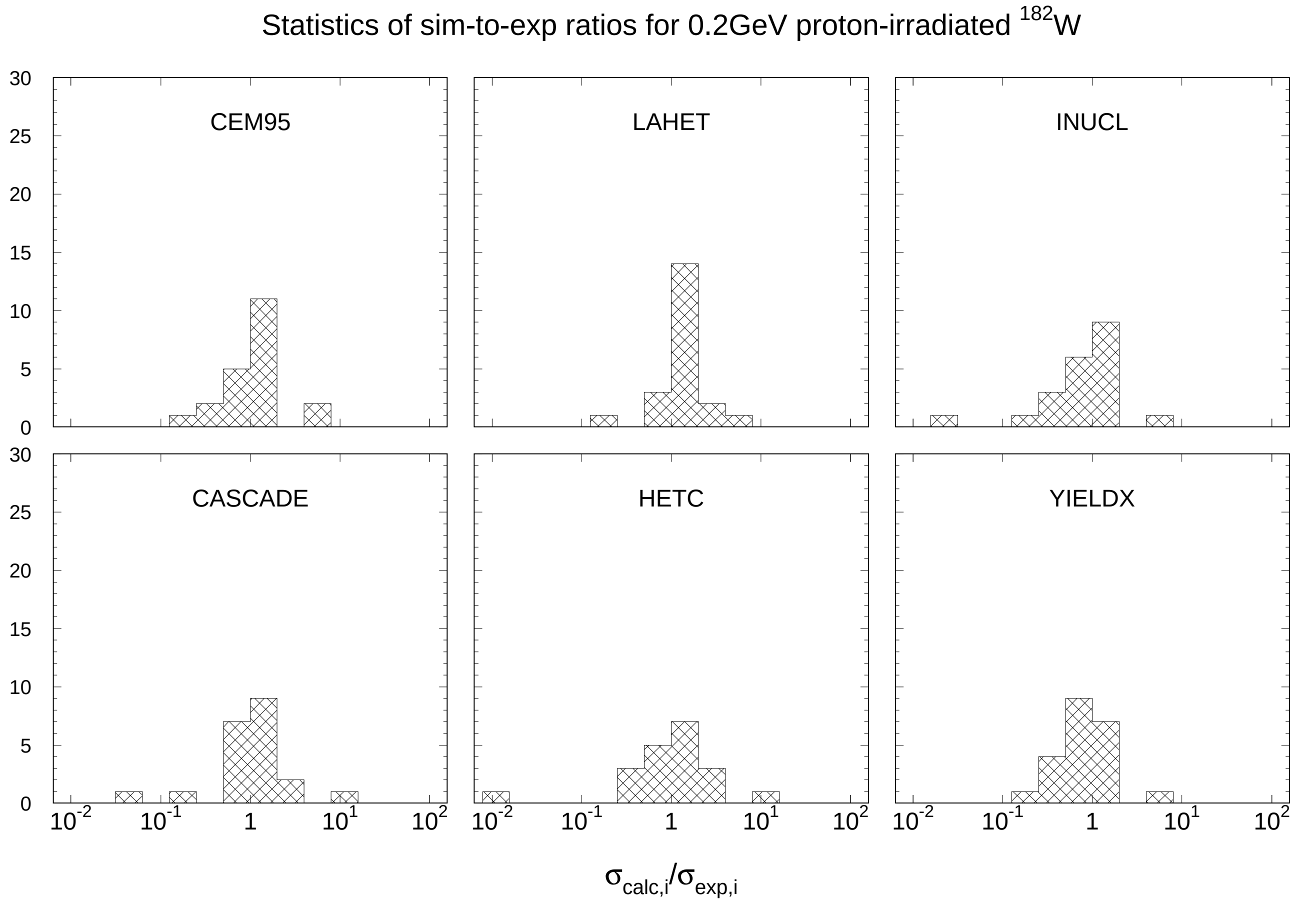

Fig. 27: Statistics of the simulation-to-experiment ratios (criterion 2) for ^{182}W irradiated with 0.2 GeV protons.

Table 66: Experimental and calculated yields from ^{182}W irradiated with 0.8 GeV protons.

Product	$T_{1/2}$	Type	Exp yield [mbarn]	Calculated Yields [mbarn] via CEM95	LAHET	CASCADE	HETC	INUCL	YIELDX
^{183}Ta	5,1d	c	1.14 ± 0.22	–	–	–	–	–	0.626
^{181}Re	19,9h	i	4.58 ± 0.72	4.34	6.98	6.55	3.97	3.36	1.86
^{177}W	135m	c	25.4 ± 2.9	22.9	28.5	21.4	26.9	26.9	26.7
^{176}Ta	8,09h	c	50.9 ± 4.3	37.2	46.8	35.1	35.8	53.7	41.7
^{175}Hf	70d	c	56.3 ± 4.1	43.1	52.2	41.4	40.6	64.2	46.5
^{174}Ta	1,14h	c	51.5 ± 5.5	34.8	42.3	38.1	35.2	50.4	37.5
^{174}Ta	1,14h	i	38.1 ± 4.8	16.8	17.7	13.6	12.6	25.9	18.5
^{173}Hf	23,6h	c	60.2 ± 4.4	45.5	49.7	46.1	41.6	66.5	53.4
^{172}Hf	1,87y	c	47.9 ± 3.3	44.5	49.2	50.8	41.3	68.2	65.4
^{172}Lu	6,70d	i(m1+m2+g)	3.68 ± 0.40	4.15	3.80	1.93	1.24	5.43	1.94
^{171}Hf	12,1h	c	48.1 ± 4.8	45.7	47.0	48.2	43.3	64.0	71.0
^{171}Lu	8,24d	i(m+g)	9.61 ± 3.79	6.86	6.24	3.84	1.49	7.49	3.42
^{170}Lu	2,012d	c	51.1 ± 4.1	49.3	49.5	52.7	41.8	68.9	44.8
^{170}Lu	2,012d	i(m+g)	4.04 ± 2.25	8.85	7.41	3.53	1.44	8.03	4.39
^{169}Yb	32,026d	c	58.0 ± 4.4	54.8	49.5	54.0	43.3	68.1	33.7
^{167}Tm	9,25d	c	60.6 ± 12.2	56.6	46.0	49.3	39.8	58.7	26.8
^{166}Tm	7,70h	c	56.2 ± 4.0	58.3	53.7	59.2	43.8	62.9	30.9
^{166}Tm	7,70h	i	3.71 ± 0.76	3.46	1.23	0.600	0.076	0.785	1.61
^{165}Tm	30,06h	c	57.3 ± 4.2	57.6	47.3	55.5	43.4	52.9	24.8
^{162}Yb	18,87m	c	44.9 ± 6.2	37.9	37.3	52.3	48.1	37.1	16.2
^{161}Tm	33m	c*	41.2 ± 7.1	50.9	39.4	51.5	49.1	33.8	37.4
^{161}Er	3,21h	c	47.3 ± 4.2	55.8	38.0	48.1	42.8	32.4	41.2
^{160}Er	28,58h	c	54.4 ± 4.3	51.8	41.0	50.9	42.2	31.2	41.3
^{159}Er	36m	c*	59.4 ± 4.2	55.7	43.5	55.3	56.2	30.0	38.4
^{159}Ho	33,05m	c	54.4 ± 4.2	50.0	36.8	43.5	42.0	24.7	35.7
^{157}Dy	8,14h	c	44.6 ± 3.4	45.5	31.7	38.5	39.1	19.5	31.2
^{156}Ho	56m	c	38.1 ± 3.0	36.6	29.6	37.1	35.9	18.4	27.0
^{155}Tb	5,32d	c	36.7 ± 3.3	34.7	28.5	22.8	0.029	13.9	28.6
^{153}Dy	6,4h	c	21.3 ± 1.8	22.6	19.9	17.3	3.40	9.95	19.1
^{153}Gd	240,4d	c	28.0 ± 2.4	26.6	22.3	17.7	3.40	10.8	–
^{152}Dy	2,38h	c	20.1 ± 1.3	18.4	19.6	15.0	8.63	9.02	19.1
^{148}Eu	54,5d	i	1.14 ± 0.23	1.06	1.34	0.073	–	0.320	0.716
^{147}Eu	24,1d	c	22.5 ± 1.9	12.2	16.3	15.9	32.1	7.23	11.9
^{146}Gd	48,27d	c	19.1 ± 1.2	9.40	13.8	15.0	25.7	7.60	12.3
^{145}Eu	5,93d	c	13.9 ± 1.0	7.09	13.2	10.7	24.3	5.42	10.6
^{139}Ce	137,640d	c	6.02 ± 0.39	0.934	6.10	2.62	7.66	2.51	6.59
^{127}Xe	36,4d	c	0.936 ± 0.086	–	0.521	0.034	–	0.451	1.47
^{88}Zr	83,4d	c	0.346 ± 0.074	–	0.209	0.825	–	0.131	1.46
^{88}Y	106,65d	c	0.836 ± 0.066	–	0.294	1.92	–	0.138	1.85
^{84}Rb	32,77d	i(m+g)	0.552 ± 0.045	–	0.076	1.77	–	0.027	0.248
^{83}Rb	86,2d	c	0.890 ± 0.122	–	0.209	2.88	–	0.148	1.39
^{74}As	17,77d	i	0.563 ± 0.066	–	0.104	0.931	–	0.047	0.277
^{59}Fe	44,472d	c	0.281 ± 0.030	–	0.133	0.123	–	0.007	0.115

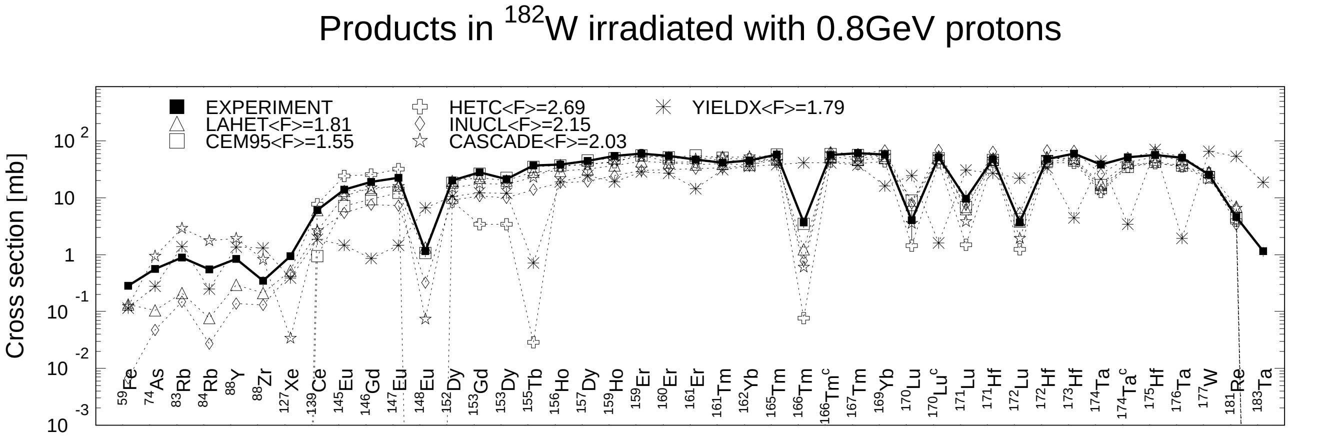

Fig. 28: Detailed comparison between experimental and simulated yields of radioactive reaction products in ^{182}W irradiated with 0.8 GeV protons. The cumulative yields are labeled -c when the respective independent yields are also shown.

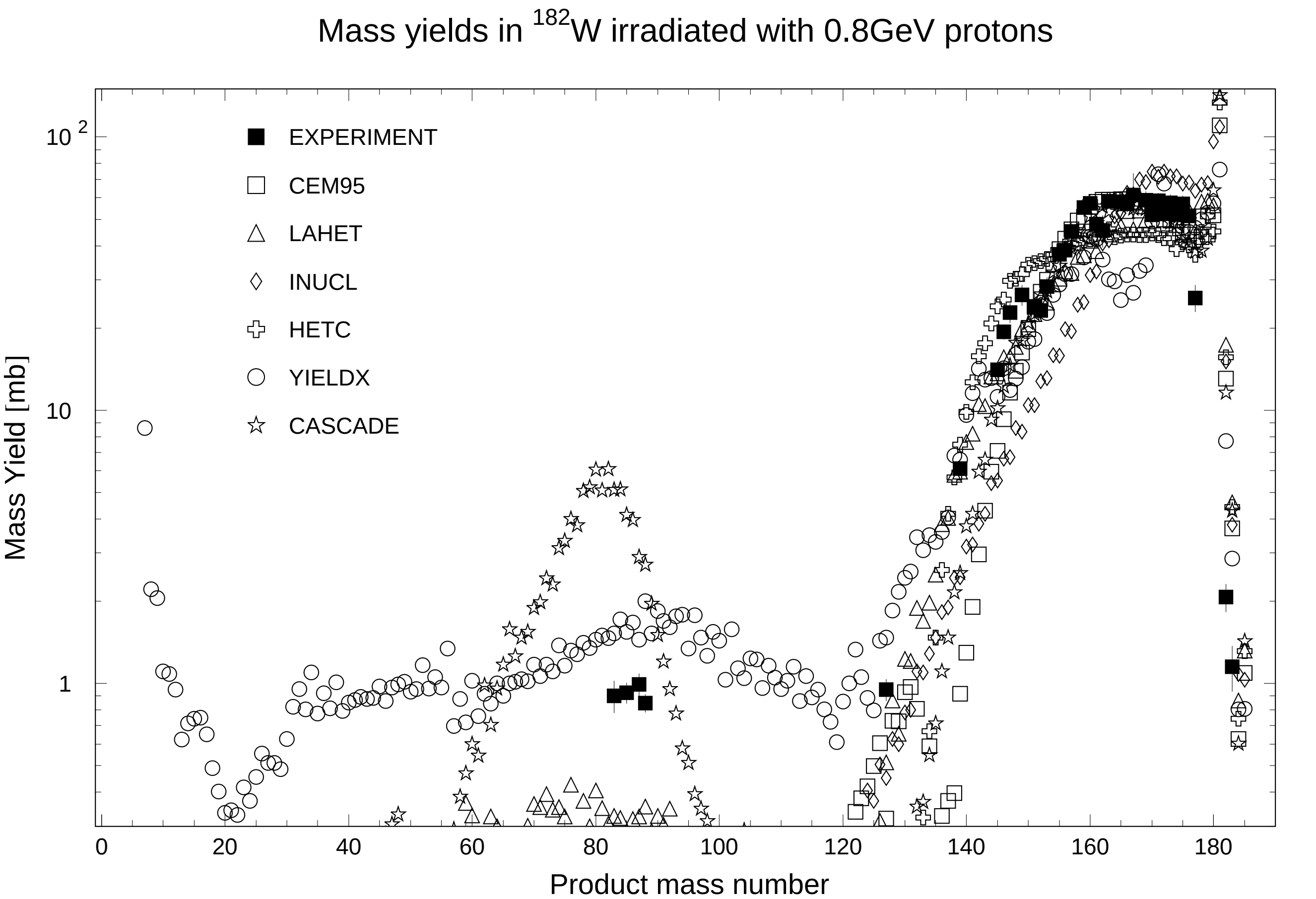

Fig. 29: The simulated mass distributions of reaction products together with the measured cumulative and supra-cumulative yields in ^{182}W irradiated with 0.8 GeV protons.

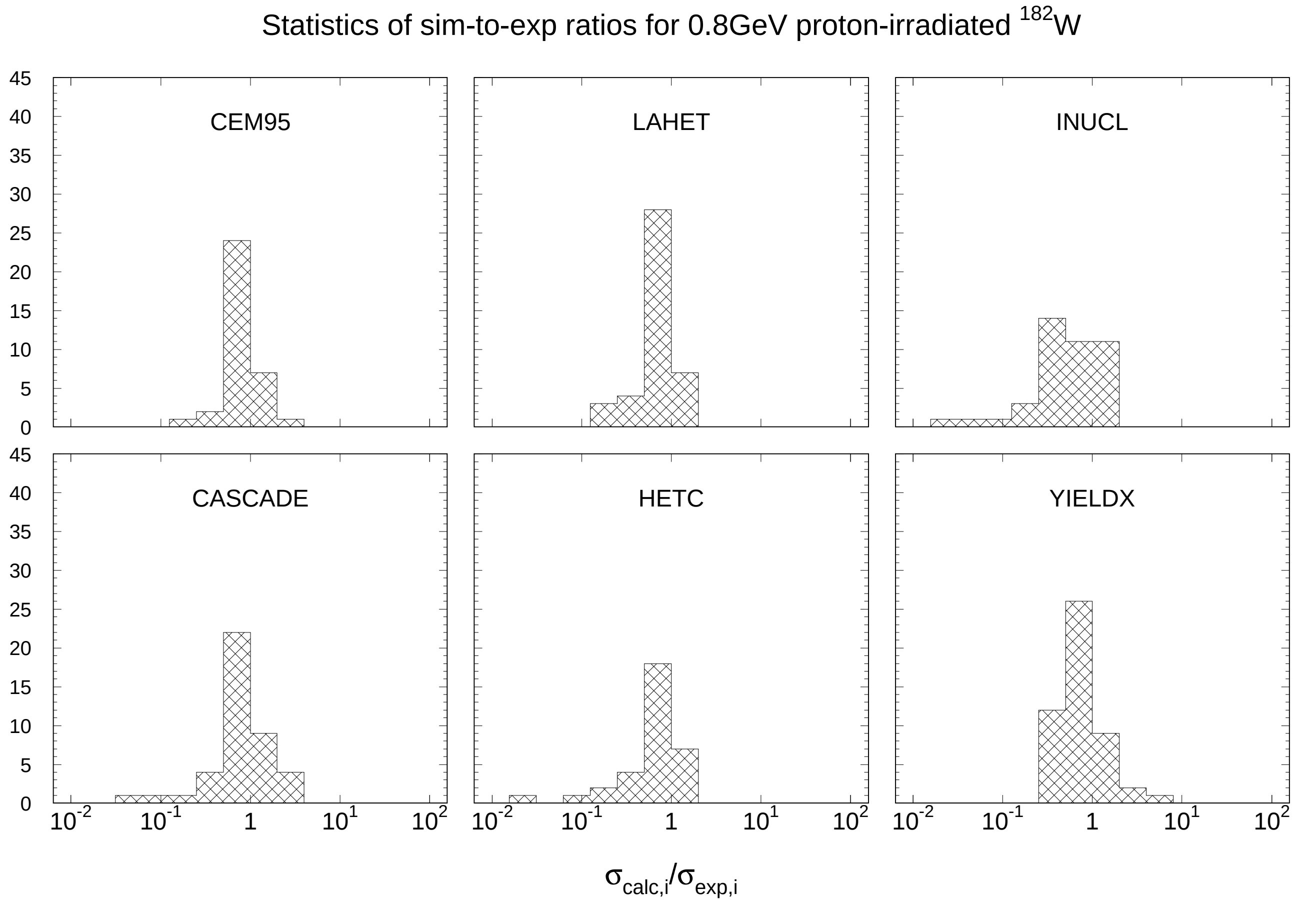

Fig. 30: Statistics of the simulation-to-experiment ratios (criterion 2) for ^{182}W irradiated with 0.8 GeV protons.

Table 67: Experimental and calculated yields from ^{182}W irradiated with 1.6 GeV protons.

Product	$T_{1/2}$	Type	Exp yield [mbarn]	Calculated Yields [mbarn] via CEM95	LAHET	CASCADE	HETC	INUCL	YIELDX
^{181}Re	19,9h	i	3.71 ± 0.61	0.502	3.36	1.95	3.21	0.252	1.15
^{177}W	135m	c	19.4 ± 2.4	14.9	17.6	14.1	19.3	17.4	19.7
^{182}Ta	114,43d	c	2.24 ± 0.34	0.017	1.50	–	0.316	–	1.21
^{176}Ta	8,09h	c	38.9 ± 3.9	23.6	28.1	24.2	27.2	36.1	32.7
^{174}Ta	1,14h	c	43.9 ± 5.9	19.0	21.6	22.3	24.2	31.7	33.3
^{181}Hf	42,39d	c	0.187 ± 0.025	0.025	0.147	–	0.058	–	0.024
^{175}Hf	70d	c	39.0 ± 3.4	27.2	29.9	26.3	29.2	44.1	41.0
^{173}Hf	23,6h	c	38.6 ± 3.2	24.9	25.2	28.0	27.6	41.6	–
^{173}Hf	23,6h	i	6.20 ± 2.75	8.09	4.79	5.71	4.50	12.3	16.9
^{172}Hf	1,87y	c	30.5 ± 2.9	23.9	23.4	28.8	26.7	43.2	83.0
^{171}Hf	12,1h	c	30.5 ± 3.3	22.7	21.6	27.5	26.1	39.9	100.
^{172}Lu	6,70d	i(m1+m2+g)	2.95 ± 0.26	2.65	2.51	1.58	1.27	4.54	1.84
^{171}Lu	8,24d	i(m+g)	4.72 ± 2.23	3.91	3.67	2.91	1.25	6.51	3.14
^{170}Lu	2,012d	c	32.2 ± 2.7	24.2	23.1	29.9	25.3	44.7	–
^{170}Lu	2,012d	i(m+g)	7.25 ± 1.97	4.78	4.17	2.75	1.73	6.98	4.01
^{169}Yb	32,026d	c	32.1 ± 2.6	27.0	23.6	30.8	26.4	47.3	33.5
^{162}Yb	18,87m	c	39.5 ± 5.7	17.7	16.8	31.1	27.9	33.1	17.6
^{167}Tm	9,25d	c	36.3 ± 5.2	27.4	20.7	29.9	23.0	44.2	24.3
^{166}Tm	7,70h	c	31.8 ± 3.2	27.2	26.0	35.0	27.3	47.6	28.2
^{166}Tm	7,70h	i	0.264 ± 0.357	1.84	0.950	0.709	0.124	1.20	2.01
^{165}Tm	30,06h	c	32.1 ± 2.8	27.0	21.6	32.7	25.4	43.0	25.5
^{161}Er	3,21h	c	28.2 ± 3.8	27.2	19.0	31.5	24.7	33.6	45.1
^{160}Er	28,58h	c	32.7 ± 3.2	26.7	20.1	34.6	25.3	34.6	44.5
^{159}Er	36m	c*	40.3 ± 6.0	31.2	22.5	37.7	32.2	35.2	41.0
^{156}Ho	56m	c	24.6 ± 4.9	25.6	16.6	30.7	22.1	25.8	27.9
^{157}Dy	8,14h	c	31.5 ± 2.9	28.3	18.4	30.6	23.4	26.6	32.6
^{153}Dy	6,4h	c	22.3 ± 2.5	21.3	12.6	18.4	2.38	17.6	19.7
^{152}Dy	2,38h	c	20.3 ± 1.7	18.9	13.8	17.2	5.85	17.1	–
^{155}Tb	5,32d	c	30.0 ± 2.5	26.0	17.8	20.6	0.259	22.0	29.5
^{153}Gd	240,4d	c	24.1 ± 2.4	25.3	14.7	19.5	2.38	19.6	23.1
^{151}Gd	124d	c	20.6 ± 2.0	27.2	15.4	24.1	18.4	19.8	18.0
^{146}Gd	48,27d	c	26.3 ± 2.1	28.5	14.0	32.5	26.2	20.0	13.3
^{147}Eu	24,1d	c	28.8 ± 2.4	30.9	15.8	28.8	26.9	18.5	12.1
^{146}Eu	4,61d	i	7.22 ± 1.00	5.65	4.26	0.885	–	2.45	2.52
^{145}Eu	5,93d	c	22.8 ± 1.9	31.0	15.7	27.0	27.3	16.2	11.6
^{144}Pm	363d	i	0.569 ± 0.074	1.00	0.794	0.125	–	0.371	1.09
^{143}Pm	265d	c	22.8 ± 2.3	32.1	16.0	26.3	26.9	15.1	14.2
^{137}Nd	38,5m	c	37.3 ± 5.1	20.6	9.79	18.0	26.6	8.96	4.03
^{136}Nd	50,65m	c	17.6 ± 1.8	15.6	10.6	16.4	23.9	7.81	2.74
^{139}Ce	137,640d	c	21.8 ± 1.8	29.1	17.0	21.9	24.4	12.2	7.82
^{135}Ce	17,7h	c	18.2 ± 1.4	24.0	14.1	16.6	24.2	9.19	4.70
^{134}Ce	3,16d	c	17.0 ± 1.6	20.9	14.9	17.2	20.4	8.77	5.04
^{132}Ce	3,51h	c	13.8 ± 1.6	14.5	14.1	13.1	21.5	6.33	–
^{133}Ba	3848,9d	c	17.2 ± 2.5	20.1	13.4	14.0	20.1	8.19	4.81
^{131}Ba	11,50d	c	14.8 ± 1.1	16.9	16.5	12.4	20.3	7.21	4.43
^{128}Ba	2,43d	c	11.6 ± 1.1	11.1	17.0	9.55	16.8	4.87	3.65
^{129}Cs	32,06h	c	14.7 ± 1.4	15.0	16.9	9.97	22.8	6.21	4.46
^{127}Xe	36,4d	c	11.1 ± 0.9	11.4	17.9	8.42	19.1	4.69	3.13
^{125}Xe	16,9h	c	9.84 ± 0.80	8.94	15.4	7.30	18.1	4.10	1.98
^{123}Xe	2,08h	c	10.9 ± 1.0	5.90	10.4	4.66	14.6	2.49	2.75
^{105}Ag	41,29d	c	1.69 ± 0.18	0.094	7.77	0.414	0.355	0.198	1.63
^{90}Nb	14,60h	c	1.12 ± 0.11	–	1.11	0.159	–	0.099	6.91
^{88}Zr	83,4d	c	1.19 ± 0.13	–	1.60	1.10	–	0.164	10.8
^{88}Y	106,65d	i(m+g)	0.550 ± 0.143	–	0.737	0.687	–	0.017	2.12
^{84}Rb	32,77d	i(m+g)	0.735 ± 0.084	–	0.376	1.38	–	0.041	1.11

Table 67, cont'd.

Product	$T_{1/2}$	Type	Exp yield [mbarn]	Calculated Yields [mbarn] via CEM95	LAHET	CASCADE	HETC	INUCL	YIELDX
^{83}Rb	86,2d	c	2.12 ± 0.28	–	0.941	3.07	–	0.245	10.1
^{75}Se	119,779d	c	1.57 ± 0.23	–	0.491	2.44	–	0.317	7.17
^{74}As	17,77d	i	0.921 ± 0.108	–	0.188	0.993	–	0.054	1.87
^{59}Fe	44,472d	c	0.503 ± 0.051	–	0.057	0.176	–	0.007	0.716
^{54}Mn	312,11d	i	1.08 ± 0.21	–	0.319	0.403	–	0.065	2.81
^{48}V	15,9735d	c	0.252 ± 0.038	–	0.205	–	–	0.036	0.942
^{48}Sc	43,67h	i	0.429 ± 0.045	–	0.065	0.074	–	0.010	0.374
^{28}Mg	20,915h	c	0.388 ± 0.042	–	–	0.006	–	–	0.286
^{24}Na	14,9590h	c	1.84 ± 0.15	–	0.074	0.028	–	–	0.899
^{7}Be	53,29d	i	5.12 ± 0.58	–	–	–	–	–	1.53

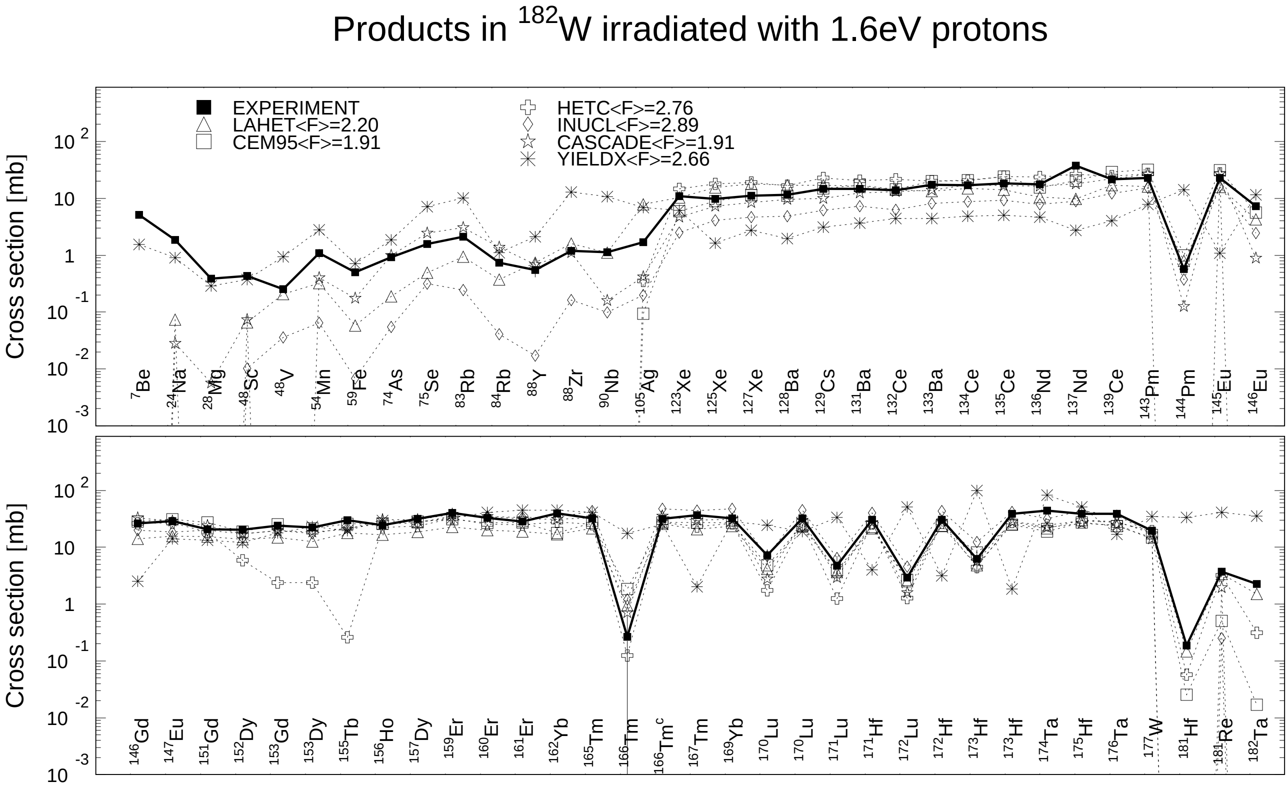

Fig. 31: Detailed comparison between experimental and simulated yields of radioactive reaction products in ^{182}W irradiated with 1.6 GeV protons. The cumulative yields are labeled -c when the respective independent yields are also shown.

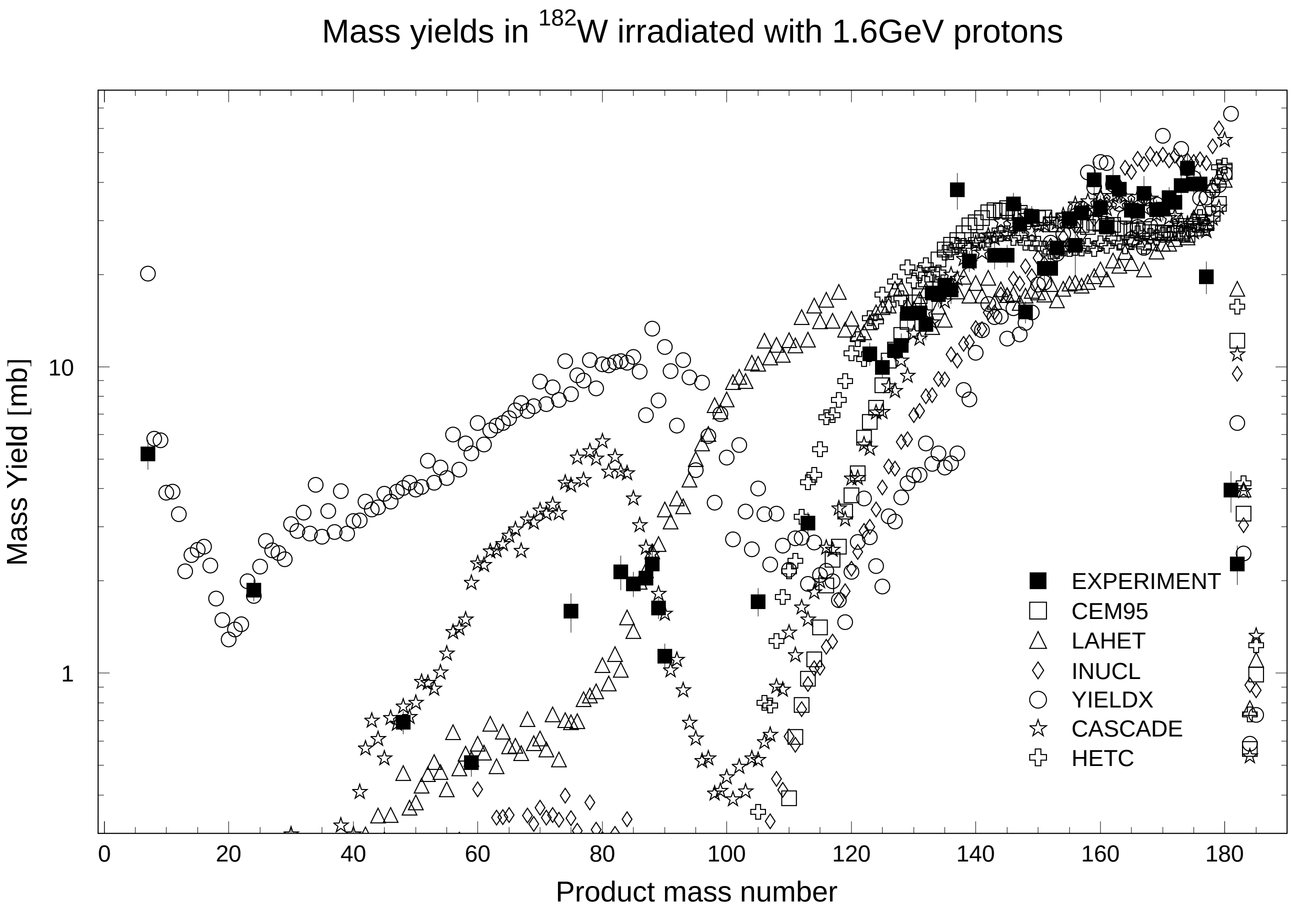

Fig. 32: The simulated mass distributions of reaction products together with the measured cumulative and supra-cumulative yields in ^{182}W irradiated with 1.6 GeV protons.

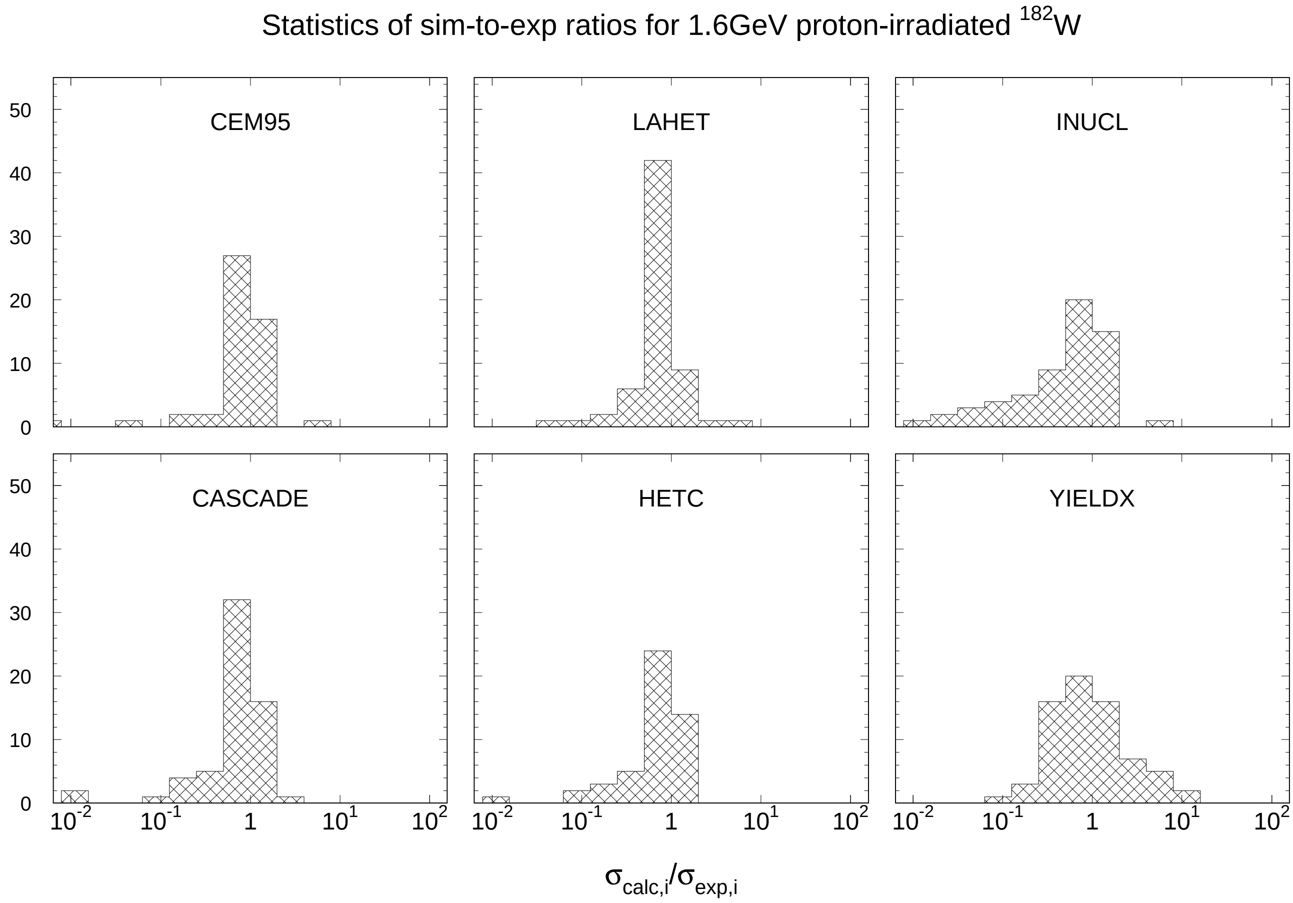

Fig. 33: Statistics of the simulation-to-experiment ratios (criterion 2) for ^{182}W irradiated with 1.6 GeV protons.

Table 68: Experimental and calculated yields from ^{183}W irradiated with 0.2 GeV protons.

Product	$T_{1/2}$	Type	Exp yield [mbarn]	Calculated Yields [mbarn] via CEM95	LAHET	CASCADE	HETC	INUCL	YIELDX
^{183}Re	70,0d	i(m+g)	5.20 ± 0.46	9.87	11.3	6.03	10.8	18.1	5.87
^{182}Re	64,0h	i	3.91 ± 0.41	20.4	15.2	26.9	14.3	22.3	12.1
^{181}Re	19,9h	i	22.4 ± 2.9	21.0	32.0	41.8	26.1	28.3	19.4
^{179}Re	19,5m	i	19.8 ± 3.7	21.9	30.6	31.3	28.2	28.9	27.3
^{178}W	21,6d	c	65.5 ± 10.5	78.9	91.2	84.1	72.4	104.	85.0
^{177}W	135m	c	64.9 ± 7.8	80.6	81.1	81.0	72.7	86.9	72.2
^{176}W	2,5h	c	74.9 ± 10.1	81.9	90.2	92.3	74.9	86.2	60.7
^{174}W	31m	c	71.8 ± 8.4	64.3	77.6	89.5	77.6	61.0	36.3
^{183}Ta	5,1d	c	2.71 ± 0.29	–	–	–	–	–	3.27
^{176}Ta	8,09h	c	118. ± 9.	121.	116.	109.	84.0	117.	92.9
^{176}Ta	8,09h	i(m+g)	39.2 ± 8.1	40.2	26.7	17.6	10.2	31.5	32.9
^{174}Ta	1,14h	i	32.0 ± 5.5	47.1	31.5	21.7	10.4	22.9	26.1
^{172}Ta	36,8m	c*	48.0 ± 5.2	66.6	89.4	115.	110.	55.7	50.3
^{171}Ta	23,3m	c*	8.16 ± 1.22	34.3	65.8	79.1	105.	33.7	23.1
^{175}Hf	70d	c	121. ± 9.	135.	114.	112.	87.7	102.	91.7
^{173}Hf	23,6h	c	107. ± 7.	117.	104.	106.	92.6	67.8	69.2
^{172}Hf	1,87y	c	76.2 ± 5.4	90.4	89.3	109.	93.2	53.6	63.7
^{171}Hf	12,1h	c	69.9 ± 5.2	59.2	74.3	85.6	98.9	37.2	37.7
^{172}Lu	6,70d	i(m1+m2+g)	1.68 ± 0.18	5.64	2.09	0.333	0.035	0.188	2.02
^{171}Lu	8,24d	i(m+g)	5.12 ± 1.25	7.08	3.35	0.592	0.044	0.293	1.97
^{170}Lu	2,012d	c	51.5 ± 3.6	37.7	54.5	69.2	95.4	25.2	18.4
^{169}Yb	32,026d	c	38.0 ± 2.6	22.7	42.0	47.0	117.	17.0	11.8
^{166}Tm	7,70h	c	11.6 ± 0.8	2.08	13.4	8.81	7.18	5.04	3.77
^{165}Tm	30,06h	c	6.75 ± 0.69	0.735	6.25	3.99	0.202	3.26	2.97

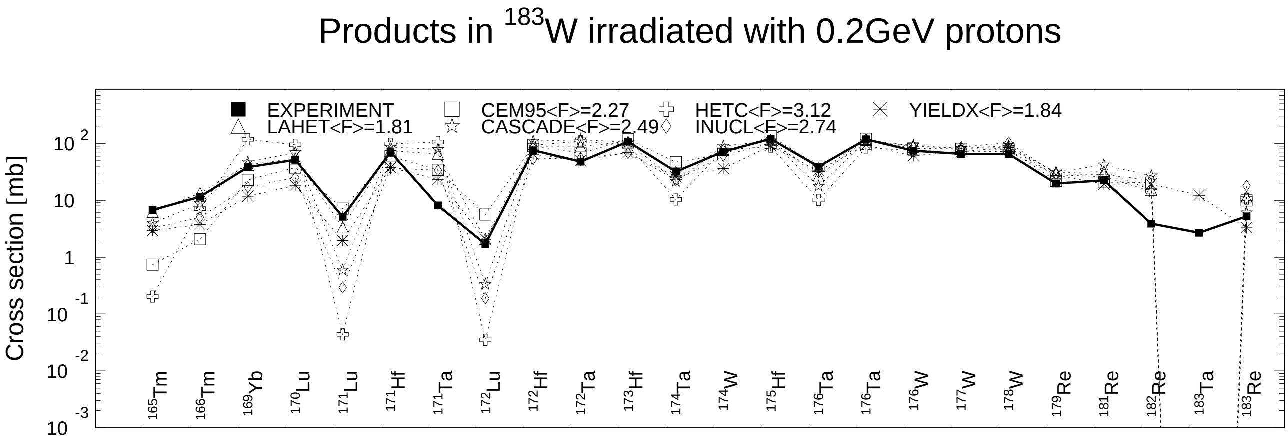

Fig. 34: Detailed comparison between experimental and simulated yields of radioactive reaction products in ^{183}W irradiated with 0.2 GeV protons. The cumulative yields are labeled -c when the respective independent yields are also shown.

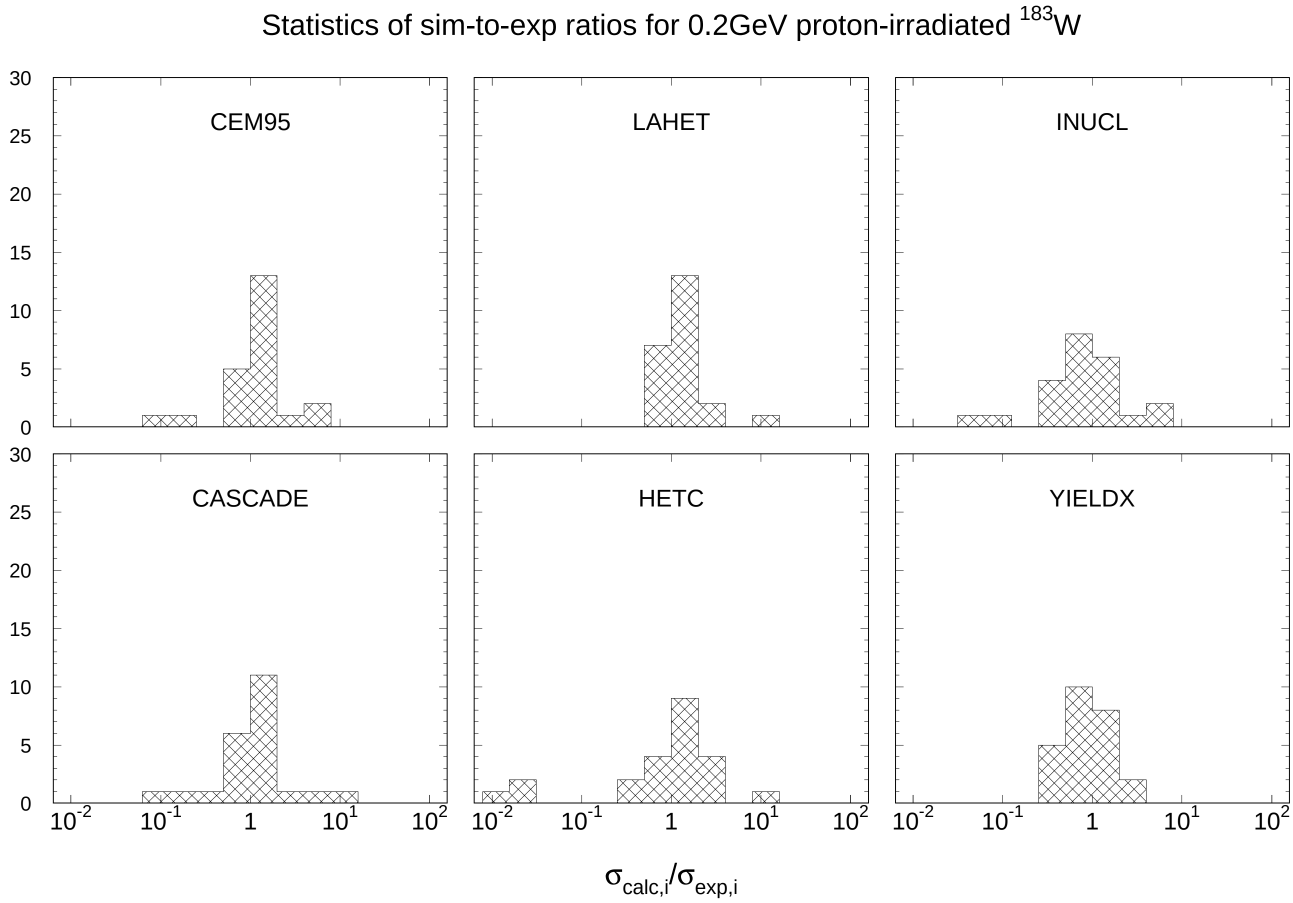

Fig. 35: Statistics of the simulation-to-experiment ratios (criterion 2) for ^{183}W irradiated with 0.2 GeV protons.

Table 69: Experimental and calculated yields from ^{183}W irradiated with 0.8 GeV protons.

Product	$T_{1/2}$	Type	Exp yield [mbarn]	Calculated Yields [mbarn] via CEM95	LAHET	CASCADE	HETC	INUCL	YIELDX
^{184}Ta	8,7h	c	0.564 ± 0.123	–	–	–	–	–	0.347
^{183}Re	70,0d	i(m+g)	1.69 ± 0.33	1.67	2.61	0.670	2.04	4.54	0.969
^{183}Ta	5,1d	c	5.53 ± 0.39	0.017	0.076	–	–	–	3.76
^{181}Re	19,9h	i	6.29 ± 0.99	4.40	8.30	7.11	5.31	3.80	3.21
^{181}Hf	42,39d	c	0.653 ± 0.074	2.26	2.47	7.01	2.88	2.07	0.192
^{177}W	135m	c	24.6 ± 2.8	21.1	27.2	21.2	26.1	26.0	29.6
^{176}Ta	8,09h	c	54.1 ± 4.7	36.4	44.8	36.1	35.3	52.9	45.3
^{175}Hf	70d	c	60.2 ± 4.3	44.2	50.9	43.3	41.0	65.6	54.2
^{174}Ta	1,14h	c	53.8 ± 5.8	33.3	39.3	37.9	36.6	49.3	39.6
^{174}Ta	1,14h	i	45.4 ± 5.8	17.1	17.7	14.4	13.6	26.6	18.2
^{173}Hf	23,6h	c	62.8 ± 4.6	45.2	49.1	46.7	40.6	65.1	57.9
^{172}Hf	1,87y	c	51.8 ± 3.6	44.5	47.2	50.5	41.2	67.7	70.4
^{172}Lu	6,70d	i(m1+m2+g)	5.56 ± 0.45	5.85	4.72	2.40	1.45	6.28	2.99
^{171}Hf	12,1h	c	48.4 ± 4.2	43.1	45.4	48.8	41.7	62.9	49.0
^{171}Lu	8,24d	i(m+g)	15.6 ± 3.0	8.54	7.78	4.27	1.41	8.87	4.53
^{170}Lu	2,012d	c	58.4 ± 4.7	48.8	48.4	52.1	42.6	67.8	32.2
^{170}Lu	2,012d	i(m+g)	13.6 ± 2.4	10.5	9.25	4.10	1.84	8.94	5.13
^{169}Yb	32,026d	c	62.9 ± 5.0	55.6	48.9	54.3	45.4	67.4	27.2
^{167}Tm	9,25d	c	64.4 ± 13.0	58.2	44.7	50.0	40.4	56.4	25.3
^{166}Tm	7,70h	c	61.2 ± 4.3	58.2	53.7	60.2	43.8	58.0	25.8
^{166}Tm	7,70h	i	6.78 ± 1.39	4.50	1.65	0.732	0.038	1.01	2.09
^{165}Tm	30,06h	c	63.6 ± 4.6	57.3	46.8	53.5	43.7	48.1	25.2
^{162}Yb	18,87m	c	40.9 ± 5.3	34.8	34.1	49.4	44.5	32.2	15.4
^{161}Tm	33m	c*	42.2 ± 7.4	46.2	35.8	51.3	49.0	29.0	35.2
^{161}Er	3,21h	c	51.8 ± 4.6	52.9	35.4	48.0	42.8	28.7	40.5
^{160}Er	28,58h	c	59.6 ± 5.3	48.6	39.1	48.5	43.4	27.1	37.1
^{159}Er	36m	c*	60.6 ± 4.2	53.1	41.8	53.5	55.4	25.9	33.6
^{159}Ho	33,05m	c	54.1 ± 5.6	49.1	36.4	42.6	41.4	21.8	33.3
^{157}Dy	8,14h	c	47.3 ± 3.6	43.1	31.0	37.8	38.8	17.3	28.4
^{156}Ho	56m	c	38.4 ± 3.2	32.8	28.5	35.3	35.2	15.2	23.9
^{156}Ho	56m	i	12.8 ± 3.5	11.3	7.27	3.02	0.010	2.48	13.6
^{155}Tb	5,32d	c	37.6 ± 3.3	32.8	28.3	22.0	0.038	12.7	25.6
^{153}Dy	6,4h	c	22.9 ± 2.0	20.3	17.9	16.6	3.30	8.14	17.3
^{153}Gd	240,4d	c	27.2 ± 2.1	24.5	20.8	17.2	3.30	9.09	–
^{152}Dy	2,38h	c	20.2 ± 1.3	15.5	18.2	14.6	8.64	7.66	15.1
^{148}Eu	54,5d	i	1.48 ± 0.34	1.25	1.56	0.130	–	0.294	0.868
^{147}Eu	24,1d	c	21.5 ± 1.8	9.83	14.4	13.1	30.8	5.97	11.3
^{146}Gd	48,27d	c	17.6 ± 1.1	7.59	11.8	13.4	24.7	6.31	9.55
^{145}Eu	5,93d	c	13.3 ± 1.0	5.72	10.9	8.67	22.6	4.46	9.50
^{139}Ce	137,640d	c	5.65 ± 0.36	0.946	4.96	1.91	6.91	2.03	5.70
^{127}Xe	36,4d	c	0.907 ± 0.091	–	0.466	0.034	–	0.392	1.31
^{88}Zr	83,4d	c	0.308 ± 0.116	–	0.171	0.625	–	0.084	1.52
^{88}Y	106,65d	c	0.970 ± 0.074	–	0.238	1.45	–	0.101	2.00
^{84}Rb	32,77d	i(m+g)	0.641 ± 0.055	–	0.105	1.58	–	0.020	0.305
^{83}Rb	86,2d	c	0.968 ± 0.113	–	0.181	2.76	–	0.112	1.45
^{74}As	17,77d	i	0.582 ± 0.058	–	0.095	0.749	–	0.037	0.332
^{59}Fe	44,472d	c	0.405 ± 0.050	–	0.048	0.039	–	0.014	0.136

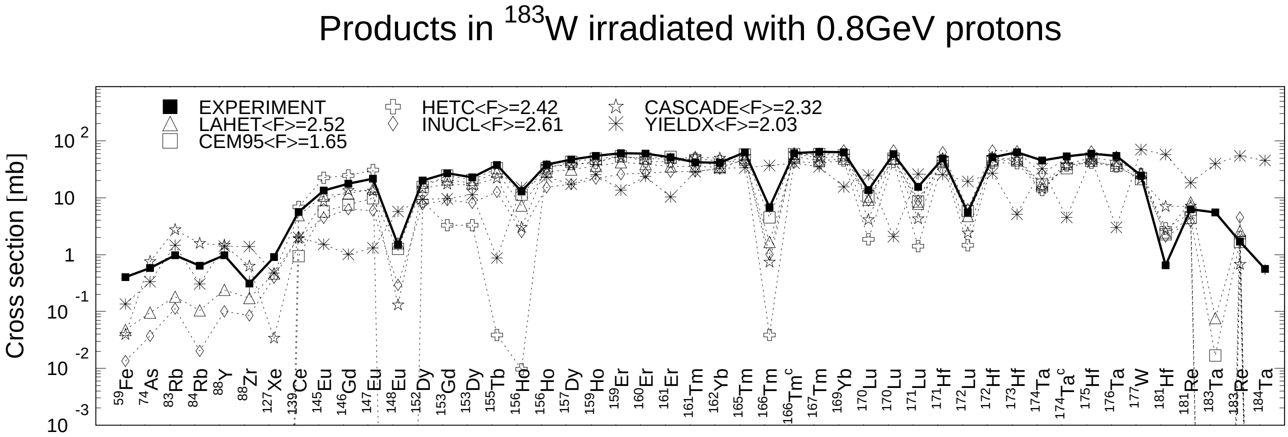

Fig. 36: Detailed comparison between experimental and simulated yields of radioactive reaction products in ^{183}W irradiated with 0.8 GeV protons. The cumulative yields are labeled -c when the respective independent yields are also shown.

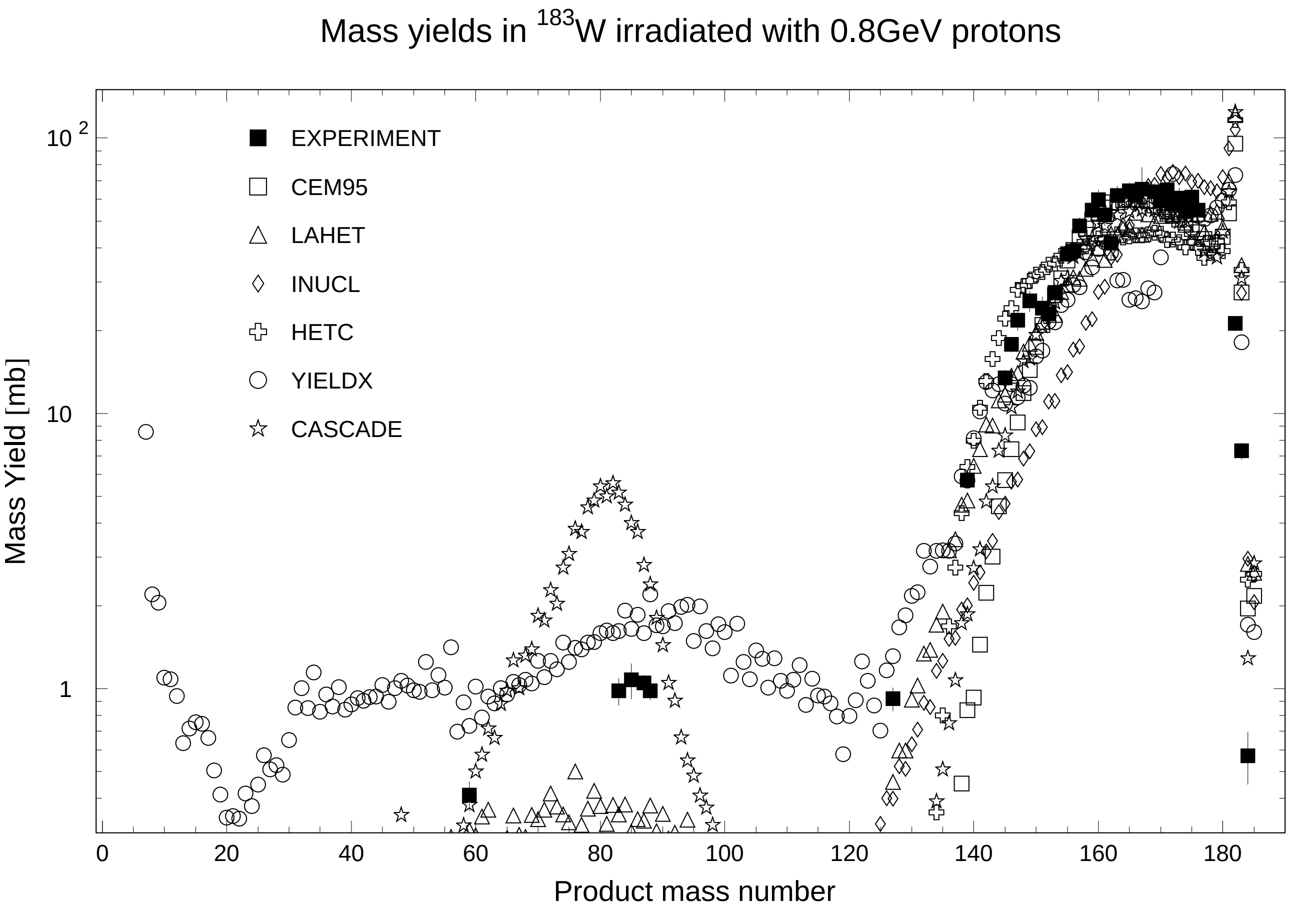

Fig. 37: The simulated mass distributions of reaction products together with the measured cumulative and supra-cumulative yields in ^{183}W irradiated with 0.8 GeV protons.

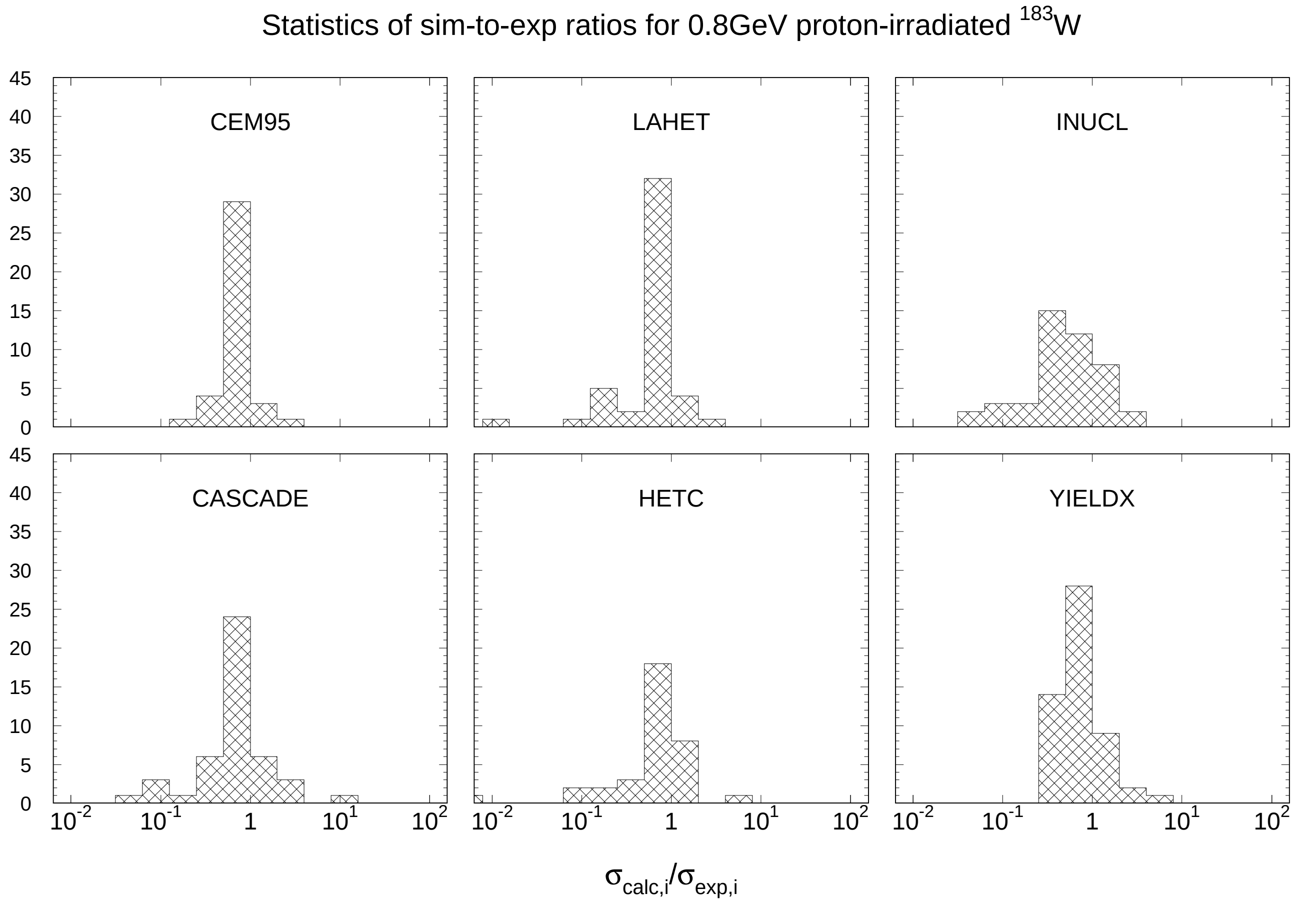

Fig. 38: Statistics of the simulation-to-experiment ratios (criterion 2) for ^{183}W irradiated with 0.8 GeV protons.

Table 70: Experimental and calculated yields from ^{183}W irradiated with 1.6 GeV protons.

Product	$T_{1/2}$	Type	Exp yield [mbarn]	Calculated Yields [mbarn] via CEM95	LAHET	CASCADE	HETC	INUCL	YIELDX
^{181}Re	19,9h	i	4.60 ± 0.76	0.880	4.17	1.65	4.67	0.731	1.49
^{177}W	135m	c	17.7 ± 2.2	13.2	14.7	13.6	18.4	15.6	22.4
^{183}Ta	5,1d	c	4.69 ± 0.45	0.034	1.81	0.006	0.413	–	2.58
^{182}Ta	114,43d	c	19.0 ± 1.5	37.7	45.9	50.8	49.6	38.6	12.1
^{176}Ta	8,09h	c	43.1 ± 4.3	22.6	24.8	24.0	25.7	34.0	38.3
^{174}Ta	1,14h	c	30.1 ± 3.9	17.6	19.8	21.4	22.6	29.2	35.6
^{174}Ta	1,14h	i	16.1 ± 5.4	9.84	9.90	8.71	8.93	16.5	16.7
^{181}Hf	42,39d	c	0.581 ± 0.064	1.83	2.77	5.75	2.96	1.31	0.163
^{175}Hf	70d	c	42.1 ± 3.7	26.2	27.7	27.1	27.6	42.6	48.7
^{173}Hf	23,6h	c	41.3 ± 3.5	23.5	23.2	27.1	26.7	41.7	–
^{173}Hf	23,6h	i	8.77 ± 2.73	8.64	5.03	6.47	4.20	13.7	15.2
^{172}Hf	1,87y	c	33.7 ± 2.9	22.1	22.4	28.4	26.5	42.4	97.7
^{171}Hf	12,1h	c	31.0 ± 3.8	21.3	21.1	26.9	25.6	39.2	62.9
^{172}Lu	6,70d	i(m1+m2+g)	4.01 ± 0.35	3.74	2.76	1.97	1.46	5.66	2.79
^{171}Lu	8,24d	i(m+g)	8.40 ± 3.05	4.89	4.67	3.38	1.36	7.70	4.26
^{170}Lu	2,012d	c	34.9 ± 3.0	24.1	22.3	30.6	24.6	45.6	–
^{170}Lu	2,012d	i(m+g)	13.0 ± 2.8	6.09	4.65	3.13	1.83	8.04	4.83
^{169}Yb	32,026d	c	36.2 ± 3.0	27.4	23.3	30.8	26.2	47.1	25.7
^{162}Yb	18,87m	c	21.7 ± 4.0	17.1	15.8	30.1	28.0	31.4	17.2
^{168}Tm	93,1d	i	0.676 ± 0.101	1.04	0.377	0.484	0.125	0.776	0.743
^{167}Tm	9,25d	c	40.4 ± 5.6	28.3	21.1	30.7	23.2	44.9	24.0
^{166}Tm	7,70h	c	36.0 ± 3.6	27.1	24.7	35.9	26.9	47.7	27.7
^{166}Tm	7,70h	i	1.08 ± 0.50	2.37	1.07	0.871	0.144	1.39	2.52
^{165}Tm	30,06h	c	36.4 ± 3.2	26.6	21.8	32.3	25.7	42.0	26.5
^{161}Er	3,21h	c	33.4 ± 3.5	28.1	17.4	31.9	25.3	33.0	43.9
^{160}Er	28,58h	c	36.6 ± 3.6	27.2	19.4	34.1	25.4	33.1	39.6
^{159}Er	36m	c*	36.0 ± 5.5	29.9	21.8	37.8	34.1	32.5	35.5
^{156}Ho	56m	c	22.5 ± 2.6	24.0	16.9	29.3	22.0	24.3	24.7
^{157}Dy	8,14h	c	35.5 ± 3.3	28.3	17.2	31.0	23.0	26.7	29.5
^{153}Dy	6,4h	c	26.2 ± 3.0	21.2	12.2	19.0	2.35	16.7	17.8
^{152}Dy	2,38h	c	22.5 ± 1.9	18.0	12.4	17.1	5.81	16.5	–
^{155}Tb	5,32d	c	32.7 ± 2.8	26.9	17.3	22.0	0.202	21.9	26.4
^{153}Gd	240,4d	c	28.8 ± 2.7	25.7	14.6	20.4	2.35	19.0	21.9
^{151}Gd	124d	c	23.4 ± 2.2	26.1	15.4	23.3	18.8	18.8	16.9
^{146}Gd	48,27d	c	28.3 ± 2.3	26.9	13.1	32.4	27.5	18.7	10.5
^{147}Eu	24,1d	c	30.9 ± 2.7	30.2	15.3	28.5	26.7	16.5	11.7
^{146}Eu	4,61d	i	6.93 ± 1.02	6.65	4.56	1.21	–	2.36	3.03
^{145}Eu	5,93d	c	25.0 ± 2.1	29.8	14.2	25.9	28.3	14.6	10.6
^{144}Pm	363d	i	0.521 ± 0.138	1.18	0.993	0.120	–	0.359	1.31
^{143}Pm	265d	c	26.1 ± 2.7	31.5	17.0	25.9	27.2	13.7	13.5
^{137}Nd	38,5m	c	29.5 ± 3.4	17.9	9.59	16.6	25.9	7.77	3.10
^{136}Nd	50,65m	c	15.9 ± 1.7	13.3	10.3	14.9	23.7	6.48	2.02
^{139}Ce	137,640d	c	24.0 ± 2.0	27.8	17.6	21.4	25.1	10.6	7.04
^{135}Ce	17,7h	c	19.4 ± 1.5	22.9	13.6	15.5	23.0	8.23	4.74
^{134}Ce	3,16d	c	17.1 ± 1.7	19.2	14.9	15.8	19.8	7.94	4.73
^{132}Ce	3,51h	c	15.9 ± 1.3	13.3	13.9	11.9	21.4	5.48	–
^{133}Ba	3848,9d	c	17.1 ± 1.8	19.3	14.4	13.6	20.2	7.09	4.56
^{131}Ba	11,50d	c	15.8 ± 1.2	16.2	16.1	11.1	20.2	6.01	4.07
^{128}Ba	2,43d	c	12.4 ± 1.2	9.69	16.6	8.96	16.4	3.85	3.45
^{129}Cs	32,06h	c	15.9 ± 1.6	14.3	17.5	9.88	22.2	5.36	4.02
^{127}Xe	36,4d	c	12.0 ± 1.0	10.8	17.9	7.75	17.8	4.00	2.95
^{125}Xe	16,9h	c	10.3 ± 0.8	8.03	15.1	6.01	17.5	3.09	1.84
^{123}Xe	2,08h	c	11.2 ± 1.0	5.05	9.75	4.07	13.9	2.08	2.91
^{105}Ag	41,29d	c	1.54 ± 0.15	0.034	7.99	0.342	0.394	0.198	1.63
^{90}Nb	14,60h	c	1.68 ± 0.23	–	0.936	0.165	–	0.068	1.59

Table 70, cont'd.

Product	$T_{1/2}$	Type	Exp yield [mbarn]	Calculated Yields [mbarn] via CEM95	LAHET	CASCADE	HETC	INUCL	YIELDX
^{88}Zr	83,4d	c	1.17 ± 0.10	–	1.49	0.917	–	0.144	11.0
^{88}Y	106,65d	c	2.20 ± 0.18	–	2.17	1.54	–	0.175	13.5
^{84}Rb	32,77d	i(m+g)	0.750 ± 0.074	–	0.369	1.34	–	0.014	1.34
^{83}Rb	86,2d	c	1.84 ± 0.21	–	1.06	2.83	–	0.178	10.1
^{75}Se	119,779d	c	1.90 ± 0.22	–	0.517	2.25	–	0.250	7.24
^{74}As	17,77d	i	0.917 ± 0.120	–	0.246	1.00	–	0.062	2.15
^{59}Fe	44,472d	c	0.659 ± 0.063	–	0.074	0.256	–	0.014	0.822
^{54}Mn	312,11d	i	1.21 ± 0.13	–	0.361	0.325	–	0.038	2.90
^{48}V	15,9735d	c	0.276 ± 0.032	–	0.181	–	–	0.032	0.844
^{48}Sc	43,67h	i	0.410 ± 0.059	–	0.041	0.085	–	0.003	0.419
^{28}Mg	20,915h	c	0.362 ± 0.070	–	–	0.034	–	–	0.318
^{24}Na	14,9590h	c	2.04 ± 0.18	–	0.066	0.011	–	–	0.962
^{7}Be	53,29d	i	4.52 ± 0.51	–	–	–	–	–	1.51

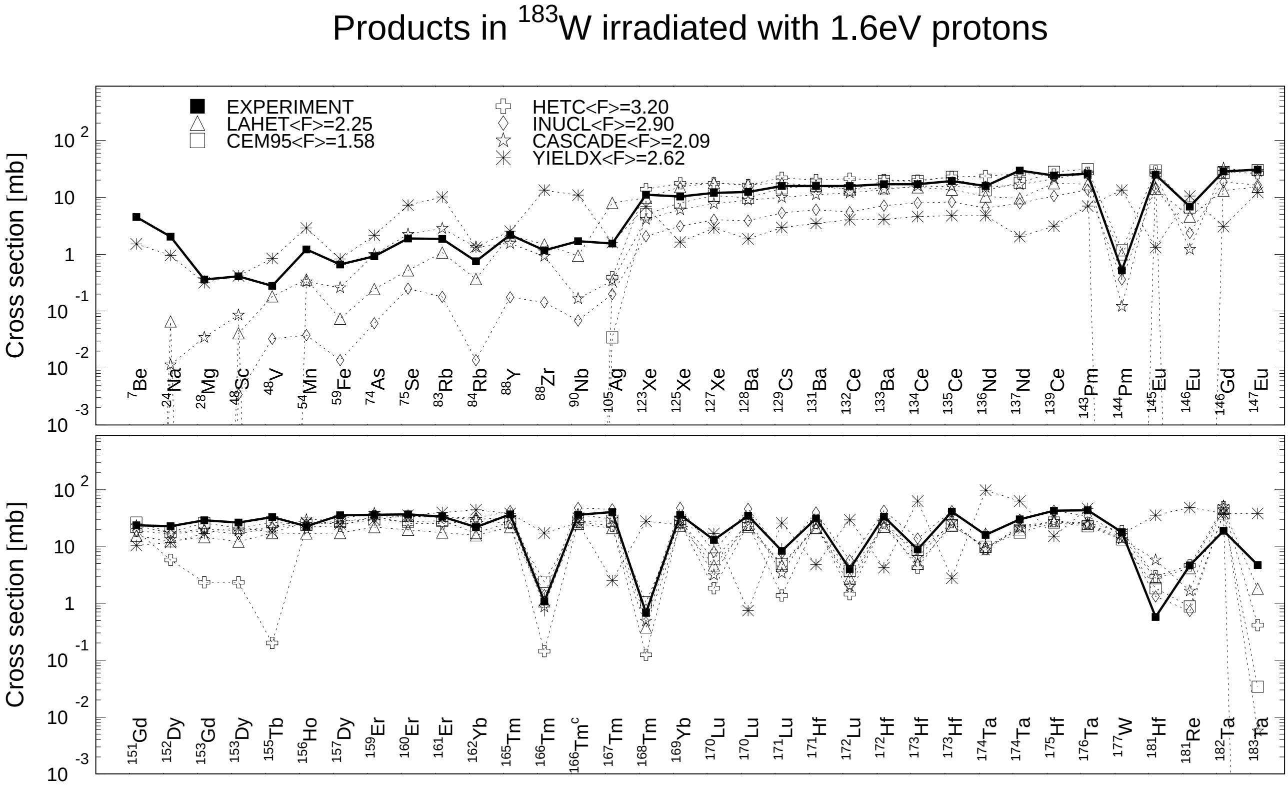

Fig. 39: Detailed comparison between experimental and simulated yields of radioactive reaction products in ^{183}W irradiated with 1.6 GeV protons. The cumulative yields are labeled -c when the respective independent yields are also shown.

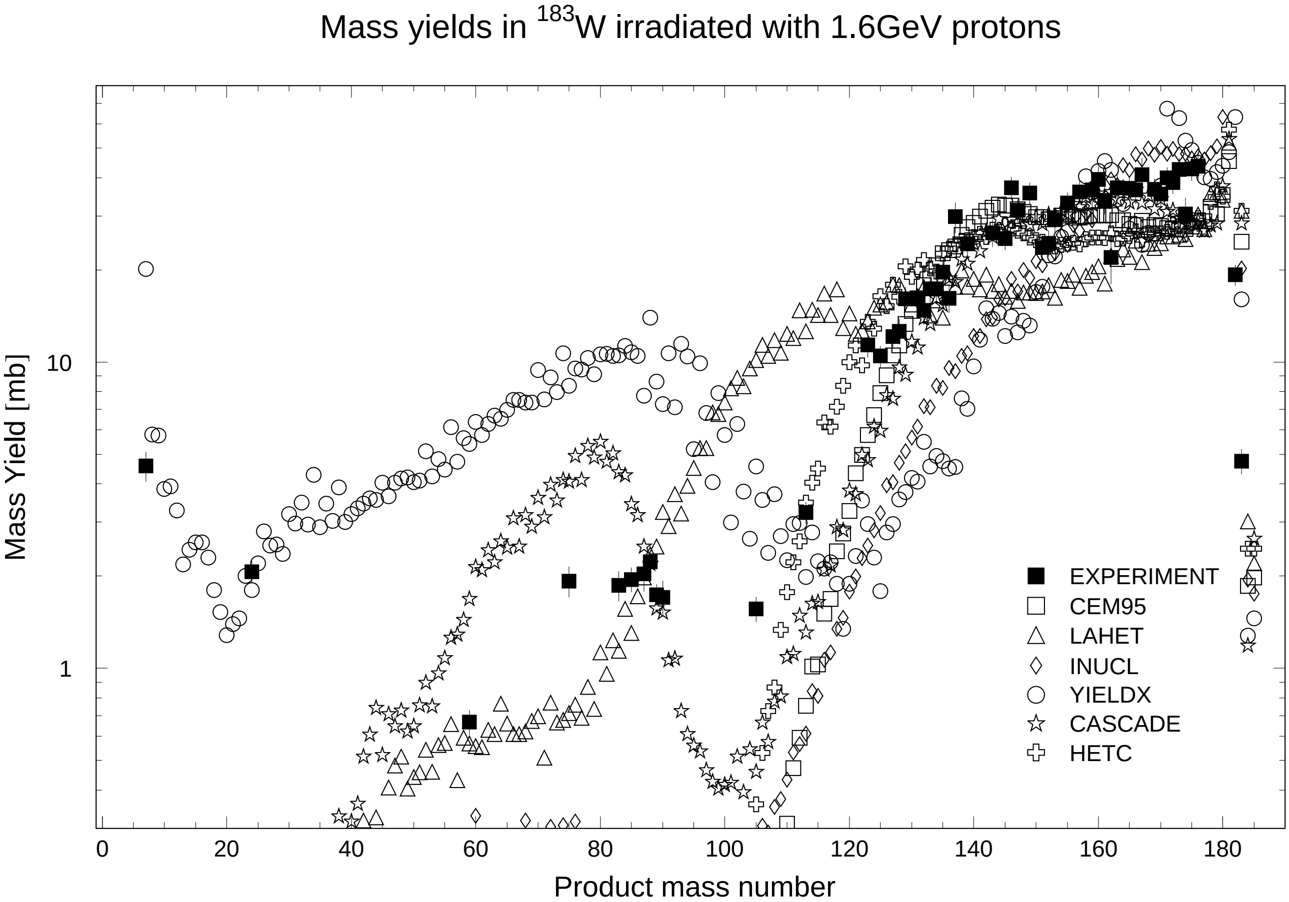

Fig. 40: The simulated mass distributions of reaction products together with the measured cumulative and supra-cumulative yields in ^{183}W irradiated with 1.6 GeV protons.

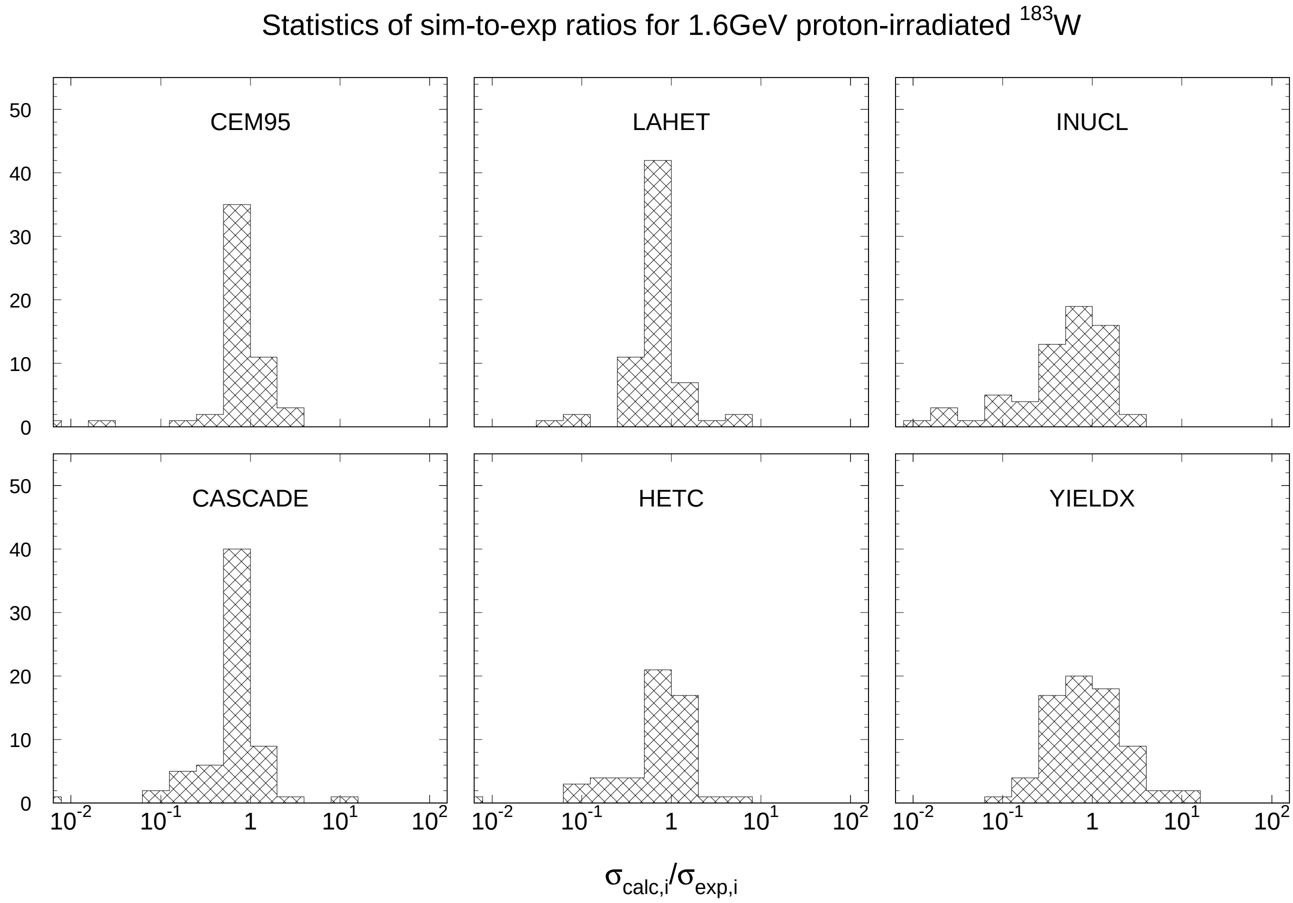

Fig. 41: Statistics of the simulation-to-experiment ratios (criterion 2) for ^{183}W irradiated with 1.6 GeV protons.

Table 71: Experimental and calculated yields from ^{184}W irradiated with 0.2 GeV protons.

Product	$T_{1/2}$	Type	Exp yield [mbarn]	Calculated Yields [mbarn] via CEM95	LAHET	CASCADE	HETC	INUCL	YIELDX
^{183}Re	70,0d	i(m+g)	11.5 ± 1.1	20.9	29.5	32.5	22.1	24.6	10.6
^{182}Re	64,0h	i	6.22 ± 0.64	21.0	16.3	27.7	18.8	24.4	18.4
^{181}Re	19,9h	i	23.9 ± 3.1	22.2	30.7	39.4	27.1	29.1	25.6
^{179}Re	19,5m	i	18.2 ± 2.0	21.5	29.9	32.1	28.3	28.1	30.2
^{178}W	21,6d	c	76.0 ± 9.3	82.7	91.3	89.4	71.7	95.9	87.8
^{177}W	135m	c	58.3 ± 6.9	81.6	82.3	83.0	75.6	79.0	75.3
^{176}W	2,5h	c	73.1 ± 6.4	78.7	86.7	93.7	79.3	77.4	63.2
^{174}W	31m	c	60.0 ± 6.9	51.6	69.5	87.1	79.3	51.1	35.4
^{183}Ta	5,1d	c	9.71 ± 0.73	42.9	27.3	36.1	22.9	80.6	12.4
^{176}Ta	8,09h	c	109. ± 8.	122.	114.	112.	88.5	104.	92.7
^{176}Ta	8,09h	i(m+g)	34.1 ± 4.0	43.6	27.6	18.8	10.6	27.6	30.3
^{174}Ta	1,14h	i	27.9 ± 4.4	42.3	30.7	20.2	9.39	18.6	22.9
^{172}Ta	36,8m	c*	40.5 ± 4.4	43.0	74.4	101.	111.	42.9	30.5
^{171}Ta	23,3m	c*	5.59 ± 0.80	18.5	50.8	65.0	107.	24.4	10.2
^{175}Hf	70d	c	111. ± 9.	132.	114.	110.	87.0	89.7	96.2
^{173}Hf	23,6h	c	93.3 ± 6.5	95.0	91.8	98.1	92.5	54.0	70.3
^{172}Hf	1,87y	c	65.9 ± 4.8	65.2	75.9	95.9	93.3	41.9	44.3
^{171}Hf	12,1h	c	44.1 ± 3.6	36.9	59.0	70.6	101.	27.6	23.0
^{172}Lu	6,70d	i(m1+m2+g)	1.77 ± 0.14	5.56	1.82	0.334	0.035	0.197	1.90
^{171}Lu	8,24d	i(m+g)	14.5 ± 2.1	5.68	3.61	0.741	0.026	0.318	1.82
^{170}Lu	2,012d	c	38.9 ± 2.7	21.1	40.4	52.7	106.	18.3	12.8
^{169}Yb	32,026d	c	28.0 ± 1.9	11.7	30.2	31.3	122.	12.0	8.39
^{166}Tm	7,70h	c	6.98 ± 0.59	0.766	8.15	5.25	0.386	3.79	2.91
^{165}Tm	30,06h	c	3.89 ± 0.31	0.206	4.05	2.04	–	2.35	2.56

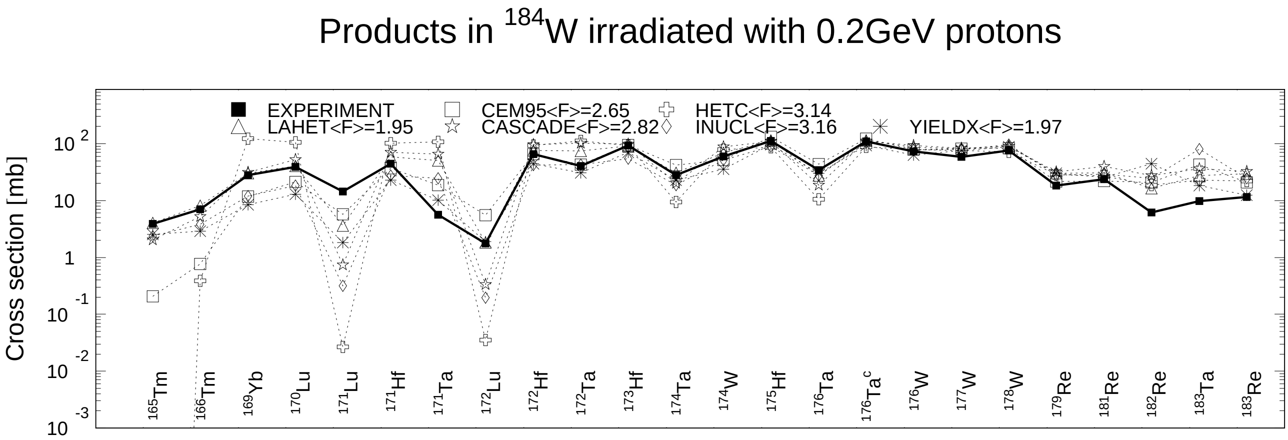

Fig. 42: Detailed comparison between experimental and simulated yields of radioactive reaction products in ^{184}W irradiated with 0.2 GeV protons. The cumulative yields are labeled -c when the respective independent yields are also shown.

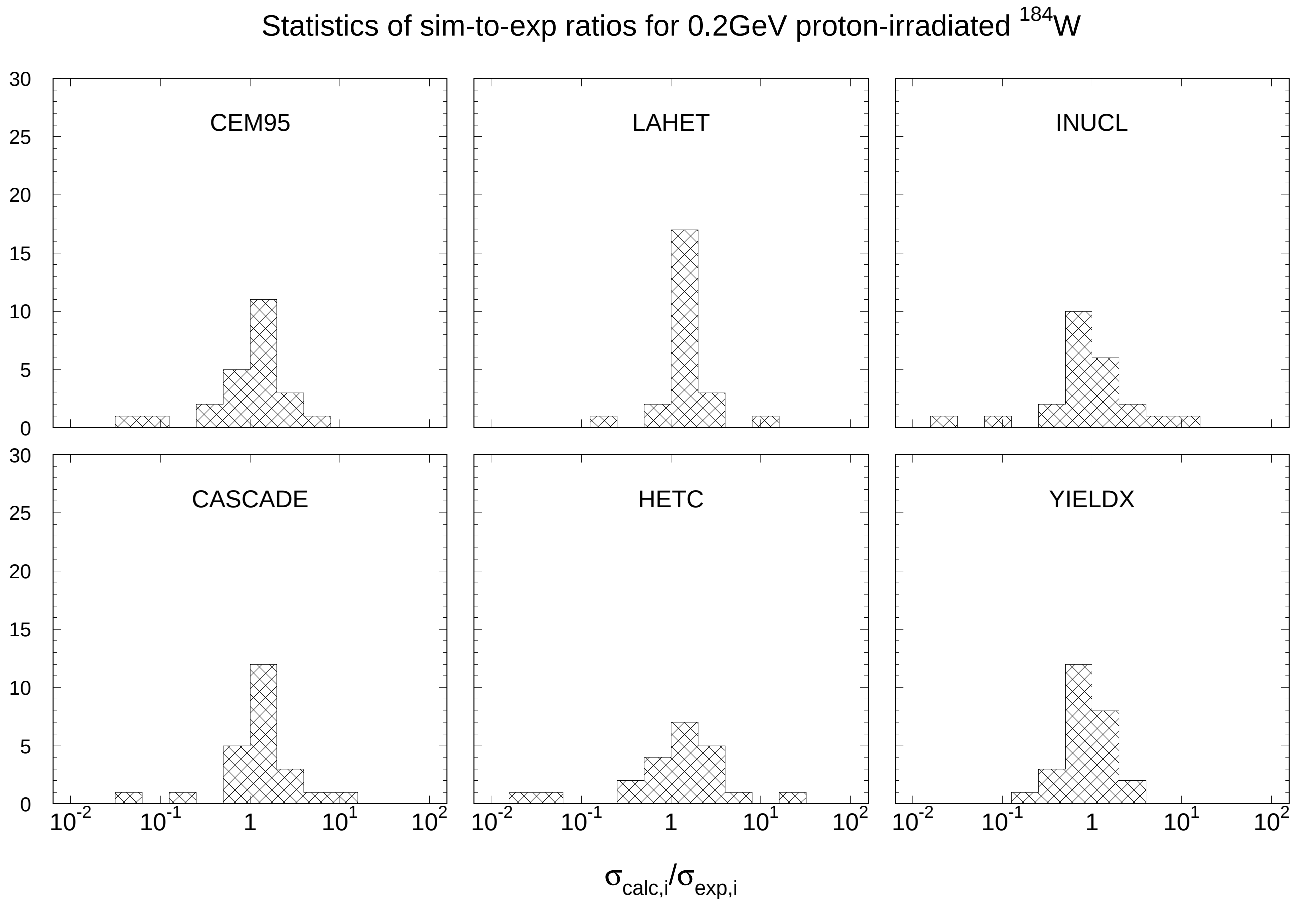

Fig. 43: Statistics of the simulation-to-experiment ratios (criterion 2) for ^{184}W irradiated with 0.2 GeV protons.

Table 72: Experimental and calculated yields from ^{184}W irradiated with 0.8 GeV protons.

Product	$T_{1/2}$	Type	Exp yield [mbarn]	Calculated Yields [mbarn] via CEM95	LAHET	CASCADE	HETC	INUCL	YIELDX
^{184}Ta	8,7h	c	0.950 ± 0.085	0.017	0.038	–	–	–	0.647
^{183}Re	70,0d	i(m+g)	3.61 ± 0.33	4.05	6.95	5.60	4.31	3.37	1.75
^{183}Ta	5,1d	c	21.2 ± 1.5	44.6	56.6	59.3	55.0	59.3	15.9
^{181}Re	19,9h	i	7.42 ± 1.16	4.27	8.74	6.82	5.14	4.26	4.25
^{181}Hf	42,39d	c	1.24 ± 0.11	3.09	2.77	6.00	2.84	5.03	0.401
^{177}W	135m	c	23.4 ± 2.7	20.1	24.8	21.1	24.2	24.4	32.4
^{176}Ta	8,09h	c	45.6 ± 4.2	35.5	42.7	37.2	35.9	50.4	46.9
^{175}Hf	70d	c	56.7 ± 4.2	45.0	51.4	44.5	40.9	64.6	61.0
^{174}Ta	1,14h	c	50.0 ± 5.5	31.1	38.5	36.7	34.8	45.6	41.0
^{174}Ta	1,14h	i	40.2 ± 5.6	17.1	18.5	14.3	12.9	24.8	18.0
^{173}Hf	23,6h	c	58.6 ± 4.4	44.6	48.4	47.2	40.1	64.3	71.7
^{173}Hf	23,6h	i	11.5 ± 2.7	16.9	9.98	10.9	5.13	20.5	16.6
^{172}Hf	1,87y	c	47.5 ± 3.3	43.6	47.0	51.6	41.2	65.7	56.3
^{172}Lu	6,70d	i(m1+m2+g)	5.89 ± 0.60	7.12	5.47	2.84	1.41	7.26	3.70
^{171}Hf	12,1h	c	44.4 ± 5.0	41.5	43.0	48.8	42.6	59.3	32.8
^{171}Lu	8,24d	i(m+g)	16.7 ± 4.2	10.2	10.2	5.39	1.54	9.62	5.34
^{170}Lu	2,012d	c	54.0 ± 4.4	48.7	46.9	53.3	41.3	65.3	26.0
^{170}Lu	2,012d	i(m+g)	5.77 ± 3.70	12.5	10.3	4.69	1.94	9.86	5.74
^{169}Yb	32,026d	c	61.4 ± 4.5	56.0	49.3	54.5	44.8	64.4	23.9
^{167}Tm	9,25d	c	61.4 ± 12.4	58.2	44.0	51.0	41.5	53.9	25.3
^{166}Tm	7,70h	c	59.0 ± 4.2	59.0	52.7	60.7	45.9	54.9	25.0
^{166}Tm	7,70h	i	5.18 ± 0.76	5.68	2.07	0.876	0.086	1.14	2.49
^{165}Tm	30,06h	c	59.3 ± 4.4	58.5	45.7	53.5	44.9	45.9	25.9
^{162}Yb	18,87m	c	42.7 ± 4.6	30.4	30.8	47.7	46.3	28.1	14.4
^{161}Tm	33m	c*	42.7 ± 7.4	41.8	34.2	49.1	49.4	26.6	31.6
^{161}Er	3,21h	c	48.0 ± 4.3	50.9	34.8	46.7	43.1	27.0	38.2
^{160}Er	28,58h	c	54.6 ± 4.6	46.2	36.4	47.2	42.4	25.7	34.6
^{159}Er	36m	c*	56.0 ± 3.9	46.3	40.5	51.1	56.1	23.5	30.5
^{159}Ho	33,05m	c	54.1 ± 3.9	45.6	36.1	40.9	41.9	20.1	31.8
^{157}Dy	8,14h	c	43.6 ± 3.4	39.5	29.1	35.9	38.3	16.6	26.6
^{156}Ho	56m	c	37.9 ± 2.9	29.5	25.7	33.5	35.0	14.1	21.7
^{156}Ho	56m	i	17.5 ± 4.6	11.4	7.64	3.61	–	2.73	13.8
^{155}Tb	5,32d	c	35.3 ± 3.2	30.8	27.5	21.7	0.038	12.3	23.3
^{153}Dy	6,4h	c	21.6 ± 1.8	18.1	16.5	15.8	3.30	8.32	15.7
^{153}Gd	240,4d	c	25.5 ± 2.2	22.5	20.0	16.4	3.30	9.42	–
^{152}Dy	2,38h	c	18.5 ± 1.2	13.1	16.5	13.5	8.10	7.53	12.2
^{148}Eu	54,5d	i	1.39 ± 0.29	1.28	1.52	0.158	–	0.333	0.991
^{147}Eu	24,1d	c	18.5 ± 1.5	7.42	13.5	11.6	27.8	5.69	10.7
^{146}Gd	48,27d	c	15.0 ± 1.0	5.64	10.5	11.8	22.0	5.78	7.70
^{145}Eu	5,93d	c	10.9 ± 0.8	4.47	10.3	7.72	20.1	4.18	8.81
^{139}Ce	137,640d	c	4.69 ± 0.31	0.433	4.23	1.63	4.54	1.85	5.16
^{127}Xe	36,4d	c	0.710 ± 0.117	–	0.410	0.034	–	0.386	1.18
^{88}Zr	83,4d	c	0.341 ± 0.133	–	0.172	0.509	–	0.068	1.52
^{88}Y	106,65d	i(m+g)	0.441 ± 0.095	–	0.133	0.848	–	0.020	0.556
^{87}Y	79,8h	c*	0.664 ± 0.063	–	0.303	1.01	–	0.082	1.45
^{84}Rb	32,77d	i(m+g)	0.496 ± 0.050	–	0.181	1.70	–	0.007	0.354
^{83}Rb	86,2d	c	0.756 ± 0.078	–	0.315	2.45	–	0.078	1.49
^{74}As	17,77d	i	0.453 ± 0.054	–	0.143	0.757	–	0.024	0.381
^{59}Fe	44,472d	c	0.287 ± 0.034	–	0.095	0.034	–	0.010	0.154

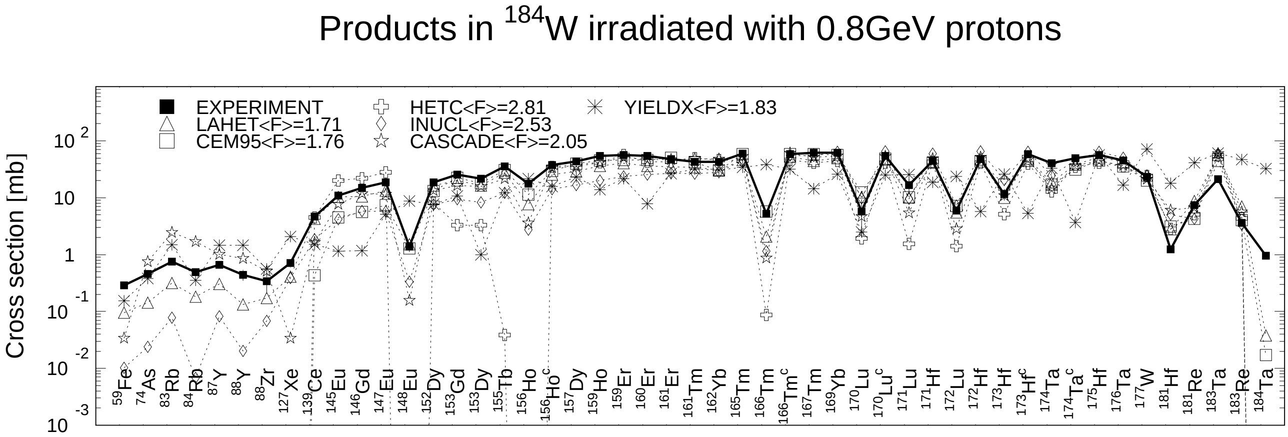

Fig. 44: Detailed comparison between experimental and simulated yields of radioactive reaction products in ^{184}W irradiated with 0.8 GeV protons. The cumulative yields are labeled -c when the respective independent yields are also shown.

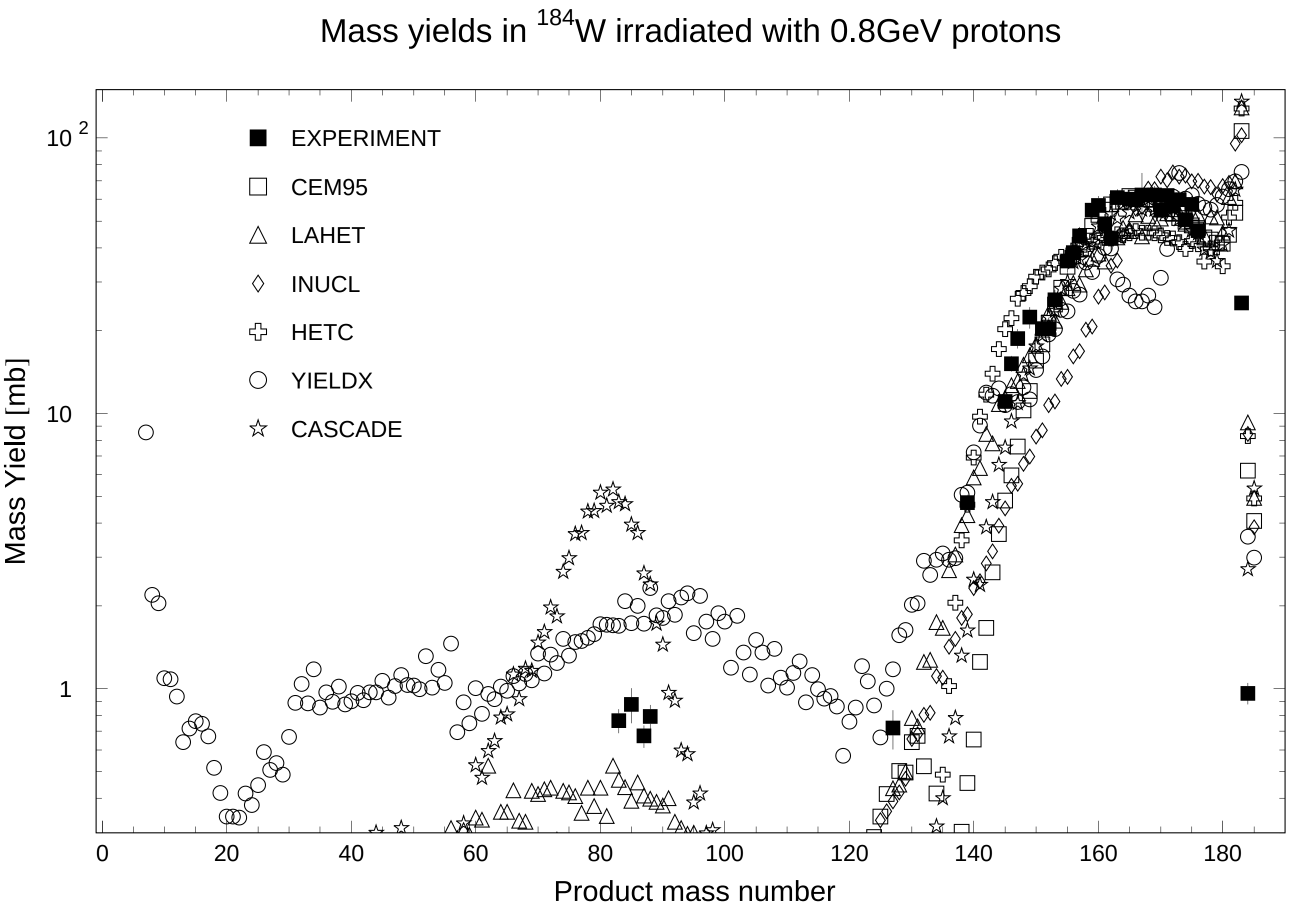

Fig. 45: The simulated mass distributions of reaction products together with the measured cumulative and supra-cumulative yields in ^{184}W irradiated with 0.8 GeV protons.

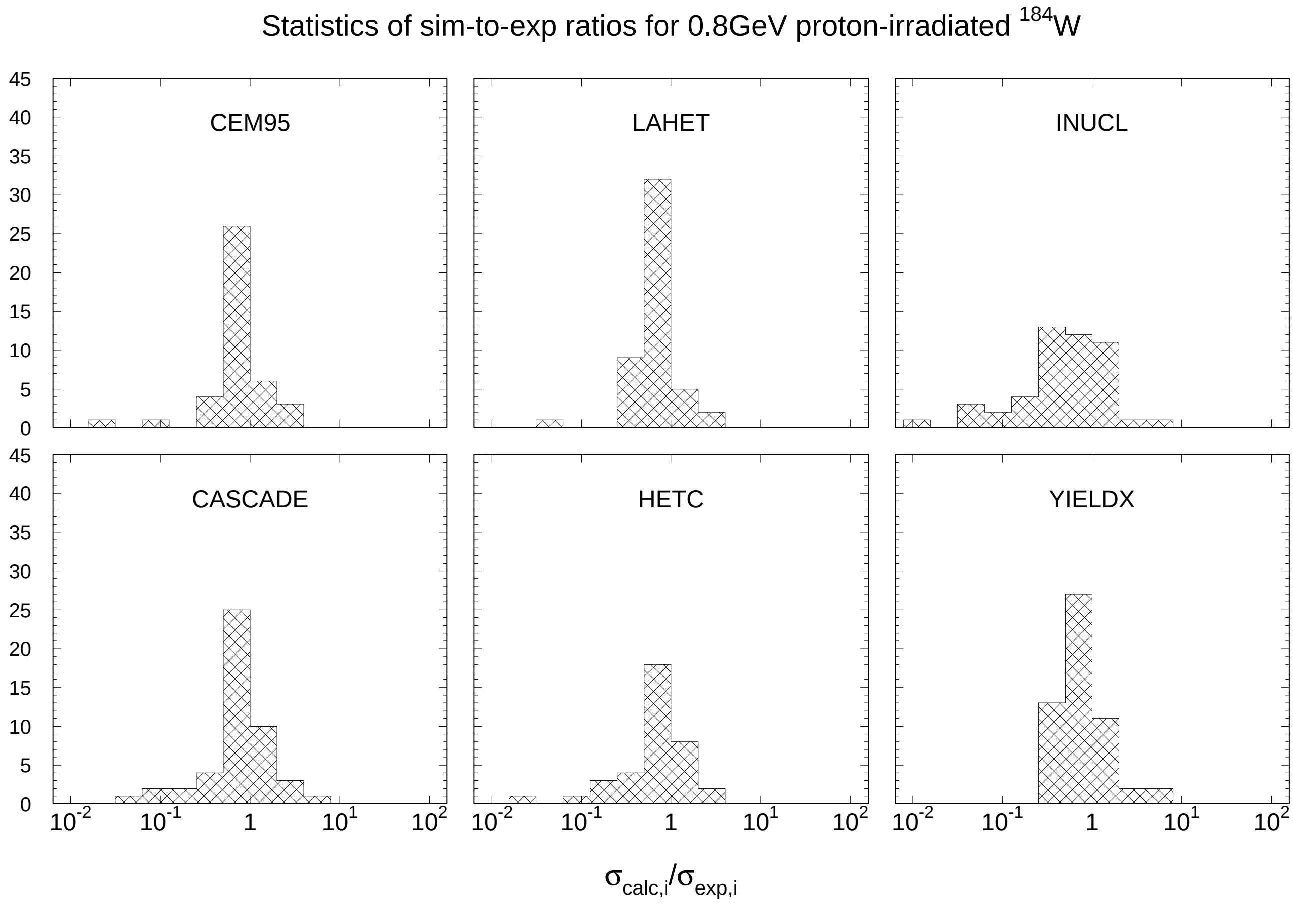

Fig. 46: Statistics of the simulation-to-experiment ratios (criterion 2) for ^{184}W irradiated with 0.8 GeV protons.

Table 73: Experimental and calculated yields from ^{184}W irradiated with 1.6 GeV protons.

Product	$T_{1/2}$	Type	Exp yield [mbarn]	Calculated Yields [mbarn] via CEM95	LAHET	CASCADE	HETC	INUCL	YIELDX
^{183}Re	70,0d	i(m+g)	3.14 ± 0.71	0.532	3.50	1.65	3.23	0.213	1.13
^{181}Re	19,9h	i	4.84 ± 0.79	1.16	3.80	1.77	4.12	1.10	1.75
^{177}W	135m	c	15.0 ± 1.9	11.6	13.9	12.8	16.4	14.1	26.0
^{184}Ta	8,7h	c	0.763 ± 0.097	0.051	1.38	–	0.212	–	0.477
^{183}Ta	5,1d	c	19.4 ± 1.6	39.1	46.7	49.9	50.2	41.1	10.9
^{182}Ta	114,43d	c	16.7 ± 1.4	17.3	17.2	27.4	20.0	35.6	13.7
^{176}Ta	8,09h	c	33.9 ± 3.7	20.1	22.3	23.1	24.6	31.2	40.0
^{174}Ta	1,14h	c	29.3 ± 3.6	16.1	18.1	20.7	22.2	27.9	37.3
^{174}Ta	1,14h	i	22.0 ± 4.1	9.20	9.56	9.08	9.29	16.1	16.8
^{181}Hf	42,39d	c	1.18 ± 0.10	2.55	2.57	5.60	3.36	3.26	0.335
^{175}Hf	70d	c	38.0 ± 3.3	24.9	25.4	27.4	27.2	41.7	55.7
^{173}Hf	23,6h	c	36.6 ± 3.2	23.2	22.4	26.6	25.9	40.4	–
^{173}Hf	23,6h	i	8.68 ± 2.34	9.61	5.46	7.05	4.74	13.8	14.7
^{172}Hf	1,87y	c	28.4 ± 2.8	21.9	21.6	28.7	25.4	41.3	73.0
^{171}Hf	12,1h	c	27.5 ± 2.8	19.8	19.4	27.1	25.2	37.6	37.9
^{172}Lu	6,70d	i(m1+m2+g)	4.46 ± 0.38	4.32	3.47	2.23	1.41	6.19	3.52
^{171}Lu	8,24d	i(m+g)	8.69 ± 1.75	5.24	5.11	3.91	1.49	8.40	5.14
^{170}Lu	2,012d	c	32.9 ± 2.8	22.5	21.6	30.0	24.4	43.9	–
^{170}Lu	2,012d	i(m+g)	9.60 ± 2.06	6.76	5.01	3.85	1.95	8.60	5.54
^{169}Yb	32,026d	c	34.0 ± 2.7	27.2	23.4	31.2	25.8	46.0	22.8
^{162}Yb	18,87m	c	25.1 ± 6.0	15.2	14.4	29.7	27.5	28.1	16.2
^{168}Tm	93,1d	i	0.900 ± 0.112	1.36	0.543	0.572	0.077	0.912	0.891
^{167}Tm	9,25d	c	37.1 ± 5.1	27.9	21.2	30.7	23.5	42.7	24.7
^{166}Tm	7,70h	c	34.2 ± 3.4	27.4	24.5	35.4	26.1	45.7	27.0
^{166}Tm	7,70h	i	1.53 ± 0.38	2.83	1.36	1.21	0.164	1.78	2.95
^{165}Tm	30,06h	c	33.9 ± 3.0	27.4	21.7	32.0	26.0	40.5	27.6
^{161}Er	3,21h	c	28.2 ± 3.0	27.1	17.4	32.0	25.8	31.6	41.0
^{160}Er	28,58h	c	34.4 ± 3.4	25.9	18.9	33.5	25.5	32.1	36.7
^{159}Er	36m	c*	35.7 ± 5.4	29.5	20.6	37.2	34.4	30.9	32.1
^{156}Ho	56m	c	23.2 ± 2.8	22.9	16.4	29.7	22.5	23.1	22.4
^{157}Dy	8,14h	c	33.0 ± 3.0	30.0	17.5	30.9	24.0	25.8	27.7
^{153}Dy	6,4h	c	25.0 ± 2.3	21.1	11.6	18.3	2.43	16.3	16.2
^{152}Dy	2,38h	c	20.8 ± 1.7	18.9	12.4	18.3	6.13	15.8	–
^{155}Tb	5,32d	c	31.8 ± 2.7	27.2	17.8	22.7	0.231	21.9	24.2
^{153}Gd	240,4d	c	27.6 ± 2.7	26.8	14.8	19.7	2.43	19.1	20.9
^{151}Gd	124d	c	21.6 ± 2.4	26.9	15.4	24.7	18.0	18.5	16.3
^{146}Gd	48,27d	c	25.1 ± 2.0	25.7	12.3	30.6	26.5	17.5	8.57
^{147}Eu	24,1d	c	28.6 ± 2.5	29.0	15.3	28.0	26.9	16.1	11.3
^{146}Eu	4,61d	i	10.1 ± 1.8	6.62	4.91	1.43	–	2.62	3.41
^{145}Eu	5,93d	c	22.7 ± 1.9	28.8	14.8	26.1	26.7	15.0	9.99
^{144}Pm	363d	i	0.612 ± 0.177	1.27	1.24	0.137	–	0.456	1.48
^{143}Pm	265d	c	23.5 ± 2.4	30.3	16.6	24.2	26.4	13.9	13.0
^{137}Nd	38,5m	c	28.4 ± 3.4	17.4	9.20	15.5	25.2	7.29	2.52
^{136}Nd	50,65m	c	15.2 ± 1.5	12.4	10.0	14.4	22.9	5.97	1.58
^{139}Ce	137,640d	c	22.1 ± 1.8	26.4	17.8	19.5	24.7	10.4	6.59
^{135}Ce	17,7h	c	18.1 ± 1.4	20.1	13.5	15.1	23.0	7.92	4.75
^{134}Ce	3,16d	c	15.0 ± 1.4	18.2	15.1	15.2	19.4	7.54	4.51
^{132}Ce	3,51h	c	14.5 ± 1.2	11.7	13.6	11.0	21.5	5.32	–
^{133}Ba	3848,9d	c	16.6 ± 1.8	17.8	13.8	12.5	20.3	6.96	4.42
^{131}Ba	11,50d	c	14.3 ± 1.1	14.6	16.7	10.8	19.4	6.00	3.86
^{128}Ba	2,43d	c	11.6 ± 1.1	8.50	16.3	7.55	16.0	3.86	3.34
^{129}Cs	32,06h	c	14.4 ± 1.4	12.8	16.9	9.05	21.2	5.28	3.70
^{127}Xe	36,4d	c	10.8 ± 0.9	8.98	17.3	6.89	17.8	3.95	2.77
^{125}Xe	16,9h	c	9.15 ± 0.76	6.97	15.2	5.47	16.0	3.07	1.78
^{123}Xe	2,08h	c	9.73 ± 0.84	4.65	9.26	3.82	12.3	1.82	2.99

Table 73, cont'd.

Product	$T_{1/2}$	Type	Exp yield	Calculated Yields [mbarn] via					
			[mbarn]	CEM95	LAHET	CASCADE	HETC	INUCL	YIELDX
^{105}Ag	41,29d	c	1.46 ± 0.15	0.009	7.30	0.309	0.250	0.192	1.63
^{90}Nb	14,60h	c	0.841 ± 0.146	–	0.938	0.177	–	0.051	1.31
^{88}Zr	83,4d	c	1.03 ± 0.10	–	1.47	0.823	–	0.185	10.7
^{88}Y	106,65d	i(m+g)	0.804 ± 0.286	–	0.700	0.657	–	0.031	2.91
^{84}Rb	32,77d	i(m+g)	0.758 ± 0.087	–	0.362	1.42	–	0.021	1.53
^{83}Rb	86,2d	c	1.51 ± 0.18	–	0.947	2.45	–	0.223	10.1
^{74}As	17,77d	i	0.796 ± 0.090	–	0.230	1.09	–	0.034	2.40
^{59}Fe	44,472d	c	0.502 ± 0.062	–	0.066	0.206	–	0.003	0.901
^{54}Mn	312,11d	i	0.859 ± 0.100	–	0.321	0.263	–	0.045	2.95
^{48}V	15,9735d	c	0.209 ± 0.042	–	0.165	0.017	–	0.010	0.774
^{48}Sc	43,67h	i	0.511 ± 0.048	–	0.074	0.120	–	0.003	0.453
^{28}Mg	20,915h	c	0.444 ± 0.042	–	–	0.029	–	–	0.342
^{24}Na	14,9590h	c	1.90 ± 0.16	–	0.107	0.029	–	–	1.01
^{7}Be	53,29d	i	4.27 ± 0.46	–	–	–	–	–	1.50

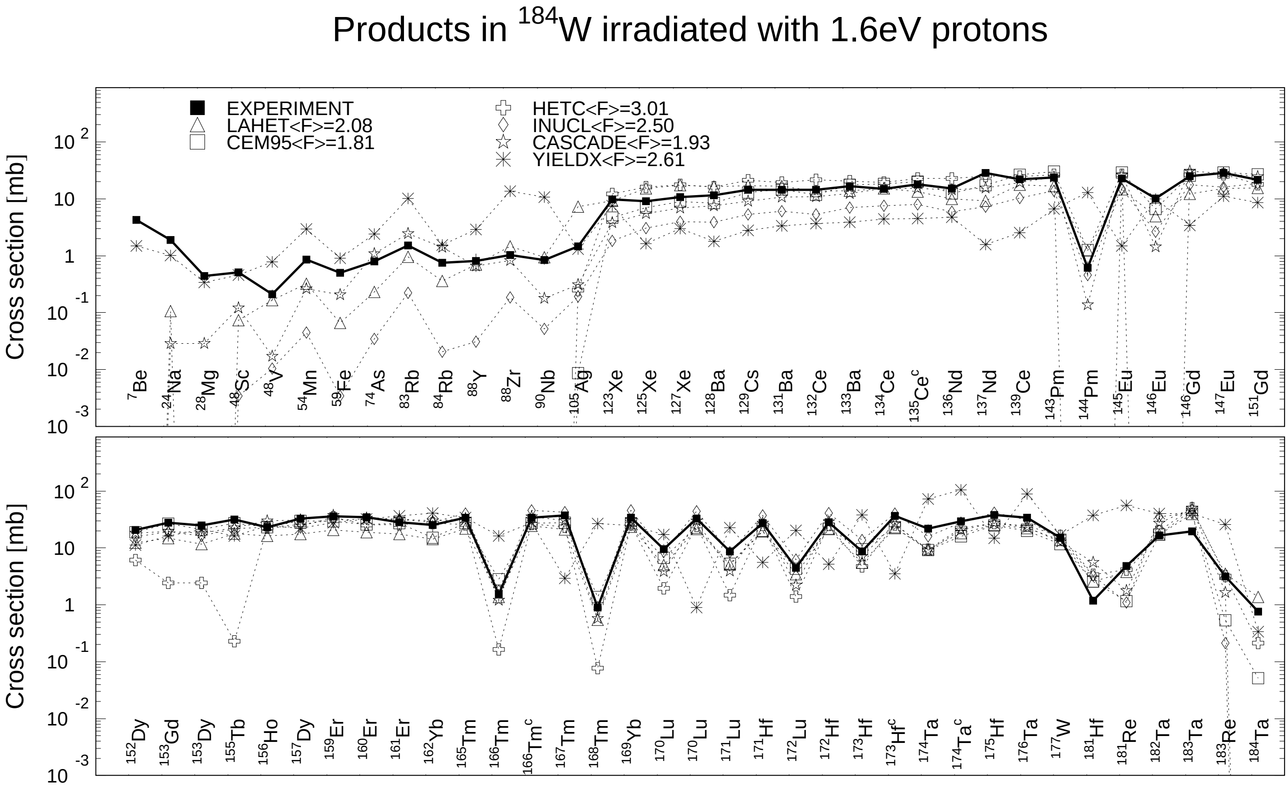

Fig. 47: Detailed comparison between experimental and simulated yields of radioactive reaction products in ^{184}W irradiated with 1.6 GeV protons. The cumulative yields are labeled -c when the respective independent yields are also shown.

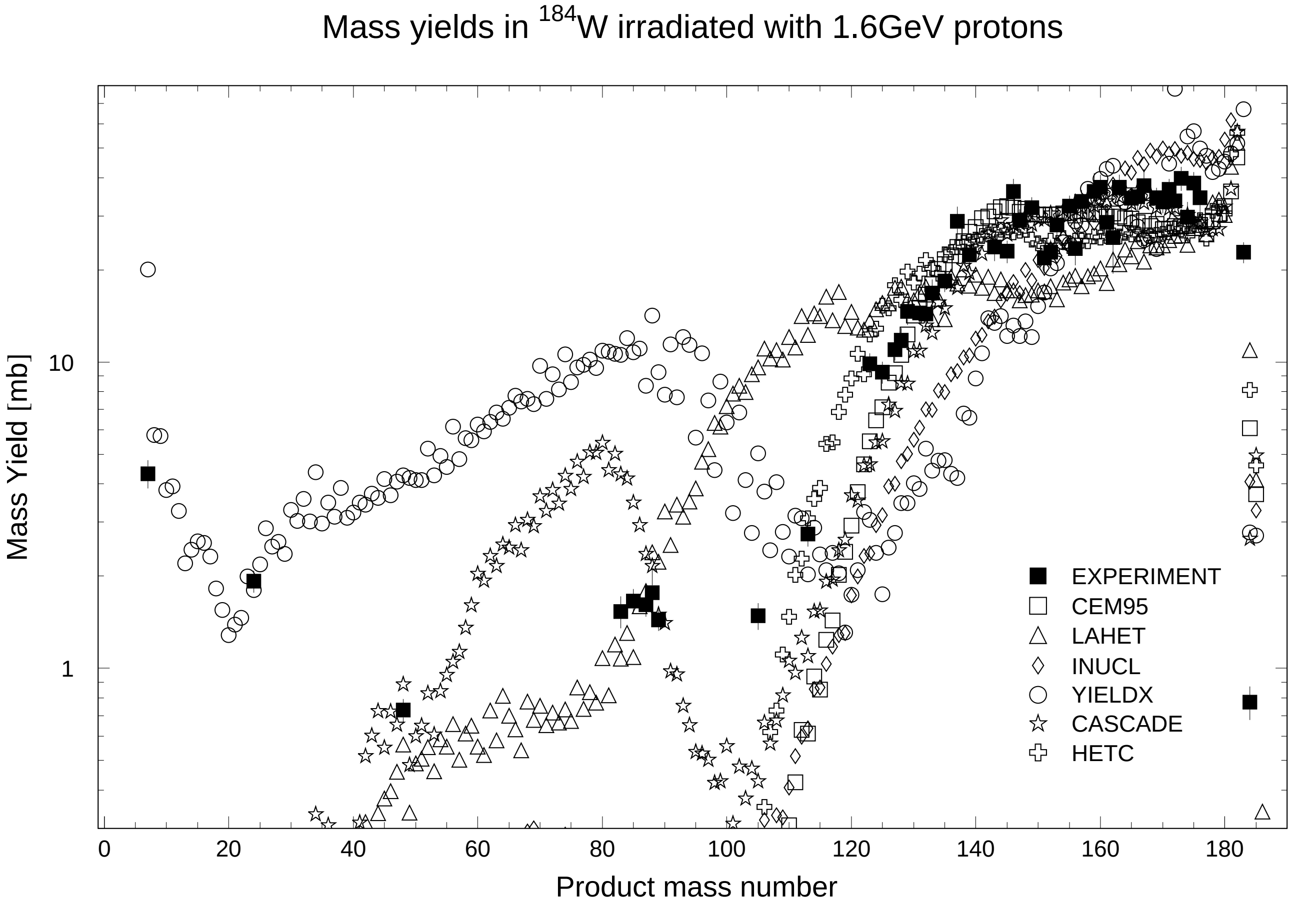

Fig. 48: The simulated mass distributions of reaction products together with the measured cumulative and supra-cumulative yields in ^{184}W irradiated with 1.6 GeV protons.

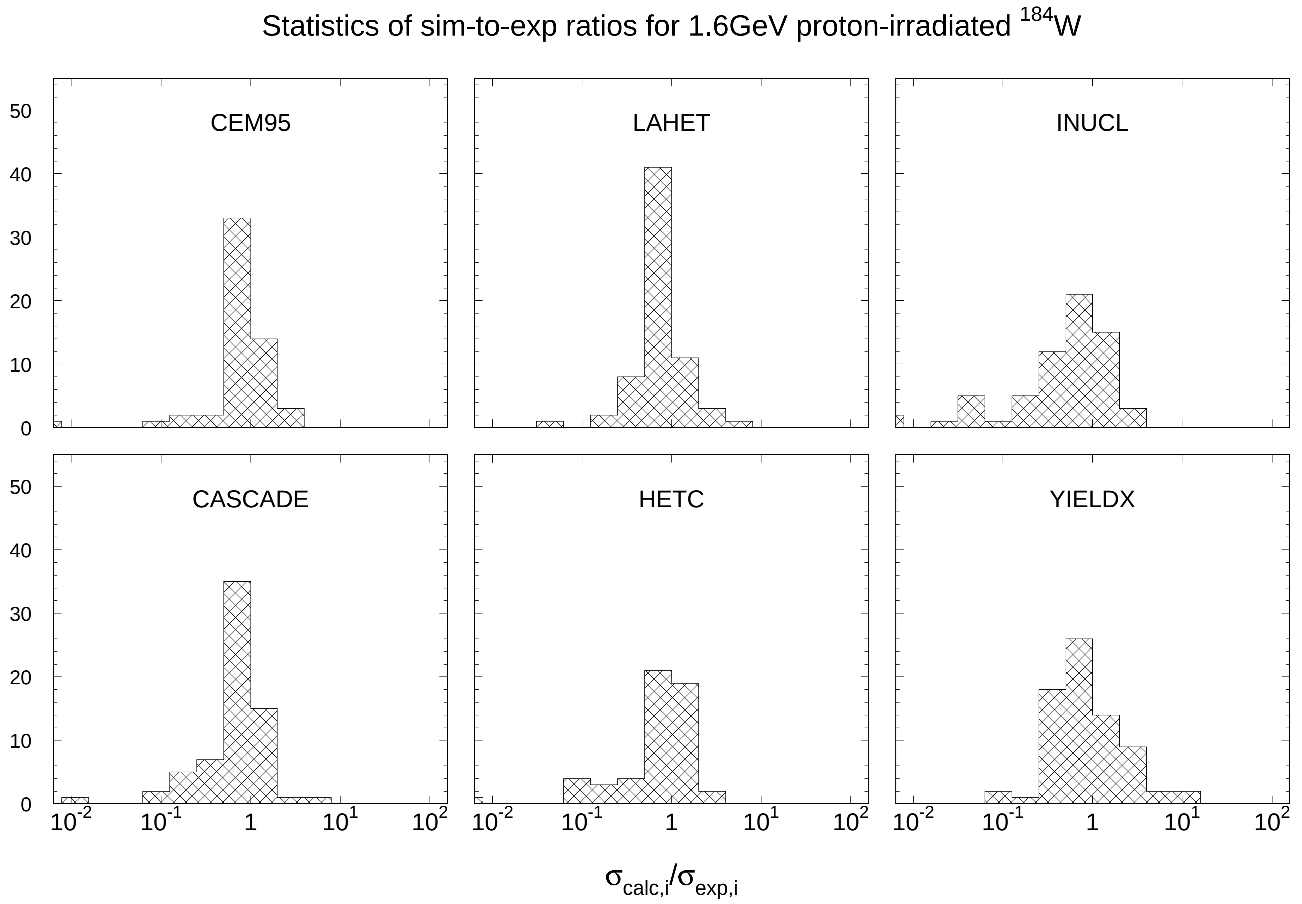

Fig. 49: Statistics of the simulation-to-experiment ratios (criterion 2) for ^{184}W irradiated with 1.6 GeV protons.

Table 74: Experimental and calculated yields from ^{186}W irradiated with 0.2 GeV protons.

Product	$T_{1/2}$	Type	Exp yield [mbarn]	Calculated Yields [mbarn] via CEM95	LAHET	CASCADE	HETC	INUCL	YIELDX
^{183}Re	70,0d	i(m+g)	26.5 ± 2.1	22.3	28.8	34.5	25.4	29.0	27.2
^{182}Re	64,0h	i	12.0 ± 1.0	20.0	15.2	24.0	18.3	24.8	33.4
^{181}Re	19,9h	i	28.8 ± 3.8	21.9	29.8	36.1	27.8	28.6	36.2
^{179}Re	19,5m	i	20.5 ± 4.0	21.0	30.5	32.7	30.2	24.8	36.0
^{178}W	21,6d	c	76.4 ± 9.2	82.5	90.6	92.2	71.9	78.7	87.3
^{177}W	135m	c	66.8 ± 7.8	72.6	77.3	83.1	77.3	62.2	71.5
^{176}W	2,5h	c	62.8 ± 9.7	61.3	75.7	91.2	80.0	58.1	54.4
^{174}W	31m	c	50.2 ± 6.0	24.4	48.6	76.7	81.6	32.7	13.7
^{183}Ta	5,1d	c	16.1 ± 1.3	20.3	18.0	10.9	8.64	41.0	44.2
^{176}Ta	8,09h	c	106. ± 9.	105.	103.	110.	88.3	76.9	76.7
^{176}Ta	8,09h	i(m+g)	39.0 ± 6.4	43.8	28.1	19.1	9.74	19.3	22.9
^{174}Ta	1,14h	i	24.2 ± 4.1	27.8	28.6	17.8	8.68	11.6	18.9
^{172}Ta	36,8m	c*	28.4 ± 3.4	12.2	42.2	68.2	124.	22.6	4.18
^{171}Ta	23,3m	c*	3.63 ± 0.61	2.99	23.8	33.8	133.	11.4	1.30
^{175}Hf	70d	c	103. ± 8.	105.	95.7	103.	89.6	60.7	74.8
^{173}Hf	23,6h	c	71.9 ± 5.3	46.5	66.7	78.2	93.6	31.6	27.9
^{172}Hf	1,87y	c	44.3 ± 3.3	24.7	47.0	65.5	104.	22.9	14.0
^{171}Hf	12,1h	c	26.3 ± 2.9	9.94	30.9	38.2	124.	14.0	7.36
^{172}Lu	6,70d	i(m1+m2+g)	2.13 ± 0.16	4.31	2.67	0.282	–	0.205	1.56
^{171}Lu	8,24d	i(m+g)	9.73 ± 2.23	3.09	3.67	0.707	–	0.273	1.45
^{170}Lu	2,012d	c	22.5 ± 1.8	5.03	20.1	21.9	96.2	8.90	5.36
^{169}Yb	32,026d	c	15.3 ± 1.1	2.58	15.3	10.7	36.8	5.80	4.14
^{166}Tm	7,70h	c	2.19 ± 0.37	0.059	2.58	1.19	–	1.61	1.79
^{165}Tm	30,06h	c	1.58 ± 0.16	0.036	1.24	0.480	–	1.01	1.87

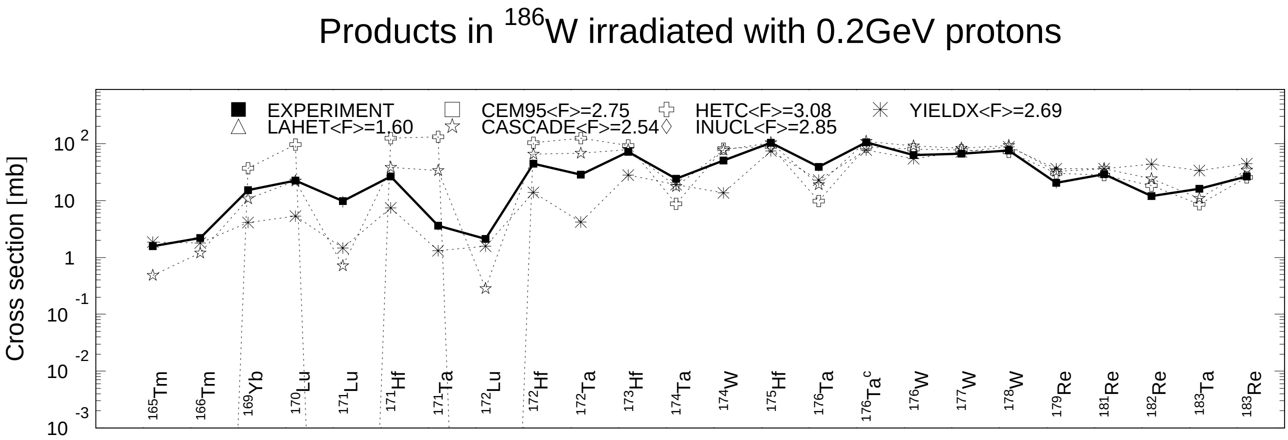

Fig. 50: Detailed comparison between experimental and simulated yields of radioactive reaction products in ^{186}W irradiated with 0.2 GeV protons. The cumulative yields are labeled -c when the respective independent yields are also shown.

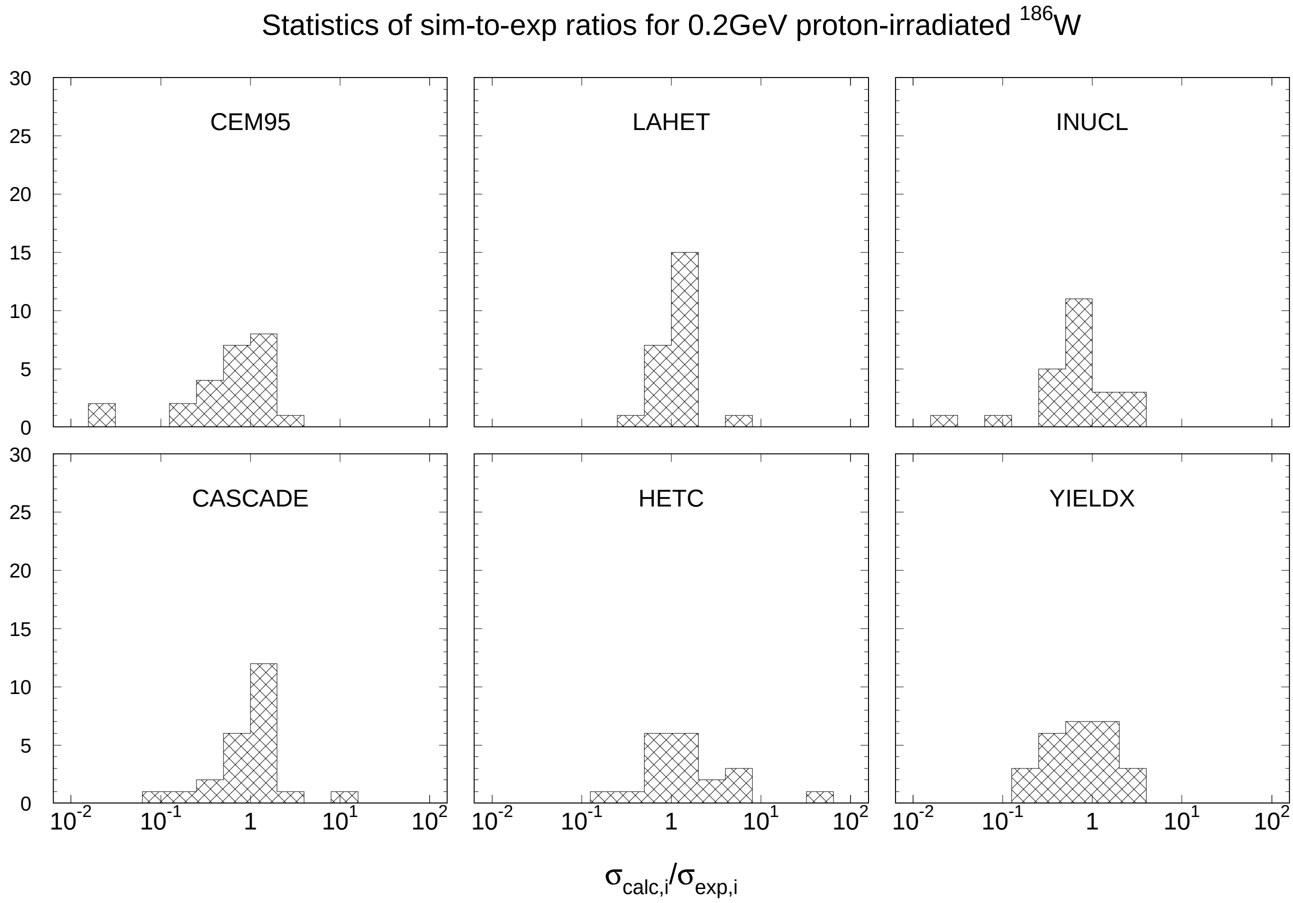

Fig. 51: Statistics of the simulation-to-experiment ratios (criterion 2) for ^{186}W irradiated with 0.2 GeV protons.

Table 75: Experimental and calculated yields from ^{186}W irradiated with 0.8 GeV protons.

Product	$T_{1/2}$	Type	Exp yield [mbarn]	Calculated Yields [mbarn] via CEM95	LAHET	CASCADE	HETC	INUCL	YIELDX
^{184}Ta	8,7h	c	15.1 ± 1.0	18.4	21.0	29.4	18.7	35.7	17.3
^{183}Re	70,0d	i(m+g)	10.5 ± 1.7	4.78	8.00	5.93	5.16	4.18	4.51
^{183}Ta	5,1d	c	20.5 ± 1.6	17.3	20.8	19.5	17.1	31.9	18.6
^{181}Re	19,9h	i	7.48 ± 1.18	4.41	7.58	6.06	5.41	4.60	6.03
^{181}Hf	42,39d	c	3.17 ± 0.41	4.37	4.24	3.44	3.18	8.63	1.14
^{177}W	135m	c	15.9 ± 1.8	18.3	21.8	20.7	23.5	21.5	34.5
^{176}Ta	8,09h	c	40.0 ± 4.3	33.4	39.7	37.9	34.8	46.2	47.8
^{175}Hf	70d	c	53.0 ± 4.0	46.6	49.6	46.6	39.5	64.3	70.3
^{174}Ta	1,14h	c	43.1 ± 4.8	27.4	35.0	36.0	34.8	41.7	39.6
^{174}Ta	1,14h	i	41.2 ± 5.1	15.8	19.3	15.1	12.9	24.1	25.6
^{173}Hf	23,6h	c	51.5 ± 3.8	42.9	46.2	48.0	41.2	61.5	38.2
^{173}Hf	23,6h	i	11.7 ± 2.4	20.0	11.4	13.1	6.06	22.7	15.5
^{172}Hf	1,87y	c	49.9 ± 8.4	41.0	42.3	51.7	40.7	62.2	23.4
^{172}Lu	6,70d	i(m1+m2+g)	7.80 ± 0.60	10.0	8.57	4.05	1.70	8.63	4.68
^{171}Hf	12,1h	c	28.6 ± 3.2	37.8	40.3	47.9	41.6	54.6	13.5
^{171}Lu	8,24d	i(m+g)	29.2 ± 3.1	12.9	12.2	6.37	1.94	11.1	6.24
^{170}Lu	2,012d	c	50.9 ± 4.4	47.1	45.6	54.7	41.7	59.3	17.2
^{170}Lu	2,012d	i(m+g)	17.0 ± 5.0	14.9	13.2	6.26	1.96	10.6	6.22
^{169}Yb	32,026d	c	58.5 ± 4.0	55.8	49.0	55.2	44.7	58.2	20.6
^{167}Tm	9,25d	c	58.2 ± 11.8	59.7	41.6	51.8	39.9	48.2	21.7
^{166}Tm	7,70h	c	55.6 ± 3.8	56.6	48.5	58.7	45.5	46.5	24.0
^{166}Tm	7,70h	i	6.67 ± 0.60	8.30	3.07	1.25	0.096	1.51	3.79
^{165}Tm	30,06h	c	53.5 ± 4.0	55.7	42.2	53.0	44.6	38.1	27.2
^{162}Yb	18,87m	c	31.7 ± 4.8	23.3	23.9	42.9	46.2	20.6	9.37
^{161}Tm	33m	c*	38.7 ± 6.8	33.0	27.7	45.0	48.6	20.0	19.9
^{161}Er	3,21h	c	44.8 ± 4.1	44.5	30.9	44.0	42.4	22.0	30.1
^{160}Er	28,58h	c	44.3 ± 3.7	38.0	32.8	44.2	43.0	20.7	30.5
^{159}Er	36m	c*	45.8 ± 3.2	36.8	32.8	46.2	55.7	17.9	22.6
^{159}Ho	33,05m	c	45.9 ± 3.5	39.3	31.7	37.8	41.5	16.4	27.5
^{157}Dy	8,14h	c	36.3 ± 2.9	33.2	27.1	30.9	37.4	13.4	24.0
^{156}Ho	56m	c	29.2 ± 2.5	21.5	21.2	28.0	33.7	11.1	14.7
^{155}Tb	5,32d	c	29.8 ± 2.7	24.3	24.3	20.3	0.048	10.1	19.4
^{153}Dy	6,4h	c	14.9 ± 1.4	12.9	13.2	13.5	3.12	6.36	9.94
^{153}Gd	240,4d	c	21.8 ± 2.6	17.6	17.4	14.2	3.12	7.70	–
^{152}Dy	2,38h	c	13.6 ± 0.9	9.19	13.0	11.3	7.50	5.89	6.95
^{147}Eu	24,1d	c	13.1 ± 1.3	4.55	10.6	8.66	22.6	4.32	8.46
^{146}Gd	48,27d	c	10.7 ± 0.8	3.14	7.09	8.35	17.5	3.94	4.27
^{145}Eu	5,93d	c	8.64 ± 0.83	2.18	7.59	4.89	16.6	3.08	7.25
^{139}Ce	137,640d	c	3.55 ± 0.49	0.145	3.31	0.849	2.73	1.35	4.05

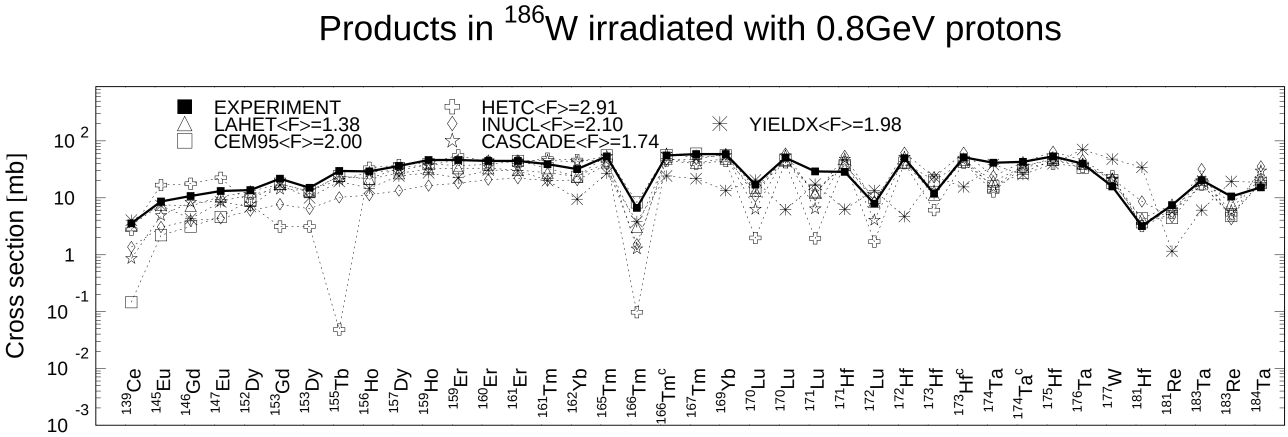

Fig. 52: Detailed comparison between experimental and simulated yields of radioactive reaction products in ^{186}W irradiated with 0.8 GeV protons. The cumulative yields are labeled -c when the respective independent yields are also shown.

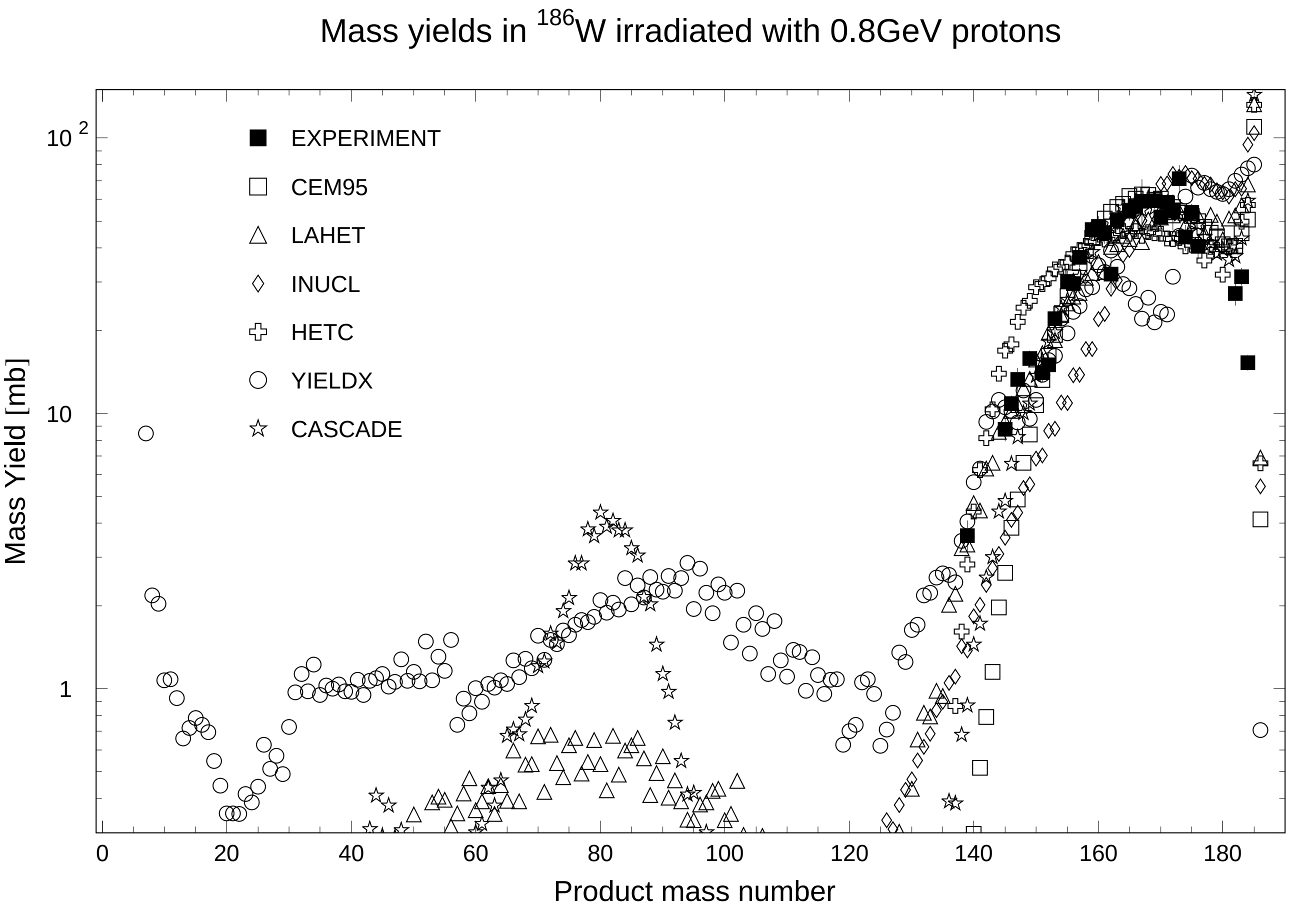

Fig. 53: The simulated mass distributions of reaction products together with the measured cumulative and supra-cumulative yields in ^{186}W irradiated with 0.8 GeV protons.

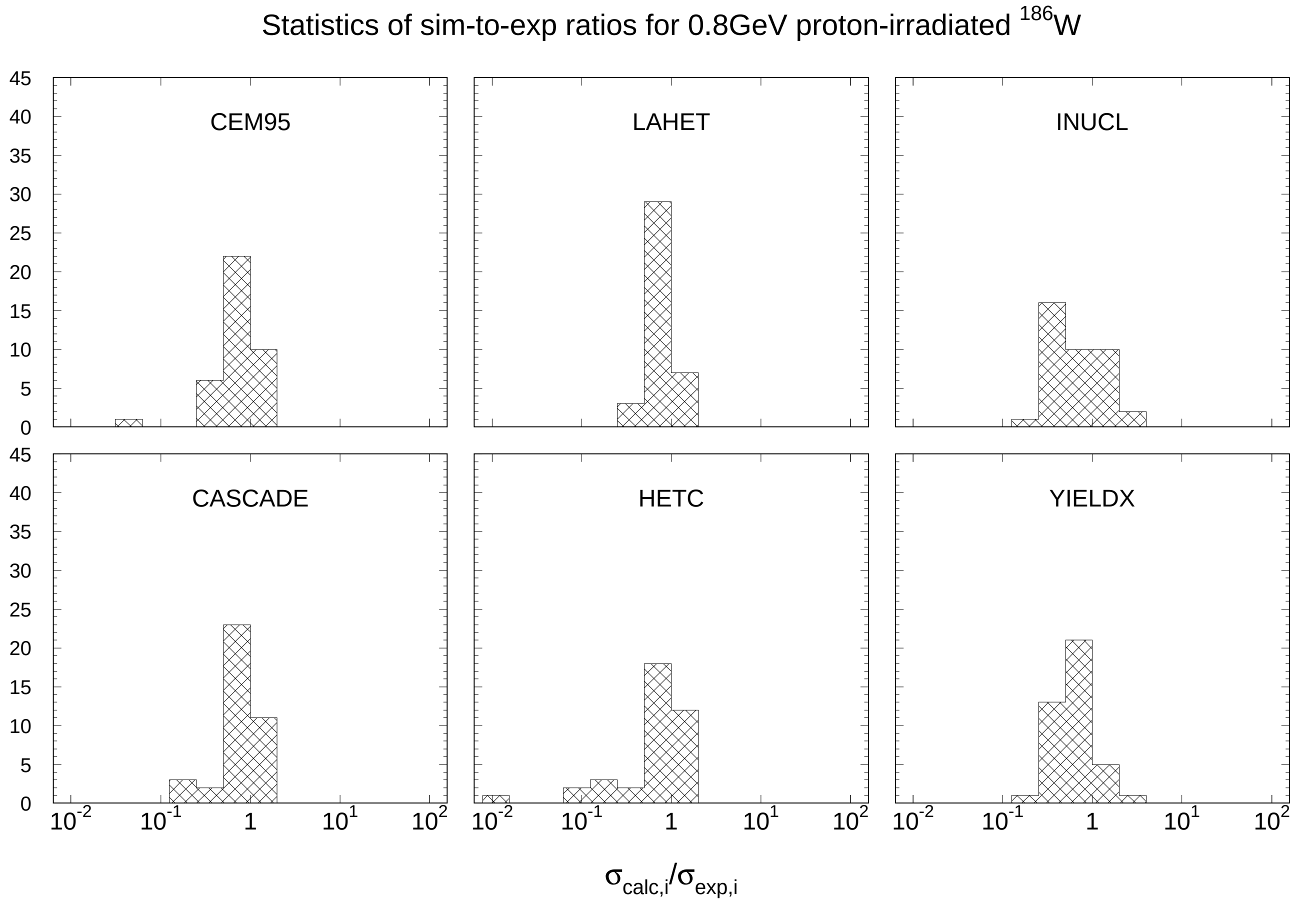

Fig. 54: Statistics of the simulation-to-experiment ratios (criterion 2) for ^{186}W irradiated with 0.8 GeV protons.

Table 76: Experimental and calculated yields from ^{186}W irradiated with 1.6 GeV protons.

Product	$T_{1/2}$	Type	Exp yield [mbarn]	Calculated Yields [mbarn] via CEM95	LAHET	CASCADE	HETC	INUCL	YIELDX
^{183}Re	70,0d	i(m+g)	3.70 ± 0.64	0.942	3.36	1.47	3.78	1.04	1.84
^{181}Re	19,9h	i	4.40 ± 0.72	1.16	3.03	1.89	3.26	1.56	2.45
^{177}W	135m	c	11.8 ± 1.4	8.87	9.81	11.7	14.6	11.6	28.1
^{184}Ta	8,7h	c	15.5 ± 1.3	16.5	17.5	25.9	19.9	35.4	12.8
^{183}Ta	5,1d	c	20.2 ± 1.7	15.3	15.5	17.5	16.4	29.5	13.8
^{182}Ta	114,43d	c	17.1 ± 1.4	13.6	13.1	12.2	14.0	25.9	14.6
^{176}Ta	8,09h	c	31.2 ± 2.9	16.4	18.5	20.6	22.2	28.4	41.4
^{174}Ta	1,14h	c	28.6 ± 3.6	12.3	15.2	19.1	20.4	24.5	59.1
^{174}Ta	1,14h	i	28.0 ± 4.8	7.75	8.45	9.03	8.34	15.0	38.8
^{181}Hf	42,39d	c	3.01 ± 0.24	3.74	3.68	3.22	3.35	6.95	0.967
^{175}Hf	70d	c	36.0 ± 3.1	23.5	23.5	27.0	25.8	40.3	99.8
^{173}Hf	23,6h	c	34.3 ± 2.9	20.0	20.8	26.6	24.3	37.7	–
^{173}Hf	23,6h	i	14.6 ± 2.7	9.83	5.78	8.39	4.64	15.9	13.6
^{172}Hf	1,87y	c	28.1 ± 2.4	18.9	19.5	29.0	24.3	38.6	24.3
^{171}Hf	12,1h	c	25.3 ± 2.6	17.8	16.9	25.6	25.6	34.1	13.3
^{172}Lu	6,70d	i(m1+m2+g)	5.97 ± 0.49	5.80	4.66	3.03	1.92	7.64	4.71
^{171}Lu	8,24d	i(m+g)	10.5 ± 1.9	6.53	6.54	4.91	1.94	10.1	6.38
^{170}Lu	2,012d	c	32.2 ± 2.7	20.2	20.9	29.6	23.8	41.6	–
^{170}Lu	2,012d	i(m+g)	14.1 ± 1.9	6.66	6.43	4.39	2.10	9.58	6.38
^{169}Yb	32,026d	c	34.0 ± 2.7	26.4	22.1	31.1	25.4	43.9	21.0
^{162}Yb	18,87m	c	22.3 ± 2.8	13.0	11.6	27.6	26.4	23.3	10.1
^{168}Tm	93,1d	i	1.42 ± 0.18	2.44	0.828	0.818	0.194	1.41	1.39
^{167}Tm	9,25d	c	37.1 ± 5.1	27.6	20.5	31.4	23.7	41.8	24.1
^{166}Tm	7,70h	c	34.8 ± 3.5	26.6	23.4	35.7	25.7	43.5	27.0
^{166}Tm	7,70h	i	2.94 ± 0.46	4.08	1.90	1.51	0.261	2.70	4.32
^{165}Tm	30,06h	c	34.6 ± 3.0	26.2	20.5	32.4	25.6	38.0	30.2
^{161}Er	3,21h	c	31.1 ± 3.2	25.9	16.6	31.2	24.9	28.6	31.9
^{160}Er	28,58h	c	34.7 ± 3.4	25.0	17.7	33.5	24.4	29.0	32.0
^{159}Er	36m	c*	34.4 ± 5.1	26.5	19.1	36.7	34.0	27.2	23.6
^{156}Ho	56m	c	35.0 ± 3.4	22.0	15.1	29.3	22.2	19.6	15.4
^{157}Dy	8,14h	c	34.5 ± 3.1	30.9	17.7	30.2	23.4	24.2	24.9
^{153}Dy	6,4h	c	24.8 ± 2.6	20.1	11.4	20.1	2.55	15.3	10.5
^{152}Dy	2,38h	c	20.0 ± 1.6	17.3	11.2	18.5	6.15	14.7	–
^{155}Tb	5,32d	c	31.7 ± 2.6	29.2	17.5	23.9	0.300	21.3	20.2
^{153}Gd	240,4d	c	28.1 ± 2.6	27.7	15.6	22.0	2.55	18.9	17.0
^{151}Gd	124d	c	24.5 ± 2.3	27.3	14.7	24.4	18.2	17.1	14.3
^{146}Gd	48,27d	c	23.3 ± 1.9	21.8	11.0	29.6	26.3	14.6	4.93
^{147}Eu	24,1d	c	29.0 ± 2.6	28.3	15.4	26.8	26.3	14.8	9.28
^{146}Eu	4,61d	i	10.7 ± 1.1	8.01	5.24	1.75	–	2.82	4.31
^{145}Eu	5,93d	c	21.5 ± 1.8	27.1	13.2	24.9	27.3	12.0	8.56
^{144}Pm	363d	i	0.899 ± 0.090	1.78	1.57	0.167	–	0.533	2.05
^{143}Pm	265d	c	23.0 ± 2.3	29.8	16.6	23.9	27.3	12.2	11.6
^{137}Nd	38,5m	c	25.8 ± 2.6	13.9	9.28	13.7	25.6	5.70	1.43
^{136}Nd	50,65m	c	12.7 ± 1.3	9.84	9.72	12.0	22.9	4.74	0.786
^{139}Ce	137,640d	c	21.4 ± 1.7	24.8	17.9	17.9	24.2	9.34	5.61
^{135}Ce	17,7h	c	16.8 ± 1.4	17.6	13.6	13.3	21.9	6.63	4.32
^{134}Ce	3,16d	c	14.3 ± 1.4	14.9	15.1	12.8	19.1	6.08	4.15
^{132}Ce	3,51h	c	12.5 ± 1.0	9.15	12.5	9.69	20.9	3.93	–
^{133}Ba	3848,9d	c	13.5 ± 1.5	15.4	13.9	10.7	19.5	5.57	4.17
^{131}Ba	11,50d	c	13.4 ± 1.1	12.3	16.2	9.03	18.5	4.60	3.54
^{128}Ba	2,43d	c	9.99 ± 0.95	6.80	16.4	6.08	14.7	3.01	3.13
^{129}Cs	32,06h	c	12.9 ± 1.3	10.6	17.1	7.44	19.8	4.16	3.08
^{127}Xe	36,4d	c	9.83 ± 0.81	8.05	17.8	6.10	16.6	3.15	2.11
^{125}Xe	16,9h	c	8.25 ± 0.67	6.04	14.1	4.50	14.9	2.35	1.83
^{123}Xe	2,08h	c	8.47 ± 0.71	3.32	8.61	2.69	10.9	1.40	2.65

Table 76, cont'd.

Product	$T_{1/2}$	Type	Exp yield [mbarn]	Calculated Yields [mbarn] via CEM95	LAHET	CASCADE	HETC	INUCL	YIELDX
^{105}Ag	41,29d	c	1.12 ± 0.11	–	6.49	0.213	0.117	0.176	1.44
^{90}Nb	14,60h	c	0.689 ± 0.124	–	0.621	0.109	–	0.079	0.917
^{88}Zr	83,4d	c	0.887 ± 0.079	–	1.28	0.582	–	0.118	8.89
^{88}Y	106,65d	i(m+g)	0.651 ± 0.075	–	0.563	0.570	–	0.017	4.09
^{84}Rb	32,77d	i(m+g)	0.679 ± 0.068	–	0.224	1.05	–	0.010	2.12
^{83}Rb	86,2d	c	1.60 ± 0.28	–	0.870	2.04	–	0.138	10.0
^{75}Se	119,779d	c	1.38 ± 0.25	–	0.588	1.95	–	0.145	7.48
^{74}As	17,77d	i	0.732 ± 0.080	–	0.182	0.898	–	0.031	3.11
^{59}Fe	44,472d	c	0.657 ± 0.064	–	0.124	0.207	–	0.010	1.14
^{54}Mn	312,11d	i	0.792 ± 0.110	–	0.315	0.265	–	0.028	2.98
^{48}V	15,9735d	c	0.183 ± 0.023	–	0.099	0.012	–	0.025	0.622
^{48}Sc	43,67h	i	0.469 ± 0.061	–	0.075	0.109	–	0.003	0.549
^{28}Mg	20,915h	c	0.406 ± 0.059	–	–	0.012	–	–	0.412
^{24}Na	14,9590h	c	1.79 ± 0.15	–	0.075	0.012	–	–	1.14
^{22}Na	2,6019y	c	1.36 ± 0.18	–	0.050	–	–	–	0.617
^{7}Be	53,29d	i	4.16 ± 0.59	–	–	–	–	–	1.46

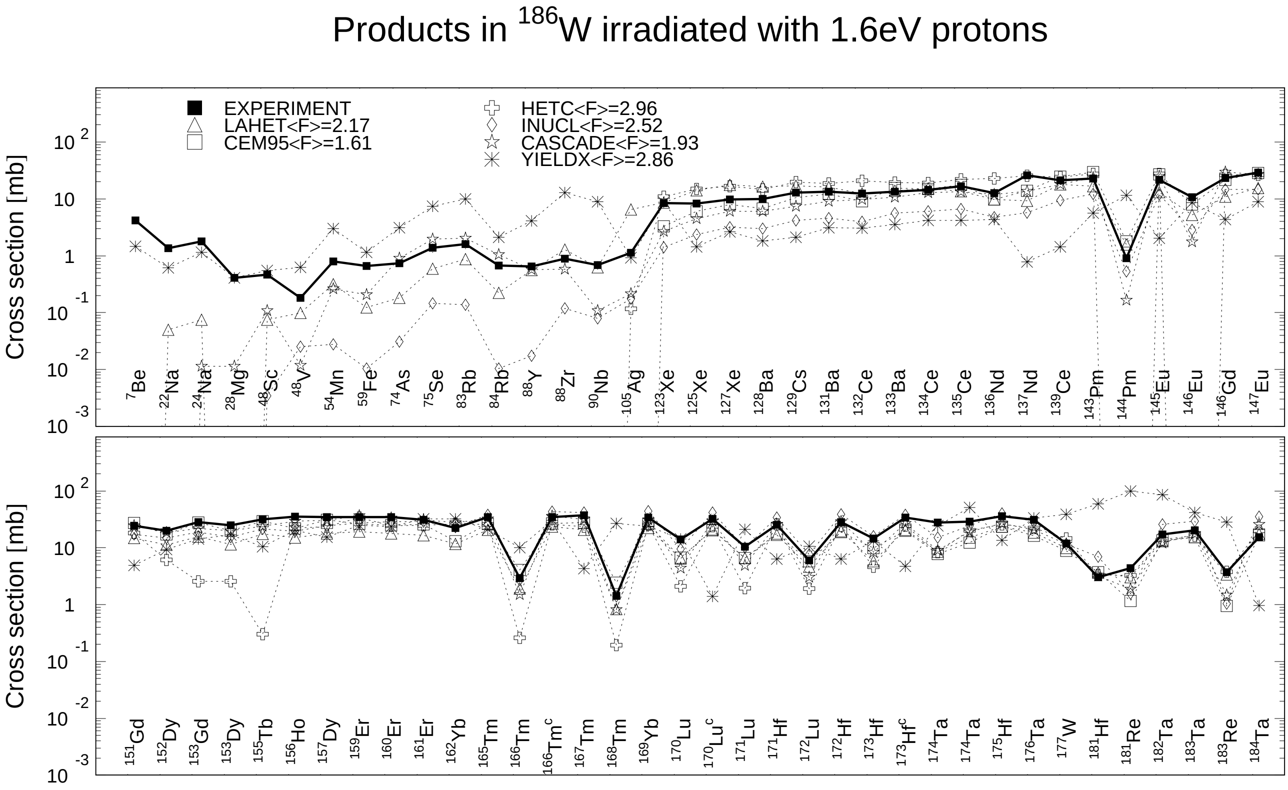

Fig. 55: Detailed comparison between experimental and simulated yields of radioactive reaction products in ^{186}W irradiated with 1.6 GeV protons. The cumulative yields are labeled -c when the respective independent yields are also shown.

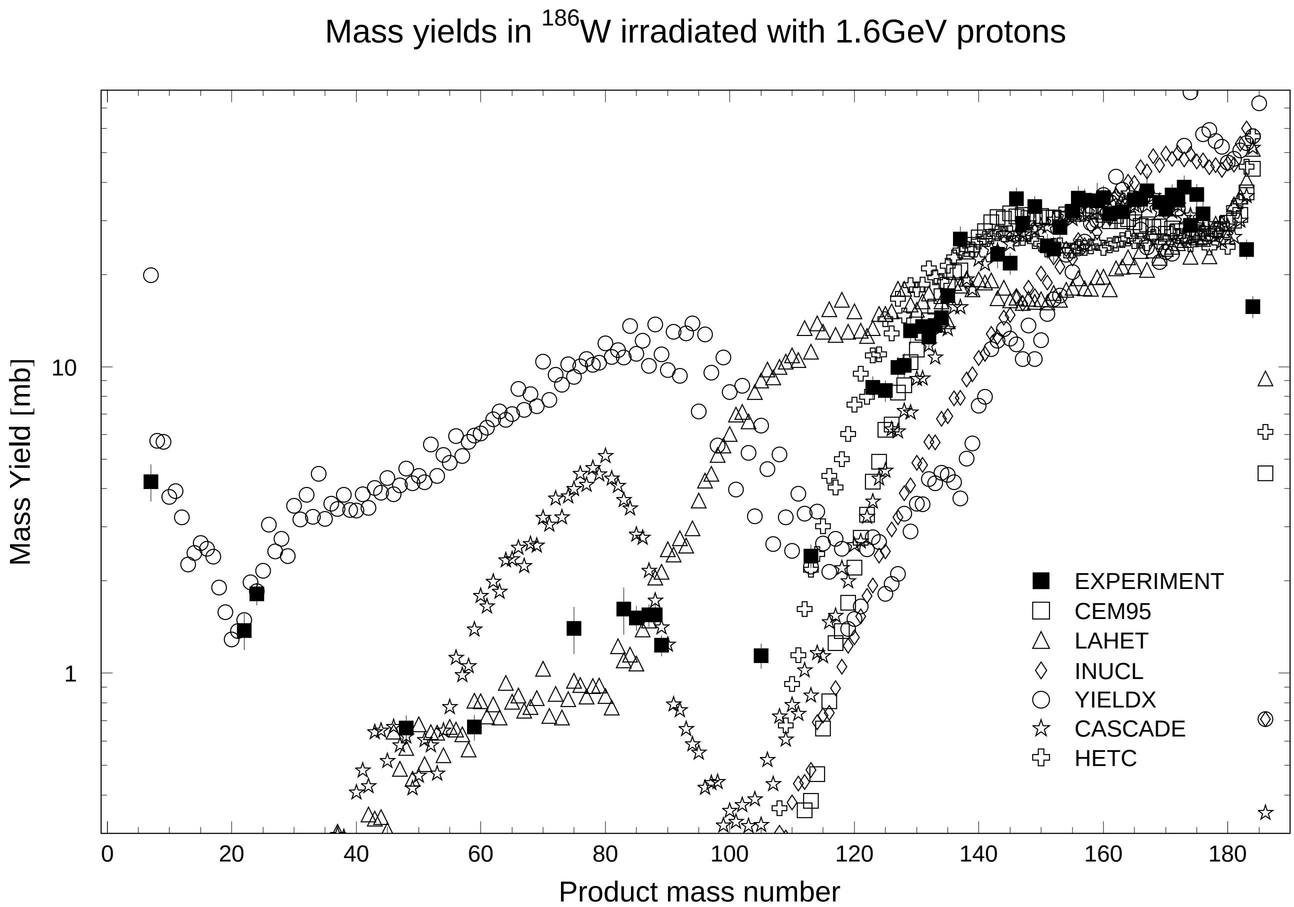

Fig. 56: The simulated mass distributions of reaction products together with the measured cumulative and supra-cumulative yields in ^{186}W irradiated with 1.6 GeV protons.

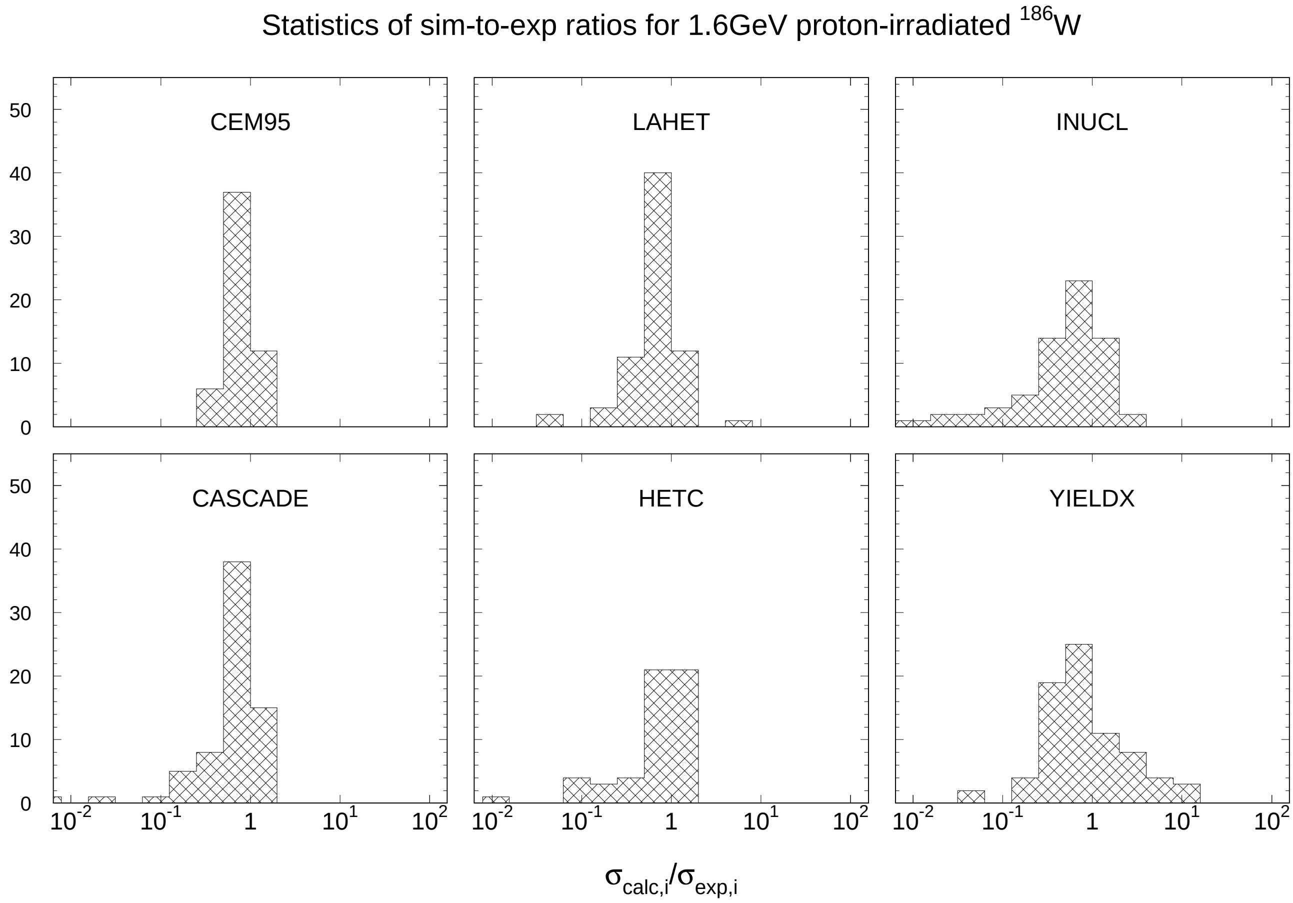

Fig. 57: Statistics of the simulation-to-experiment ratios (criterion 2) for ^{186}W irradiated with 1.6 GeV protons.

Table 77: Experimental and calculated yields from ^{nat}W irradiated with 2.6 GeV protons.

Product	$T_{1/2}$	Type	Exp yield [mbarn]	Calculated Yields [mbarn] via CEM95	CEM2k	LAHET	CASCADE	HETC	INUCL	YIELDX
^{181}Re	19,9h	i	3.51 ± 0.58	0.632	1.01	2.96	1.54	3.10	0.754	1.43
^{177}W	135m	c	13.0 ± 1.6	6.64	7.73	11.2	7.97	13.6	10.4	23.6
^{176}W	2,5h	c	7.86 ± 2.51	6.67	6.94	11.0	8.79	13.2	10.9	22.3
^{184}Ta	8,7h	c	4.39 ± 0.44	4.17	1.29	5.07	7.11	1.12	8.27	3.74
^{183}Ta	5,1d	c	10.4 ± 1.0	16.1	7.07	17.4	18.1	44.0	20.5	7.35
^{176}Ta	8,09h	c	29.3 ± 3.4	13.8	13.5	19.3	15.2	20.5	24.4	38.0
^{174}Ta	1,14h	c	25.5 ± 2.8	10.5	11.6	15.1	14.4	17.7	19.7	36.6
^{181}Hf	42,39d	c	1.24 ± 0.12	1.92	0.272	1.83	3.57	2.34	2.35	0.398
^{175}Hf	70d	c	33.0 ± 3.0	18.1	16.6	21.5	19.0	22.8	32.5	54.6
^{173}Hf	23,6h	c	29.5 ± 2.5	16.3	15.8	18.1	18.8	21.1	30.1	53.8
^{173}Hf	23,6h	i	5.52 ± 2.43	6.63	5.24	4.13	5.26	3.70	11.5	15.9
^{172}Hf	1,87y	c	21.7 ± 2.1	15.2	13.6	17.3	21.0	21.3	31.9	51.5
^{171}Hf	12,1h	c	19.4 ± 2.4	13.9	13.2	14.9	20.1	19.6	27.7	39.3
^{172}Lu	6,70d	i(m1+m2+g)	3.68 ± 0.50	3.00	2.10	3.09	1.66	1.01	4.59	3.47
^{171}Lu	8,24d	i(m+g)	10.7 ± 2.0	4.42	2.56	3.93	3.17	1.63	7.20	5.13
^{170}Lu	2,012d	c	24.5 ± 2.2	17.8	15.0	17.8	23.3	19.8	34.7	28.5
^{169}Yb	32,026d	c	27.4 ± 2.5	18.9	15.5	17.9	23.8	21.1	35.5	26.0
^{162}Yb	18,87m	c	18.6 ± 3.3	9.37	10.2	10.9	21.0	19.3	23.6	15.2
^{167}Tm	9,25d	c	28.9 ± 6.0	20.1	15.3	16.2	24.0	18.1	34.2	25.1
^{166}Tm	7,70h	c	26.9 ± 2.4	19.3	16.0	18.6	26.7	20.1	36.5	27.7
^{166}Tm	7,70h	i	2.34 ± 0.45	2.20	1.24	1.06	1.13	0.150	1.59	2.37
^{165}Tm	30,06h	c	26.8 ± 2.5	18.9	14.7	16.1	24.0	17.8	33.4	27.4
^{161}Er	3,21h	c	24.0 ± 2.5	17.3	14.4	11.8	23.5	18.9	25.1	36.2
^{160}Er	28,58h	c	23.6 ± 2.2	16.6	14.1	14.4	25.1	18.7	26.8	34.8
^{159}Er	36m	c*	25.0 ± 3.8	18.0	15.6	13.9	27.5	24.2	28.7	30.6
^{156}Ho	56m	c	19.4 ± 1.8	14.1	13.4	11.7	22.2	16.2	21.6	22.8
^{157}Dy	8,14h	c	23.9 ± 2.3	18.6	13.9	12.8	22.2	17.5	23.1	28.4
^{153}Dy	6,4h	c	13.9 ± 1.9	11.9	9.56	7.96	13.3	1.93	15.9	17.5
^{152}Dy	2,38h	c	15.4 ± 1.3	11.4	8.96	8.37	12.9	4.10	16.5	15.3
^{155}Tb	5,32d	c	22.4 ± 1.9	16.3	11.2	11.4	16.5	0.366	19.8	26.1
^{153}Gd	240,4d	c	26.7 ± 2.6	15.5	11.1	9.76	15.0	1.93	19.2	22.8
^{151}Gd	124d	c	18.8 ± 2.2	16.7	12.0	11.0	17.9	13.5	19.7	19.1
^{146}Gd	48,27d	c	18.6 ± 1.6	16.9	14.6	8.46	24.6	18.5	19.3	12.0
^{147}Eu	24,1d	c	22.2 ± 2.0	19.3	14.0	10.9	22.7	17.6	18.3	14.3
^{146}Eu	4,61d	i	3.60 ± 0.32	3.99	1.92	3.29	1.25	–	2.93	4.51
^{145}Eu	5,93d	c	17.6 ± 1.6	19.5	15.1	9.75	21.1	17.8	17.5	13.7
^{143}Pm	265d	c	20.1 ± 2.2	21.2	14.8	10.8	21.8	17.3	18.4	18.6
^{139}Ce	137,640d	c	19.6 ± 1.7	22.3	14.8	12.6	20.8	17.8	16.0	10.6
^{135}Ce	17,7h	c	17.6 ± 1.5	20.4	14.0	8.92	18.5	17.4	14.6	7.74
^{134}Ce	3,16d	c	17.7 ± 1.8	19.6	14.1	9.76	20.5	16.0	13.3	8.01
^{132}Ce	3,51h	c	16.1 ± 2.7	15.0	13.0	9.68	17.1	17.3	10.8	7.48
^{133}Ba	3848,9d	c	18.2 ± 4.1	21.6	14.1	9.79	18.2	16.4	13.2	7.97
^{131}Ba	11,50d	c	16.0 ± 1.3	20.5	14.1	10.9	17.6	16.1	13.0	7.31
^{128}Ba	2,43d	c	15.4 ± 1.5	16.5	13.5	11.3	16.0	15.8	9.73	6.58
^{126}Ba	100m	c	7.86 ± 1.12	10.8	11.6	1.52	10.4	0.043	5.95	4.07
^{129}Cs	32,06h	c	18.6 ± 1.7	20.8	14.1	10.6	15.4	19.4	11.9	6.72
^{127}Xe	36,4d	c	15.2 ± 1.3	19.8	13.6	12.0	16.0	18.5	11.4	5.35
^{125}Xe	16,9h	c	14.1 ± 1.2	19.0	13.1	10.9	13.9	18.2	8.98	3.64
^{123}Xe	2,08h	c	15.5 ± 1.3	15.4	12.3	6.61	10.8	18.2	6.24	5.64
^{122}Xe	20,1h	c	11.6 ± 1.0	13.0	11.5	3.58	11.1	14.1	5.57	6.00
^{117}Te	62m	c	8.71 ± 0.79	10.1	9.42	7.40	8.18	14.2	3.57	2.29
^{115}Sb	32,1m	c*	9.74 ± 0.89	10.8	11.6	10.6	6.41	16.7	3.03	3.15
^{111}In	2,8047d	c	7.33 ± 0.63	10.0	9.22	9.98	8.19	14.7	3.09	3.02
^{109}In	4,2h	c	5.06 ± 0.44	7.06	7.77	5.55	5.04	13.8	1.64	2.27
^{105}Ag	41,29d	c	5.27 ± 0.69	5.73	6.95	10.1	4.29	11.9	0.994	2.90

Table 77, cont'd.

Product	$T_{1/2}$	Type	Exp yield [mbarn]	Calculated Yields [mbarn] via CEM95	CEM2k	LAHET	CASCADE	HETC	INUCL	YIELDX
^{100}Pd	3,63d	c	1.18 ± 0.26	1.21	3.40	3.15	2.14	8.73	0.240	0.754
^{97}Ru	2,791d	c	3.08 ± 0.30	2.15	4.09	8.21	2.09	7.83	0.257	2.14
^{90}Nb	14,60h	c	2.55 ± 0.23	0.748	2.23	5.00	0.497	3.33	0.103	4.28
^{88}Zr	83,4d	c	2.53 ± 0.27	0.351	1.41	9.45	1.49	2.28	0.103	14.0
^{88}Y	106,65d	i(m+g)	1.54 ± 0.22	0.213	0.812	3.98	0.651	–	–	2.64
^{83}Sr	32,41h	c	1.94 ± 0.92	0.122	0.650	6.47	0.960	0.645	0.240	9.18
^{84}Rb	32,77d	i(m+g)	1.29 ± 0.14	–	0.211	2.00	0.806	–	–	1.38
^{83}Rb	86,2d	c	3.30 ± 0.58	0.213	0.941	11.5	2.33	0.645	0.257	13.0
^{77}Kr	74,4m	c	1.69 ± 0.18	–	0.145	2.51	0.326	0.172	0.189	2.56
^{75}Se	119,779d	c	2.35 ± 0.22	0.057	0.247	6.03	2.47	0.022	0.240	10.9
^{74}As	17,77d	i	1.37 ± 0.16	–	0.044	1.87	1.08	–	0.017	2.34
^{59}Fe	44,472d	c	0.845 ± 0.103	–	–	0.033	0.326	–	–	0.842
^{54}Mn	312,11d	i	2.48 ± 0.41	–	0.004	0.661	0.446	–	0.034	5.61
^{51}Cr	27,7025d	c	4.48 ± 1.34	–	–	0.264	0.840	–	0.103	3.92
^{48}V	15,9735d	c	0.551 ± 0.060	–	–	0.066	0.051	–	0.034	1.48
^{48}Sc	43,67h	i	0.660 ± 0.088	–	–	0.066	0.086	–	–	0.442
^{43}K	22,3h	c	0.673 ± 0.081	–	–	0.033	0.326	–	–	0.982
^{28}Mg	20,915h	c	0.899 ± 0.087	–	–	–	0.017	–	–	0.622
^{24}Na	14,9590h	c	4.04 ± 0.34	–	–	0.099	0.069	–	–	1.92
^{7}Be	53,29d	i	8.61 ± 1.01	–	–	–	–	–	–	3.45

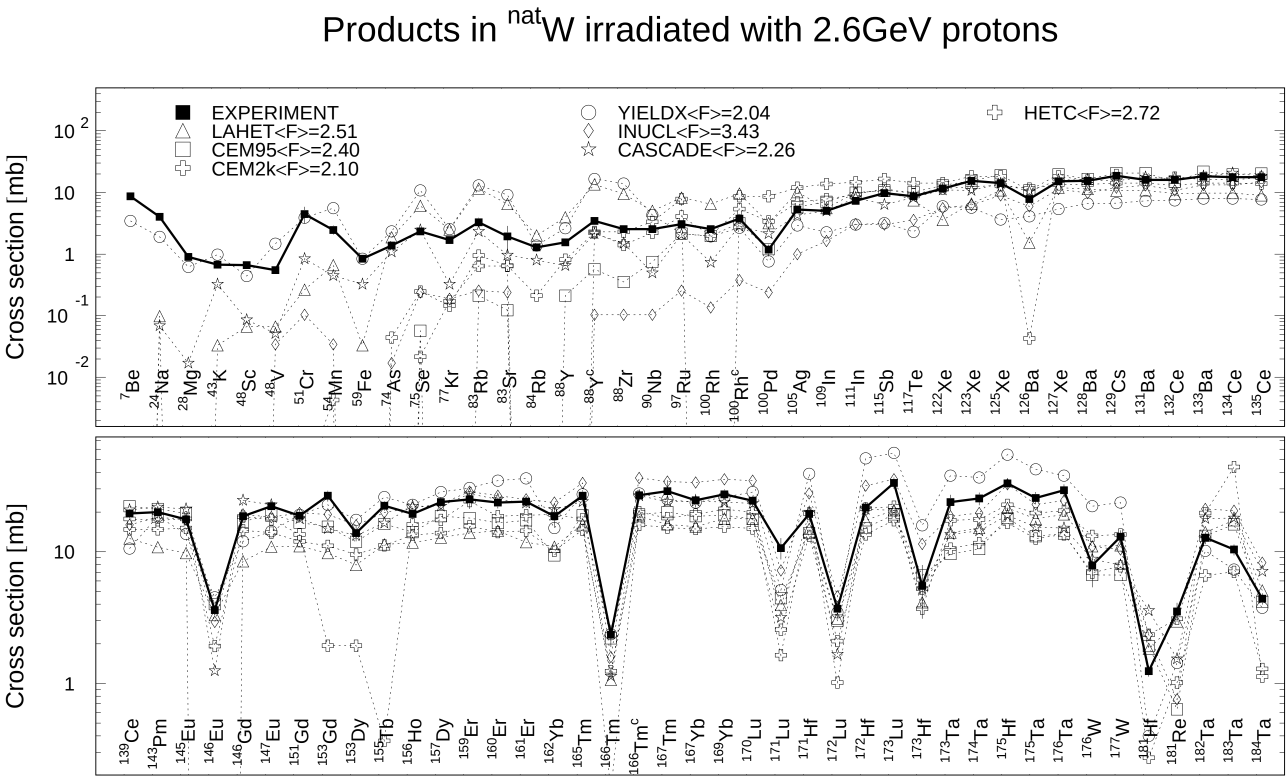

Fig. 58: Detailed comparison between experimental and simulated yields of radioactive reaction products in ^{nat}W irradiated with 2.6 GeV protons. The cumulative yields are labeled -c when the respective independent yields are also shown.

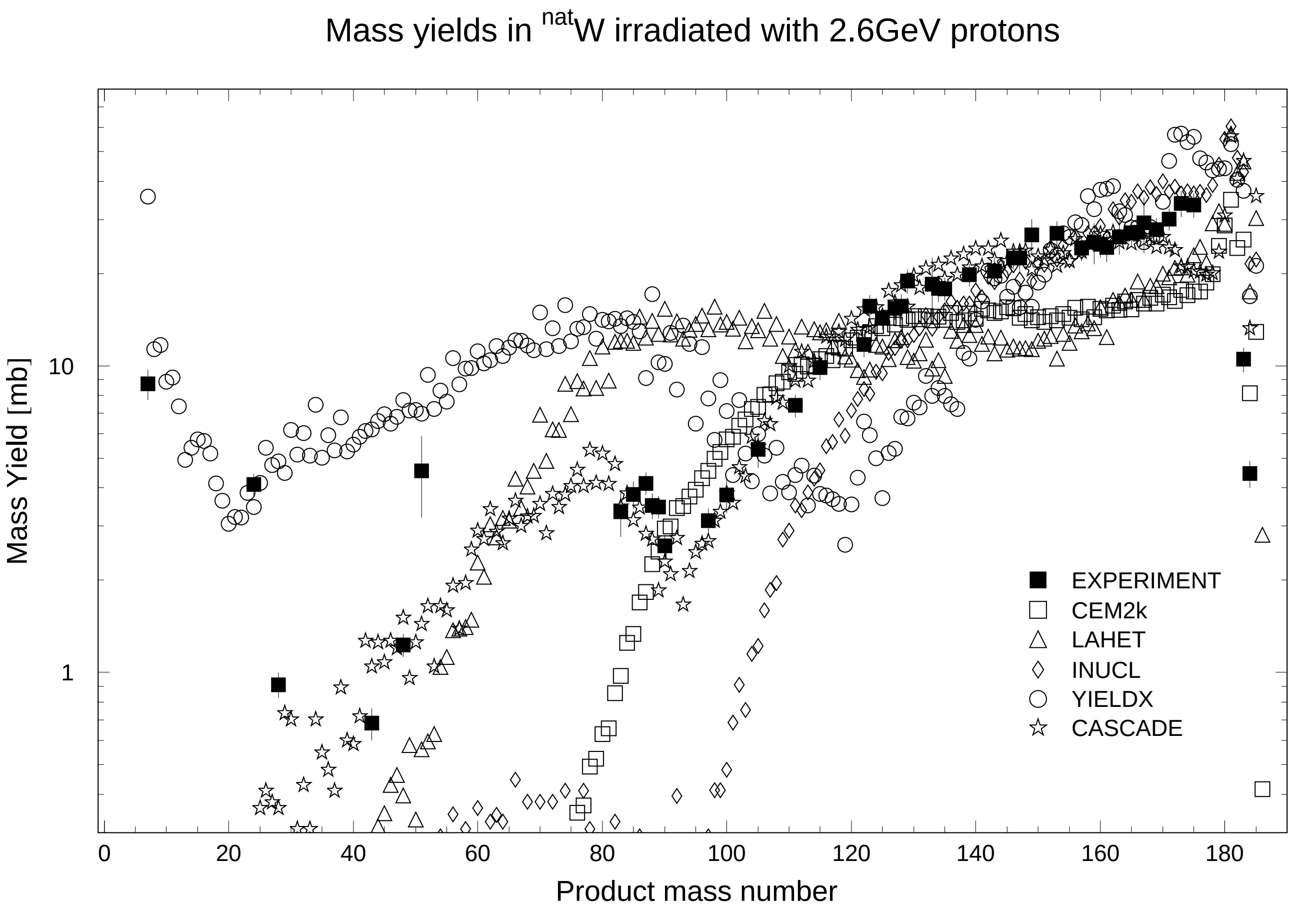

Fig. 59: The simulated mass distributions of reaction products together with the measured cumulative and supra-cumulative yields in ^{nat}W irradiated with 2.6 GeV protons.

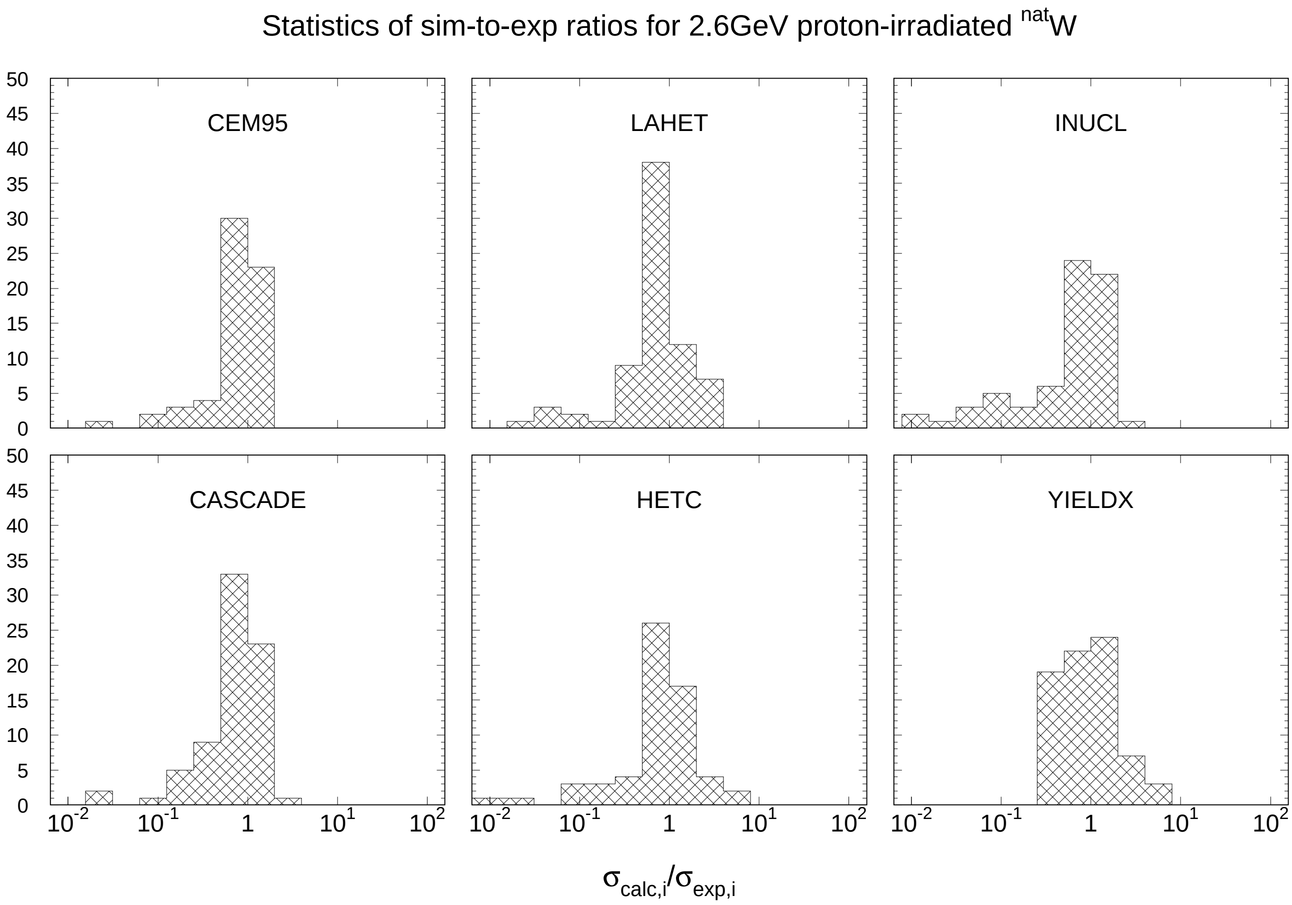

Fig. 60: Statistics of the simulation-to-experiment ratios (criterion 2) for ^{nat}W irradiated with 2.6 GeV protons.

Table 78: Experimental and calculated yields from ^{232}Th irradiated with 0.1 GeV protons.

Product	$T_{1/2}$	Type	Exp yield [mbarn]	Calculated Yields [mbarn] via LAHET	CASCADE	CASCADO-IPPE	INUCL	ALICE-IPPE
^{228}Ac	6,15h	i	19.8 ± 1.7	13.0	3.28	6.58	18.3	9.65
^{227}Th	18,72d	c	51.0 ± 6.4	35.5	31.6	42.7	101.	42.3
^{226}Ac	29,37h	i	8.29 ± 0.87	12.9	0.966	3.52	12.9	5.50
^{224}Ac	2,78h	i	5.72 ± 0.72	6.81	0.163	0.698	6.20	1.24
^{143}Ce	33,039h	c	14.8 ± 1.1	16.6	1.45	8.16	0.864	–
^{142}La	91,1m	c	16.5 ± 1.3	15.2	0.864	5.15	1.00	–
^{141}Ce	32,501d	c	24.2 ± 2.6	23.8	4.39	11.4	1.42	–
^{141}Ba	18,27m	c	15.6 ± 2.0	14.3	0.413	2.97	0.923	–
^{140}La	1,6781d	i	4.93 ± 0.38	4.66	3.20	7.31	0.500	–
^{140}Ba	12,752d	c	15.5 ± 1.3	15.7	1.50	5.66	1.53	–
^{139}Ba	83,06m	c	20.2 ± 3.8	22.2	3.49	9.44	2.94	–
^{136}Cs	13,16d	i(m+g)	9.97 ± 0.81	7.23	15.2	12.3	7.97	–
^{135}Xe	9,14h	i(m+g)	13.4 ± 1.1	8.04	24.0	10.9	14.3	–
^{135}I	6,57h	c	10.1 ± 0.8	14.4	5.85	0.917	3.76	–
^{134}Te	41,8m	c	5.41 ± 0.68	9.92	0.485	0.115	2.15	–
^{133}I	20,8h	c	17.9 ± 1.5	21.2	71.0	11.8	31.6	–
^{132}Te	3,204d	c	9.60 ± 0.85	17.3	33.3	5.16	27.8	–
^{131}I	8,02070d	c	25.4 ± 1.9	26.3	149.	27.0	47.8	–
^{129}Sb	4,40h	c	5.66 ± 0.60	13.8	45.8	6.35	21.3	–
^{128}Sn	59,07m	c	2.43 ± 0.35	10.8	9.38	1.42	11.1	–
^{127}Sb	3,85d	c	16.4 ± 1.5	20.1	68.4	22.3	27.6	–
^{122}Sb	2,7238d	i(m+g)	6.20 ± 0.48	4.93	1.28	0.956	0.827	–
^{112}Ag	3,130h	i	11.0 ± 1.6	6.77	0.133	3.37	0.616	–
^{112}Ag	3,130h	c	69.5 ± 8.5	33.2	1.65	54.4	9.16	–
^{111}Ag	7,45d	c	72.4 ± 8.0	30.2	1.06	55.0	8.97	–
^{107}Rh	21,7m	c*	66.2 ± 7.9	34.7	1.29	62.9	9.81	–
^{105}Ru	4,44h	c	58.6 ± 4.3	28.9	1.73	54.8	10.5	–
^{104}Tc	18,3m	c	49.9 ± 4.2	23.8	2.62	54.4	12.8	–
^{103}Ru	39,26d	c	53.4 ± 4.1	31.8	8.52	52.7	14.6	–
^{101}Tc	14,22m	c	50.1 ± 9.8	30.5	29.4	45.0	20.3	–
^{99}Mo	65,94h	c	46.7 ± 3.5	16.1	22.7	12.8	14.1	–
^{97}Zr	16,744h	c	36.1 ± 2.6	19.9	80.2	34.4	28.0	–
^{96}Nb	23,35h	i	2.08 ± 0.23	6.20	0.904	0.201	2.60	–
^{95}Zr	64,02d	c	41.6 ± 3.4	28.5	134.	36.2	32.4	–
^{94}Y	18,7m	i	37.8 ± 3.8	8.56	66.0	20.7	17.3	–
^{92}Y	3,54h	i	19.0 ± 3.8	7.36	20.4	3.86	9.10	–
^{92}Y	3,54h	c	48.2 ± 6.7	33.5	167.	30.3	42.6	–
^{91}Sr	9,63h	c	40.5 ± 3.2	26.6	145.	26.0	31.0	–
^{89}Rb	15,15m	c*	35.8 ± 3.6	33.0	80.8	30.0	19.1	–
^{88}Kr	2,84h	c	26.9 ± 2.1	21.1	26.2	15.6	8.76	–
^{87}Kr	76,3m	c	29.7 ± 3.3	19.3	25.7	17.8	18.9	–
^{78}As	90,7m	i	2.63 ± 0.78	2.28	0.512	1.84	0.251	–
^{78}Ge	88m	c	4.23 ± 0.37	6.71	0.942	7.23	0.135	–
^{73}Ga	4,86h	c	1.87 ± 0.16	3.02	0.184	5.56	0.038	–

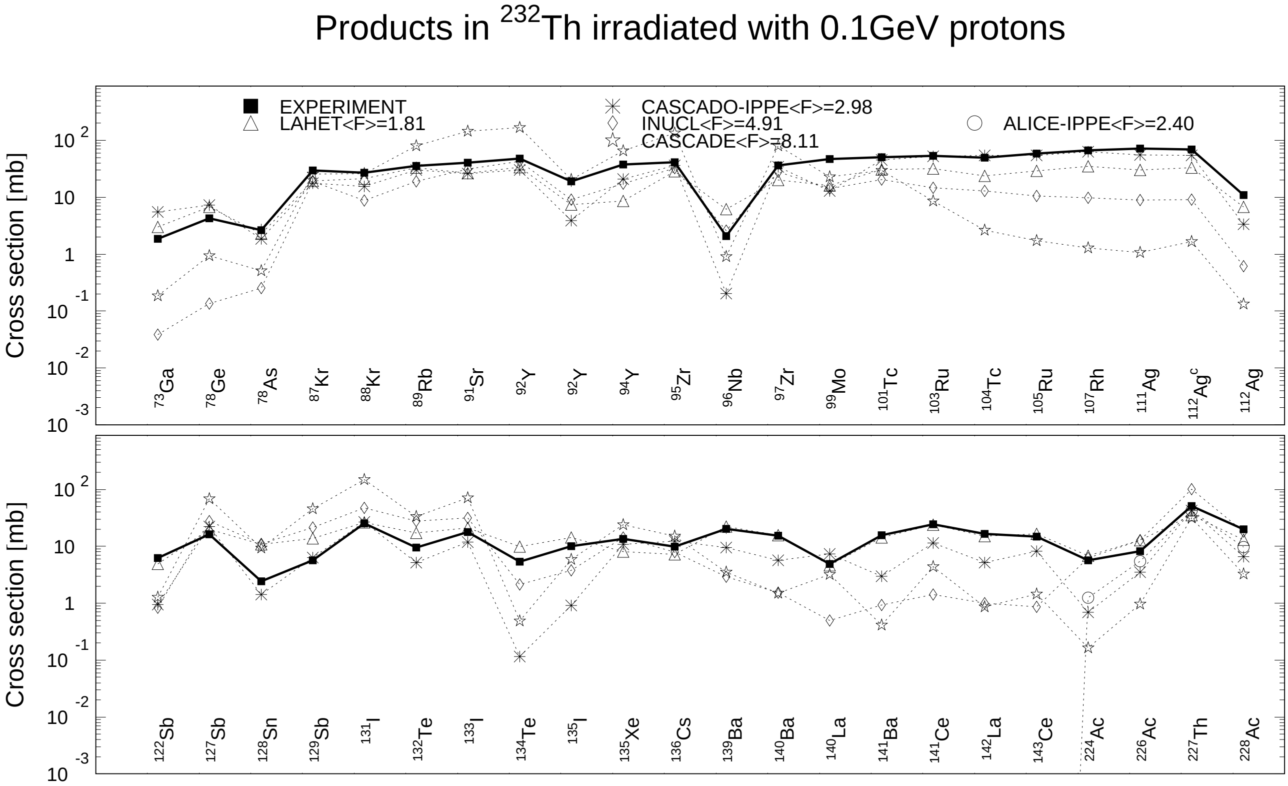

Fig. 61: Detailed comparison between experimental and simulated yields of radioactive reaction products in ^{232}Th irradiated with 0.1 GeV protons. The cumulative yields are labeled -c when the respective independent yields are also shown.

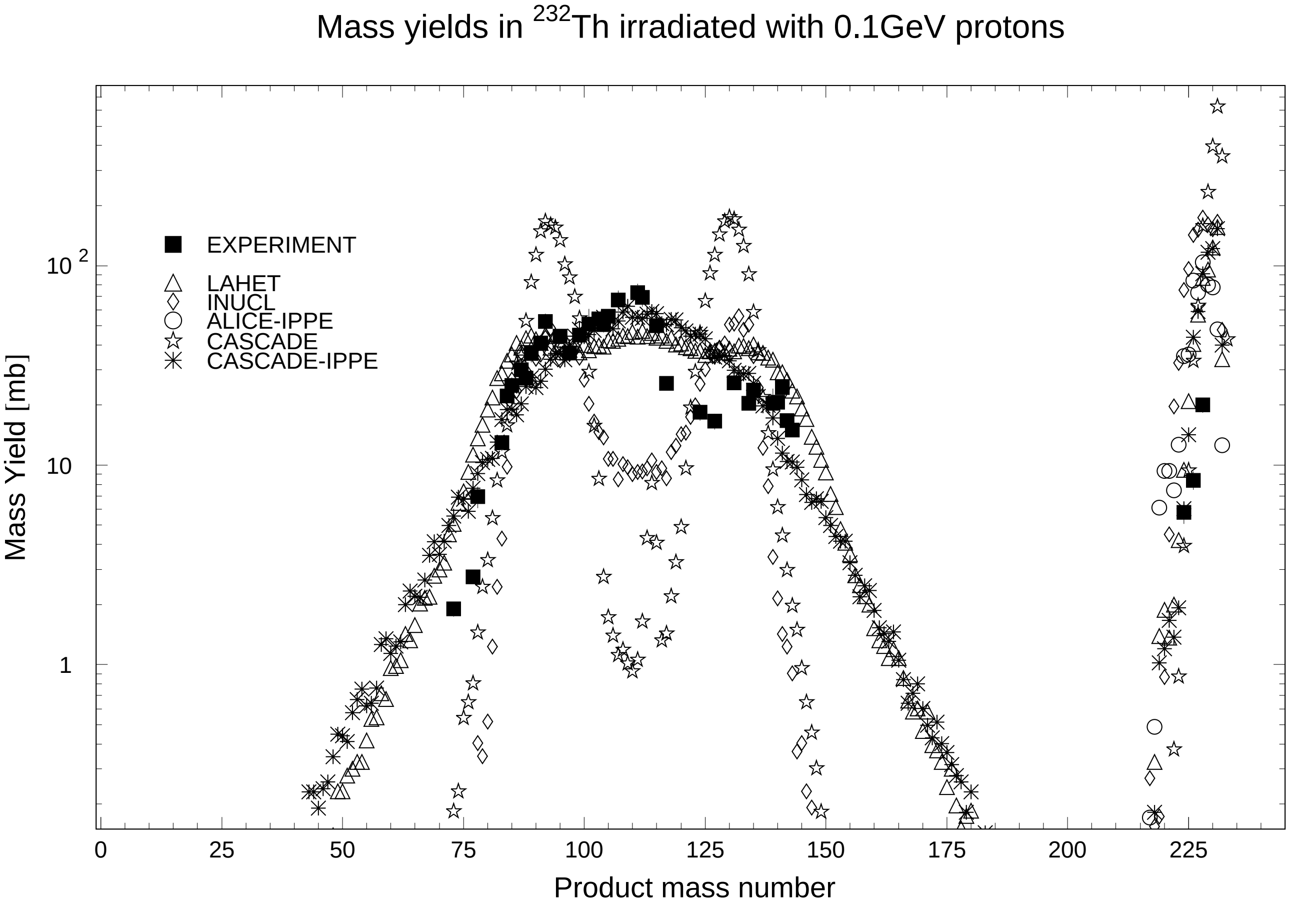

Fig. 62: The simulated mass distributions of reaction products together with the measured cumulative and supra-cumulative yields in ^{232}Th irradiated with 0.1 GeV protons.

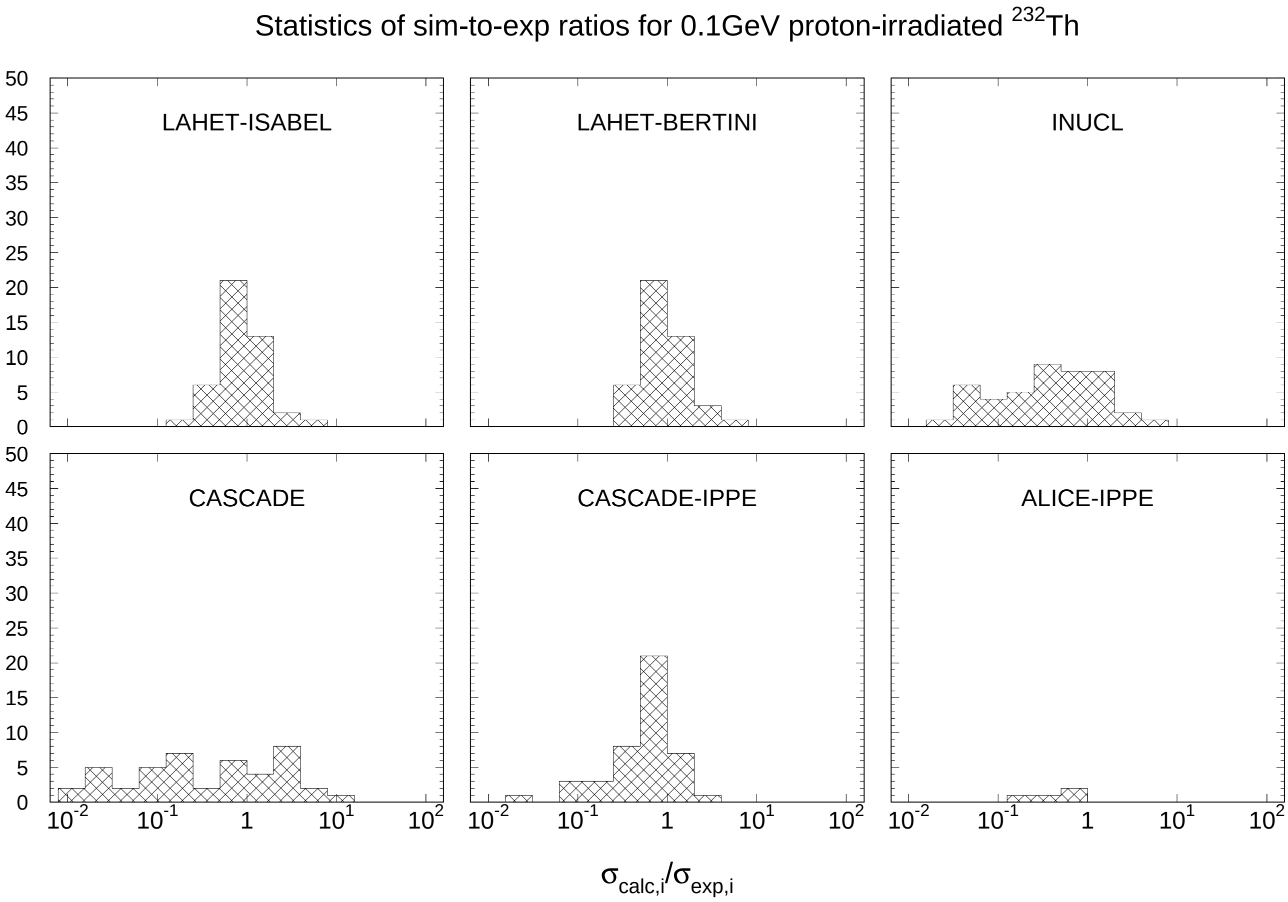

Fig. 63: Statistics of the simulation-to-experiment ratios (criterion 2) for ^{232}Th irradiated with 0.1 GeV protons.

Table 79: Experimental and calculated yields from ^{232}Th irradiated with 0.2 GeV protons.

Product	$T_{1/2}$	Type	Exp yield [mbarn]	Calculated Yields [mbarn] via LAHET	CASCADE	INUCL	ALICE-IPPE
^{233}Pa	26,967d	i	1.67 ± 0.22	–	0.527	–	–
^{229}Ac	62,7m	c	0.828 ± 0.126	14.9	45.7	40.9	10.0
^{228}Ac	6,15h	i	21.2 ± 2.1	12.3	21.3	28.4	8.13
^{227}Th	18,72d	c	28.1 ± 3.5	18.8	69.8	52.8	19.4
^{226}Ac	29,37h	i	17.0 ± 1.8	15.4	15.9	29.6	8.55
^{225}Ac	10,0d	c	19.4 ± 1.6	20.5	23.2	39.0	11.9
^{224}Ac	2,78h	i	17.0 ± 1.4	17.9	8.30	28.3	10.4
^{223}Ra	11,435d	c	36.0 ± 3.2	22.1	71.8	56.5	19.6
^{211}Rn	14,6h	c	3.21 ± 0.26	2.07	0.653	1.90	1.89
^{210}At	8,1h	c	4.82 ± 0.39	1.83	0.062	0.162	0.331
^{209}At	5,41h	c*	4.35 ± 0.37	2.95	0.534	0.449	1.17
^{208}At	1,63h	c*	1.40 ± 0.16	1.09	0.315	0.394	0.637
^{206}Bi	6,243d	c	2.78 ± 0.23	0.597	0.058	0.427	1.02
^{204}Bi	11,22h	c	0.498 ± 0.063	0.050	0.004	0.276	–
^{147}Nd	10,98d	c	2.99 ± 0.61	8.11	0.092	0.141	–
^{146}Pr	24,15m	c	2.59 ± 0.57	7.65	0.152	0.141	–
^{143}Ce	33,039h	c	7.78 ± 0.63	10.7	0.567	0.327	–
^{142}La	91,1m	c	8.15 ± 0.69	10.0	0.353	0.590	–
^{141}Ce	32,501d	c	12.3 ± 1.0	15.9	1.39	0.873	–
^{141}Ba	18,27m	c	7.65 ± 1.03	9.18	0.194	0.490	–
^{140}La	1,6781d	i	2.64 ± 0.27	3.26	0.978	0.245	–
^{140}Ba	12,752d	c	8.91 ± 0.85	10.5	0.639	0.960	–
^{139}Ba	83,06m	c	11.6 ± 2.2	14.6	1.80	1.69	–
^{136}Cs	13,16d	i(m+g)	5.08 ± 0.40	5.11	9.72	5.31	–
^{135}Xe	9,14h	i(m+g)	7.17 ± 0.69	5.37	14.7	10.7	–
^{135}I	6,57h	c	5.42 ± 0.47	8.69	3.72	2.79	–
^{134}Te	41,8m	c	3.16 ± 0.42	6.85	0.387	1.32	–
^{133}I	20,8h	c	9.28 ± 0.80	13.9	42.5	22.3	–
^{132}Cs	6,479d	i	2.85 ± 0.69	3.52	14.4	1.58	–
^{132}Te	3,204d	c	5.07 ± 0.43	10.9	21.8	15.9	–
^{131}I	8,02070d	c	13.9 ± 1.1	18.3	92.5	30.3	–
^{129}Sb	4,40h	c	3.11 ± 0.39	8.81	29.2	11.2	–
^{128}Sn	59,07m	c	1.24 ± 0.12	7.06	5.92	5.41	–
^{127}Xe	36,4d	c	1.76 ± 0.18	3.46	3.41	0.287	–
^{127}Sb	3,85d	c	8.75 ± 0.77	13.7	46.8	17.2	–
^{126}I	13,11d	i	4.28 ± 0.60	4.51	11.1	1.22	–
^{125}Xe	16,9h	c	0.317 ± 0.039	1.43	0.133	0.024	–
^{124}I	4,1760d	i	2.07 ± 0.42	2.65	1.68	0.176	–
^{122}Sb	2,7238d	i(m+g)	8.25 ± 0.65	5.00	8.27	2.52	–
^{112}Ag	3,130h	i	14.3 ± 1.7	6.00	0.530	2.05	–
^{112}Ag	3,130h	c	57.0 ± 6.5	25.6	2.25	8.90	–
^{111}Ag	7,45d	c	54.6 ± 5.5	25.5	2.00	8.62	–
^{107}Rh	21,7m	c*	55.9 ± 6.8	30.4	1.12	10.4	–
^{106}Ru	373,59d	c	43.1 ± 5.1	22.6	0.641	8.15	–
^{105}Ag	41,29d	c	3.50 ± 0.43	1.34	–	0.003	–
^{105}Ru	4,44h	c	50.0 ± 3.9	24.6	1.05	9.13	–
^{104}Tc	18,3m	c	37.2 ± 3.2	20.6	1.17	8.07	–
^{103}Ru	39,26d	c	48.0 ± 3.9	28.2	4.98	11.7	–
^{101}Tc	14,22m	c	45.4 ± 5.1	26.5	14.4	14.9	–
^{101}Tc	14,22m	i	7.49 ± 3.97	6.92	0.686	2.45	–
^{99}Mo	65,94h	c	40.3 ± 3.3	14.8	13.0	9.51	–
^{97}Zr	16,744h	c	26.4 ± 2.1	16.2	42.1	18.2	–
^{96}Nb	23,35h	i	5.37 ± 0.42	5.78	3.41	3.91	–
^{95}Zr	64,02d	c	32.4 ± 2.5	23.0	76.6	24.4	–
^{94}Y	18,7m	i	23.7 ± 2.4	7.02	35.7	10.7	–

Table 79, cont'd.

Product	$T_{1/2}$	Type	Exp yield [mbarn]	Calculated Yields [mbarn] via LAHET	CASCADE	INUCL	ALICE-IPPE
^{92}Y	3,54h	i	7.10 ± 2.08	6.31	26.3	7.81	–
^{92}Y	3,54h	c	32.3 ± 4.6	25.7	119.	30.3	–
^{91}Sr	9,63h	c	27.9 ± 2.6	19.8	104.	24.6	–
^{89}Rb	15,15m	c*	24.0 ± 2.2	25.4	73.6	14.2	–
^{88}Rb	17,78m	i	8.74 ± 1.95	6.23	39.6	12.9	–
^{88}Rb	17,78m	c	27.0 ± 3.1	21.1	66.1	19.2	–
^{88}Kr	2,84h	c	16.0 ± 1.3	14.6	26.4	6.24	–
^{87}Kr	76,3m	c	20.2 ± 1.9	14.2	29.2	16.0	–
^{78}As	90,7m	i	2.95 ± 0.64	2.63	1.68	0.269	–
^{78}Ge	88m	c	3.30 ± 0.29	7.45	0.671	0.104	–
^{73}Ga	4,86h	c	2.38 ± 0.21	4.77	0.272	0.066	–
^{72}Ga	14,10h	i(m+g)	0.871 ± 0.120	1.25	0.114	0.034	–
^{72}Zn	46,5h	c	1.72 ± 0.18	2.79	0.102	0.045	–

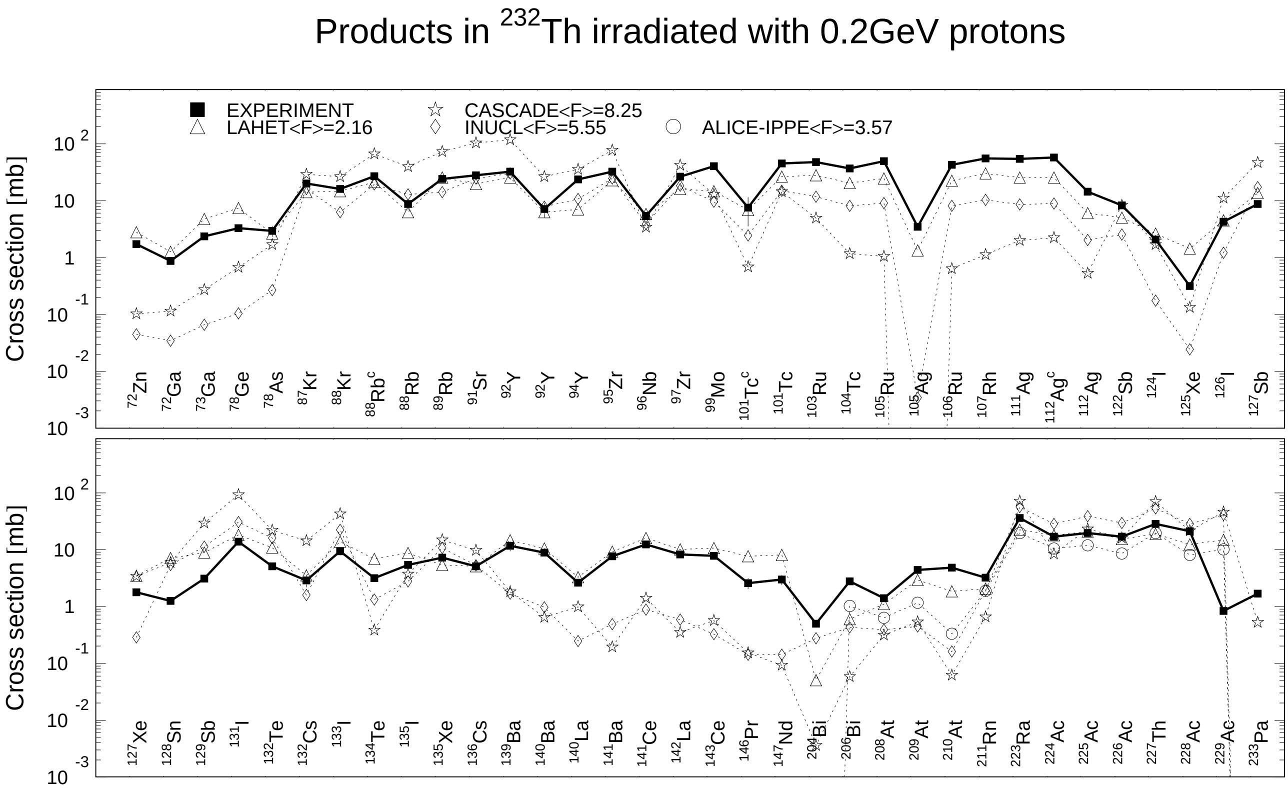

Fig. 64: Detailed comparison between experimental and simulated yields of radioactive reaction products in ^{232}Th irradiated with 0.2 GeV protons. The cumulative yields are labeled -c when the respective independent yields are also shown.

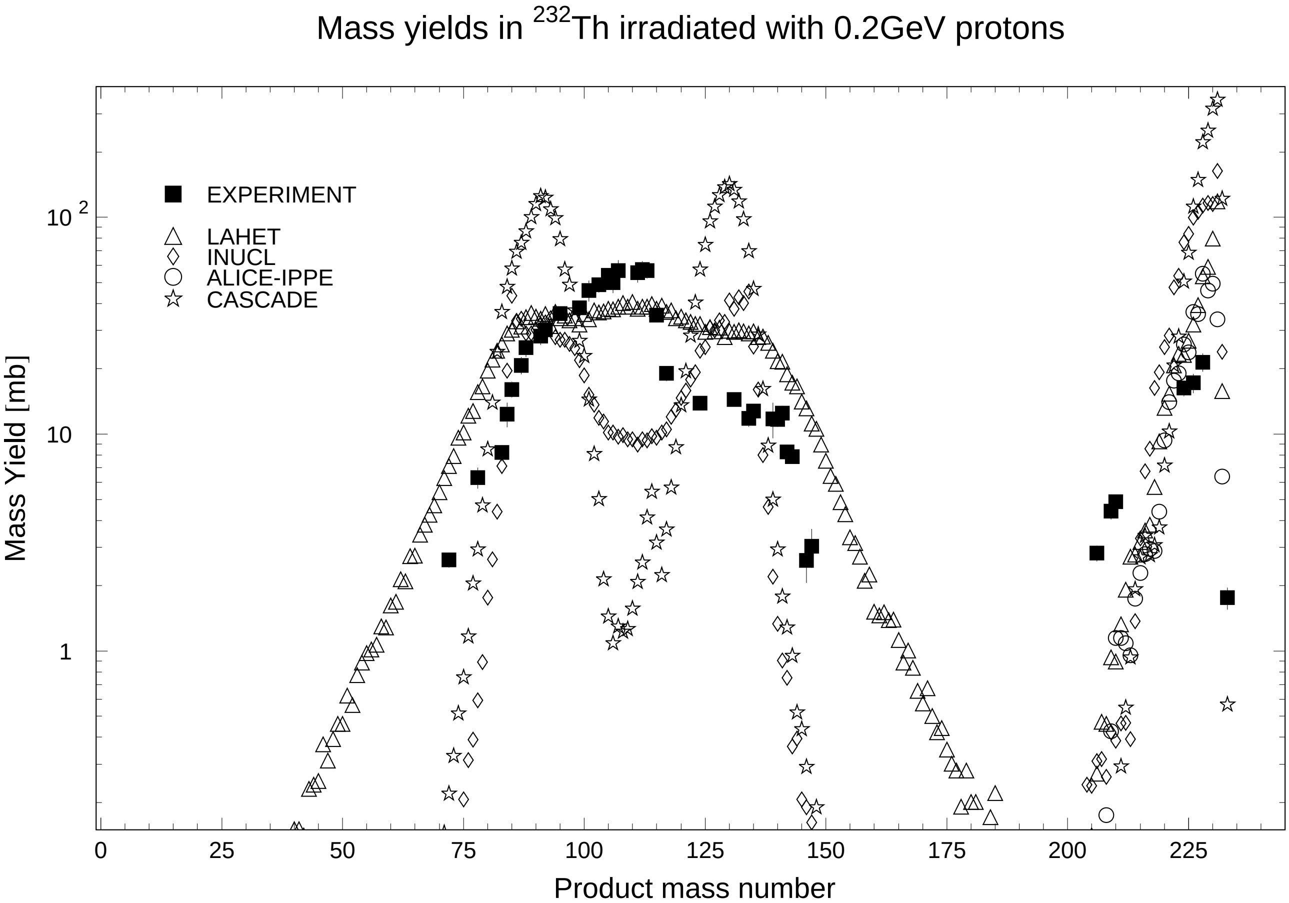

Fig. 65: The simulated mass distributions of reaction products together with the measured cumulative and supra-cumulative yields in ^{232}Th irradiated with 0.2 GeV protons.

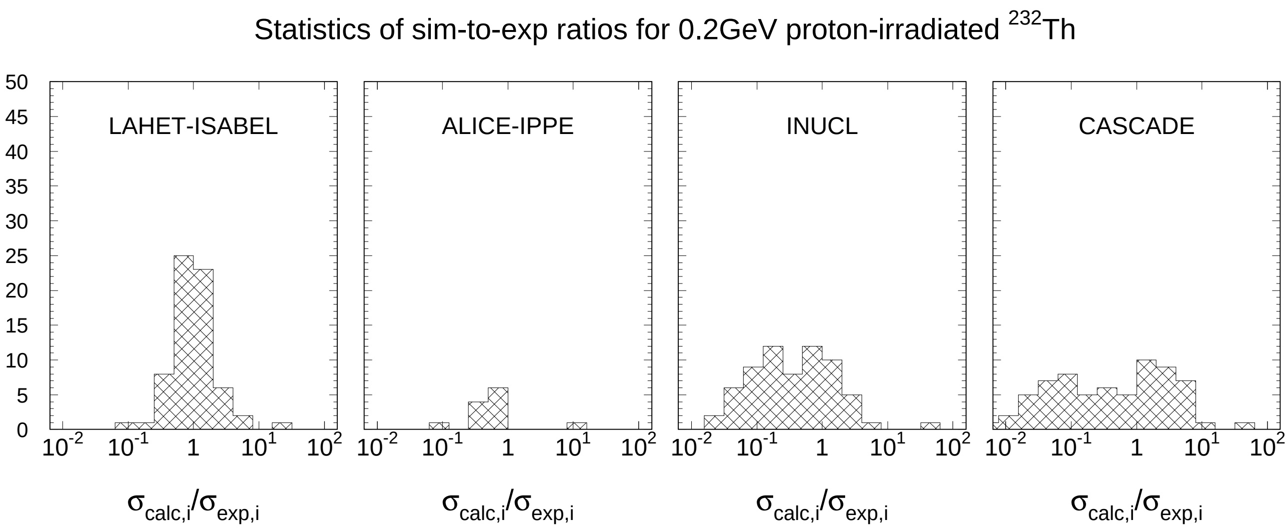

Fig. 66: Statistics of the simulation-to-experiment ratios (criterion 2) for ^{232}Th irradiated with 0.2 GeV protons.

Table 80: Experimental and calculated yields from ^{232}Th irradiated with 0.8 GeV protons.

Product	$T_{1/2}$	Type	Exp yield [mbarn]	Calculated Yields [mbarn] via LAHET	CASCADE	CASCADO-IPPE	INUCL
^{229}Ac	62,7m	c	1.30 ± 0.21	20.9	47.1	19.2	34.2
^{228}Ac	6,15h	i	20.1 ± 2.1	12.3	25.2	13.2	20.5
^{226}Ac	29,37h	i	16.6 ± 1.6	12.0	29.3	12.2	20.2
^{225}Ac	10,0d	c	20.3 ± 5.1	14.7	48.6	14.7	26.4
^{224}Ac	2,78h	i	12.0 ± 0.9	12.3	26.5	12.7	20.4
^{211}Rn	14,6h	c	9.89 ± 0.75	8.77	18.2	13.5	30.9
^{210}At	8,1h	c	11.0 ± 0.8	8.85	6.49	6.22	10.7
^{209}At	5,41h	c*	17.8 ± 1.2	17.0	32.5	10.0	21.9
^{208}At	1,63h	c*	10.5 ± 0.9	13.4	39.2	5.52	15.9
^{207}At	1,80h	c	16.5 ± 1.4	17.1	46.7	4.32	19.5
^{206}At	30,6m	c*	10.3 ± 0.8	12.5	33.3	1.25	16.5
^{206}Bi	6,243d	c	20.1 ± 1.5	21.8	44.6	11.7	22.1
^{205}Bi	15,31d	c	18.2 ± 1.7	19.1	45.4	8.47	20.1
^{204}Bi	11,22h	c	13.2 ± 1.0	18.3	35.3	8.50	15.2
^{203}Pb	51,873h	c	10.3 ± 0.7	14.7	10.2	10.9	2.01
^{202}Bi	1,72h	c	11.2 ± 0.8	14.4	12.0	6.61	3.95
^{201}Pb	9,33h	i(m+g)	7.22 ± 2.56	2.46	1.08	7.78	0.278
^{201}Pb	9,33h	c	9.62 ± 0.99	14.4	11.2	13.3	4.23
^{200}Pb	21,5h	c	7.70 ± 0.56	13.3	13.4	14.9	4.23
^{200}Tl	26,1h	i(m+g)	0.980 ± 0.204	0.733	0.175	0.956	0.020
^{192}Hg	4,85h	c	6.11 ± 0.55	7.96	11.5	10.2	0.278
^{190}Au	42,8m	c*	5.48 ± 0.79	8.07	9.47	8.61	0.040
^{186}Pt	2,08h	c	2.88 ± 0.83	6.42	3.93	4.29	–
^{184}Ir	3,09h	c*	2.65 ± 0.33	7.11	1.84	3.43	–
^{182}Os	22,10h	c	2.76 ± 0.29	5.56	0.888	2.50	–
^{181}Re	19,9h	c	2.13 ± 0.35	4.86	0.597	1.98	–
^{143}Ce	33,039h	c	4.15 ± 0.30	5.86	0.089	1.58	0.179
^{140}La	1,6781d	i	1.47 ± 0.15	1.84	0.259	1.40	0.119
^{140}Ba	12,752d	c	5.24 ± 0.91	5.09	0.233	0.684	0.438
^{135}Ce	17,7h	c	1.94 ± 0.20	1.57	0.634	1.30	0.060
^{135}Xe	9,14h	i(m+g)	3.93 ± 0.40	2.73	5.70	1.39	3.98
^{135}I	6,57h	c	2.93 ± 0.28	4.38	1.63	0.060	1.10
^{133}I	20,8h	c	4.59 ± 0.35	7.25	15.9	1.05	9.08
^{132}Ce	3,51h	c	0.563 ± 0.215	0.884	0.213	0.048	0.020
^{132}Te	3,204d	c	2.55 ± 0.22	5.38	9.41	0.428	5.13
^{131}I	8,02070d	c	6.82 ± 0.52	10.2	37.2	3.95	13.7
^{127}Xe	36,4d	c	8.38 ± 0.98	5.51	22.8	5.44	1.47
^{127}Sb	3,85d	c	5.11 ± 0.51	7.93	18.7	2.53	8.28
^{125}Xe	16,9h	c	4.26 ± 0.32	2.93	11.7	1.58	0.616
^{124}I	4,1760d	i	4.67 ± 0.69	3.87	13.8	3.14	0.955
^{122}Sb	2,7238d	i(m+g)	8.72 ± 0.61	4.78	15.8	8.55	7.54
^{121}I	2,12h	c	3.07 ± 0.27	2.70	4.02	0.384	0.139
^{112}Ag	3,130h	i	22.8 ± 3.0	5.55	1.68	12.0	6.36
^{112}Ag	3,130h	c	49.4 ± 5.9	20.1	2.75	25.2	13.8
^{111}In	2,8047d	c	3.02 ± 0.33	3.49	3.59	1.14	0.636
^{105}Ru	4,44h	c	43.0 ± 2.9	19.6	0.797	22.9	13.6
^{104}Tc	18,3m	c	30.5 ± 2.8	15.9	0.374	12.3	6.86
^{103}Ru	39,26d	c	61.0 ± 4.4	24.2	1.89	33.1	18.0
^{101}Tc	14,22m	c	61.3 ± 7.0	24.0	4.70	32.9	18.2
^{101}Tc	14,22m	i	32.1 ± 7.0	7.61	1.29	15.4	8.42
^{99}Mo	65,94h	c	45.0 ± 3.1	14.3	4.74	17.6	12.9
^{97}Zr	16,744h	c	19.1 ± 1.3	12.4	12.1	9.59	8.75
^{96}Nb	23,35h	i	14.8 ± 1.0	6.00	1.39	13.0	8.55
^{95}Zr	64,02d	c	31.5 ± 2.9	18.0	22.6	21.0	17.4
^{94}Y	18,7m	i	20.0 ± 2.3	5.99	9.32	8.14	6.16

Table 80, cont'd.

Product	$T_{1/2}$	Type	Exp yield [mbarn]	LAHET	CASCADE	CASCADO-IPPE	INUCL
				Calculated Yields [mbarn] via			
^{92}Y	3,54h	i	13.0 ± 5.0	6.24	9.83	14.1	11.2
^{92}Y	3,54h	c	30.5 ± 4.6	20.1	42.8	22.9	20.8
^{91}Sr	9,63h	c	22.8 ± 2.1	14.6	38.5	14.4	16.2
^{90}Nb	14,60h	c	0.820 ± 0.097	1.23	0.023	0.020	0.080
^{89}Rb	15,15m	c*	23.6 ± 3.3	17.6	33.3	9.61	11.3
^{88}Kr	2,84h	c	10.6 ± 0.9	11.2	14.9	3.52	3.03
^{87}Kr	76,3m	c	13.4 ± 1.5	10.5	18.5	7.46	8.92
^{86}Y	14,74h	c	1.28 ± 0.12	2.46	0.174	0.096	0.358
^{78}As	90,7m	i	7.09 ± 1.61	3.34	9.80	7.52	1.75
^{78}Ge	88m	c	2.94 ± 0.87	6.87	2.22	3.33	0.398
^{76}As	1,0778d	i	5.03 ± 0.43	2.92	8.69	5.54	1.59
^{73}Ga	4,86h	c	4.55 ± 0.36	6.22	2.82	8.18	0.936
^{72}Zn	46,5h	c	2.00 ± 0.20	3.94	0.618	4.60	0.418
^{48}Sc	43,67h	i	0.940 ± 0.180	0.259	–	1.63	–
^{24}Na	14,9590h	c	0.806 ± 0.131	0.022	–	0.396	–

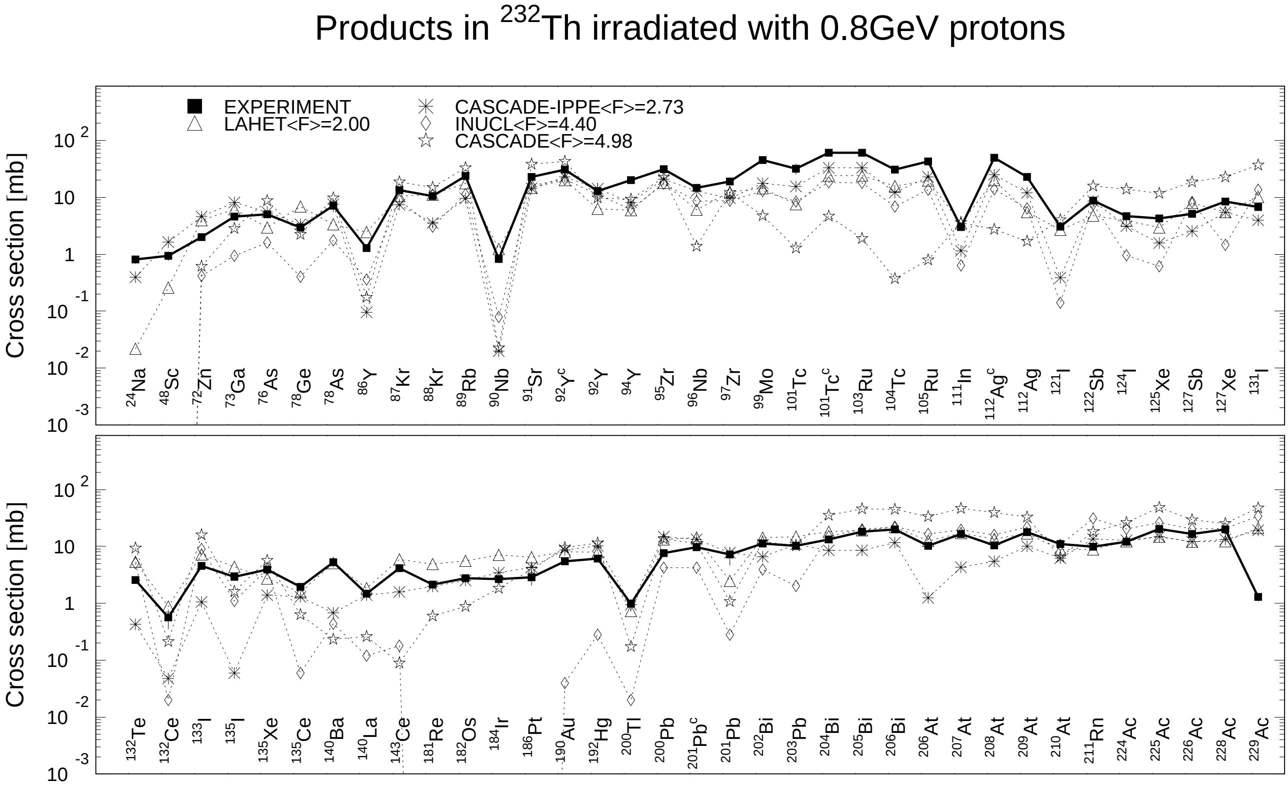

Fig. 67: Detailed comparison between experimental and simulated yields of radioactive reaction products in ^{232}Th irradiated with 0.8 GeV protons. The cumulative yields are labeled -c when the respective independent yields are also shown.

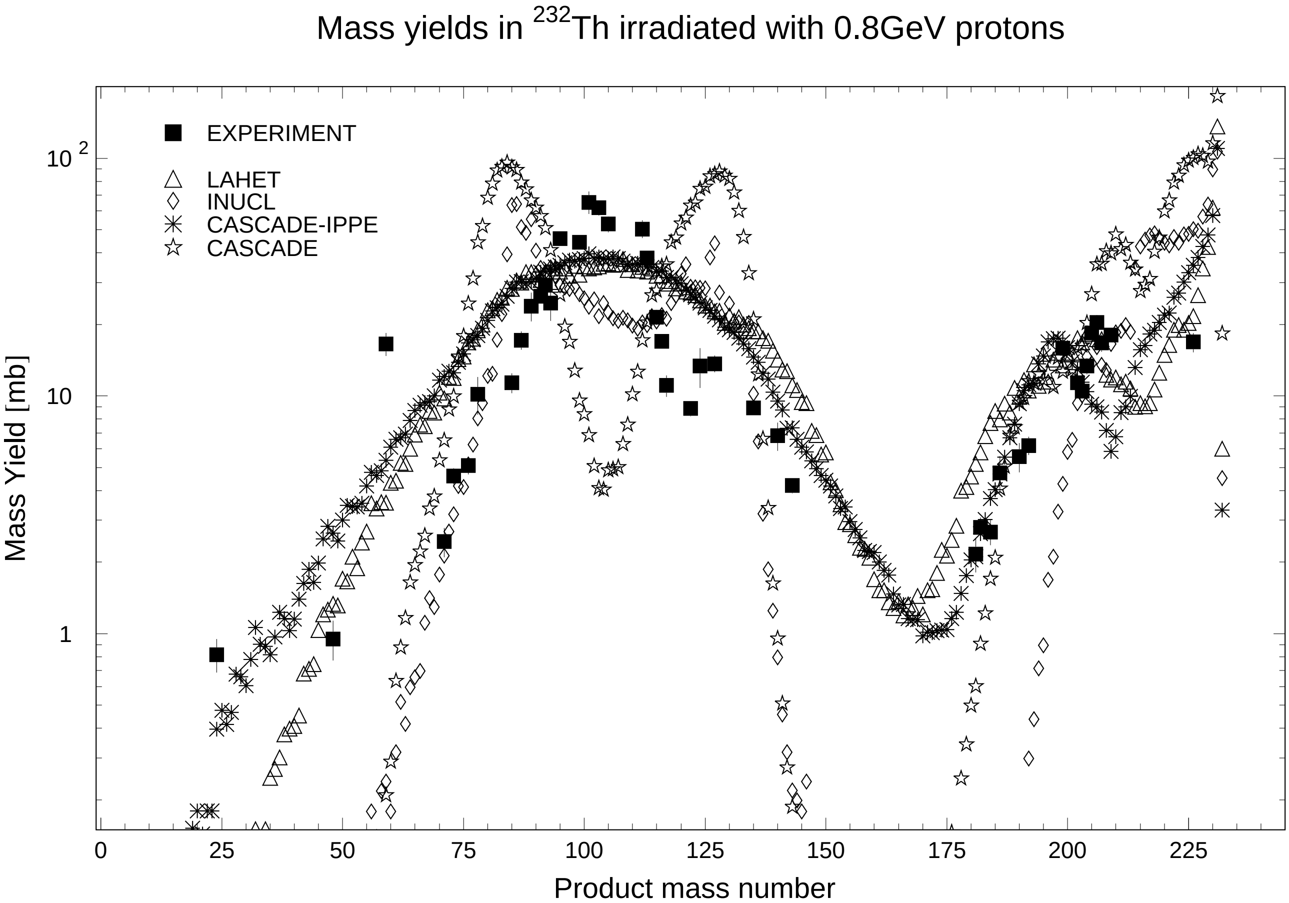

Fig. 68: The simulated mass distributions of reaction products together with the measured cumulative and supra-cumulative yields in ^{232}Th irradiated with 0.8 GeV protons.

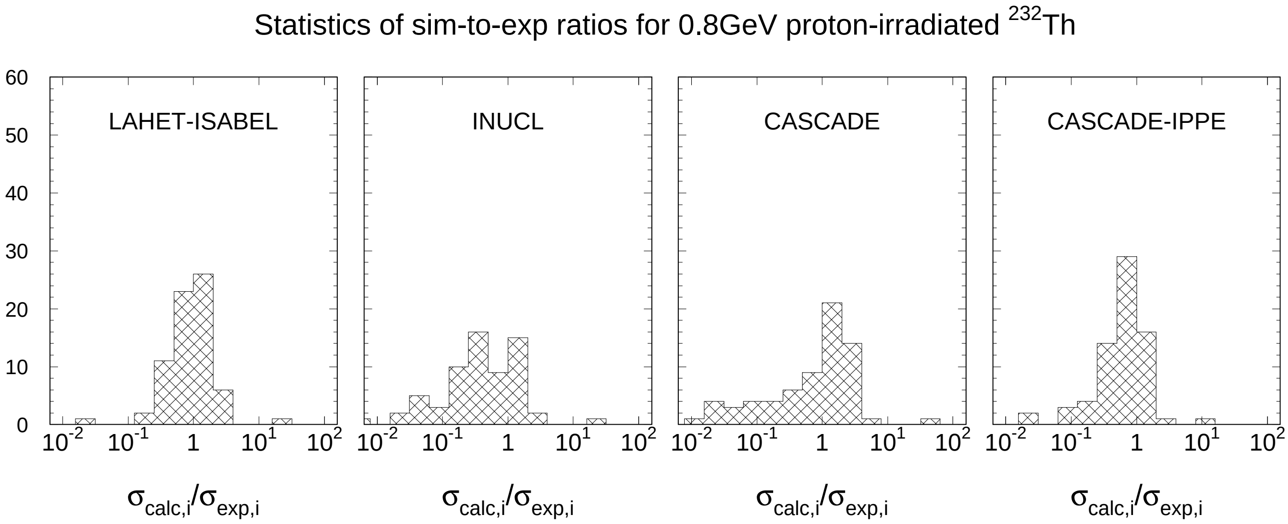

Fig. 69: Statistics of the simulation-to-experiment ratios (criterion 2) for ^{232}Th irradiated with 0.8 GeV protons.

Table 81: Experimental and calculated yields from ^{232}Th irradiated with 1.2 GeV protons.

Product	$T_{1/2}$	Type	Exp yield [mbarn]	Calculated Yields [mbarn] via LAHET	CASCADE	INUCL
^{233}Pa	26,967d	i	2.81 ± 0.33	–	–	–
^{229}Ac	62,7m	c	1.23 ± 0.18	17.2	39.6	31.0
^{228}Ac	6,15h	i	19.3 ± 1.5	9.28	19.1	18.2
^{227}Th	18,72d	c	13.5 ± 1.6	5.96	21.4	13.9
^{226}Ac	29,37h	i	17.1 ± 1.7	8.77	20.3	16.5
^{225}Ac	10,0d	c	19.5 ± 1.5	10.8	32.5	21.0
^{225}Ra	14,9d	c	4.18 ± 0.37	4.23	14.5	8.92
^{224}Ac	2,78h	i	12.5 ± 1.0	8.01	17.7	17.0
^{223}Ra	11,435d	c	21.8 ± 1.7	10.9	43.7	26.1
^{211}Rn	14,6h	c	9.76 ± 0.76	4.81	18.5	26.9
^{210}At	8,1h	c	10.6 ± 0.8	6.03	7.83	10.9
^{209}At	5,41h	c*	19.3 ± 1.4	11.3	32.3	22.6
^{208}At	1,63h	c*	9.95 ± 0.88	8.20	36.6	17.8
^{207}At	1,80h	c	14.2 ± 1.4	9.93	45.9	20.9
^{206}At	30,6m	c*	9.08 ± 0.83	7.46	33.2	17.3
^{206}Bi	6,243d	c	18.9 ± 1.4	14.1	49.5	24.8
^{205}Bi	15,31d	c	14.2 ± 1.1	11.8	48.3	22.0
^{204}Bi	11,22h	c	15.2 ± 1.2	12.6	40.6	16.1
^{203}Pb	51,873h	i(m1+m2+g)	1.14 ± 0.46	0.630	2.05	0.241
^{203}Pb	51,873h	c	11.7 ± 0.9	10.0	15.8	3.18
^{202}Bi	1,72h	c	12.2 ± 0.9	10.2	15.8	4.28
^{201}Pb	9,33h	i(m+g)	3.45 ± 1.05	2.50	3.22	0.542
^{201}Pb	9,33h	c	11.2 ± 1.1	10.9	16.7	5.03
^{200}Pb	21,5h	c	9.35 ± 0.72	10.4	20.3	4.95
^{200}Tl	26,1h	i(m+g)	1.36 ± 0.16	0.818	0.972	0.114
^{198}Bi	11,6m	c*	8.66 ± 1.49	2.98	8.93	2.43
^{192}Hg	4,85h	c	11.6 ± 1.0	9.39	26.8	0.387
^{191}Pt	2,802d	c	9.98 ± 1.13	16.2	25.4	0.336
^{190}Au	42,8m	c	11.1 ± 1.3	11.2	27.0	0.254
^{188}Pt	10,2d	c	11.0 ± 1.0	13.0	24.1	0.178
^{186}Pt	2,08h	c	10.8 ± 2.5	12.4	21.7	0.074
^{185}Os	93,6d	c	11.2 ± 0.9	16.2	11.8	0.093
^{184}Ir	3,09h	c*	9.71 ± 0.95	15.9	13.3	0.051
^{183}Re	70,0d	c	9.69 ± 0.82	17.1	8.68	0.040
^{182}Os	22,10h	c	11.1 ± 1.0	16.0	9.96	0.054
^{181}Re	19,9h	c	9.96 ± 1.40	16.8	7.54	0.013
^{180}Re	21,5m	c	10.8 ± 1.0	16.1	7.59	0.027
^{177}W	135m	c	5.85 ± 0.72	14.1	2.35	0.054
^{176}Ta	8,09h	c	6.31 ± 0.83	13.9	3.99	0.020
^{175}Hf	70d	c	6.43 ± 0.54	14.7	3.05	0.034
^{174}Ta	1,14h	c	6.36 ± 0.76	13.2	2.81	0.007
^{173}Hf	23,6h	c	5.55 ± 0.57	12.0	2.34	0.007
^{171}Lu	8,24d	c	4.76 ± 0.38	12.8	0.942	–
^{170}Lu	2,012d	c	4.58 ± 0.50	11.2	1.36	0.006
^{169}Yb	32,026d	c	5.75 ± 0.47	11.8	0.928	–
^{167}Tm	9,25d	c	3.43 ± 0.71	10.2	0.462	0.007
^{166}Yb	56,7h	c	3.03 ± 0.30	10.4	0.526	–
^{160}Er	28,58h	c	2.20 ± 0.24	6.76	0.072	–
^{157}Dy	8,14h	c	1.63 ± 0.17	6.33	0.031	–
^{155}Dy	9,9h	c*	1.49 ± 0.13	5.14	0.065	–
^{152}Dy	2,38h	c	0.702 ± 0.156	2.27	0.001	–
^{147}Eu	24,1d	c	1.11 ± 0.17	2.45	–	–
^{146}Gd	48,27d	c	0.677 ± 0.068	1.25	–	–
^{146}Eu	4,61d	i	0.589 ± 0.054	1.30	–	–
^{143}Ce	33,039h	c	4.05 ± 0.31	3.90	0.062	0.228

Table 81, cont'd.

Product	$T_{1/2}$	Type	Exp yield [mbarn]	Calculated Yields [mbarn] via LAHET	CASCADE	INUCL
^{141}Ce	32,501d	c	6.41 ± 0.49	5.22	0.145	0.408
^{140}La	1,6781d	i	1.24 ± 0.10	1.23	0.191	0.047
^{140}Ba	12,752d	c	5.57 ± 0.42	3.16	0.151	0.281
^{139}Ce	137,640d	c	4.54 ± 0.55	5.29	0.313	0.348
^{136}Cs	13,16d	i(m+g)	2.18 ± 0.16	1.90	2.71	1.57
^{135}Ce	17,7h	c	3.11 ± 0.27	1.84	0.426	0.100
^{135}Xe	9,14h	i(m+g)	3.00 ± 0.35	2.13	3.91	2.87
^{135}I	6,57h	c	3.65 ± 0.45	2.88	1.30	0.842
^{133}I	20,8h	c	4.52 ± 0.37	4.48	12.1	6.52
^{132}Ce	3,51h	c	1.28 ± 0.20	1.05	0.371	0.047
^{132}Cs	6,479d	i	3.50 ± 0.29	1.97	6.54	1.30
^{132}Te	3,204d	c	2.76 ± 0.21	3.45	7.24	4.15
^{131}Ba	11,50d	c	4.97 ± 0.42	3.74	3.95	0.355
^{131}I	8,02070d	c	6.31 ± 0.47	5.61	27.8	10.2
^{128}Ba	2,43d	c	2.40 ± 0.22	2.34	1.98	0.094
^{127}Xe	36,4d	c	8.91 ± 0.71	4.20	16.6	1.43
^{127}Sb	3,85d	c	3.82 ± 0.32	4.82	15.1	6.49
^{126}I	13,11d	i	5.80 ± 0.67	2.61	13.3	3.09
^{125}Xe	16,9h	c	6.04 ± 0.47	2.67	9.63	0.582
^{124}I	4,1760d	i	5.37 ± 0.50	3.30	10.7	1.26
^{122}Sb	2,7238d	i(m+g)	8.03 ± 0.60	3.05	11.8	7.46
^{121}I	2,12h	c	4.61 ± 0.36	2.83	4.46	0.214
^{112}Ag	3,130h	i	19.1 ± 3.8	3.84	1.87	7.09
^{112}Ag	3,130h	c	42.1 ± 7.8	12.6	2.73	15.0
^{111}In	2,8047d	c	4.87 ± 0.38	4.38	7.01	1.71
^{111}Ag	7,45d	c	45.0 ± 4.3	13.4	4.44	19.4
^{106}Ru	373,59d	c	38.4 ± 3.1	10.7	0.309	12.4
^{105}Ag	41,29d	c	2.66 ± 0.26	3.44	1.85	1.13
^{105}Rh	35,36h	i(m+g)	24.8 ± 4.2	6.14	2.98	9.17
^{105}Ru	4,44h	c	38.2 ± 3.0	12.2	0.725	15.9
^{104}Tc	18,3m	c	26.1 ± 2.3	9.89	0.339	8.15
^{103}Ru	39,26d	c	52.4 ± 4.0	16.3	2.58	25.5
^{101}Tc	14,22m	c	54.2 ± 5.9	15.4	4.04	22.9
^{101}Tc	14,22m	i	26.5 ± 4.9	5.46	1.63	12.0
^{99}Mo	65,94h	c	43.0 ± 3.3	11.6	6.41	17.9
^{97}Zr	16,744h	c	18.2 ± 1.3	7.41	9.17	7.71
^{96}Nb	23,35h	i	17.6 ± 1.4	5.01	1.66	11.4
^{95}Zr	64,02d	c	30.8 ± 2.2	12.1	16.2	19.1
^{94}Y	18,7m	i	15.8 ± 1.6	3.78	6.21	6.40
^{92}Y	3,54h	i	11.5 ± 2.8	4.32	6.22	11.4
^{92}Y	3,54h	c	34.2 ± 4.8	13.7	30.8	20.5
^{91}Sr	9,63h	c	20.7 ± 1.6	9.59	28.8	14.3
^{90}Nb	14,60h	c	1.83 ± 0.14	2.20	0.120	0.428
^{89}Rb	15,15m	c*	20.2 ± 2.2	11.6	24.2	9.07
^{88}Zr	83,4d	c	2.29 ± 0.18	4.64	2.00	2.69
^{88}Y	106,65d	i(m+g)	10.4 ± 0.8	5.16	8.78	5.27
^{88}Kr	2,84h	c	9.65 ± 0.76	7.34	11.1	3.25
^{87}Kr	76,3m	c	12.6 ± 1.4	6.76	13.2	7.97
^{86}Y	14,74h	c	2.54 ± 0.19	3.58	0.387	0.857
^{86}Rb	18,631d	i(m+g)	16.6 ± 1.3	5.42	25.5	22.2
^{83}Rb	86,2d	c	8.74 ± 0.75	8.05	8.99	4.75
^{78}As	90,7m	i	8.43 ± 1.42	2.71	8.18	2.91
^{78}Ge	88m	c	2.74 ± 0.60	5.02	1.79	0.991
^{77}Br	57,036h	c	2.47 ± 0.21	4.19	1.53	1.21
^{76}As	1,0778d	i	7.54 ± 0.65	3.13	9.39	3.11

Table 81, cont'd.

Product	$T_{1/2}$	Type	Exp yield [mbarn]	Calculated Yields [mbarn] via LAHET	CASCADE	INUCL
^{75}Se	119,779d	c	2.98 ± 0.28	3.71	4.19	2.21
^{74}As	17,77d	i	4.90 ± 0.49	3.65	3.97	1.81
^{73}Ga	4,86h	c	5.50 ± 0.49	5.48	3.31	1.62
^{72}Ga	14,10h	i(m+g)	5.31 ± 0.47	2.06	3.39	1.39
^{72}Zn	46,5h	c	2.48 ± 0.20	3.09	0.876	0.616
^{59}Fe	44,472d	c	3.42 ± 0.29	2.10	0.544	0.241
^{58}Co	70,86d	i(m+g)	0.851 ± 0.081	1.01	0.183	0.087
^{56}Mn	2,5789h	c	3.99 ± 0.55	2.14	0.275	0.147
^{48}V	15,9735d	c	0.232 ± 0.025	0.310	–	0.013
^{48}Sc	43,67h	i	0.923 ± 0.071	0.555	0.038	0.007
^{46}Sc	83,79d	i(m+g)	0.980 ± 0.094	0.367	–	0.007
^{43}K	22,3h	c	1.19 ± 0.10	0.789	–	–
^{28}Mg	20,915h	c	0.562 ± 0.048	–	–	–
^{24}Na	14,9590h	c	1.51 ± 0.12	0.226	–	–

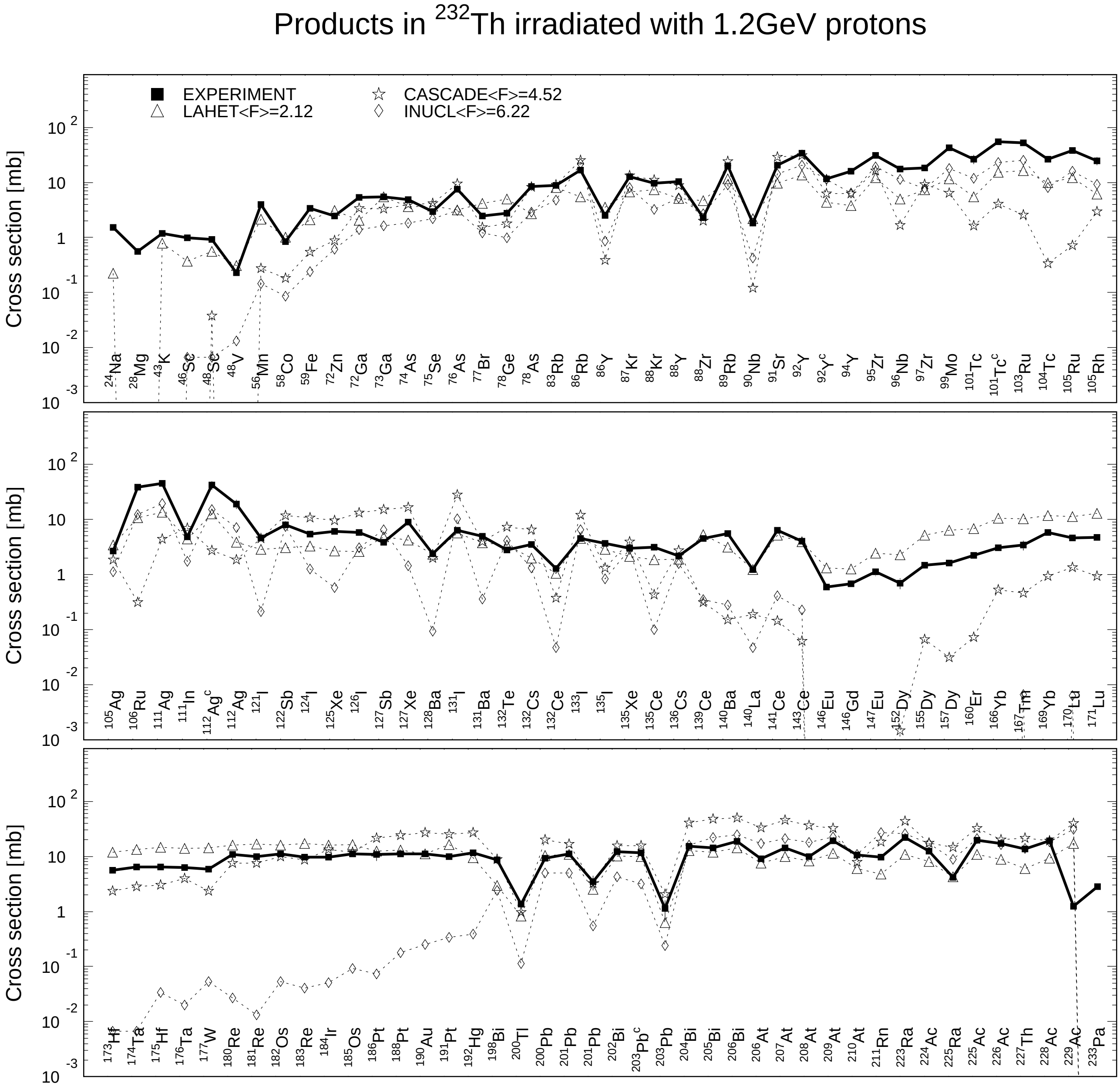

Fig. 70: Detailed comparison between experimental and simulated yields of radioactive reaction products in ^{232}Th irradiated with 1.2 GeV protons. The cumulative yields are labeled -c when the respective independent yields are also shown.

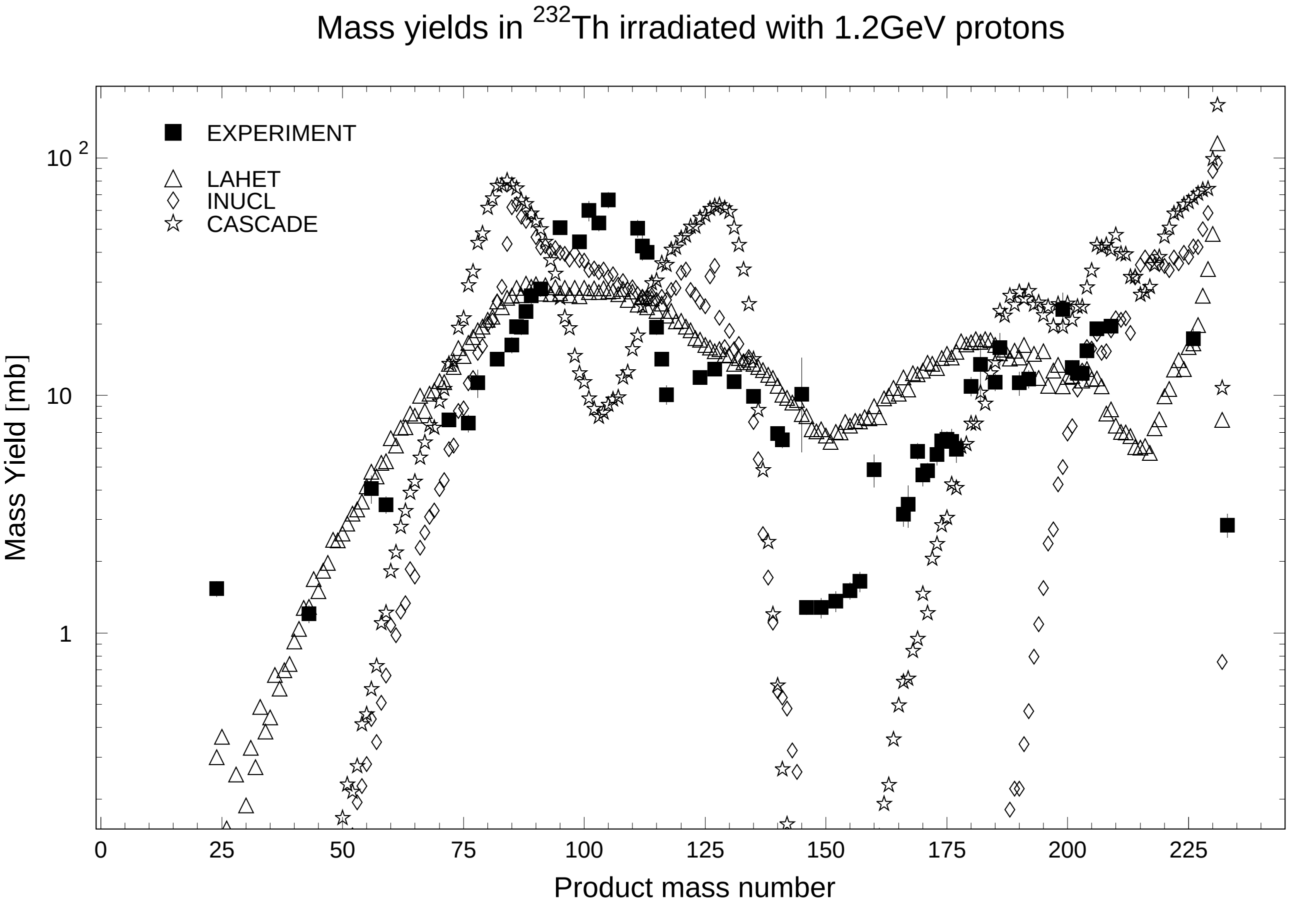

Fig. 71: The simulated mass distributions of reaction products together with the measured cumulative and supra-cumulative yields in ^{232}Th irradiated with 1.2 GeV protons.

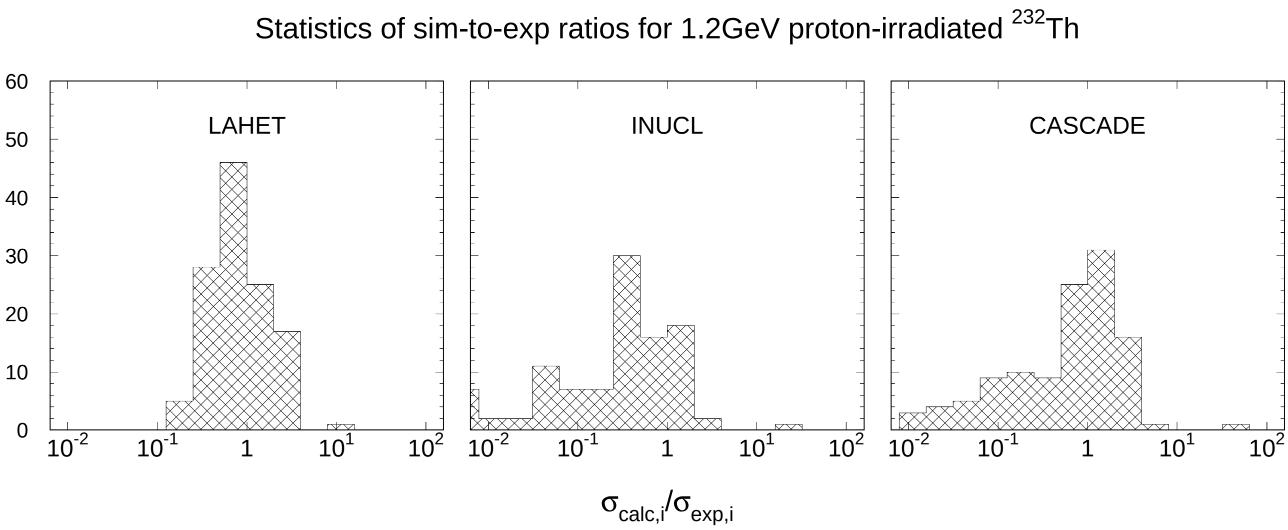

Fig. 72: Statistics of the simulation-to-experiment ratios (criterion 2) for ^{232}Th irradiated with 1.2 GeV protons.

Table 82: Experimental and calculated yields from ^{232}Th irradiated with 1.6 GeV protons.

Product	$T_{1/2}$	Type	Exp yield [mbarn]	Calculated Yields [mbarn] via LAHET	CASCADE	INUCL
^{233}Pa	26,967d	i	3.12 ± 0.30	–	31.0	–
^{229}Ac	62,7m	c	1.09 ± 0.17	17.4	10.9	30.8
^{228}Ac	6,15h	i	17.8 ± 1.6	8.48	6.96	17.9
^{227}Th	18,72d	c	12.3 ± 1.6	5.87	18.4	13.2
^{226}Ac	29,37h	i	15.1 ± 1.6	8.35	9.57	15.3
^{225}Ac	10,0d	c	18.5 ± 1.5	9.56	15.4	17.9
^{225}Ra	14,9d	c	3.87 ± 0.41	3.52	8.10	7.96
^{224}Ac	2,78h	i	11.8 ± 1.1	7.47	8.98	14.6
^{223}Ra	11,435d	c	20.6 ± 2.0	10.1	31.2	24.2
^{211}Rn	14,6h	c	7.57 ± 0.63	4.17	10.6	22.9
^{210}At	8,1h	c	8.92 ± 0.74	4.28	4.52	9.91
^{209}At	5,41h	c*	16.5 ± 1.3	7.93	18.7	20.9
^{208}At	1,63h	c*	7.94 ± 0.66	6.53	21.5	15.9
^{207}At	1,80h	c	11.6 ± 1.2	7.74	25.8	18.8
^{206}At	30,6m	c*	8.31 ± 0.82	5.84	19.3	15.4
^{206}Bi	6,243d	c	15.7 ± 1.3	11.2	30.2	22.7
^{205}Bi	15,31d	c	11.8 ± 1.0	9.03	32.3	20.2
^{204}Bi	11,22h	c	12.2 ± 1.1	9.21	26.2	15.1
^{203}Pb	51,873h	c	9.88 ± 0.81	7.89	10.9	3.22
^{202}Bi	1,72h	c	10.5 ± 0.9	7.30	10.1	4.20
^{201}Pb	9,33h	i(m+g)	5.79 ± 1.07	1.67	2.70	0.563
^{201}Pb	9,33h	c	10.0 ± 1.0	7.87	11.9	4.82
^{200}Pb	21,5h	c	7.97 ± 0.69	7.71	14.0	4.92
^{200}Tl	26,1h	i(m+g)	1.08 ± 0.16	0.525	1.12	0.105
^{198}Bi	11,6m	c*	5.61 ± 1.05	1.85	5.72	2.16
^{192}Hg	4,85h	c	11.0 ± 1.4	7.01	21.6	0.694
^{191}Pt	2,802d	c	10.1 ± 1.5	11.3	21.5	0.669
^{190}Au	42,8m	c	11.3 ± 1.3	8.25	24.1	0.535
^{188}Pt	10,2d	c	11.9 ± 1.1	9.18	23.4	0.588
^{186}Pt	2,08h	c	12.2 ± 2.8	9.25	22.6	0.483
^{185}Os	93,6d	c	13.1 ± 1.2	12.6	12.8	0.454
^{184}Ir	3,09h	c*	12.9 ± 1.3	11.1	16.5	0.473
^{183}Re	70,0d	c	12.7 ± 1.1	13.4	10.8	0.419
^{182}Os	22,10h	c	14.3 ± 1.2	12.4	12.3	0.407
^{181}Re	19,9h	c	13.1 ± 1.9	13.9	10.5	0.350
^{180}Re	21,5m	c	12.8 ± 1.3	12.9	11.7	0.390
^{177}W	135m	c	9.66 ± 1.20	12.2	3.43	0.250
^{176}Ta	8,09h	c	12.0 ± 1.4	12.9	7.53	0.278
^{175}Hf	70d	c	11.2 ± 1.0	12.7	6.01	0.233
^{174}Ta	1,14h	c	10.4 ± 1.3	12.0	5.83	0.173
^{173}Hf	23,6h	c	10.8 ± 1.1	11.8	5.12	0.141
^{171}Lu	8,24d	c	10.7 ± 0.9	12.6	3.17	0.119
^{170}Lu	2,012d	c	7.89 ± 0.79	11.4	3.76	0.111
^{169}Yb	32,026d	c	9.66 ± 0.90	12.2	3.24	0.133
^{167}Tm	9,25d	c	8.40 ± 1.75	11.7	1.84	0.101
^{166}Yb	56,7h	c	7.98 ± 0.82	12.1	2.22	0.097
^{160}Er	28,58h	c	6.11 ± 0.66	10.0	0.669	0.008
^{157}Dy	8,14h	c	4.27 ± 0.41	11.1	0.497	0.016
^{155}Dy	9,9h	c*	3.70 ± 0.35	10.1	0.283	0.004
^{152}Dy	2,38h	c	2.24 ± 0.21	5.39	0.072	0.004
^{147}Eu	24,1d	c	2.84 ± 0.41	9.22	0.027	0.004
^{146}Gd	48,27d	c	1.98 ± 0.18	4.77	0.045	–
^{146}Eu	4,61d	i	0.879 ± 0.092	3.49	–	–
^{145}Eu	5,93d	c	3.87 ± 0.89	6.65	0.030	0.009
^{143}Ce	33,039h	c	3.75 ± 0.31	2.92	0.335	0.145

Table 82, cont'd.

Product	$T_{1/2}$	Type	Exp yield [mbarn]	Calculated Yields [mbarn] via LAHET	CASCADE	INUCL
^{141}Ce	32,501d	c	5.66 ± 0.53	4.77	0.838	0.350
^{140}La	1,6781d	i	0.986 ± 0.092	1.16	0.436	0.141
^{140}Ba	12,752d	c	5.00 ± 0.43	2.83	0.469	0.205
^{139}Ce	137,640d	c	6.40 ± 0.53	11.4	0.838	0.314
^{136}Cs	13,16d	i(m+g)	1.87 ± 0.17	1.48	2.58	1.23
^{135}Ce	17,7h	c	3.52 ± 0.32	5.73	0.811	0.097
^{135}Xe	9,14h	i(m+g)	2.25 ± 0.46	1.26	3.52	2.58
^{135}I	6,57h	c	3.65 ± 0.46	2.40	2.31	0.611
^{133}I	20,8h	c	4.29 ± 0.38	3.37	12.1	5.63
^{132}Ce	3,51h	c	1.89 ± 0.26	4.08	0.496	0.020
^{132}Cs	6,479d	i	4.14 ± 0.45	1.43	6.32	1.14
^{132}Te	3,204d	c	2.57 ± 0.23	2.82	10.2	3.91
^{131}Ba	11,50d	c	5.15 ± 0.49	7.24	5.65	0.535
^{131}I	8,02070d	c	5.60 ± 0.45	4.75	29.1	8.37
^{128}Ba	2,43d	c	3.15 ± 0.30	4.67	3.06	0.105
^{127}Xe	36,4d	c	8.42 ± 0.69	7.01	20.8	1.78
^{127}Sb	3,85d	c	3.35 ± 0.31	4.05	21.2	5.45
^{126}I	13,11d	i	4.07 ± 0.54	2.59	13.4	2.79
^{125}Xe	16,9h	c	6.51 ± 0.55	3.93	13.6	0.768
^{124}I	4,1760d	i	4.61 ± 0.45	3.04	12.1	1.35
^{122}Sb	2,7238d	i(m+g)	6.89 ± 0.57	2.51	11.3	7.17
^{121}I	2,12h	c	5.48 ± 0.47	3.44	7.13	0.310
^{112}Ag	3,130h	i	15.2 ± 3.9	3.03	1.45	8.04
^{112}Ag	3,130h	c	35.0 ± 7.0	10.4	2.14	15.8
^{111}In	2,8047d	c	5.70 ± 0.47	3.49	9.65	2.54
^{111}Ag	7,45d	c	36.7 ± 3.7	11.2	3.75	19.7
^{106}Ru	373,59d	c	26.6 ± 6.6	8.76	3.35	12.1
^{105}Ag	41,29d	c	3.35 ± 0.32	3.92	2.56	1.71
^{105}Rh	35,36h	i(m+g)	14.4 ± 4.6	4.68	3.18	10.4
^{105}Ru	4,44h	c	31.6 ± 2.6	9.60	5.30	16.9
^{104}Tc	18,3m	c	19.7 ± 2.1	7.60	7.91	8.51
^{103}Ru	39,26d	c	44.0 ± 3.7	12.4	16.0	27.6
^{101}Tc	14,22m	c	33.2 ± 4.0	12.5	24.0	23.9
^{101}Tc	14,22m	i	8.76 ± 3.39	4.45	1.98	12.7
^{99}Mo	65,94h	c	36.4 ± 3.0	11.0	15.8	20.8
^{97}Zr	16,744h	c	15.3 ± 1.2	6.08	20.9	7.30
^{96}Nb	23,35h	i	14.3 ± 1.4	4.28	4.61	12.4
^{95}Zr	64,02d	c	25.2 ± 2.1	9.41	25.8	18.0
^{94}Y	18,7m	i	14.6 ± 1.6	2.95	11.0	5.72
^{92}Y	3,54h	i	12.6 ± 3.3	3.46	12.4	10.8
^{92}Y	3,54h	c	29.8 ± 4.4	10.7	29.4	19.3
^{91}Sr	9,63h	c	17.1 ± 1.7	7.62	20.1	13.1
^{90}Nb	14,60h	c	2.29 ± 0.20	2.09	0.322	0.934
^{89}Rb	15,15m	c*	17.4 ± 1.9	9.49	14.1	8.40
^{88}Zr	83,4d	c	2.96 ± 0.28	6.02	3.76	5.60
^{88}Y	106,65d	c	13.2 ± 1.2	11.7	16.2	12.9
^{88}Kr	2,84h	c	8.48 ± 0.81	5.51	4.53	2.91
^{87}Kr	76,3m	c	11.1 ± 1.3	5.31	6.47	7.02
^{86}Y	14,74h	c	3.24 ± 0.26	4.75	0.905	1.68
^{86}Rb	18,631d	i(m+g)	16.5 ± 1.4	4.75	24.4	21.0
^{83}Rb	86,2d	c	10.1 ± 0.9	8.98	13.6	7.65
^{78}As	90,7m	i	7.12 ± 1.09	2.36	5.85	3.12
^{78}Ge	88m	c	2.26 ± 0.41	4.01	0.972	1.12
^{77}Br	57,036h	c	2.70 ± 0.24	5.14	2.52	2.10
^{76}As	1,0778d	i	7.88 ± 0.73	2.95	8.33	4.37

Table 82, cont'd.

Product	$T_{1/2}$	Type	Exp yield [mbarn]	Calculated Yields [mbarn] via LAHET	CASCADE	INUCL
^{75}Se	119,779d	c	3.47 ± 0.29	5.07	6.56	3.95
^{74}As	17,77d	i	5.50 ± 0.59	3.79	4.64	2.77
^{73}Ga	4,86h	c	4.20 ± 0.55	4.27	2.61	1.98
^{72}Ga	14,10h	i(m+g)	5.22 ± 0.53	2.07	2.95	1.90
^{72}Zn	46,5h	c	2.22 ± 0.19	2.57	0.623	0.748
^{59}Fe	44,472d	c	3.97 ± 0.35	2.38	0.757	0.382
^{58}Co	70,86d	i(m+g)	1.26 ± 0.12	2.09	0.221	0.318
^{56}Mn	2,5789h	c	3.50 ± 0.59	2.36	0.402	0.185
^{48}V	15,9735d	c	0.283 ± 0.084	0.469	–	–
^{48}Sc	43,67h	i	1.21 ± 0.10	0.873	0.034	0.008
^{46}Sc	83,79d	i(m+g)	1.42 ± 0.16	0.807	0.034	0.004
^{43}K	22,3h	c	1.66 ± 0.15	1.03	0.013	0.008
^{28}Mg	20,915h	c	0.894 ± 0.075	–	–	–
^{24}Na	14,9590h	c	2.62 ± 0.22	0.516	–	–

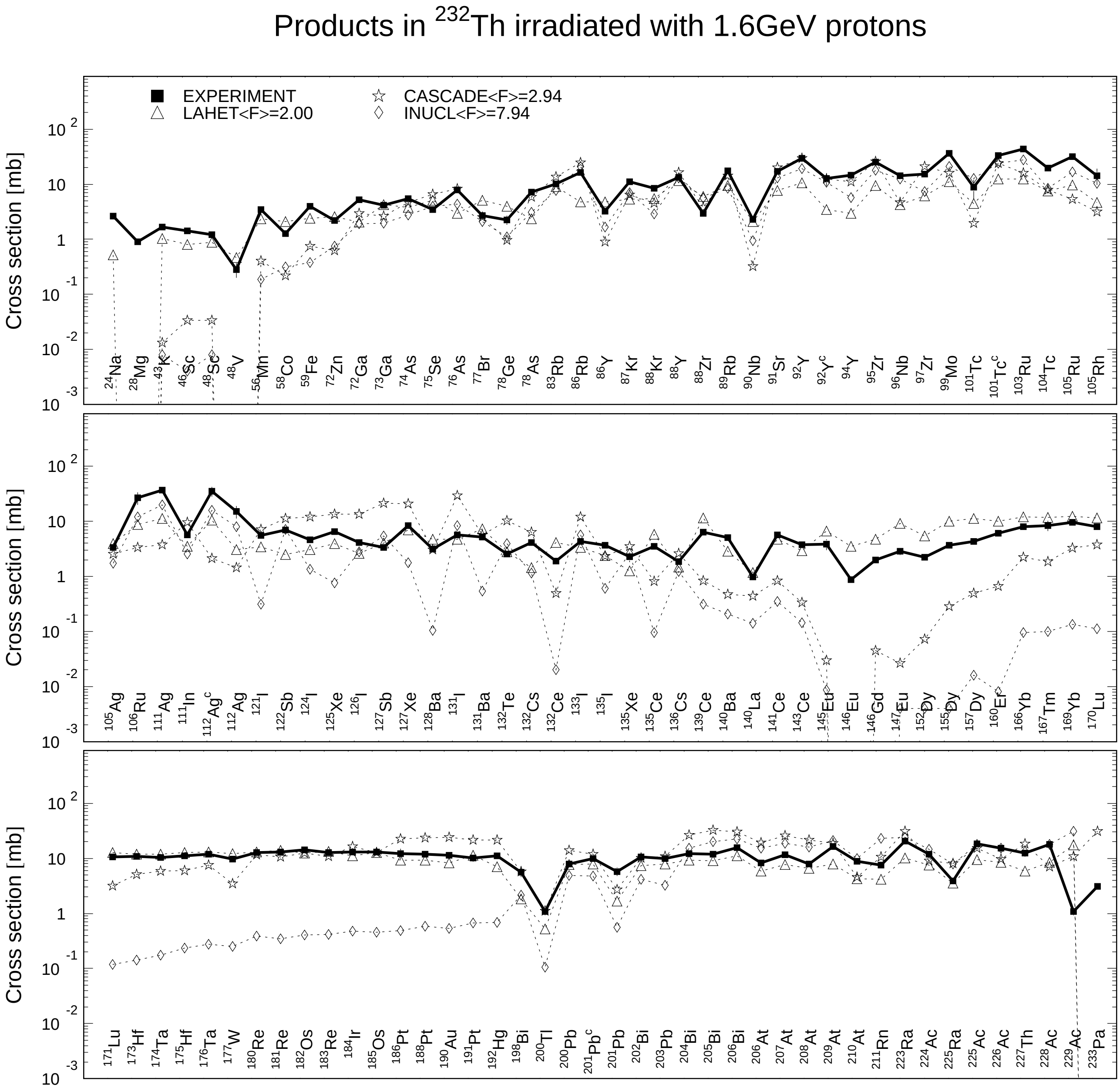

Fig. 73: Detailed comparison between experimental and simulated yields of radioactive reaction products in ^{232}Th irradiated with 1.6 GeV protons. The cumulative yields are labeled -c when the respective independent yields are also shown.

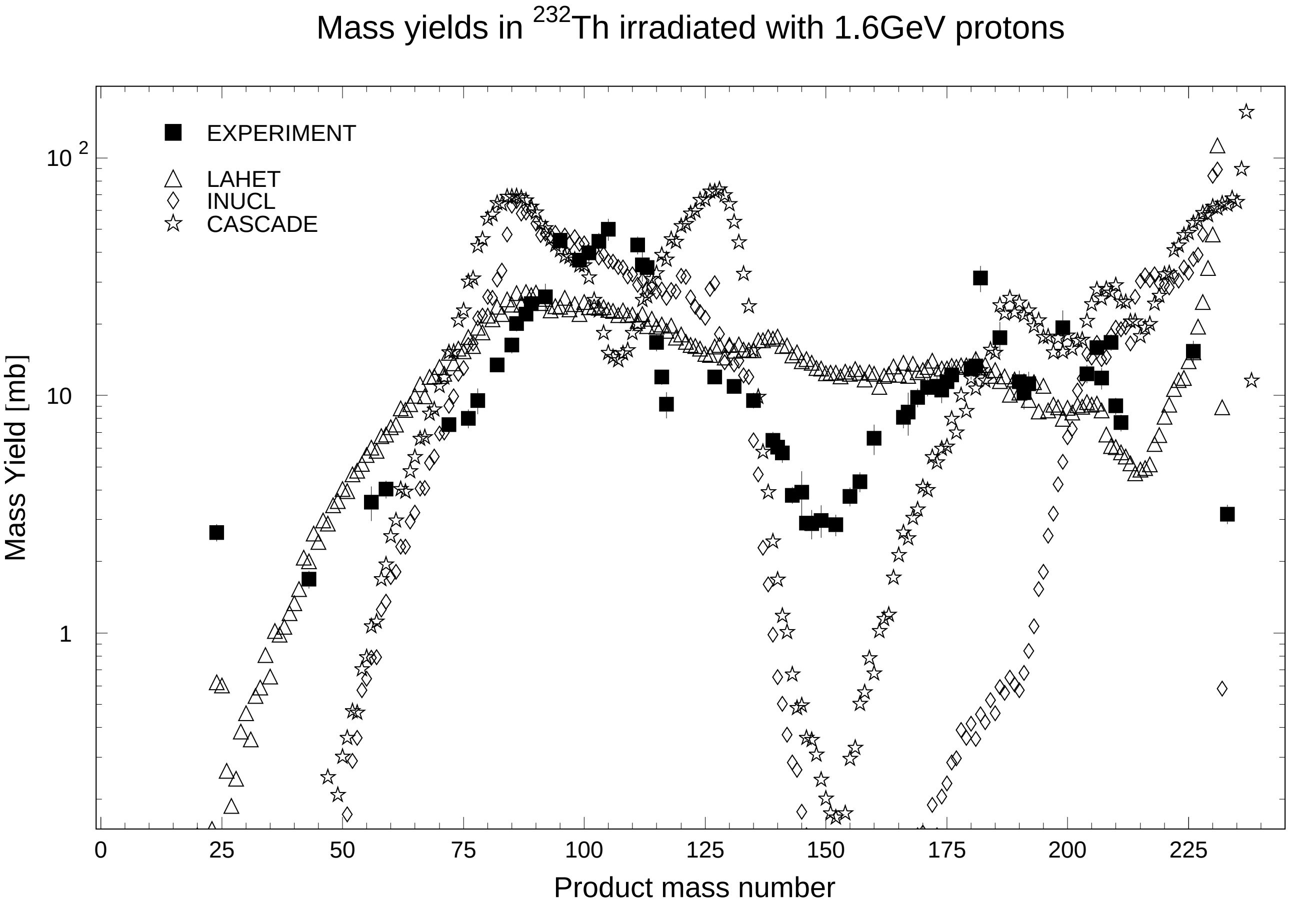

Fig. 74: The simulated mass distributions of reaction products together with the measured cumulative and supra-cumulative yields in ^{232}Th irradiated with 1.6 GeV protons.

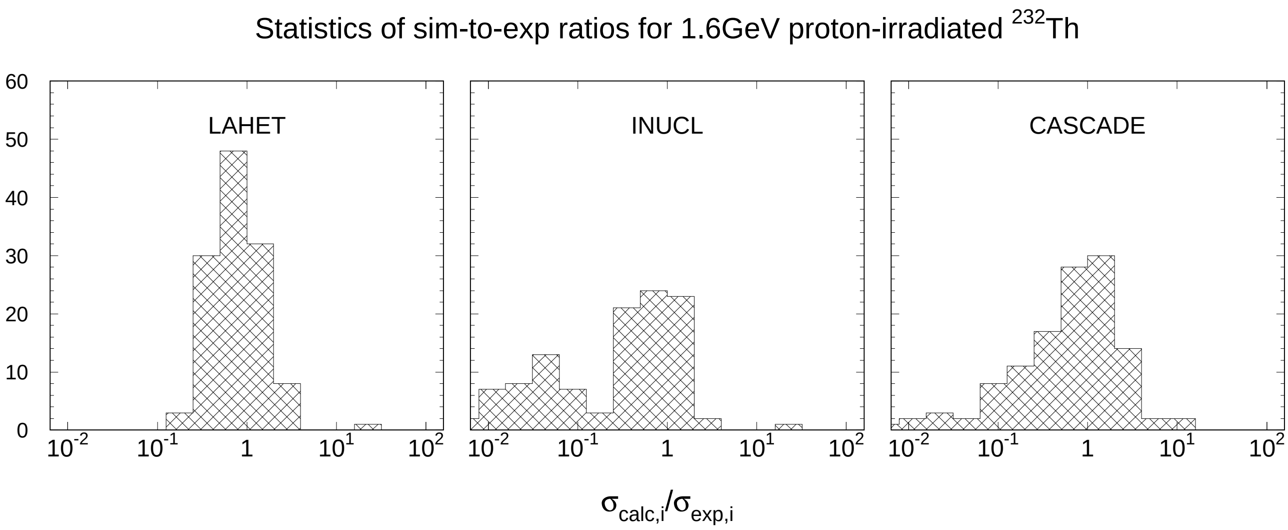

Fig. 75: Statistics of the simulation-to-experiment ratios (criterion 2) for ^{232}Th irradiated with 1.6 GeV protons.

Table 83: Experimental and calculated yields from ^{nat}U irradiated with 0.1 GeV protons.

Product	$T_{1/2}$	Type	Exp yield [mbarn]	Calculated Yields [mbarn] via LAHET	CASCADE	CASCADO-IPPE	INUCL	ALICE-IPPE
^{238}Np	2,117d	i	2.93 ± 0.28	13.9	266.	17.2	16.4	4.55
^{237}U	6,75d	c	95.3 ± 8.0	113.	216.	101.	124.	45.0
^{233}Pa	26,967d	c	5.09 ± 0.41	10.2	3.32	4.73	19.5	13.5
^{232}Pa	1,31d	i	3.75 ± 0.33	5.33	0.624	1.46	11.8	6.01
^{228}Pa	22h	c	2.45 ± 0.37	0.106	0.005	0.004	1.10	3.84
^{227}Th	18,72d	c	3.66 ± 0.81	0.152	0.005	0.013	0.032	1.52
^{146}Pr	24,15m	c	15.3 ± 2.3	13.5	0.161	13.5	0.666	–
^{143}Ce	33,039h	c	24.9 ± 1.9	20.3	0.185	17.7	1.23	–
^{141}Ce	32,501d	c	34.1 ± 2.7	29.0	0.505	21.7	2.20	–
^{139}Ce	137,640d	c	1.46 ± 0.22	4.86	0.028	0.008	0.039	–
^{142}La	91,1m	c	25.1 ± 2.4	20.0	0.126	13.9	1.66	–
^{140}La	1,6781d	i	7.23 ± 0.62	5.51	0.417	10.1	1.04	–
^{141}Ba	18,27m	c	23.6 ± 2.8	17.8	0.087	9.99	0.979	–
^{140}Ba	12,752d	c	24.9 ± 1.9	21.7	0.419	14.2	2.50	–
^{139}Ba	83,06m	c	32.1 ± 5.9	29.5	1.26	20.8	2.84	–
^{136}Cs	13,16d	i(m+g)	13.9 ± 1.1	9.35	8.84	17.8	6.83	–
^{134}Cs	2,0648y	i(m+g)	9.31 ± 1.20	7.08	10.4	8.47	4.98	–
^{132}Cs	6,479d	i	3.48 ± 0.40	4.89	0.928	0.102	0.431	–
^{135}Xe	9,14h	i(m+g)	17.8 ± 1.6	11.4	13.4	21.4	12.4	–
^{135}I	6,57h	c	19.0 ± 1.5	19.2	8.39	6.73	5.54	–
^{133}I	20,8h	c	32.4 ± 2.7	29.3	59.3	31.3	44.9	–
^{131}I	8,02070d	c	43.1 ± 3.3	36.6	134.	50.2	81.4	–
^{126}I	13,11d	i	2.38 ± 0.39	4.37	0.175	0.004	0.098	–
^{134}Te	41,8m	c	11.4 ± 1.0	14.7	3.36	1.59	4.02	–
^{132}Te	3,204d	c	18.1 ± 1.4	24.5	55.6	19.0	86.4	–
^{131}Sb	23,03m	c	8.91 ± 1.04	15.6	18.5	3.95	17.0	–
^{129}Sb	4,40h	c	11.8 ± 1.2	19.6	79.8	23.7	37.5	–
^{127}Sb	3,85d	c	27.0 ± 2.3	28.4	104.	47.6	57.3	–
^{125}Sb	2,75856y	c	46.4 ± 5.4	31.3	103.	64.1	53.0	–
^{122}Sb	2,7238d	i(m+g)	5.78 ± 0.44	6.27	2.47	0.430	1.07	–
^{128}Sn	59,07m	c	6.48 ± 0.59	17.1	17.5	9.41	28.3	–
^{112}Ag	3,130h	c	65.8 ± 8.1	37.2	9.45	71.0	18.2	–
^{112}Ag	3,130h	i	9.10 ± 1.60	7.24	0.892	1.50	1.20	–
^{111}Ag	7,45d	c	57.5 ± 5.6	34.5	10.5	71.9	19.1	–
^{107}Rh	21,7m	c*	63.7 ± 7.6	41.4	60.8	80.6	36.7	–
^{106}Ru	373,59d	c	59.8 ± 5.7	34.5	68.6	63.3	45.3	–
^{105}Ru	4,44h	c	60.8 ± 4.9	37.0	92.8	66.8	57.3	–
^{103}Ru	39,26d	c	61.1 ± 4.7	41.8	149.	60.9	63.8	–
^{104}Tc	18,3m	c	55.1 ± 4.8	32.8	118.	64.8	77.2	–
^{101}Tc	14,22m	c	64.2 ± 7.5	44.4	180.	54.8	55.3	–
^{99}Mo	65,94h	c	62.9 ± 5.0	23.4	48.1	18.9	27.7	–
^{96}Nb	23,35h	i	1.86 ± 0.16	7.01	1.70	0.117	3.87	–
^{97}Zr	16,744h	c	50.1 ± 3.8	31.9	79.0	40.8	44.9	–
^{95}Zr	64,02d	c	52.8 ± 3.9	39.0	61.8	40.8	30.0	–
^{94}Y	18,7m	i	46.3 ± 4.4	11.2	27.9	18.4	12.0	–
^{92}Y	3,54h	c	50.4 ± 7.0	40.1	26.5	31.5	22.5	–
^{92}Y	3,54h	i	15.0 ± 2.7	7.31	5.39	2.32	6.50	–
^{91}Sr	9,63h	c	40.3 ± 3.3	30.0	15.9	28.4	10.5	–
^{89}Rb	15,15m	c*	35.7 ± 3.3	31.0	4.00	32.4	3.40	–
^{88}Rb	17,78m	c	36.5 ± 3.6	22.5	2.21	26.0	3.76	–
^{88}Rb	17,78m	i	10.3 ± 2.1	4.82	1.42	7.14	2.35	–
^{88}Kr	2,84h	c	24.2 ± 1.9	17.5	0.789	18.6	1.40	–
^{87}Kr	76,3m	c	26.0 ± 2.9	13.9	0.768	19.1	2.10	–
^{78}Ge	88m	c	3.61 ± 0.35	3.75	0.082	8.12	0.098	–
^{73}Ga	4,86h	c	1.68 ± 0.15	2.14	–	5.41	0.059	–

Table 83, cont'd.

Product	$T_{1/2}$	Type	Exp yield [mbarn]	Calculated Yields [mbarn] via LAHET	CASCADE	CASCADO-IPPE	INUCL	ALICE-IPPE
^{72}Ga	14,10h	i(m+g)	0.434 ± 0.174	0.376	–	0.090	0.039	–
^{72}Zn	46,5h	c	1.27 ± 0.18	1.40	–	4.42	0.039	–
^{24}Na	14,9590h	c	0.386 ± 0.046	–	–	–	–	–

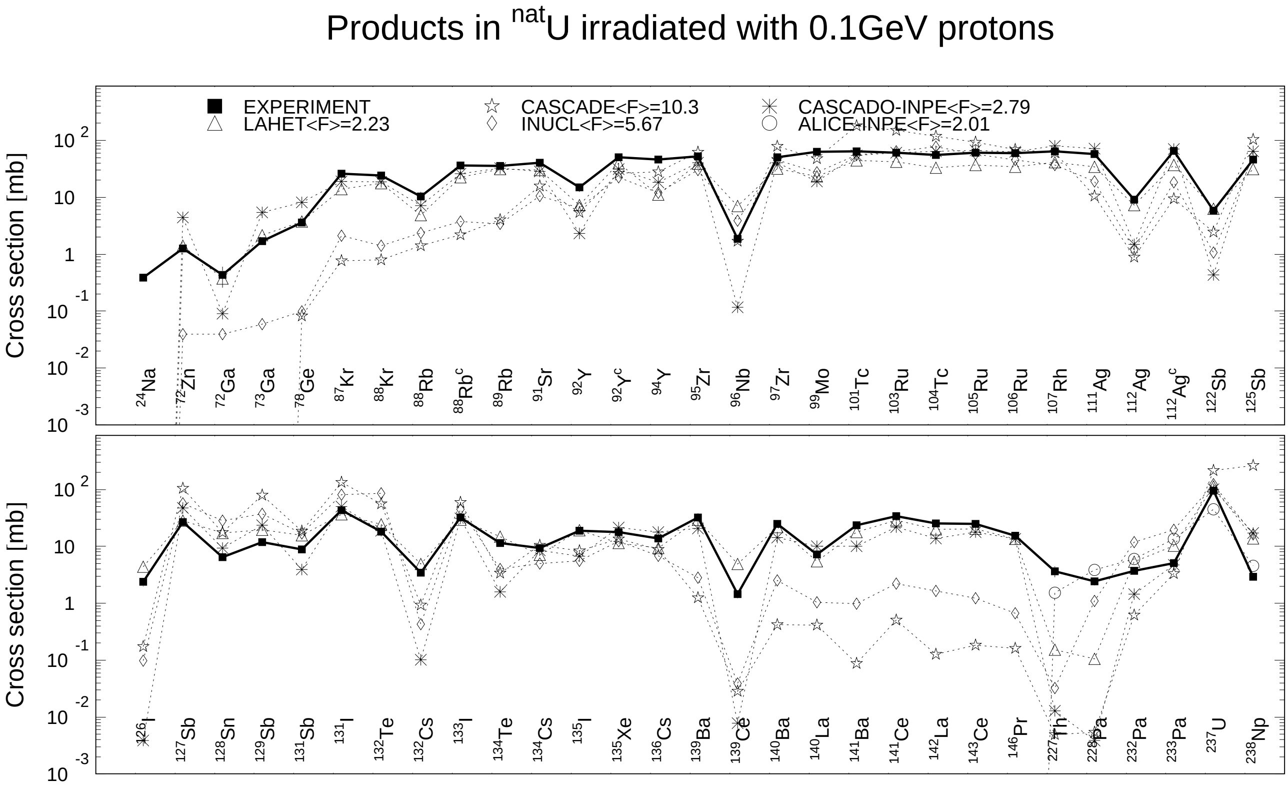

Fig. 76: Detailed comparison between experimental and simulated yields of radioactive reaction products in ^{nat}U irradiated with 0.1 GeV protons. The cumulative yields are labeled -c when the respective independent yields are also shown.

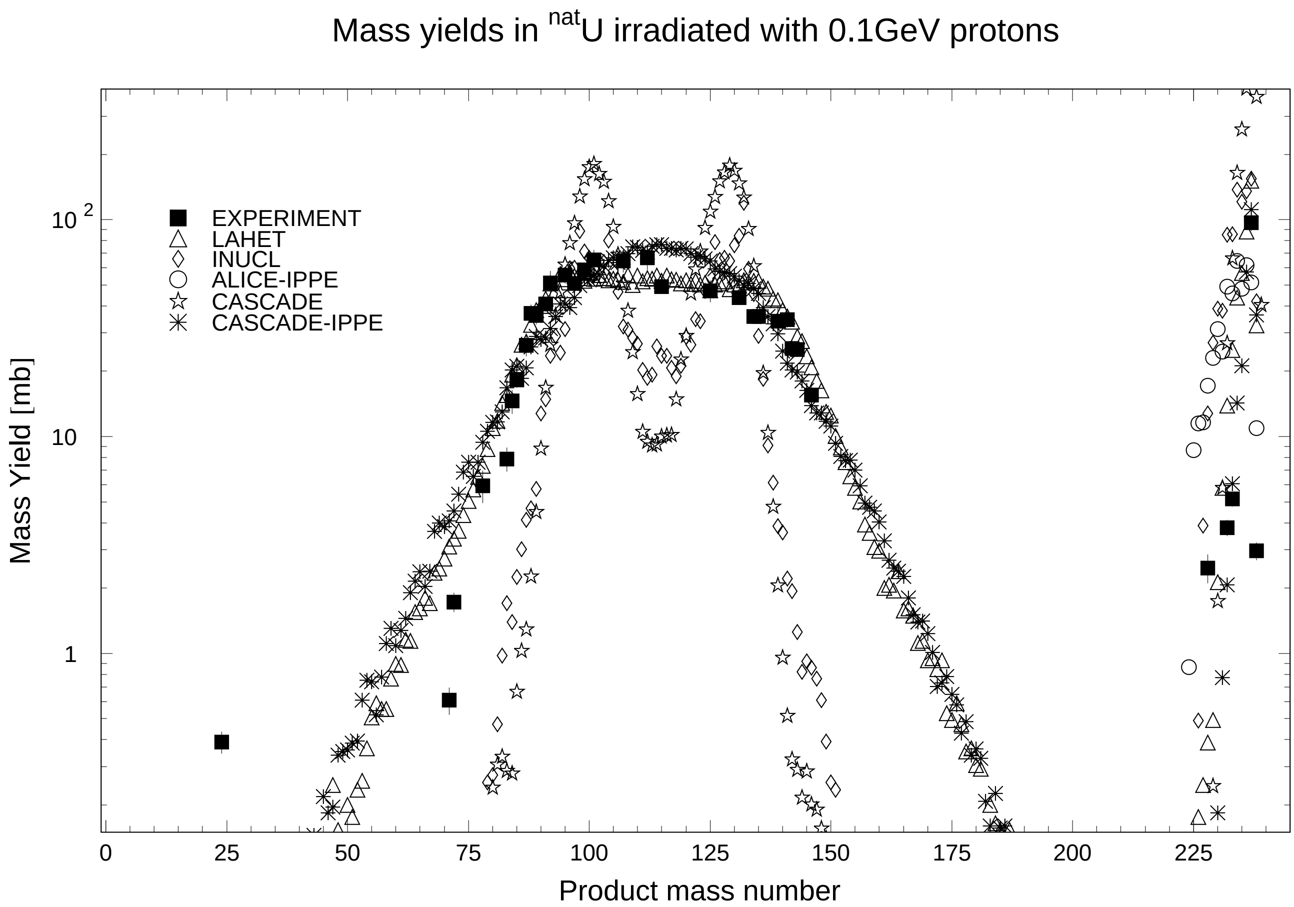

Fig. 77: The simulated mass distributions of reaction products together with the measured cumulative and supra-cumulative yields in ^{nat}U irradiated with 0.1 GeV protons.

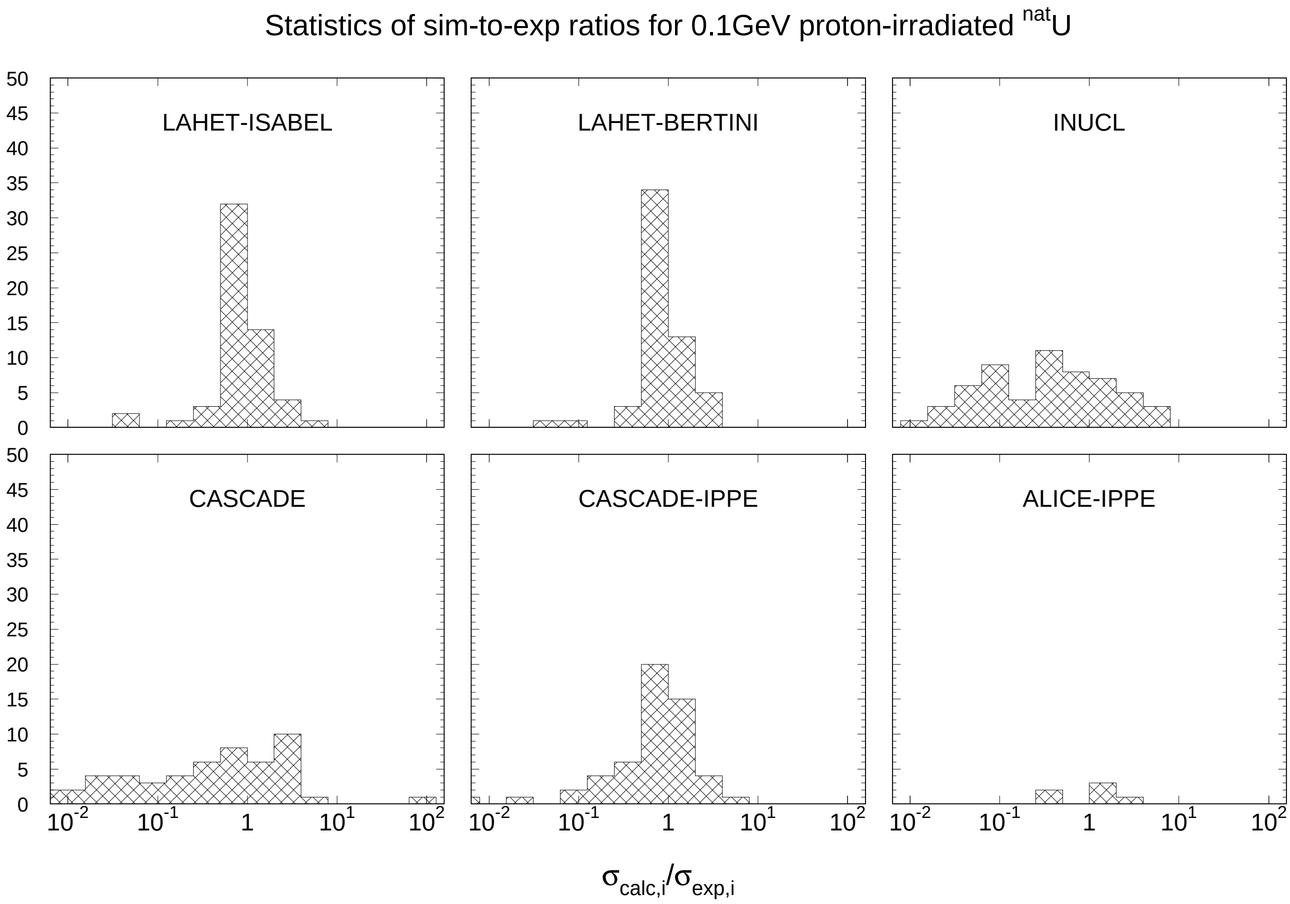

Fig. 78: Statistics of the simulation-to-experiment ratios (criterion 2) for ^{nat}U irradiated with 0.1 GeV protons.

Table 84: Experimental and calculated yields from ^{nat}U irradiated with 0.2 GeV protons.

Product	$T_{1/2}$	Type	Exp yield [mbarn]	Calculated Yields [mbarn] via LAHET	CASCADE	INUCL
^{238}Np	2,117d	i	1.09 ± 0.12	6.66	83.4	11.7
^{237}U	6,75d	c	76.9 ± 6.0	101.	203.	137.
^{233}Pa	26,967d	c	9.87 ± 0.68	11.2	37.7	34.1
^{232}Pa	1,31d	i	8.52 ± 0.64	6.51	16.9	24.2
^{230}Pa	17,4d	i	3.88 ± 0.48	3.31	6.30	14.1
^{228}Pa	22h	c	1.55 ± 0.21	0.938	2.17	11.2
^{227}Th	18,72d	c	2.63 ± 0.49	1.30	0.924	3.40
^{147}Nd	10,98d	c	9.16 ± 0.98	11.4	0.548	0.581
^{146}Pr	24,15m	c	12.4 ± 1.4	9.86	0.579	0.615
^{146}Pr	24,15m	i	7.60 ± 2.06	2.63	0.203	0.130
^{143}Ce	33,039h	c	17.3 ± 1.2	14.8	0.864	0.966
^{141}Ce	32,501d	c	25.0 ± 1.8	21.0	1.51	1.93
^{139}Ce	137,640d	c	3.58 ± 0.32	6.45	0.789	0.204
^{142}La	91,1m	c	17.1 ± 1.6	13.8	0.545	1.11
^{140}La	1,6781d	i	5.13 ± 0.42	4.54	0.787	0.875
^{141}Ba	18,27m	c	16.0 ± 1.8	11.6	0.373	0.826
^{140}Ba	12,752d	c	17.6 ± 1.1	14.6	0.942	1.96
^{139}Ba	83,06m	c	21.2 ± 3.8	20.2	1.83	2.72
^{136}Cs	13,16d	i(m+g)	9.79 ± 0.66	7.18	6.79	5.94
^{134}Cs	2,0648y	i(m+g)	10.1 ± 2.1	6.59	11.5	6.57
^{132}Cs	6,479d	i	5.30 ± 0.43	4.37	9.34	2.07
^{135}Xe	9,14h	i(m+g)	13.0 ± 1.0	7.21	10.6	10.8
^{127}Xe	36,4d	c	2.08 ± 0.22	4.24	2.86	0.243
^{135}I	6,57h	c	13.3 ± 0.9	13.6	5.73	3.93
^{133}I	20,8h	c	22.3 ± 1.7	21.1	39.4	31.9
^{131}I	8,02070d	c	30.2 ± 2.0	27.8	90.3	56.5
^{126}I	13,11d	i	5.45 ± 0.63	4.97	8.98	1.10
^{134}Te	41,8m	c	7.93 ± 0.67	9.63	2.07	2.38
^{132}Te	3,204d	c	12.5 ± 0.8	17.0	33.7	52.2
^{131}Sb	23,03m	c	5.32 ± 0.57	11.3	10.8	11.9
^{129}Sb	4,40h	c	8.17 ± 0.80	13.9	49.2	27.5
^{127}Sb	3,85d	c	19.2 ± 1.5	20.0	70.6	38.3
^{125}Sb	2,75856y	c	34.7 ± 4.2	24.6	71.2	38.8
^{122}Sb	2,7238d	i(m+g)	9.45 ± 0.63	6.49	12.2	3.10
^{128}Sn	59,07m	c	4.03 ± 0.40	11.1	11.2	17.6
^{112}Ag	3,130h	c	60.8 ± 7.2	33.0	6.09	20.1
^{112}Ag	3,130h	i	14.2 ± 1.8	7.55	2.24	3.51
^{111}Ag	7,45d	c	56.5 ± 5.1	31.0	7.24	19.8
^{107}Rh	21,7m	c*	57.1 ± 6.5	37.8	27.6	29.0
^{106}Ru	373,59d	c	39.8 ± 4.1	29.4	28.5	31.4
^{105}Ru	4,44h	c	56.1 ± 3.8	31.2	38.9	37.7
^{103}Ru	39,26d	c	57.0 ± 3.8	35.5	77.7	46.0
^{104}Tc	18,3m	c	45.4 ± 3.4	26.5	52.8	47.8
^{101}Tc	14,22m	c	55.3 ± 5.2	36.3	112.	48.4
^{101}Tc	14,22m	i	7.19 ± 2.89	8.01	8.90	5.23
^{99}Mo	65,94h	c	54.7 ± 3.9	18.8	42.7	22.5
^{96}Nb	23,35h	i	4.45 ± 0.32	7.07	14.8	5.80
^{97}Zr	16,744h	c	39.5 ± 2.6	24.1	66.2	36.2
^{95}Zr	64,02d	c	46.2 ± 3.0	30.4	79.2	31.2
^{94}Y	18,7m	i	34.6 ± 3.1	9.07	33.4	12.0
^{92}Y	3,54h	c	44.6 ± 6.0	33.4	61.4	26.0
^{92}Y	3,54h	i	15.7 ± 2.8	7.12	28.2	7.86
^{88}Y	106,65d	c	2.44 ± 0.45	2.79	0.082	0.333
^{88}Y	106,65d	i(m+g)	1.14 ± 0.34	1.91	0.082	0.326
^{91}Sr	9,63h	c	34.5 ± 2.5	24.1	35.0	17.2

Table 84, cont'd.

Product	$T_{1/2}$	Type	Exp yield [mbarn]	Calculated Yields [mbarn] via LAHET	CASCADE	INUCL
^{89}Rb	15,15m	c*	28.9 ± 2.3	25.9	15.1	5.93
^{88}Rb	17,78m	c	31.7 ± 2.6	22.2	13.1	7.26
^{88}Rb	17,78m	i	9.79 ± 1.41	5.57	9.58	5.48
^{88}Kr	2,84h	c	20.1 ± 1.4	16.4	3.50	1.77
^{87}Kr	76,3m	c	22.4 ± 2.3	13.4	4.46	3.24
^{78}Ge	88m	c	3.42 ± 0.26	5.53	0.615	0.081
^{73}Ga	4,86h	c	2.46 ± 0.18	3.93	0.094	0.049
^{72}Ga	14,10h	i(m+g)	0.747 ± 0.096	0.978	0.026	0.039
^{72}Zn	46,5h	c	1.77 ± 0.16	2.41	0.084	0.035
^{24}Na	14,9590h	c	0.196 ± 0.023	–	–	–

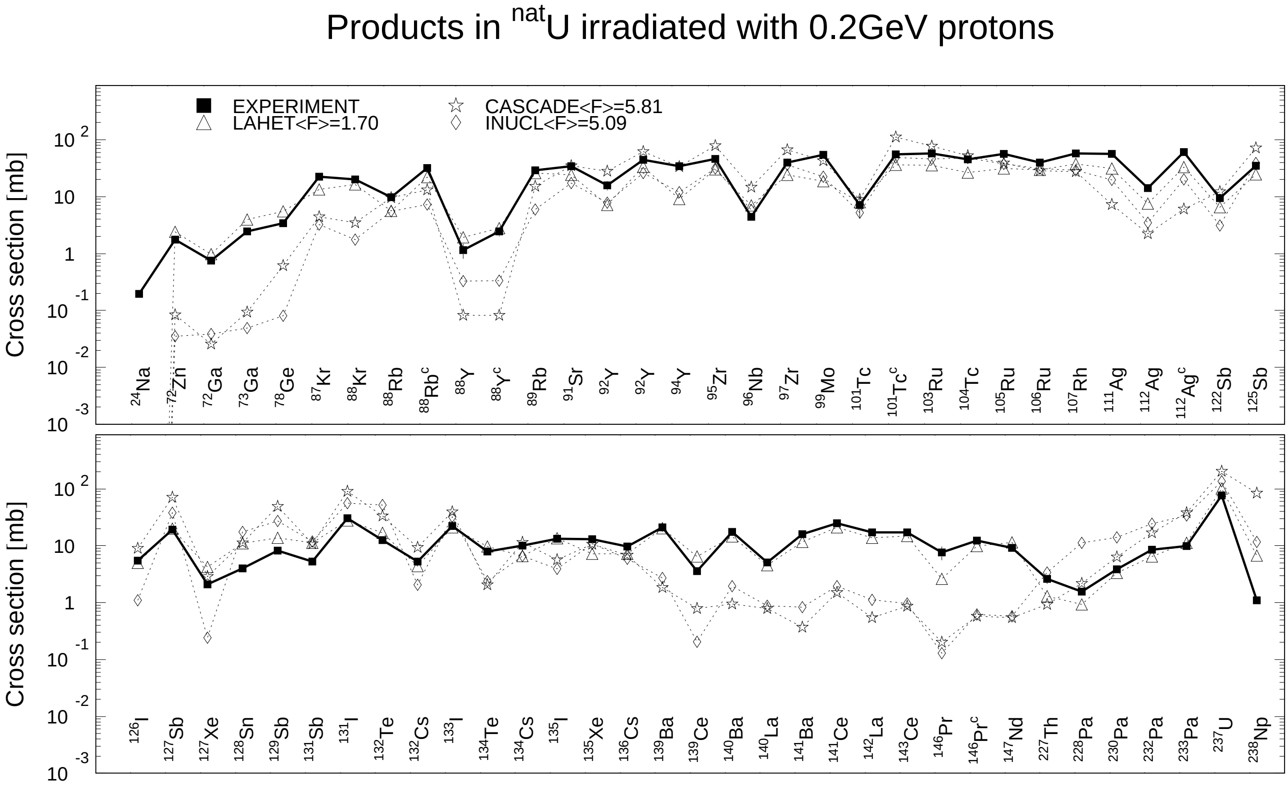

Fig. 79: Detailed comparison between experimental and simulated yields of radioactive reaction products in ^{nat}U irradiated with 0.2 GeV protons. The cumulative yields are labeled -c when the respective independent yields are also shown.

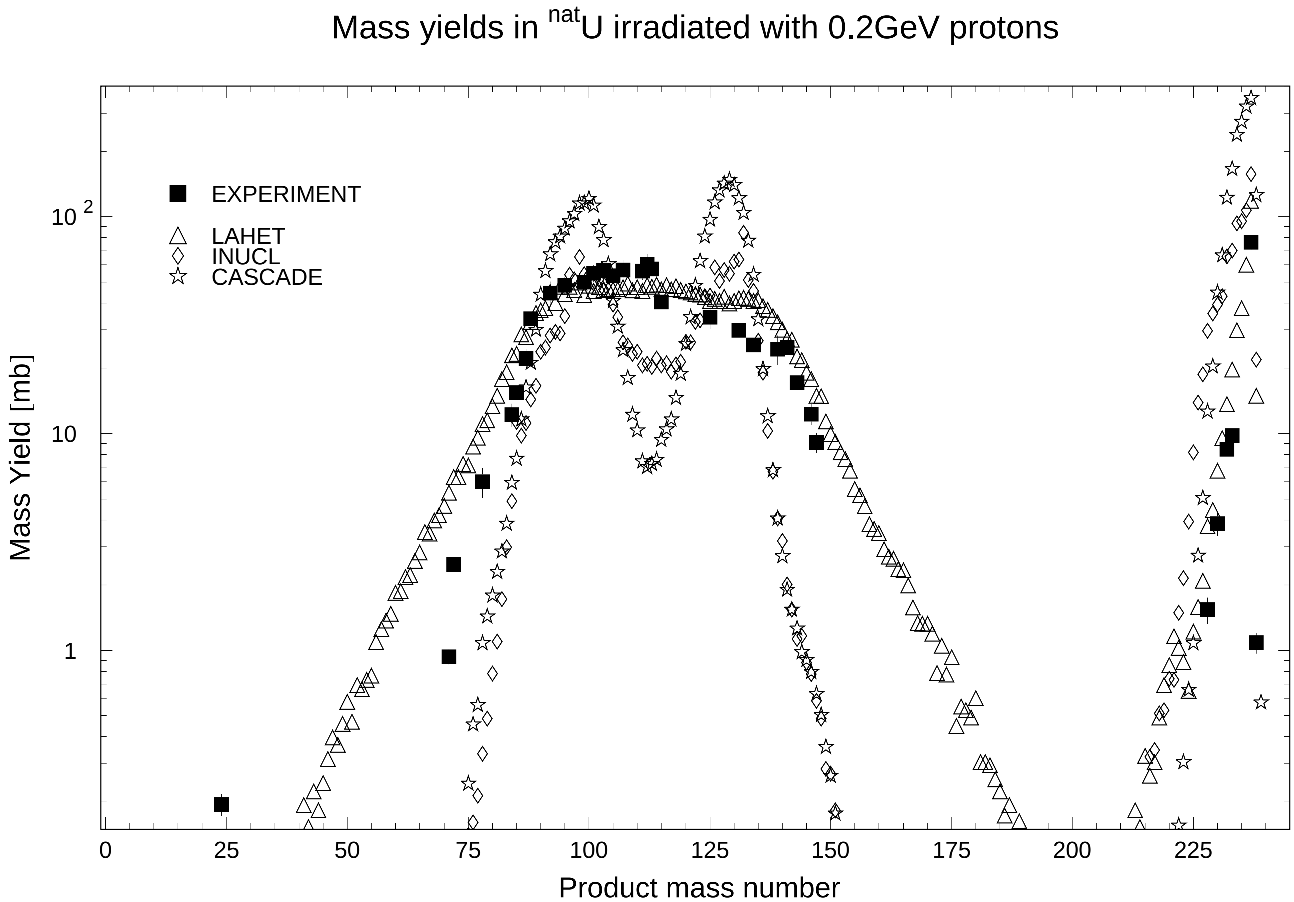

Fig. 80: The simulated mass distributions of reaction products together with the measured cumulative and supra-cumulative yields in ^{nat}U irradiated with 0.2 GeV protons.

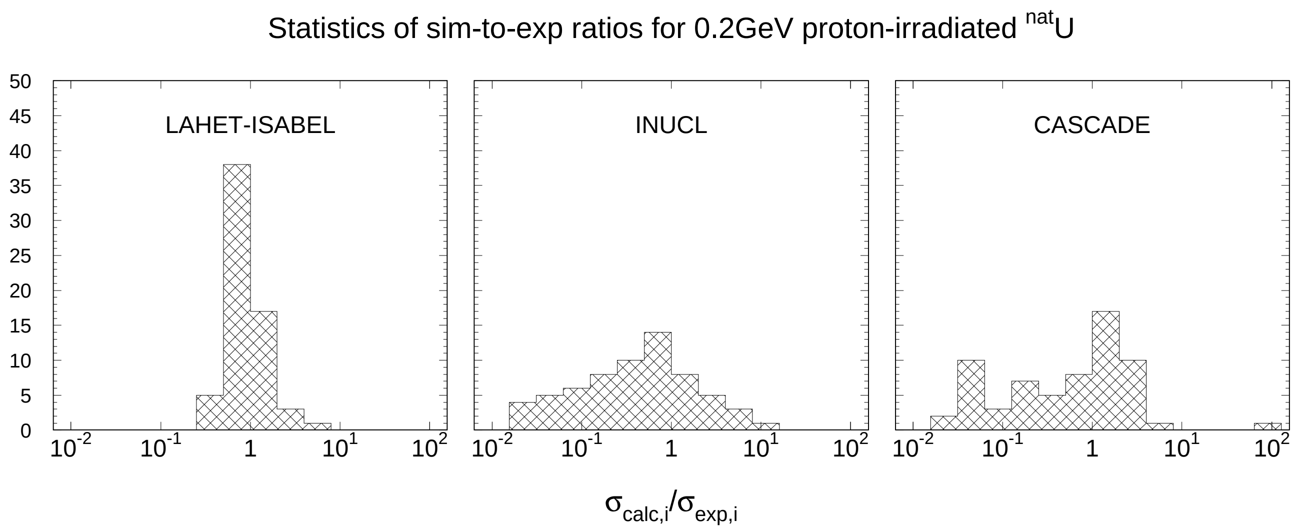

Fig. 81: Statistics of the simulation-to-experiment ratios (criterion 2) for ^{nat}U irradiated with 0.2 GeV protons.

Table 85: Experimental and calculated yields from ^{nat}U irradiated with 0.8 GeV protons.

Product	$T_{1/2}$	Type	Exp yield [mbarn]	Calculated Yields [mbarn] via LAHET	CASCADE	CASCADO-IPPE	INUCL
^{239}Np	2,3565d	i	3.46 ± 0.28	–	0.004	–	–
^{237}U	6,75d	c	107. ± 9.	133.	165.	105.	101.
^{233}Pa	26,967d	c	14.2 ± 0.9	12.3	65.3	16.8	27.3
^{232}Pa	1,31d	i	8.88 ± 0.63	5.74	35.9	12.0	15.2
^{230}Pa	17,4d	i	3.60 ± 0.34	2.36	30.9	10.3	11.8
^{228}Pa	22h	c	1.98 ± 0.64	0.678	24.5	6.74	11.1
^{227}Th	18,72d	c	3.87 ± 0.60	2.08	30.9	5.91	11.6
^{226}Ac	29,37h	i	2.18 ± 0.22	1.76	12.8	1.56	4.63
^{225}Ac	10,0d	c	3.31 ± 0.23	2.78	20.6	2.21	6.64
^{223}Ra	11,435d	c	4.45 ± 0.40	2.74	40.9	6.75	13.1
^{211}Rn	14,6h	c	4.03 ± 0.28	4.49	6.86	4.76	8.74
^{210}At	8,1h	c	4.67 ± 0.32	4.78	2.01	1.87	2.05
^{209}At	5,41h	c	9.02 ± 0.58	10.1	11.4	3.17	4.72
^{208}At	1,63h	c*	4.73 ± 0.51	8.66	14.8	1.76	4.86
^{207}At	1,80h	c	8.43 ± 0.84	10.6	18.9	1.53	6.76
^{206}At	30,6m	c*	4.82 ± 0.38	7.62	13.9	0.360	6.35
^{206}Po	8,8d	c	8.85 ± 0.55	14.6	17.8	4.19	8.25
^{205}Po	1,66h	c*	7.10 ± 0.79	13.2	24.4	2.09	12.4
^{204}Po	3,53h	c*	8.11 ± 0.57	10.3	15.2	1.82	7.49
^{202}Bi	1,72h	c	5.24 ± 0.37	8.72	3.98	3.04	1.75
^{203}Pb	51,873h	c	5.25 ± 0.35	9.38	2.91	4.69	1.11
^{203}Pb	51,873h	i(m1+m2+g)	1.24 ± 0.24	0.546	0.162	1.74	0.020
^{201}Pb	9,33h	c	4.94 ± 0.47	9.06	3.99	6.40	1.75
^{201}Pb	9,33h	i(m+g)	3.86 ± 0.92	1.81	0.353	3.76	0.061
^{200}Pb	21,5h	c	3.21 ± 0.28	8.58	4.53	7.13	2.09
^{200}Tl	26,1h	i(m+g)	1.29 ± 0.13	0.459	0.033	0.488	–
^{192}Hg	4,85h	c	2.37 ± 0.24	4.35	3.58	3.93	0.162
^{191}Pt	2,802d	c	1.48 ± 0.52	6.41	2.61	4.10	0.061
^{188}Pt	10,2d	c	1.29 ± 0.13	3.97	1.65	1.97	–
^{185}Os	93,6d	c	2.59 ± 0.31	3.96	0.422	1.57	–
^{182}Os	22,10h	c	1.20 ± 0.13	2.28	0.156	0.793	–
^{177}W	135m	c	2.13 ± 0.30	0.994	0.007	0.541	–
^{172}Ta	36,8m	c*	1.86 ± 0.26	0.230	–	0.322	–
^{175}Hf	70d	c	0.578 ± 0.071	0.798	0.004	0.879	–
^{171}Lu	8,24d	c	0.938 ± 0.103	0.467	–	0.874	–
^{157}Dy	8,14h	c	0.752 ± 0.107	0.809	–	1.70	–
^{155}Dy	9,9h	c*	0.722 ± 0.137	0.455	–	1.11	–
^{156}Tb	5,35d	i(m1+m2+g)	0.472 ± 0.051	0.634	–	0.928	–
^{155}Tb	5,32d	c	1.48 ± 0.23	1.22	–	2.27	–
^{153}Tb	2,34d	c*	1.05 ± 0.13	0.781	–	1.24	–
^{146}Gd	48,27d	c	0.309 ± 0.050	0.226	0.007	0.159	–
^{146}Eu	4,61d	i	0.567 ± 0.053	0.382	0.004	0.688	–
^{144}Pm	363d	i	1.32 ± 0.23	1.58	0.096	1.79	0.020
^{147}Nd	10,98d	c	6.56 ± 0.64	7.28	0.313	3.83	0.263
^{144}Ce	284,893d	c	11.6 ± 1.0	9.82	0.372	2.73	0.929
^{143}Ce	33,039h	c	12.4 ± 0.8	8.85	0.581	3.55	0.425
^{141}Ce	32,501d	c	19.0 ± 1.3	13.4	1.48	7.36	1.05
^{139}Ce	137,640d	c	8.20 ± 0.54	7.97	1.83	9.57	0.304
^{135}Ce	17,7h	c	3.08 ± 0.25	2.72	1.33	1.60	0.061
^{132}Ce	3,51h	c	0.701 ± 0.186	1.28	0.486	0.094	–
^{142}La	91,1m	c	13.3 ± 1.0	7.86	0.464	2.10	0.809
^{140}La	1,6781d	i	3.22 ± 0.23	2.94	0.865	3.08	0.364
^{140}Ba	12,752d	c	13.5 ± 0.8	8.66	0.626	2.22	1.11
^{131}Ba	11,50d	c	6.51 ± 0.45	6.30	8.73	3.32	0.405
^{128}Ba	2,43d	c	2.16 ± 0.28	2.85	3.68	0.293	0.061

Table 85, cont'd.

Product	$T_{1/2}$	Type	Exp yield [mbarn]	Calculated Yields [mbarn] via LAHET	CASCADE	cascsh	INUCL
^{136}Cs	13,16d	i(m+g)	5.96 ± 0.36	4.50	3.72	4.43	5.28
^{134}Cs	2,0648y	i(m+g)	6.43 ± 0.52	4.10	8.03	6.55	7.81
^{132}Cs	6,479d	i	6.95 ± 0.48	4.49	11.6	7.49	3.85
^{135}Xe	9,14h	i(m+g)	8.19 ± 0.66	4.51	5.16	3.97	8.72
^{127}Xe	36,4d	c	11.6 ± 0.8	7.00	31.5	6.80	2.02
^{125}Xe	16,9h	c	6.09 ± 0.39	3.53	17.3	1.66	0.749
^{135}I	6,57h	c	12.0 ± 0.8	7.59	3.07	0.378	2.79
^{133}I	20,8h	c	16.7 ± 1.2	11.9	17.1	4.01	19.7
^{131}I	8,02070d	c	20.4 ± 1.3	16.6	42.2	10.0	35.2
^{126}I	13,11d	i	9.74 ± 0.89	6.02	22.6	7.67	4.80
^{124}I	4,1760d	i	7.83 ± 0.52	6.02	17.5	3.95	1.32
^{121}I	2,12h	c	3.16 ± 0.23	3.65	5.69	0.403	0.081
^{132}Te	3,204d	c	10.3 ± 0.7	9.81	13.3	1.75	23.8
^{127}Sb	3,85d	c	12.0 ± 0.8	12.8	31.4	7.35	22.7
^{125}Sb	2,75856y	c	24.3 ± 2.1	17.1	35.5	16.2	28.8
^{122}Sb	2,7238d	i(m+g)	14.0 ± 0.9	6.00	16.4	11.0	9.45
^{111}In	2,8047d	c	3.47 ± 0.27	4.62	3.28	1.45	0.931
^{112}Ag	3,130h	c	67.3 ± 7.7	27.8	2.97	36.8	24.1
^{112}Ag	3,130h	i	26.5 ± 3.2	7.48	1.52	14.5	8.86
^{111}Ag	7,45d	c	66.7 ± 5.8	28.6	4.60	43.2	24.6
^{105}Ag	41,29d	c	1.53 ± 0.18	3.15	0.401	0.533	0.405
^{107}Rh	21,7m	c*	63.4 ± 7.1	31.4	6.48	42.7	25.7
^{106}Ru	373,59d	c	44.0 ± 6.1	22.5	6.16	28.3	22.8
^{105}Ru	4,44h	c	60.0 ± 3.7	27.0	9.11	33.2	28.4
^{103}Ru	39,26d	c	75.9 ± 4.7	31.8	22.1	43.5	36.1
^{104}Tc	18,3m	c	41.4 ± 3.3	21.0	13.2	21.9	24.9
^{101}Tc	14,22m	c	63.5 ± 7.3	32.1	35.7	41.3	39.6
^{99}Mo	65,94h	c	65.7 ± 4.6	18.7	19.1	21.4	22.0
^{96}Nb	23,35h	i	17.6 ± 1.1	8.33	8.40	14.2	12.6
^{90}Nb	14,60h	c*	0.807 ± 0.064	1.72	0.068	0.045	0.252
^{97}Zr	16,744h	c	35.3 ± 2.3	17.7	31.2	15.1	22.6
^{95}Zr	64,02d	c	50.9 ± 3.2	24.5	43.7	27.1	31.6
^{88}Zr	83,4d	c	1.04 ± 0.08	3.41	1.31	0.118	0.607
^{94}Y	18,7m	i	34.0 ± 2.9	7.31	19.4	10.7	12.2
^{92}Y	3,54h	c	50.5 ± 6.7	26.6	51.7	28.4	32.5
^{92}Y	3,54h	i	20.8 ± 3.7	6.93	24.9	15.6	14.5
^{88}Y	106,65d	i(m+g)	6.74 ± 0.52	4.52	9.61	3.25	3.20
^{86}Y	14,74h	c	1.10 ± 0.08	2.37	0.372	0.094	0.304
^{91}Sr	9,63h	c	34.4 ± 2.1	18.7	34.0	18.8	23.9
^{89}Rb	15,15m	c*	29.6 ± 2.4	21.9	21.8	14.2	12.7
^{86}Rb	18,631d	i(m+g)	15.8 ± 1.0	6.97	32.9	12.1	20.8
^{83}Rb	86,2d	c	4.75 ± 0.40	5.96	9.90	1.67	2.02
^{88}Kr	2,84h	c	16.4 ± 1.1	14.0	6.44	6.35	4.12
^{87}Kr	76,3m	c	20.6 ± 1.8	12.6	9.71	9.78	8.19
^{77}Br	57,036h	c	1.13 ± 0.10	2.39	0.868	0.159	0.344
^{75}Se	119,779d	c	1.38 ± 0.17	2.28	1.89	0.277	0.465
^{78}As	90,7m	i	7.10 ± 0.94	3.80	5.56	8.35	1.13
^{76}As	1,0778d	i	5.68 ± 0.45	3.01	5.82	5.61	1.23
^{74}As	17,77d	i	2.85 ± 0.27	2.44	1.93	1.32	0.283
^{78}Ge	88m	c	3.70 ± 0.38	7.36	1.26	4.69	0.223
^{73}Ga	4,86h	c	6.32 ± 0.47	6.64	1.86	10.1	0.344
^{72}Ga	14,10h	i(m+g)	4.83 ± 0.39	2.31	1.48	5.98	0.486
^{72}Zn	46,5h	c	2.89 ± 0.21	4.29	0.585	5.24	0.182
^{66}Ni	54,6h	c	2.62 ± 0.24	2.61	0.247	5.87	0.081
^{58}Co	70,86d	i(m+g)	0.334 ± 0.043	0.525	–	0.220	0.020

Table 85, cont'd.

Product	$T_{1/2}$	Type	Exp yield [mbarn]	Calculated Yields [mbarn] via LAHET	CASCADE	CASCADO-IPPE	INUCL
^{59}Fe	44,472d	c	2.96 ± 0.28	1.72	0.033	4.79	0.081
^{48}V	15,9735d	c	0.203 ± 0.030	0.164	–	–	–
^{48}Sc	43,67h	i	0.573 ± 0.065	0.361	–	1.64	–
^{43}K	22,3h	c	0.503 ± 0.057	0.350	–	1.66	–
^{28}Mg	20,915h	c	0.295 ± 0.027	0.011	–	0.325	–
^{7}Be	53,29d	i	3.91 ± 0.47	–	–	–	–

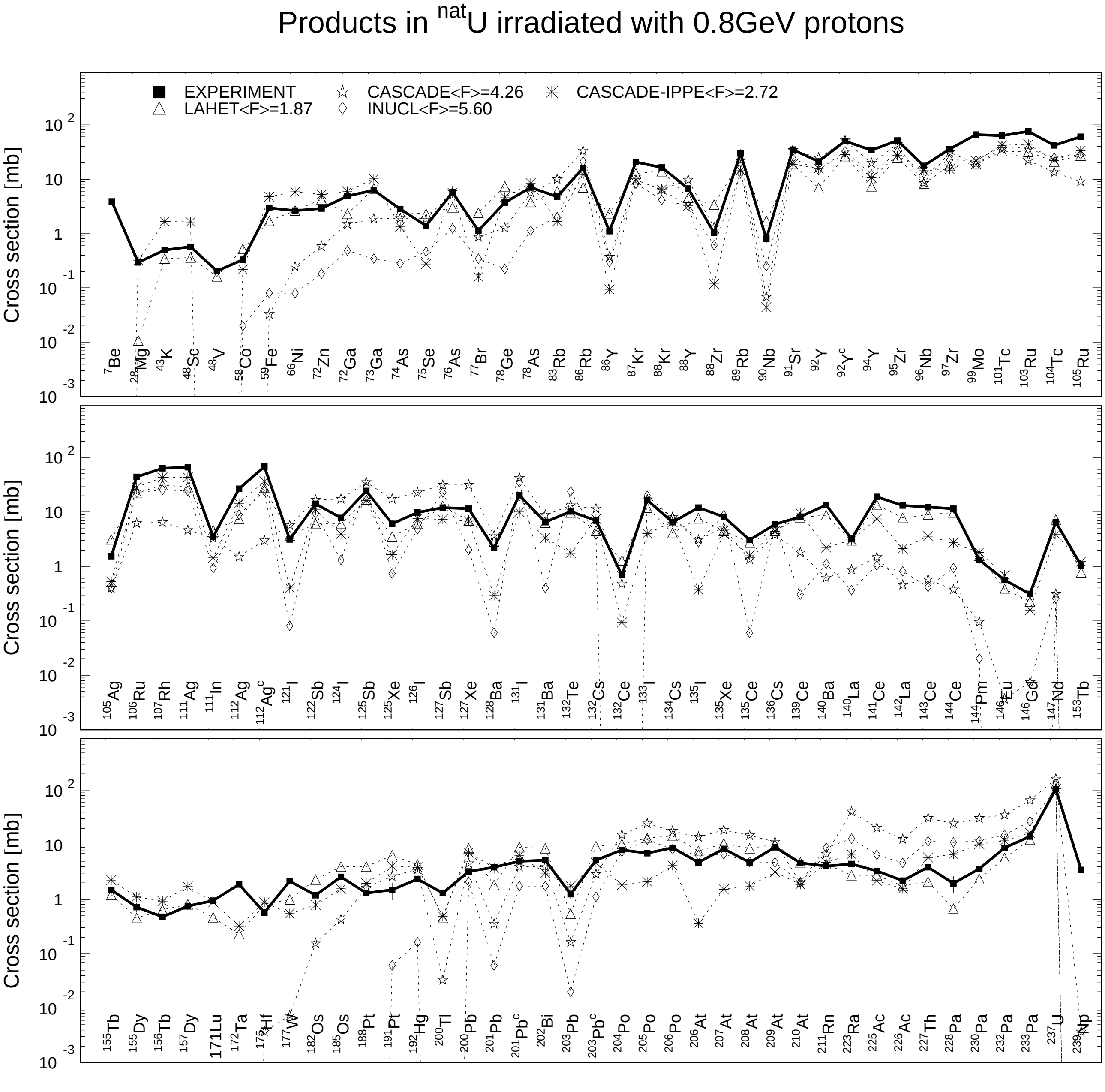

Fig. 82: Detailed comparison between experimental and simulated yields of radioactive reaction products in ^{nat}U irradiated with 0.8 GeV protons. The cumulative yields are labeled -c when the respective independent yields are also shown.

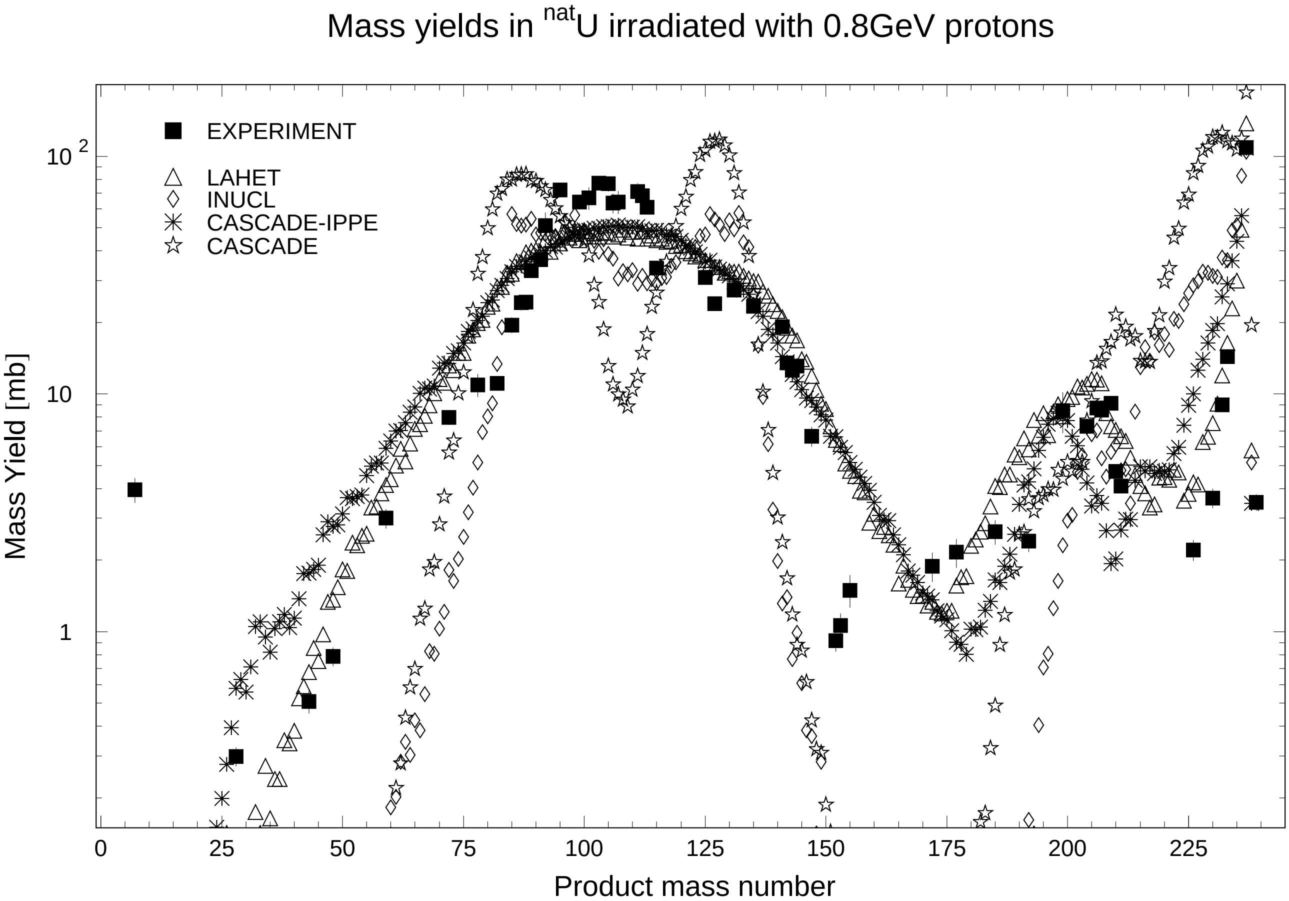

Fig. 83: The simulated mass distributions of reaction products together with the measured cumulative and supra-cumulative yields in ^{nat}U irradiated with 0.8 GeV protons.

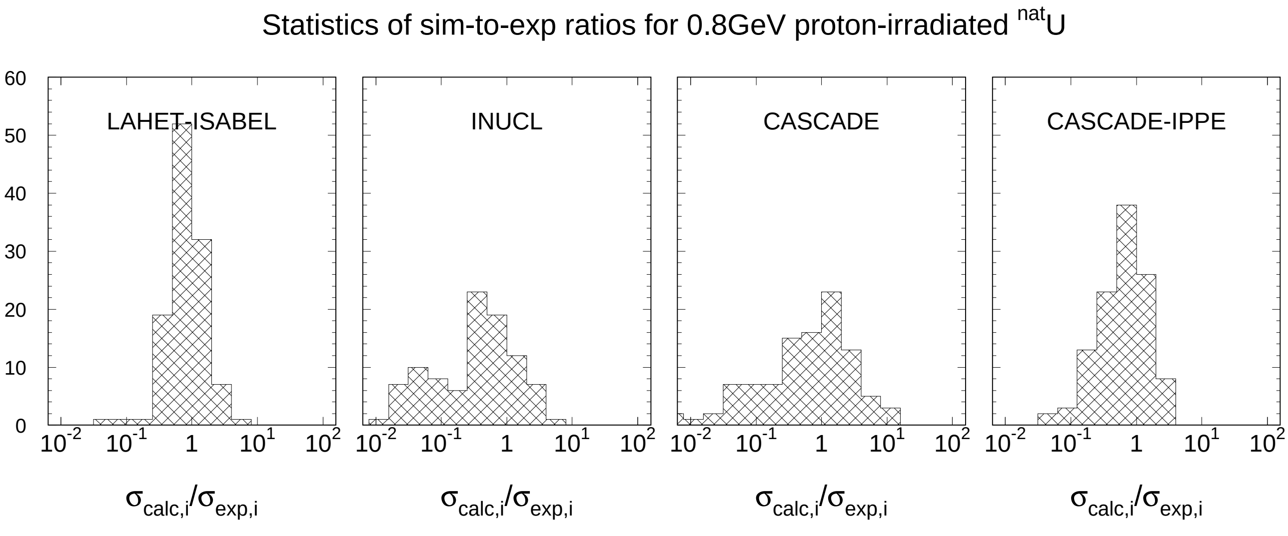

Fig. 84: Statistics of the simulation-to-experiment ratios (criterion 2) for ^{nat}U irradiated with 0.8 GeV protons.

Table 86: Experimental and calculated yields from ^{nat}U irradiated with 1.2 GeV protons.

Product	$T_{1/2}$	Type	Exp yield [mbarn]	Calculated Yields [mbarn] via LAHET	CASCADE	INUCL
^{239}Np	2,3565d	i	3.69 ± 0.32	–	–	–
^{237}U	6,75d	c	115. ± 9.	113.	160.	93.9
^{233}Pa	26,967d	c	14.0 ± 1.1	9.65	49.2	24.3
^{232}Pa	1,31d	i	7.95 ± 0.70	3.84	25.2	13.1
^{230}Pa	17,4d	i	2.99 ± 0.37	1.67	21.2	8.93
^{227}Th	18,72d	c	4.28 ± 0.63	1.60	24.0	9.95
^{226}Ac	29,37h	i	2.34 ± 0.29	1.58	11.6	4.38
^{225}Ac	10,0d	c	2.99 ± 0.23	2.37	20.2	6.71
^{223}Ra	11,435d	c	3.66 ± 0.33	2.34	37.9	12.1
^{211}Rn	14,6h	c	3.88 ± 0.31	3.34	10.3	12.2
^{210}At	8,1h	c	4.49 ± 0.34	3.78	4.05	2.75
^{209}At	5,41h	c	8.93 ± 0.66	7.36	18.8	7.72
^{208}At	1,63h	c*	4.84 ± 0.56	5.94	21.9	7.45
^{207}At	1,80h	c	8.12 ± 0.87	7.52	27.5	10.1
^{206}At	30,6m	c*	5.17 ± 0.50	5.73	21.1	9.28
^{206}Po	8,8d	c	9.29 ± 0.66	10.9	30.2	12.4
^{205}Po	1,66h	c*	8.19 ± 0.90	9.89	38.7	18.7
^{204}Po	3,53h	c*	8.72 ± 0.82	8.87	26.7	11.3
^{202}Bi	1,72h	c	7.26 ± 0.56	8.00	8.99	2.92
^{203}Pb	51,873h	c	6.69 ± 0.50	8.03	7.98	1.66
^{203}Pb	51,873h	i(m1+m2+g)	1.34 ± 0.40	0.515	0.881	0.020
^{201}Pb	9,33h	c	7.12 ± 0.70	8.43	9.83	3.48
^{201}Pb	9,33h	i(m+g)	5.64 ± 0.99	2.05	1.72	0.061
^{200}Pb	21,5h	c	5.36 ± 0.53	8.72	11.6	3.13
^{200}Tl	26,1h	i(m+g)	1.58 ± 0.22	0.668	0.445	0.041
^{192}Hg	4,85h	c	6.68 ± 0.66	7.34	16.3	0.368
^{192}Au	4,94h	c	8.91 ± 1.20	10.3	16.4	0.430
^{191}Pt	2,802d	c	5.82 ± 0.60	13.2	14.7	0.123
^{188}Pt	10,2d	c	5.72 ± 0.61	10.3	13.8	–
^{186}Pt	2,08h	c	5.30 ± 1.23	10.4	10.9	–
^{184}Ir	3,09h	c	5.44 ± 0.55	11.7	5.92	0.020
^{185}Os	93,6d	c	5.32 ± 1.44	13.6	5.98	–
^{182}Os	22,10h	c	6.27 ± 0.49	12.8	4.80	–
^{183}Re	70,0d	c	5.84 ± 0.51	14.2	4.44	–
^{181}Re	19,9h	c	5.99 ± 0.84	13.4	3.67	–
^{177}W	135m	c	4.85 ± 0.58	11.2	0.927	–
^{176}Ta	8,09h	c	3.79 ± 0.54	11.5	1.48	–
^{174}Ta	1,14h	c	3.59 ± 0.49	9.48	1.08	–
^{172}Ta	36,8m	c*	4.04 ± 0.58	7.90	0.757	–
^{175}Hf	70d	c	3.67 ± 0.32	11.5	1.12	–
^{173}Lu	1,37y	c	4.42 ± 0.61	10.5	0.840	–
^{171}Lu	8,24d	c	3.08 ± 0.26	10.2	0.396	–
^{166}Yb	56,7h	c	1.70 ± 0.21	7.47	0.136	–
^{160}Er	28,58h	c	1.91 ± 0.23	4.73	0.018	–
^{157}Dy	8,14h	c	1.29 ± 0.15	4.36	0.009	–
^{155}Dy	9,9h	c*	1.32 ± 0.17	3.38	–	–
^{155}Tb	5,32d	c	2.98 ± 0.40	4.16	–	–
^{153}Tb	2,34d	c*	1.90 ± 0.21	3.12	–	–
^{146}Gd	48,27d	c	0.804 ± 0.081	0.869	–	–
^{147}Eu	24,1d	c	0.772 ± 0.226	2.15	–	–
^{146}Eu	4,61d	i	0.858 ± 0.088	0.878	0.005	–
^{144}Pm	363d	i	1.50 ± 0.14	1.41	0.050	–
^{147}Nd	10,98d	c	6.16 ± 0.78	4.64	0.223	0.266
^{144}Ce	284,893d	c	12.1 ± 1.1	6.15	0.386	0.408
^{143}Ce	33,039h	c	11.7 ± 0.9	6.28	0.441	0.409

Table 86, cont'd.

Product	$T_{1/2}$	Type	Exp yield [mbarn]	Calculated Yields [mbarn] via LAHET	CASCADE	INUCL
^{141}Ce	32,501d	c	17.5 ± 1.4	8.80	1.22	0.981
^{139}Ce	137,640d	c	8.33 ± 0.62	6.16	1.06	0.450
^{135}Ce	17,7h	c	4.28 ± 0.36	2.38	1.04	0.286
^{132}Ce	3,51h	c	1.45 ± 0.20	1.69	0.495	0.041
^{142}La	91,1m	c	11.5 ± 1.0	5.55	0.422	0.389
^{140}La	1,6781d	i	2.60 ± 0.24	1.83	0.545	0.592
^{140}Ba	12,752d	c	12.7 ± 0.9	5.40	0.495	1.06
^{131}Ba	11,50d	c	7.28 ± 0.58	5.09	7.26	0.511
^{128}Ba	2,43d	c	3.05 ± 0.45	3.33	3.93	0.020
^{136}Cs	13,16d	i(m+g)	4.83 ± 0.34	2.97	2.92	3.88
^{134}Cs	2,0648y	i(m+g)	4.78 ± 0.43	2.62	5.94	6.03
^{132}Cs	6,479d	i	5.72 ± 0.56	2.42	8.01	3.33
^{135}Xe	9,14h	i(m+g)	6.94 ± 0.60	3.28	3.83	6.68
^{127}Xe	36,4d	c	13.0 ± 0.9	6.48	26.8	2.53
^{125}Xe	16,9h	c	7.57 ± 0.58	3.66	16.9	0.776
^{135}I	6,57h	c	11.9 ± 1.0	4.91	2.26	2.41
^{133}I	20,8h	c	15.8 ± 1.3	8.27	13.7	16.6
^{131}I	8,02070d	c	18.2 ± 1.3	10.5	34.2	29.4
^{126}I	13,11d	i	8.62 ± 1.02	4.86	17.5	4.74
^{124}I	4,1760d	i	7.90 ± 0.61	4.91	15.1	1.76
^{121}I	2,12h	c	5.01 ± 0.40	4.10	7.30	0.245
^{132}Te	3,204d	c	10.0 ± 0.8	6.25	11.7	19.8
^{127}Sb	3,85d	c	10.5 ± 0.9	8.04	25.6	17.8
^{125}Sb	2,75856y	c	19.7 ± 1.6	11.2	26.4	23.3
^{122}Sb	2,7238d	i(m+g)	11.6 ± 0.9	4.31	13.9	9.77
^{111}In	2,8047d	c	5.45 ± 0.43	5.47	7.29	1.00
^{112}Ag	3,130h	c	58.2 ± 6.4	17.7	2.42	21.8
^{112}Ag	3,130h	i	23.2 ± 2.6	5.25	1.65	8.10
^{111}Ag	7,45d	c	57.7 ± 5.4	19.7	4.46	25.4
^{105}Ag	41,29d	c	2.82 ± 0.28	5.02	1.34	0.777
^{107}Rh	21,7m	c*	58.2 ± 6.9	20.9	3.80	26.8
^{105}Rh	35,36h	i(m+g)	10.4 ± 3.6	8.07	2.48	9.05
^{106}Ru	373,59d	c	38.8 ± 3.1	15.2	3.87	20.1
^{105}Ru	4,44h	c	52.4 ± 3.8	17.4	6.47	26.4
^{103}Ru	39,26d	c	70.1 ± 5.4	23.3	18.1	37.8
^{104}Tc	18,3m	c	34.2 ± 2.9	13.9	9.32	19.8
^{101}Tc	14,22m	c	52.7 ± 8.9	21.6	27.8	37.5
^{99}Mo	65,94h	c	61.0 ± 4.4	16.9	16.2	24.0
^{96}Nb	23,35h	i	19.3 ± 1.4	6.38	5.33	13.0
^{90}Nb	14,60h	c*	1.89 ± 0.14	2.50	0.199	0.534
^{97}Zr	16,744h	c	31.9 ± 2.3	12.3	23.8	19.3
^{95}Zr	64,02d	c	46.3 ± 3.3	17.5	32.2	29.1
^{88}Zr	83,4d	c	2.27 ± 0.18	5.89	2.22	1.82
^{94}Y	18,7m	i	34.2 ± 3.2	5.51	14.1	10.6
^{92}Y	3,54h	c	45.9 ± 6.4	18.6	37.2	29.4
^{92}Y	3,54h	i	15.4 ± 3.5	5.69	16.4	14.5
^{88}Y	106,65d	i(m+g)	10.9 ± 0.8	6.24	10.2	4.85
^{86}Y	14,74h	c	2.56 ± 0.19	4.79	0.463	0.531
^{91}Sr	9,63h	c	30.6 ± 2.3	13.0	25.1	20.9
^{83}Sr	32,41h	c	1.33 ± 0.63	3.31	1.71	0.879
^{89}Rb	15,15m	c*	28.1 ± 3.2	16.0	17.7	10.6
^{86}Rb	18,631d	i(m+g)	18.6 ± 1.4	6.61	29.2	22.3
^{83}Rb	86,2d	c	8.99 ± 0.76	9.56	13.2	3.35
^{88}Kr	2,84h	c	14.4 ± 1.3	8.90	5.56	3.40
^{87}Kr	76,3m	c	18.4 ± 1.7	8.26	7.61	7.23

Table 86, cont'd.

Product	$T_{1/2}$	Type	Exp yield [mbarn]	Calculated Yields [mbarn] via LAHET	CASCADE	INUCL
^{77}Br	57,036h	c	1.57 ± 0.15	4.96	2.21	0.879
^{75}Se	119,779d	c	2.99 ± 0.26	4.26	5.02	1.49
^{78}As	90,7m	i	8.23 ± 1.53	3.28	6.31	1.70
^{76}As	1,0778d	i	8.12 ± 0.70	3.69	9.05	2.41
^{74}As	17,77d	i	4.99 ± 0.50	3.63	3.85	1.41
^{78}Ge	88m	c	3.18 ± 0.38	5.07	1.39	0.634
^{73}Ga	4,86h	c	6.61 ± 0.54	6.15	2.63	1.02
^{72}Ga	14,10h	i(m+g)	5.84 ± 0.47	2.43	2.64	0.838
^{72}Zn	46,5h	c	2.88 ± 0.24	3.32	0.690	0.286
^{65}Zn	244,26d	c	1.41 ± 0.16	2.06	0.531	0.368
^{66}Ni	54,6h	c	3.23 ± 0.43	2.68	0.595	0.306
^{58}Co	70,86d	i(m+g)	0.831 ± 0.068	1.26	0.023	0.041
^{59}Fe	44,472d	c	4.34 ± 0.35	2.48	0.309	0.143
^{56}Mn	2,5789h	c	3.72 ± 0.40	2.18	0.141	0.082
^{48}V	15,9735d	c	0.141 ± 0.038	0.219	–	–
^{48}Sc	43,67h	i	1.17 ± 0.11	0.630	0.014	–
^{46}Sc	83,79d	i(m+g)	1.00 ± 0.10	0.420	–	–
^{43}K	22,3h	c	1.42 ± 0.11	0.849	–	–
^{28}Mg	20,915h	c	0.608 ± 0.052	–	–	–
^{24}Na	14,9590h	c	1.27 ± 0.11	0.238	–	–
^{7}Be	53,29d	i	5.78 ± 1.23	–	–	–

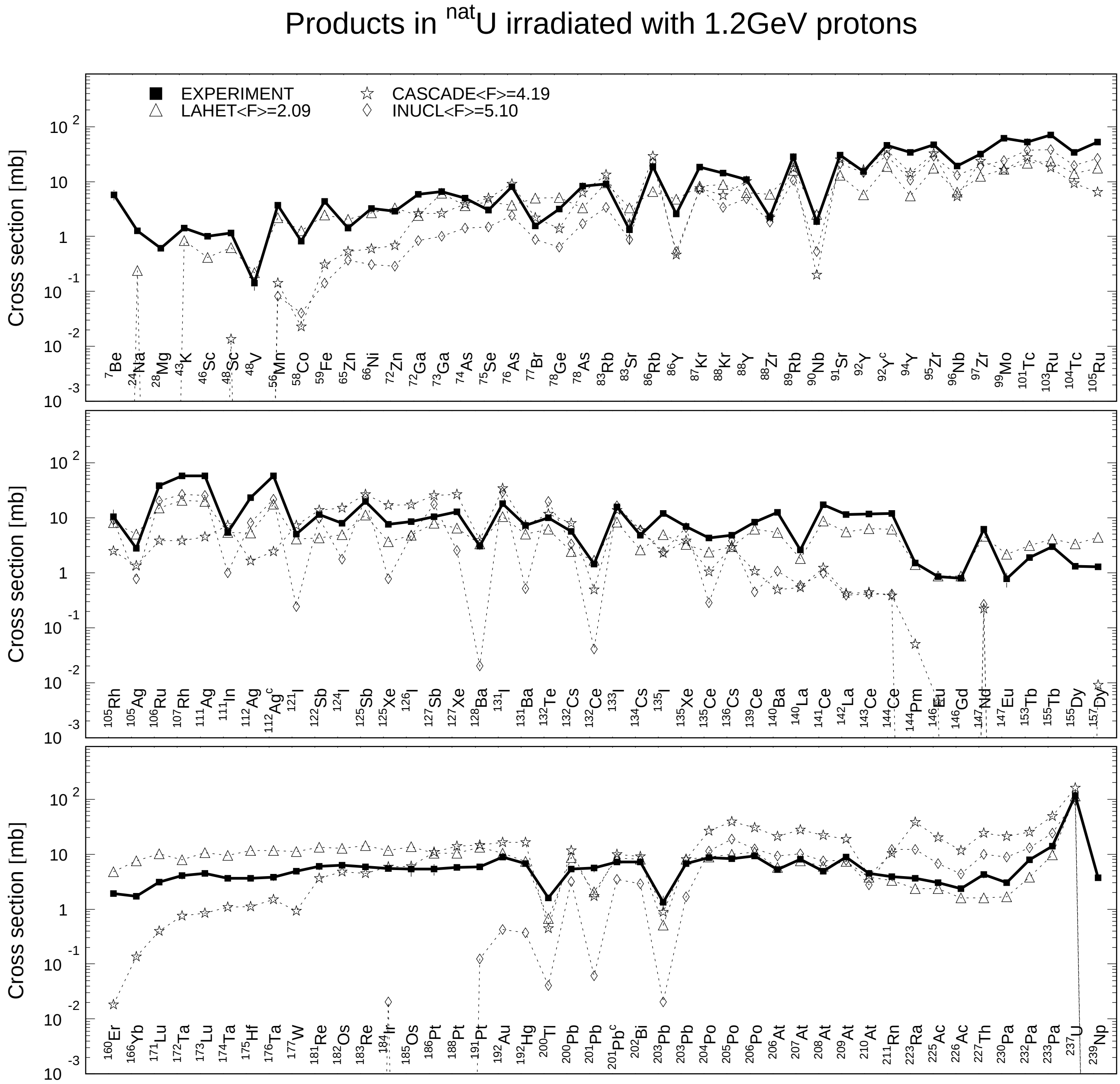

Fig. 85: Detailed comparison between experimental and simulated yields of radioactive reaction products in ^{nat}U irradiated with 1.2 GeV protons. The cumulative yields are labeled -c when the respective independent yields are also shown.

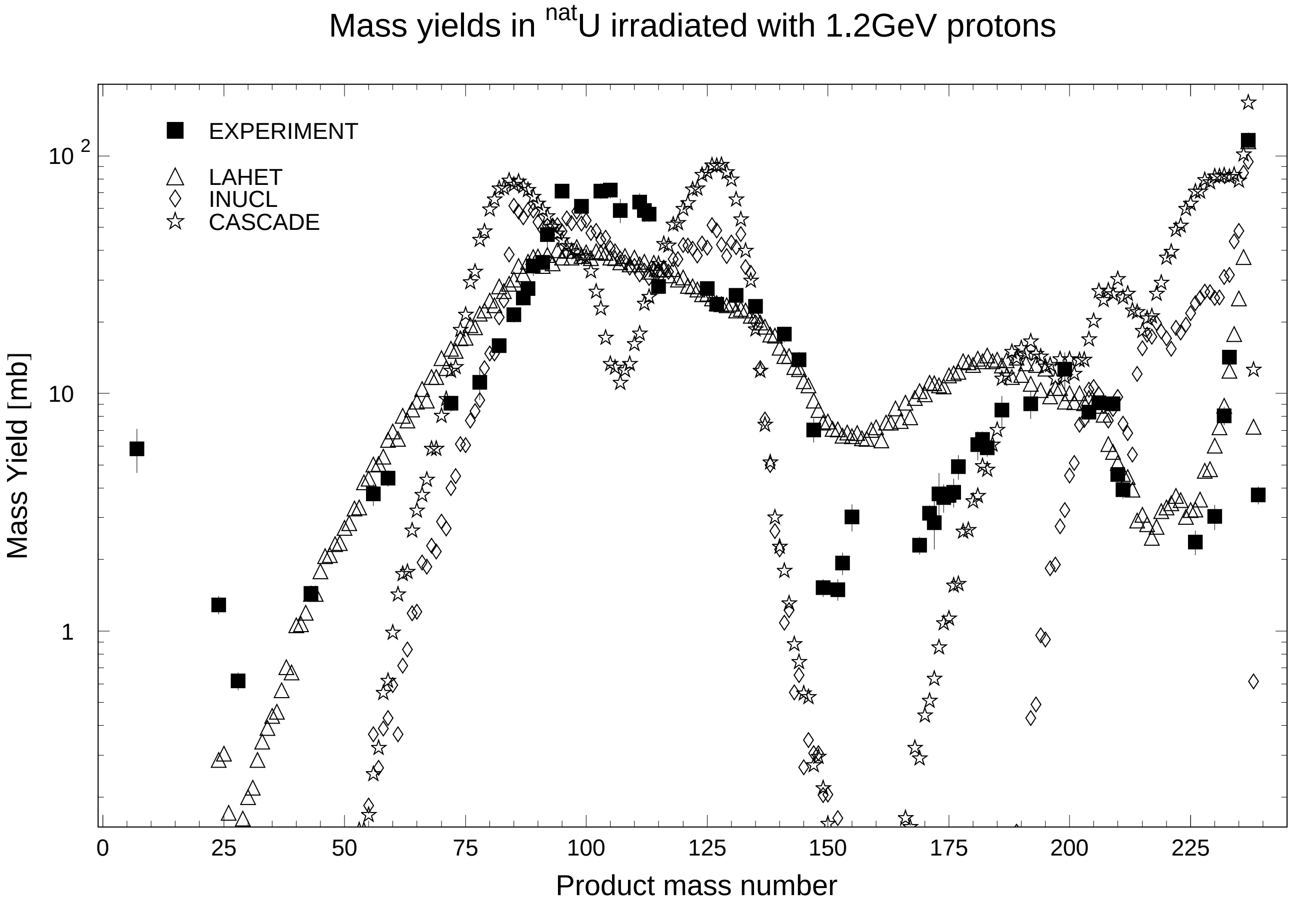

Fig. 86: The simulated mass distributions of reaction products together with the measured cumulative and supra-cumulative yields in ^{nat}U irradiated with 1.2 GeV protons.

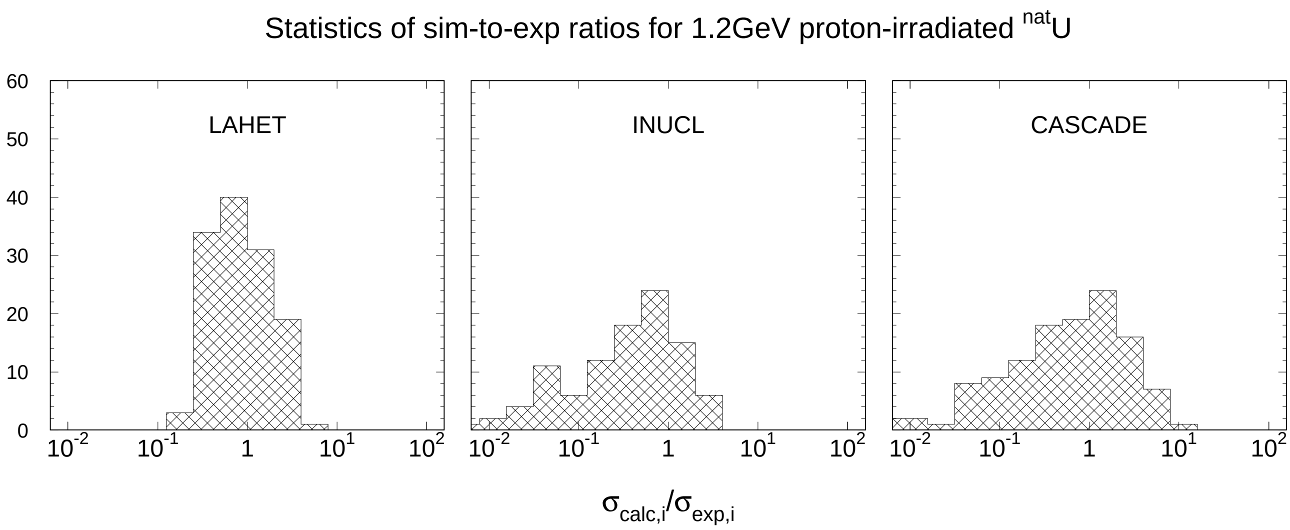

Fig. 87: Statistics of the simulation-to-experiment ratios (criterion 2) for ^{nat}U irradiated with 1.2 GeV protons.

Table 87: Experimental and calculated yields from ^{nat}U irradiated with 1.6 GeV protons.

Product	$T_{1/2}$	Type	Exp yield [mbarn]	Calculated Yields [mbarn] via LAHET	CASCADE	INUCL
^{239}Np	2,3565d	i	3.51 ± 0.47	–	–	–
^{237}U	6,75d	c	108. ± 10.	111.	152.	88.4
^{233}Pa	26,967d	c	12.7 ± 1.1	8.83	40.2	23.5
^{232}Pa	1,31d	i	7.18 ± 0.70	3.72	20.2	12.3
^{230}Pa	17,4d	i	2.73 ± 0.34	1.33	16.6	7.39
^{228}Pa	22h	c	1.25 ± 0.32	0.314	12.9	6.83
^{227}Th	18,72d	c	2.95 ± 0.44	1.34	18.7	9.05
^{226}Ac	29,37h	i	1.80 ± 0.21	1.34	9.74	3.81
^{223}Ra	11,435d	c	2.65 ± 0.50	1.98	31.8	10.7
^{211}Rn	14,6h	c	3.17 ± 0.30	2.61	10.8	11.8
^{210}At	8,1h	c	3.54 ± 0.32	2.77	4.60	2.96
^{209}At	5,41h	c	7.03 ± 0.62	5.54	19.0	8.00
^{208}At	1,63h	c*	4.20 ± 0.47	4.45	21.9	7.67
^{207}At	1,80h	c	6.07 ± 0.85	5.55	26.3	10.8
^{206}At	30,6m	c*	4.65 ± 0.54	4.19	19.7	9.26
^{206}Po	8,8d	c	7.66 ± 0.65	8.13	31.2	12.4
^{205}Po	1,66h	c*	7.27 ± 0.98	7.25	40.6	20.0
^{204}Po	3,53h	c*	7.53 ± 0.69	5.81	28.0	11.9
^{202}Bi	1,72h	c	6.69 ± 0.61	5.69	10.2	3.38
^{203}Pb	51,873h	c	5.66 ± 0.48	5.74	11.1	1.53
^{201}Pb	9,33h	c	6.21 ± 0.67	5.81	12.2	2.78
^{201}Pb	9,33h	i(m+g)	4.07 ± 0.93	1.40	2.75	0.103
^{200}Pb	21,5h	c	4.88 ± 0.42	5.81	14.2	3.66
^{200}Tl	26,1h	i(m+g)	0.923 ± 0.362	0.657	1.14	0.021
^{192}Hg	4,85h	c	8.00 ± 0.80	5.60	22.0	0.344
^{192}Au	4,94h	c	10.8 ± 1.6	7.62	22.6	0.344
^{191}Pt	2,802d	c	6.27 ± 0.87	9.85	21.9	0.246
^{188}Pt	10,2d	c	6.94 ± 0.85	7.87	23.8	0.061
^{186}Pt	2,08h	c	7.82 ± 1.82	8.37	23.0	0.021
^{184}Ir	3,09h	c	8.24 ± 0.87	9.82	15.3	0.102
^{185}Os	93,6d	c	7.54 ± 1.52	11.3	13.0	0.021
^{182}Os	22,10h	c	10.0 ± 0.9	11.5	12.6	0.082
^{183}Re	70,0d	c	8.81 ± 0.85	11.8	11.0	0.041
^{181}Re	19,9h	c	9.61 ± 1.41	11.4	10.7	–
^{177}W	135m	c	7.20 ± 0.90	10.9	3.49	0.021
^{176}Ta	8,09h	c	7.93 ± 1.02	11.2	7.67	0.021
^{174}Ta	1,14h	c	8.15 ± 1.03	10.5	5.93	0.021
^{175}Hf	70d	c	7.73 ± 0.72	11.1	6.11	–
^{172}Hf	1,87y	c	6.80 ± 0.70	10.9	5.59	0.021
^{173}Lu	1,37y	c	5.99 ± 0.88	11.0	5.23	–
^{171}Lu	8,24d	c	7.22 ± 0.64	11.1	3.22	–
^{170}Lu	2,012d	c	5.94 ± 1.01	10.6	3.83	0.019
^{169}Yb	32,026d	c	6.44 ± 0.62	10.8	3.30	0.041
^{166}Yb	56,7h	c	5.43 ± 0.53	10.0	2.26	–
^{160}Er	28,58h	c	4.22 ± 0.48	8.73	0.682	–
^{157}Dy	8,14h	c	3.38 ± 0.33	9.78	0.506	–
^{155}Dy	9,9h	c*	2.66 ± 0.28	7.92	0.288	–
^{155}Tb	5,32d	c	4.38 ± 0.48	9.24	0.273	–
^{153}Tb	2,34d	c*	2.81 ± 0.32	8.78	0.083	–
^{146}Gd	48,27d	c	1.71 ± 0.16	3.72	0.045	–
^{147}Eu	24,1d	c	2.65 ± 0.31	7.38	0.027	–
^{146}Eu	4,61d	i	1.05 ± 0.10	3.28	–	–
^{145}Eu	5,93d	c	2.19 ± 0.31	4.97	0.031	–
^{144}Pm	363d	i	1.28 ± 0.16	2.09	0.014	–
^{147}Nd	10,98d	c	6.28 ± 0.74	4.00	0.246	0.184

Table 87, cont'd.

Product	$T_{1/2}$	Type	Exp yield [mbarn]	Calculated Yields [mbarn] via LAHET	CASCADE	INUCL
^{144}Ce	284,893d	c	11.6 ± 1.3	5.02	0.327	0.572
^{143}Ce	33,039h	c	10.4 ± 0.9	5.48	0.341	0.532
^{141}Ce	32,501d	c	15.4 ± 1.3	7.45	0.853	0.819
^{139}Ce	137,640d	c	7.82 ± 0.68	10.2	0.853	0.697
^{135}Ce	17,7h	c	4.64 ± 0.43	4.82	0.826	0.246
^{132}Ce	3,51h	c	2.01 ± 0.21	2.94	0.505	0.021
^{142}La	91,1m	c	10.4 ± 1.1	4.77	0.321	0.471
^{140}La	1,6781d	i	2.18 ± 0.30	1.52	0.444	0.266
^{140}Ba	12,752d	c	11.7 ± 1.0	5.04	0.478	0.655
^{131}Ba	11,50d	c	6.67 ± 0.64	6.83	5.75	0.962
^{128}Ba	2,43d	c	3.54 ± 0.46	4.89	3.11	0.164
^{136}Cs	13,16d	i(m+g)	3.87 ± 0.33	2.66	2.63	3.41
^{134}Cs	2,0648y	i(m+g)	3.97 ± 0.38	2.10	4.99	4.87
^{132}Cs	6,479d	i	4.94 ± 0.48	2.33	6.43	2.87
^{135}Xe	9,14h	i(m+g)	5.88 ± 0.58	2.29	3.58	5.53
^{127}Xe	36,4d	c	11.8 ± 1.0	7.30	21.2	2.52
^{125}Xe	16,9h	c	7.83 ± 0.67	4.21	13.8	0.942
^{135}I	6,57h	c	11.0 ± 0.9	4.05	2.35	1.88
^{133}I	20,8h	c	14.5 ± 1.3	6.56	12.3	14.5
^{131}I	8,02070d	c	15.6 ± 1.3	9.60	29.6	24.8
^{126}I	13,11d	i	6.40 ± 0.73	3.88	13.6	4.30
^{124}I	4,1760d	i	6.29 ± 0.67	3.77	12.4	2.04
^{121}I	2,12h	c	6.14 ± 0.54	3.96	7.26	0.430
^{132}Te	3,204d	c	8.93 ± 0.78	5.30	10.4	19.2
^{127}Sb	3,85d	c	9.13 ± 0.85	7.53	21.6	16.5
^{125}Sb	2,75856y	c	14.9 ± 1.8	8.68	21.4	19.4
^{122}Sb	2,7238d	i(m+g)	9.26 ± 0.79	3.38	11.5	9.19
^{111}In	2,8047d	c	6.47 ± 0.56	5.11	9.82	2.28
^{112}Ag	3,130h	c	48.7 ± 6.2	14.7	2.18	21.1
^{112}Ag	3,130h	i	18.8 ± 2.4	3.97	1.47	9.23
^{111}Ag	7,45d	c	46.6 ± 4.8	14.2	3.81	25.1
^{105}Ag	41,29d	c	3.56 ± 0.32	5.05	2.61	1.27
^{107}Rh	21,7m	c*	52.3 ± 6.6	17.2	3.41	26.0
^{105}Rh	35,36h	i(m+g)	18.0 ± 3.7	6.89	3.23	10.8
^{106}Ru	373,59d	c	31.3 ± 2.9	12.8	3.41	19.7
^{105}Ru	4,44h	c	42.3 ± 3.5	14.0	5.39	25.4
^{103}Ru	39,26d	c	57.0 ± 4.8	18.4	16.2	38.4
^{104}Tc	18,3m	c	35.8 ± 3.6	11.7	8.05	19.8
^{101}Tc	14,22m	c	50.8 ± 9.0	17.3	24.4	34.7
^{99}Mo	65,94h	c	51.5 ± 4.5	15.3	16.1	26.5
^{96}Nb	23,35h	i	16.5 ± 1.5	5.28	4.69	13.6
^{90}Nb	14,60h	c*	2.51 ± 0.21	3.02	0.416	0.511
^{97}Zr	16,744h	c	27.1 ± 2.3	9.65	21.2	16.8
^{95}Zr	64,02d	c	39.4 ± 3.5	14.1	26.3	27.2
^{88}Zr	83,4d	c	2.96 ± 0.25	7.54	3.83	4.34
^{94}Y	18,7m	i	31.7 ± 3.5	4.55	11.2	9.58
^{92}Y	3,54h	c	40.8 ± 5.9	15.6	29.9	27.6
^{92}Y	3,54h	i	17.4 ± 3.5	5.15	12.7	14.3
^{88}Y	106,65d	i(m+g)	11.2 ± 0.9	6.70	12.6	7.00
^{86}Y	14,74h	c	3.21 ± 0.27	5.71	0.921	1.41
^{91}Sr	9,63h	c	25.5 ± 2.2	11.3	20.5	19.4
^{83}Sr	32,41h	c	1.69 ± 0.80	4.28	2.21	2.28
^{89}Rb	15,15m	c*	31.1 ± 4.4	12.9	14.4	10.3
^{86}Rb	18,631d	i(m+g)	17.5 ± 1.5	5.60	24.8	22.2
^{83}Rb	86,2d	c	10.2 ± 1.0	11.4	13.9	5.92

Table 87, cont'd.

Product	$T_{1/2}$	Type	Exp yield [mbarn]	Calculated Yields [mbarn] via LAHET	CASCADE	INUCL
^{88}Kr	2,84h	c	13.0 ± 1.1	7.46	4.61	3.34
^{87}Kr	76,3m	c	15.8 ± 1.9	6.60	6.58	6.90
^{77}Br	57,036h	c	2.42 ± 0.25	7.20	2.57	1.62
^{75}Se	119,779d	c	3.75 ± 0.34	6.10	6.67	3.07
^{78}As	90,7m	i	9.02 ± 1.36	2.72	5.96	2.38
^{76}As	1,0778d	i	8.36 ± 0.79	3.52	8.48	3.03
^{74}As	17,77d	i	5.96 ± 0.64	5.05	4.72	2.06
^{78}Ge	88m	c	2.78 ± 0.50	4.25	0.989	0.655
^{73}Ga	4,86h	c	6.74 ± 0.68	4.79	2.66	1.53
^{72}Ga	14,10h	i(m+g)	5.69 ± 0.55	2.10	3.00	1.29
^{72}Zn	46,5h	c	2.34 ± 0.23	2.92	0.635	0.676
^{65}Zn	244,26d	c	1.74 ± 0.26	3.52	1.17	0.942
^{66}Ni	54,6h	c	2.81 ± 0.44	2.34	0.730	0.266
^{58}Co	70,86d	i(m+g)	1.30 ± 0.16	2.11	0.225	0.123
^{59}Fe	44,472d	c	4.50 ± 0.39	2.65	0.771	0.144
^{56}Mn	2,5789h	c	4.00 ± 0.45	2.41	0.409	0.123
^{54}Mn	312,11d	i	1.56 ± 0.22	2.29	0.246	0.123
^{48}V	15,9735d	c	0.252 ± 0.040	0.495	–	–
^{48}Sc	43,67h	i	1.40 ± 0.12	0.781	0.034	–
^{46}Sc	83,79d	i(m+g)	1.77 ± 0.15	0.933	0.034	–
^{43}K	22,3h	c	1.91 ± 0.17	1.12	0.014	–
^{28}Mg	20,915h	c	1.02 ± 0.09	–	–	–
^{24}Na	14,9590h	c	2.42 ± 0.22	0.352	–	–
^{7}Be	53,29d	i	5.82 ± 0.61	–	–	–

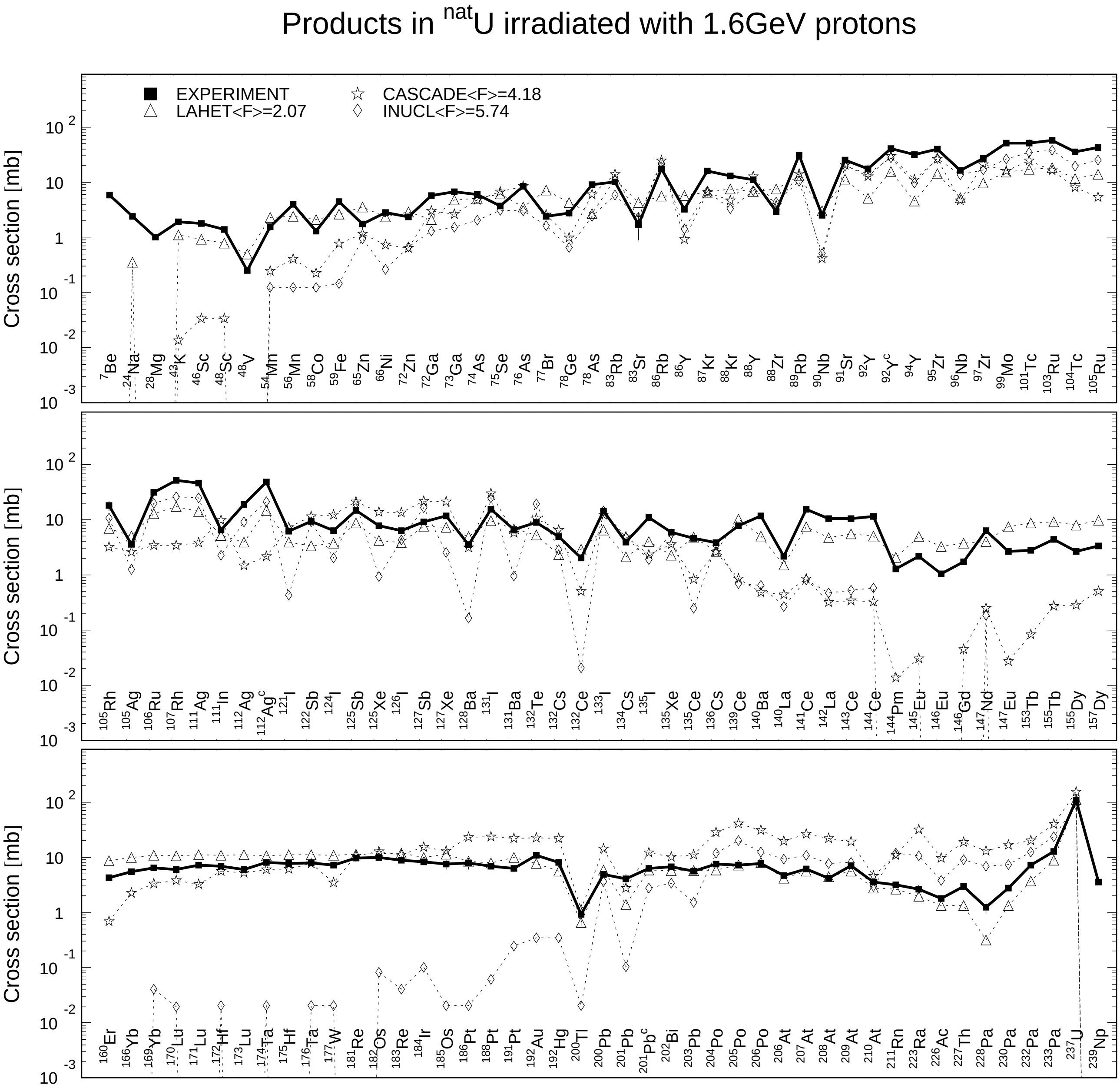

Fig. 88: Detailed comparison between experimental and simulated yields of radioactive reaction products in ^{nat}U irradiated with 1.6 GeV protons. The cumulative yields are labeled -c when the respective independent yields are also shown.

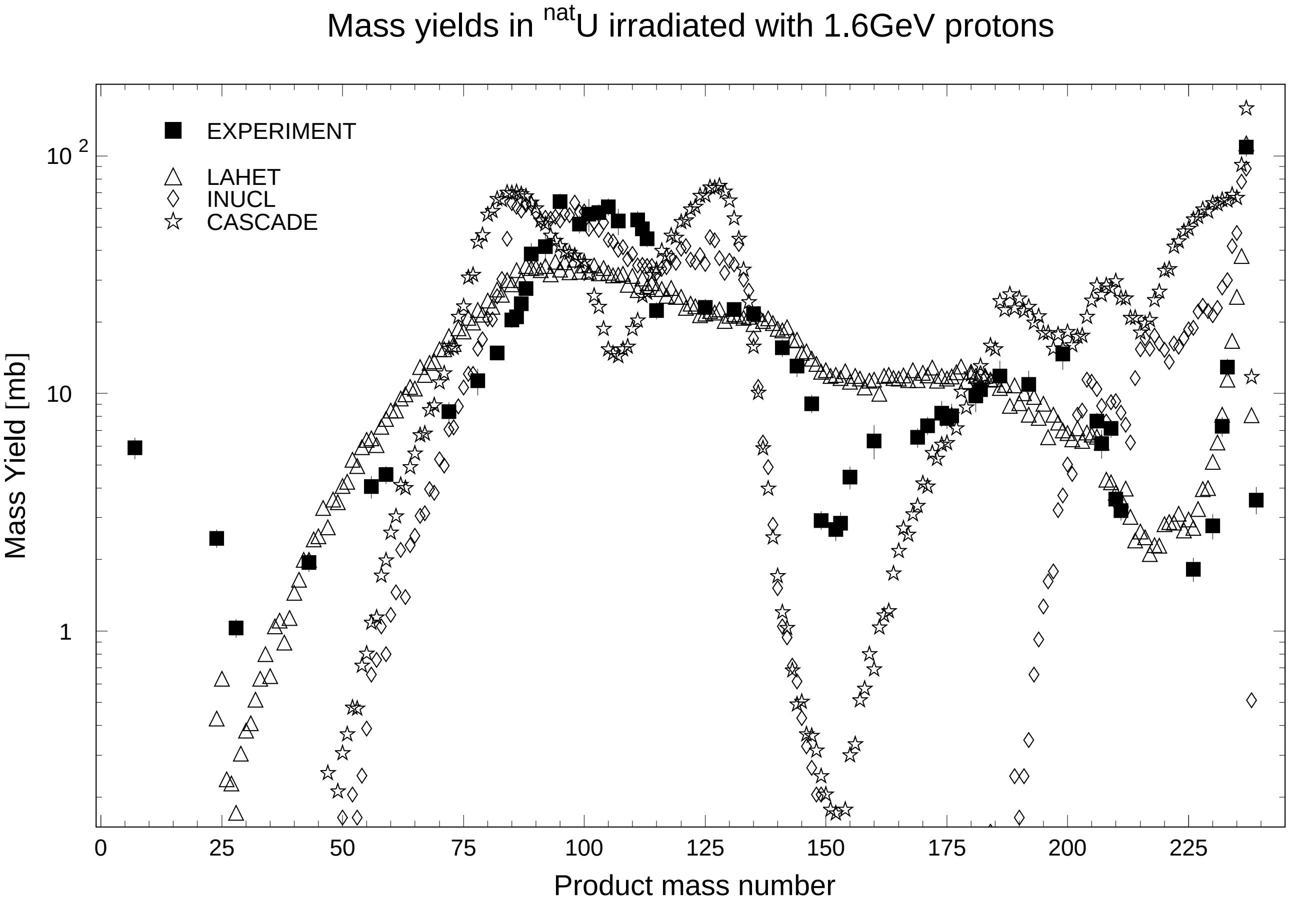

Fig. 89: The simulated mass distributions of reaction products together with the measured cumulative and supra-cumulative yields in ^{nat}U irradiated with 1.6 GeV protons.

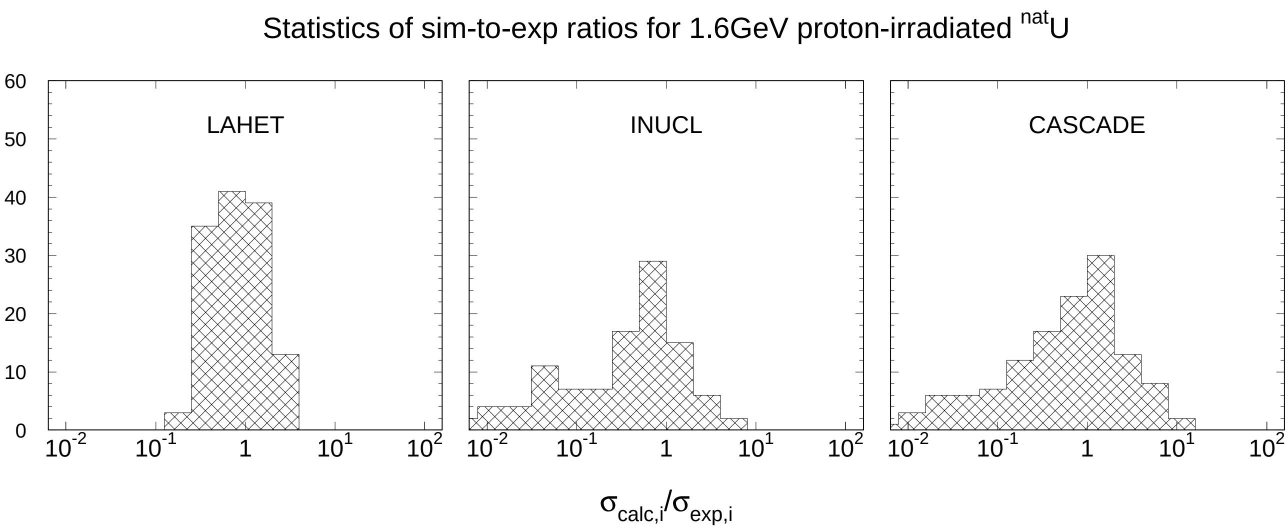

Fig. 90: Statistics of the simulation-to-experiment ratios (criterion 2) for ^{nat}U irradiated with 1.6 GeV protons.

Table 88: Experimental and calculated yields from ^{99}Tc irradiated with 0.1 GeV protons.

Product	$T_{1/2}$	Type	Exp yield [mbarn]	Calculated Yields [mbarn] via CEM95	LAHET	CASCADE	HETC	INUCL	YIELDX
^{97}Ru	2,791d	i	32.4 ± 2.5	39.2	37.9	48.2	35.9	31.5	28.0
^{95}Ru	1,643h	i	18.1 ± 1.6	17.4	31.8	46.0	52.1	33.7	13.7
^{94}Ru	51,8m	i	7.28 ± 0.80	1.30	8.86	41.4	65.2	33.9	5.52
^{90}Mo	5,56h	c	4.50 ± 0.39	0.054	1.37	4.15	–	3.60	6.69
^{90}Nb	14,60h	i(m1+m2+g)	27.0 ± 2.2	6.35	9.39	1.73	–	1.63	6.80

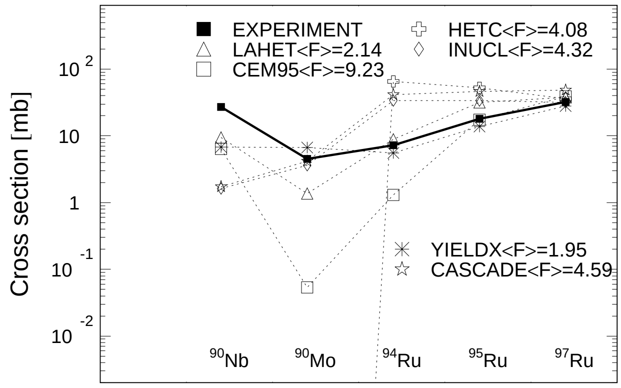

Fig. 91: Detailed comparison between experimental and simulated yields of radioactive reaction products in ^{99}Tc irradiated with 0.1 GeV protons. The cumulative yields are labeled -c when the respective independent yields are also shown.

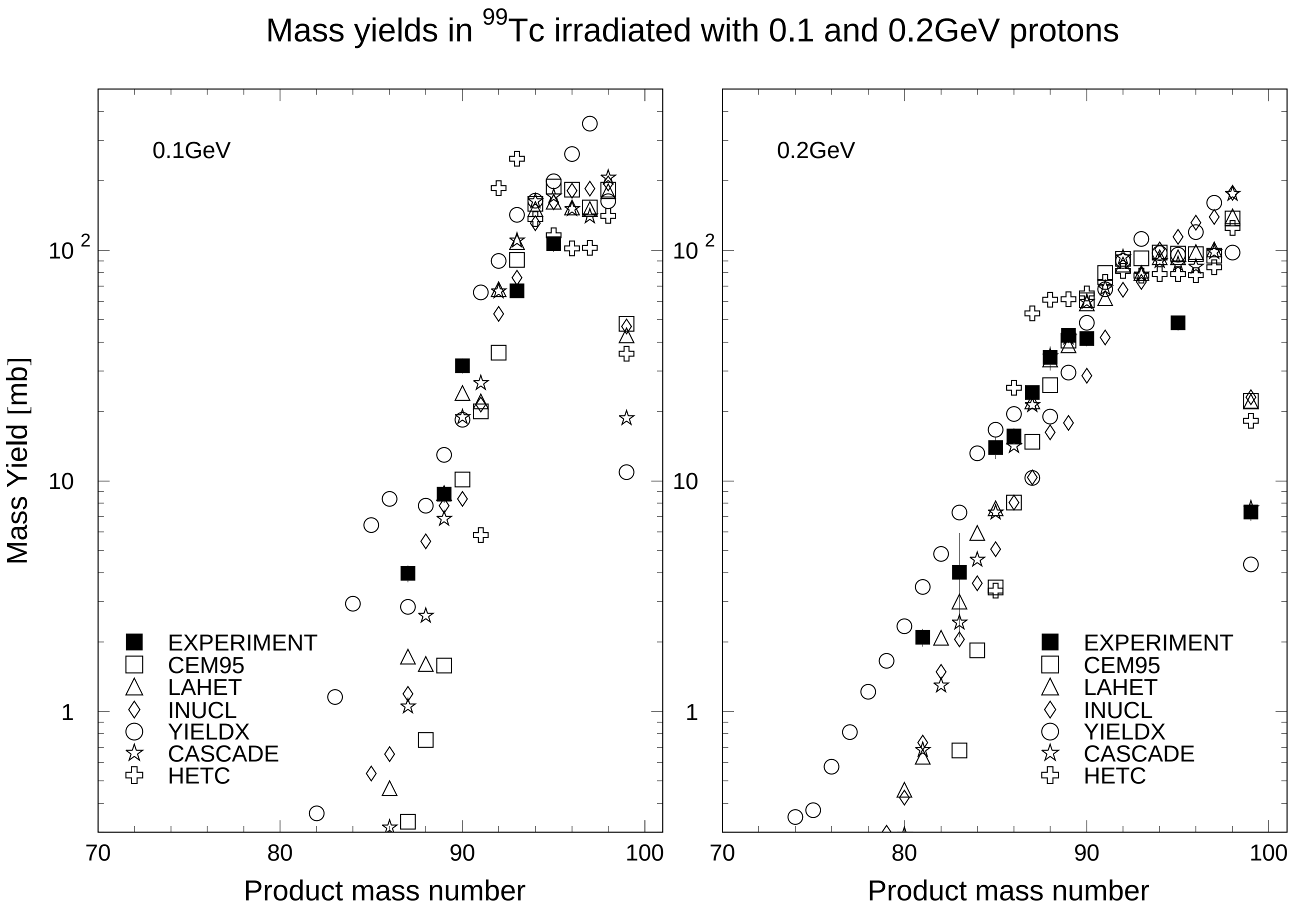

Fig. 92: The simulated mass distributions of reaction products together with the measured cumulative and supra-cumulative yields in ^{99}Tc irradiated with 0.1 and 0.2 GeV protons.

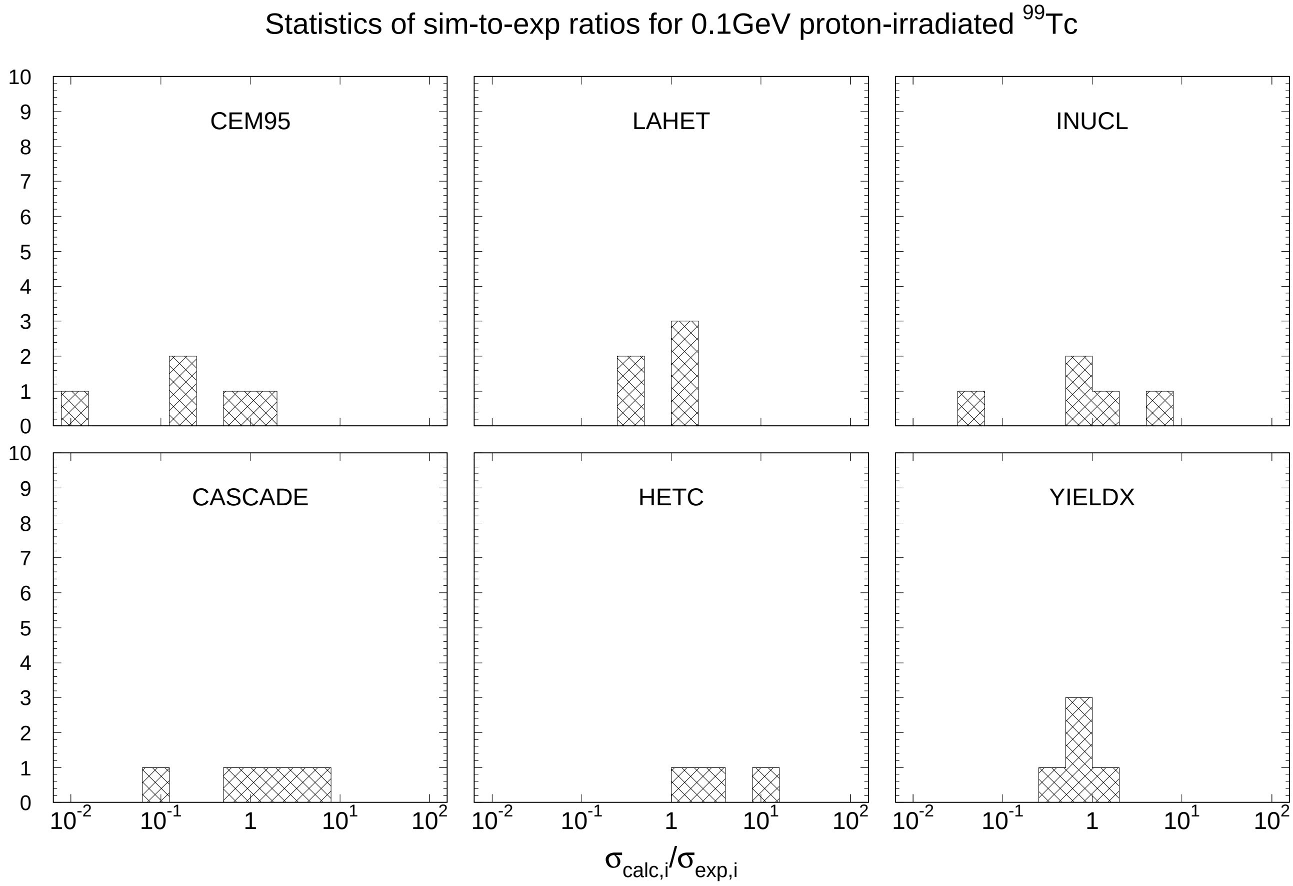

Fig. 93: Statistics of the simulation-to-experiment ratios (criterion 2) for ^{99}Tc irradiated with 0.1 GeV protons.

Table 89: Experimental and calculated yields from ^{99}Tc irradiated with 0.2 GeV protons.

Product	$T_{1/2}$	Type	Exp yield [mbarn]	Calculated Yields [mbarn] via CEM95	LAHET	CASCADE	HETC	INUCL	YIELDX
^{97}Ru	2,791d	i	14.0 ± 1.0	18.3	19.4	25.0	22.9	20.4	11.3
^{95}Ru	1,643h	i	6.30 ± 0.60	6.21	12.5	16.0	24.0	16.4	5.58
^{94}Ru	51,8m	i	2.31 ± 0.30	0.731	3.01	12.4	20.8	14.9	2.26
^{90}Mo	5,56h	c	7.06 ± 0.59	1.15	4.28	15.5	9.49	15.5	15.7
^{97}Nb	72,1m	i(m+g)	0.447 ± 0.054	3.03	0.797	3.01	0.832	3.93	0.277
^{90}Nb	14,60h	i(m1+m2+g)	35.0 ± 2.4	39.2	23.5	6.38	55.1	3.78	13.8
^{88}Zr	83,4d	c	28.3 ± 2.2	16.7	28.3	29.9	60.9	15.1	14.8
^{87}Zr	1,68h	c	15.6 ± 1.2	4.26	13.1	10.4	53.2	7.98	4.11
^{86}Zr	16,5h	c	5.09 ± 0.36	0.256	6.11	5.13	25.3	4.82	1.26
^{88}Y	106,65d	i(m+g)	8.43 ± 1.12	8.64	4.90	3.59	0.023	1.07	3.19
^{86}Y	14,74h	i(m+g)	11.1 ± 0.8	5.48	5.82	1.45	–	1.25	14.7
^{83}Sr	32,41h	c	4.06 ± 1.96	0.438	2.15	1.65	–	1.72	5.42

Table 90: Experimental and GNASH-calculated yields from ^{99}Tc irradieted with 0.2GeV protons.

Product	$T_{1/2}$	Type	Exp yield [mbarn]	Calculated Yields [mbarn] via GNASH
^{87m}Y	13,37h	i(m)	8.83 ± 0.85	11.4
^{94}Tc	293m	i	27.4± 1.8	22.0
^{94m}Tc	52.0m	i(m)	8.68 ± 0.78	2.8
^{96}Tc	4.28d	i(m+g)	50.0 ± 3.4	119
^{94}Ru	51.8m	i	2.31 ± 0.30	0.4
^{95}Ru	1.643h	i	6.30 ± 0.60	1.60
^{97}Ru	2.791d	i	14.0 ± 1.0	13.5

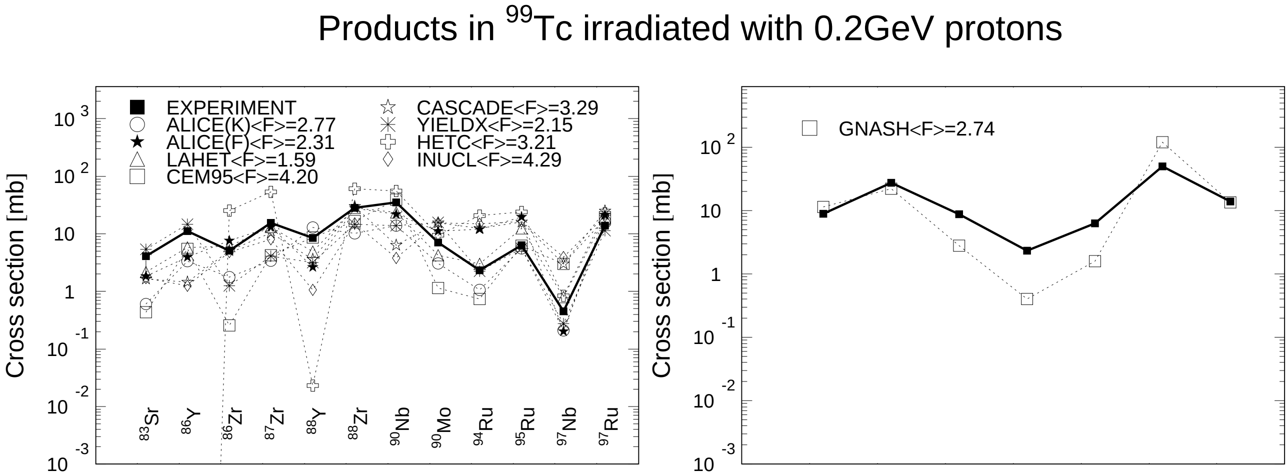

Fig. 94: Detailed comparison between experimental and simulated yields of radioactive reaction products in ^{99}Tc irradiated with 0.2 GeV protons. The cumulative yields are labeled -c when the respective independent yields are also shown.

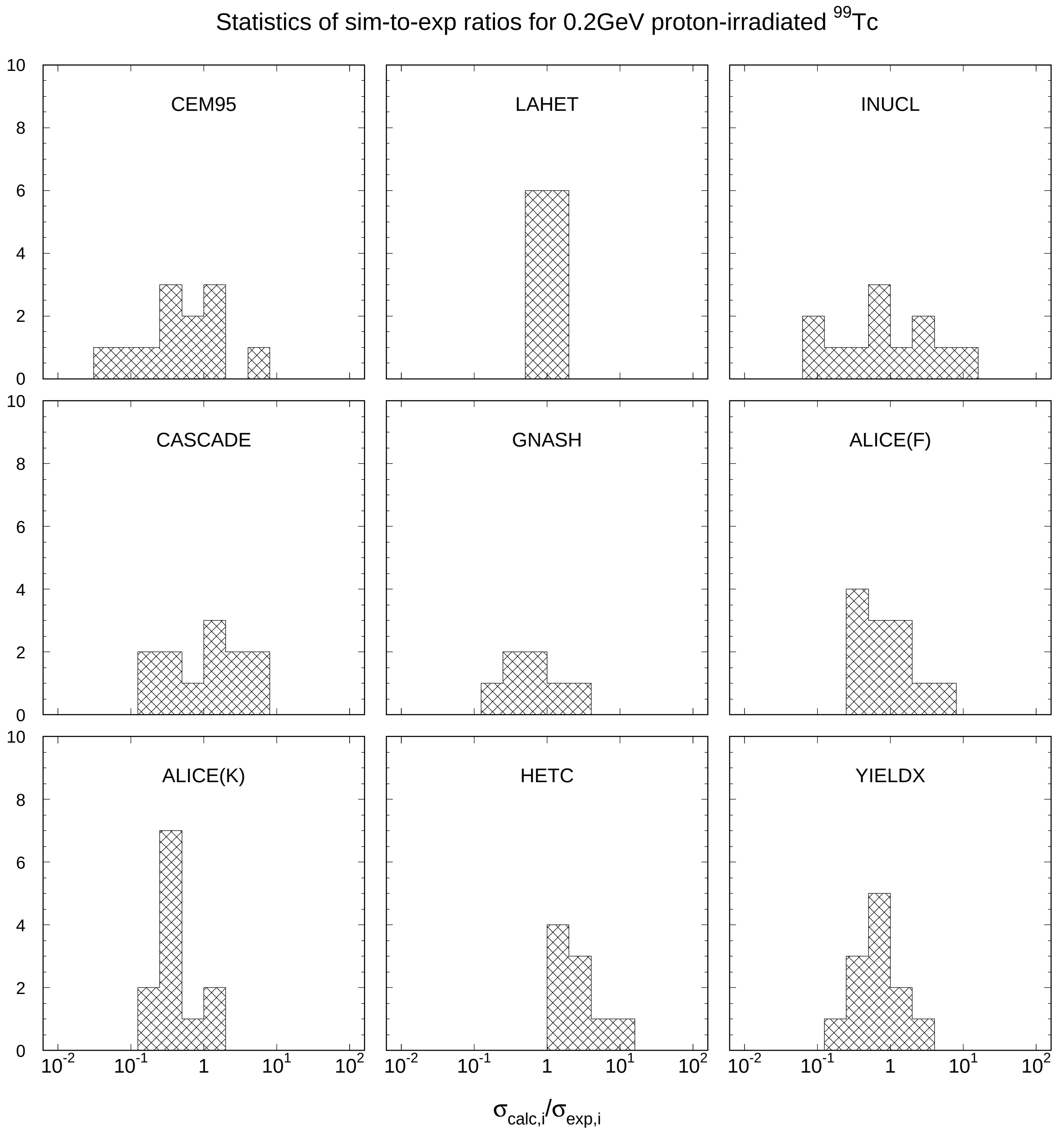

Fig. 95: Statistics of the simulation-to-experiment ratios (criterion 2) for ^{99}Tc irradiated with 0.2 GeV protons.

Table 91: Experimental and calculated yields from ^{99}Tc irradiated with 0.8 GeV protons.

Product	$T_{1/2}$	Type	Exp yield [mbarn]	Calculated Yields [mbarn] via CEM95	LAHET	CASCADE	HETC	INUCL	YIELDX
^{97}Ru	2,791d	i	3.58 ± 0.23	3.91	4.95	4.68	3.47	2.62	1.84
^{95}Ru	1,643h	i	1.66 ± 0.17	1.43	3.32	3.05	3.84	2.85	0.917
^{94}Ru	51,8m	i	0.692 ± 0.176	0.211	1.01	2.12	3.23	3.90	0.373
^{90}Mo	5,56h	c	4.56 ± 0.35	1.13	3.52	9.22	4.16	20.6	11.8
^{96}Nb	23,35h	i	3.21 ± 0.21	4.12	3.56	7.66	2.74	8.58	1.90
^{90}Nb	14,60h	i(m1+m2+g)	27.9 ± 1.7	27.7	20.5	4.62	34.1	7.58	14.2
^{88}Zr	83,4d	c	35.4 ± 2.2	28.2	41.2	39.9	41.0	47.6	15.4
^{87}Zr	1,68h	c	23.5 ± 1.7	13.9	24.0	18.3	41.6	31.4	4.23
^{86}Zr	16,5h	c	11.0 ± 0.7	2.64	18.3	14.5	43.7	23.5	1.29
^{88}Y	106,65d	i(m+g)	11.8 ± 0.8	14.3	9.91	6.89	0.823	5.57	10.3
^{86}Y	14,74h	i(m+g)	25.0 ± 1.5	30.5	16.8	5.51	1.40	7.34	15.2
^{83}Sr	32,41h	c	28.1 ± 7.6	23.2	21.3	23.4	41.2	22.7	25.3
^{82}Sr	25,55d	c	17.4 ± 1.4	9.98	16.2	18.2	42.2	16.7	15.9
^{81}Sr	22,3m	c	3.83 ± 0.70	1.32	1.73	2.58	8.82	7.45	3.85
^{80}Sr	106,3m	c	1.70 ± 0.27	0.222	0.060	2.78	–	3.85	1.09
^{84}Rb	32,77d	i(m+g)	4.99 ± 0.34	6.80	3.54	3.59	0.052	2.16	3.69
^{83}Rb	86,2d	c	39.8 ± 2.9	37.2	29.6	34.6	41.3	27.5	35.8
^{79}Rb	22,9m	c*	6.63 ± 0.88	3.81	1.69	2.49	8.75	1.95	5.50
^{79}Kr	35,04h	c	22.6 ± 1.5	24.2	15.4	19.8	32.0	11.4	27.2
^{77}Kr	74,4m	c	8.22 ± 0.65	4.94	7.11	6.02	29.2	5.40	5.91
^{76}Kr	14,8h	c	2.48 ± 0.38	0.811	2.01	3.87	10.0	2.97	2.17
^{77}Br	57,036h	c	18.9 ± 1.3	22.5	15.4	15.2	29.2	8.02	24.5
^{76}Br	16,2h	i(m+g)	11.4 ± 0.8	14.9	9.44	1.14	17.7	1.25	13.9
^{75}Se	119,779d	c	18.1 ± 1.3	18.3	11.1	12.9	24.1	5.16	19.5
^{72}Se	8,40d	c	2.93 ± 0.21	1.15	1.17	3.17	15.1	1.95	3.10
^{74}As	17,77d	i	3.53 ± 0.33	3.76	2.19	2.09	–	0.477	3.30
^{72}As	26,0h	i	7.97 ± 0.55	9.61	4.97	0.673	0.114	0.755	10.9
^{71}As	65,28h	c	7.77 ± 0.52	5.81	3.64	2.49	13.6	1.38	7.69
^{69}Ge	39,05h	c	4.66 ± 0.50	5.06	2.76	3.33	9.22	1.48	6.84
^{67}Ge	18,9m	c	0.840 ± 0.138	0.122	0.081	0.247	0.009	0.300	0.640
^{67}Ga	3,2612d	c	5.28 ± 0.52	4.39	2.19	2.19	5.49	0.766	7.05
^{66}Ga	9,49h	c*	2.80 ± 0.22	2.46	0.886	0.348	4.45	0.283	2.54
^{65}Zn	244,26d	c	4.35 ± 0.53	2.91	1.29	1.95	3.04	0.810	5.87
^{58}Co	70,86d	i(m+g)	1.33 ± 0.14	0.211	0.161	0.101	–	0.089	1.91
^{48}V	15,9735d	c*	0.333 ± 0.029	–	–	–	–	0.012	0.071
^{24}Na	14,9590h	c	0.341 ± 0.038	–	–	–	–	–	0.119
^{7}Be	53,29d	i	4.16 ± 0.91	–	–	–	–	–	0.845

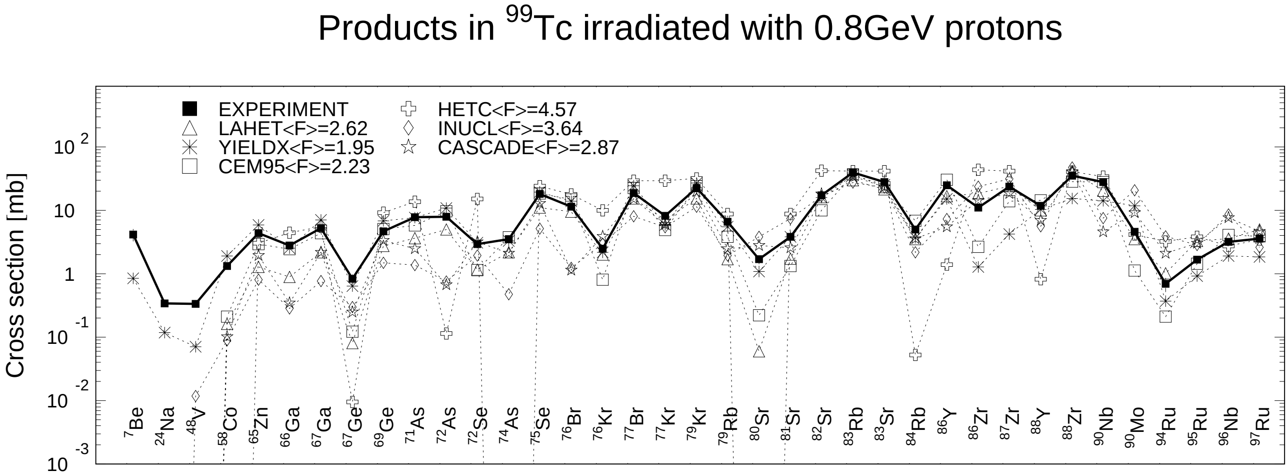

Fig. 96: Detailed comparison between experimental and simulated yields of radioactive reaction products in ^{99}Tc irradiated with 0.8 GeV protons. The cumulative yields are labeled -c when the respective independent yields are also shown.

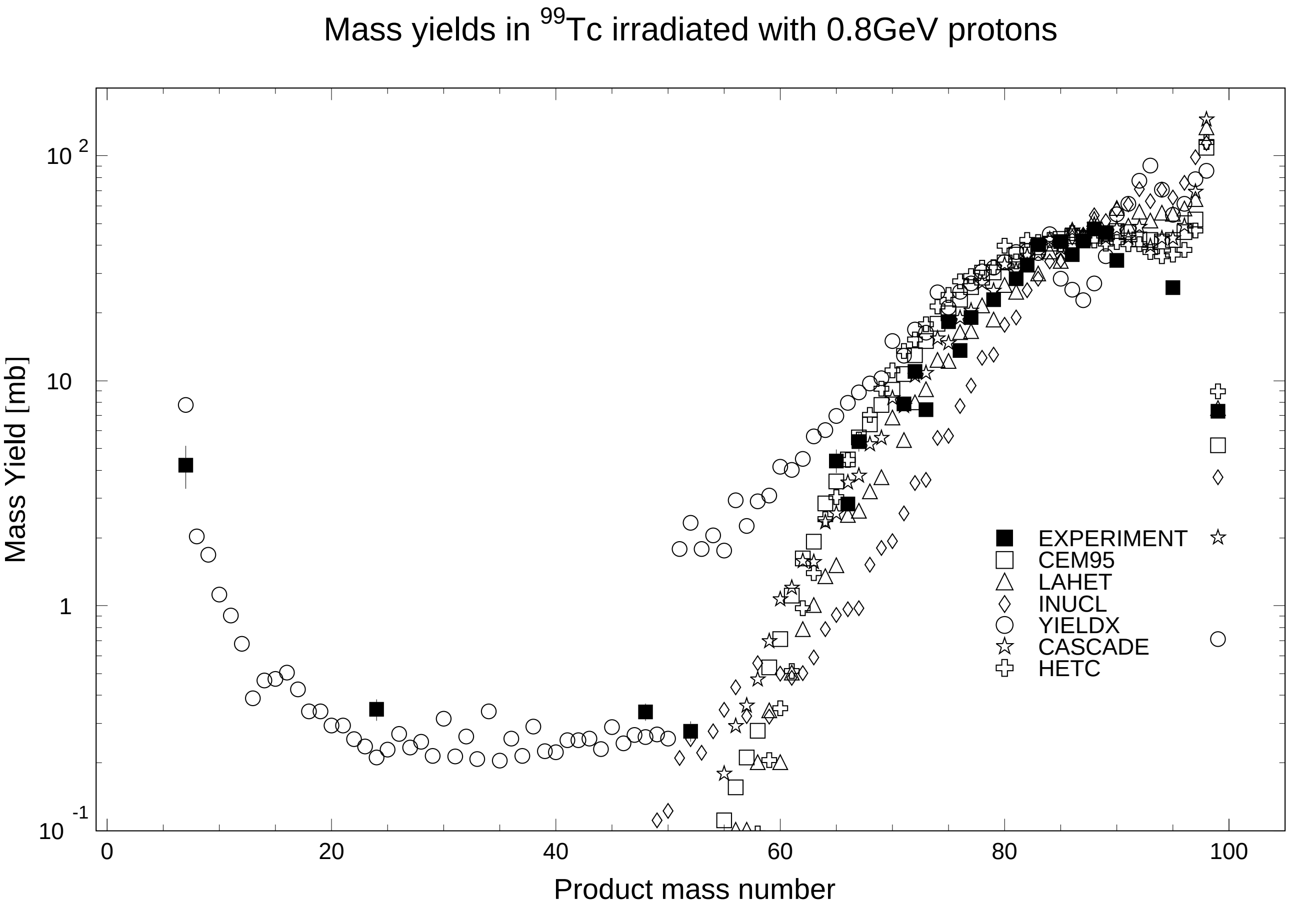

Fig. 97: The simulated mass distributions of reaction products together with the measured cumulative and supra-cumulative yields in ^{99}Tc irradiated with 0.8 GeV protons.

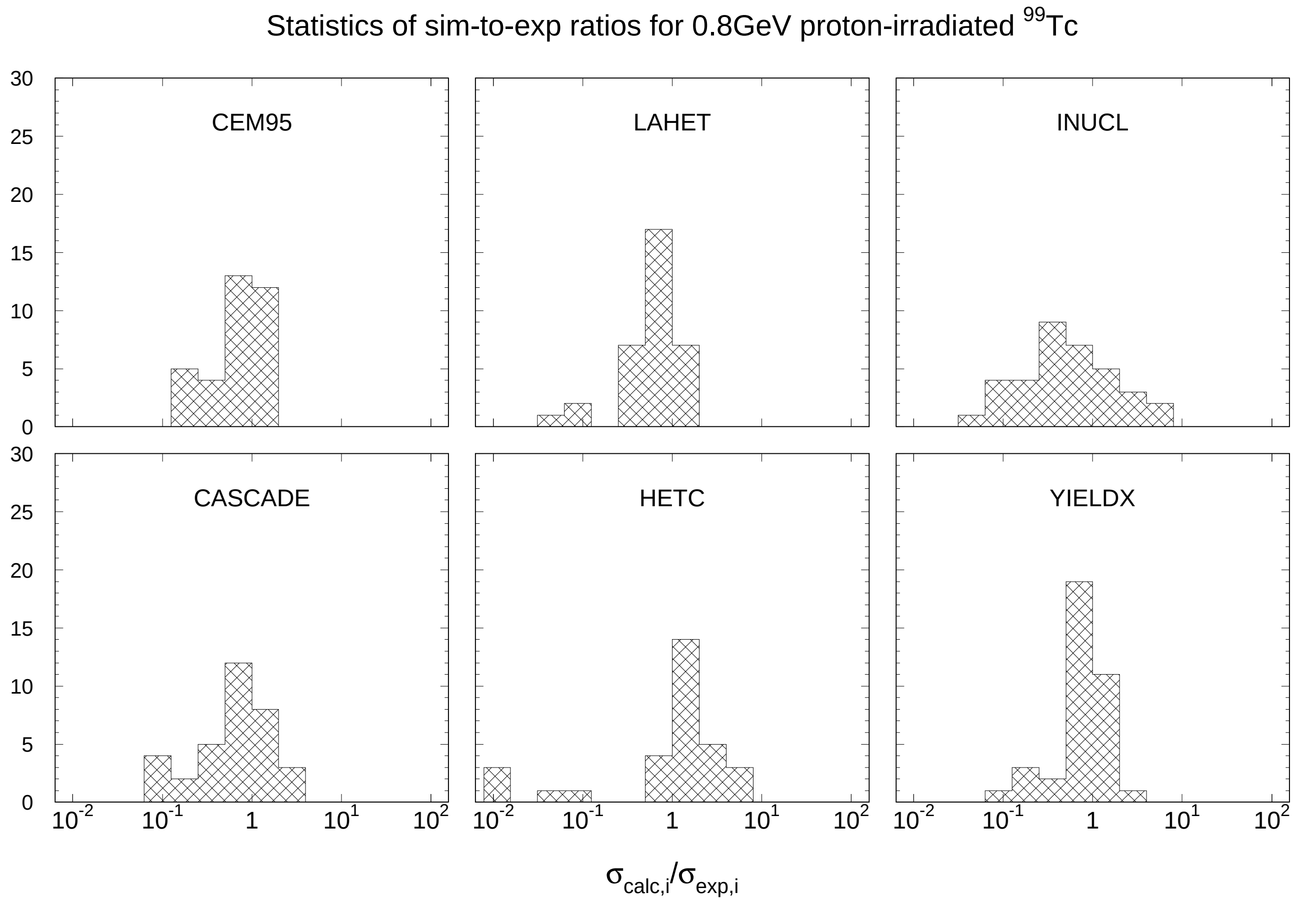

Fig. 98: Statistics of the simulation-to-experiment ratios (criterion 2) for ^{99}Tc irradiated with 0.8 GeV protons.

Table 92: Experimental and calculated yields from ^{99}Tc irradiated with 1.2 GeV protons.

Product	$T_{1/2}$	Type	Exp yield [mbarn]	Calculated Yields [mbarn] via CEM95	LAHET	CASCADE	HETC	INUCL	YIELDX
^{97}Ru	2,791d	i	4.02 ± 0.33	1.30	3.16	1.62	1.90	1.05	1.10
^{95}Ru	1,643h	i	1.40 ± 0.11	0.908	2.14	1.21	2.46	2.04	0.545
^{90}Mo	5,56h	c	3.96 ± 0.36	0.404	1.94	6.29	2.74	16.6	15.8
^{96}Nb	23,35h	i	3.30 ± 0.38	3.75	2.82	7.05	2.27	7.05	1.90
^{90}Nb	14,60h	i(m1+m2+g)	25.1 ± 2.0	19.0	11.3	3.15	25.0	6.89	14.5
^{88}Zr	83,4d	c	31.4 ± 2.5	20.4	22.8	31.0	27.9	43.8	15.7
^{87}Zr	1,68h	c	20.5 ± 1.9	10.0	14.0	14.4	28.5	30.3	4.30
^{86}Zr	16,5h	c	9.44 ± 0.78	2.31	11.0	11.0	30.3	23.1	1.31
^{88}Y	106,65d	i(m+g)	13.2 ± 3.7	11.2	6.07	5.61	0.739	5.61	9.48
^{86}Y	14,74h	i(m+g)	22.8 ± 1.7	22.1	10.1	4.19	1.45	7.24	15.4
^{83}Sr	32,41h	c	27.9 ± 7.8	17.8	16.7	21.0	29.8	25.4	20.7
^{81}Sr	22,3m	c	4.69 ± 0.76	1.13	1.20	2.57	5.96	9.47	2.90
^{80}Sr	106,3m	c	1.53 ± 0.29	0.067	0.053	2.97	–	5.37	0.796
^{83}Rb	86,2d	c	39.6 ± 4.2	28.6	23.2	31.3	30.0	30.3	29.1
^{79}Rb	22,9m	c*	7.62 ± 0.71	3.41	1.41	2.72	7.68	3.01	3.90
^{79}Kr	35,04h	c	24.2 ± 1.9	22.5	17.1	21.4	28.4	17.4	19.2
^{77}Kr	74,4m	c	10.0 ± 0.9	5.33	9.32	6.65	27.9	8.08	3.99
^{76}Kr	14,8h	c	3.76 ± 0.89	0.864	2.63	4.53	10.8	5.38	1.43
^{77}Br	57,036h	c	23.6 ± 1.9	23.4	18.8	17.6	28.0	12.4	16.6
^{76}Br	16,2h	i(m+g)	13.7 ± 1.7	16.5	13.8	1.28	18.3	2.30	9.19
^{75}Se	119,779d	c	26.7 ± 3.3	22.1	17.2	17.8	28.6	9.45	12.8
^{72}Se	8,40d	c	2.49 ± 1.10	2.12	3.87	5.78	24.1	4.00	2.20
^{74}As	17,77d	i	6.27 ± 0.82	5.04	3.53	2.90	–	1.02	2.22
^{72}As	26,0h	i	11.5 ± 1.1	15.9	11.8	1.03	0.382	1.50	7.72
^{71}As	65,28h	c	13.1 ± 1.1	11.3	10.5	4.64	24.2	2.77	5.59
^{70}As	52,6m	i	4.70 ± 0.66	2.78	2.79	0.261	22.0	0.201	1.66
^{67}Ge	18,9m	c	1.53 ± 0.17	0.493	0.582	0.668	–	1.02	0.519
^{67}Ga	3,2612d	c	14.8 ± 2.4	13.6	12.6	5.99	18.6	2.22	5.71
^{66}Ga	9,49h	c*	6.79 ± 0.63	8.26	5.58	0.872	18.1	0.698	2.12
^{56}Mn	2,5789h	c	0.811 ± 0.098	0.168	0.724	0.113	–	0.011	0.321
^{24}Na	14,9590h	c	0.911 ± 0.100	–	–	–	–	–	0.290

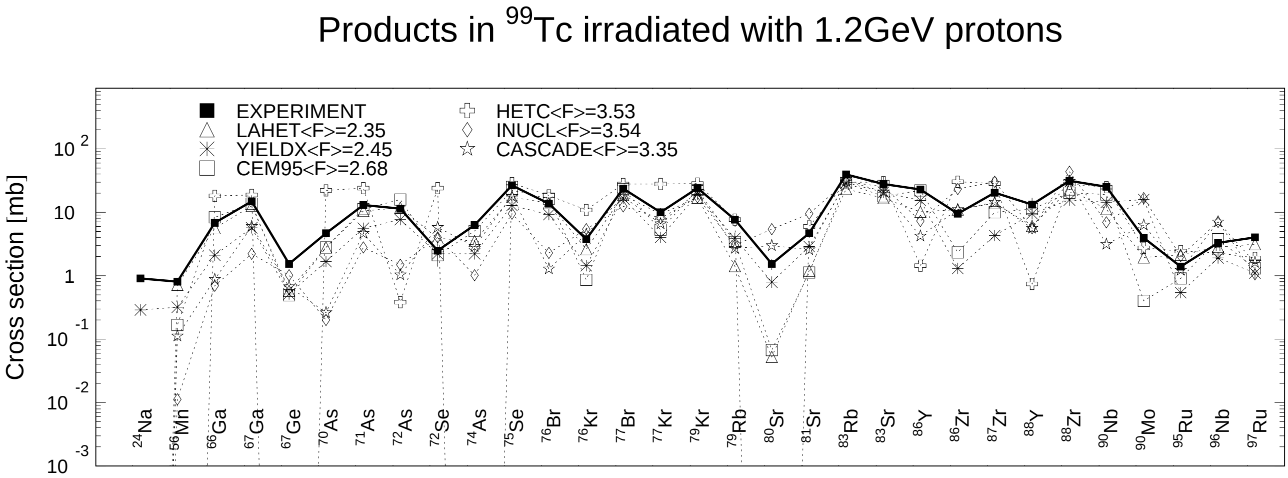

Fig. 99: Detailed comparison between experimental and simulated yields of radioactive reaction products in ^{99}Tc irradiated with 1.2 GeV protons. The cumulative yields are labeled -c when the respective independent yields are also shown.

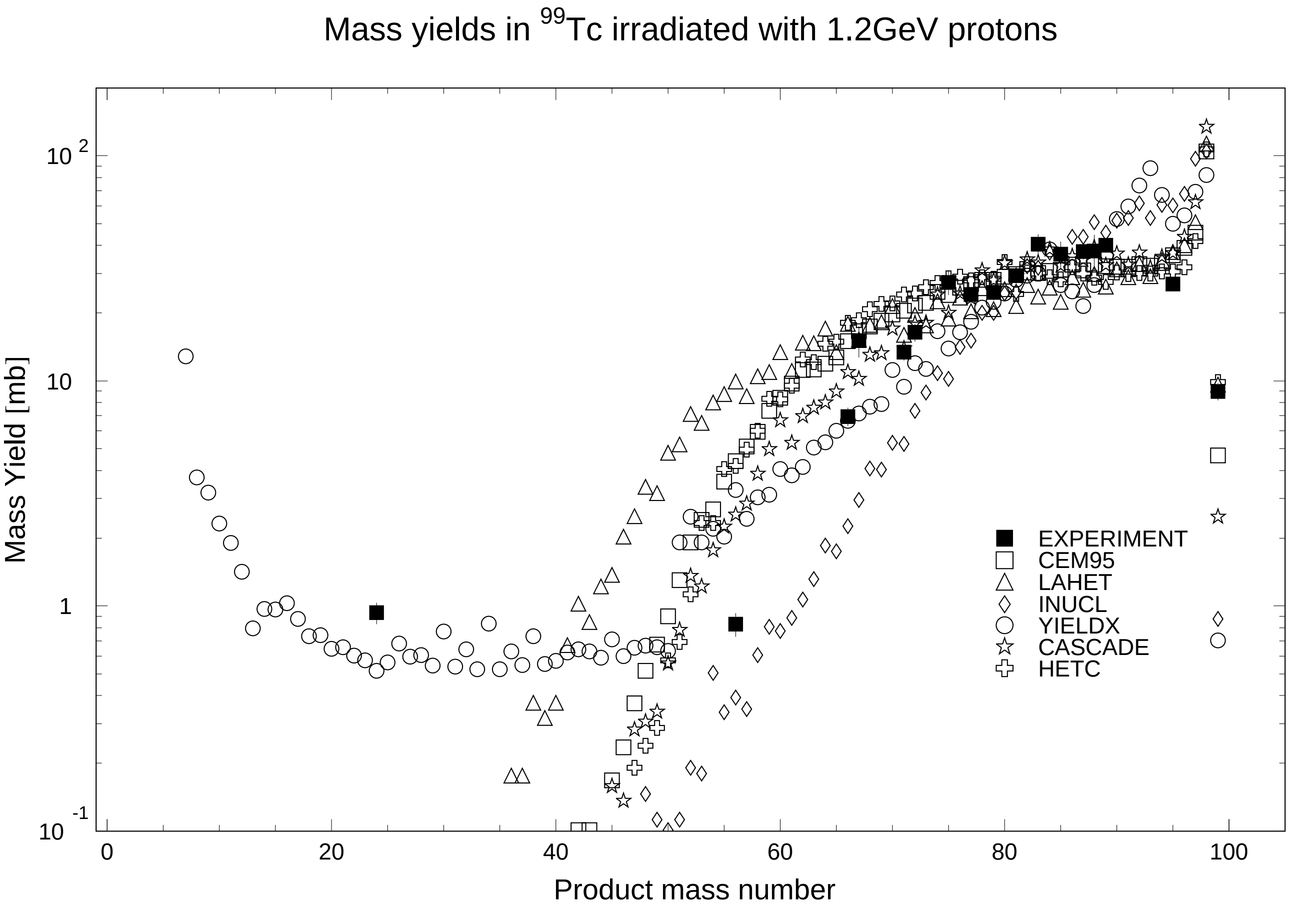

Fig. 100: The simulated mass distributions of reaction products together with the measured cumulative and supra-cumulative yields in ^{99}Tc irradiated with 1.2 GeV protons.

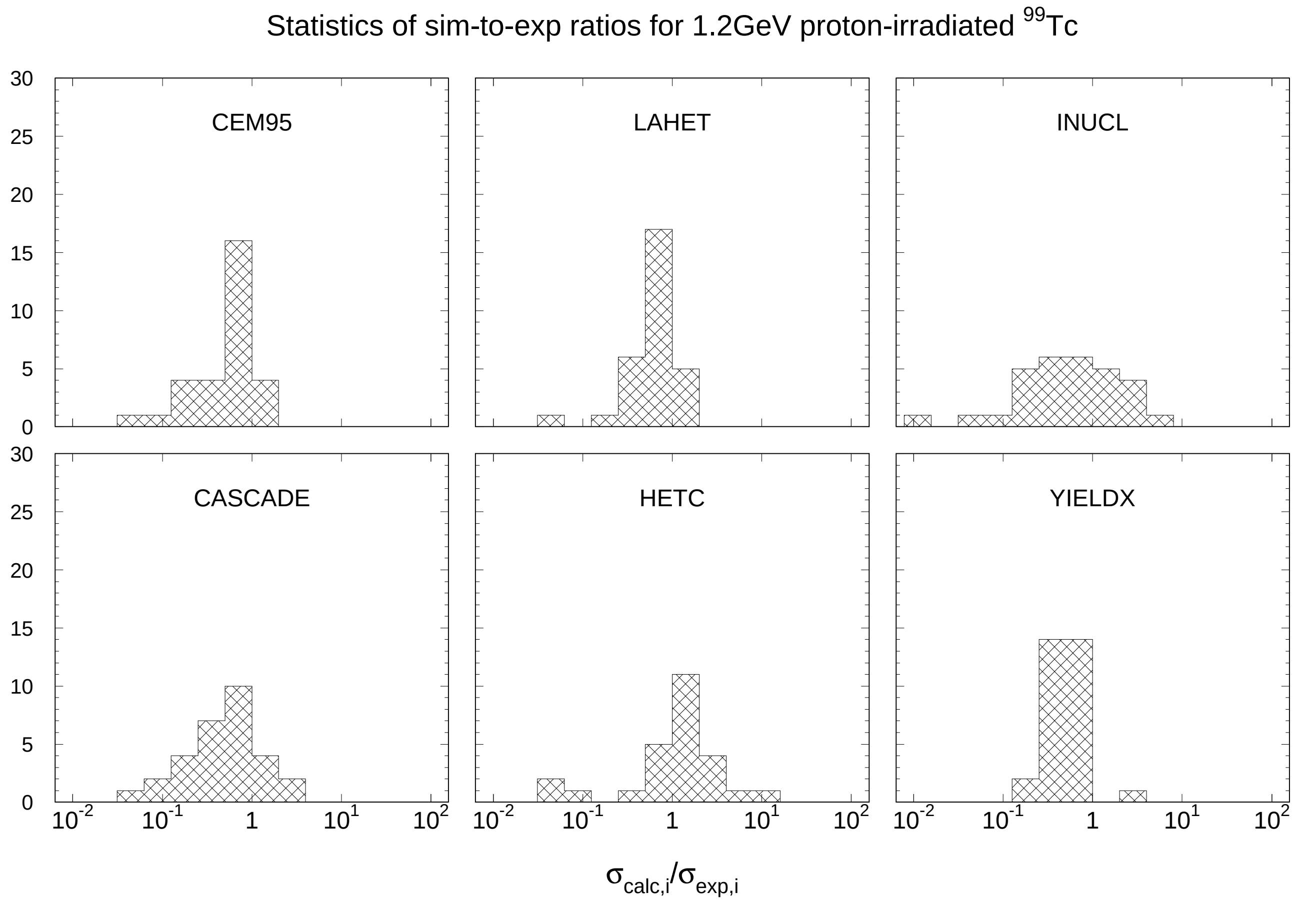

Fig. 101: Statistics of the simulation-to-experiment ratios (criterion 2) for ^{99}Tc irradiated with 1.2 GeV protons.

Table 93: Experimental and calculated yields from ^{99}Tc irradiated with 1.6 GeV protons.

Product	$T_{1/2}$	Type	Exp yield [mbarn]	Calculated Yields [mbarn] via CEM95	LAHET	CASCADE	HETC	INUCL	YIELDX
^{97}Ru	2,791d	i	2.28 ± 0.23	1.07	2.35	1.30	1.42	0.663	0.884
^{95}Ru	1,643h	i	1.05 ± 0.21	0.517	1.50	1.01	1.59	1.17	0.375
^{90}Mo	5,56h	c	2.78 ± 0.36	0.505	1.70	5.34	2.55	14.5	14.5
^{96}Nb	23,35h	i	2.97 ± 0.28	3.91	2.61	6.51	2.26	6.57	1.90
^{90}Nb	14,60h	i(m1+m2+g)	19.1 ± 1.6	15.5	8.95	2.51	19.6	5.78	14.8
^{88}Zr	83,4d	c	24.3 ± 2.1	15.3	19.2	26.0	22.3	40.0	16.0
^{87}Zr	1,68h	c	12.8 ± 1.6	7.69	11.0	12.5	22.6	26.2	4.42
^{86}Zr	16,5h	c	6.66 ± 0.59	1.52	8.74	8.71	23.4	21.5	1.35
^{88}Y	106,65d	i(m+g)	8.00 ± 0.75	8.56	5.19	4.91	0.603	5.25	9.72
^{86}Y	14,74h	i(m+g)	17.2 ± 1.5	16.8	8.14	3.69	1.23	7.04	15.8
^{83}Sr	32,41h	c	20.5 ± 5.7	14.0	12.6	16.8	24.0	25.2	20.3
^{82}Sr	25,55d	c	13.5 ± 1.4	5.76	11.0	14.6	25.7	21.7	12.2
^{81}Sr	22,3m	c	4.22 ± 0.73	0.797	1.02	2.23	5.30	10.0	2.88
^{80}Sr	106,3m	c	1.49 ± 0.31	0.112	0.018	2.50	–	5.67	0.801
^{84}Rb	32,77d	i(m+g)	4.20 ± 0.39	4.16	2.03	3.14	0.096	2.49	3.00
^{83}Rb	86,2d	c	28.4 ± 2.8	22.9	17.8	25.3	24.1	30.8	28.6
^{79}Rb	22,9m	c*	5.12 ± 0.55	3.22	1.25	2.38	6.15	3.64	3.96
^{79}Kr	35,04h	c	20.0 ± 1.8	19.0	14.0	18.1	21.9	19.8	19.5
^{77}Kr	74,4m	c	7.72 ± 0.77	4.13	6.89	6.44	22.6	10.3	4.16
^{76}Kr	14,8h	c	2.94 ± 0.96	0.809	1.94	5.28	8.27	6.93	1.50
^{77}Br	57,036h	c	17.8 ± 1.6	19.0	14.6	16.8	22.6	16.0	17.3
^{76}Br	16,2h	i(m+g)	13.1 ± 1.6	13.8	12.0	1.15	15.6	2.59	9.67
^{75}Se	119,779d	c	21.4 ± 1.8	19.8	14.9	17.9	23.1	13.6	13.6
^{74}As	17,77d	i	4.66 ± 0.51	4.54	3.07	2.94	–	1.71	2.40
^{72}As	26,0h	i	11.3 ± 1.3	14.2	11.0	1.36	0.120	2.49	8.55
^{71}As	65,28h	c	11.6 ± 1.0	11.2	9.34	5.72	21.5	4.51	6.27
^{70}As	52,6m	i	2.78 ± 0.57	2.57	2.58	0.227	21.2	0.370	1.89
^{69}Ge	39,05h	c	8.92 ± 1.82	12.4	9.89	9.30	22.0	5.78	6.07
^{67}Ge	18,9m	c	1.43 ± 0.24	0.595	0.406	0.692	0.048	1.70	0.617
^{67}Ga	3,2612d	c	13.0 ± 1.2	14.7	11.7	8.02	19.6	3.31	6.80
^{66}Ga	9,49h	c*	6.77 ± 0.78	10.2	5.37	1.29	20.2	1.55	2.56
^{65}Zn	244,26d	c	12.8 ± 1.4	14.4	11.6	9.27	18.5	3.11	6.20
^{58}Co	70,86d	i(m+g)	6.31 ± 0.56	10.5	8.62	2.47	–	0.360	2.69
^{56}Co	77,233d	c	1.56 ± 0.30	5.39	2.24	0.477	12.7	0.101	0.342
^{56}Mn	2,5789h	c	1.12 ± 0.11	0.438	1.08	0.363	–	0.011	0.449
^{54}Mn	312,11d	i	7.24 ± 0.81	5.14	8.55	1.15	–	0.056	2.20
^{48}V	15,9735d	c*	1.71 ± 0.16	2.04	4.17	0.104	4.47	0.024	0.316
^{46}Sc	83,79d	i(m+g)	1.91 ± 0.27	1.26	3.27	0.238	–	0.023	0.476
^{41}Ar	109,34m	c	0.443 ± 0.073	0.011	0.088	0.011	–	–	0.064
^{24}Na	14,9590h	c	1.06 ± 0.12	–	0.035	–	–	–	0.527
^{7}Be	53,29d	i	9.89 ± 1.77	–	–	–	–	–	2.84

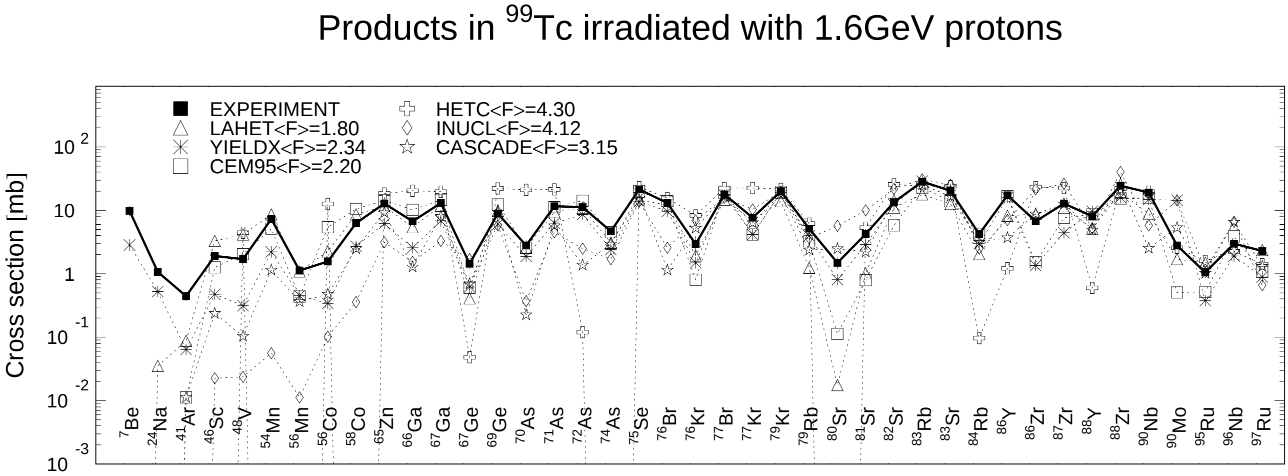

Fig. 102: Detailed comparison between experimental and simulated yields of radioactive reaction products in ^{99}Tc irradiated with 1.6 GeV protons. The cumulative yields are labeled -c when the respective independent yields are also shown.

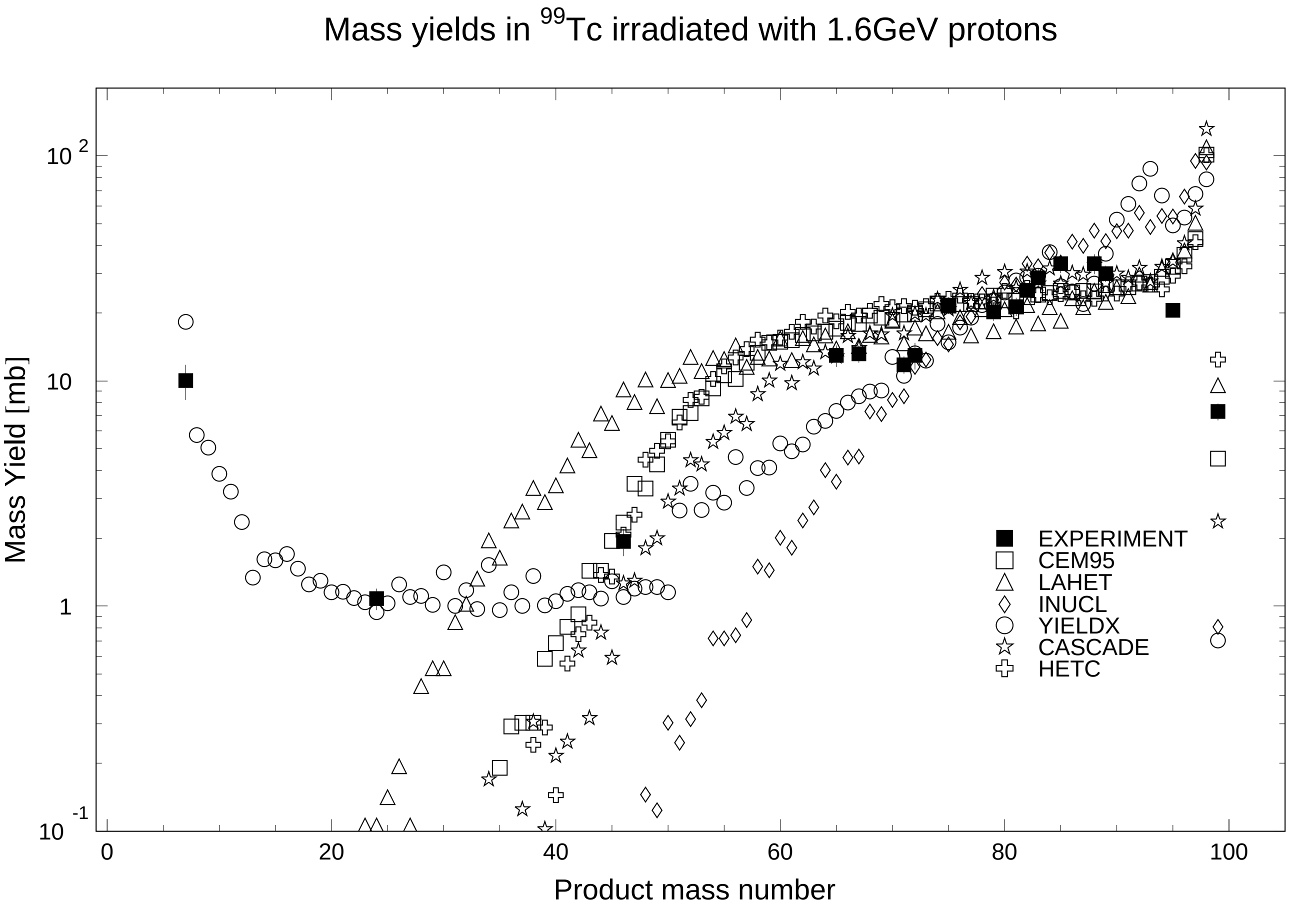

Fig. 103: The simulated mass distributions of reaction products together with the measured cumulative and supra-cumulative yields in ^{99}Tc irradiated with 1.6 GeV protons.

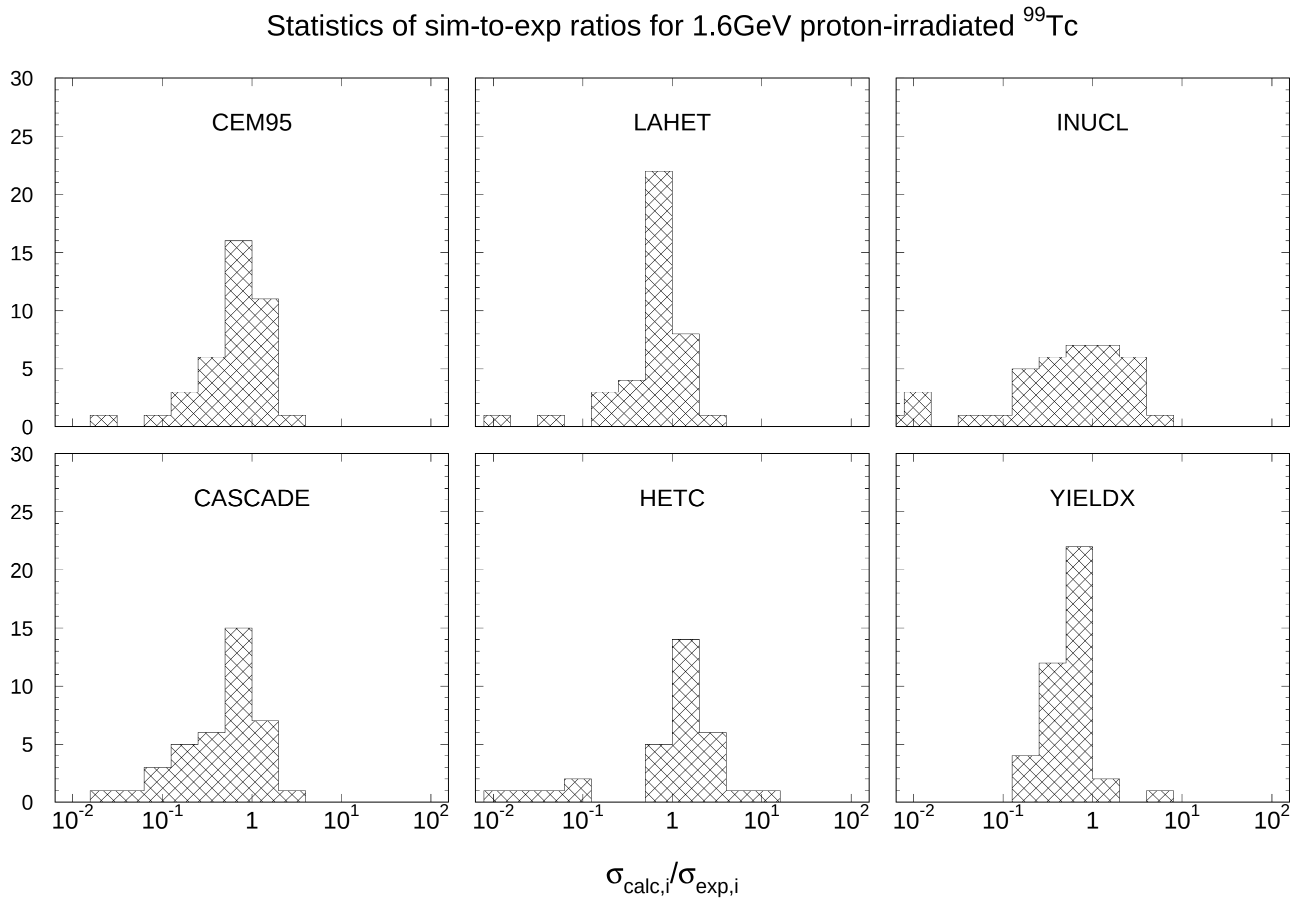

Fig. 104: Statistics of the simulation-to-experiment ratios (criterion 2) for ^{99}Tc irradiated with 1.6 GeV protons.

Table 94: Experimental and calculated yields from ^{59}Co irradiated with 0.2 GeV protons.

Product	$T_{1/2}$	Type	Exp yield [mbarn]	Calculated Yields [mbarn] via CEM95	LAHET	CASCADE	HETC	INUCL	YIELDX
^{57}Ni	35,60h	c	0.781 ± 0.074	1.49	1.45	3.68	1.45	4.54	0.500
^{58}Co	70,86d	i(m+g)	63.5 ± 5.7	72.2	85.5	89.4	71.5	51.2	71.3
^{57}Co	271,79d	c	49.2 ± 4.4	50.8	57.9	51.9	66.2	44.2	40.2
^{56}Co	77,233d	c	15.8 ± 1.4	32.0	21.6	8.42	56.2	35.7	8.65
^{55}Co	17,53h	c	2.53 ± 0.23	3.97	1.34	3.33	0.910	9.13	2.34
^{56}Mn	2,5789h	c	4.54 ± 0.41	7.38	3.49	3.23	1.25	18.4	17.6
^{54}Mn	312,11d	i	35.8 ± 3.2	33.4	40.0	10.4	2.94	51.3	59.9
^{51}Cr	27,7025d	c	31.4 ± 2.9	34.2	22.5	29.8	41.0	30.5	22.7
^{49}Cr	42,3m	c	2.82 ± 0.28	1.11	1.12	1.57	2.86	4.81	1.08
^{48}Cr	21,56h	c	0.252 ± 0.023	0.044	0.096	0.547	–	0.311	0.136
^{48}V	15,9735d	c	8.43 ± 0.75	6.56	5.68	1.65	22.0	11.0	4.11
^{48}Sc	43,67h	i	0.186 ± 0.017	0.149	0.176	0.089	–	1.30	0.433
^{47}Sc	3,3492d	i	1.09 ± 0.10	0.355	0.638	0.670	–	0.853	1.35
^{46}Sc	83,79d	i(m+g)	2.52 ± 0.26	1.49	1.13	0.615	–	3.69	2.79
^{43}Sc	3,891h	c	0.491 ± 0.048	0.041	0.080	0.075	–	0.711	0.470
^{47}Ca	4,536d	c	0.051 ± 0.009	0.010	–	0.021	–	0.027	0.058
^{43}K	22,3h	c	0.107 ± 0.010	0.003	–	0.027	–	0.122	0.216
^{42}K	12,360h	i	0.357 ± 0.033	0.020	–	0.082	–	0.474	0.515
^{41}Ar	109,34m	c	0.036 ± 0.004	–	–	0.007	–	0.020	0.077

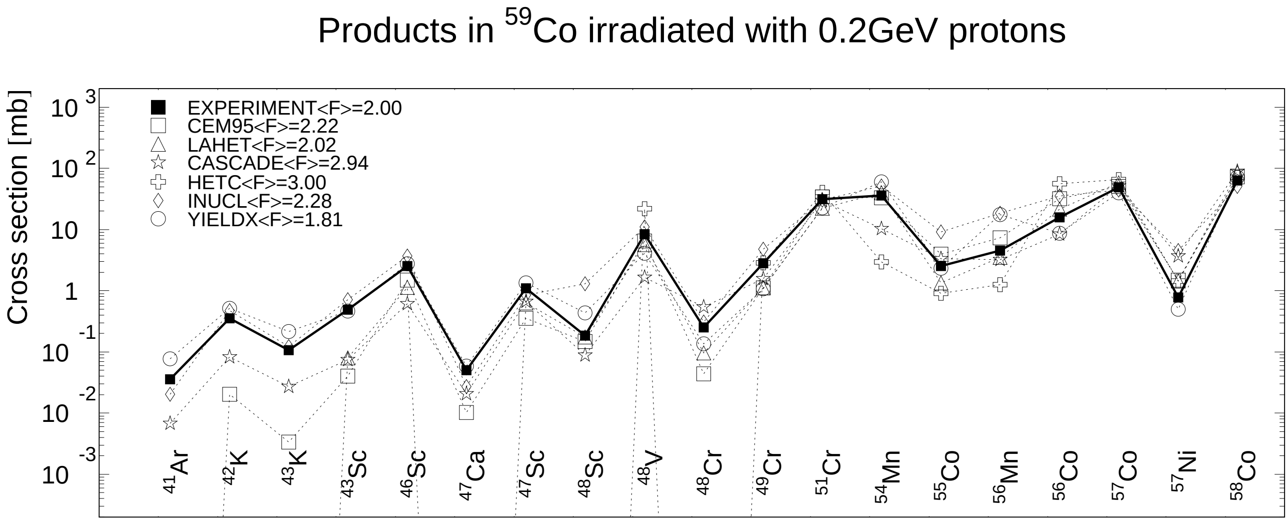

Fig. 105: Detailed comparison between experimental and simulated yields of radioactive reaction products in ^{59}Co irradiated with 0.2 GeV protons. The cumulative yields are labeled -c when the respective independent yields are also shown.

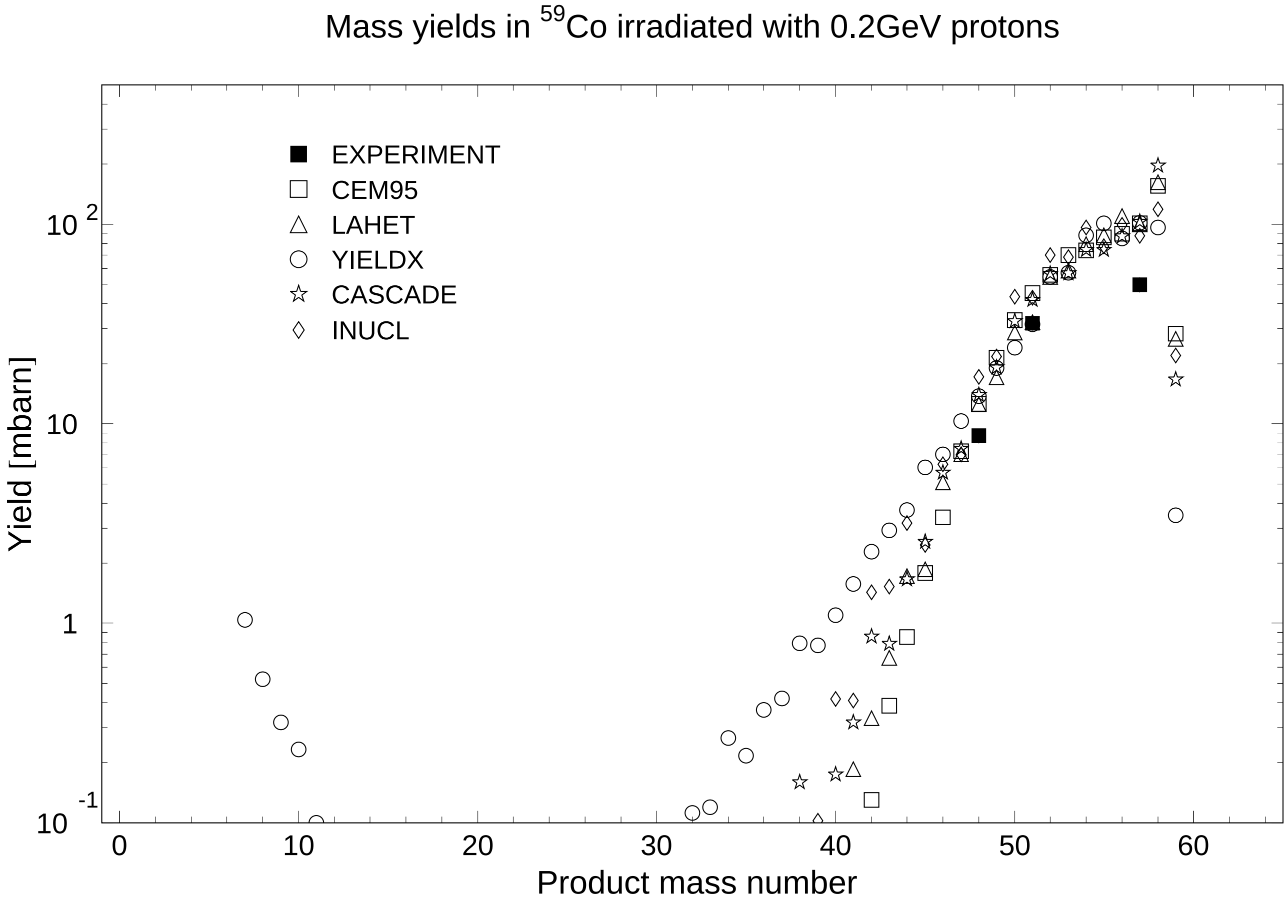

Fig. 106: The simulated mass distributions of reaction products together with the measured cumulative and supra-cumulative yields in ^{59}Co irradiated with 0.2 GeV protons.

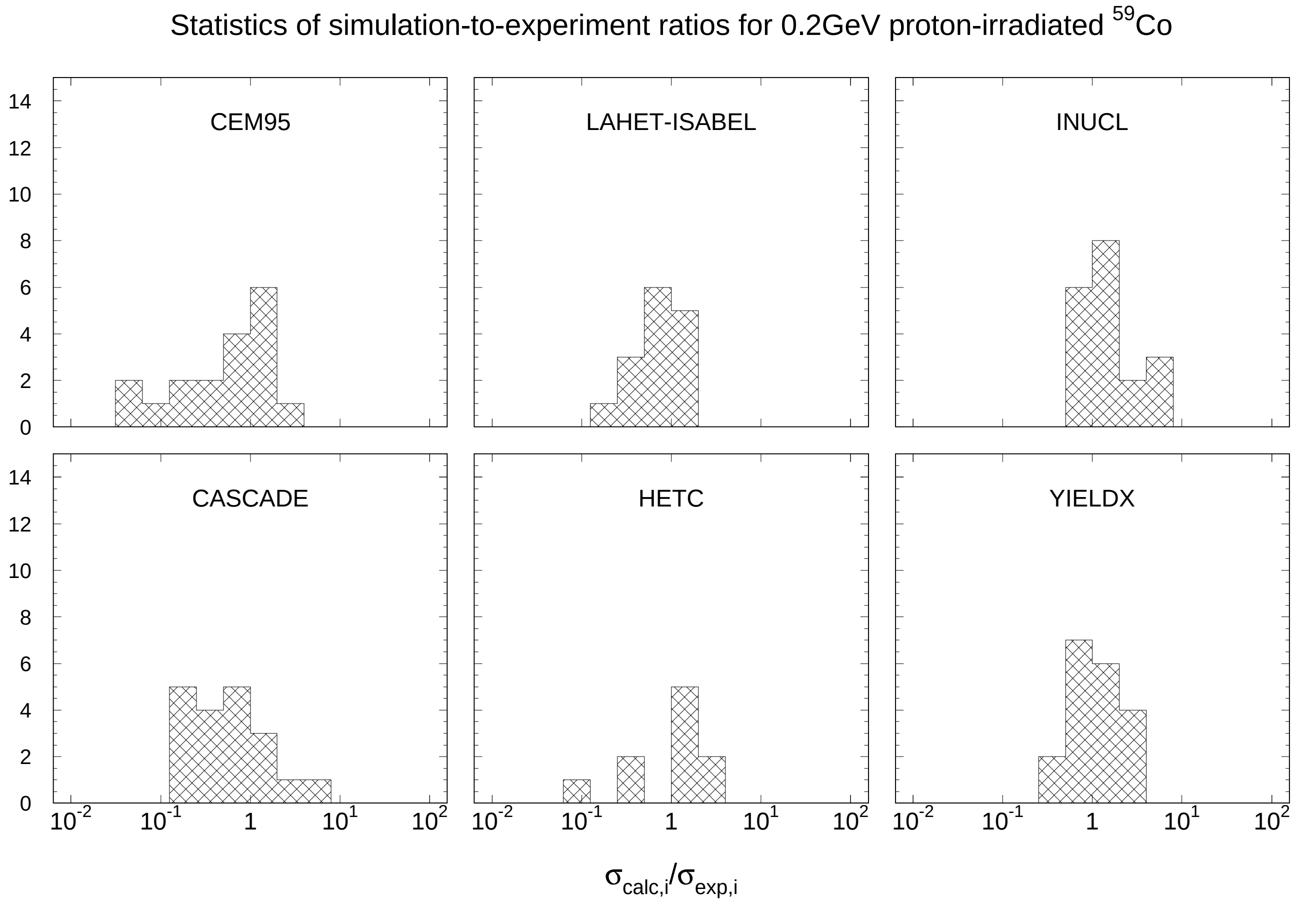

Fig. 107: Statistics of the simulation-to-experiment ratios (criterion 2) for ^{59}Co irradiated with 0.2 GeV protons.

Table 95: Experimental and calculated yields from ^{59}Co irradiated with 1.2 GeV protons.

Product	$T_{1/2}$	Type	Exp yield [mbarn]	CEM95	LAHET	CASCADE	HETC	INUCL	YIELDX	NUCLEUS	QMD
				Calculated Yields [mbarn] via							
^{57}Ni	35,60h	c	0.274 ± 0.021	0.237	0.355	0.574	0.304	0.371	0.047	1.21	0.150
^{58}Co	70,86d	i(m+g)	51.3 ± 3.7	56.5	53.9	68.9	58.0	32.1	56.6	70.5	71.9
^{57}Co	271,79d	c	27.2 ± 1.9	21.3	23.1	24.1	30.3	22.5	18.0	28.3	20.1
^{56}Co	77,233d	c	6.91 ± 0.48	11.6	7.75	6.23	20.3	11.4	4.07	15.9	2.30
^{55}Co	17,53h	c	1.00 ± 0.08	1.36	0.551	2.25	0.322	2.69	1.09	4.14	0.535
^{59}Fe	44,472d	c	0.555 ± 0.043	0.032	0.902	–	0.059	–	–	1.18	–
^{56}Mn	2,5789h	c	5.94 ± 0.42	6.07	4.63	11.0	4.64	10.2	6.88	9.69	–
^{54}Mn	312,11d	i	26.8 ± 1.9	16.4	19.5	8.22	7.52	20.7	34.5	15.4	19.2
^{51}Cr	27,7025d	c	29.0 ± 2.2	23.4	17.5	23.7	28.0	19.4	26.9	22.9	17.5
^{49}Cr	42,3m	c	3.64 ± 0.30	1.97	1.98	4.84	2.36	6.08	1.97	7.27	0.649
^{48}Cr	21,56h	c	0.456 ± 0.034	0.205	0.255	3.31	0.004	0.663	0.306	0.778	0.053
^{48}V	15,9735d	c	14.9 ± 1.0	14.2	12.0	6.25	26.2	18.8	9.21	15.8	8.96
^{48}Sc	43,67h	i	0.785 ± 0.055	0.394	0.843	0.359	0.020	4.21	0.970	0.869	0.543
^{47}Sc	3,3492d	i	4.03 ± 0.30	1.75	3.25	2.18	0.048	3.51	3.74	1.68	2.03
^{46}Sc	83,79d	i(m+g)	9.91 ± 0.70	11.4	6.70	3.38	0.105	13.2	9.56	3.04	7.67
^{43}Sc	3,891h	c	4.64 ± 0.37	3.46	1.65	3.38	1.01	7.59	3.07	7.95	2.54
^{47}Ca	4,536d	c	0.087 ± 0.010	0.079	0.109	0.104	0.002	0.165	0.162	0.175	0.013
^{43}K	22,3h	c	1.70 ± 0.12	0.631	0.989	0.845	0.004	2.56	1.45	0.947	0.572
^{42}K	12,360h	i	5.15 ± 0.38	2.29	2.96	1.59	0.004	12.0	4.13	2.79	3.39
^{41}Ar	109,34m	c	0.929 ± 0.068	0.237	0.223	0.598	–	1.22	0.796	0.736	0.508
^{39}Cl	55,6m	c	0.608 ± 0.045	0.079	0.242	0.199	–	1.18	0.550	0.189	–
^{38}Cl	37,24m	i(m+g)	2.01 ± 0.15	0.647	0.929	0.486	–	8.68	1.73	0.834	–
^{38}S	170,3m	c	0.064 ± 0.006	0.032	0.009	0.072	–	0.150	0.103	0.021	–
^{29}Al	6,56m	c	1.48 ± 0.20	0.300	1.29	0.247	–	2.52	1.44	0.512	–
^{28}Mg	20,915h	c	0.264 ± 0.019	–	0.009	0.072	–	0.392	0.336	0.084	–
^{27}Mg	9,462m	c	0.819 ± 0.089	0.158	0.178	0.167	–	0.791	0.916	0.491	–
^{24}Na	14,9590h	c	2.13 ± 0.16	1.20	2.21	0.215	–	4.17	1.81	0.827	–
^{22}Na	2,6019y	c	1.35 ± 0.16	1.33	1.98	0.112	1.57	2.62	0.964	1.23	–
^{7}Be	53,29d	i	5.52 ± 0.52	–	–	–	–	–	5.57	–	–

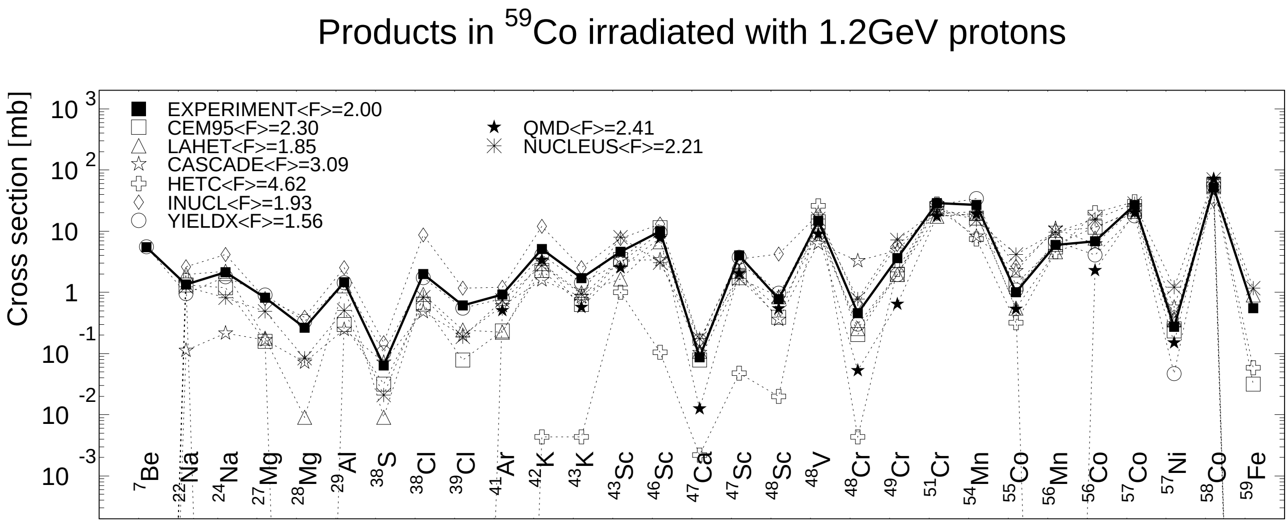

Fig. 108: Detailed comparison between experimental and simulated yields of radioactive reaction products in ^{59}Co irradiated with 1.2 GeV protons. The cumulative yields are labeled -c when the respective independent yields are also shown.

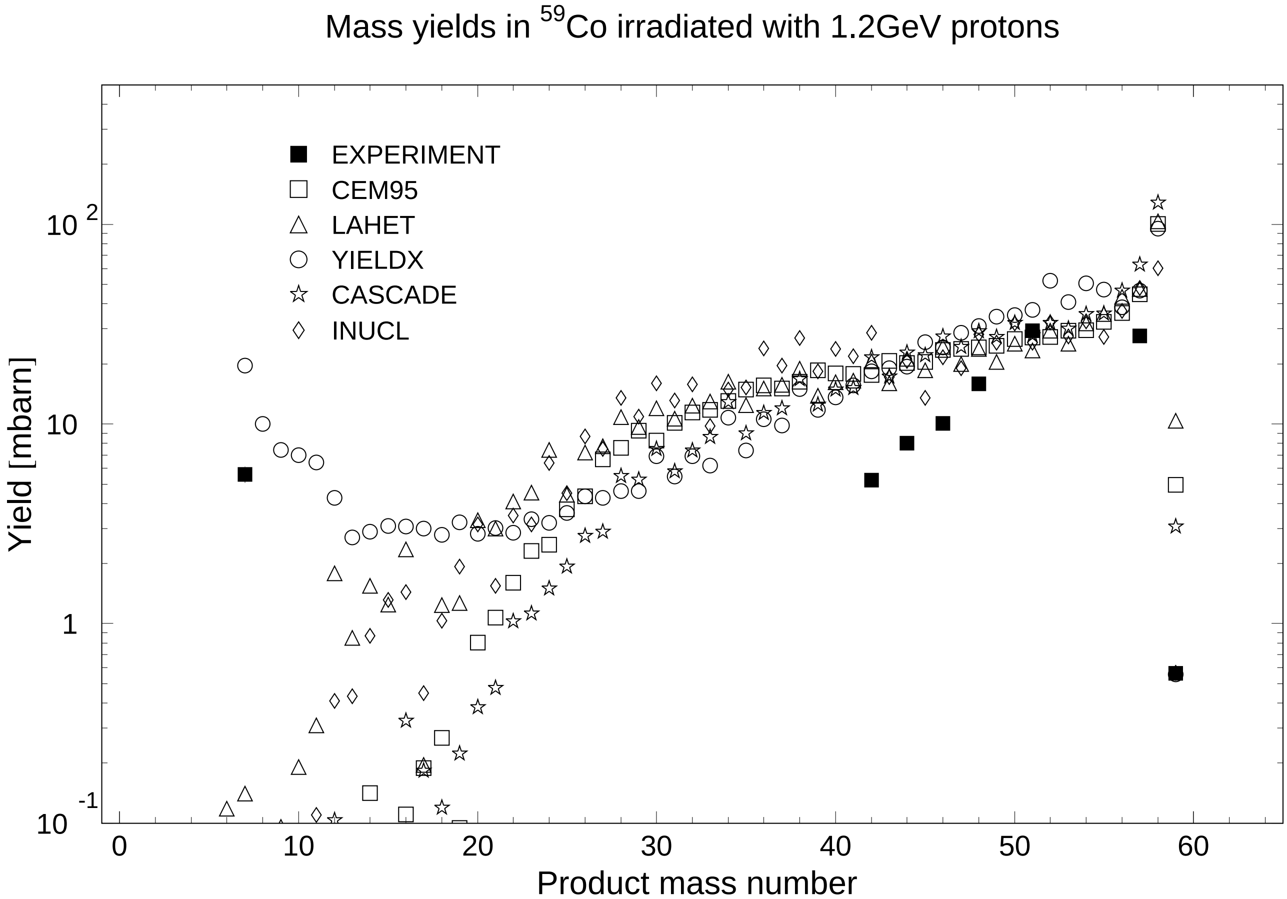

Fig. 109: The simulated mass distributions of reaction products together with the measured cumulative and supra-cumulative yields in ^{59}Co irradiated with 1.2 GeV protons.

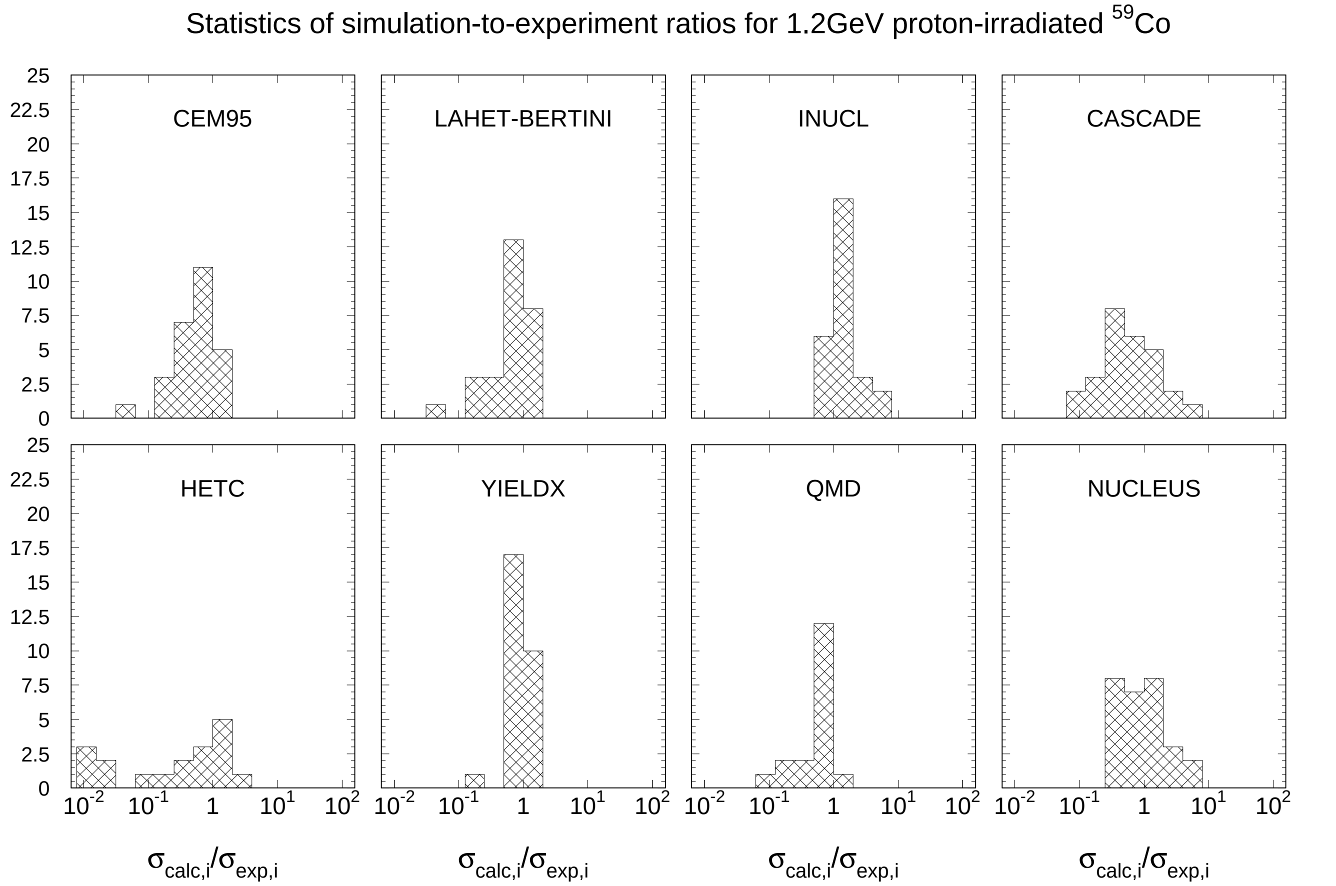

Fig. 110: Statistics of the simulation-to-experiment ratios (criterion 2) for ^{59}Co irradiated with 1.2 GeV protons.

Table 96: Experimental and calculated yields from ^{59}Co irradiated with 1.6 GeV protons.

Product	$T_{1/2}$	Type	Exp yield [mbarn]	Calculated Yields [mbarn] via CEM95	LAHET	CASCADE	HETC	INUCL	YIELDX
^{57}Ni	35,60h	c	0.246 ± 0.020	0.134	0.283	0.502	0.255	0.273	0.039
^{58}Co	70,86d	i(m+g)	50.1 ± 4.1	52.8	53.0	66.5	57.4	31.8	56.1
^{57}Co	271,79d	c	26.0 ± 2.1	20.9	22.0	21.5	28.3	22.4	17.6
^{56}Co	77,233d	c	6.31 ± 0.50	10.7	7.09	5.03	18.6	10.3	3.99
^{55}Co	17,53h	c	0.905 ± 0.076	1.20	0.520	1.78	0.331	2.45	0.931
^{59}Fe	44,472d	c	0.583 ± 0.049	0.071	1.30	–	0.329	–	–
^{56}Mn	2,5789h	c	5.61 ± 0.45	4.86	4.55	10.3	4.32	9.68	5.84
^{54}Mn	312,11d	i	24.5 ± 2.0	14.0	17.4	8.07	6.84	18.2	29.9
^{51}Cr	27,7025d	c	25.3 ± 2.1	19.2	14.8	19.6	24.6	16.5	25.4
^{49}Cr	42,3m	c	3.25 ± 0.29	1.48	1.86	2.36	1.96	4.85	1.91
^{48}Cr	21,56h	c	0.390 ± 0.033	0.142	0.196	1.15	0.002	0.601	0.301
^{48}V	15,9735d	c	13.0 ± 1.0	11.6	10.0	3.54	22.8	16.5	9.05
^{48}Sc	43,67h	i	0.693 ± 0.058	0.517	0.629	0.450	0.033	3.62	0.954
^{47}Sc	3,3492d	i	3.60 ± 0.30	1.53	2.79	2.95	0.070	3.03	3.73
^{46}Sc	83,79d	i(m+g)	8.84 ± 0.71	9.36	5.69	3.49	0.150	11.5	9.67
^{43}Sc	3,891h	c	4.22 ± 0.37	3.11	1.61	1.90	0.936	6.73	3.24
^{47}Ca	4,536d	c	0.099 ± 0.010	0.040	0.050	0.155	0.002	0.170	0.161
^{43}K	22,3h	c	1.64 ± 0.13	0.683	0.893	1.42	0.009	2.50	1.53
^{42}K	12,360h	i	4.81 ± 0.39	2.35	2.72	2.22	0.007	10.6	4.42
^{41}Ar	109,34m	c	0.918 ± 0.075	0.221	0.333	1.10	0.004	1.01	0.863
^{39}Cl	55,6m	c	0.630 ± 0.053	0.111	0.210	0.402	–	1.22	0.614
^{38}Cl	37,24m	i(m+g)	2.14 ± 0.18	0.635	0.966	0.705	–	8.75	1.96
^{38}S	170,3m	c	0.064 ± 0.006	–	–	0.124	–	0.194	0.117
^{29}Al	6,56m	c	2.36 ± 0.23	0.343	1.63	0.886	–	3.67	1.78
^{28}Mg	20,915h	c	0.353 ± 0.028	0.016	0.009	0.434	–	0.523	0.430
^{27}Mg	9,462m	c	1.43 ± 0.18	0.383	0.228	0.815	–	1.34	1.16
^{24}Na	14,9590h	c	2.88 ± 0.23	2.29	3.35	0.815	–	6.70	2.39
^{22}Na	2,6019y	c	1.74 ± 0.15	2.73	3.73	0.255	4.80	3.96	1.22
^{7}Be	53,29d	i	6.58 ± 0.66	–	0.451	–	–	–	6.41

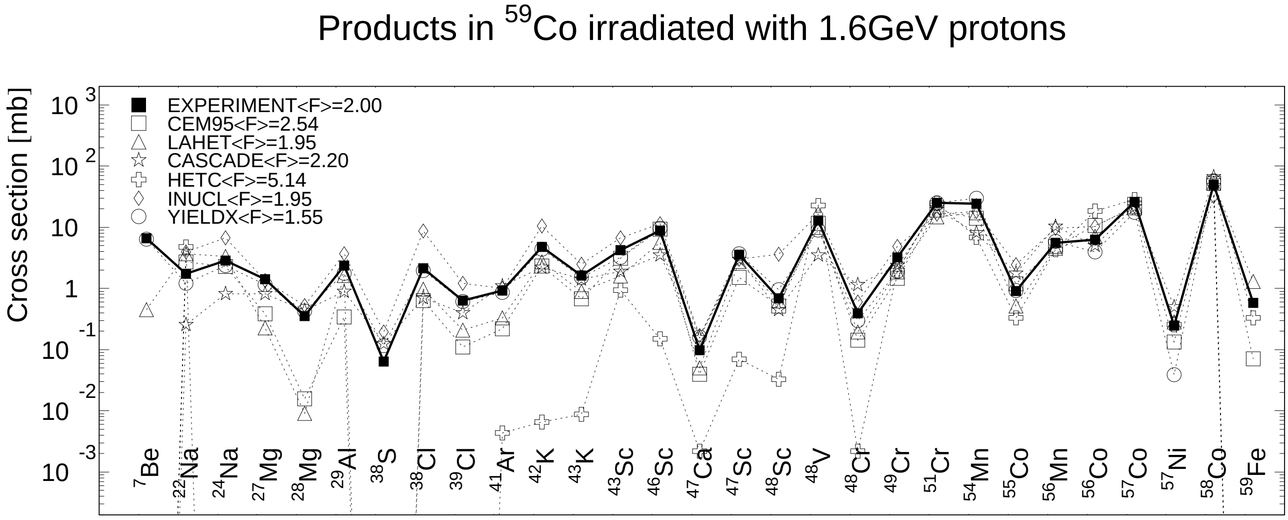

Fig. 111: Detailed comparison between experimental and simulated yields of radioactive reaction products in ^{59}Co irradiated with 1.6 GeV protons. The cumulative yields are labeled -c when the respective independent yields are also shown.

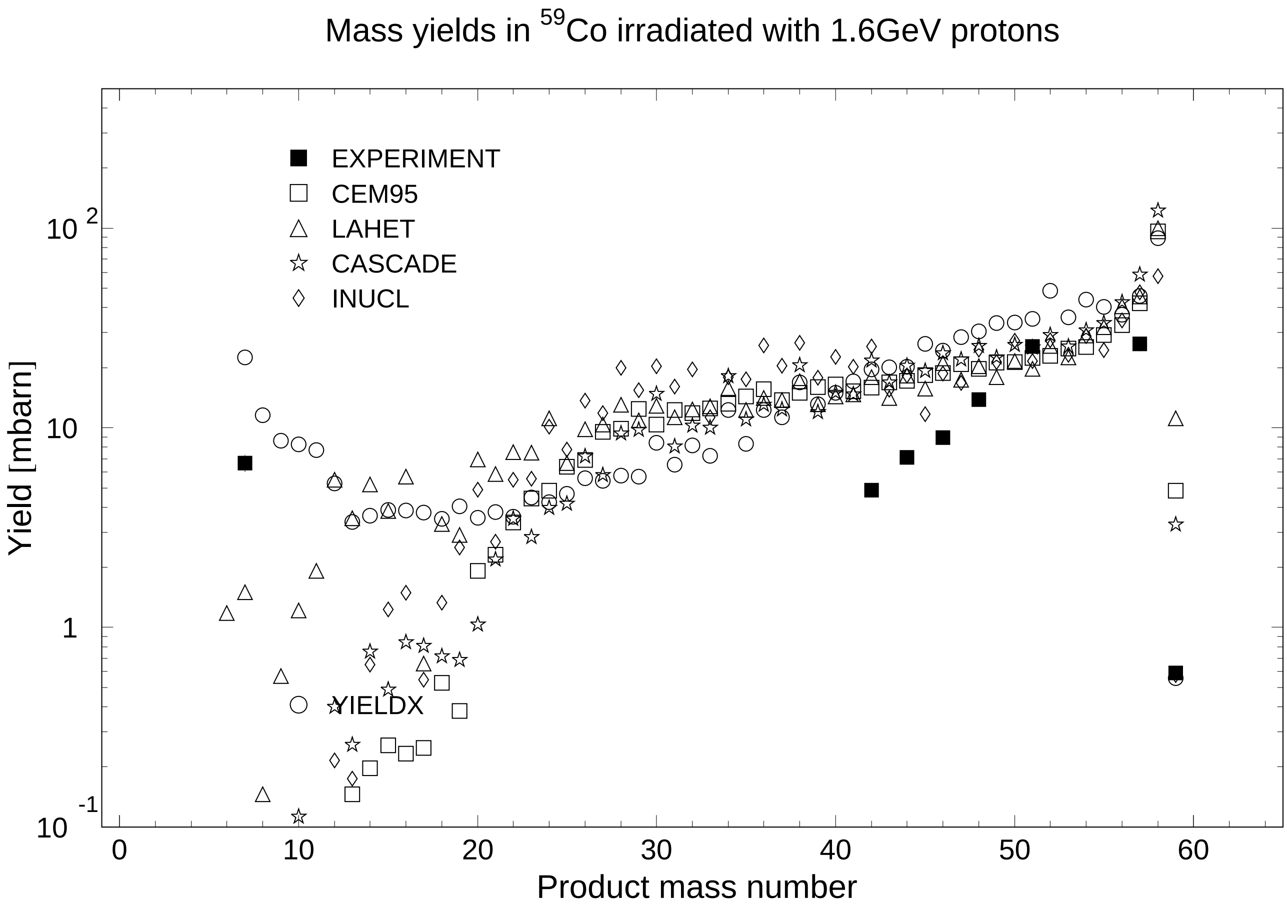

Fig. 112: The simulated mass distributions of reaction products together with the measured cumulative and supra-cumulative yields in ^{59}Co irradiated with 1.6 GeV protons.

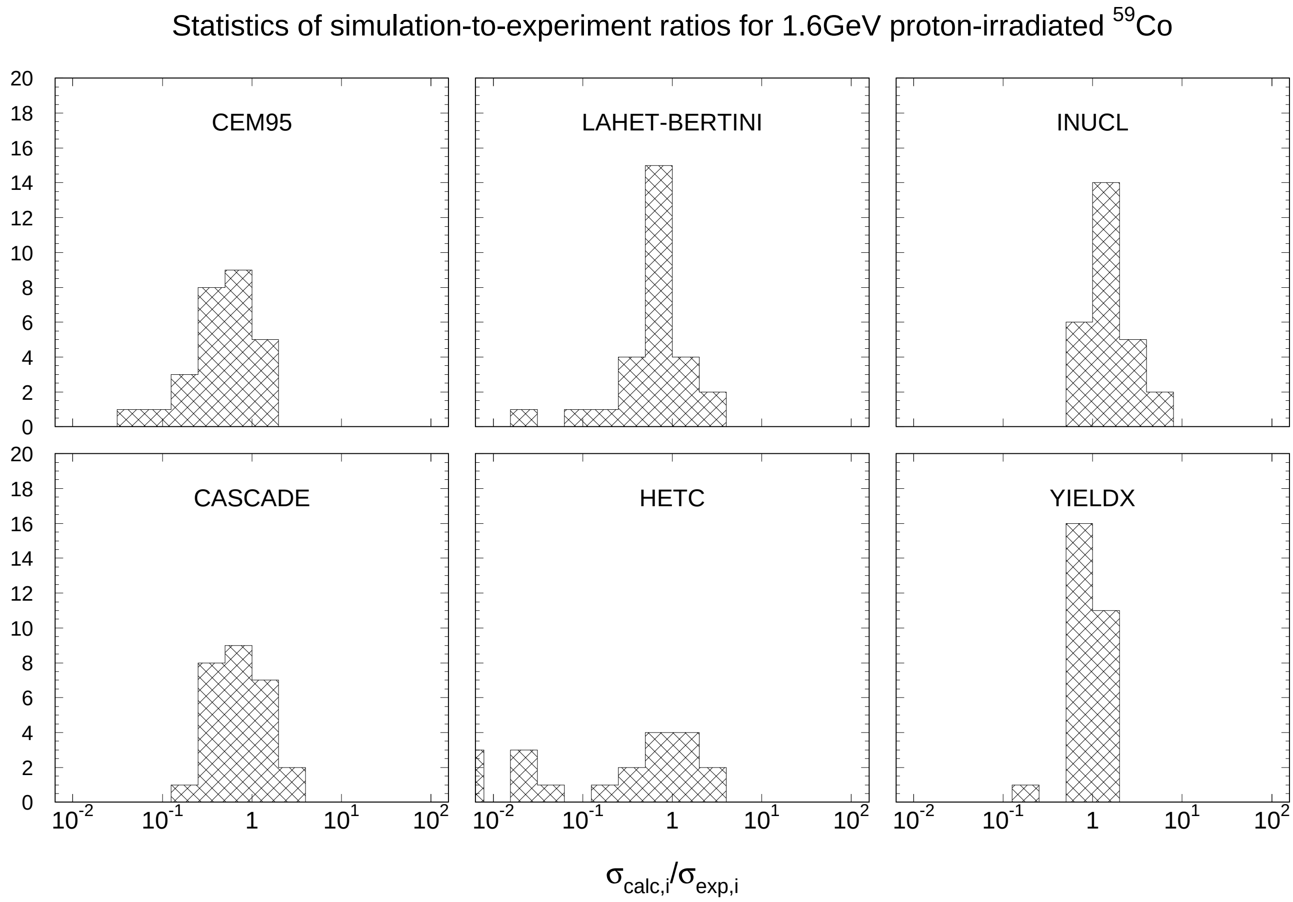

Fig. 113: Statistics of the simulation-to-experiment ratios (criterion 2) for ^{59}Co irradiated with 1.6 GeV protons.

Table 97: Experimental and calculated yields from ^{59}Co irradiated with 2.6 GeV protons.

Product	$T_{1/2}$	Type	Exp yield [mbarn]	Calculated Yields [mbarn] via CEM95	LAHET	CASCADE	HETC	INUCL	YIELDX
^{57}Ni	35,60h	c	0.223 ± 0.020	0.106	0.262	0.381	0.147	0.252	0.039
^{58}Co	70,86d	i(m+g)	47.8 ± 3.9	47.6	52.4	61.6	55.0	29.7	55.9
^{57}Co	271,79d	c	24.2 ± 2.0	16.0	20.4	18.4	26.4	23.7	17.5
^{56}Co	77,233d	c	5.63 ± 0.45	7.57	6.26	4.89	16.9	9.35	3.98
^{55}Co	17,53h	c	0.762 ± 0.065	0.943	0.400	1.86	0.305	2.12	0.677
^{59}Fe	44,472d	c	0.537 ± 0.048	0.055	1.50	–	1.55	–	–
^{56}Mn	2,5789h	c	4.99 ± 0.41	4.64	3.48	10.1	3.74	9.25	4.24
^{54}Mn	312,11d	i	21.3 ± 1.8	10.9	14.8	7.11	5.65	15.7	22.3
^{51}Cr	27,7025d	c	21.4 ± 1.8	15.0	12.5	16.4	20.9	13.4	20.6
^{49}Cr	42,3m	c	2.61 ± 0.24	1.04	1.32	1.98	1.82	3.97	1.63
^{48}Cr	21,56h	c	0.317 ± 0.027	0.106	0.189	1.16	0.004	0.481	0.264
^{48}V	15,9735d	c	10.6 ± 0.9	8.77	8.70	3.24	19.2	13.2	7.96
^{48}Sc	43,67h	i	0.625 ± 0.051	0.355	0.699	0.463	0.033	2.91	0.839
^{47}Sc	3,3492d	i	3.12 ± 0.26	1.20	2.64	2.81	0.068	2.64	3.37
^{46}Sc	83,79d	i(m+g)	7.42 ± 0.60	6.96	4.54	2.92	0.105	9.55	8.98
^{43}Sc	3,891h	c	3.46 ± 0.31	2.48	1.17	1.68	0.801	5.53	3.27
^{47}Ca	4,536d	c	0.082 ± 0.010	0.043	0.046	0.216	0.004	0.186	0.146
^{43}K	22,3h	c	1.42 ± 0.11	0.438	0.777	1.40	0.018	2.15	1.54
^{42}K	12,360h	i	4.17 ± 0.35	1.98	2.19	2.06	0.007	8.87	4.57
^{41}Ar	109,34m	c	0.836 ± 0.070	0.182	0.211	0.934	0.002	0.926	0.918
^{39}Cl	55,6m	c	0.566 ± 0.049	0.087	0.198	0.563	–	1.16	0.690
^{38}Cl	37,24m	i(m+g)	1.93 ± 0.17	0.481	0.662	0.871	0.004	7.69	2.26
^{38}S	170,3m	c	0.066 ± 0.007	0.008	–	0.200	–	0.210	0.135
^{29}Al	6,56m	c	2.56 ± 0.24	0.363	1.80	1.48	–	4.60	2.61
^{28}Mg	20,915h	c	0.432 ± 0.035	0.008	0.014	0.740	–	0.848	0.652
^{27}Mg	9,462m	c	1.53 ± 0.14	0.387	0.225	1.31	–	1.88	1.80
^{24}Na	14,9590h	c	3.77 ± 0.31	2.48	3.84	1.85	–	10.9	4.03
^{22}Na	2,6019y	c	2.46 ± 0.22	3.69	4.53	0.692	8.00	7.10	2.01
^{7}Be	53,29d	i	8.78 ± 0.89	–	2.89	–	0.002	–	8.21

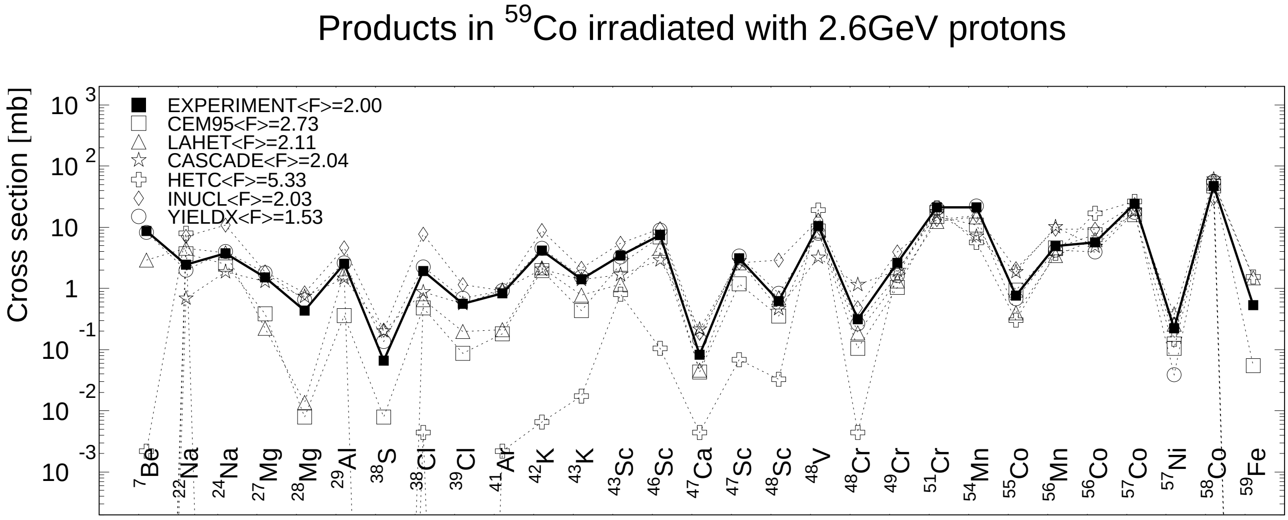

Fig. 114: Detailed comparison between experimental and simulated yields of radioactive reaction products in ^{59}Co irradiated with 2.6 GeV protons. The cumulative yields are labeled -c when the respective independent yields are also shown.

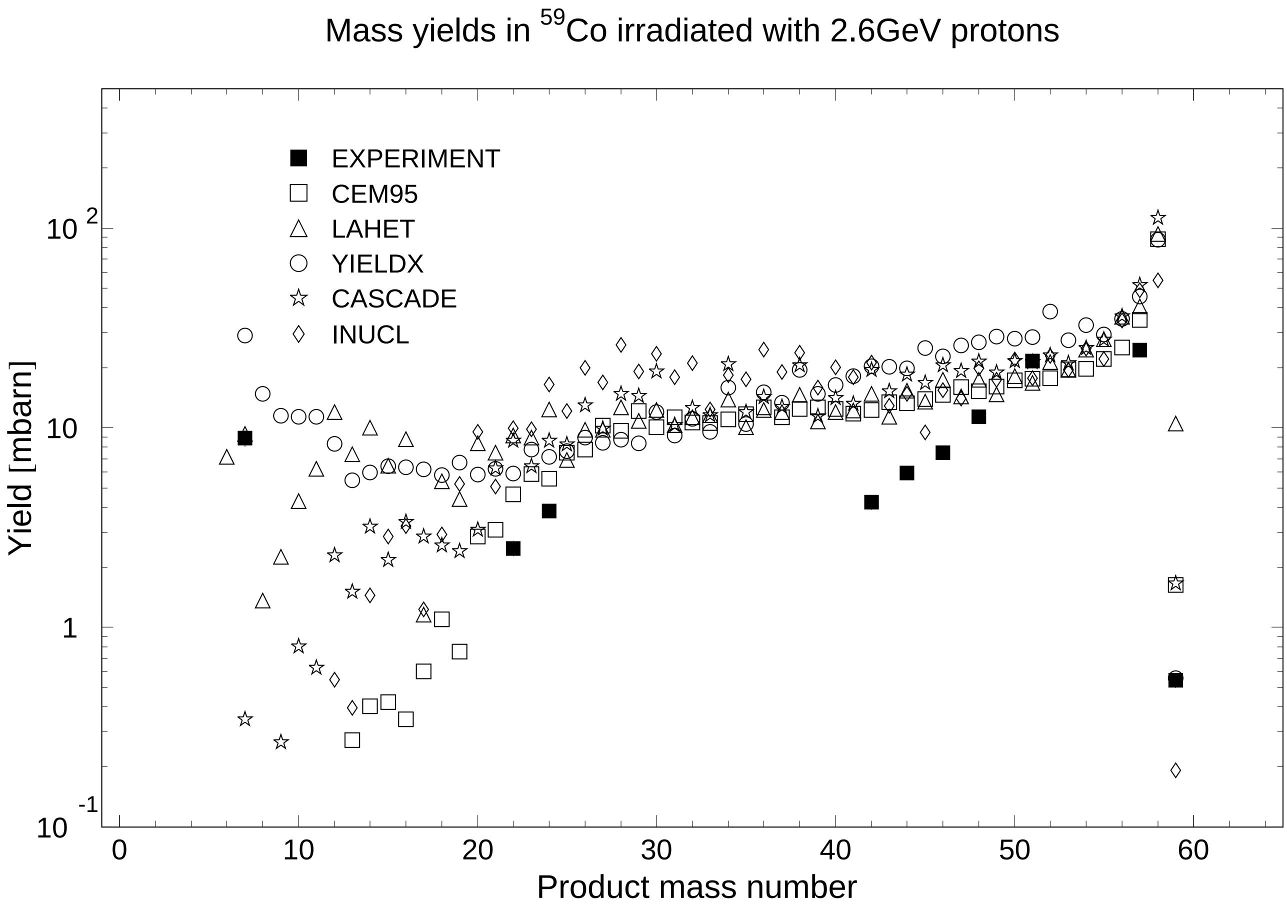

Fig. 115: The simulated mass distributions of reaction products together with the measured cumulative and supra-cumulative yields in ^{59}Co irradiated with 2.6 GeV protons.

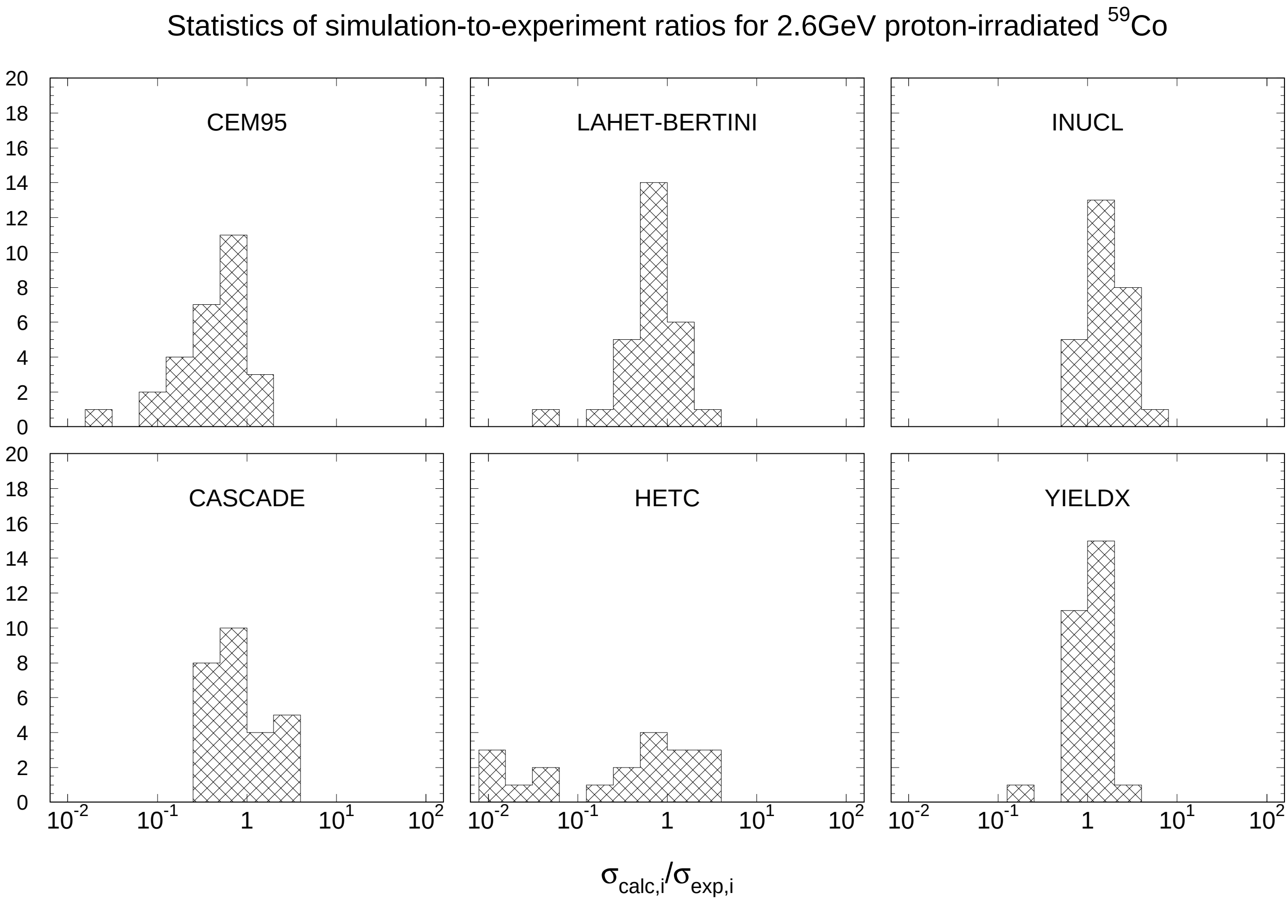

Fig. 116: Statistics of the simulation-to-experiment ratios (criterion 2) for ^{59}Co irradiated with 2.6 GeV protons.

Table 98: Experimental and calculated yields from ^{63}Cu irradiated with 0.2 GeV protons.

Product	$T_{1/2}$	Type	Exp yield [mbarn]	Calculated Yields [mbarn] via CEM95	LAHET	CASCADE	HETC	INUCL	YIELDX
^{63}Zn	38,47m	i	2.17 ± 0.33	9.76	3.35	6.57	8.92	6.90	3.16
^{62}Zn	9,26h	i	2.06 ± 0.17	3.56	4.46	19.7	3.58	3.41	1.87
^{61}Cu	3,333h	c	29.5 ± 3.0	43.8	41.3	39.8	65.5	29.9	21.2
^{60}Cu	23,7m	c*	8.44 ± 0.57	11.0	8.60	3.22	7.82	21.5	4.79
^{57}Ni	35,60h	c	2.16 ± 0.19	2.87	1.51	6.21	3.97	8.64	3.94
^{56}Ni	5,9d	i	0.147 ± 0.011	0.117	0.115	2.97	–	0.549	0.467
^{60}Co	5,2714y	i(m+g)	9.43 ± 1.30	8.26	6.97	3.56	1.36	25.0	18.4
^{58}Co	70,86d	i(m+g)	42.2 ± 2.8	48.9	42.5	12.9	2.71	56.9	101.
^{57}Co	271,79d	c	44.0 ± 2.9	50.5	42.5	41.6	55.2	41.7	78.9
^{56}Co	77,233d	c	14.1 ± 0.9	29.7	15.0	8.16	52.1	30.2	18.3
^{55}Co	17,53h	c	2.28 ± 0.16	3.32	0.777	3.55	0.640	6.78	3.48
^{59}Fe	44,472d	c	0.468 ± 0.065	0.956	0.436	0.477	0.062	1.18	4.50
^{56}Mn	2,5789h	c	1.73 ± 0.11	1.13	1.57	0.423	0.014	7.48	6.74
^{54}Mn	312,11d	i	17.4 ± 1.2	14.6	19.0	4.22	0.029	27.8	28.7
^{51}Cr	27,7025d	c	12.8 ± 0.9	7.64	7.78	9.21	15.4	13.4	18.4
^{49}Cr	42,3m	c	1.04 ± 0.09	0.124	0.345	0.342	0.029	1.32	1.33
^{48}Cr	21,56h	i	0.084 ± 0.006	0.004	0.034	0.101	–	0.074	0.205
^{48}V	15,9735d	c	2.67 ± 0.17	0.602	1.17	0.305	0.052	2.97	3.88
^{47}Sc	3,3492d	c	0.241 ± 0.017	0.067	0.120	0.135	–	0.138	0.533
^{46}Sc	83,79d	i(m+g)	0.605 ± 0.062	0.074	0.134	0.080	–	0.834	1.16

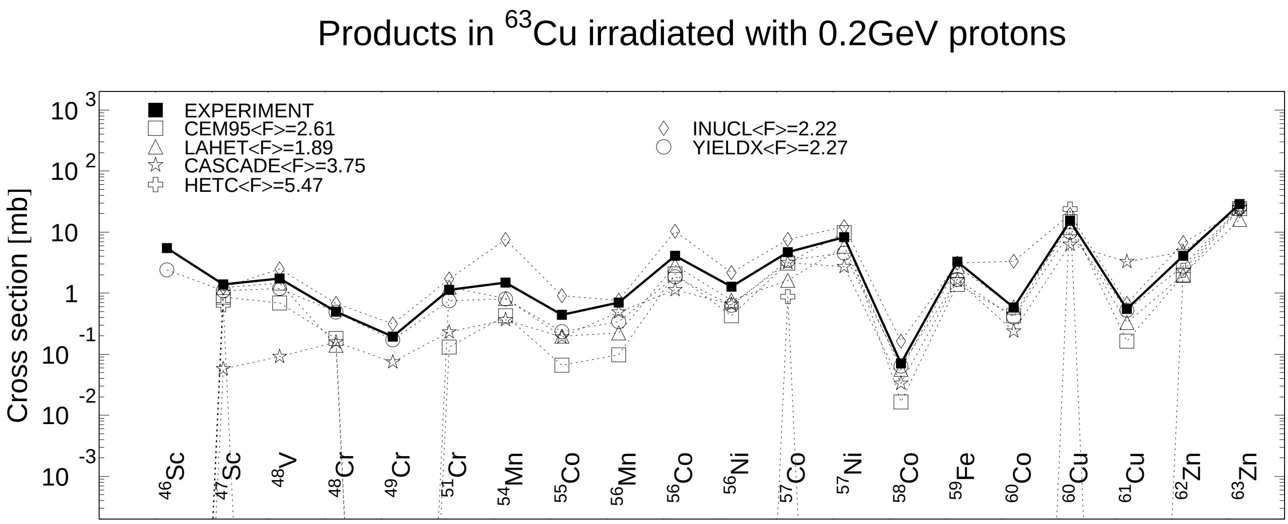

Fig. 117: Detailed comparison between experimental and simulated yields of radioactive reaction products in ^{63}Cu irradiated with 0.2 GeV protons. The cumulative yields are labeled -c when the respective independent yields are also shown.

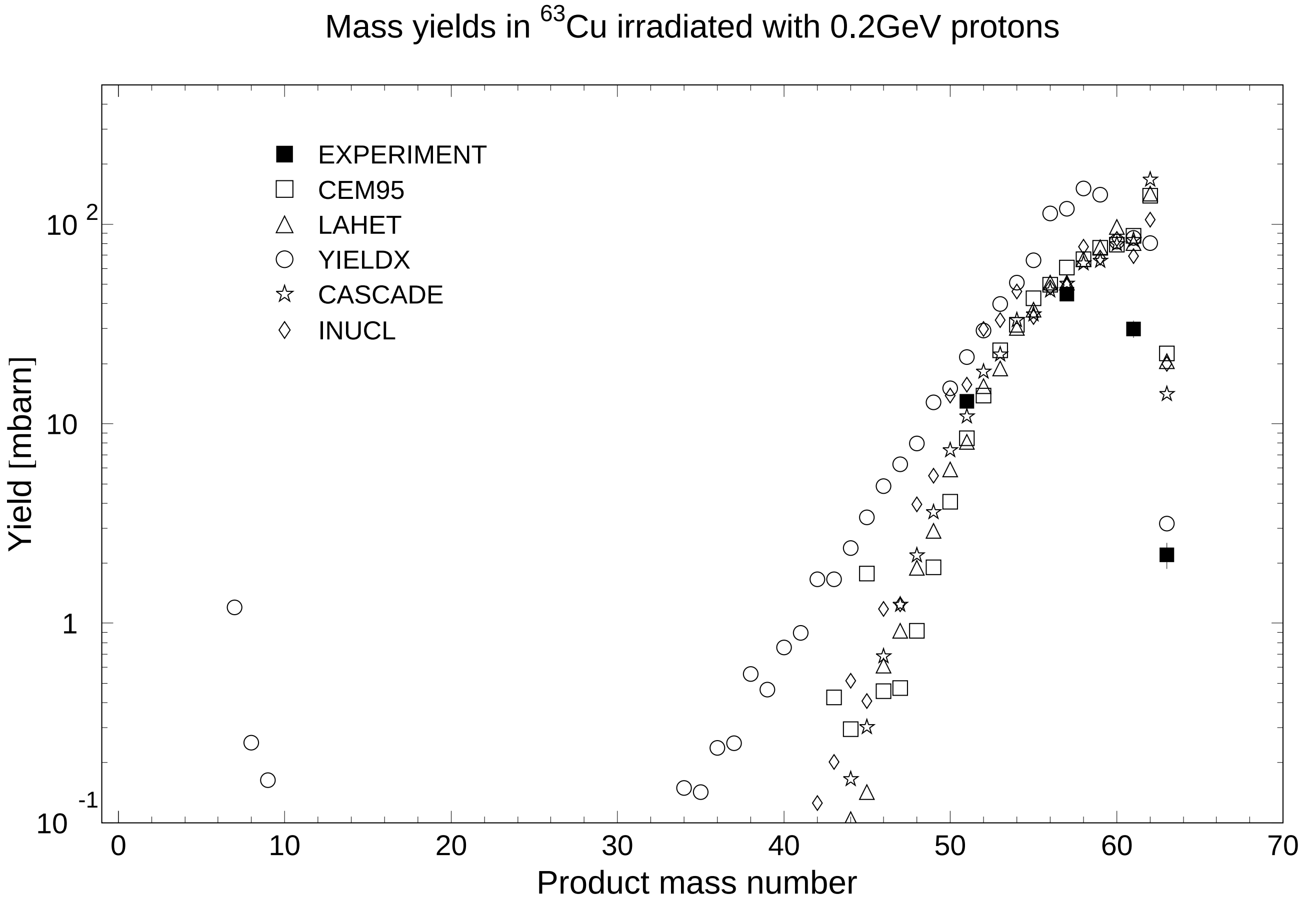

Fig. 118: The simulated mass distributions of reaction products together with the measured cumulative and supra-cumulative yields in ^{63}Cu irradiated with 0.2 GeV protons.

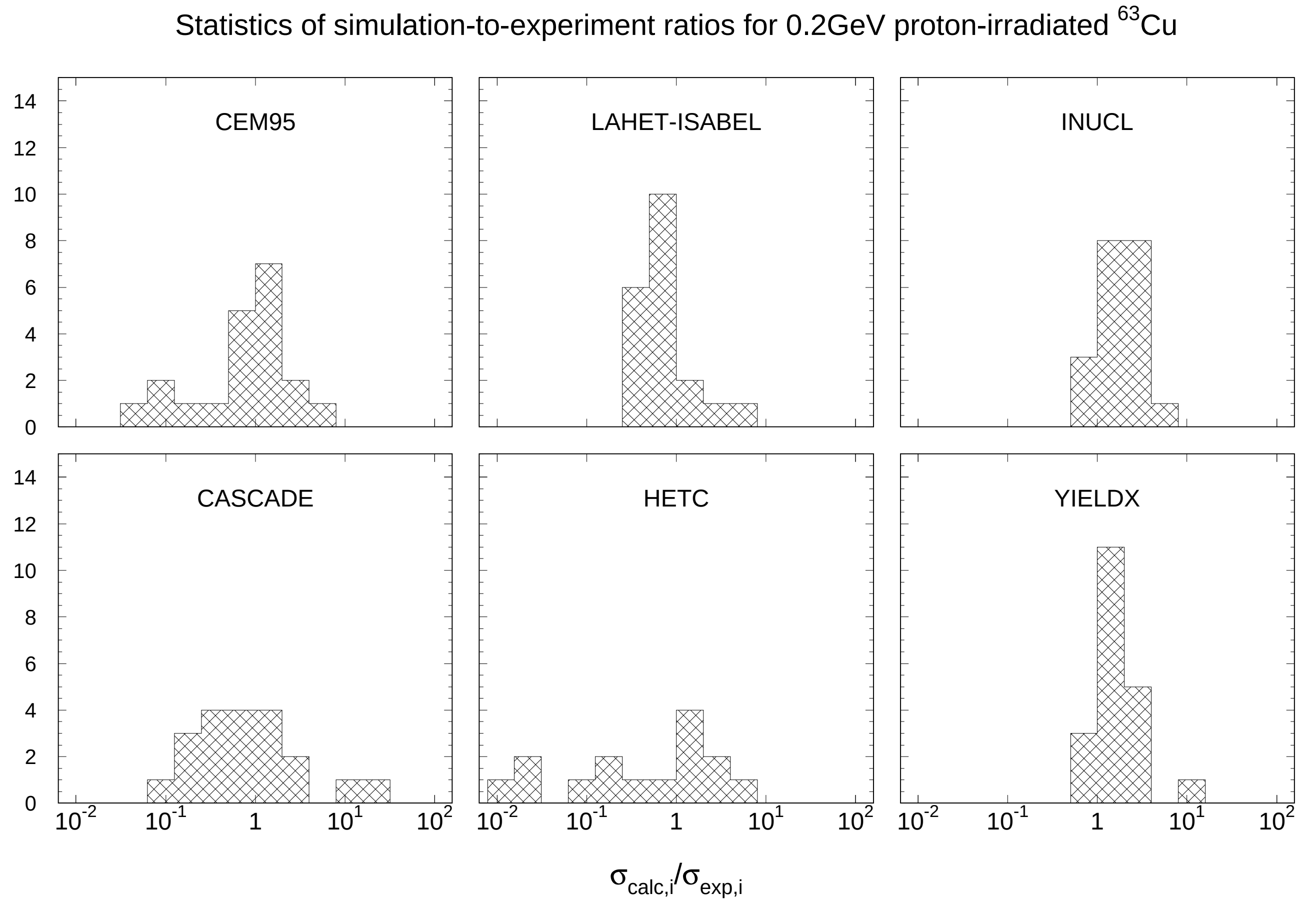

Fig. 119: Statistics of the simulation-to-experiment ratios (criterion 2) for ^{63}Cu irradiated with 0.2 GeV protons.

Table 99: Experimental and calculated yields from ^{63}Cu irradiated with 1.2 GeV protons.

Product	$T_{1/2}$	Type	Exp yield [mbarn]	CEM95	LAHET	CASCADE	HETC	INUCL	YIELDX	QMD
				Calculated Yields [mbarn] via						
^{63}Zn	38,47m	i	1.33 ± 0.20	0.247	1.01	0.100	1.00	0.025	0.522	0.060
^{62}Zn	9,26h	i	0.481 ± 0.053	0.445	0.854	1.31	0.924	0.132	0.204	0.259
^{61}Cu	3,333h	c	14.9 ± 1.7	19.6	16.2	20.4	28.6	15.7	9.56	13.0
^{60}Cu	23,7m	c*	3.46 ± 0.25	3.48	2.51	4.17	2.80	7.50	2.27	1.18
^{57}Ni	35,60h	c	1.18 ± 0.10	1.20	0.652	5.23	2.15	4.10	1.49	0.237
^{56}Ni	5,9d	i	0.086 ± 0.012	0.165	0.075	3.15	–	0.403	0.233	0.051
^{61}Co	1,650h	c	5.29 ± 1.92	3.77	4.57	9.61	4.84	3.20	1.57	7.08
^{60}Co	5,2714y	i(m+g)	9.27 ± 0.68	5.82	5.85	9.07	4.78	11.1	7.60	8.46
^{58}Co	70,86d	i(m+g)	31.0 ± 2.2	20.7	18.8	8.89	6.14	21.8	37.7	22.7
^{57}Co	271,79d	i	27.1 ± 2.0	20.5	17.5	17.3	29.2	14.2	28.5	13.9
^{56}Co	77,233d	c	9.68 ± 0.67	15.0	6.62	6.70	28.4	15.1	9.10	2.70
^{55}Co	17,53h	c	1.73 ± 0.13	1.96	0.606	3.91	0.373	4.37	2.13	0.203
^{59}Fe	44,472d	c	0.931 ± 0.070	0.873	0.667	3.30	0.849	1.09	1.74	2.12
^{53}Fe	8,51m	c*	2.19 ± 0.37	1.65	0.737	4.19	0.060	5.23	2.23	0.395
^{56}Mn	2,5789h	c	2.56 ± 0.18	1.14	1.39	1.32	0.238	5.32	3.37	2.66
^{54}Mn	312,11d	i	21.7 ± 1.5	12.0	15.8	4.21	0.774	20.2	21.5	18.5
^{51}Cr	27,7025d	c	28.8 ± 2.2	24.5	16.0	25.0	24.9	22.5	25.6	18.6
^{49}Cr	42,3m	c	4.08 ± 0.34	1.98	2.01	4.79	2.37	6.69	2.78	0.358
^{48}Cr	21,56h	c	0.558 ± 0.041	0.165	0.329	3.31	–	0.676	0.528	–
^{48}V	15,9735d	c	15.2 ± 1.1	14.9	11.8	6.27	24.0	19.5	9.99	9.71
^{48}Sc	43,67h	i	0.581 ± 0.041	0.428	0.596	0.241	–	3.32	0.405	0.184
^{47}Sc	3,3492d	c	3.31 ± 0.24	1.40	2.78	1.62	–	3.10	1.68	1.71
^{46}Sc	83,79d	i(m+g)	8.29 ± 0.58	9.87	5.90	2.72	–	12.2	4.51	7.56
^{43}Sc	3,891h	c	4.72 ± 0.87	3.13	1.62	3.18	0.879	7.59	3.43	2.18
^{47}Ca	4,536d	c	0.071 ± 0.009	0.016	0.056	0.033	–	0.165	0.064	–
^{43}K	22,3h	c	1.28 ± 0.09	0.428	0.760	0.657	–	2.19	0.630	0.425
^{42}K	12,360h	i	4.09 ± 0.30	2.08	2.85	1.13	–	10.4	1.85	3.56
^{41}Ar	109,34m	c	0.708 ± 0.053	0.099	0.225	0.491	–	0.766	0.345	0.185
^{39}Cl	55,6m	c	0.442 ± 0.034	0.066	0.197	0.191	–	0.906	0.234	0.227
^{38}Cl	37,24m	c	1.50 ± 0.12	0.428	0.822	0.366	–	7.61	0.807	1.32
^{29}Al	6,56m	c	1.13 ± 0.14	0.132	1.26	0.233	–	1.70	0.750	0.733
^{28}Mg	20,915h	c	0.195 ± 0.014	–	–	0.075	–	0.313	0.174	–
^{27}Mg	9,462m	c	0.503 ± 0.074	0.181	0.141	0.158	–	0.676	0.487	0.132
^{24}Na	14,9590h	c	1.73 ± 0.12	0.692	1.47	0.091	–	2.48	1.19	0.638
^{22}Na	2,6019y	c	1.39 ± 0.20	0.857	1.24	0.058	0.641	1.24	1.10	0.429
^{7}Be	53,29d	i	5.47 ± 0.51	–	–	–	–	–	2.40	–

Products in ^{63}Cu irradiated with 1.2GeV protons

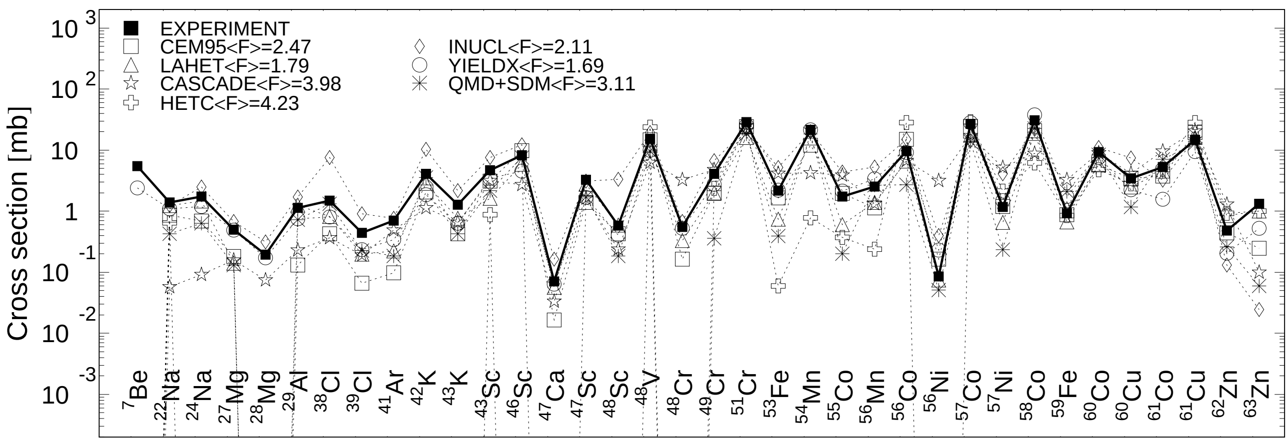

Fig. 120: Detailed comparison between experimental and simulated yields of radioactive reaction products in ^{63}Cu irradiated with 1.2 GeV protons. The cumulative yields are labeled -c when the respective independent yields are also shown.

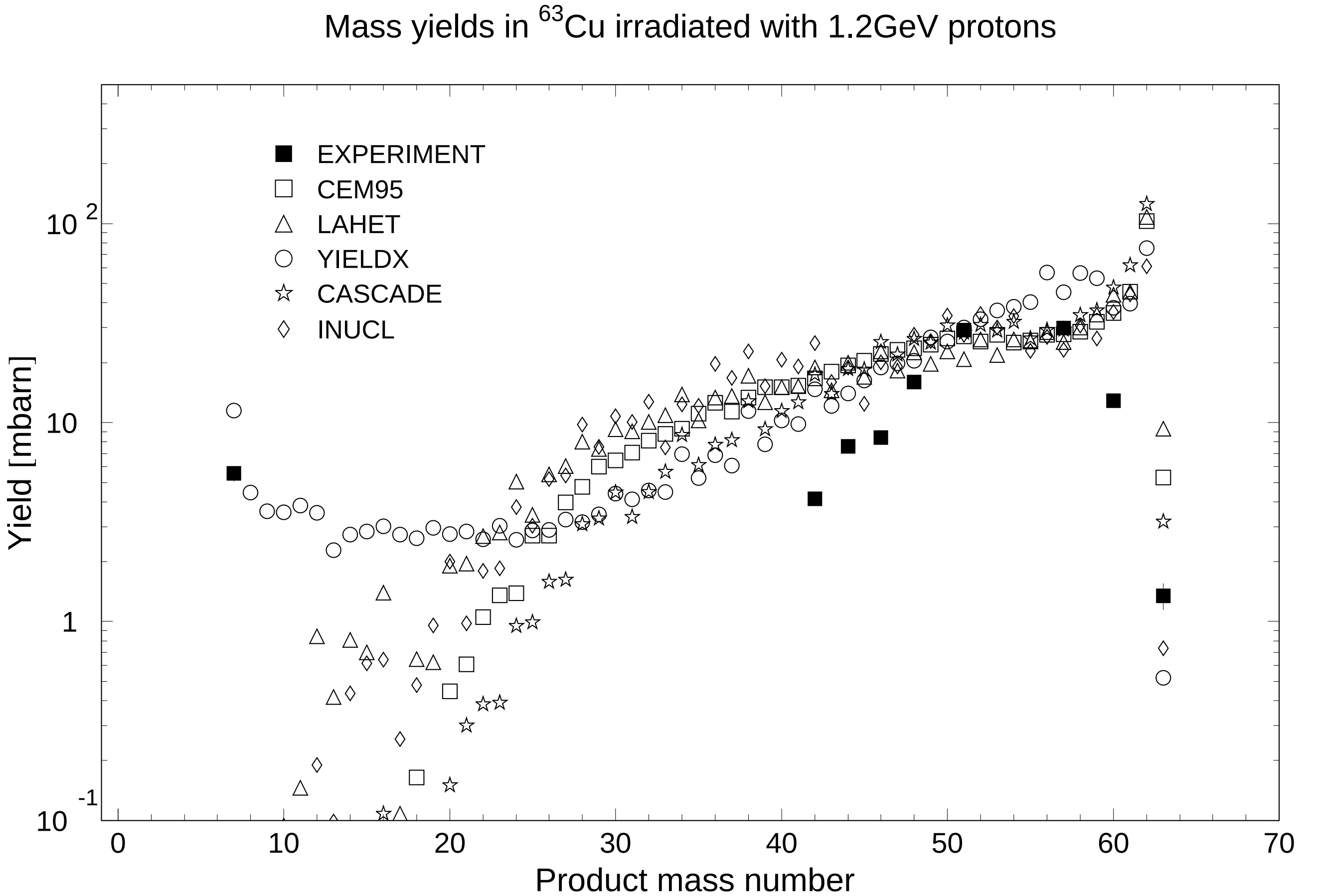

Fig. 121: The simulated mass distributions of reaction products together with the measured cumulative and supra-cumulative yields in ^{63}Cu irradiated with 1.2 GeV protons.

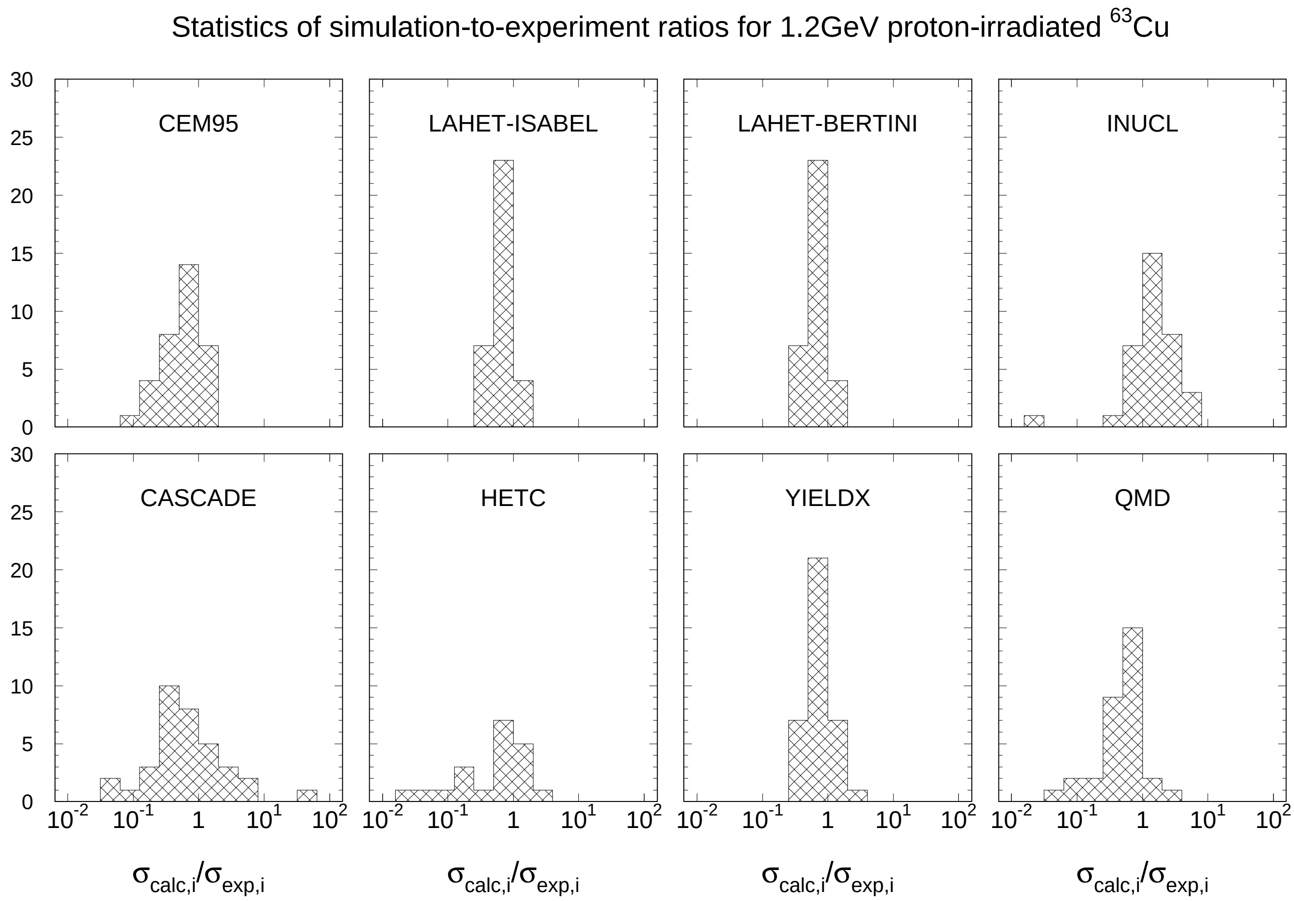

Fig. 122: Statistics of the simulation-to-experiment ratios (criterion 2) for ^{63}Cu irradiated with 1.2 GeV protons.

Table 100: Experimental and calculated yields from ^{63}Cu irradiated with 1.6 GeV protons.

Product	$T_{1/2}$	Type	Exp yield [mbarn]	Calculated Yields [mbarn] via CEM95	LAHET	CASCADE	HETC	INUCL	YIELDX
^{62}Zn	9,26h	i	0.328 ± 0.036	0.210	0.757	1.20	0.733	0.124	0.204
^{61}Cu	3,333h	c	12.2 ± 1.5	17.6	15.4	18.5	27.7	15.9	9.37
^{60}Cu	23,7m	c*	2.76 ± 0.23	3.41	2.33	4.03	2.57	7.31	2.23
^{57}Ni	35,60h	c	0.824 ± 0.069	1.03	0.635	2.87	1.73	3.17	1.36
^{60}Co	5,2714y	i(m+g)	6.74 ± 0.55	5.51	5.31	8.81	4.40	10.5	6.78
^{58}Co	70,86d	i(m+g)	23.7 ± 1.9	18.4	16.9	7.97	6.17	19.0	34.1
^{57}Co	271,79d	c	22.1 ± 1.8	18.4	15.6	17.0	27.0	15.2	27.4
^{56}Co	77,233d	c	7.10 ± 0.57	12.5	6.12	4.06	25.7	12.7	8.72
^{55}Co	17,53h	c	1.28 ± 0.11	1.82	0.400	1.98	0.344	3.74	2.06
^{59}Fe	44,472d	c	0.757 ± 0.065	0.891	0.785	3.17	0.578	1.04	1.57
^{56}Mn	2,5789h	c	2.03 ± 0.16	0.973	1.34	1.43	0.314	4.60	3.22
^{54}Mn	312,11d	i	16.4 ± 1.3	10.1	13.4	4.21	0.863	17.2	21.0
^{51}Cr	27,7025d	c	21.7 ± 1.8	19.3	13.8	20.5	21.5	19.1	25.7
^{49}Cr	42,3m	c	3.20 ± 0.29	1.74	1.79	2.34	2.14	5.66	2.85
^{48}Cr	21,56h	i	0.427 ± 0.035	0.165	0.249	1.34	–	0.594	0.546
^{48}V	15,9735d	c	11.6 ± 0.9	11.9	9.70	3.87	21.2	17.4	10.3
^{48}Sc	43,67h	i	0.483 ± 0.039	0.272	0.639	0.335	–	2.97	0.419
^{47}Sc	3,3492d	i	2.56 ± 0.21	1.32	2.38	2.64	0.010	2.57	1.69
^{46}Sc	83,79d	i(m+g)	6.68 ± 0.55	8.42	5.60	3.06	0.005	10.7	4.77
^{47}Ca	4,536d	c	0.064 ± 0.009	0.016	0.052	0.168	–	0.141	0.067
^{43}K	22,3h	c	1.13 ± 0.09	0.375	0.808	1.18	–	2.02	0.692
^{42}K	12,360h	i	3.57 ± 0.30	1.97	2.40	1.83	–	9.66	2.06
^{41}Ar	109,34m	c	0.645 ± 0.053	0.116	0.273	0.753	–	0.831	0.388
^{39}Cl	55,6m	c	0.436 ± 0.037	0.062	0.160	0.360	–	1.05	0.271
^{38}Cl	37,24m	c	1.55 ± 0.13	0.478	0.762	0.635	–	8.01	0.949
^{29}Al	6,56m	c	1.56 ± 0.17	0.322	1.50	0.685	–	3.02	0.976
^{28}Mg	20,915h	c	0.245 ± 0.020	0.012	0.009	0.283	–	0.460	0.230
^{27}Mg	9,462m	c	0.713 ± 0.079	0.243	0.244	0.465	–	1.06	0.656
^{24}Na	14,9590h	c	2.16 ± 0.18	1.49	2.94	0.514	–	4.87	1.55
^{22}Na	2,6019y	c	1.45 ± 0.13	1.84	3.05	0.151	3.42	2.60	1.44
^{7}Be	53,29d	i	5.85 ± 0.59	–	–	–	–	–	3.84

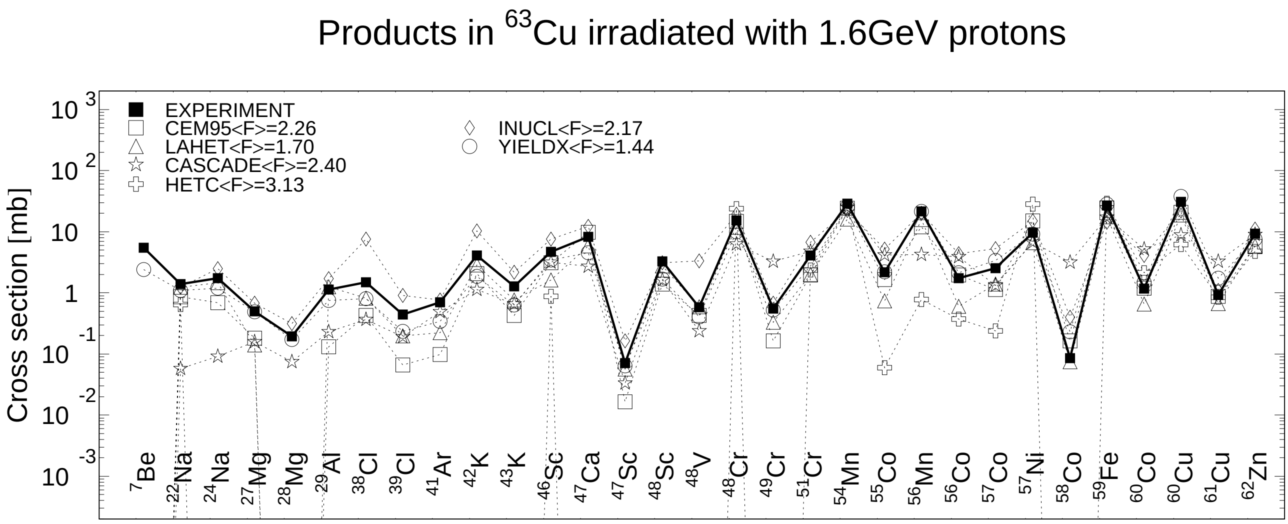

Fig. 123: Detailed comparison between experimental and simulated yields of radioactive reaction products in ^{63}Cu irradiated with 1.6 GeV protons. The cumulative yields are labeled -c when the respective independent yields are also shown.

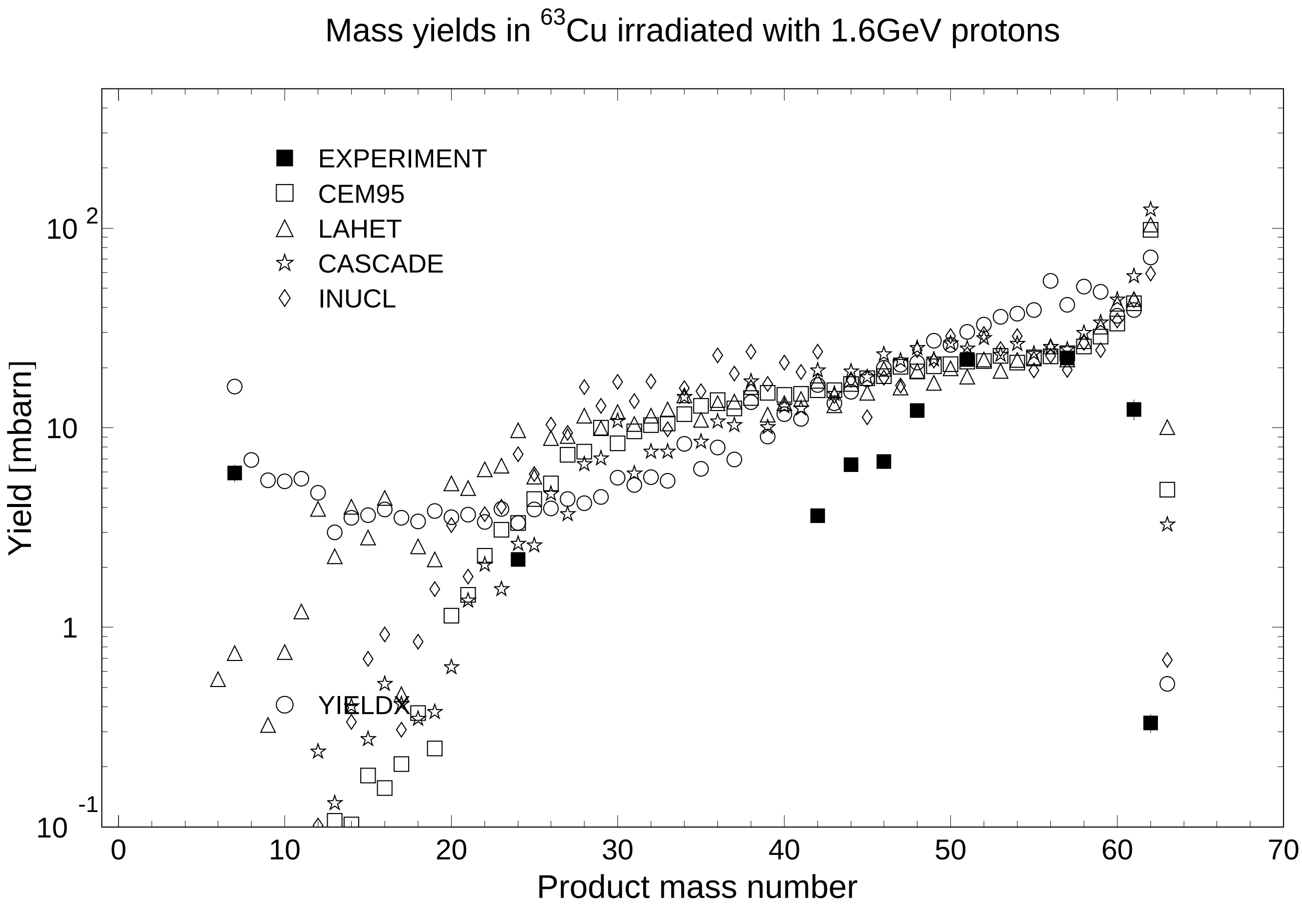

Fig. 124: The simulated mass distributions of reaction products together with the measured cumulative and supra-cumulative yields in ^{63}Cu irradiated with 1.6 GeV protons.

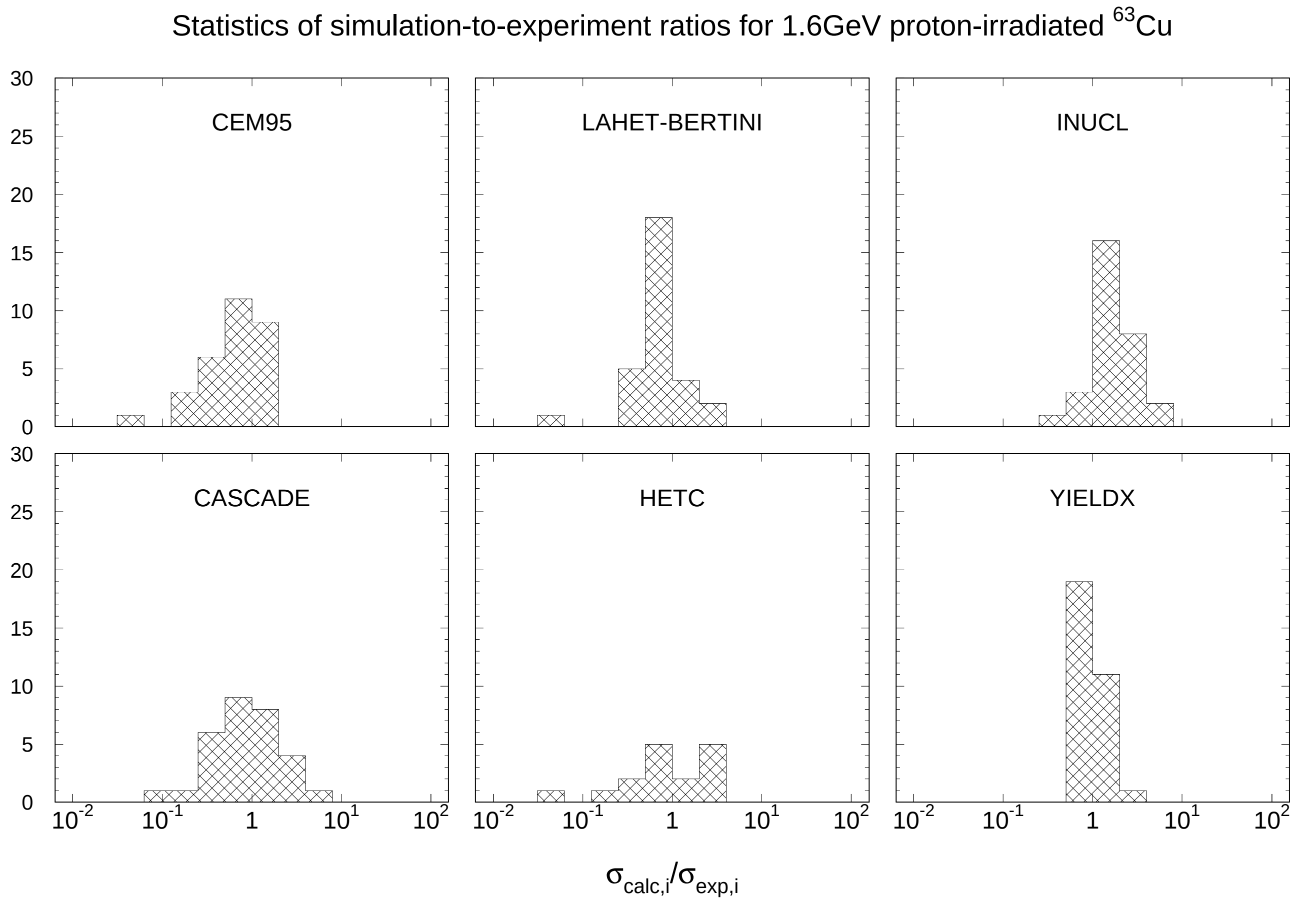

Fig. 125: Statistics of the simulation-to-experiment ratios (criterion 2) for ^{63}Cu irradiated with 1.6 GeV protons.

Table 101: Experimental and calculated yields from ^{63}Cu irradiated with 2.6 GeV protons.

Product	$T_{1/2}$	Type	Exp yield [mbarn]	Calculated Yields [mbarn] via CEM95	LAHET	CASCADE	HETC	INUCL	YIELDX
^{62}Zn	9,26h	i	0.336 ± 0.035	0.206	0.707	1.04	0.792	0.091	0.204
^{61}Cu	3,333h	c	12.6 ± 1.5	13.7	14.4	16.8	25.5	16.0	9.34
^{60}Cu	23,7m	c*	2.62 ± 0.22	2.73	2.21	4.15	2.28	6.59	2.22
^{57}Ni	35,60h	c	0.777 ± 0.074	0.891	0.384	2.43	1.38	2.57	1.04
^{60}Co	5,2714y	i(m+g)	8.39 ± 0.88	4.81	4.43	8.48	3.57	10.5	4.79
^{58}Co	70,86d	i(m+g)	23.1 ± 1.9	13.9	14.4	6.76	5.18	16.3	25.4
^{57}Co	271,79d	c	21.5 ± 1.8	13.6	14.0	13.6	22.4	12.7	20.9
^{56}Co	77,233d	c	6.94 ± 0.57	9.21	5.20	3.56	21.3	10.9	7.02
^{55}Co	17,53h	c	1.17 ± 0.10	1.39	0.370	1.83	0.316	3.04	1.69
^{59}Fe	44,472d	c	0.757 ± 0.078	0.850	0.560	3.18	0.591	0.832	1.15
^{56}Mn	2,5789h	c	1.91 ± 0.16	0.887	1.12	1.41	0.265	3.94	2.59
^{54}Mn	312,11d	i	15.4 ± 1.3	7.86	11.3	3.59	0.797	13.7	17.8
^{51}Cr	27,7025d	c	19.8 ± 1.7	14.8	11.0	17.3	17.4	14.9	23.7
^{49}Cr	42,3m	c	2.78 ± 0.26	1.21	1.29	2.18	1.74	4.55	2.78
^{48}Cr	21,56h	i	0.383 ± 0.033	0.124	0.228	1.14	–	0.462	0.547
^{48}V	15,9735d	c	10.6 ± 0.9	9.38	8.37	3.29	17.7	13.9	10.4
^{48}Sc	43,67h	i	0.451 ± 0.040	0.190	0.451	0.292	–	2.40	0.420
^{47}Sc	3,3492d	i	2.43 ± 0.21	1.13	2.06	2.38	0.010	2.29	1.74
^{46}Sc	83,79d	i(m+g)	6.37 ± 0.56	6.41	4.40	2.77	0.010	9.03	5.05
^{47}Ca	4,536d	c	0.065 ± 0.014	0.025	0.043	0.118	–	0.147	0.069
^{43}K	22,3h	c	1.10 ± 0.09	0.280	0.717	1.22	–	1.87	0.793
^{42}K	12,360h	i	3.51 ± 0.30	1.58	2.07	1.83	–	8.60	2.42
^{41}Ar	109,34m	c	0.683 ± 0.058	0.083	0.218	0.886	–	0.845	0.469
^{39}Cl	55,6m	c	0.479 ± 0.050	0.041	0.128	0.456	–	1.04	0.345
^{38}Cl	37,24m	c	1.64 ± 0.15	0.474	0.570	0.886	–	7.47	1.24
^{29}Al	6,56m	c	1.83 ± 0.49	0.268	1.60	1.26	–	4.25	1.53
^{28}Mg	20,915h	c	0.357 ± 0.030	0.008	0.009	0.573	–	0.706	0.368
^{27}Mg	9,462m	c	1.15 ± 0.15	0.318	0.204	1.13	–	1.75	1.06
^{24}Na	14,9590h	c	3.31 ± 0.28	2.33	3.74	1.49	–	9.46	2.36
^{22}Na	2,6019y	c	2.72 ± 0.90	2.99	4.34	0.544	7.11	5.83	2.18
^{7}Be	53,29d	i	8.71 ± 0.92	–	2.48	–	0.005	–	7.94

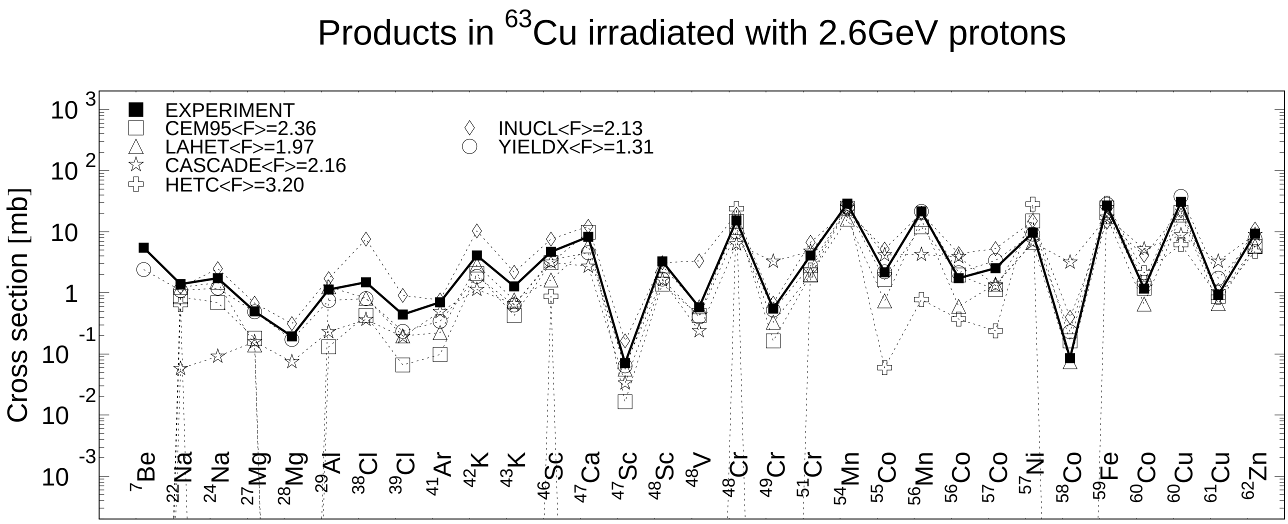

Fig. 126: Detailed comparison between experimental and simulated yields of radioactive reaction products in ^{63}Cu irradiated with 2.6 GeV protons. The cumulative yields are labeled -c when the respective independent yields are also shown.

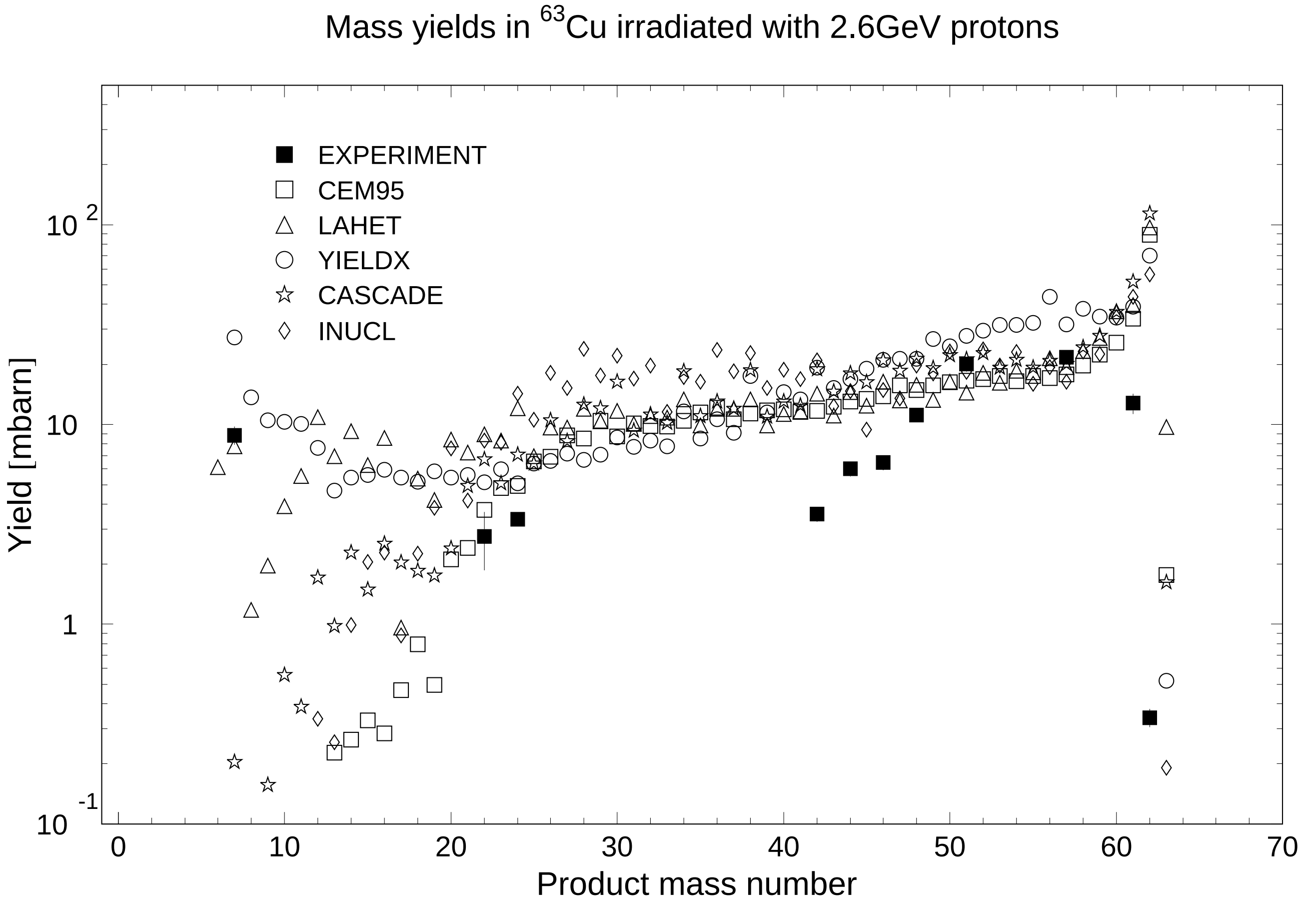

Fig. 127: The simulated mass distributions of reaction products together with the measured cumulative and supra-cumulative yields in ^{63}Cu irradiated with 2.6 GeV protons.

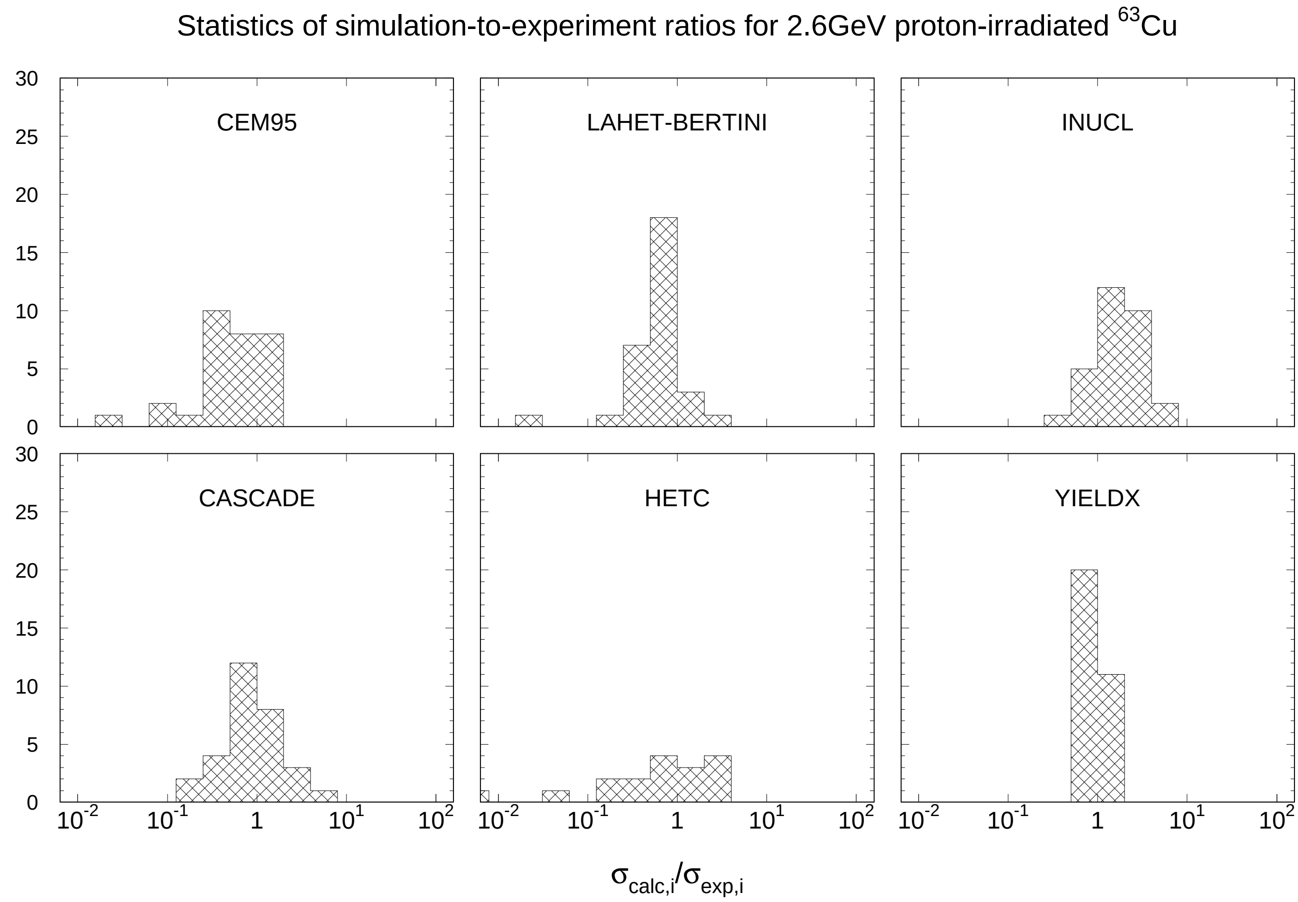

Fig. 128: Statistics of the simulation-to-experiment ratios (criterion 2) for ^{63}Cu irradiated with 2.6 GeV protons.

Table 102: Experimental and calculated yields from ^{65}Cu irradiated with 0.2 GeV protons.

Product	$T_{1/2}$	Type	Exp yield [mbarn]	Calculated Yields [mbarn] via CEM95	LAHET	CASCADE	HETC	INUCL	YIELDX
^{65}Zn	244,26d	i	2.88 ± 0.22	11.2	4.36	3.87	7.10	5.77	4.00
^{63}Zn	38,47m	i	4.34 ± 0.33	2.70	5.11	4.13	16.4	6.07	4.04
^{62}Zn	9,26h	i	0.970 ± 0.087	0.242	1.41	3.82	0.077	1.10	1.87
^{64}Cu	12,700h	i	68.1 ± 4.8	68.5	70.7	93.8	71.3	48.6	79.2
^{61}Cu	3,333h	c	14.0 ± 1.5	22.1	19.3	11.7	49.5	19.2	31.5
^{60}Cu	23,7m	c*	3.10 ± 0.21	3.72	2.36	0.369	5.61	11.3	5.61
^{57}Ni	35,60h	c	0.572 ± 0.040	0.724	0.310	2.61	3.07	4.29	0.643
^{61}Co	1,650h	c	5.11 ± 0.68	8.18	8.09	3.63	1.67	8.85	15.6
^{60}Co	5,2714y	i(m+g)	19.9 ± 1.5	15.0	14.5	5.53	2.34	33.7	35.5
^{58}Co	70,86d	i(m+g)	34.3 ± 2.3	41.8	32.1	13.3	3.15	46.2	62.9
^{57}Co	271,79d	c	24.6 ± 1.6	30.0	23.1	24.2	45.6	29.4	25.2
^{56}Co	77,233d	c	5.95 ± 0.40	13.4	6.02	3.08	41.7	16.8	4.59
^{55}Co	17,53h	c	0.681 ± 0.049	0.876	0.184	0.912	0.489	2.96	0.616
^{59}Fe	44,472d	c	2.65 ± 0.19	3.03	1.61	1.43	0.187	1.96	8.40
^{56}Mn	2,5789h	c	3.49 ± 0.23	2.17	2.24	0.835	0.019	8.41	7.86
^{54}Mn	312,11d	i	13.1 ± 0.9	9.06	11.5	3.47	0.034	19.8	21.9
^{51}Cr	27,7025d	c	6.06 ± 0.46	2.28	2.75	3.88	0.763	5.51	7.20
^{48}V	15,9735d	c	0.906 ± 0.061	0.188	0.300	0.060	–	0.583	1.27
^{48}Sc	43,67h	i	0.055 ± 0.006	0.007	0.010	0.007	–	0.119	0.179
^{47}Sc	3,3492d	c	0.248 ± 0.018	0.033	0.053	0.043	–	0.057	0.582

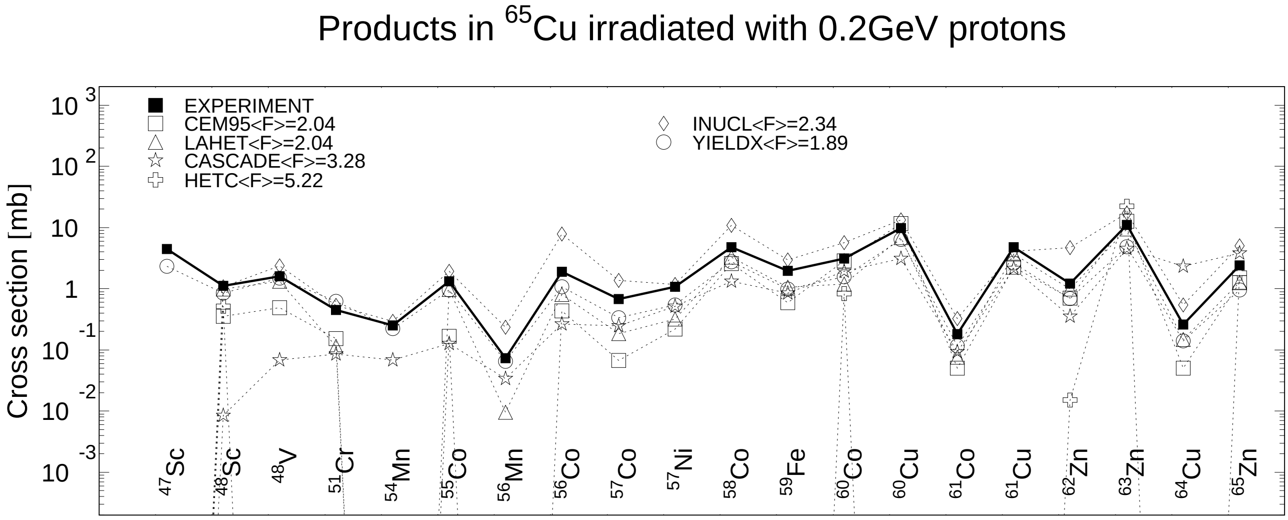

Fig. 129: Detailed comparison between experimental and simulated yields of radioactive reaction products in ^{65}Cu irradiated with 0.2 GeV protons. The cumulative yields are labeled -c when the respective independent yields are also shown.

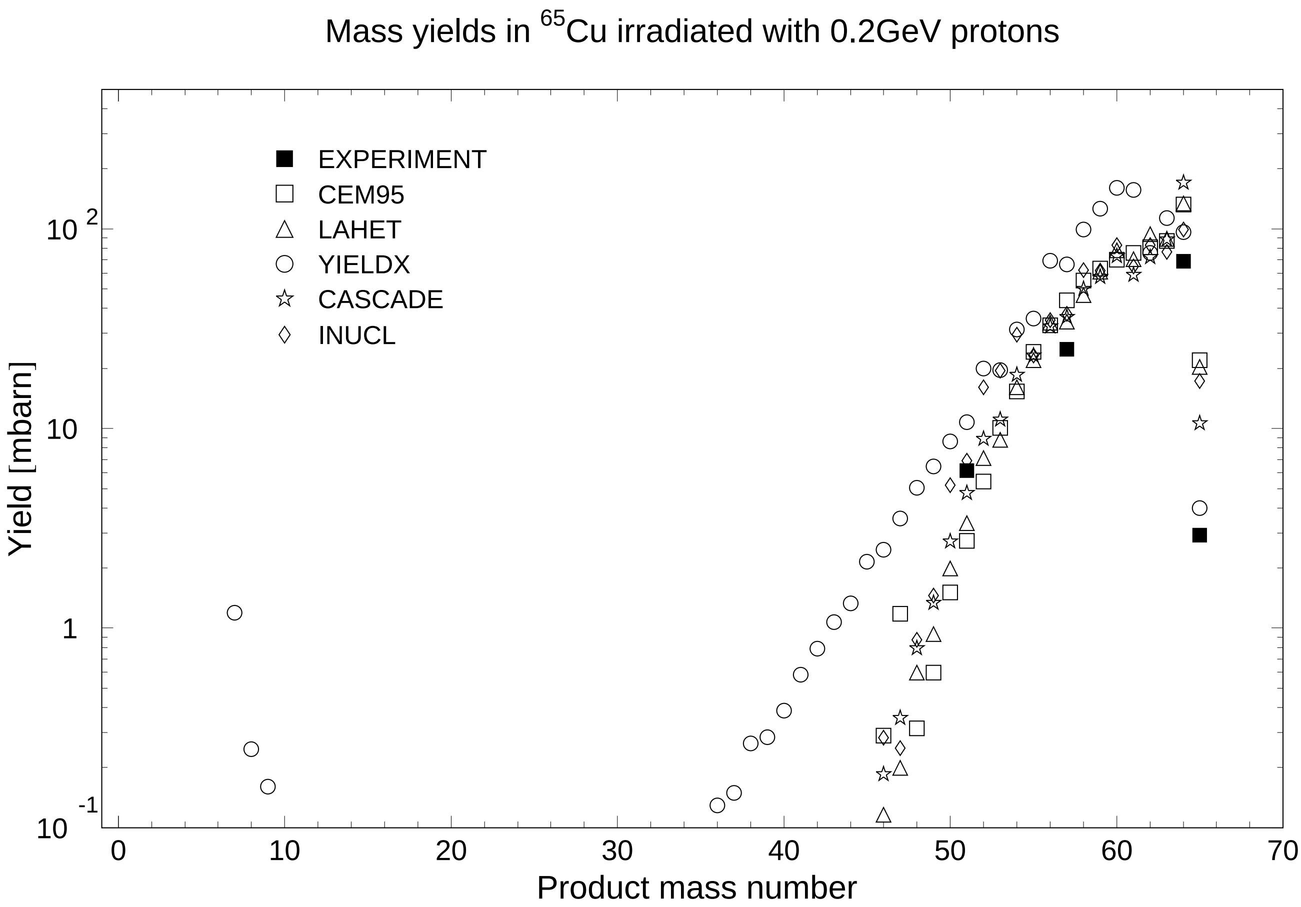

Fig. 130: The simulated mass distributions of reaction products together with the measured cumulative and supra-cumulative yields in ^{65}Cu irradiated with 0.2 GeV protons.

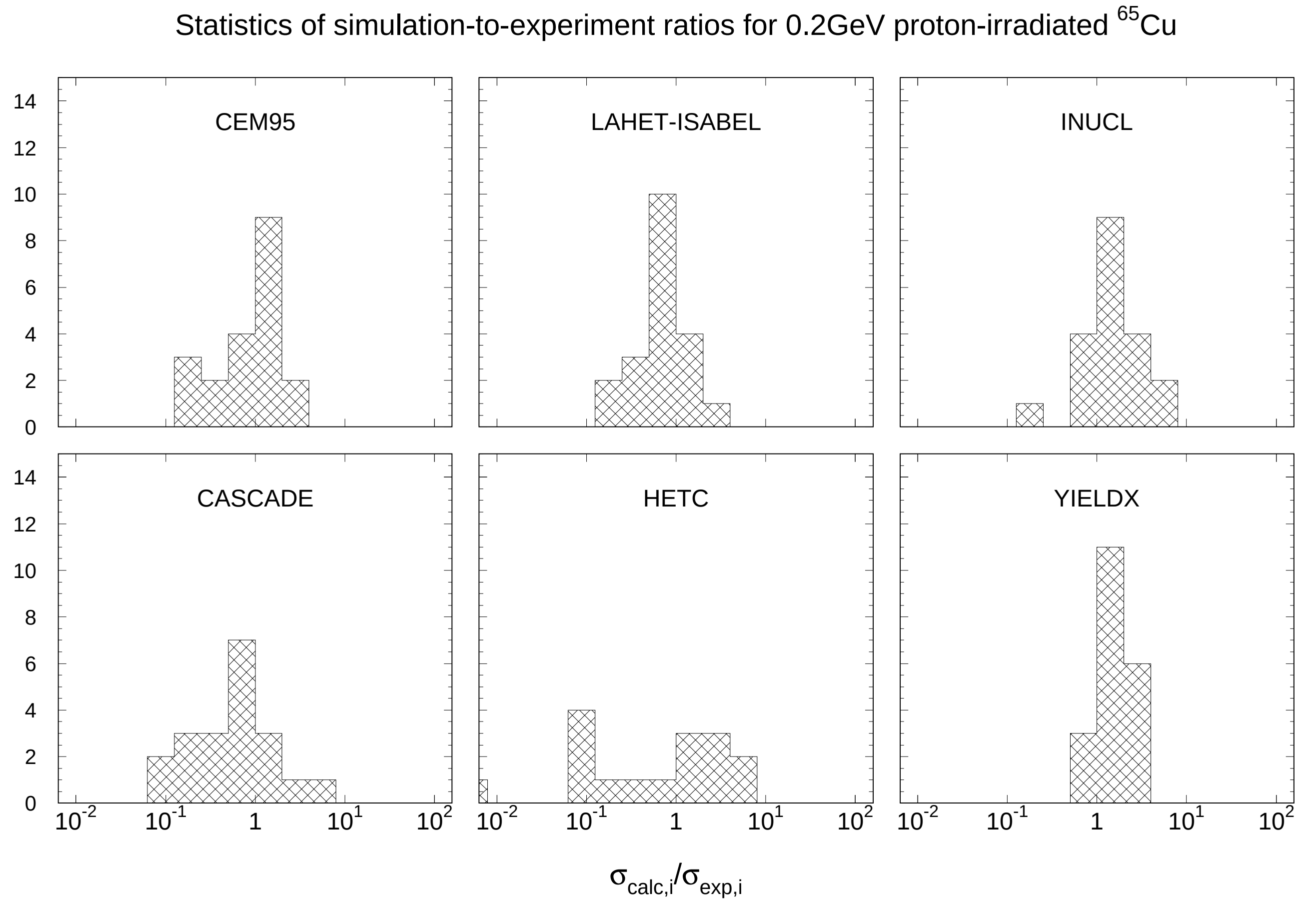

Fig. 131: Statistics of the simulation-to-experiment ratios (criterion 2) for ^{65}Cu irradiated with 0.2 GeV protons.

Table 103: Experimental and calculated yields from ^{65}Cu irradiated with 1.2 GeV protons.

Product	$T_{1/2}$	Type	Exp yield [mbarn]	Calculated Yields [mbarn] via CEM95	LAHET	CASCADE	HETC	INUCL	YIELDX	QMD
^{65}Zn	244,26d	i	1.73 ± 0.13	0.236	1.02	0.017	0.861	0.017	0.661	0.250
^{63}Zn	38,47m	i	1.32 ± 0.26	0.387	0.811	0.706	2.94	0.564	0.395	0.089
^{62}Zn	9,26h	i	0.219 ± 0.027	0.034	0.210	0.595	0.030	0.211	0.183	–
^{64}Cu	12,700h	i	61.4 ± 4.7	54.1	53.8	70.7	59.1	29.9	63.4	85.8
^{61}Cu	3,333h	c	5.42 ± 0.62	6.95	5.85	5.32	16.5	5.60	12.2	4.39
^{60}Cu	23,7m	c*	1.08 ± 0.08	1.04	0.549	0.493	1.64	3.14	2.13	0.275
^{65}Ni	2,51719h	c	0.390 ± 0.043	0.034	0.806	–	0.106	–	–	–
^{57}Ni	35,60h	c	0.392 ± 0.035	0.488	0.215	2.98	1.51	1.89	0.390	0.027
^{56}Ni	5,9d	i	0.356 ± 0.084	0.034	0.010	1.93	–	0.126	0.044	–
^{61}Co	1,650h	c	6.52 ± 0.87	5.86	7.89	10.2	6.07	6.70	6.09	8.13
^{60}Co	5,2714y	i(m+g)	16.8 ± 1.2	8.36	8.97	6.54	5.93	14.1	13.6	9.73
^{58}Co	70,86d	i(m+g)	25.4 ± 1.8	18.3	15.4	9.17	7.26	20.2	31.1	18.1
^{57}Co	271,79d	i	18.5 ± 1.3	16.4	11.9	14.2	24.3	12.0	14.9	9.16
^{56}Co	77,233d	c	5.08 ± 0.36	10.3	4.10	4.25	25.4	10.3	3.41	1.13
^{55}Co	17,53h	c	0.739 ± 0.056	1.11	0.167	2.24	0.438	2.39	0.563	0.045
^{59}Fe	44,472d	c	4.19 ± 0.33	2.66	2.05	3.31	1.77	2.23	3.28	4.26
^{53}Fe	8,51m	c*	1.30 ± 0.43	0.656	0.296	2.80	0.030	3.58	0.641	0.158
^{56}Mn	2,5789h	c	6.04 ± 0.43	2.59	2.63	1.71	0.695	7.71	5.85	4.62
^{54}Mn	312,11d	i	22.5 ± 1.6	13.5	16.2	5.47	1.42	19.6	24.5	16.2
^{51}Cr	27,7025d	c	23.5 ± 1.8	22.0	14.8	22.5	23.2	20.4	15.0	16.5
^{49}Cr	42,3m	c	2.40 ± 0.20	1.26	1.29	3.80	1.79	5.03	0.955	0.541
^{48}Cr	21,56h	c	0.260 ± 0.019	0.051	0.148	2.32	–	0.547	0.140	0.021
^{48}V	15,9735d	c	11.0 ± 0.8	12.7	9.55	4.58	22.3	17.3	4.86	8.76
^{48}Sc	43,67h	i	1.21 ± 0.09	0.707	0.992	0.357	0.015	4.69	0.688	0.553
^{47}Sc	3,3492d	i	4.81 ± 0.35	2.26	3.73	2.15	–	4.10	2.64	2.17
^{46}Sc	83,79d	i(m+g)	9.77 ± 0.68	11.6	6.89	3.13	–	13.4	6.41	7.57
^{43}Sc	3,891h	c	3.10 ± 0.76	2.85	1.20	1.94	0.831	5.70	1.57	1.82
^{47}Ca	4,536d	c	0.182 ± 0.014	0.051	0.076	0.094	–	0.328	0.116	0.141
^{43}K	22,3h	c	1.98 ± 0.14	0.589	1.06	0.842	–	2.98	0.993	0.999
^{42}K	12,360h	i	4.82 ± 0.35	2.58	3.27	1.32	–	10.9	2.77	4.10
^{41}Ar	109,34m	c	1.08 ± 0.08	0.219	0.320	0.519	–	1.18	0.541	0.268
^{39}Cl	55,6m	c	0.679 ± 0.051	0.067	0.186	0.247	–	1.38	0.337	0.164
^{38}Cl	37,24m	i(m+g)	1.90 ± 0.14	0.438	0.806	0.264	–	7.87	1.08	1.36
^{38}S	170,3m	c	0.073 ± 0.008	–	0.010	0.034	–	0.235	0.065	0.002
^{29}Al	6,56m	c	1.32 ± 0.14	0.168	0.973	0.127	–	1.94	0.951	0.404
^{28}Mg	20,915h	c	0.251 ± 0.018	–	–	0.068	–	0.293	0.224	0.052
^{27}Mg	9,462m	c	0.452 ± 0.068	0.152	0.115	0.085	–	0.531	0.625	0.111
^{24}Na	14,9590h	c	1.61 ± 0.13	0.488	1.33	0.068	–	2.36	1.50	0.427
^{22}Na	2,6019y	c	1.12 ± 0.11	0.354	0.983	0.009	0.513	1.08	0.849	0.102
^{7}Be	53,29d	i	4.50 ± 0.42	–	–	–	–	–	2.34	–

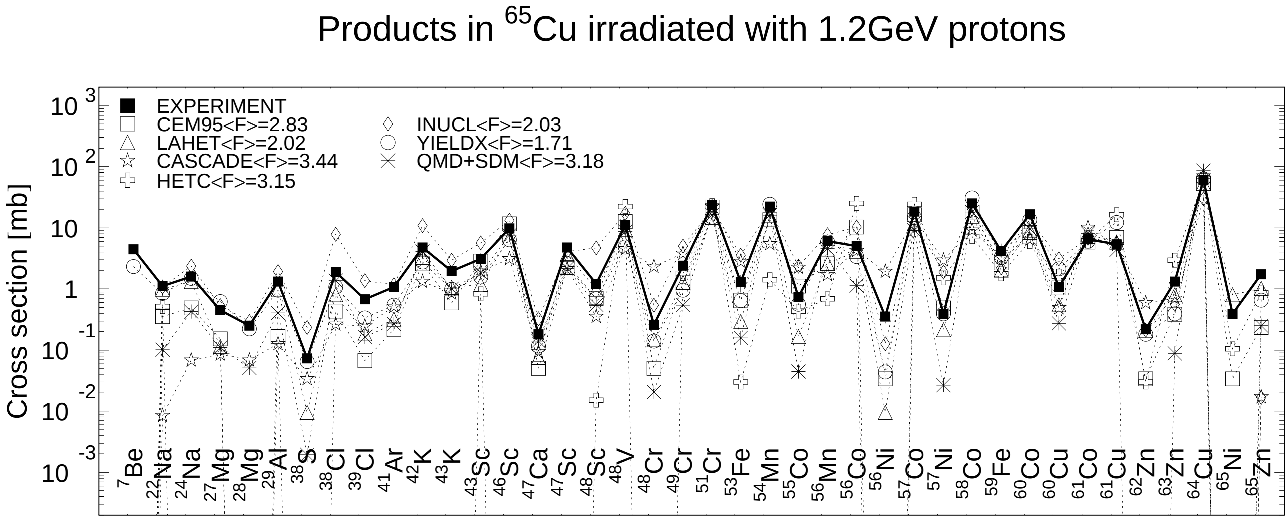

Fig. 132: Detailed comparison between experimental and simulated yields of radioactive reaction products in ^{65}Cu irradiated with 1.2 GeV protons. The cumulative yields are labeled -c when the respective independent yields are also shown.

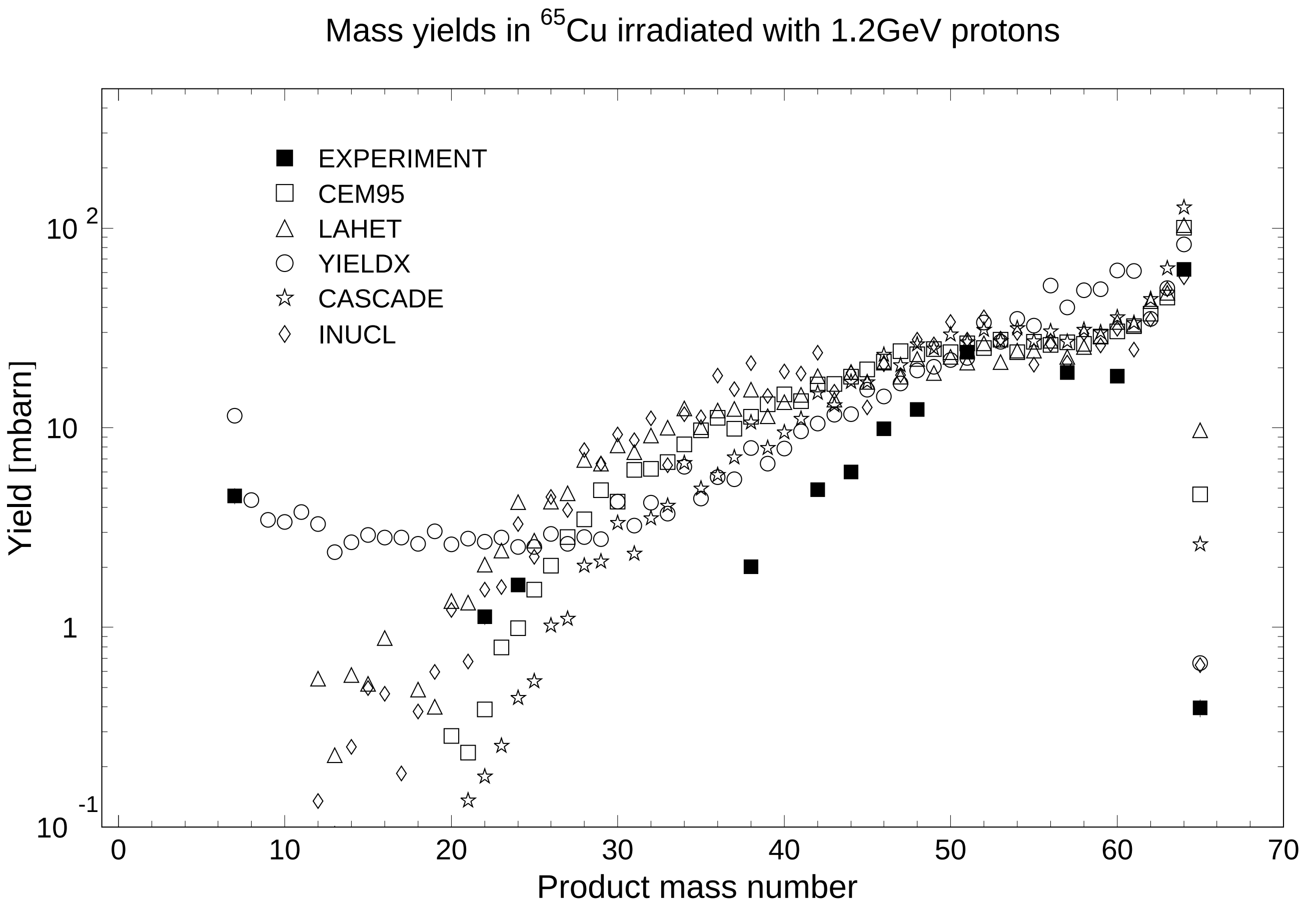

Fig. 133: The simulated mass distributions of reaction products together with the measured cumulative and supra-cumulative yields in ^{65}Cu irradiated with 1.2 GeV protons.

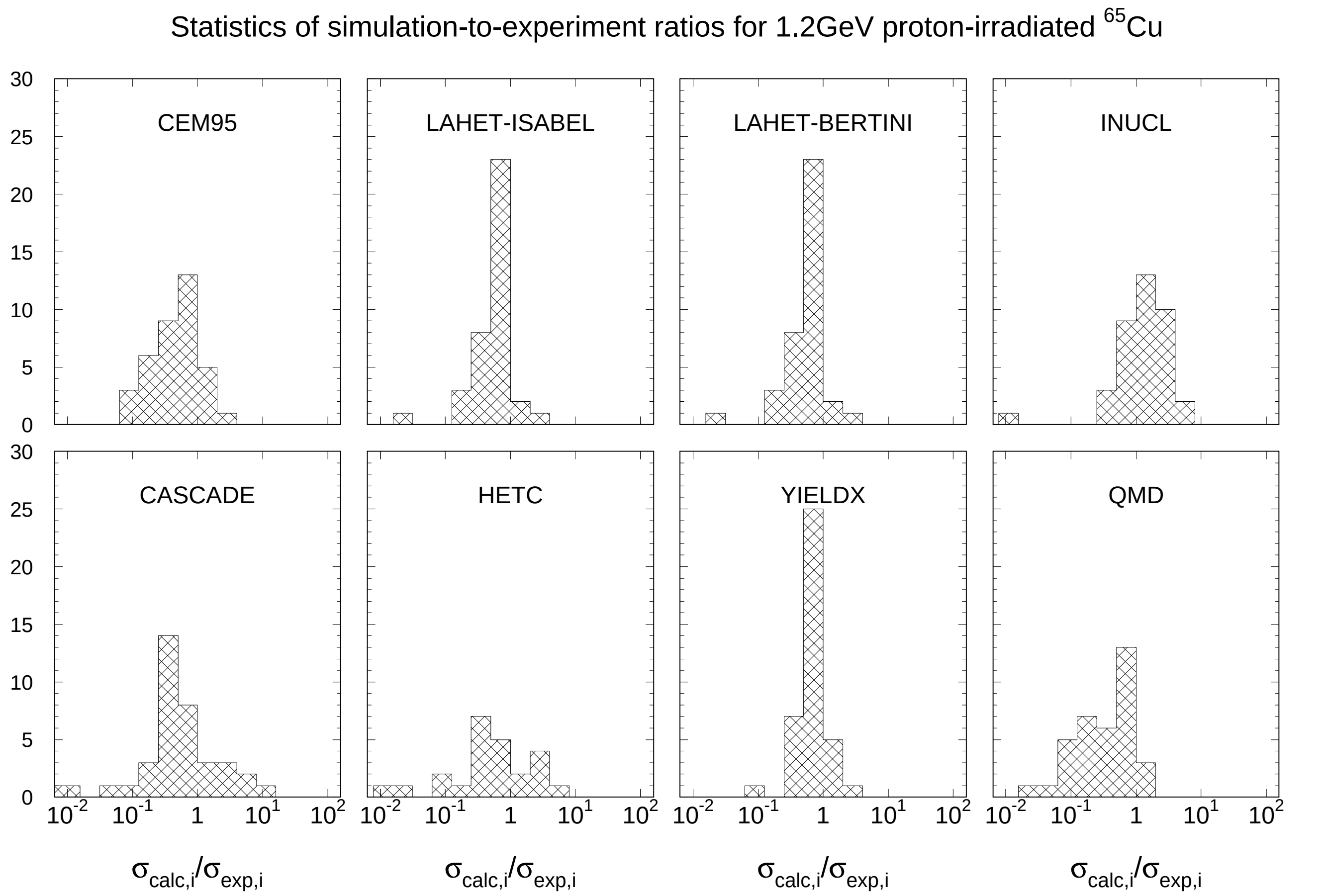

Fig. 134: Statistics of the simulation-to-experiment ratios (criterion 2) for ^{65}Cu irradiated with 1.2 GeV protons.

Table 104: Experimental and calculated yields from ^{65}Cu irradiated with 1.6 GeV protons.

Product	$T_{1/2}$	Type	Exp yield [mbarn]	Calculated Yields [mbarn] via CEM95	LAHET	CASCADE	HETC	INUCL	YIELDX
^{65}Zn	244,26d	i	1.54 ± 0.15	0.185	0.945	0.028	0.635	0.007	0.661
^{62}Zn	9,26h	i	0.159 ± 0.023	0.034	0.258	0.396	0.060	0.066	0.126
^{64}Cu	12,700h	i	62.5 ± 5.4	53.0	53.2	69.6	58.8	30.0	62.9
^{61}Cu	3,333h	c	4.98 ± 0.60	6.39	5.04	3.71	15.4	4.81	10.9
^{60}Cu	23,7m	c*	0.893 ± 0.076	1.13	0.559	0.517	1.49	2.73	1.93
^{57}Ni	35,60h	c	0.311 ± 0.026	0.375	0.139	1.26	1.06	1.64	0.376
^{61}Co	1,650h	c	7.40 ± 0.89	5.84	7.33	10.4	5.46	6.15	5.45
^{60}Co	5,2714y	i(m+g)	15.7 ± 1.3	7.60	8.41	6.37	5.91	12.4	12.2
^{58}Co	70,86d	i(m+g)	22.0 ± 1.8	15.6	14.1	7.23	6.66	16.5	29.7
^{57}Co	271,79d	c	15.9 ± 1.3	13.6	10.4	12.1	23.2	12.1	14.8
^{56}Co	77,233d	c	4.35 ± 0.35	7.89	3.17	2.02	22.2	8.16	3.31
^{55}Co	17,53h	c	0.600 ± 0.062	0.860	0.186	0.905	0.368	1.81	0.551
^{59}Fe	44,472d	c	4.01 ± 0.33	2.22	1.89	3.55	1.60	2.06	2.98
^{56}Mn	2,5789h	c	5.53 ± 0.45	2.35	2.56	1.87	0.696	6.06	5.68
^{54}Mn	312,11d	i	19.4 ± 1.6	11.7	13.4	5.77	1.18	16.3	24.3
^{51}Cr	27,7025d	c	20.5 ± 1.7	17.7	12.4	19.8	20.6	18.2	15.2
^{49}Cr	42,3m	c	2.13 ± 0.20	1.05	1.10	1.76	1.86	4.50	0.994
^{48}Cr	21,56h	c	0.233 ± 0.019	0.072	0.196	0.930	–	0.491	0.147
^{48}V	15,9735d	c	9.79 ± 0.78	10.5	8.26	2.84	20.6	15.5	5.11
^{48}Sc	43,67h	i	1.16 ± 0.09	0.619	0.974	0.567	0.020	4.07	0.723
^{47}Sc	3,3492d	i	4.60 ± 0.38	1.83	3.33	3.19	0.010	3.63	2.81
^{46}Sc	83,79d	i(m+g)	9.34 ± 0.75	9.48	6.23	3.46	0.035	12.0	6.90
^{47}Ca	4,536d	c	0.174 ± 0.017	0.059	0.057	0.261	–	0.246	0.123
^{43}K	22,3h	c	2.07 ± 0.16	0.581	1.18	1.68	–	2.80	1.11
^{42}K	12,360h	i	5.25 ± 0.43	2.78	2.85	2.16	–	10.8	3.14
^{41}Ar	109,34m	c	1.22 ± 0.10	0.324	0.248	1.03	–	1.21	0.623
^{39}Cl	55,6m	c	0.788 ± 0.066	0.143	0.205	0.435	–	1.40	0.394
^{38}Cl	37,24m	i(m+g)	2.23 ± 0.19	0.674	0.836	0.657	–	8.95	1.24
^{38}S	170,3m	c	0.136 ± 0.025	0.008	0.010	0.098	–	0.241	0.075
^{29}Al	6,56m	c	1.71 ± 0.21	0.287	1.54	0.649	–	3.18	1.27
^{28}Mg	20,915h	c	0.385 ± 0.031	0.008	0.005	0.292	–	0.562	0.304
^{27}Mg	9,462m	c	1.08 ± 0.12	0.198	0.234	0.458	–	1.09	0.843
^{24}Na	14,9590h	c	2.54 ± 0.21	1.14	2.99	0.376	–	4.17	1.95
^{7}Be	53,29d	i	5.68 ± 0.58	–	–	–	–	–	3.75

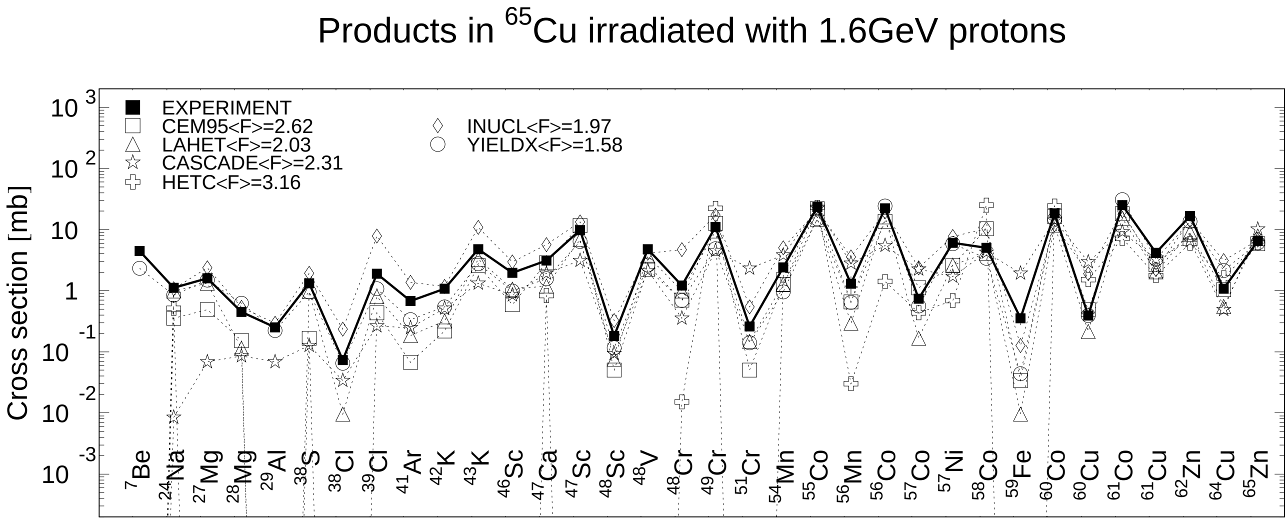

Fig. 135: Detailed comparison between experimental and simulated yields of radioactive reaction products in ^{65}Cu irradiated with 1.6 GeV protons. The cumulative yields are labeled -c when the respective independent yields are also shown.

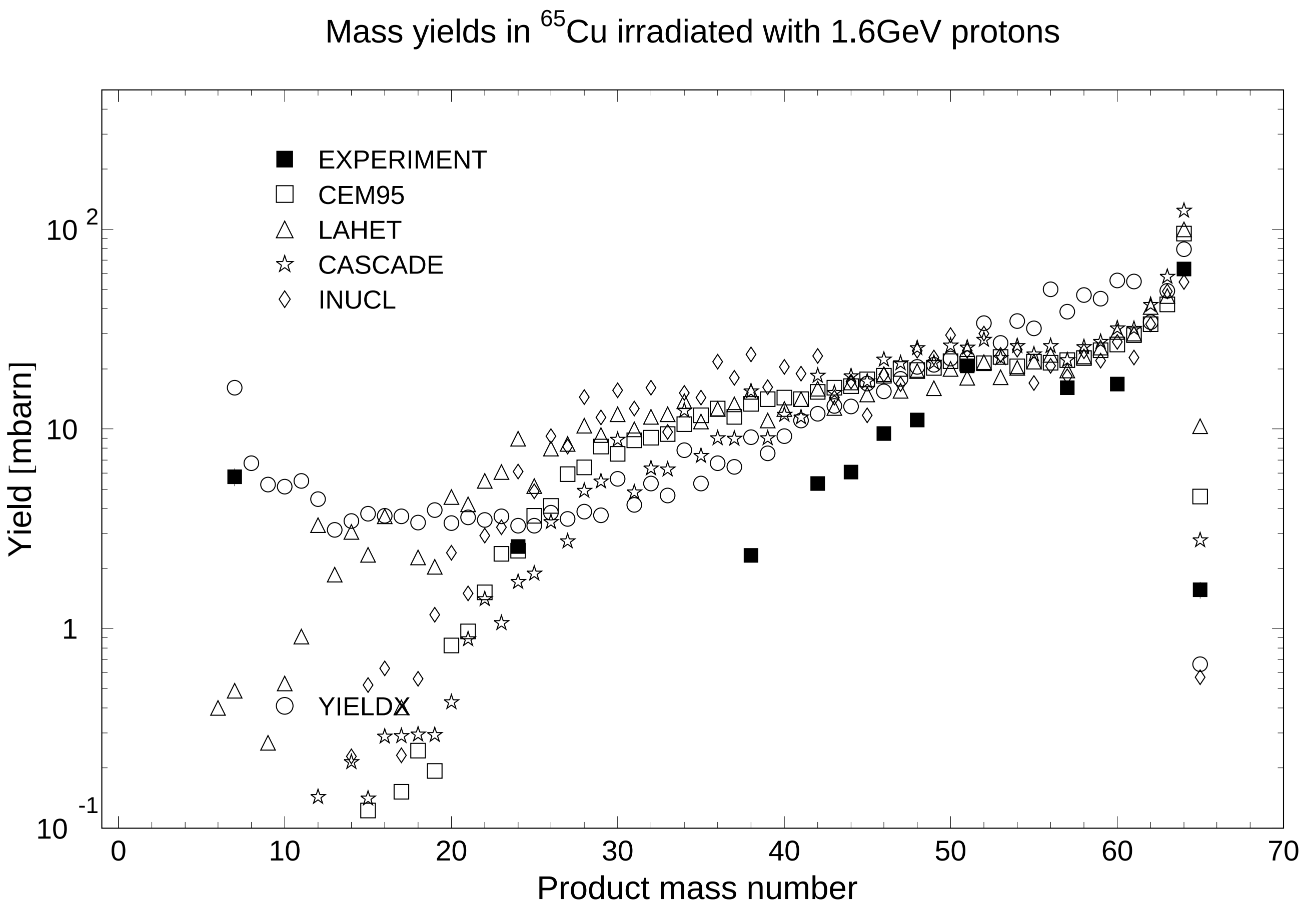

Fig. 136: The simulated mass distributions of reaction products together with the measured cumulative and supra-cumulative yields in ^{65}Cu irradiated with 1.6 GeV protons.

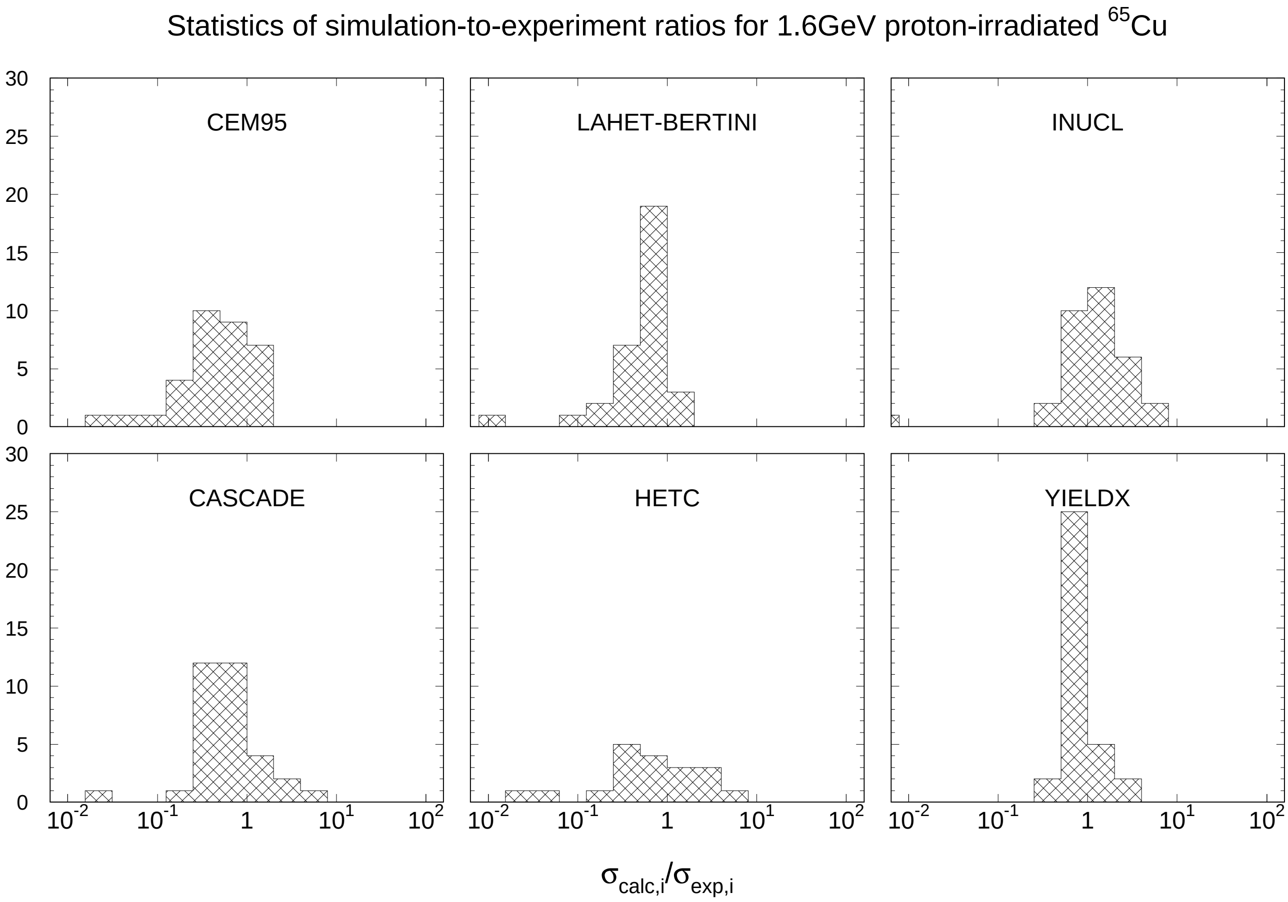

Fig. 137: Statistics of the simulation-to-experiment ratios (criterion 2) for ^{65}Cu irradiated with 1.6 GeV protons.

Table 105: Experimental and calculated yields from ^{65}Cu irradiated with 2.6 GeV protons.

Product	$T_{1/2}$	Type	Exp yield [mbarn]	Calculated Yields [mbarn] via CEM95	LAHET	CASCADE	HETC	INUCL	YIELDX
^{65}Zn	244,26d	i	2.19 ± 0.25	0.122	1.09	0.023	1.02	0.007	0.661
^{62}Zn	9,26h	i	0.147 ± 0.022	0.034	0.178	0.351	0.030	0.077	0.116
^{64}Cu	12,700h	i	60.2 ± 5.4	46.5	53.0	64.5	56.4	27.8	62.6
^{61}Cu	3,333h	c	4.06 ± 0.51	4.44	4.52	3.05	13.1	3.98	7.74
^{60}Cu	23,7m	c*	0.770 ± 0.070	0.952	0.467	0.562	1.28	2.22	1.40
^{65}Ni	2,51719h	c	0.348 ± 0.036	0.046	1.34	–	1.20	–	–
^{57}Ni	35,60h	c	0.251 ± 0.023	0.299	0.116	1.01	1.03	1.21	0.308
^{61}Co	1,650h	c	6.25 ± 1.11	4.93	5.76	9.72	4.61	5.75	3.87
^{60}Co	5,2714y	i(m+g)	14.4 ± 1.3	6.25	6.75	5.37	4.62	10.8	8.92
^{58}Co	70,86d	i(m+g)	19.4 ± 1.6	12.0	11.7	5.61	5.43	13.2	23.7
^{57}Co	271,79d	c	13.7 ± 1.2	10.2	8.51	9.48	18.7	9.69	12.1
^{56}Co	77,233d	c	3.70 ± 0.32	6.25	2.77	1.73	18.1	6.55	2.80
^{55}Co	17,53h	c	0.498 ± 0.046	0.632	0.135	0.742	0.258	1.46	0.478
^{59}Fe	44,472d	c	3.75 ± 0.33	1.96	1.69	3.44	1.24	1.89	2.24
^{56}Mn	2,5789h	c	4.92 ± 0.41	1.96	2.11	1.91	0.581	5.14	4.79
^{54}Mn	312,11d	i	16.4 ± 1.4	9.22	11.6	4.59	1.17	12.9	21.6
^{51}Cr	27,7025d	c	17.1 ± 1.5	13.4	10.7	16.0	17.9	14.4	14.8
^{49}Cr	42,3m	c	1.75 ± 0.17	0.864	1.03	1.51	1.64	3.54	1.02
^{48}Cr	21,56h	c	0.192 ± 0.017	0.038	0.116	0.865	–	0.389	0.155
^{48}V	15,9735d	c	8.21 ± 0.69	8.31	6.66	2.61	17.0	12.8	5.39
^{48}Sc	43,67h	i	1.03 ± 0.09	0.413	0.670	0.511	0.005	3.46	0.764
^{47}Sc	3,3492d	i	4.00 ± 0.34	1.50	2.77	3.10	0.020	3.17	3.05
^{46}Sc	83,79d	i(m+g)	7.82 ± 0.66	7.53	4.73	3.33	0.045	10.4	7.70
^{47}Ca	4,536d	c	0.168 ± 0.020	0.072	0.082	0.264	0.005	0.233	0.134
^{43}K	22,3h	c	1.91 ± 0.16	0.586	0.891	1.74	–	2.57	1.35
^{42}K	12,360h	i	4.77 ± 0.41	2.09	2.38	2.38	–	9.60	3.90
^{41}Ar	109,34m	c	1.20 ± 0.10	0.253	0.255	1.21	–	1.14	0.794
^{39}Cl	55,6m	c	0.812 ± 0.071	0.122	0.198	0.539	–	1.38	0.512
^{38}Cl	37,24m	i(m+g)	2.10 ± 0.19	0.518	0.785	0.902	–	8.78	1.66
^{38}S	170,3m	c	0.111 ± 0.011	0.004	–	0.143	–	0.259	0.100
^{29}Al	6,56m	c	2.08 ± 0.22	0.308	1.70	1.31	–	4.70	2.07
^{28}Mg	20,915h	c	0.531 ± 0.045	0.008	0.019	0.551	–	0.860	0.520
^{27}Mg	9,462m	c	1.30 ± 0.19	0.308	0.193	1.15	–	1.87	1.42
^{24}Na	14,9590h	c	3.76 ± 0.32	1.90	3.86	1.30	–	8.77	2.96
^{7}Be	53,29d	i	7.40 ± 0.80	–	2.38	–	–	–	8.09

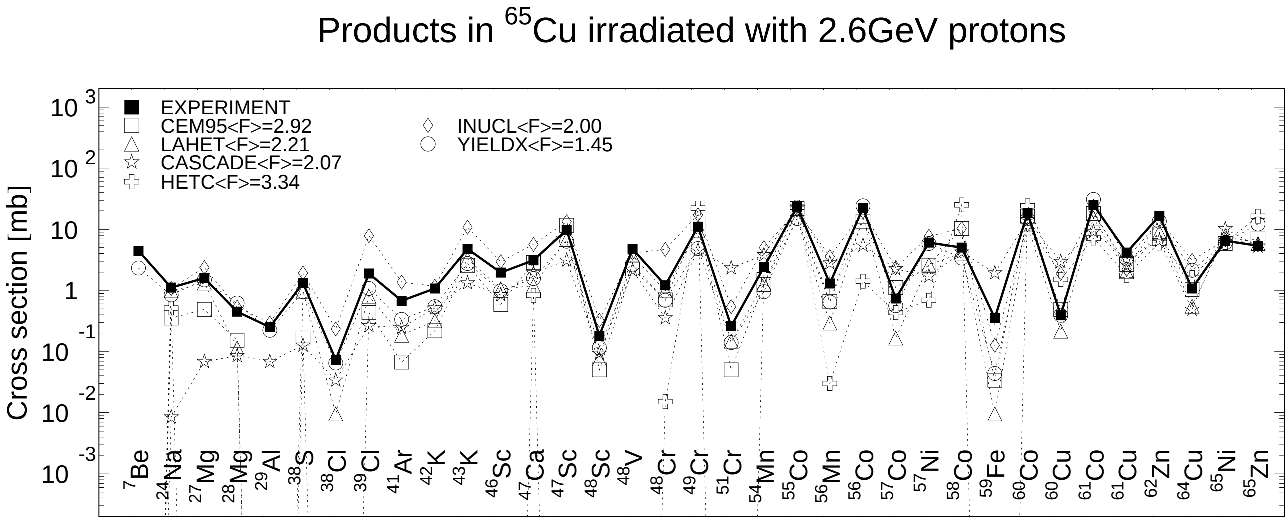

Fig. 138: Detailed comparison between experimental and simulated yields of radioactive reaction products in ^{65}Cu irradiated with 2.6 GeV protons. The cumulative yields are labeled -c when the respective independent yields are also shown.

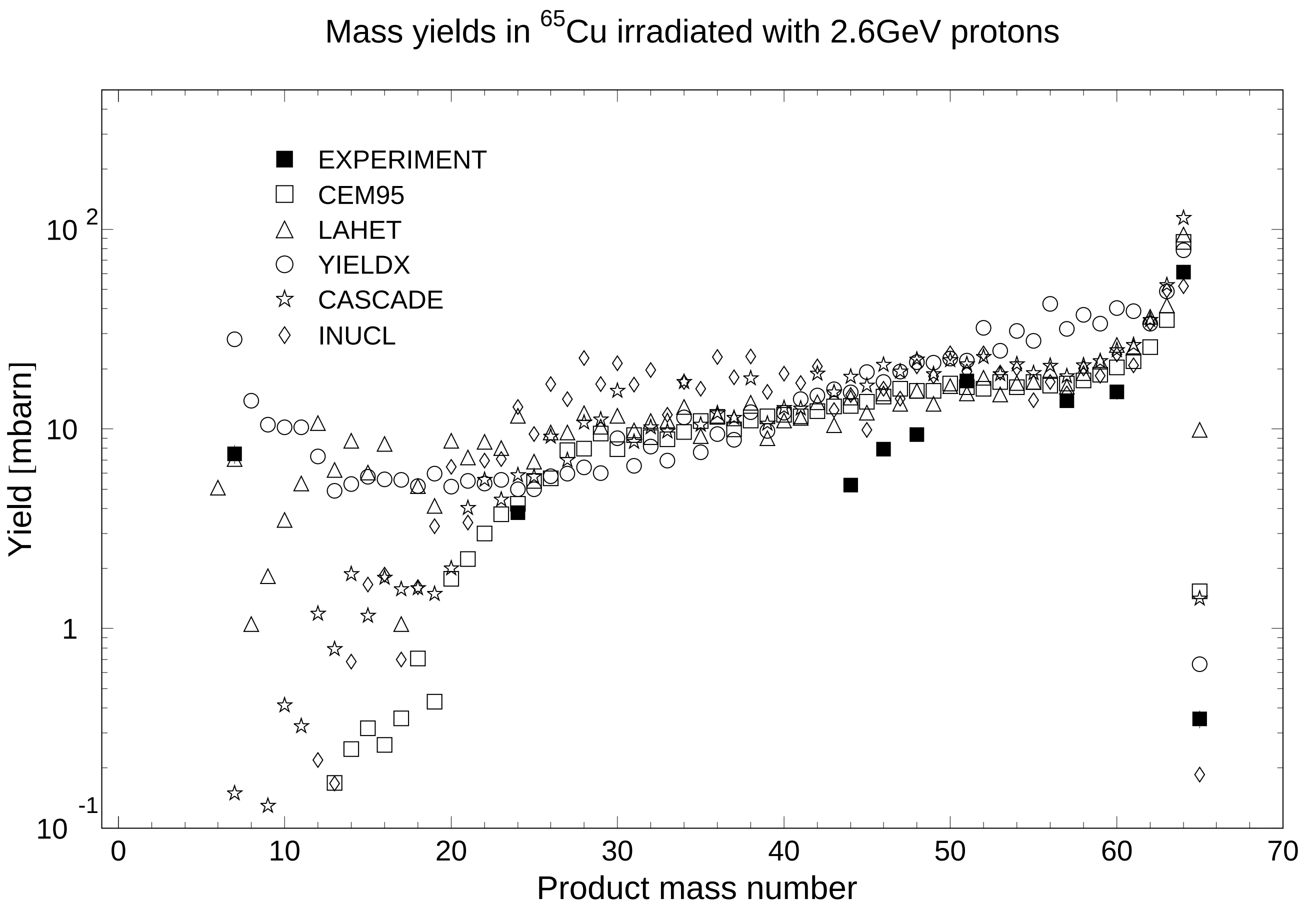

Fig. 139: The simulated mass distributions of reaction products together with the measured cumulative and supra-cumulative yields in ^{65}Cu irradiated with 2.6 GeV protons.

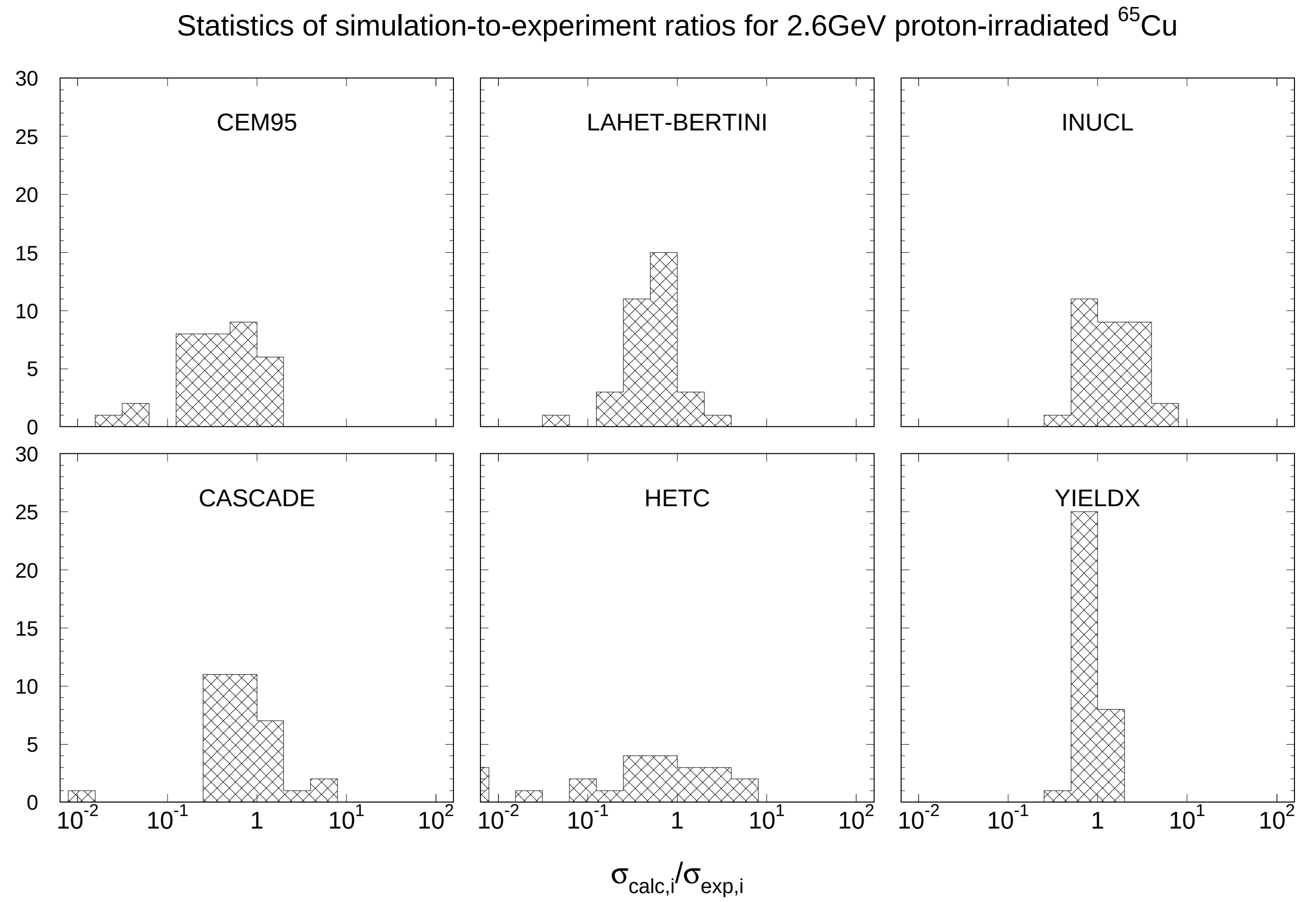

Fig. 140: Statistics of the simulation-to-experiment ratios (criterion 2) for ^{65}Cu irradiated with 2.6 GeV protons.

Table 106: Experimental and calculated yields from ^{nat}Hg irradiated with 0.1 GeV protons.

Product	$T_{1/2}$	Type	Exp yield [mbarn]	Calculated Yields [mbarn] via					
				CEM95	CEM2k	LAHET	CASCADE	HETC	INUCL
^{202}Tl	12,23d	i	4.73 ± 0.37	10.4	11.3	9.30	5.29	–	9.18
^{201}Tl	72,912h	i(m+g)	13.7 ± 1.1	19.3	19.1	29.4	26.7	10.9	19.1
^{200}Tl	26,1h	i(m+g)	23.7 ± 2.3	30.6	30.9	32.2	28.3	25.0	24.9
^{199}Tl	7,42h	i(m+g)	38.8 ± 5.4	41.0	42.5	62.5	50.0	46.2	42.4
^{197}Tl	2,84h	i(m+g)	112. ± 37.	64.0	66.0	84.8	84.6	52.0	59.7
^{195}Tl	1,16h	i(m+g)	100. ± 10.	73.9	87.9	101.	121.	80.1	67.6
^{194}Tl	32,8m	i(m+g)	125. ± 16.	68.6	88.4	36.2	115.	54.7	59.2
^{203}Hg	46,612d	c	9.63 ± 0.75	10.5	5.29	8.61	10.7	–	10.1
^{197}Hg	64,14h	c	194. ± 18.	183.	150.	183.	164.	102.	184.
^{192}Hg	4,85h	c	107. ± 9.	79.5	90.4	82.6	140.	383.	86.5
^{190}Hg	20,0m	c*	8.48 ± 1.96	10.9	14.3	20.5	57.8	26.2	21.8
^{199}Au	3,139d	c	6.83 ± 0.56	22.8	9.00	17.2	8.50	9.05	26.8
^{198}Au	2,69517d	i(m+g)	7.80 ± 0.61	26.7	12.7	17.3	7.80	5.54	24.2
^{196}Au	6,183d	i(m1+m2+g)	9.58 ± 0.75	29.6	18.8	15.6	5.73	4.34	17.5
^{195}Au	186,098d	c	284. ± 33.	103.	105.	118.	126.	84.5	84.0
^{194}Au	38,02h	i(m1+m2+g)	10.6 ± 0.9	27.2	15.8	9.76	4.06	2.90	9.09
^{192}Au	4,94h	c	132. ± 13.	93.0	99.4	88.4	141.	383.	89.7
^{192}Au	4,94h	i(m1+m2+g)	13.3 ± 5.2	13.5	8.94	5.78	1.34	–	3.20
^{191}Au	3,18h	c	58.3 ± 9.6	56.5	65.0	81.5	141.	332.	66.5
^{191}Pt	2,802d	c	48.7 ± 4.4	44.6	50.1	63.0	104.	245.	49.7
^{189}Pt	10,87h	c	9.22 ± 0.96	3.18	3.74	8.55	18.8	0.170	5.47
^{188}Ir	41,5h	c	3.55 ± 0.37	1.09	1.34	2.65	3.36	–	1.06
^{188}Ir	41,5h	i	0.217 ± 0.090	0.041	0.015	0.021	–	–	–
^{103}Ru	39,26d	c	1.05 ± 0.09	–	–	0.083	0.609	–	0.070
^{96}Nb	23,35h	i	0.378 ± 0.064	–	–	0.041	0.087	–	0.070
^{97}Zr	16,744h	c	0.411 ± 0.035	–	–	0.062	0.017	–	0.017
^{95}Zr	64,02d	c	1.15 ± 0.23	–	–	0.019	0.139	–	0.174

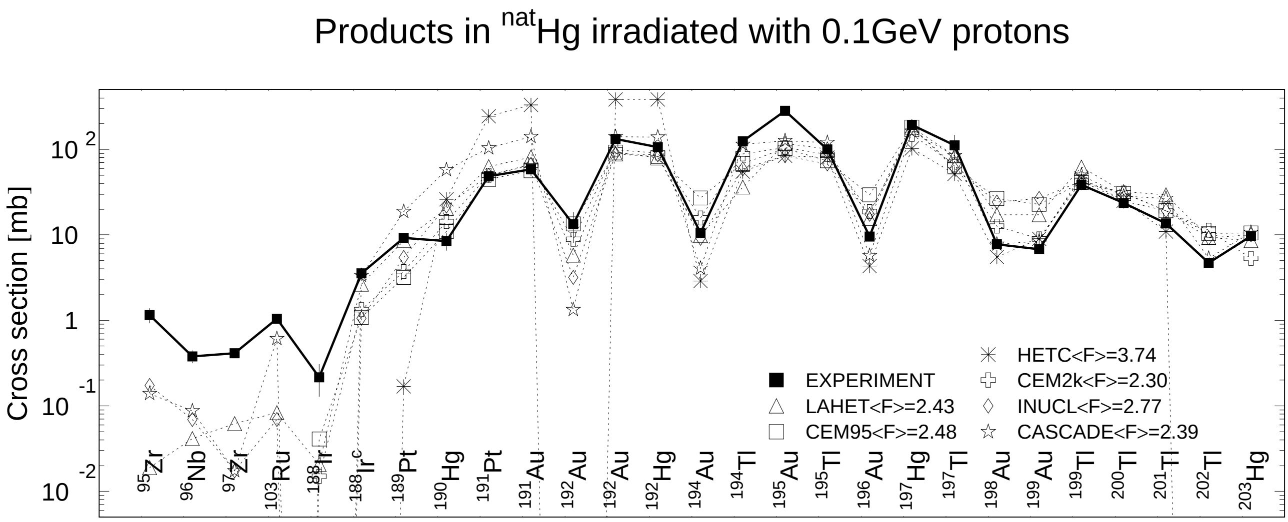

Fig. 141: Detailed comparison between experimental and simulated yields of radioactive reaction products in ^{nat}Hg irradiated with 0.1 GeV protons. The cumulative yields are labeled -c when the respective independent yields are also shown.

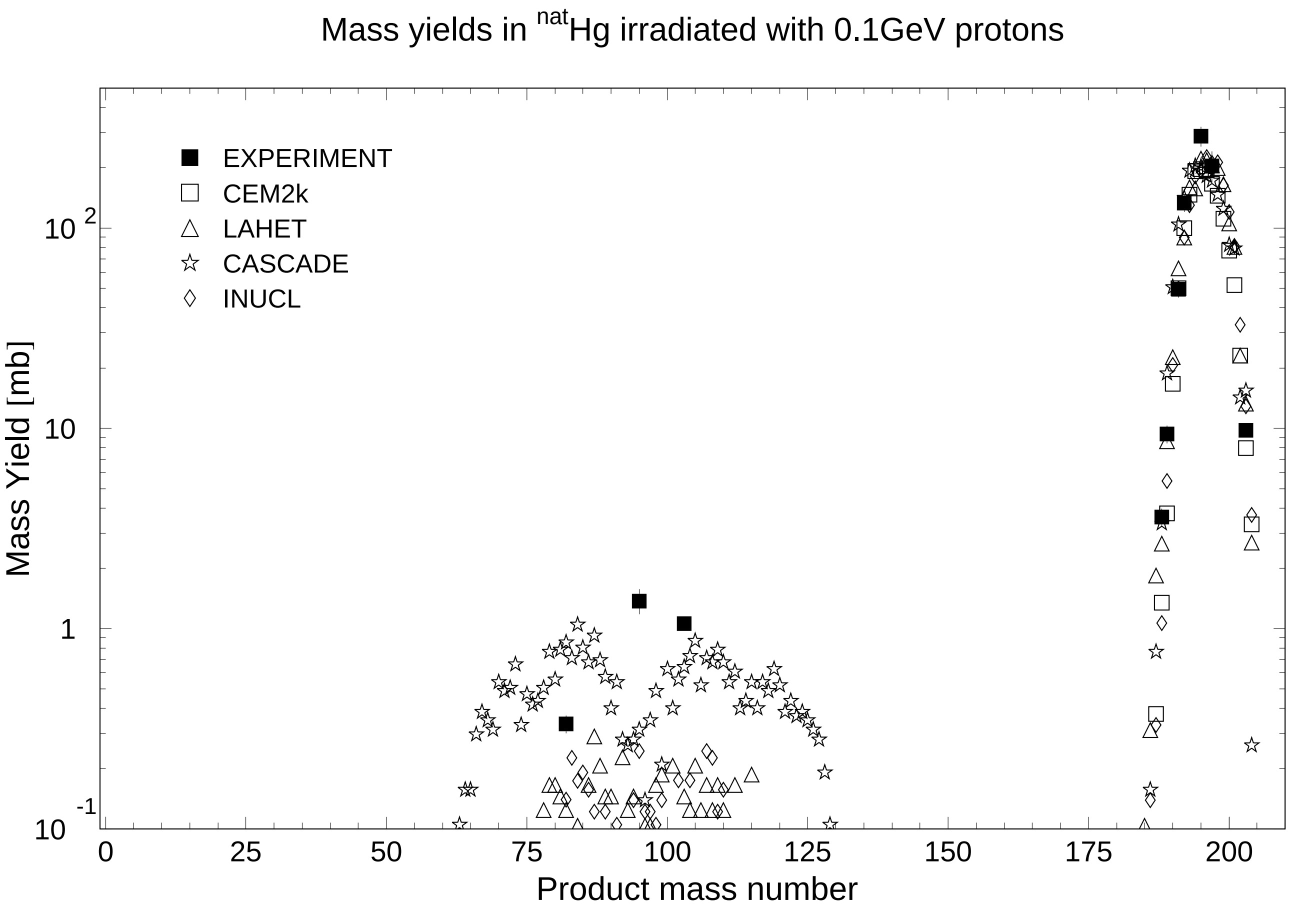

Fig. 142: The simulated mass distributions of reaction products together with the measured cumulative and supra-cumulative yields in ^{nat}Hg irradiated with 0.1 GeV protons.

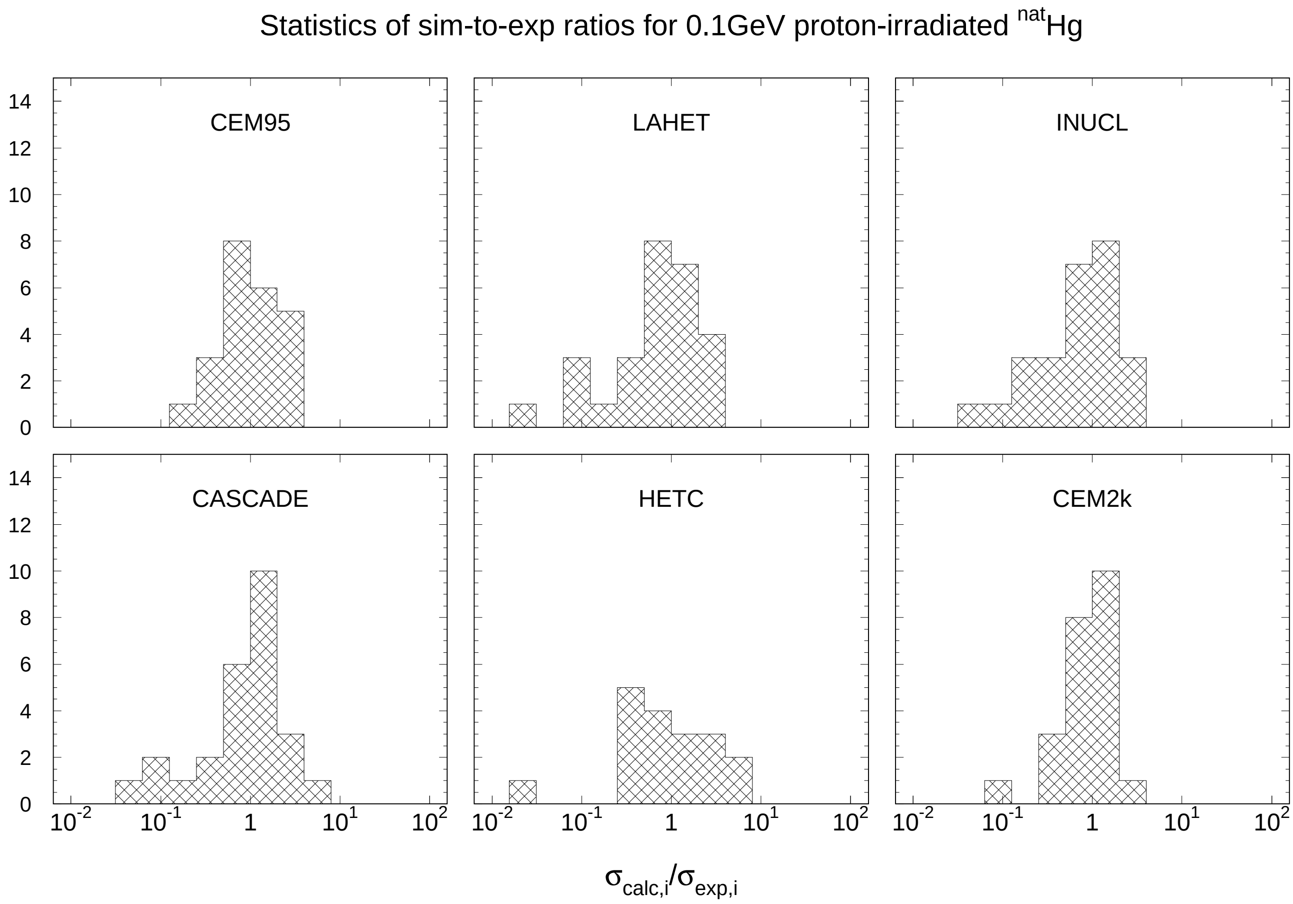

Fig. 143: Statistics of the simulation-to-experiment ratios (criterion 2) for ^{nat}Hg irradiated with 0.1 GeV protons.

Table 107: Experimental and calculated yields from ^{nat}Hg irradiated with 0.2 GeV protons.

Product	$T_{1/2}$	Type	Exp yield [mbarn]	Calculated Yields [mbarn] via CEM2k	LAHET	CASCADE	HETC	INUCL	YIELDX
^{202}Tl	12,23d	i	2.00 ± 0.14	6.95	4.09	2.55	–	6.34	2.70
^{201}Tl	72,912h	i(m+g)	5.93 ± 0.47	11.3	14.1	14.9	5.45	12.8	5.78
^{200}Tl	26,1h	i(m+g)	9.53 ± 0.87	16.8	14.2	13.8	15.1	15.5	10.7
^{199}Tl	7,42h	i(m+g)	14.9 ± 2.0	21.3	27.8	26.1	27.6	25.9	16.9
^{197}Tl	2,84h	i(m+g)	35.9 ± 11.7	25.0	31.8	35.9	29.9	30.0	29.2
^{195}Tl	1,16h	i(m+g)	22.9 ± 2.6	26.9	30.1	38.6	32.6	30.3	34.3
^{194}Tl	32,8m	i(m+g)	22.9 ± 2.3	28.4	11.0	31.6	15.7	23.7	32.9
^{203}Hg	46,612d	c	6.80 ± 0.48	4.26	7.88	9.90	–	10.5	6.40
^{197}Hg	64,14h	c	96.8 ± 9.4	74.3	90.3	84.8	71.2	99.8	121.
^{192}Hg	4,85h	c	83.4 ± 6.8	77.0	59.3	97.5	60.7	71.1	67.2
^{190}Hg	20,0m	c*	61.9 ± 10.8	64.9	67.4	101.	89.5	48.6	36.4
^{199}Au	3,139d	c	11.8 ± 0.9	10.8	17.6	15.5	16.8	41.3	25.5
^{198}Au	2,69517d	i(m+g)	13.2 ± 0.9	14.4	17.6	13.9	9.01	38.2	34.4
^{196}Au	6,183d	i(m1+m2+g)	18.7 ± 1.4	21.4	18.7	11.6	8.89	34.4	40.7
^{195}Au	186,098d	c	141. ± 15.	48.5	55.3	54.8	41.4	70.0	72.0
^{194}Au	38,02h	i(m1+m2+g)	26.9 ± 2.0	23.8	21.3	15.6	8.85	31.7	34.7
^{192}Au	4,94h	c	118. ± 14.	105.	84.8	115.	69.7	95.9	94.8
^{192}Au	4,94h	i(m1+m2+g)	27.8 ± 6.5	28.4	25.5	17.1	9.02	24.8	27.5
^{191}Au	3,18h	c	100. ± 8.	127.	124.	149.	116.	98.5	91.9
^{191}Au	3,18h	i(m+g)	68.6 ± 8.6	30.0	31.9	22.3	9.09	23.7	24.4
^{190}Au	42,8m	c	85.7 ± 9.1	93.2	79.6	112.	85.6	63.0	55.2
^{191}Pt	2,802d	c	94.2 ± 7.9	111.	107.	118.	88.9	82.0	93.8
^{189}Pt	10,87h	c	85.9 ± 7.6	115.	104.	138.	129.	64.2	74.7
^{187}Pt	2,35h	c	37.2 ± 4.3	49.7	48.3	73.8	109.	24.0	30.0
^{186}Pt	2,08h	c	28.9 ± 2.2	31.5	35.6	55.9	122.	15.9	16.7
^{188}Ir	41,5h	c	64.3 ± 6.0	72.0	63.3	90.4	96.3	38.6	47.1
^{188}Ir	41,5h	i	1.90 ± 0.43	1.87	1.68	0.094	0.020	0.172	2.33
^{187}Ir	10,5h	c	57.8 ± 5.9	51.9	51.8	74.1	109.	24.2	32.3
^{185}Os	93,6d	c	21.6 ± 1.5	20.3	28.5	19.7	25.5	8.49	11.8
^{182}Os	22,10h	c	6.34 ± 0.60	2.99	9.87	3.08	0.145	2.10	3.71
^{183}Re	70,0d	c	9.72 ± 0.73	6.09	14.9	5.25	0.712	3.16	5.38
^{182}Re	12,7h	c	6.76 ± 0.70	3.03	9.97	3.08	0.145	2.10	4.07
^{181}Re	19,9h	c*	3.76 ± 0.51	1.40	5.13	1.09	–	1.12	2.79
^{103}Ru	39,26d	c	1.55 ± 0.11	–	0.429	1.80	–	0.610	0.787
^{96}Nb	23,35h	i	0.954 ± 0.069	–	0.131	1.17	–	0.422	0.499
^{97}Zr	16,744h	c	0.284 ± 0.020	–	0.201	0.016	–	0.016	0.100
^{95}Zr	64,02d	c	0.956 ± 0.075	–	0.295	0.094	–	0.156	0.421
^{88}Y	106,65d	c	0.461 ± 0.037	–	0.224	1.31	–	0.391	2.22
^{74}As	17,77d	i	0.195 ± 0.029	–	–	0.047	–	0.156	0.255

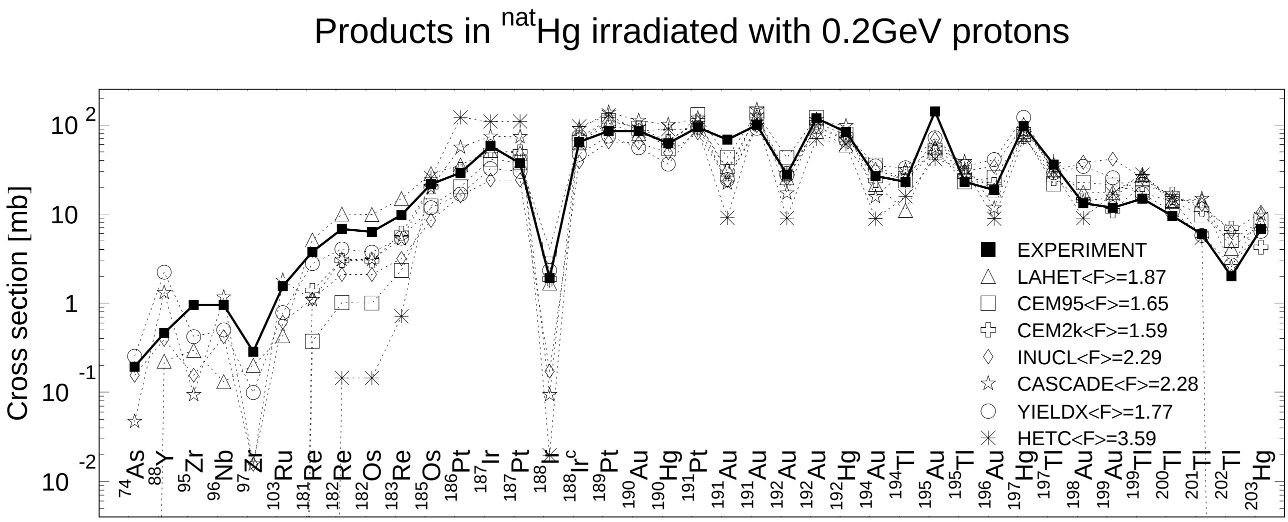

Fig. 144: Detailed comparison between experimental and simulated yields of radioactive reaction products in ^{nat}Hg irradiated with 0.2 GeV protons. The cumulative yields are labeled -c when the respective independent yields are also shown.

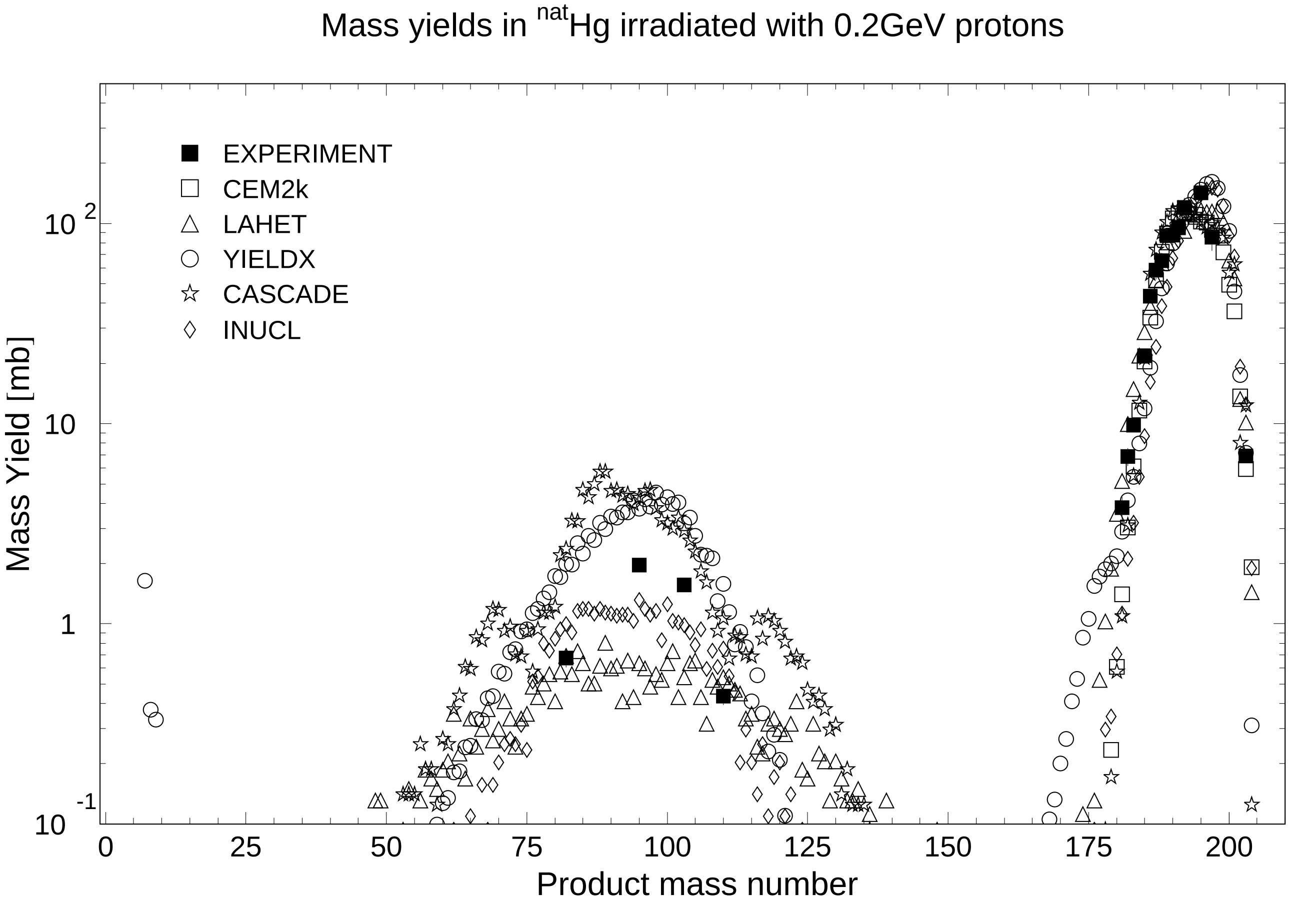

Fig. 145: The simulated mass distributions of reaction products together with the measured cumulative and supra-cumulative yields in ^{nat}Hg irradiated with 0.2 GeV protons.

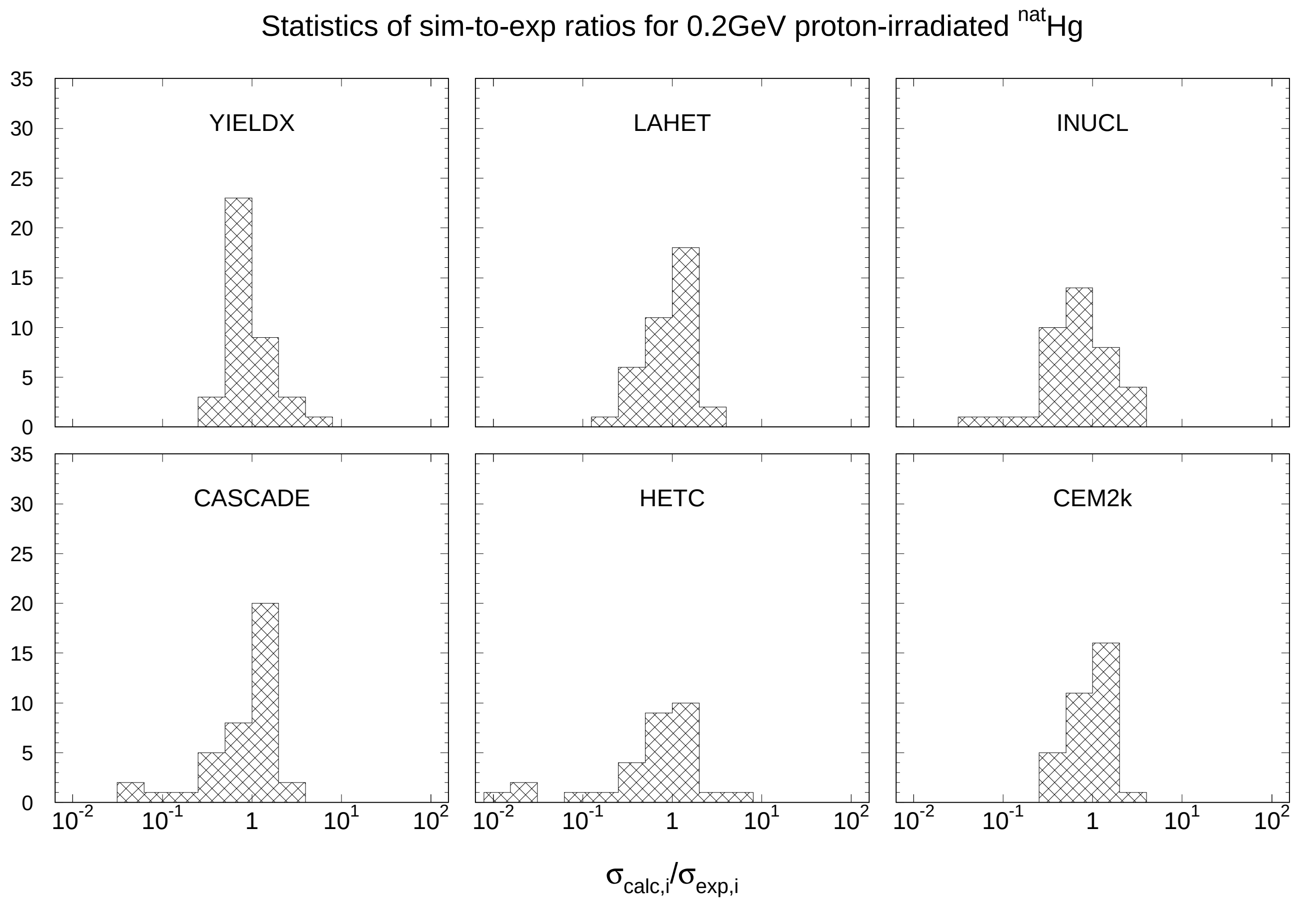

Fig. 146: Statistics of the simulation-to-experiment ratios (criterion 2) for ^{nat}Hg irradiated with 0.2 GeV protons.

Table 108: Experimental and calculated yields from ^{nat}Hg irradiated with 0.8 GeV protons.

Product	$T_{1/2}$	Type	Exp yield [mbarn]	Calculated Yields [mbarn] via CEM2k	LAHET	CASCADE	HETC	INUCL	YIELDX
^{202}Tl	12,23d	i	0.811 ± 0.070	1.62	1.04	0.450	–	1.64	0.440
^{200}Tl	26,1h	i(m+g)	5.00 ± 0.48	4.05	3.80	2.70	2.33	2.93	1.75
^{199}Tl	7,42h	i(m+g)	4.70 ± 0.97	5.03	7.61	3.85	6.14	3.92	2.77
^{194}Tl	32,8m	i(m+g)	6.30 ± 0.74	5.20	2.28	5.45	2.79	3.83	5.44
^{203}Hg	46,612d	c	8.99 ± 0.62	3.93	9.19	9.59	–	7.38	5.49
^{192}Hg	4,85h	c	26.8 ± 2.2	19.0	17.0	26.9	15.3	25.1	28.5
^{190}Hg	20,0m	c*	15.8 ± 2.0	17.2	17.8	29.8	22.2	21.2	21.3
^{199}Au	3,139d	c	19.4 ± 1.4	10.5	28.6	24.4	38.8	33.5	11.3
^{198}Au	2,69517d	i(m+g)	18.8 ± 1.3	12.7	21.0	22.1	14.5	30.4	14.1
^{196}Au	6,183d	i(m1+m2+g)	20.5 ± 1.4	16.6	16.8	12.3	11.5	24.5	15.6
^{194}Au	38,02h	i(m1+m2+g)	24.9 ± 2.0	13.2	15.9	12.2	11.1	24.1	15.3
^{192}Au	4,94h	c	50.6 ± 8.1	32.1	33.8	41.8	27.9	50.9	43.7
^{192}Au	4,94h	i(m1+m2+g)	24.6 ± 4.3	13.1	16.9	14.9	12.6	25.8	15.2
^{191}Au	3,18h	c	44.7 ± 3.5	38.1	47.3	51.7	43.1	57.1	52.4
^{190}Au	42,8m	c	42.7 ± 4.2	30.5	27.3	44.7	28.5	45.6	39.1
^{190}Au	42,8m	i	27.2 ± 3.7	14.1	9.85	15.9	7.53	24.7	18.2
^{191}Pt	2,802d	c	47.1 ± 4.9	38.4	49.8	50.6	39.9	67.1	57.3
^{189}Pt	10,87h	c	53.8 ± 4.3	37.6	48.3	55.3	40.7	64.1	52.2
^{187}Pt	2,35h	c	35.8 ± 6.6	36.2	39.2	55.5	41.9	58.9	33.9
^{186}Pt	2,08h	c	42.9 ± 3.2	34.1	39.2	69.0	39.9	57.8	22.1
^{189}Ir	13,2d	c	58.3 ± 7.7	40.2	52.2	58.7	41.8	71.5	54.8
^{188}Ir	41,5h	c	62.5 ± 6.8	40.7	42.1	62.8	40.0	70.4	48.4
^{188}Ir	41,5h	i	6.92 ± 0.99	3.49	4.64	3.20	1.55	7.12	3.06
^{184}Ir	3,09h	c*	49.2 ± 4.5	41.6	47.3	65.3	48.2	63.7	19.5
^{185}Os	93,6d	c	55.8 ± 4.0	42.2	48.4	66.7	37.8	64.2	22.5
^{182}Os	22,10h	c	58.6 ± 4.2	40.2	46.6	59.0	40.0	52.7	23.4
^{183}Re	70,0d	c	59.1 ± 4.1	43.0	46.9	51.8	36.0	55.4	21.8
^{182}Re	12,7h	c	60.0 ± 4.5	42.0	47.6	59.7	40.0	53.7	25.7
^{181}Re	19,9h	c*	57.9 ± 7.7	42.1	48.4	51.8	43.2	46.0	24.0
^{179}Re	19,5m	c*	59.2 ± 5.9	56.5	57.1	69.3	17.2	51.8	34.4
^{177}W	135m	c	46.9 ± 6.4	32.7	41.0	29.1	1.18	23.7	37.9
^{176}Ta	8,09h	c	43.5 ± 4.0	42.0	39.7	41.4	44.0	27.3	40.1
^{174}Ta	1,14h	c	41.9 ± 4.4	38.4	34.7	36.2	37.7	20.3	33.7
^{175}Hf	70d	c	44.3 ± 3.3	39.7	35.7	36.2	44.8	22.2	33.1
^{173}Hf	23,6h	c*	46.9 ± 5.4	42.5	34.8	37.7	51.4	19.3	31.8
^{172}Hf	1,87y	c	34.3 ± 2.4	35.9	32.0	37.4	42.0	16.7	27.8
^{172}Lu	6,70d	i(m1+m2+g)	0.178 ± 0.050	0.444	0.640	–	–	–	0.431
^{171}Lu	8,24d	c*	35.7 ± 2.5	25.9	31.9	22.7	–	10.6	25.1
^{170}Lu	2,012d	c	32.6 ± 2.3	30.1	25.9	25.5	38.6	11.6	22.3
^{169}Yb	32,026d	c	32.4 ± 2.2	26.7	24.7	23.1	37.4	8.90	20.1
^{166}Yb	56,7h	c	21.3 ± 1.5	20.6	23.4	15.5	33.9	6.80	16.5
^{167}Tm	9,25d	c	27.3 ± 5.7	20.6	21.4	13.5	27.2	6.60	16.9
^{165}Tm	30,06h	c	20.4 ± 1.6	19.4	18.9	14.7	30.5	5.60	14.5
^{160}Er	28,58h	c	11.8 ± 1.4	9.90	10.4	6.77	19.7	2.32	9.46
^{157}Dy	8,14h	c	6.91 ± 0.55	5.32	6.63	3.01	11.2	1.29	6.85
^{155}Tb	5,32d	c	5.87 ± 0.58	2.43	5.28	1.44	–	1.15	5.62
^{153}Gd	240,4d	c	2.85 ± 0.55	1.58	3.29	0.752	0.327	0.670	4.47
^{146}Gd	48,27d	c	1.29 ± 0.12	0.380	0.784	0.101	–	0.280	2.36
^{147}Eu	24,1d	c	1.83 ± 0.23	0.280	1.18	0.126	–	0.269	1.87
^{146}Eu	4,61d	i	0.430 ± 0.219	0.025	0.360	0.018	–	0.036	0.293
^{139}Ce	137,640d	c	0.557 ± 0.058	0.012	0.320	0.018	–	0.018	0.923
^{111}In	2,8047d	c	0.802 ± 0.081	–	0.320	0.917	–	0.324	9.00
^{103}Ru	39,26d	c	1.78 ± 0.13	–	0.380	1.13	–	0.252	0.890
^{96}Nb	23,35h	i	1.39 ± 0.12	–	0.240	1.87	–	0.216	0.548
^{95}Zr	64,02d	c	1.03 ± 0.08	–	0.180	0.270	–	0.090	0.142
^{88}Zr	83,4d	c	0.843 ± 0.062	–	0.660	4.44	–	1.82	8.37
^{88}Y	106,65d	i(m+g)	2.46 ± 0.23	–	0.300	11.4	–	1.08	3.17
^{83}Rb	86,2d	c	2.73 ± 0.28	–	0.760	8.38	–	2.32	7.99
^{77}Br	57,036h	c	0.983 ± 0.176	–	0.400	0.935	–	0.612	5.30
^{75}Se	119,779d	c	1.31 ± 0.11	–	0.400	1.19	–	1.18	4.66
^{74}As	17,77d	i	1.51 ± 0.16	–	0.440	0.756	–	0.485	1.91
^{59}Fe	44,472d	c	0.717 ± 0.063	–	0.200	0.576	–	0.090	0.721
^{48}Sc	43,67h	i	0.380 ± 0.042	–	0.120	0.144	–	–	0.214
^{24}Na	14,9590h	c	0.303 ± 0.042	–	–	–	–	–	0.375

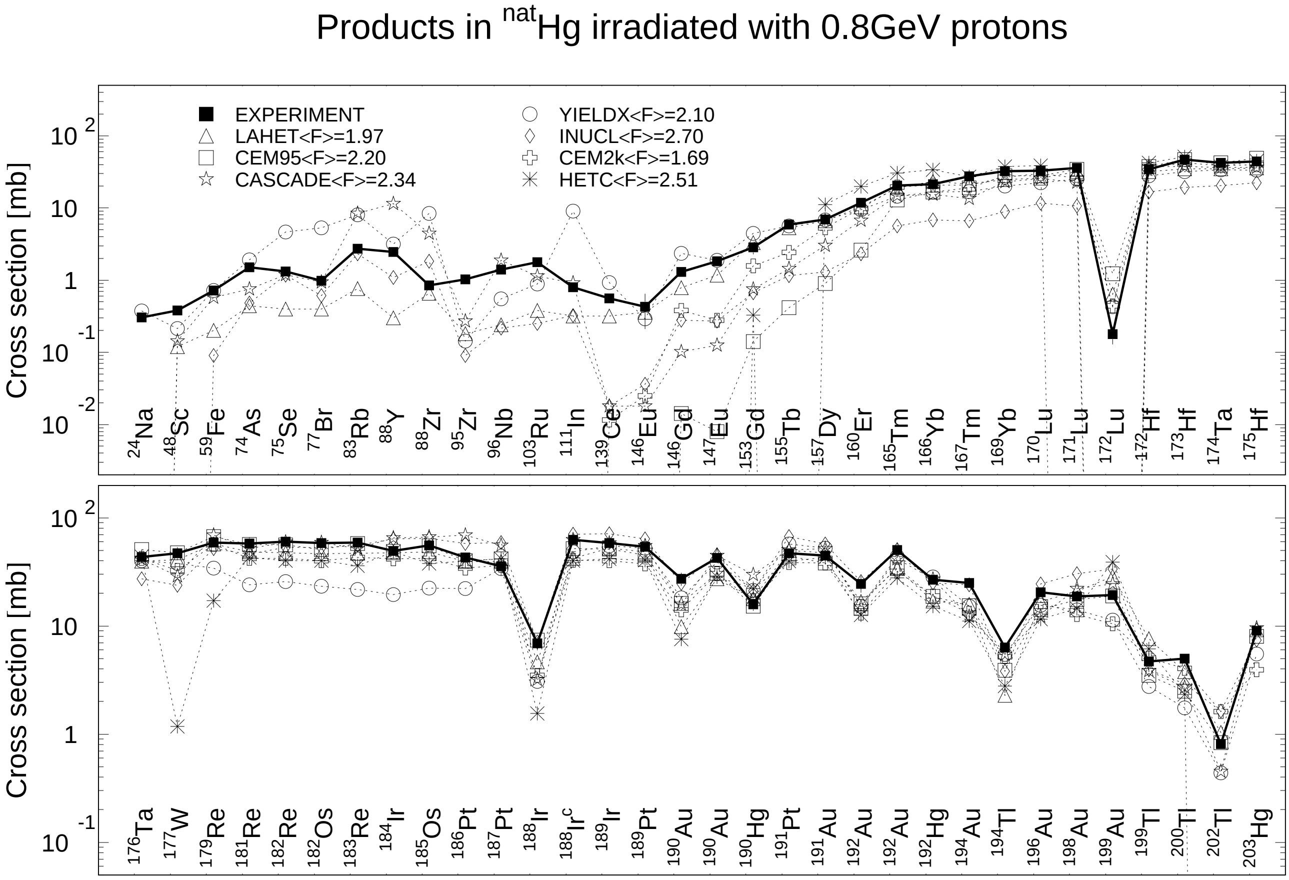

Fig. 147: Detailed comparison between experimental and simulated yields of radioactive reaction products in ^{nat}Hg irradiated with 0.8 GeV protons. The cumulative yields are labeled -c when the respective independent yields are also shown.

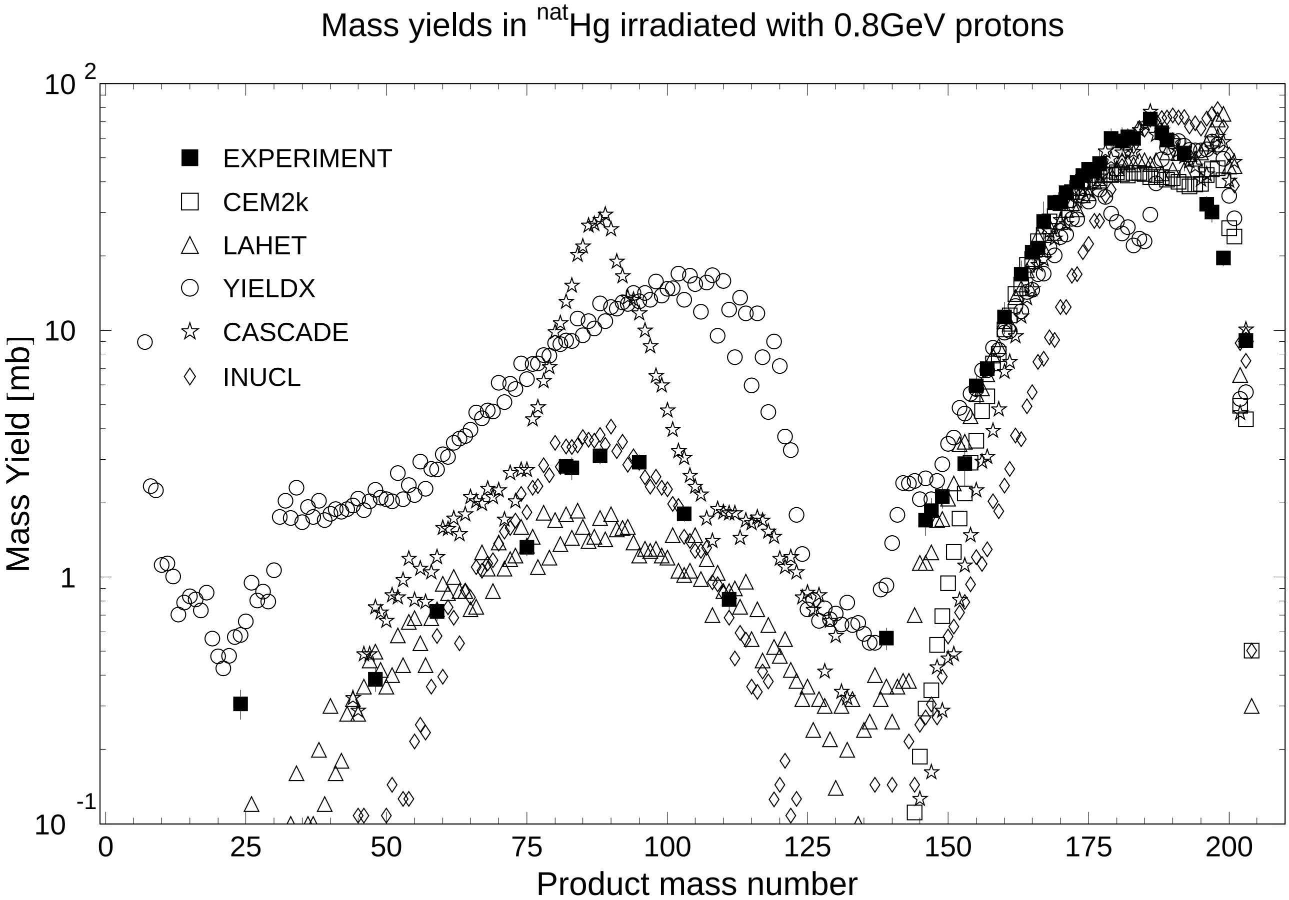

Fig. 148: The simulated mass distributions of reaction products together with the measured cumulative and supra-cumulative yields in ^{nat}Hg irradiated with 0.8 GeV protons.

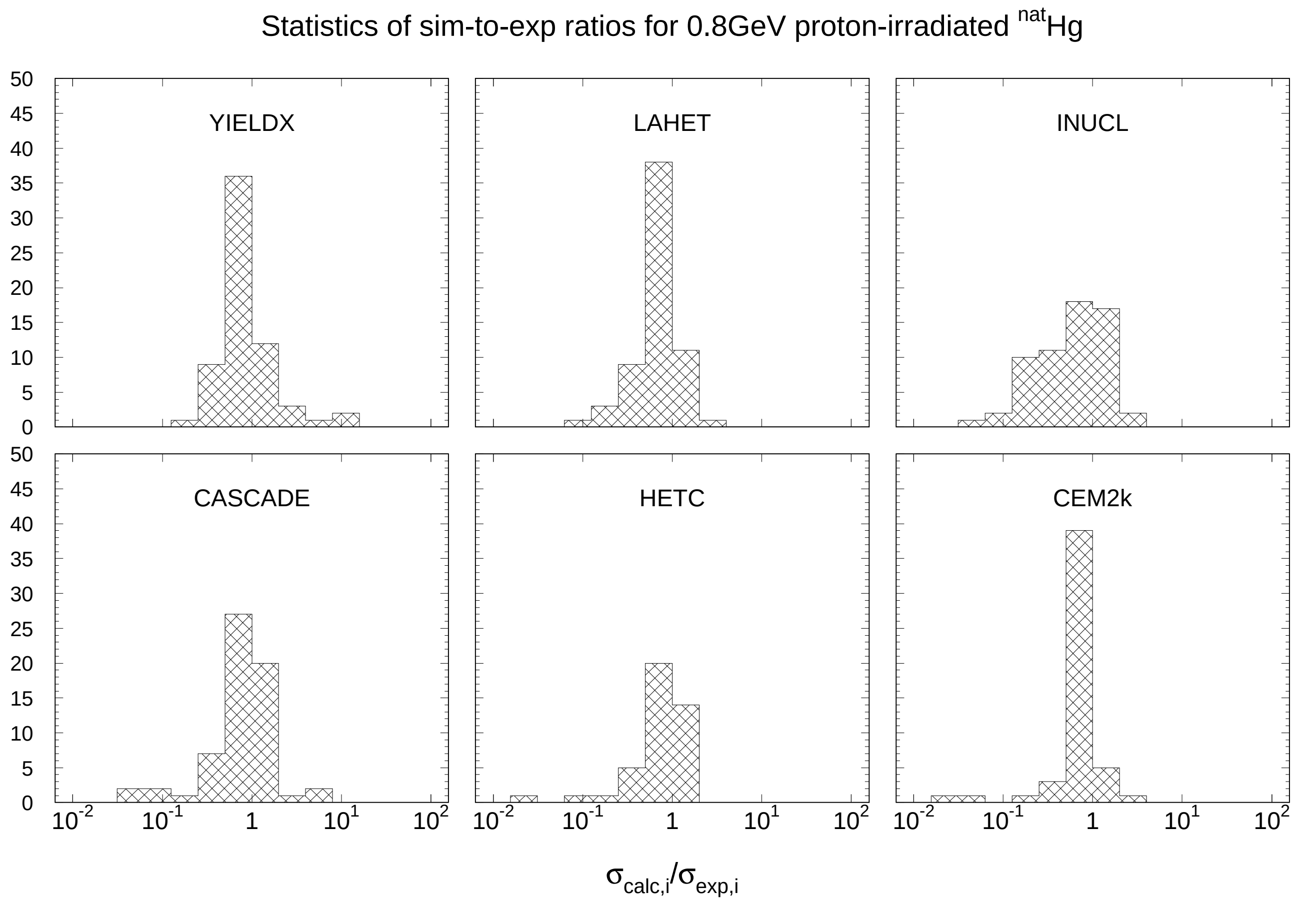

Fig. 149: Statistics of the simulation-to-experiment ratios (criterion 2) for ^{nat}Hg irradiated with 0.8 GeV protons.

Table 109: Experimental and calculated yields from ^{nat}Hg irradiated with 2.6 GeV protons.

Product	$T_{1/2}$	Type	Exp yield [mbarn]	Calculated Yields [mbarn] via CEM95	CEM2k	LAHET	CASCADE	HETC	INUCL	YIELDX
^{200}Tl	26,1h	i(m+g)	2.79 ± 1.43	0.485	0.498	1.73	0.637	2.24	0.346	0.896
^{203}Hg	46,612d	c	9.22 ± 0.78	6.76	3.21	6.66	8.50	–	5.55	4.90
^{192}Hg	4,85h	c	14.8 ± 1.5	6.61	6.38	6.45	9.50	8.94	10.5	20.0
^{198}Au	2,69517d	i(m+g)	16.2 ± 1.4	13.5	10.5	15.0	16.0	12.9	21.7	8.65
^{196}Au	6,183d	i(m1+m2+g)	17.1 ± 1.4	9.41	13.2	9.80	8.72	8.80	18.4	10.1
^{194}Au	38,02h	i(m1+m2+g)	20.8 ± 2.1	7.40	8.54	8.27	5.82	8.04	13.0	10.7
^{192}Au	4,94h	c	34.8 ± 5.1	13.6	13.1	13.9	16.4	16.2	22.5	31.8
^{192}Au	4,94h	i(m1+m2+g)	17.6 ± 2.7	6.97	6.73	7.40	6.93	7.26	12.0	11.8
^{191}Pt	2,802d	c	26.0 ± 3.0	17.7	16.0	20.9	20.8	22.8	29.9	50.0
^{189}Pt	10,87h	c	29.0 ± 3.5	16.2	14.3	17.5	22.8	21.1	28.4	50.3
^{186}Pt	2,08h	c	17.6 ± 1.6	12.9	11.9	13.0	24.8	17.4	26.4	20.6
^{189}Ir	13,2d	c	27.6 ± 3.6	19.1	15.9	19.8	25.0	22.1	34.5	52.6
^{188}Ir	41,5h	c	28.1 ± 3.7	18.3	15.6	15.9	24.4	19.0	34.9	47.8
^{188}Ir	41,5h	i	3.02 ± 0.88	3.46	1.85	2.53	1.80	1.30	5.28	2.97
^{184}Ir	3,09h	c*	20.8 ± 1.8	14.6	14.2	15.9	26.8	21.1	32.4	18.5
^{185}Os	93,6d	c	25.8 ± 2.1	18.5	15.4	16.5	28.0	16.5	35.6	22.2
^{182}Os	22,10h	c	28.3 ± 2.3	16.5	13.8	15.8	25.6	18.2	32.8	25.1
^{183}Re	70,0d	c	25.9 ± 2.3	18.1	15.5	16.5	24.1	16.9	34.0	22.8
^{182}Re	12,7h	c	28.6 ± 2.8	18.6	14.8	16.3	26.5	18.3	34.6	27.4
^{181}Re	19,9h	c*	19.8 ± 3.4	19.1	16.0	16.9	27.0	21.5	35.8	28.1
^{179}Re	19,5m	c*	24.5 ± 6.2	20.8	19.0	19.9	31.2	11.5	40.3	38.4
^{178}W	21,6d	c	17.7 ± 2.5	17.1	14.4	15.1	26.6	17.6	31.9	37.7
^{177}W	135m	c	19.0 ± 2.7	14.8	10.7	13.2	15.1	1.60	23.9	37.7
^{176}Ta	8,09h	c	19.9 ± 2.4	17.3	14.9	14.2	23.0	18.8	30.2	43.7
^{174}Ta	1,14h	c	22.1 ± 2.5	16.7	14.2	13.5	23.2	15.8	29.2	36.5
^{175}Hf	70d	c	21.3 ± 1.9	18.7	14.4	12.6	22.3	19.7	28.9	35.3
^{173}Hf	23,6h	c*	25.5 ± 2.3	20.3	16.5	14.3	25.1	21.6	29.9	35.2
^{172}Hf	1,87y	c	19.1 ± 1.6	18.0	14.4	12.8	25.5	18.3	28.3	31.5
^{171}Lu	8,24d	c*	22.3 ± 1.9	18.7	11.2	12.6	17.5	0.424	22.7	29.2
^{170}Lu	2,012d	c	20.5 ± 1.8	18.1	13.6	10.9	21.4	17.6	24.0	26.6
^{169}Yb	32,026d	c	21.9 ± 1.9	17.8	12.9	11.7	21.4	18.0	23.6	24.6
^{166}Yb	56,7h	c	20.0 ± 1.8	18.6	12.5	12.2	19.2	18.3	21.2	22.2
^{167}Tm	9,25d	c	21.5 ± 3.0	19.0	11.8	11.1	17.6	14.3	18.6	22.0
^{165}Tm	30,06h	c	21.7 ± 2.2	20.1	13.4	10.7	21.5	17.3	21.7	20.2
^{161}Tm	33m	c*	17.0 ± 3.1	19.0	14.1	8.80	22.6	20.0	16.2	15.1
^{160}Er	28,58h	c	21.1 ± 2.6	18.4	13.7	10.1	22.3	16.9	18.3	16.0
^{157}Dy	8,14h	c	19.6 ± 1.8	19.6	12.8	9.65	20.5	16.6	14.2	13.1
^{152}Dy	2,38h	c	11.9 ± 1.0	12.8	8.32	6.63	11.5	4.06	9.65	9.46
^{155}Tb	5,32d	c	18.4 ± 1.9	16.5	8.57	10.1	13.5	–	13.1	11.8
^{153}Gd	240,4d	c	15.5 ± 1.9	16.3	9.21	8.26	13.5	1.65	11.9	10.3
^{151}Gd	124d	c	13.6 ± 1.5	16.6	11.2	8.11	16.8	12.5	10.7	8.87
^{146}Gd	48,27d	c	16.0 ± 1.4	17.9	15.1	6.39	21.4	18.8	10.0	8.02
^{148}Eu	54,5d	i	0.725 ± 0.062	1.26	0.386	1.09	0.400	–	0.491	0.309
^{147}Eu	24,1d	c	18.8 ± 1.6	17.9	10.3	8.62	11.9	18.7	8.98	6.30
^{146}Eu	4,61d	i	2.59 ± 0.23	3.64	1.30	3.17	1.11	–	1.98	1.10
^{145}Eu	5,93d	c	13.2 ± 1.2	19.0	14.8	8.28	18.3	19.2	8.28	6.96
^{136}Nd	50,65m	c	9.34 ± 1.09	9.74	10.4	5.84	12.8	18.5	3.57	1.56
^{139}Ce	137,640d	c	14.7 ± 1.3	18.1	12.9	11.4	17.0	18.2	7.06	5.47
^{135}Ce	17,7h	c	12.9 ± 1.3	16.4	11.5	8.77	13.7	17.6	5.69	3.82
^{130}Ce	25m	c	6.53 ± 0.65	4.79	7.75	–	5.59	–	1.28	1.21
^{131}Ba	11,50d	c	10.9 ± 0.9	14.4	10.9	11.7	10.7	16.6	4.65	3.27
^{129}Cs	32,06h	c	12.1 ± 1.2	13.1	10.5	10.2	9.72	18.0	3.72	3.11
^{127}Xe	36,4d	c	9.61 ± 0.79	12.0	9.85	11.9	8.66	17.4	2.40	2.68
^{123}Xe	2,08h	c	10.4 ± 1.2	7.91	8.53	6.09	5.39	15.2	1.53	3.43
^{117}Te	62m	c	5.09 ± 0.51	4.01	5.65	7.20	3.02	10.7	0.491	2.07

Table 109, cont'd.

Product	$T_{1/2}$	Type	Exp yield [mbarn]	Calculated Yields [mbarn] via CEM95	CEM2k	LAHET	CASCADE	HETC	INUCL	YIELDX
^{115}Sb	32,1m	c*	5.53 ± 0.49	3.29	6.52	10.4	2.69	12.7	0.421	2.84
^{111}In	2,8047d	c	4.66 ± 0.47	2.63	4.67	10.8	3.49	7.55	0.782	10.0
^{109}In	4,2h	c	3.43 ± 0.31	1.67	3.69	5.60	1.78	6.66	0.419	2.10
^{105}Ag	41,29d	c	3.29 ± 0.27	0.781	2.81	9.81	1.91	4.47	0.619	13.6
^{100}Pd	3,63d	c	0.818 ± 0.082	0.081	1.17	2.77	0.764	2.06	0.764	0.717
^{103}Ru	39,26d	c	0.967 ± 0.111	–	0.005	0.503	0.382	–	0.164	0.276
^{97}Ru	2,791d	c	2.01 ± 0.25	0.125	1.29	8.03	1.20	1.47	1.25	10.4
^{95}Zr	64,02d	c	0.512 ± 0.046	–	–	0.139	0.164	–	–	0.041
^{88}Zr	83,4d	c	2.31 ± 0.21	0.006	0.268	8.15	3.93	0.089	3.28	17.1
^{88}Y	106,65d	i(m+g)	2.21 ± 0.19	0.018	0.187	3.80	5.77	–	0.764	2.85
^{83}Sr	32,41h	c	1.66 ± 0.79	–	0.109	4.27	2.88	–	2.87	11.2
^{82}Sr	25,55d	c	0.945 ± 0.101	–	0.050	2.91	1.42	–	1.82	7.21
^{84}Rb	32,77d	i(m+g)	2.08 ± 0.18	–	0.036	1.94	4.46	–	0.965	1.49
^{83}Rb	86,2d	c	4.19 ± 0.42	–	0.163	8.44	8.34	–	4.42	15.4
^{77}Br	57,036h	c	2.50 ± 0.25	–	0.048	4.61	3.00	–	2.62	13.2
^{75}Se	119,779d	c	2.69 ± 0.23	–	0.023	4.44	4.68	–	3.80	12.2
^{74}As	17,77d	i	1.97 ± 0.21	–	0.005	1.84	1.69	–	1.27	2.52
^{65}Zn	244,26d	c	1.88 ± 0.17	–	–	2.36	2.17	–	2.31	10.2
^{59}Fe	44,472d	c	1.23 ± 0.11	–	–	0.416	0.619	–	0.145	0.924
^{54}Mn	312,11d	i	1.74 ± 0.14	–	–	1.60	0.546	–	0.582	6.22
^{51}Cr	27,7025d	c	1.26 ± 0.14	–	–	1.35	1.07	–	0.983	5.27
^{48}V	15,9735d	c	0.419 ± 0.034	–	–	0.659	0.018	–	0.164	2.03
^{48}Sc	43,67h	i	0.843 ± 0.092	–	–	0.451	0.382	–	0.036	0.495
^{46}Sc	83,79d	i(m+g)	1.82 ± 0.16	–	–	0.832	0.491	–	0.200	3.65
^{28}Mg	20,915h	c	1.18 ± 0.11	–	–	–	–	–	–	0.924
^{24}Na	14,9590h	c	4.46 ± 0.37	–	–	0.382	0.018	–	–	2.51
^{22}Na	2,6019y	c	0.677 ± 0.071	–	–	0.035	–	–	–	1.45

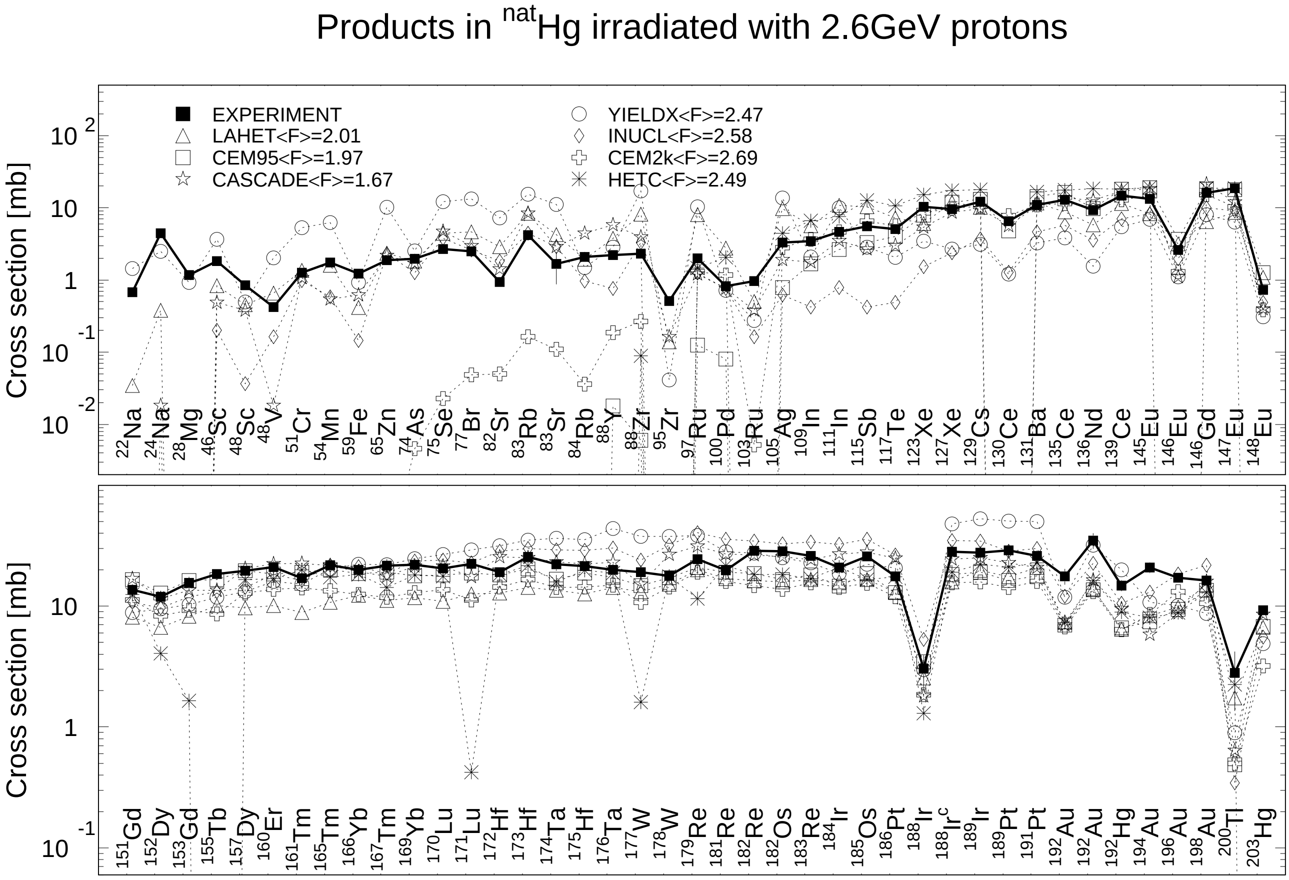

Fig. 150: Detailed comparison between experimental and simulated yields of radioactive reaction products in ^{nat}Hg irradiated with 2.6 GeV protons. The cumulative yields are labeled -c when the respective independent yields are also shown.

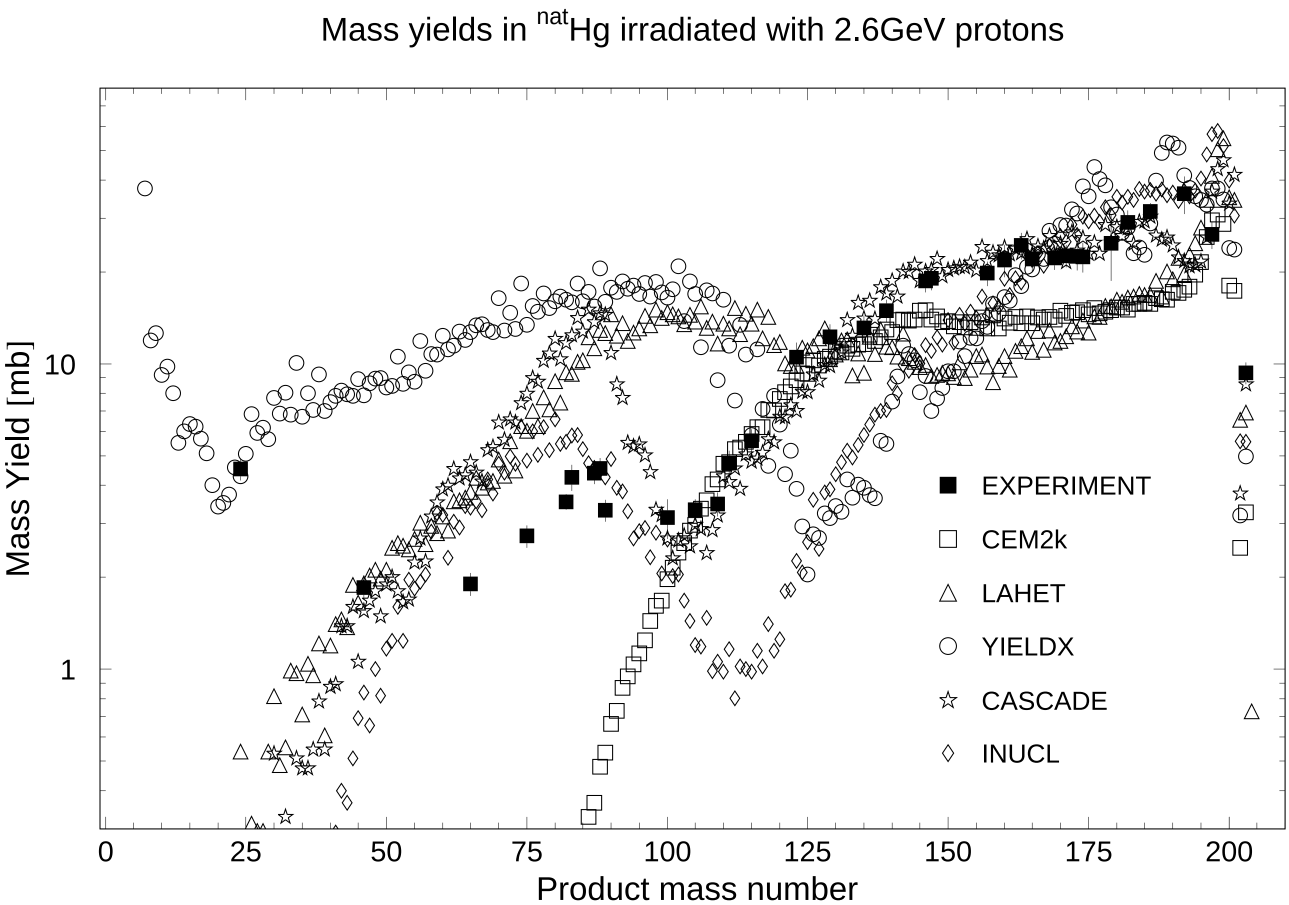

Fig. 151: The simulated mass distributions of reaction products together with the measured cumulative and supra-cumulative yields in ^{nat}Hg irradiated with 2.6 GeV protons.

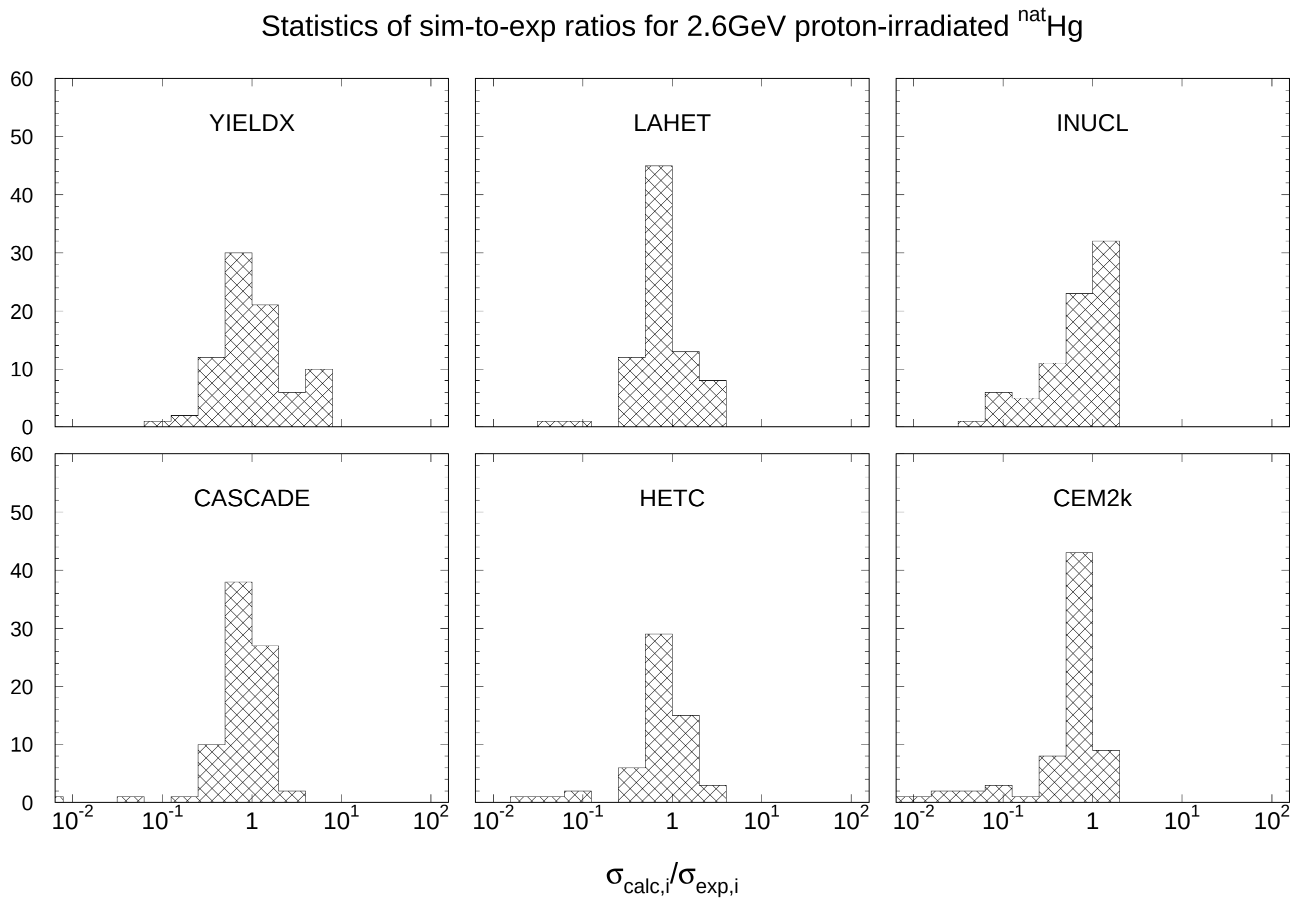

Fig. 152: Statistics of the simulation-to-experiment ratios (criterion 2) for ^{nat}Hg irradiated with 2.6 GeV protons.

Table 110: Experimental and calculated yields from ^{56}Fe irradiated with 2.6 GeV protons.

Product	$T_{1/2}$	Type	Exp yield [mbarn]	Calculated Yields [mbarn] via CEM95	LAHET	CASCADE	HETC	INUCL	YIELDX
^{57}Co	271,79d	c	0.365 ± 0.033	–	–	–	–	–	–
^{56}Co	77,233d	c	1.02 ± 0.09	0.118	1.04	0.023	1.38	0.039	0.469
^{55}Co	17,53h	c	0.274 ± 0.025	0.156	0.363	0.921	0.261	0.122	0.118
^{53}Fe	8,51m	c*	2.44 ± 0.32	1.44	1.57	4.77	0.908	2.71	3.29
^{56}Mn	2,5789h	c	0.861 ± 0.072	0.038	1.75	–	1.70	0.001	–
^{54}Mn	312,11d	i	32.8 ± 2.7	18.2	25.6	24.3	18.8	29.3	45.4
^{51}Cr	27,7025d	c	27.9 ± 2.4	17.4	16.9	18.6	24.1	13.0	22.1
^{49}Cr	42,3m	c	4.00 ± 0.35	1.72	2.06	2.86	1.83	4.23	2.07
^{48}Cr	21,56h	c	0.506 ± 0.043	0.194	0.327	1.54	0.022	0.584	0.342
^{48}V	15,9735d	c	13.4 ± 1.1	10.2	10.3	4.30	20.9	12.3	9.16
^{48}Sc	43,67h	i	0.428 ± 0.039	0.282	0.511	0.543	0.058	2.13	0.898
^{47}Sc	3,3492d	c	2.69 ± 0.23	1.22	2.14	2.66	0.131	1.98	3.76
^{46}Sc	83,79d	i(m+g)	7.18 ± 0.61	6.88	4.58	2.48	0.146	7.47	9.76
^{43}Sc	3,891h	c	4.11 ± 0.37	2.87	1.44	2.16	0.799	5.41	3.95
^{47}Ca	4,536d	c	0.067 ± 0.017	0.027	0.054	0.238	–	0.107	0.155
^{43}K	22,3h	c	1.17 ± 0.10	0.464	0.538	1.28	0.015	1.43	1.64
^{42}K	12,360h	i	3.91 ± 0.33	1.80	2.07	1.86	0.044	7.26	4.90
^{41}Ar	109,34m	c	0.703 ± 0.060	0.186	0.184	0.898	–	0.658	0.973
^{39}Cl	55,6m	c	0.521 ± 0.045	0.103	0.121	0.398	–	0.695	0.660
^{38}Cl	37,24m	i(m+g)	1.72 ± 0.16	0.529	0.672	0.748	–	6.00	2.15
^{38}S	170,3m	c	0.055 ± 0.008	0.004	0.004	0.178	–	0.119	0.141
^{29}Al	6,56m	c	1.63 ± 0.30	0.339	1.52	1.60	–	3.57	2.80
^{28}Mg	20,915h	c	0.387 ± 0.033	0.023	0.004	0.727	–	0.572	0.695
^{27}Mg	9,462m	c	1.56 ± 0.15	0.441	0.242	1.43	–	1.62	1.93
^{24}Na	14,9590h	c	3.70 ± 0.32	2.88	3.82	2.05	–	11.7	4.35
^{22}Na	2,6019y	c	3.10 ± 0.29	4.49	4.76	0.908	8.39	9.84	2.62
^{7}Be	53,29d	i	8.95 ± 0.91	–	3.42	–	0.007	0.325	9.04

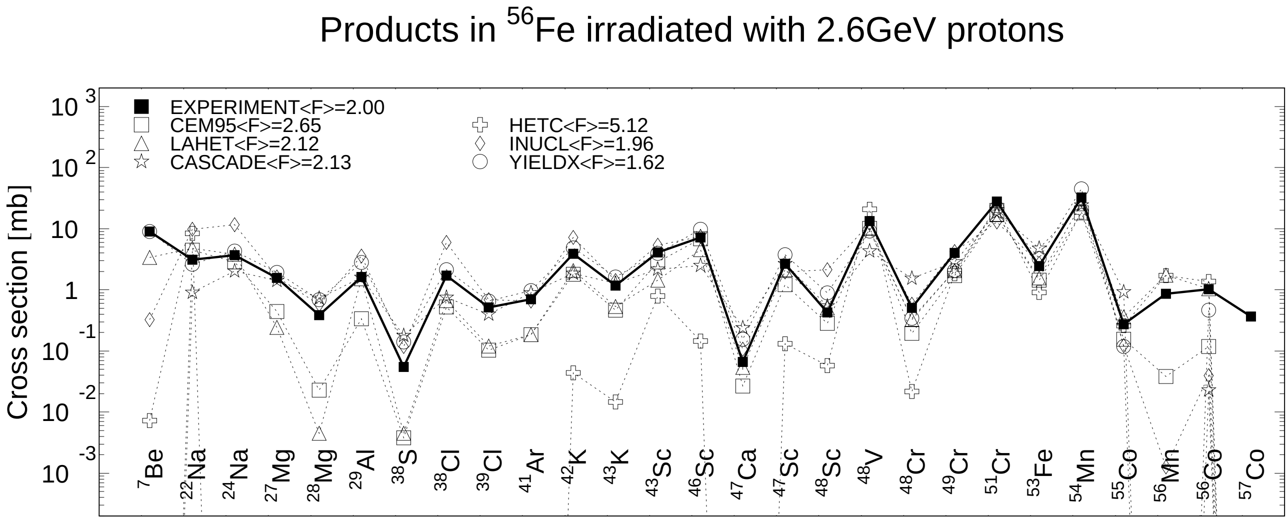

Fig. 153: Detailed comparison between experimental and simulated yields of radioactive reaction products in ^{56}Fe irradiated with 2.6 GeV protons. The cumulative yields are labeled -c when the respective independent yields are also shown.

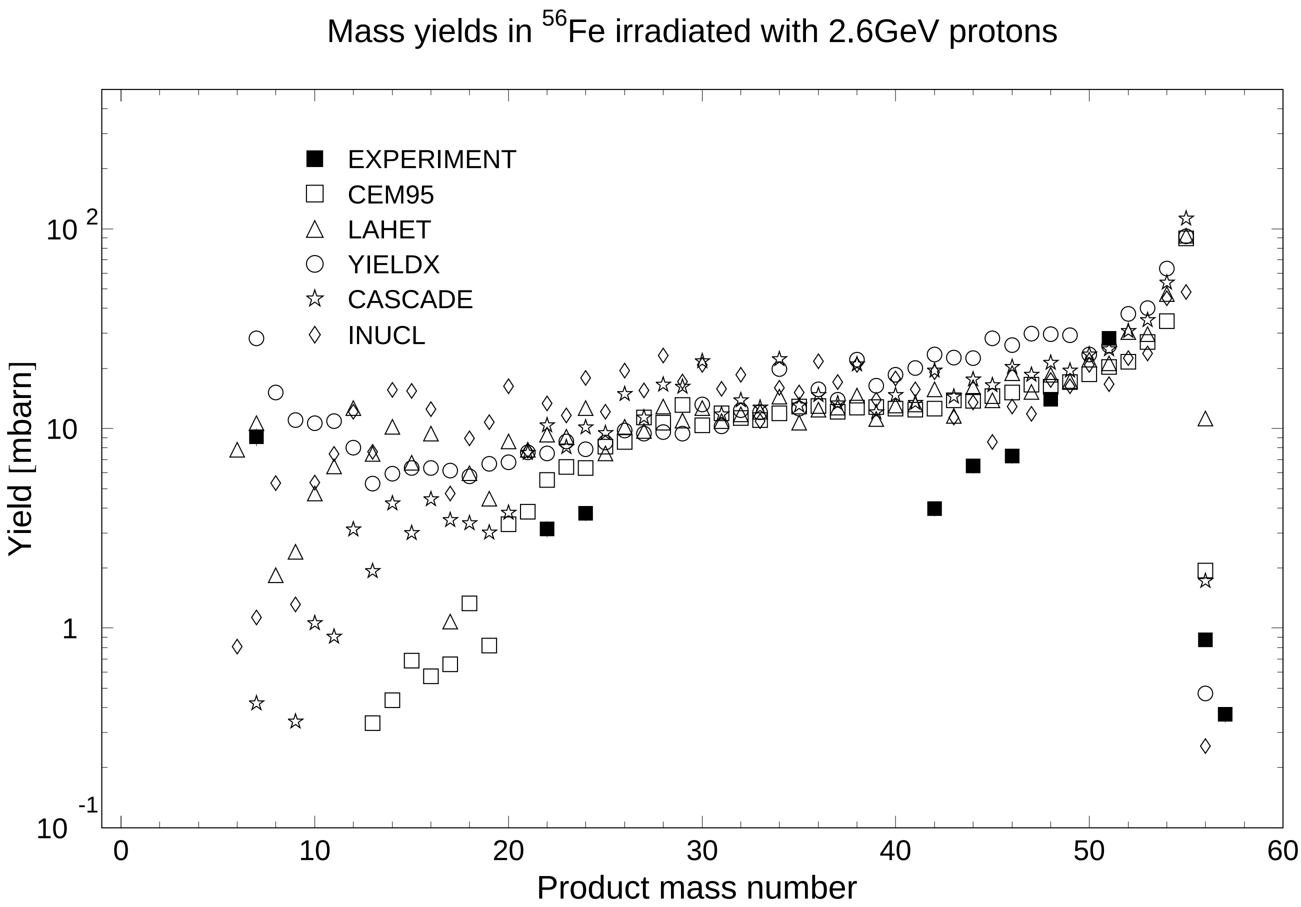

Fig. 154: The simulated mass distributions of reaction products together with the measured cumulative and supra-cumulative yields in ^{56}Fe irradiated with 2.6 GeV protons.

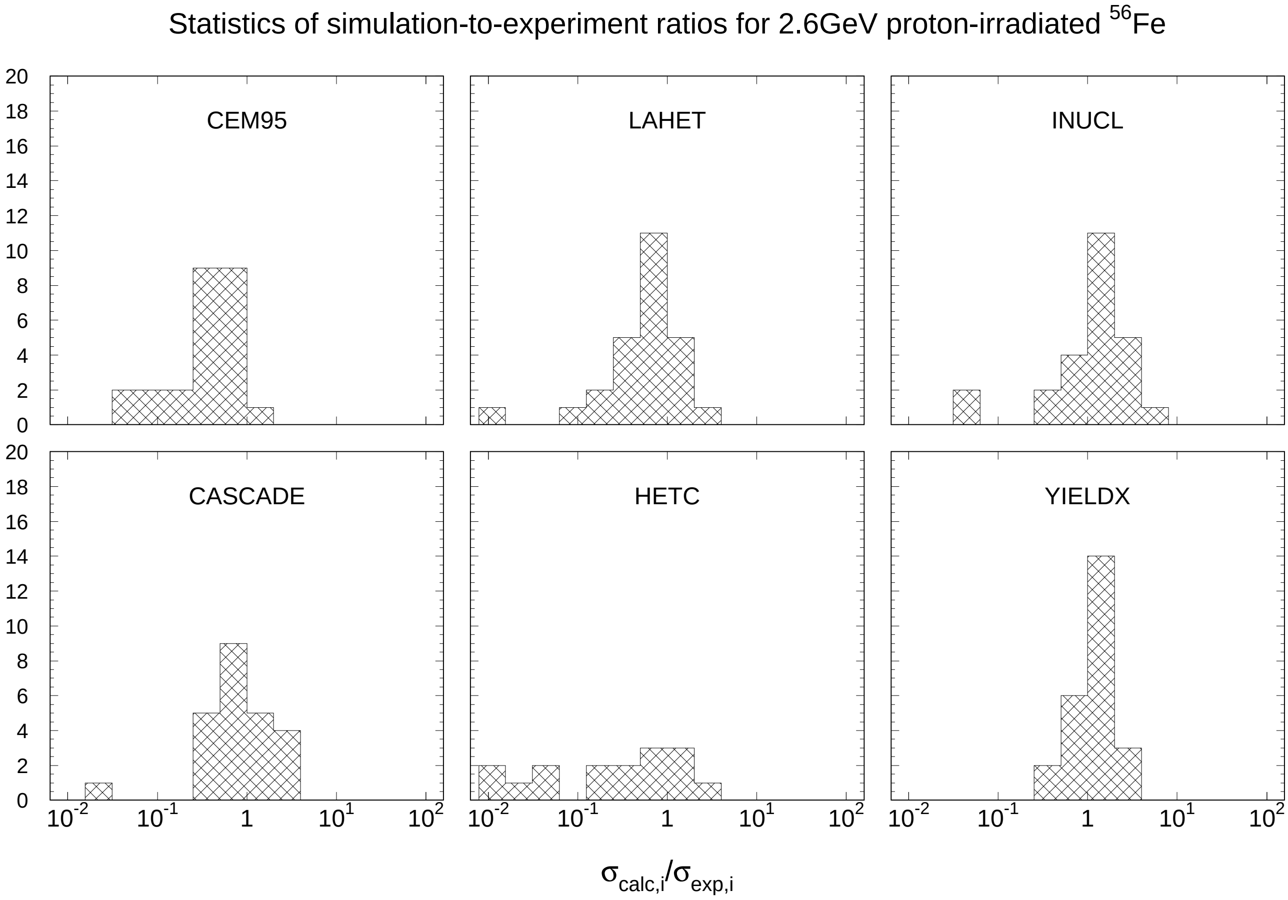

Fig. 155: Statistics of the simulation-to-experiment ratios (criterion 2) for ^{56}Fe irradiated with 2.6 GeV protons.

Table 111: Experimental and calculated yields from ^{58}Ni irradiated with 2.6 GeV protons.

Product	$T_{1/2}$	Type	Exp yield [mbarn]	Calculated Yields [mbarn] via CEM95	LAHET	CASCADE	HETC	INUCL	YIELDX
^{57}Ni	35,60h	c	30.7 ± 2.6	45.6	44.4	58.8	49.9	33.5	37.7
^{56}Ni	5,9d	i	2.56 ± 0.21	6.45	6.21	14.4	7.18	4.26	2.75
^{58}Co	70,86d	i(m+g)	6.21 ± 0.52	0.078	2.16	0.005	2.60	–	–
^{57}Co	271,79d	c	82.1 ± 6.7	91.2	92.2	113.	102.	60.2	79.8
^{57}Co	271,79d	i	50.8 ± 4.4	45.6	47.8	54.3	51.6	26.8	42.1
^{56}Co	77,233d	i	33.5 ± 2.8	23.3	27.3	25.3	36.4	42.2	29.7
^{55}Co	17,53h	c	11.1 ± 0.9	8.62	7.32	16.7	7.35	11.8	27.6
^{53}Fe	8,51m	c*	4.12 ± 0.78	4.86	3.92	7.84	2.61	8.20	4.89
^{54}Mn	312,11d	i	9.90 ± 0.82	4.88	9.34	3.60	0.809	9.07	10.7
^{51}Cr	27,7025d	c	28.4 ± 2.5	17.3	15.0	18.3	21.4	15.6	28.7
^{49}Cr	42,3m	c	8.08 ± 0.74	3.60	3.41	4.25	2.30	7.36	6.85
^{48}Cr	21,56h	c	1.65 ± 0.14	0.748	0.634	2.66	0.102	1.39	1.96
^{48}V	15,9735d	c	17.4 ± 1.4	12.2	11.8	6.42	19.5	17.1	20.1
^{48}Sc	43,67h	i	0.076 ± 0.017	1.15	0.119	0.091	–	1.00	0.238
^{47}Sc	3,3492d	c	0.794 ± 0.067	0.577	0.876	1.31	0.007	0.980	1.11
^{46}Sc	83,79d	i(m+g)	3.63 ± 0.30	4.60	2.72	1.67	0.022	5.97	3.25
^{43}Sc	3,891h	c	6.21 ± 0.55	3.48	1.80	3.23	0.888	7.79	9.53
^{43}K	22,3h	c	0.411 ± 0.034	0.125	0.374	0.611	0.007	0.782	0.502
^{42}K	12,360h	i	1.94 ± 0.16	0.951	1.47	1.07	–	6.29	1.58
^{41}Ar	109,34m	c	0.240 ± 0.021	0.109	0.078	0.450	–	0.383	0.292
^{39}Cl	55,6m	c	0.183 ± 0.019	0.016	0.091	0.234	–	0.401	0.228
^{38}Cl	37,24m	i(m+g)	0.886 ± 0.078	0.203	0.443	0.434	–	4.94	0.838
^{29}Al	6,56m	c	1.28 ± 0.15	0.203	1.36	1.23	–	3.47	1.28
^{28}Mg	20,915h	c	0.206 ± 0.018	0.094	0.018	0.502	–	0.390	0.311
^{27}Mg	9,462m	c	0.710 ± 0.087	0.312	0.187	1.12	–	1.45	0.917
^{24}Na	14,9590h	c	2.92 ± 0.28	2.76	3.30	1.75	–	11.0	2.60
^{22}Na	2,6019y	c	3.64 ± 0.32	4.58	5.01	0.941	8.10	8.73	3.70
^{7}Be	53,29d	i	12.4 ± 1.3	–	3.33	–	–	–	10.9

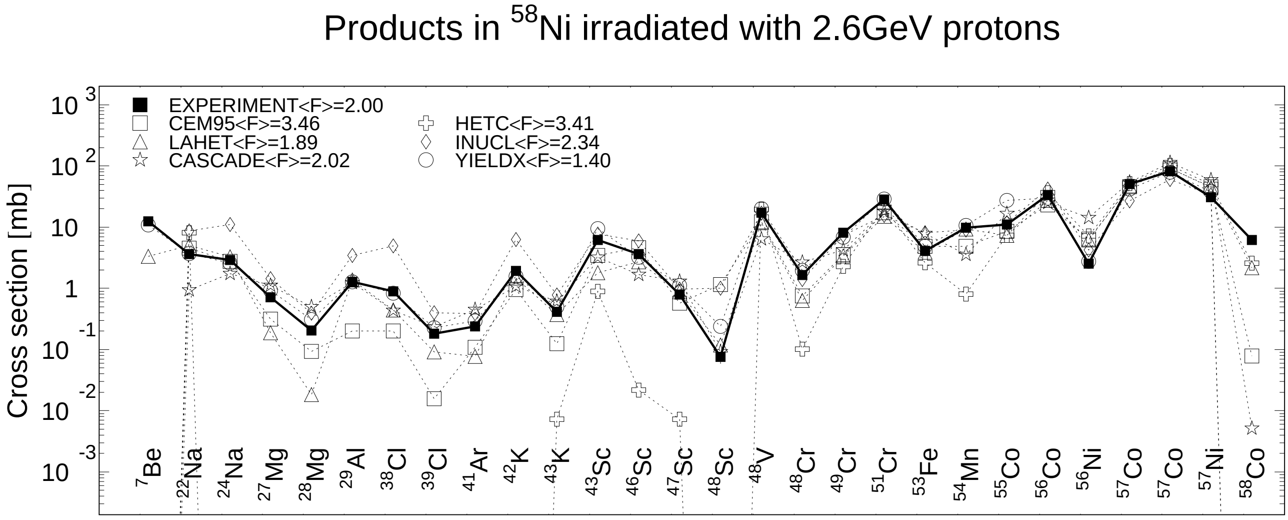

Fig. 156: Detailed comparison between experimental and simulated yields of radioactive reaction products in ^{58}Ni irradiated with 2.6 GeV protons. The cumulative yields are labeled -c when the respective independent yields are also shown.

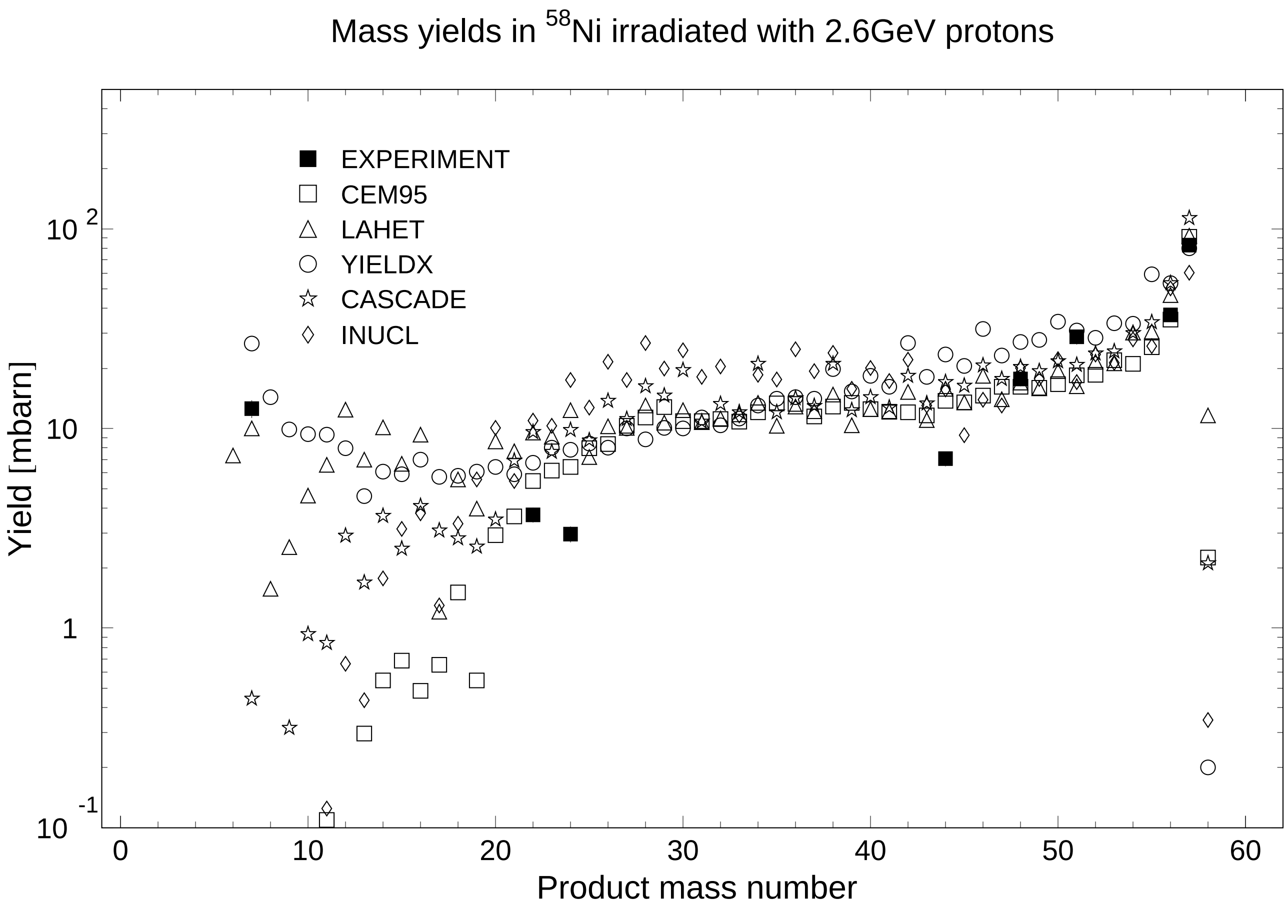

Fig. 157: The simulated mass distributions of reaction products together with the measured cumulative and supra-cumulative yields in ^{58}Ni irradiated with 2.6 GeV protons.

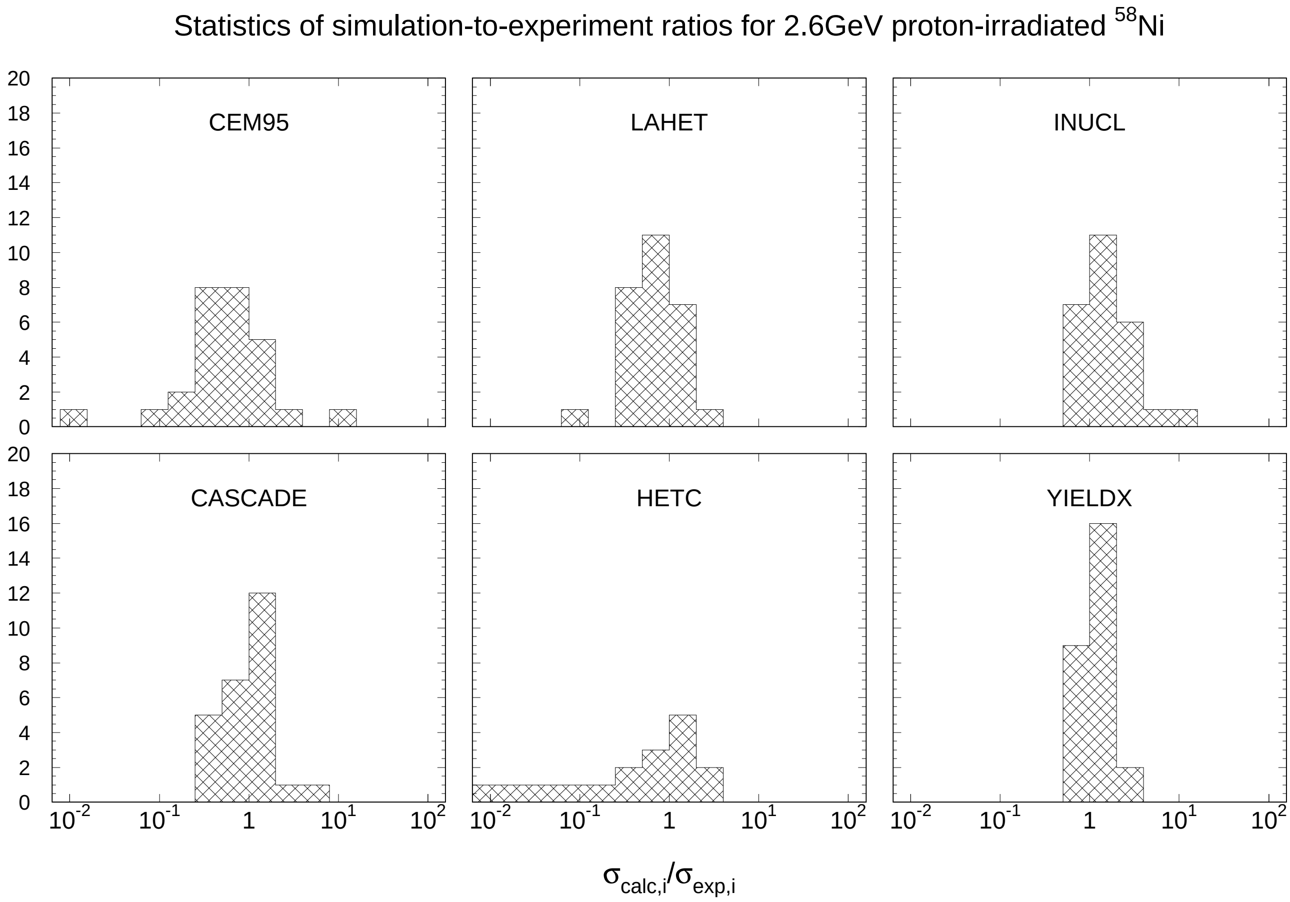

Fig. 158: Statistics of the simulation-to-experiment ratios (criterion 2) for ^{58}Ni irradiated with 2.6 GeV protons.

Table 112: Experimental and calculated yields from ^{93}Nb irradiated with 2.6 GeV protons.

Product	$T_{1/2}$	Type	Exp yield [mbarn]	Calculated Yields [mbarn] via CEM95	LAHET	CASCADE	HETC	INUCL	YIELDX
^{90}Mo	5,56h	c	0.584 ± 0.069	0.075	0.483	0.549	0.434	0.154	0.278
^{90}Nb	14,60h	c	21.1 ± 1.7	10.5	11.4	5.82	20.3	9.68	17.2
^{88}Zr	83,4d	c	27.8 ± 2.2	12.2	21.4	16.2	24.0	6.97	33.3
^{87}Zr	1,68h	c	13.8 ± 1.6	5.65	11.1	7.69	20.8	5.72	31.0
^{86}Zr	16,5h	c	5.92 ± 0.48	1.15	9.04	6.32	19.2	1.51	31.4
^{88}Y	106,65d	c	40.9 ± 3.3	20.4	28.0	22.7	28.7	15.5	66.2
^{88}Y	106,65d	i(m+g)	12.8 ± 1.1	8.23	6.68	6.49	4.74	8.58	32.9
^{86}Y	14,74h	c	23.3 ± 1.9	14.3	17.0	9.47	24.8	8.31	49.8
^{86}Y	14,74h	i(m+g)	17.6 ± 1.4	13.1	7.97	3.14	5.55	6.80	18.4
^{83}Sr	32,41h	c	18.8 ± 3.9	10.7	11.4	12.8	19.5	3.79	22.8
^{82}Sr	25,55d	c	12.3 ± 1.2	4.61	9.73	12.1	18.7	2.88	15.4
^{81}Sr	22,3m	c	4.37 ± 0.80	0.603	1.06	1.73	3.97	2.97	4.27
^{84}Rb	32,77d	i(m+g)	3.86 ± 0.34	2.80	1.89	2.25	0.539	1.85	4.93
^{83}Rb	86,2d	c	28.5 ± 2.6	16.6	15.6	19.3	20.1	7.46	33.6
^{79}Rb	22,9m	c	6.67 ± 0.73	2.20	1.33	2.41	4.74	3.96	6.04
^{79}Kr	35,04h	c	18.9 ± 1.7	13.1	12.0	15.4	17.4	11.8	25.8
^{77}Kr	74,4m	c	7.60 ± 0.65	3.41	6.42	5.97	17.4	5.70	8.14
^{76}Kr	14,8h	c	2.27 ± 0.20	0.635	2.05	4.88	6.36	1.32	3.48
^{77}Br	57,036h	c	17.0 ± 1.4	13.9	12.7	14.2	17.6	13.3	24.7
^{76}Br	16,2h	i(m+g)	10.6 ± 0.9	10.2	9.56	1.07	11.6	9.09	16.8
^{75}Se	119,779d	c	19.6 ± 1.6	14.0	12.1	15.7	17.1	10.3	21.4
^{72}Se	8,40d	c	3.62 ± 0.44	1.68	2.77	6.71	15.8	2.32	5.51
^{74}As	17,77d	i	3.83 ± 0.37	2.73	2.08	2.32	0.008	4.86	2.87
^{72}As	26,0h	c	14.9 ± 1.4	12.1	11.8	8.08	16.0	12.0	18.8
^{72}As	26,0h	i	11.3 ± 1.0	10.5	9.06	1.37	0.233	9.72	13.3
^{71}As	65,28h	c	11.8 ± 1.0	9.05	7.67	6.30	15.4	9.83	13.2
^{70}As	52,6m	c	4.75 ± 0.49	2.30	2.30	0.893	15.3	7.82	4.56
^{69}Ge	39,05h	c	9.65 ± 1.22	10.2	8.68	10.6	14.2	10.5	13.0
^{67}Ge	18,9m	c	1.91 ± 0.22	0.614	0.431	1.10	0.016	3.37	1.73
^{67}Ga	3,2612d	c	14.5 ± 1.2	12.0	9.64	9.60	14.4	13.6	14.6
^{65}Ga	15,2m	c	2.32 ± 0.60	2.04	0.512	1.34	0.869	3.42	2.38
^{65}Zn	244,26d	c	14.4 ± 1.3	12.3	9.03	12.0	13.5	10.3	12.8
^{62}Zn	9,26h	c	1.44 ± 0.23	2.22	0.955	3.17	0.885	4.12	3.14
^{61}Cu	3,333h	c	5.19 ± 0.99	7.50	3.83	3.42	13.6	7.36	3.33
^{60}Cu	23,7m	c	0.832 ± 0.138	1.49	0.500	0.158	1.66	4.91	0.723
^{57}Ni	35,60h	c	0.207 ± 0.026	0.458	0.075	0.962	0.957	1.89	0.137
^{60}Co	5,2714y	i(m+g)	9.24 ± 0.99	1.84	2.12	1.64	–	8.67	1.85
^{58}Co	70,86d	i(m+g)	8.97 ± 0.77	12.2	7.66	4.56	–	17.2	6.27
^{57}Co	271,79d	c	7.68 ± 0.66	11.8	6.14	9.29	12.9	12.6	3.85
^{56}Co	77,233d	c	2.46 ± 0.26	7.67	2.08	1.58	13.6	8.42	1.03
^{55}Co	17,53h	c	0.318 ± 0.044	0.963	0.132	0.606	0.161	1.76	0.208
^{59}Fe	44,472d	c	0.779 ± 0.088	0.242	0.339	0.750	–	0.601	0.404
^{56}Mn	2,5789h	c	1.54 ± 0.14	0.603	0.886	0.750	–	4.31	0.784
^{51}Cr	27,7025d	c	7.86 ± 0.77	12.8	7.77	10.4	12.2	14.1	4.51
^{48}Cr	21,56h	c	0.084 ± 0.010	0.027	0.086	0.337	–	0.324	0.072
^{48}V	15,9735d	c	3.44 ± 0.28	6.88	5.23	1.12	12.0	11.4	1.83
^{48}Sc	43,67h	i	0.388 ± 0.033	0.151	0.633	0.226	–	3.39	0.138
^{47}Sc	3,3492d	c	1.62 ± 0.14	0.823	2.27	1.62	–	3.18	0.596
^{46}Sc	83,79d	i(m+g)	2.91 ± 0.26	5.07	4.03	1.66	–	10.0	1.05
^{43}K	22,3h	c	0.760 ± 0.080	0.162	0.719	0.685	–	2.47	0.207
^{42}K	12,360h	i	1.79 ± 0.17	1.07	1.85	0.829	–	8.20	0.647
^{41}Ar	109,34m	c	0.505 ± 0.058	0.032	0.178	0.420	–	0.920	0.136
^{39}Cl	55,6m	c	0.464 ± 0.086	0.027	0.161	0.162	–	1.12	0.115
^{28}Mg	20,915h	c	0.326 ± 0.037	0.032	0.006	0.093	–	0.418	0.224
^{27}Mg	9,462m	c	0.634 ± 0.140	0.038	0.178	0.136	–	0.803	0.625

Table 112, cont'd.

Product	$T_{1/2}$	Type	Exp yield [mbarn]	Calculated Yields [mbarn] via CEM95	LAHET	CASCADE	HETC	INUCL	YIELDX
^{24}Na	14,9590h	c	2.50 ± 0.21	0.135	2.50	0.111	–	3.33	1.30
^{7}Be	53,29d	i	10.0 ± 1.1	–	–	–	–	0.004	6.61

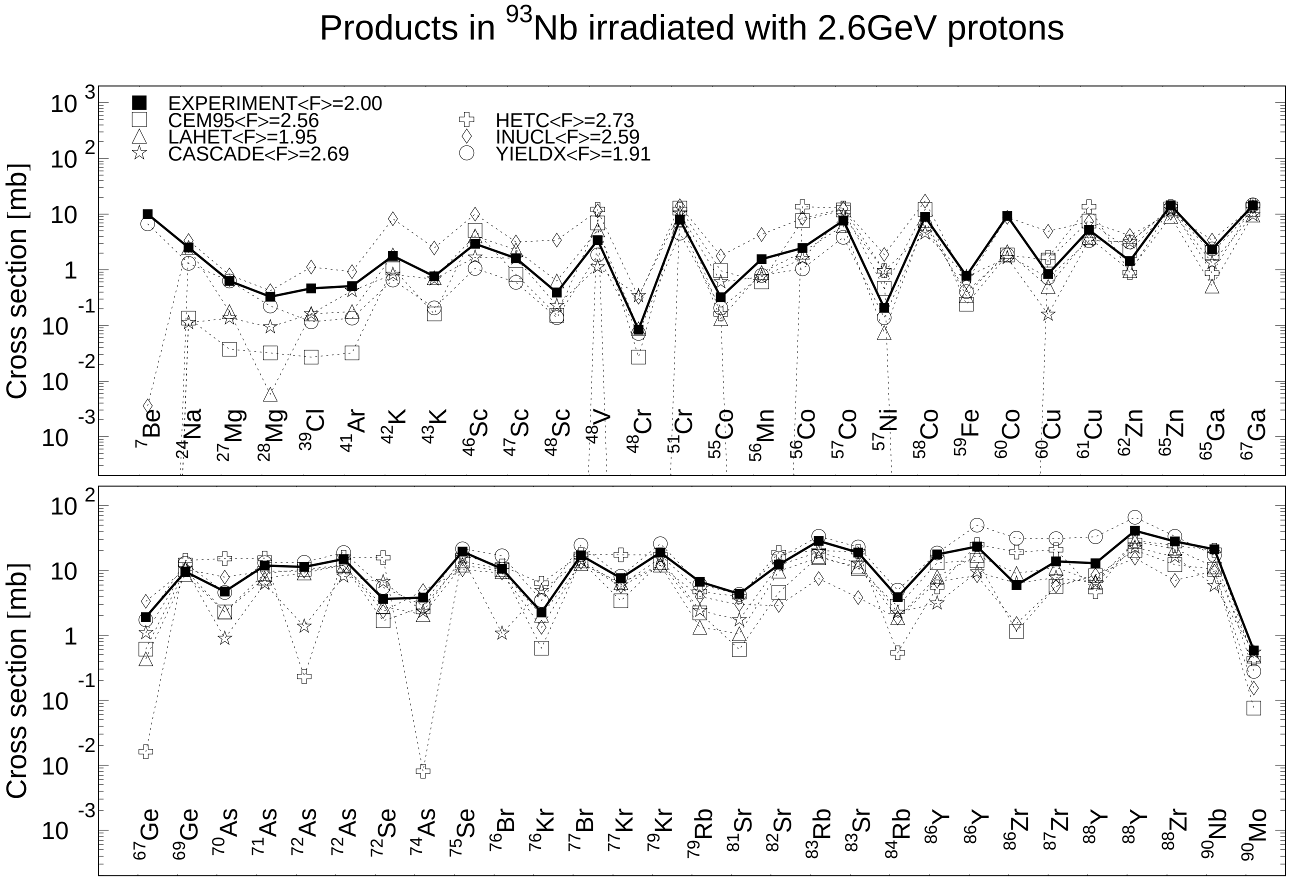

Fig. 159: Detailed comparison between experimental and simulated yields of radioactive reaction products in ^{93}Nb irradiated with 2.6 GeV protons. The cumulative yields are labeled -c when the respective independent yields are also shown.

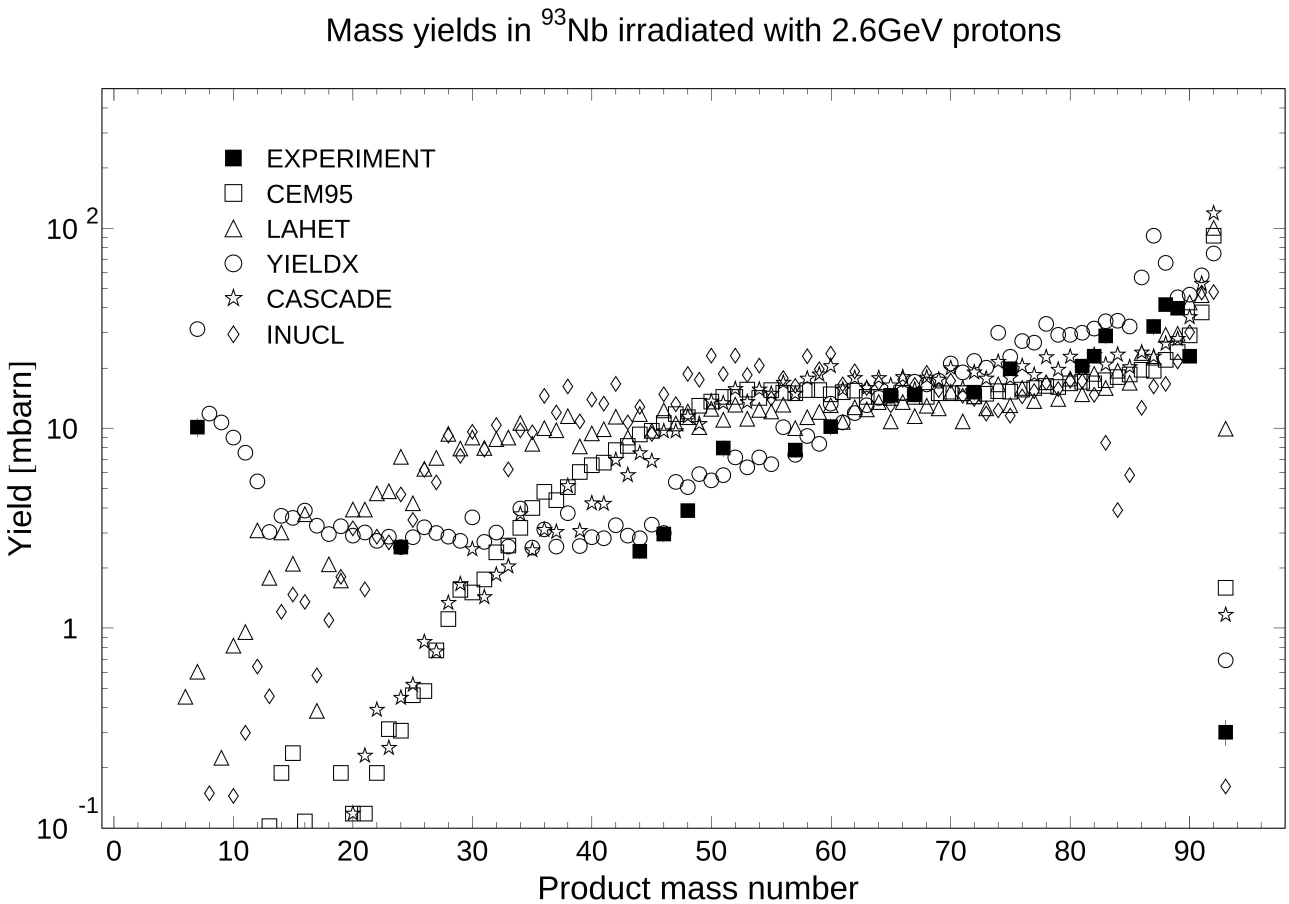

Fig. 160: The simulated mass distributions of reaction products together with the measured cumulative and supra-cumulative yields in ^{93}Nb irradiated with 2.6 GeV protons.

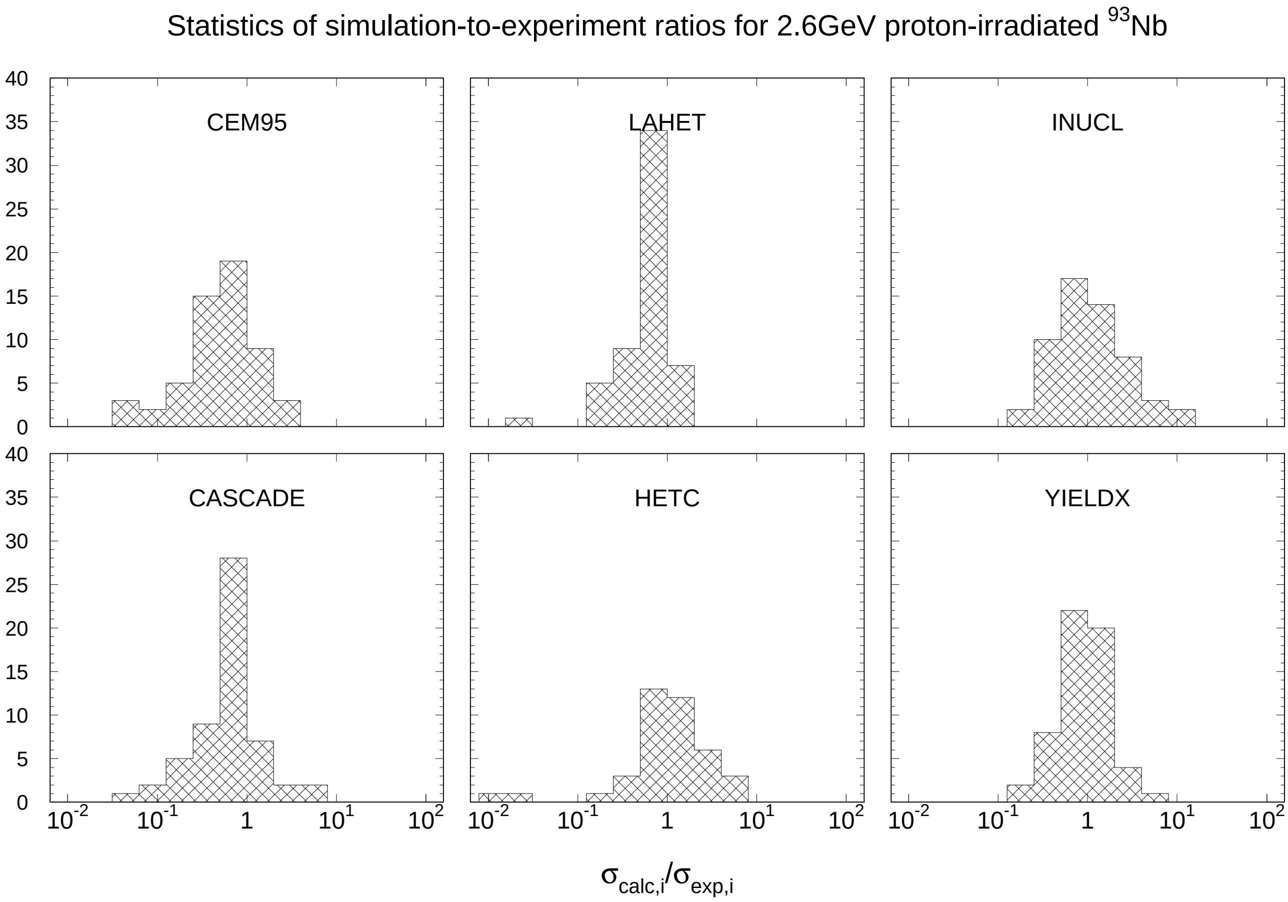

Fig. 161: Statistics of the simulation-to-experiment ratios (criterion 2) for ^{93}Nb irradiated with 2.6 GeV protons.

Table 113: Experimental and calculated yields from ^{208}Pb irradiated with 1.0 GeV protons.

Product	$T_{1/2}$	Type	Exp YIELD	Calculated Yields [mbarn] via							
			[mbarn]	CEM95	CEM2k	LAHET	CASCADE-INPE	CASCADE	HETC	INUCL	YIELDX
^{206}Bi	6,243d	i	4.60 ± 0.29	2.71	3.90	7.51	2.65	2.71	5.73	1.78	2.41
^{205}Bi	15,31d	i	6.20 ± 0.40	2.53	3.58	8.30	3.18	4.14	4.95	2.72	3.51
^{204}Bi	11,22h	i(m1+m2+g)	5.29 ± 0.80	2.60	4.13	6.11	3.03	3.44	3.87	2.72	4.30
^{203}Bi	11,76h	i(m+g)	4.84 ± 0.59	3.19	3.93	6.85	3.15	4.83	5.02	3.22	4.66
^{203}Pb	51,873h	c	31.5 ± 2.1	22.5	22.0	27.3	23.4	22.3	21.8	24.0	28.7
^{201}Pb	9,33h	c*	26.9 ± 2.4	15.5	18.8	22.3	18.5	19.0	20.0	19.8	27.7
^{200}Pb	21,5h	c	18.2 ± 1.2	13.9	18.9	24.1	18.2	21.7	19.7	23.5	26.5
^{198}Pb	2,4h	c	8.86 ± 2.11	11.8	15.7	18.5	15.6	21.3	19.5	18.5	23.0
^{202}Tl	12,23d	c	18.8 ± 1.2	33.4	33.6	45.0	35.0	33.1	31.0	45.2	36.8
^{201}Tl	72,912h	c	43.7 ± 2.9	31.7	34.5	44.7	34.9	34.9	36.1	47.5	42.0
^{200}Tl	26,1h	c	40.6 ± 2.6	27.6	32.0	39.0	31.1	34.5	30.5	45.8	36.1
^{200}Tl	26,1h	i(m+g)	22.7 ± 1.5	13.8	13.0	15.0	12.9	12.8	10.8	22.4	9.63
^{199}Tl	7,42h	c	38.5 ± 5.2	26.5	28.7	35.6	31.1	34.3	29.7	43.0	34.4
^{203}Hg	46,612d	c	4.03 ± 0.27	4.35	1.48	4.28	4.95	4.22	3.91	8.40	0.514
^{192}Hg	4,85h	c	35.2 ± 2.8	27.1	30.5	17.3	37.2	47.7	29.0	44.8	9.13
^{198}Au	2,69517d	i(m+g)	2.11 ± 0.22	2.97	1.52	2.00	1.40	1.75	0.932	4.22	0.789
^{196}Au	6,183d	i(m1+m2+g)	4.13 ± 0.35	4.12	2.74	2.86	2.26	2.84	1.38	6.30	1.91
^{195}Au	186,098d	c	48.7 ± 5.5	25.7	26.6	28.5	30.0	40.2	28.2	43.7	21.9
^{194}Au	38,02h	i(m1+m2+g)	7.06 ± 0.75	6.84	4.79	5.27	3.21	4.11	1.90	8.77	3.30
^{192}Au	4,94h	c	46.9 ± 6.6	36.3	37.7	25.6	41.8	52.7	30.8	55.7	13.8
^{192}Au	4,94h	i(m1+m2+g)	11.6 ± 1.7	9.18	7.20	8.23	4.60	5.00	1.75	10.9	4.70
^{191}Pt	2,9d	c	40.1 ± 4.4	43.0	40.4	30.2	44.6	54.7	35.7	52.8	16.5
^{189}Pt	10,87h	c	46.8 ± 4.8	45.0	39.0	33.0	42.4	54.3	37.3	47.8	18.8
^{186}Pt	2,0h	c*	34.5 ± 2.4	36.1	35.5	32.2	37.2	63.2	24.1	33.5	19.1
^{188}Ir	41,5h	c	43.2 ± 3.2	47.2	40.8	33.0	42.4	58.7	34.5	46.6	25.6
^{188}Ir	41,5h	i	2.93 ± 0.69	6.02	2.18	3.27	0.650	1.28	0.148	1.74	2.63
^{184}Ir	3,09h	c*	39.5 ± 3.0	40.2	38.2	37.8	34.8	44.2	39.6	29.7	30.0
^{185}Os	93,6d	c	41.8 ± 2.8	45.0	39.5	38.8	36.0	44.6	12.0	33.0	35.2
^{182}Os	22,10h	c	42.0 ± 2.8	42.7	38.1	38.3	33.5	41.7	21.0	25.2	44.4
^{183}Re	70,0d	c	41.7 ± 2.9	47.5	39.9	39.2	32.2	36.1	11.4	27.1	41.8
^{181}Re	19,9h	c	43.1 ± 5.9	41.9	38.9	38.7	30.7	36.5	34.7	21.9	32.5
^{179}Re	19,7m	c*	48.2 ± 4.2	38.2	37.1	33.5	28.4	30.7	1.57	17.2	26.6
^{177}W	135m	c	30.1 ± 3.5	30.4	25.7	28.9	22.5	16.4	0.074	10.8	25.9
^{176}W	2,5h	c	28.0 ± 3.9	34.3	36.6	29.3	25.9	29.2	37.6	12.5	23.9
^{176}Ta	8,09h	c	35.0 ± 3.6	38.1	37.8	30.7	26.2	29.4	37.6	12.7	25.5
^{172}Ta	36,8m	c*	17.3 ± 2.3	19.1	31.0	22.4	19.6	24.2	34.7	7.47	15.9
^{175}Hf	70d	c	31.3 ± 2.3	35.1	35.4	28.4	24.4	25.1	36.4	10.9	22.7
^{173}Hf	23,6h	c	28.4 ± 2.6	30.0	33.4	26.3	21.7	23.7	35.7	7.85	19.0
^{172}Hf	1,87y	c	24.1 ± 1.6	24.1	32.8	24.7	22.0	24.7	34.7	8.30	19.5
^{171}Hf	12,1h	c	18.2 ± 2.8	22.4	29.9	23.5	20.1	18.0	33.2	5.70	16.5
^{172}Lu	6,70d	i(m1+m2+g)	0.190 ± 0.046	1.49	0.444	0.679	0.081	0.019	–	0.093	0.430
^{171}Lu	8,24d	c	26.1 ± 1.8	23.0	22.6	24.8	20.0	14.4	–	5.15	17.3
^{170}Lu	2,012d	c	21.7 ± 2.9	21.9	29.3	22.0	18.9	19.1	34.1	6.06	17.0
^{169}Yb	32,026d	c	20.9 ± 1.5	17.3	25.1	19.8	17.3	16.0	31.4	4.87	15.2
^{166}Yb	56,7h	c	16.1 ± 1.1	10.3	19.5	17.9	13.3	11.3	27.8	2.99	12.7
^{167}Tm	9,25d	c	19.4 ± 4.0	12.0	19.2	16.5	14.7	9.14	22.8	3.48	12.6
^{165}Tm	30,06h	c	14.4 ± 1.4	8.25	18.3	14.2	12.3	10.4	26.0	2.56	10.8
^{160}Er	28,58h	c	8.77 ± 0.57	2.38	10.4	8.52	5.84	5.14	14.1	1.04	7.63
^{157}Dy	8,14h	c	5.73 ± 0.45	0.776	6.05	5.06	3.56	2.60	8.50	0.446	5.72
^{155}Tb	5,32d	c	4.16 ± 0.39	0.297	3.01	4.20	2.54	1.34	–	0.594	5.26
^{153}Gd	240,4d	c	2.60 ± 0.23	0.334	2.14	2.88	1.59	0.732	0.350	0.260	4.14
^{146}Gd	48,27d	c	1.26 ± 0.09	–	0.659	0.732	0.390	0.203	0.074	0.185	2.26
^{147}Eu	24,1d	c	0.978 ± 0.306	–	0.520	0.864	0.424	0.056	0.186	0.074	2.06
^{146}Eu	4,61d	i	0.370 ± 0.045	–	0.078	0.288	0.045	–	–	–	0.416
^{143}Pm	265d	c	1.02 ± 0.13	–	0.182	0.720	0.171	0.019	–	0.112	2.82
^{139}Ce	137,640d	c	0.832 ± 0.064	–	0.022	0.494	0.027	0.019	–	–	1.29
^{105}Ag	41,29d	c	0.646 ± 0.119	–	–	0.432	0.930	0.947	–	0.781	15.0
^{105}Rh	35,36h	c	4.63 ± 0.54	–	–	0.885	1.61	2.10	–	3.74	1.05
^{103}Ru	39,26d	c	3.84 ± 0.26	–	–	0.638	1.48	1.71	–	3.31	0.624
^{96}Nb	23,35h	i	2.31 ± 0.19	–	–	0.535	0.993	1.86	–	2.57	0.375
^{95}Zr	64,02d	c	2.34 ± 0.15	–	–	0.741	0.289	0.279	–	1.32	0.094
^{88}Zr	83,4d	c	0.765 ± 0.082	–	–	0.659	0.966	5.22	–	2.63	11.2
^{88}Y	106,65d	i(m+g)	3.41 ± 0.25	–	–	0.535	4.84	13.9	–	3.14	4.73
^{86}Rb	18,631d	i(m+g)	5.48 ± 0.66	–	–	0.967	2.61	5.24	–	2.67	0.504
^{83}Rb	86,2d	c	3.46 ± 0.28	–	–	1.13	3.67	8.25	–	3.68	11.0
^{75}Se	119,779d	c	1.34 ± 0.09	–	–	0.453	1.15	1.65	–	2.22	6.81
^{74}As	17,77d	i	1.86 ± 0.18	–	–	0.515	1.54	0.966	–	1.41	2.89
^{59}Fe	44,472d	c	0.913 ± 0.081	–	–	0.391	1.46	0.836	–	0.148	1.02
^{65}Zn	244,26d	c	0.785 ± 0.193	–	–	0.432	0.280	0.483	–	0.836	3.41
^{46}Sc	83,79d	i(m+g)	0.355 ± 0.062	–	–	0.144	0.199	0.186	–	–	2.35

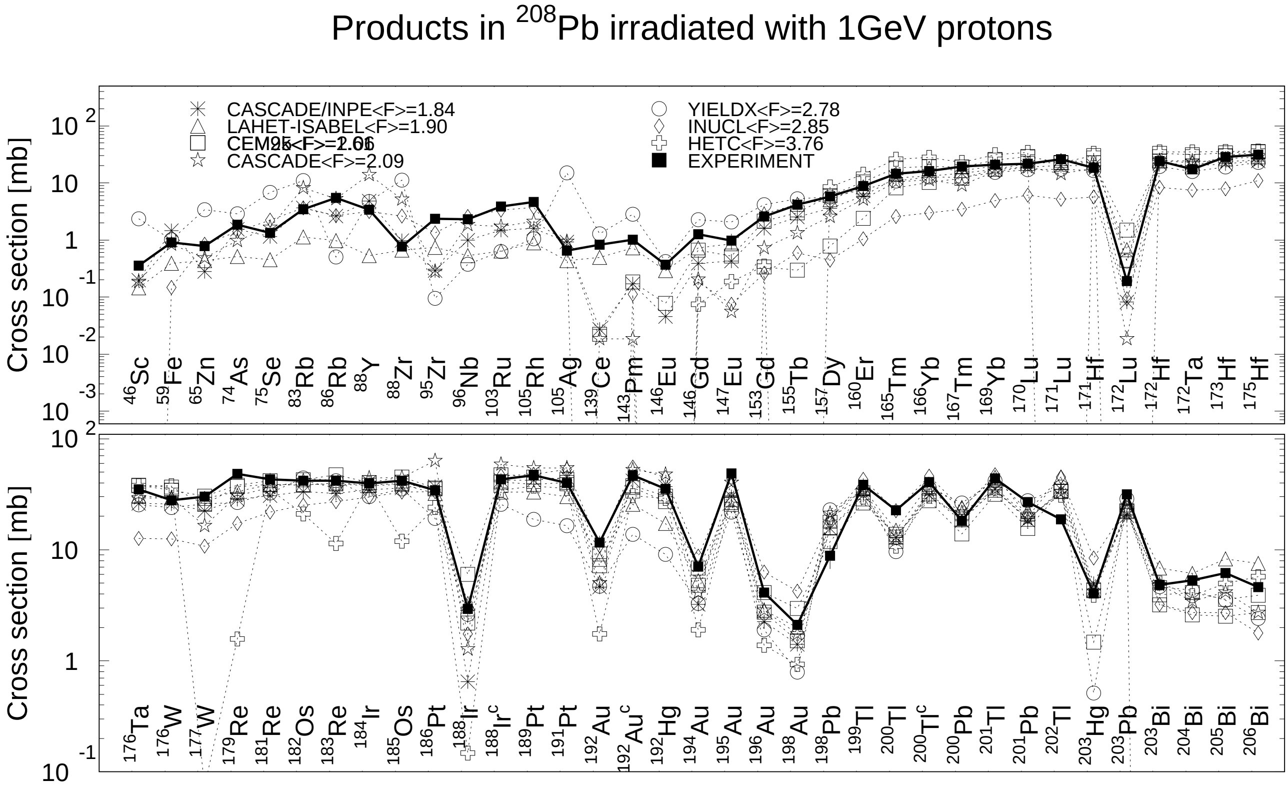

Fig. 162: Detailed comparison between experimental and simulated yields of radioactive reaction products in ^{208}Pb irradiated with 1.0 GeV protons. The cumulative yields are labeled -c when the respective independent yields are also shown.

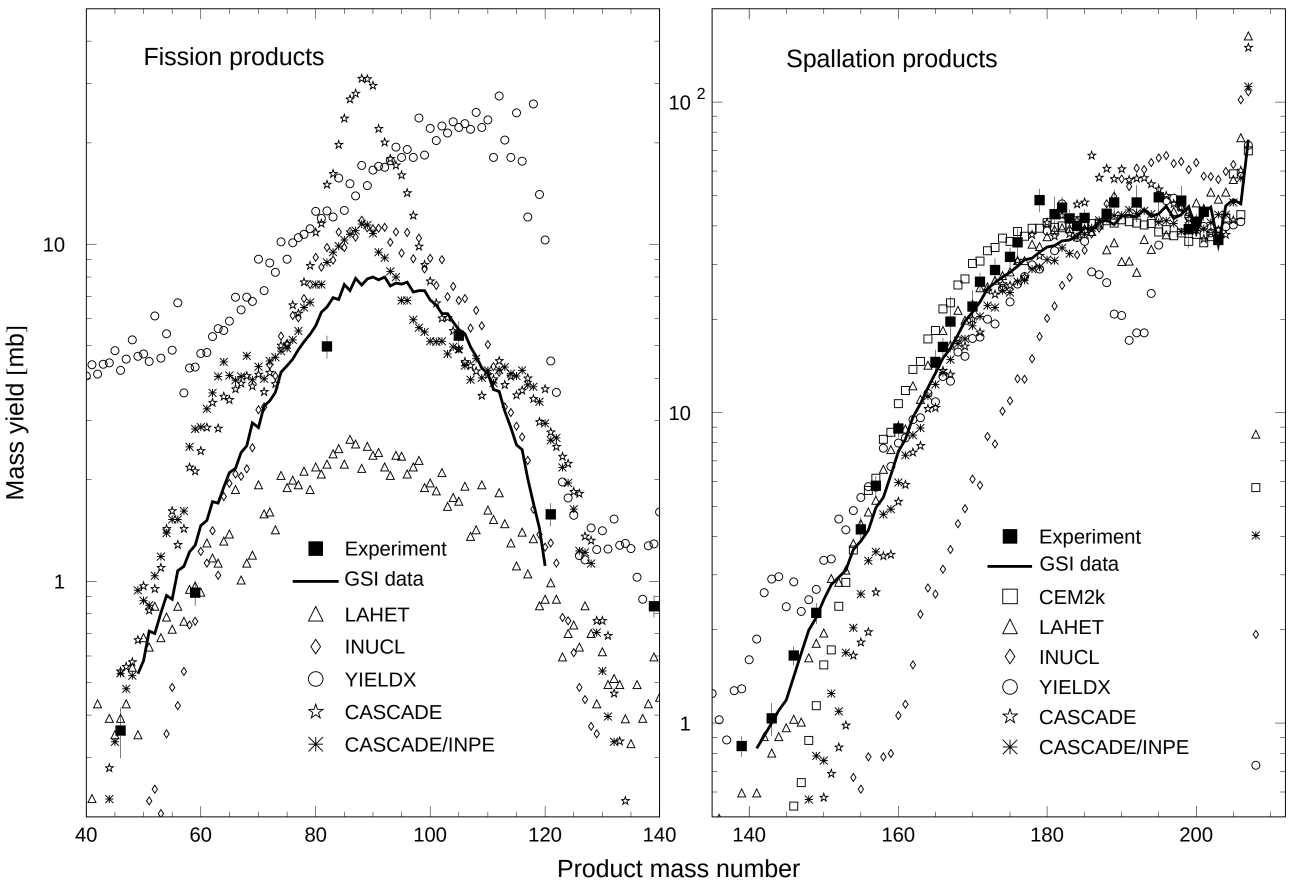

Fig. 163: The simulated mass distributions of reaction products together with the measured cumulative and supra-cumulative yields in ^{208}Pb irradiated with 1.0 GeV protons.

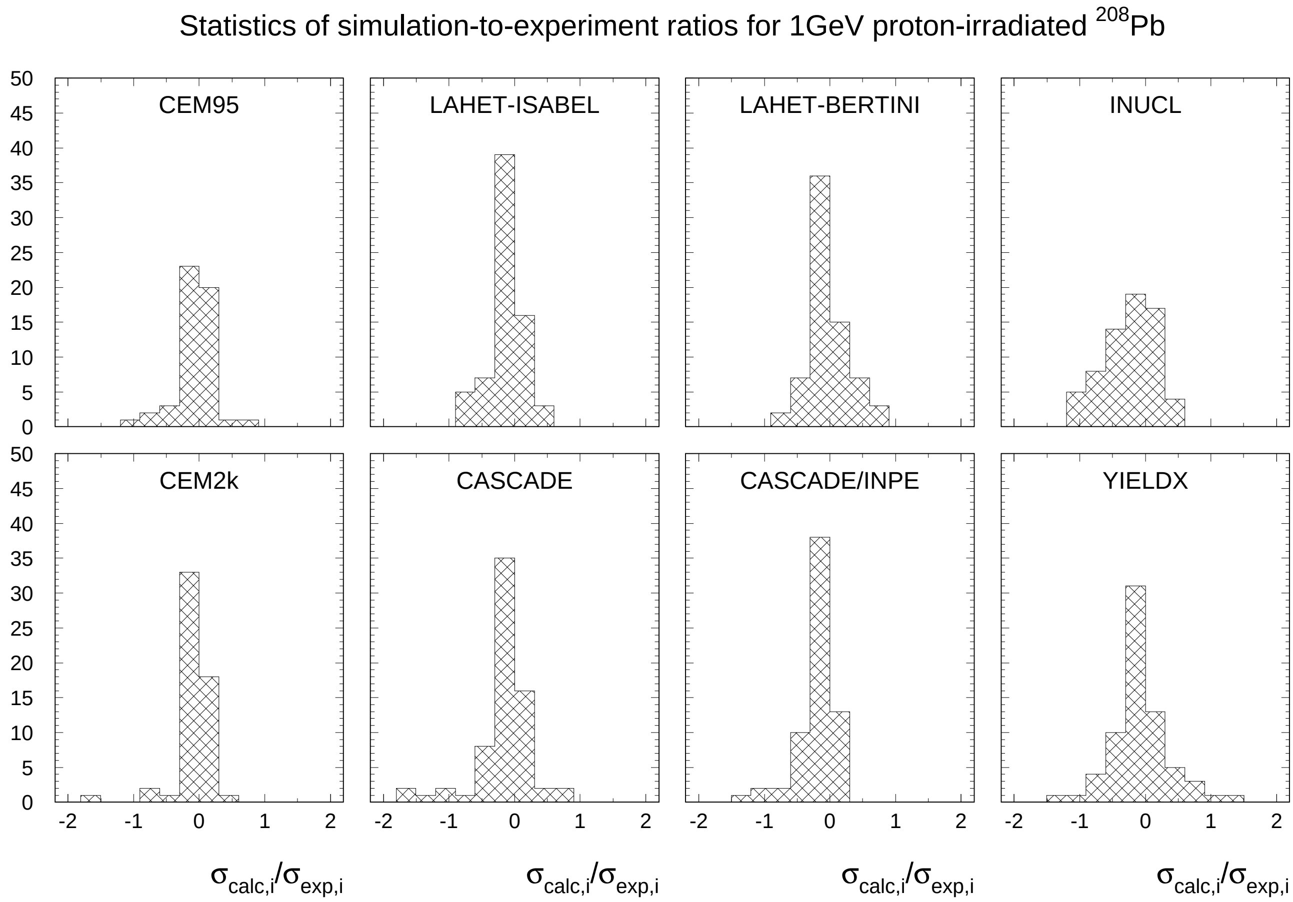

Fig. 164: Statistics of the simulation-to-experiment ratios (criterion 2) for ^{208}Pb irradiated with 1.0 GeV protons.

8 Annex 2. List of publications.

1. Yu. E. Titarenko, O. V. Shvedov, V. F. Batyaev, E. I. Karpikhin, V. M. Zhivun, A. B. Koldobsky, M. M. Igumnov, I. S. Sklokin, R. D. Mulambetov, A.N. Sosnin, H. Yasuda, H. Takada, S. Chiba, Y. Kasugai, S. G. Mashnik, R. E. Prael, M. B. Chadwick, T. A. Gabriel, M. Blann, "Experimental and Computer Simulation Study of Radionuclide Yields in the ADT Materials Irradiated with Intermediate Energy Protons", 3rd Specialists' Meeting on High Energy Nuclear Data, March 30-31 at JAERI, Tokai, Ibaraki-ken, Japan, 1998, 125-135.

2. Yu.E. Titarenko, O.V. Shvedov, E.I. Karpikhin, A.B. Koldobsky, V.M. Zhivun, R. Michel, M. Gloris, S.G. Mashnik, A.N. Sosnin, V.F. Batyaev, N.V. Stepanov, V.D. Kazaritsky, M.B. Chadwick, R.E. Prael, T.A. Gabriel, M. Blann, "Consultancy on review the draft of a database of experimental facilities and computer codes for accelerator-driven systems related R&D", Moscow, ITEP, 27-31 July 1998.

3. Yu. E. Titarenko, O. V. Shvedov, V. F. Batyaev, E. I. Karpikhin, V. M. Zhivun, A. B. Koldobsky, M. M. Igumnov, I. S. Sklokin, R. D. Mulambetov, A.N. Sosnin, H. Yasuda, H. Ta Takada, S. Chiba, Y. Kasugai, S. G. Mashnik, R. E. Prael, M. B. Chadwick, T. A. Gabriel, M. Blann, "Experimental and Computer Simulation Study of Radionuclide Formation in the ADT Materials Irradiated with Intermediate Energy Protons", Second Int. Topical Meeting on Nuclear Applications of Accelerator Technology (AccApp'98), Gatlinburg, USA, Sept. 20-23, 1998, 164-171.

4. Yu. E. Titarenko, O. V. Shvedov, V. F. Batyaev, E. I. Karpikhin, M. M. Igumnov, V.I. Volk, A.Yu. Vakhrushin, S.V. Shepelkov, A.V. Lopatkin, A.N. Sosnin, S. G. Mashnik, R. E. Prael, M. B. Chadwick T. A. Gabriel, "Experimental measurement and computer simulation of integral parameters of subcritical systems based on accelerator-driven neutron source", Second Int. Topical Meeting on Nuclear Applications of Accelerator Technology (AccApp'98)", Gatlinburg, USA, Sept. 20-23, 1998, 172-176.

5. Y.E. Titarenko, O.V. Shvedov, V.F. Batyaev, E.I. Karpikhin, V.M. Zhivun, R.D. Mulambetov, A. N. Sosnin, S.G. Mashnik, R.E. Prael, T.A. Gabriel, "Experimental and theoretical study of the yields of radionuclides produced in ^{59}Co thin and stacked targets irradiated by 70 - 200 MeV protons", 3rd International Conference on Accelerator-Driven Transmutation Technologies and Applications, Praha, June 7-11, 1999, CDRom Edition ADTTA'99, P-C27.

6. Y.E. Titarenko, O.V. Shvedov, V.F. Batyaev, E.I. Karpikhin, V.M. Zhivun, R.D. Mulambetov, S.G. Mashnik, R.E. Prael, "Nuclei product yields in ^{99}Tc transmutation under 0.1-2.6 GeV proton bombardment", 3rd International Conference on Accelerator-Driven Transmutation Technologies and Applications, Praha, June 7-11, 1999, CDRom Edition ADTTA'99, P-C26.

7. Yury E. Titarenko, Oleg V. Shvedov, Vyacheslav F. Batyaev, Eugeny I. Karpikhin, Valery M. Zhivun, Ruslan D. Mulambetov, Stepan G. Mashnik, Richard E. Prael, "Experimental and theoretical study of the yields of radionuclides produced in ^{232}Th thin targets irradiated by 100 and 800 MeV protons", 3rd International Conference on Accelerator-Driven Transmutation Technologies and Applications, Praha, June 7-11, 1999, CDRom Edition ADTTA'99, P-C24.

8. Yury E. Titarenko, Oleg V. Shvedov, Vyacheslav F. Batyaev, Eugeny I. Karpikhin, Valery M. Zhivun, Ruslan D. Mulambetov, Stepan G. Mashnik, Richard E. Prael, "Experimental and theoretical study of the yields of radionuclides produced in ^{nat}U thin targets irradiated by

100 and 800 MeV protons", 3rd International Conference on Accelerator-Driven Transmutation Technologies and Applications, Praha, June 7-11, 1999, CDRom Edition ADTTA'99, P-C25.

9. Yu. E. Titarenko, O. V. Shvedov, V. F. Batyaev, E. I. Karpikhin, V. M. Zhivun, R. D. Mulambetov, A. N. Sosnin S. G. Mashnik, R. E. Prael, T. A. Gabriel, M. Blann, "Experimental and computer simulation study of radionuclide production in heavy materials irradiated by intermediate energy protons", 3rd International Topical meeting on Nuclear Applications of Accelerator Technology (AccAppŸ99), Long Beach, CA, USA, November 14-18, 1999, 212-223; Los Alamos Preprint LA-UR-99-4489(1999).

10. Yu. E. Titarenko, O. V. Shvedov, V. F. Batyaev, E. I. Karpikhin, V. M. Zhivun, R. D. Mulambetov, S. G. Mashnik, R. E. Prael, W.B. Wilson, "Experimental and computer simulation study of radioactivity of materials irradiated by intermediate energy protons", 3rd International Topical meeting on Nuclear Applications of Accelerator Technology (AccAppŸ99), Long Beach, CA, USA, November 14-18, 1999 203-211; nucl-ex/9908015; Los Alamos Preprint LA-UR-99-4090(1999).

11. Yu. E. Titarenko, O. V. Shvedov, V. F. Batyaev, E. I. Karpikhin, V. M. Zhivun, R. D. Mulambetov, S. G. Mashnik, R. E. Prael, W.B. Wilson "Experimental and computer simulation study of radioactivity of materials irradiated with protons of intermediate energies", Proc. Intern. Conf. on Subcritical Accelerator- Driven Sysytems, ITEP, Moscow 11-15 October 1999, pp.183-183. Los Alamos Preprint LA-UR-99-4090 (1999).

12. Yu.E. Titarenko, O.V. Shvedov, V.F. Batyaev, E.I. Karpikhin, V.M. Zhivun, R.D. Mulambetov, "Spallation and fission reaction products in ^{209}Bi and ^{206,207,208}Pb irradiated by 1.5 GeV protons", Proc. Intern. Conf. on Subcritical Accelerator-Driven Sysytems, ITEP, Moscow 11-15 October 1999, p.194-199.

13. Yu. E. Titarenko, O. V. Shvedov, V. F. Batyaev, E. I. Karpikhin, V. M. Zhivun, R. D. Mulambetov, S. G. Mashnik, R. E. Prael, M. Blann, "Nuclear Product Yield in ^{99}Tc transmutation under 0.1-2.6 GeV proton bombardment", ITEP, 11-15 October 1999, p.204-211.

14. Yu.E. Titarenko, O.V. Shvedov, V.F. Batyaev, E.I. Karpikhin, V.M. Zhivun, R.D. Mulambetov, A.N. Sosnin, H. Yasuda, H. Takada, S. Chiba, Y. Kasugai, S. G. Mashnik, R. E. Prael, M. B. Chadwick, T. A. Gabriel, M. Blann, "Measurements of Radioactive Product Nuclide Yields in Intermediate-Energy Proton-Irradiated Thin Targets Made of ADT Materials", MIPhI-99 Scientific Session, Collected Works, Moscow, 1999, v. 5, p 32 (in Russian).

15. Y.E. Titarenko, O.V. Shvedov, V.F. Batyaev, E.I. Karpikhin, V.M. Zhivun, R.D. Mulambetov, A.N. Sosnin, H. Yasuda, H. Takada, S. Chiba, Y. Kasugai, S. G. Mashnik, R. E. Prael, M. B. Chadwick, T. A. Gabriel, M. Blann, "Study of Comparative Ability to Work of Codes that Simulate Interactions of ADS Materials Nuclei with Intermediate-Energy Protons", MIPhI-99 Scientific Session, Collected Works, Moscow, 1999, v.5, p. 233.

16. Yu.E. Titarenko, O.V. Shvedov, V.F. Batyaev, V.M. Zhivun, E.I. Karpikhin, R.D. Mulambetov, D.V. Fischenko, S.V. Kvasova, S.G. Mashnik, R.E. Prael, "Study of residual product nuclide yields in 1.0 GeV proton-irradiated ^{208}Pb and 2.6 GeV proton-irradiated ^{nat}W thin targets", Fifth Specialists Meeting on Shielding Aspects of Accelerators, Targets and Irradiation Facilities (SATIF-5), nucl-ex/0008011, 20-21 July 2000, Paris, France.

17. Yu.E. Titarenko, O.V. Shvedov, V.F. Batyaev, V.M. Zhivun, E.I. Karpikhin, R.D. Mulambetov, D.V. Fischenko, S.V. Kvasova, V.E. LuckŸyashin, S.G. Mashnik, R.E. Prael, "Study of residual product nuclide yields in 0.1, 0.2, 0.8, and 2.6 GeV proton-irradiated thin Hg

targets", Fifth Specialists Meeting on Shielding Aspects of Accelerators, Targets and Irradiation Facilities", (SATIF-5), 20-21 July 2000, Paris, France, nucl-ex/0008012, Los Alamos Preprint LA-UR-00-3600

18. Yu.E. Titarenko, O.V. Shvedov, V.F. Batyaev, E.I. Karpikhin, V.M. Zhivun, A.B. Koldobsky, R.D. Mulambetov, D.V. Fischenko, S.V. Kvasova, A.N. Sosnin, S.G. Mashnik, R.E. Prael, A.J. Sierk, T.A. Gabriel, M. Saito, H. Yasuda, "Cross sections for nuclide production in 1 GeV proton-irradiated ^{208}Pb". nucl- th/0011083 23 Nov 2000, Los Alamos Preprint LA-UR-00-4779, Submitted to Phys. Rev. C.

19. Yu.E. Titarenko, O.V. Shvedov, V.F. Batyaev, V.M. Zhivun, E.I. Karpikhin, R.D. Mulambetov, D.V. Fischenko, S.V. Kvasova, S.G. Mashnik, R.E. Prael, A.J. Sierk, "Fission product yields in hybrid (ADS) target material induced by high-energy protons", Proc. of the 15th Int. Workshop on Fission Physics, Obninsk, Russia, October 2-6, 2000. Los Alamos Preprint LA-UR-00-5848.

20. Yu.E. Titarenko, V.F. Batyaev, E.I. Karpikhin, V.M. Zhivun, A.B. Koldobsky, R.D. Mulambetov, D.V. Fischenko, S.V. Kvasova, A.N. Sosnin, S.G. Mashnik, R.E. Prael, A.J. Sierk, T.A. Gabriel, M. Saito and H. Yasuda, "Experimental and Theoretical Study of the Residual Product Nuclide Yields in 100-2600 MeV Proton-irradiated Thin Targets"; Los Alamos Preprint LA-UR-00-6007; Summary submitted to the International Conference on Nuclear Data for Science and Technology, October 7-12, 2001, Tsukuba, Japan.

21. V.F. Batyaev, S.V. Kvasova, R.D. Mulambetov, Yu.E. Titarenko, S.G. Mashnik, R.E. Prael, A.J. Sierk, "Benchmarking Ten Codes Against the Recent GSI Measurements of the Nuclide Yields from ^{208}Pb, ^{197}Au and U Reactions at 1 GeV nucleon"; Los Alamos Preprint LA-UR-00-6008; Summary submitted to the International Conference on Nuclear Data for Science and Technology, October 7-12, 2001, Tsukuba, Japan.

Nuclear Data Section
International Atomic Energy Agency
P.O. Box 100
A-1400 Vienna
Austria

e-mail: services@iaeand.iaea.org
fax: (43-1) 26007
cable: INATOM VIENNA
telex: 1-12645
telephone: (43-1) 2600-21710

Online: TELNET or FTP: iaeand.iaea.org
username: IAEANDS for interactive Nuclear Data Information System
usernames: ANONYMOUS for FTP file transfer;
FENDL2 for FTP file transfer of FENDL-2.0;
RIPL for FTP file transfer of RIPL;
NDSONL for FTP access to files sent to NDIS "open" area.
Web: http://www-nds.iaea.org